

Institute of Electrophysics, Ural Branch of RAS
Institute of High Current Electronics, Siberian Branch of RAS
Institute of Metal Physics, Ural Branch of RAS
Institute of Metallurgy, Ural Branch of RAS
Ural Branch of the Russian Academy of Sciences
Ural Federal University
LLC "Signifika"

15th International Conference
“Gas Discharge Plasmas
and Their Applications”
GDP 2021

Abstracts

September 5–10, 2021
Ekaterinburg, Russia

Ekaterinburg 2021

UDC 533.9
BBC 22.333.3

15th International Conference "Gas Discharge Plasmas and Their Applications" GDP 2021 (Ekaterinburg, September 5–10, 2021): Abstracts. – Ekaterinburg: IEP UB RAS, 2021. – 260 p.

Edited by Dr Nikolay Zubarev.

ISBN 978-5-6046849-0-0

The book contains abstracts of oral and poster reports presented at the 15th International Conference "Gas Discharge Plasmas and Their Applications" (GDP 2021). This event is a continuation of conferences on gas discharge physics held in Russia since 1984, as well as seminars and conferences on the technological application of low-temperature plasma. The conference is held every 2 years in different cities of the Russian Federation. This year, the wonderful city of Ekaterinburg, located in the heart of the Urals on the border of Europe and Asia, was chosen as the venue. The program of the Conference covers a wide range of technical areas and modern aspects of the physical processes occurring in generators of low temperature plasma, low and high-pressure discharges, pulsed plasma sources, surface modification, and other gas-discharge technologies.

Science Edition

Published in author's version

ISBN 978-5-6046849-0-0

© IEP UB RAS

CONTENT

Section 1. FUNDAMENTAL PROCESSES IN LOW-TEMPERATURE PLASMA: low and high pressure discharges, near-electrode phenomena, radiation, ultrafast processes, diagnostics.....	18
DIFFERENT MODES OF RUNAWAY ELECTRON BEAMS IN HIGH-PRESSURE GASES V.F. Tarasenko, D.V. Beloplotov, D.A. Sorokin, M.I. Lomaev, E.Kh. Baksh, A.G. Burachenko	19
FEATURES OF THE LOW-PRESSURE HOLLOW-CATHODE GLOW DISCHARGE SUSTAINING FOR THE CONDITIONS OF ENHANCED EMISSIVITY OF THE CATHODE SURFACE N.V. Landl, Y.D. Korolev, O.B. Frants, G.A. Argunov, V.G. Geyman, V.O. Nekhoroshev	20
INVESTIGATION OF DISCHARGES WITH THE EMISSION OF ELECTRONS FROM COLD CATHODES IN PURE GASES FEATURES E.V. Belskaya, P.A. Bokhan, P.P. Gugin, V.A. Kim, G.V. Shevchenko, D.E. Zakrevsky	21
INVESTIGATION OF THE CHARGE STATE VARIATION OF THE CATHODE MATERIAL IONS IN THE LOW CURRENT VACUUM ARC PLASMA Yu.A. Zemskov, I.V. Uimanov.....	22
SUBNANOSECOND BREAKDOWN OF AIR-INSULATED COAXIAL LINE INITIATED BY RUNAWAY ELECTRONS IN THE PRESENCE OF STRONG AXIAL MAGNETIC FIELD G.A. Mesyats, E.A. Osipenko, K.A. Sharypov, V.G. Shpak, S.A. Shunailov, M.I. Yalandin, N.M. Zubarev	23
ELECTRICAL PROPERTIES OF HE-INDUCED W "FUZZ" WITHIN THE PRE-BREAKDOWN AND BREAKDOWN REGIMES Yu.A. Zemskov, Yu.I. Mamontov, I.V. Uimanov	24
MEASUREMENT OF THE EXPANSION VELOCITY OF THE PLASMA HIGH-CURRENT VACUUM ARC DISCHARGE A.S. Zhigalin, A.G. Rousskikh, V.I. Oreshkin, A.P. Artyomov.....	25
RUNAWAY ELECTRON FLOWS IN MAGNETIZED COAXIAL GAS DIODES G.A. Mesyats, K.A. Sharypov, V.G. Shpak, S.A. Shunailov, M.I. Yalandin, N.M. Zubarev.....	26
METHODS TO ACHIEVE A BETTER EFFECT OF SYNTHETIC SOUND GENERATED BY REPETITIVE NANOSECOND PULSE DISCHARGE Handong Li, Yutai Li, Xinxin Wang, Haiyun Luo	27
THE INFLUENCE OF BOTH AN EXTERNAL ELECTRODE SECTIONING AND THE PRESENCE OF PLASMA INSIDE A LONG CAPILLARY TUBE ON THE IONIZATION WAVE PROPAGATION IN IT Yu.S. Akishev, V.B. Karalnik, A.V. Petryakov.....	28
METHOD OF TRIGGERING A COLD CATHODE THYRATRON WITH NANOSECOND STABILITY G.A. Argunov, N.V. Landl, Y.D. Korolev, O.B. Frants, V.G. Geyman, V.O. Nekhoroshev	29
A SOURCE OF POWERFUL SUBNANOSECOND VUV-UV RADIATION PULSES BASED ON A HIGH-PRESSURE GAS DISCHARGE V.I. Baryshnikov, V.L. Paperny	30
STUDY OF THE GENERATION OF RUNAWAY ELECTRONS WITH REFERENCE TO THE FORMATION OF A STREAMER IN A SHARPLY INHOMOGENEOUS ELECTRIC FIELD D.V. Beloplotov, V.F. Tarasenko, V.A. Shklyayev, D.A. Sorokin	31
DYNAMICS AND FEATURES OF STREAMER FORMATION IN A SHARPLY INHOMOGENEOUS ELECTRIC FIELD D.V. Beloplotov, M.I. Lomaev, D.A. Sorokin, V.F. Tarasenko	32

NANOSECOND BREAKDOWN IN A PULSED OPEN DISCHARGE P.A. Bokhan, N.A. Glubokov, P.P. Gugin, D.E. Zakrevsky	33
INVESTIGATION OF THE RADIAL DENSITY DISTRIBUTION OF THE NEAR-SURFACE MATTER IN THE CYLINDRICAL CONDUCTORS SKIN EXPLOSION I.M. Datsko, N.A. Labetskaya, V.A. Van'kevich	34
THE INITIAL STAGE OF THE PLASMA FORMATION AT THE SKIN EXPLOSION OF CYLINDRICAL CONDUCTORS I.M. Datsko, N.A. Labetskaya, S.A. Chaikovsky, V.A. Van'kevich, V.I. Oreshkin	35
FORMATION OF THE SPATIAL STRUCTURE OF A DIFFUSE DISCHARGE IN EXCIMER LASERS Yu. N. Panchenko, A.V. Puchikin, M.V. Andreev, E.V. Gorlov, V.I. Zharkov	36
PLASMA CHANNEL DYNAMICS IN SUB- AND MICROSECOND DISCHARGES IN WATER N.S. Semeniuk, A.V. Kozyrev, A.A. Zherlitsyn, S.S. Kondratiev, V.M. Alexeenko	37
THE DYNAMICS OF THE FORMATION OF INITIAL STAGES OF A TRANSVERSE NANOSECOND DISCHARGE WITH AN EXTENDED SLOT CATHODE IN ARGON N.A. Ashurbekov, K.O. Iminov, M.Z. Zakaryeva, G.S. Shakhshinov, K.M. Rabadanov	38
THE MEASUREMENTS OF VACUUM ARC BEHAVIOR AT THRESHOLD CURRENTS I.L. Muzyukin, P.S. Mikhailov	39
IONIC WIND PRODUCED BY POINT-TO-PLATE DIELECTRIC BARRIER DISCHARGES E. Moreau, E. Defoort	40
ROLE OF THE SURFACE FINISH ON THE DIFFERENT DISCHARGE REGIMES OF POINT-TO- PLATE DC CORONAS H. Yan, N. Benard, E. Moreau	41
INVESTIGATION OF THE ALUMINUM ELECTRODES EROSION OF A PLASMA GUN DURING THE OPERATION OF A HIGH-CURRENT VACUUM ARC DISCHARGE A.P. Artyomov, A.G. Rousskikh, A.S. Zhigalin, I.A. Rousskikh, A.G. Tyukavkin, V.I. Oreshkin	42
DETERMINATION OF THE CONDUCTOR RESISTANCE DURING THEIR EXPLOSION IN VACUUM UNDER CONDITIONS OF SKINNING THE CURRENT A.G. Rousskikh, A.S. Zhigalin, V.I. Oreshkin	43
METHODS FOR INTRODUCING NEGATIVE FEEDBACK FOR BEAM CURRENT CONTROL IN SOURCES WITH A PLASMA CATHODE BASED ON A LOW PRESSURE ARC M.S. Vorobyov, V.I. Shin, V.N. Devyatkov, P.V. Moskvina, N.N. Koval	44
OES OF NITROGEN ATOMS CONCENTRATION DURING PLASMA PROCESSING S.V. Avtaeva	45
THE DEVELOPMENT OF HYDRODYNAMIC AND THERMAL INSTABILITIES IN A LIQUID METAL JETS IN THE CATHODE SPOT OF A VACUUM ARC I.V. Uimanov, G.A. Mesyats	46
SURFACE DISCHARGE DURING ELECTRICAL EXPLOSION OF CONDUCTORS IN STRONG MAGNETIC FIELDS V.I. Oreshkin, S.A. Chaikovsky, E.V. Oreshkin	47
RESEARCH OF THE LIFE CHARACTERISTICS OF THERMOCATHODES IN ARC PLASMA TORCH A.S. Anshakov, P.V. Domarov	48
DETERMINATION OF THE VOLTAGE DROP ON A HIGH-CURRENT VACUUM ARC DISCHARGE UNDER CONDITIONS OF A LIMITED CROSS-SECTION OF THE PLASMA FLOW A.G. Rousskikh, A.S. Zhigalin, V.I. Oreshkin, A.P. Artyomov	49

COMPARATIVE CHARACTERISTICS OF A GLOWING ANOMALOUS, AN OPEN AND A HOLLOW CATHODE DISCHARGES E.V. Belskaya, P.A. Bokhan, P.P. Gugin, A.A. Kvashnina, D.E. Zakrevsky	50
FEATURES OF THE ELECTRON AVALANCHE FORMATION PROCESS IN A STRONGLY INHOMOGENEOUS ELECTRIC FIELD UNDER HIGH OVERVOLTAGES Y.I. Mamontov, V.V. Lisenkov	51
ELECTRON EMISSION FROM AN EXPANDING PLASMA FRONT WITHIN THE FOREVACUUM PRESSURE RANGE IN SPHERICAL GEOMETRY Y.I. Mamontov, I.V. Uimanov	52
NUMERICAL INVESTIGATION OF A HIGH-PRESSURE GAS MEDIUM PRE-IONIZATION BY RUNAWAY ELECTRONS V.V. Lisenkov, Y.I. Mamontov	53
SOME ISSUES OF THE OPERATION OF PLASMA OPENING SWITCHES S.V. Loginov	54
INTERRELATION FORMS THE CHANNEL THE HIGH FREQUENCY TORCH DISCHARGE TO THE CHARACTERISTICS OF ITS ELEMENTS TO THE ELECTROMAGNETIC FIELD Y.Y. Lutsenko, A.E. Myusova	55
FEATURES OF THE IONIZATION WAVE DEVELOPMENT PRECEDING THE BREAKDOWN IN A LONG CAPILLARY TUBE SURROUNDED BY A CONTINUOUS OR SECTIONED ELECTRODE Yu.S. Akishev, V.B. Karalnik, A.V. Petryakov	56
SPATIAL SPECTROSCOPY OF MAGNETRON DISCHARGE ARGON PLASMA USING A RADIATIVE-COLLISIONAL MODEL S.V. Serushkin	57
FEATURES OF PLASMA SUSTAINING IN A LARGE-VOLUME HOLLOW ANODE N.V. Landl, Y.D. Korolev, I.V. Lopatin, S.S. Kovalsky, V.S. Kasyanov, V.O. Nekhoroshev	58
GENERATION OF A PLASMA OF A NON-SELF-SUSTAINING GLOW DISCHARGE AT LOW PRESSURE INSIDE LONG CAVITIES D.Y. Ignatov, S.S. Kovalsky, I.V. Lopatin	59
INFLUENCE OF MOLECULAR OXYGEN ON ENERGY CHARACTERISTICS OF A GAS DISCHARGE OF ATMOSPHERIC PRESSURE IN AIR WITH ADDITION OF CARBON OXIDE V.V. Osipov, A.N. Orlov, V.V. Lisenkov, S.M. Armyninov	60
SIMULATION OF NEGATIVE CORONA DISCHARGE IN ATMOSPHERIC AIR: FROM MODE OF TRICHEL PULSES TO STATIONARY DISCHARGE A.O. Kokovin, A.V. Kozyrev, V.Y. Kozhevnikov	61
THE PROBLEM OF "ANOMALOUS" ION TRANSPORT IN HIGH-CURRENT VACUUM DISCHARGES V.Y. Kozhevnikov, A.V. Kozyrev, A.O. Kokovin	62
"ELECTRICAL WIND" IN CO ₂ -LASER MIXTURES AT SUPERATMOSPHERIC PRESSURES B.A. Kozlov, D.S. Makhanko	63
FORMATION OF VOLUME DISCHARGES IN DENSE GASES AT PULSE REPETITION RATES UP TO 10 kHz B.A. Kozlov	64
ELECTRIC EXPLOSION OF FLAT COPPER CONDUCTORS IN ASYMMETRIC AND SYMMETRIC CONFIGURATIONS IN THE CURRENT SKINNING MODE N.A. Labetskaya, I.M. Datsko, S.A. Chaikovsky, V.A. Van'kevich, E.V. Oreshkin, V.I. Oreshkin	65
ARC DISCHARGES OPERATION IN "ELION" MODE I.V. Lopatin, Yu.H. Akhmadeev, S.S. Kovalsky, D.Yu. Ignatov	66

TRAPPED RUNAWAY MODE OF ELECTRONS ACCELERATION AND IONIZATION PROCESSES IN PULSED DISCHARGE M.M. Tsventoukh	67
AVERAGE ION-CHARGE STATE AND EXPLOSIVE EMISSION PLASMA MOMENTUM DERIVATION FROM CRITICAL TEMPERATURE OF METAL M.M. Tsventoukh	68
MODELING DC DISCHARGES: FROM TOWNSEND TO ARC MODE IN ATOMIC AND MOLECULAR GASES A.I. Saifutdinov, B.A. Timerkaev, A.R. Sorokina, A.A. Saifutdinova	69
DYNAMICS OF THE FORMATION AND CONTRACTION OF A MICROWAVE DISCHARGE AND FAST GAS HEATING IN NITROGEN A.I. Saifutdinov, E.V. Kustova	70
NUMERICAL STUDIES OF THE DYNAMICS OF A SURFACE BARRIER DISCHARGE IN MOLECULAR GASES AND GAS HEATING IN THE REGION OF THE DISCHARGE FORMATION A.A. Saifutdinova, B.A. Timerkaev, A.I. Saifutdinov	71
ON HYBRID TYPE OF CATHODE ATTACHMENT IN HIGH CURRENT VACUUM ARCS D.L. Shmelev, S.A. Chaikovskiy, I.V. Uimanov	72
2D KINETIC SIMULATION OF CATHODE SPOT PLASMA EXPANSION D.L. Shmelev, S.A. Barenholts, M.M. Tsventoukh, I.V. Uimanov	73
MECHANISM OF ADDITIONAL SELF-FOCUSING OF AN ELECTRON BEAM GENERATED DURING A HIGH-VOLTAGE NANOSECOND DISCHARGE IN A GAS-FILLED DIODE M.I. Lomaev, A.V. Dyatlov, V.F. Tarasenko, D.A. Sorokin	74
SPLITTING OF THE IONIZATION WAVE DURING THE DEVELOPMENT OF GAS BREAKDOWN IN A MULTICHANNEL DISCHARGE SYSTEM A.I. Shishpanov, P.S. Bazhin, A.V. Meschanov	75
HOLE SIZE EFFECT ON MICROHOLLOW CATHODE DISCHARGE IN AIR S.I. Moshkunov, S.V. Nebogatkin, K.I. Romanov, E.A. Shershunova	76
FORMATION OF PLASMA JETS BY A HIGH-CURRENT DISCHARGE IN METAL VAPOR V.A. Kokshenev, N.E. Kurmaev	77
DENSE PLASMA FORMATION ON THE SURFACE OF A STAINLESS STEEL CONDUCTOR IN ULTRAHIGH MAGNETIC FIELDS V.A. Kokshenev, N.E. Kurmaev	78
MECHANISMS FOR INCREASING THE DIFFUSE CHANNELS DENSITY IN PUMP DISCHARGES OF EXCIMER LASERS A.G. Yastremskii, S.A. Yampolskaya	79
RUNAWAY OF ELECTRONS AND INITIATION OF EXPLOSIVE ELECTRON EMISSION DURING PULSE BREAKDOWN OF DENSE GASES G.A. Mesyats, N.M. Zubarev	80
EXPERIMENTAL INSTALLATION FOR STUDYING CATHODE PLASMA PROCESSES IN VACUUM GAP OF PULSED ELECTRON ACCELERATOR WITH GAS OR LIQUIDE INJECTION I.S. Egorov, A.V. Klimkin, A.V. Poloskov, M.A. Serebrennikov, M.V. Trigub	81
OES INVESTIGATION OF A LOW-PREASSURE NON-SELF-SUSTAINED GLOW DISCHARGE PLASMA IN Ar:N ₂ GAS MIXTURE S.S. Kovalsky, V.V. Denisov, E.V. Ostroverkhov, V.E. Prokop'ev	82
PRELIMINARY EXPERIMENTAL STUDY ON HIGH REPETITIVE AND SHORT NANOSECOND PULSED DISCHARGE IN AIR AT ATMOSPHERIC PRESSURE Yutai Li, Handong Li, Zhigang Liu, Yangyang Fu, Xiaobing Zou, Xinxin Wang	83

CURRENT AND VOLTAGE IN PLANAR DIODE WITH A MOVING CONDUCTING CHANNEL V.A. Shklyayev, S.Ya. Belomytsev, A.A. Grishkov	84
ON THE SCALING LAWS FOR LOW-TEMPERATURE PLASMAS AT MACRO AND MICRO SCALES Yangyang Fu, Xinxin Wang, Bocong Zheng, Peng Zhang, Qi Hua Fan, John P. Verboncoeur	85
INITIATION MECHANISMS AND DYNAMICS OF DEVELOPMENT AT THE PREBREAKDOWN STAGE OF A SELF-SUSTAINED SUBNANOSECOND DISCHARGE IN HIGH-PRESSURE NITROGEN S.N. Ivanov, V.V. Lisenkov, Y.I. Mamontov	86
STUDY OF RADIATIVE CHARACTERISTICS OF A COMPLETED PARTIAL DISCHARGE E.A. Yakovlev, V.V. Yugay, L.A. Zinovyev, A.R. Kashlev, V.O. Bezrukov	87
MAGNETIC FIELD INFLUENCE ON THE PENNING DISCHARGE CHARACTERISTICS N.V. Mamedov, A.S. Rohmanenkov, A.A. Solodovnikov	88
STUDY OF ANODE AND CATHODE PLASMAS FORMATION IN AN ELECTRON DIODE WITH AN EXPLOSIVE EMISSION CATHODE A.I. Pushkarev, A.I. Prima	89
DYNAMICS OF CHARGE SYSTEM IN OWN FIELD A.S. Chikhachev	90
GENERATION OF PLASMA IN LOW-PRESSURE DISCHARGE S.P. Nikulin	91
EFFECT OF BREMSSTRAHLUNG ON THE CHARACTERISTIC GROWTH LENGTH OF AN AVALANCHE OF RUNAWAY ELECTRONS E.V. Oreshkin	92
Section 2. GAS-DISCHARGE METHODS FOR SURFACE MODIFICATION AND COATING DEPOSITION:	
surface modification, ion implantation, combined methods of surface treatment	93
MULTI-CYCLE MODIFICATION OF 40Cr STEEL BY IRRADIATING THE "FILM (Si (0.2 μm) + Nb (0.2 μm)) / SUBSTRATE (40Cr STEEL)" SYSTEM BY AN INTENSIVE PULSED ELECTRON BEAM N.N. Koval, Yu.F. Ivanov, V.V. Shugurov, A.D. Teresov, E.A. Petrikova	94
CHARGE AND ELEMENTAL COMPOSITION OF PLASMA GENERATED BY SPUTTERING OF POWDER TARGET FROM AMORPHOUS BORON Yu.F. Ivanov, V.V. Shugurov, O.V. Krygina, V.E. Prokop'ev	95
STRUCTURE AND PROPERTIES OF HIGH-CHROMIUM STEEL IRRADIATED WITH A PULSED ELECTRON BEAM AND NITRIDED IN A LOW-PRESSURE GAS DISCHARGE PLASMA Yu.F. Ivanov, E.A. Petrikova, A.D. Teresov, S.V. Lykov, M.E. Rygina	96
NUMERICAL ESTIMATION OF THE SPUTTERING COEFFICIENT OF COPPER ANODE OF A PLANAR MAGNETRON BY A BEAM OF ACCELERATED ARGON IONS WITH ENERGY OF 1- 10 keV A.P. Semenov, I.A. Semenova, D.B-D. Tsyrenov, E.O. Nikolaev	97
FEATURES OF THE DISCHARGE AND DEPOSITION OF THE CrN _x COATINGS WHEN USING MAGNETRON WITH A HOT TARGET G.A. Bleykher, V.A. Grudin, D.V. Sidelev, V.P. Krivobokov	98
DEVELOPMENT OF THE COMPUTER MODEL OF THE PLASMA INSTALLATION R.A. Okulov, E.V. Popov, B.R. Gelchinski, A.A. Rempel	99

BALANCED CONTROL OF THERMAL IMPACT ON METAL MATERIALS IN ELECTRON SOURCE WITH A PLASMA CATHODE K.T. Ashurova, T.V. Koval, M.S. Vorobyov, My Kim An Tran, V.I. Shin, P.V. Moskvin, N.N. Koval	100
PLASMA MODIFICATION OF THE SURFACE OF A STEEL PRODUCT USING THE MAK-10 INSTALLATION S.A. Il'inyh, S.A. Ahmetshin, V.A. Krashaninin, B.R. Gelchinski, A.A. Rempel	101
DEPOSITION OF TiSiCN COATINGS BY DECOMPOSITION OF HEXAMETHYLDISILAZANE AND ANODIC EVAPORATION OF TITANIUM IN A LOW-PRESSURE ARC DISCHARGE A.I. Men'shakov, Yu.A. Bryuhanova, Yu.S. Surkov, A.V. Chukin	102
EFFECT OF 3D IONS IMPLANTATION ON ELECTRONIC STRUCTURE OF V ₂ O ₅ BASED CATHODE FOR LITHIUM-ION BATTERIES I.S. Zhidkov, A.I. Kukharenko, D.A. Erzunov, S.O. Cholakh, N.V. Gavrilov, E.Z. Kurmaev	103
METHOD OF A STRUCTURAL STEELS COMPLEX TREATMENT COMBINING ELECTRON-ION-PLASMA ALITIZING AND NITRIDING IN A SINGLE VACUUM CYCLE Yu.H. Akhmadeev, I.V. Lopatin, Yu.F. Ivanov, O.V. Krysina, E.A. Petrikova, M.E. Rygina	104
DEPOSITION OF Al ₂ O ₃ COATINGS IN Ar-O ₂ LOW-PRESSURE DISCHARGE PLASMA UNDER HIGH DISSOCIATION DEGREE OF O ₂ P.V. Tretnikov, N.V. Gavrilov, A.S. Kamenetskikh, S.V. Krivoshapko, A.V. Chukin	105
IMPROVEMENT OF VACUUM SURFACE FLASHOVER VOLTAGE FOR POLYMER BY ATMOSPHERIC PRESSURE PLASMA JET Chengyan Ren, Chuansheng Zhang, Kun Xie, Cheng Zhang, Tao Shao	106
THE EFFECT OF O ₂ DISSOCIATION DEGREE ON THE RATE OF ANODIC EVAPORATION OF Al IN LOW-PRESSURE ARC S.V. Krivoshapko, N.V. Gavrilov, A.S. Kamenetskikh, P.V. Tretnikov, A.V. Chukin	107
INFLUENCE OF ELECTRON-BEAM HEATING MODES ON THE STRUCTURE OF COMPOSITE ZrO ₂ -Al ₂ O ₃ CERAMICS A.S. Klimov, I.Yu. Bakeev, A.A. Zenin	108
ELECTRON BEAM SINTERING OF Mn-Zn FERRITES USING A FOREVACUUM PLASMA ELECTRON SOURCE A.S. Klimov, I.Yu. Bakeev, A.A. Zenin	109
FEATURES OF BORIDING DIE STEEL D5 BY ELECTRON BEAMS A.S. Milonov, D.E. Dasheev, N.N. Smirnyagina, A.E. Lapina	110
EFFECT OF PLASMA ASSISTANCE ON THE PROPERTIES OF COATINGS BASED ON ALUMINUM OXIDE A.Yu. Nazarov, E.L. Vardanyan, R.Sh. Nagimov, A.A. Maslov	111
Nb/NbN MULTILAYER COATINGS DEPOSITED BY THE VACUUM-ARC PLASMA-ASSISTED METHOD: SYNTHESIS, PROPERTIES, STRUCTURE O.V. Krysina, N.A. Prokopenko, Yu.F. Ivanov, V.V. Shugurov, E.A. Petrikova, O.S. Tolkachev, M.E. Rygina	112
STRUCTURAL AND PHASE DEPENDENCIES OF COATINGS FORMATION BASED ON INTERMETALLIDES Ti-Al SYSTEMS FOR INCREASING THE DURABILITY OF CUTTING TOOLS E.L. Vardanyan, K.N. Ramazanov, A.Yu. Nazarov, R.Sh. Nagimov, A.A. Maslov	113
Ti ₂ AlC MAX PHASE COATINGS MADE BY REACTIVE CATHODIC ARC DEPOSITION (ARC-PVD) A.A. Maslov, A.Yu. Nazarov, E.L. Vardanyan	114

EFFECT OF ION NITRIDING BY GLOW DISCHARGE ON THE PHYSICOMECHANICAL PROPERTIES OF THE PLASTICALLY DEFORMED TOOL STEEL R6M5 R.K. Vafin, A.V. Asylbaev, D.V. Mamontov, I.D. Sklizkov, G.I. Raab, E.F. Khairtdinov, R.S. Esipov	115
MODELING OF ION-PLASMA SYNTHESIS OF LINEAR-CHAINED CARBON E.A. Buntov, A.F. Zatsepin, A.I. Matitsev, V.A. Dutov, K.P. Arslanov	116
ADVANTAGES OF USING OF PLASMA OF PULSE-PERIODIC LOW-PRESSURE DISCHARGES FOR SURFACE TREATMENT V.V. Denisov, Yu.A. Denisova, S.S. Kovalsky, A.A. Leonov, E.V. Ostroverkhov, V.N. Tishchenko, V.V. Yakovlev	117
INVESTIGATION OF TUNGSTEN SURFACE CARBIDIZATION UNDER PLASMA IRRADIATION A.Zh. Miniyazov, T.R. Tulenbergenov, I.A. Sokolov, G.K. Zhanbolatova, O.S. Bukina, Ye.A. Kozhahmetov, M.K. Skakov	118
STUDY OF THE TiN-Cu FILMS DEPOSITED ON ALLOY T15K6 BY PLASMA OF LOW PRESSURE VACUUM-ARC AND MAGNETRON DISCHARGES D.B-D. Tsyrenov, A.P. Semenov, E.O. Nikolaev, N.S. Ulakhanov	119
FORMATION OF CATALYTIC AND CORROSION PROTECTIVE LAYERS WITH USE OF ION BEAM ASSISTED DEPOSITION OF METALS FROM VACUUM ARC DISCHARGE PLASMA V.V. Poplavsky	120
INFLUENCE OF PULSE-PERIODIC LOW-PRESSURE ARC DISCHARGE MODE ON COATING PROPERTIES M.V. Savchuk, V.V. Yakovlev, V.V. Denisov, A.A. Leonov, A.O. Egorov	121
EFFECT OF TEMPERATURE ON THE FORMATION OF TUNGSTEN CARBIDE IN A BEAM-PLASMA DISCHARGE G.K. Zhanbolatova, V.V. Baklanov, M.K. Skakov, I.A. Sokolov, O.S. Bukina, Ye.A. Kozhahmetov, N.A. Orazgaliev	122
TiCrN VACUUM ARC COATING TO INCREASE WEAR RESISTANCE OF DIE STEELS A.A. Leonov, Yu.A. Denisova, V.V. Denisov, M.V. Savchuk, V.N. Tishchenko	123
COMPARATIVE STUDY ON HIGH-VOLTAGE NANOSECOND PULSES AND DIELECTRIC BARRIER DISCHARGE EFFECTS ON SURFACE MORPHOLOGY AND PHYSICO-CHEMICAL PROPERTIES OF NATURAL PYRRHOTITE I.Zh. Bunin, I.A. Khabarova	124
EFFECT OF POWER OF ULTRASOUND DURING MICRO-ARC OXIDATION ON PHASE COMPOSITION AND MORPHOLOGY OF CALCIUM PHOSPHATE COATINGS E.A. Kazantseva, E.G. Komarova, Y.P. Shakreev	125
EFFECT OF BIAS VOLTAGE ON THE PERFORMANCE OF MAGNETRON DEPOSITED MoS ₂ COATINGS M.M. Kharkov, G.I. Rykunov, A.V. Kaziev, M.S. Kukushkina, D.V. Kolodko, M.V. Prozhega, E.O. Reschikov, I.S. Babinets, P.P. Beschapov, A.M. Stasenko, S.V. Chernyshov	126
SURFACE ENGINEERING OF TITANIUM: INFLUENCE OF ICP ETCHING AND CALCIUM-PHOSPHATE-BASED COATING DEPOSITION M.M. Kharkov, A.V. Kaziev, G.I. Rykunov, M.S. Kukushkina, K.A. Prosolov, M.A. Khimich, Yu.P. Sharkeev	127
PVD GRADIENT AND MULTILAYER COATINGS DEPOSITED BY VACUUM-ARC PLASMA-ASSISTED METHOD O.V. Krygina, N.N. Koval, Yu.F. Ivanov, N.A. Prokopenko, V.V. Shugurov	128

COMPUTER SIMULATION OF TEMPERATURE FIELDS IN THE Cr (FILM) – Zn (SUBSTRATE) SYSTEM DURING PULSED ELECTRON BEAM IRRADIATION A.B. Markov, A.V. Solovov, E.V. Yakovlev, E.A. Pesterev	129
FIELD ELECTRON EMISSION FROM NANOSTRUCTURED TUNGSTEN SURFACE I.L. Muzyukin, P.S. Mikhailov	130
EFFECT OF ION IRRADIATION ON THE STRUCTURAL STATE AND MECHANICAL PROPERTIES OF NATURALLY-AGED HOT-PRESSED D16 (Al-Cu-Mg) ALLOY PROFILES N.V. Gushchina, V.V. Ovchinnikov, L.I. Kaigorodova, D.Y. Rasposienko, D.I. Vichuzhanin	131
POSSIBILITY OF ANNEALING OF A DEFORMED Ni–13.9 WT.% W ALLOY WITH A BEAM OF ACCELERATED ARGON IONS N.V. Gushchina, V.V. Ovchinnikov, V.I. Bobrovskii, V.I. Voronin	132
ION CURRENT OPTIMIZATION IN A MAGNETRON WITH TUNABLE MAGNETIC FIELD A.V. Kaziev, D.G. Ageychenkov, A.V. Tumarkin, D.V. Kolodko, N.S. Sergeev, M.M. Kharkov	133
APPLICATION OF COMPOSITE SHS-CATHODES IN RECENT PVD TECHNOLOGIES FOR MANUFACTURING OF PROTECTIVE UHTC-BASED COATINGS Ph. Kiryukhantsev-Korneev, E. Levashov	134
INVESTIGATION OF THE STRUCTURE OF CRATERS ON THE SURFACE OF STEEL 12X18H10T AFTER ITS TREATMENT WITH A HIGH PULSE POWER BEAM OF CARBON IONS M.V. Zhidkov, A.E. Ligachev, G.V. Potemkin, G.E. Remnev	135
FORMATION OF A Cr-Zr SURFACE ALLOY USING A LOW-ENERGY HIGH-CURRENT ELECTRON BEAM A.B. Markov, E.V. Yakovlev, A.V. Solovov, E.A. Pesterev, M.S. Slobodyan, V.I. Petrov	136
MODIFICATION OF STAINLESS STEEL BASED ON SYNERGISTIC OF LOW-ENERGY HIGH-INTENSITY ION IMPLANTATION AND HIGH-CURRENT ELECTRON BEAM IMPACT ON THE SURFACE LAYER A.I. Ryabchikov, O.S. Korneva, D.O. Sivin, A.I. Ivanova, I.V. Lopatin, I.A. Bozhko	137
Ti-W SURFACE ALLOYS SYNTHETIZED BY PVD-LEHCEB AND OXIDIZED BY PEO F. Morini, A. Palmeri, S. Franz, A. Vincenzo, M. Bestetti	138
INFLUENCE OF ION NITRIDING ON THE PROPERTIES OF DUPLEX SURFACE TREATMENT OF HIGH-SPEED STEEL R.Sh. Nagimov, E.L. Vardanyan, A.A. Nikolaev, A.V. Oleinik, A.Yu. Nazarov	139
FORMATION OF WEAR-RESISTANCE NEAR SURFACE LAYERS IN Al-Si ALLOYS WITH AN ELECTRON-BEAM TREATMENT E.A. Petrikova, Yu.F. Ivanov, N.A. Prokopenko, A.D. Teresov	140
ENERGY DENSITY DISTRIBUTION OF A MODULATED ELECTRON BEAM IN A SOURCE WITH A PLASMA CATHODE BASED ON A LOW PRESSURE ARC V.I. Shin, P.V. Moskvina, M.S. Vorobyov, V.N. Devyatkov, N.N. Koval	141
FORMATION OF A SILICON-NIOBIUM-BASED SURFACE ALLOY USING ELECTRON-ION-PLASMA SURFACE ENGINEERING V.V. Shugurov, N.N. Koval, Yu.F. Ivanov, A.D. Teresov, E.A. Petrikova	142
DEPOSITION OF BORON FILMS BY DISCHARGE SYSTEM WITH HOT ANODE FROM BORON POWDER V.V. Shugurov, Yu.F. Ivanov	143
MODIFICATION AND OPTICAL DEGRADATION OF THIN MULTILAYERS UNDER VUV/VU RADIATION FROM COMPRESSED PLASMA FLOWS A.S. Skriabin, V.D. Telekh, A.V. Pavlov, D.A. Chesnokov, V.G. Zhupanov, P.A. Novikov	144

PROCESSING OF THE TITANIUM ALLOY BY HIGH-SPEED STEEL TOOLS WITH COMBINE SURFACE TREATMENT	
S.V. Fedorov, Tet Oo, E.S. Mustafaev	145
INTERACTION OF PLASMA WITH BERYLLIUM	
I.A. Sokolov, M.K. Skakov, A.Z. Miniyazov, T.R. Tulenbergenov, G.K. Zhanbolatova	146
HYSTERESIS OF THE MAGNETRON DEPOSITION PROCESS WITH ALUMINUM AND ZINC TARGETS IN A REACTIVE MIXTURE OF GASES	
D.G. Ageychenkov, A.V. Kaziev, D.V. Kolodko, N.S. Sergeev, A.S. Isakova, A.V. Tumarkin	147
EFFECT OF THE ANNEALING TEMPERATURE ON THE STRUCTURAL AND CHARACTERISTICS OF Hf NANOFILMS BY MAGNETRON SPUTTERING	
A.P. Kuzmenko, Thant Sin Win, A.S. Petrov, Myo Min Than	148
ELECTRON-BEAM DEPOSITION OF THERMOCONDUCTING CERAMIC COATINGS FOR MICROELECTRONIC DEVICES	
E.M. Oks, A.V. Tyunkov, Yu.G. Yushkov, D.B. Zolotukhin	149
EVALUATION OF EFFECTIVE MAGNETIZATION OF THIN MAGNETO-DIELECTRIC FILMS DEPOSITED FROM BEAM PLASMA IN MEDIUM VACUUM	
A.V. Tyunkov, Yu.G. Yushkov, D.B. Zolotukhin	150
TWO-STAGE PVD METHOD FOR PROTECTIVE COATINGS FORMATION	
V.A. Burdovitsin, A.V. Tyunkov, Y.G. Yushkov, D.B. Zolotukhin	151
PLASMA NITRIDING IN COMPLEX POST-PROCESSING OF STAINLESS STEEL PARTS OBTAINED BY ADDITIVE LASER TECHNOLOGY	
A.V. Makarov, V.P. Kuznetsov, P.A. Skorynina, V.A. Sirosh, A.B. Vladimirov, N.V. Lezhnin, S.V. Kolmakov	152
AEROSOL ASSISTED ATMOSPHERIC PRESSURE PLASMA DEPOSITION FOR SILVER-CONTAINING ANTIBACTERIAL COATINGS	
L. Wang, C. Lo Porto, F. Palumbo, M. Modic, U. Cvelbar, C. Leys, A. Nikiforov	153
FORMATION OF ALLOYED LAYERS ON THE SURFACE OF MA-2 MAGNESIUM ALLOY BY METHODS OF COMBINED ELECTRON-ION-PLASMA TREATMENT	
A.D. Teresov, Yu.A. Denisova, V.V. Denisov, A.A. Leonov, S.S. Kovalsky	154
STRUCTURE AND MECHANICAL PROPERTIES OF STAINLESS-STEEL SPECIMENS, MADE BY ADDITIVE METHOD, AFTER PULSED ELECTRON BEAM TREATMENT	
A.D. Teresov, Yu.H. Akhmadeev, E.A. Petrikova, O.V. Krygina, Yu.F. Ivanov, G.V. Semenov	155
EFFECT OF ULTRAVIOLET IRRADIATION OR PLASMA OF DIFFUSE DISCHARGE ON THE SURFACE PROPERTIES OF MAO CALCIUM PHOSPHATE COATINGS	
E.G. Komarova, E.A. Kazantseva, V.S. Ripenko, A. Zharin, Y.P. Sharkeev	156
LEAD EVAPORATION BY VUV RADIATION OF VARIOUS SPECTRAL RANGES	
A.V. Pavlov, Y.Y. Protasov, V.D. Telekh, T.S. Shchepanuk	157
GAS-DISCHARGE PLASMA APPLICATION FOR ION-BEAM TREATMENT OF THE HOLES' INNER SURFACES	
D.O. Sivin, O.S. Korneva, A.I. Ivanova, D.O. Vakhrushev	158
HIGH-ENTROPY ZrTiCrNiCu COATING	
V.M. Yurov, V.I. Goncharenko, V.S. Oleshko	159
EFFECT OF IRRADIATION WITH IONS OF DIFFERENT ATOMIC MASSES (Ar ⁺ AND Xe ⁺) ON THE PROPERTIES OF CO ₉₀ Fe ₁₀ /Cu MAGNETIC SUPERLATTICES	
N.V. Gushchina, V.V. Ovchinnikov, K.V. Shalomov, N.S. Bannikova, R.S. Zavornitsyn, M.A. Milyaev	160
INVESTIGATION OF THE EFFECT OF ION IRRADIATION ON THE PROCESS OF NANOCRYSTALLIZATION OF AN Fe _{72.5} Cu ₁ Nb ₂ Mo _{1.5} Si ₁₄ B ₉ ALLOY USING THE IN SITU	

RESISTIVITY MEASUREMENT METHOD K.V. Shalomov, V.V. Ovchinnikov	161
FORMATION OF AUSTENITE PARTICLES ENRICHED IN MANGANESE UP TO 20 AT.% AND MORE, IN VOLUME OF Fe-6.35 AT.% Mn ALLOY IN TEMPERATURE RANGE OF 300-450°C DURING IRRADIATION WITH Ar ⁺ 20 keV IONS E.V. Makarov, V.V. Ovchinnikov	162
ELECTRONIC-ION-PLASMA MODIFICATION OF THE STRUCTURE AND PROPERTIES OF SILUMIN Yu.F. Ivanov, A.A. Klopotov, A.M. Ustinov, D.V. Zaguliaev, A.D. Teresov, Yu.A. Abzaev, O.M. Loskutov	163
ADHESION STRENGTH OF Ti _{1-x} C _x – DLC MULTILAYER NANOCOMPOSITE THIN FILMS COATED BY ION-PLASMA DEPOSITION ON MARTENSITIC STAINLESS STEEL PRODUCED BY SELECTIVE LASER MELTING FOLLOWED BY PLASMA-NITRIDING AND DIAMOND BURNISHING N.V. Lezhnin, A.V. Makarov, V.P. Kuznetsov, A.B. Vladimirov, P.A. Skorynina, V.A. Sirosh	164
Section 3. PLASMA-CHEMICAL, ELECTROPHYSICAL AND LASER TECHNOLOGIES: environmental applications, production of nanopowders and functional materials	165
ANALYSIS OF THE SIZE AND MORPHOLOGICAL COMPOSITION OF ABLATED CERIUM DIOXIDE NANOPARTICLES AFTER ULTRASONIC DISPERSION AND CENTRIFUGATION IN AQUATIC MEDIUM M.A. Pugachevskii, V.A. Mamontov, A.Yu. Ryzhenkova	166
INVESTIGATION OF EFFECTIVENESS OF ANTIMICROBIAL TREATMENT OF POULTRY PRODUCTS BY ELECTROPHYSICAL METHODS R.A. Vazirov, S.Yu. Sokovnin, A.S. Krivonogova, A.G. Isaeva	167
PREPARATION OF CERIUM (III) FLUORIDE NANOPOWDERS BY PULSED ELECTRON BEAM EVAPORATION IN VACUUM V.G. Ilves, S.Yu. Sokovnin, M.A. Uimin	168
PRODUCTION OF IRON OXIDE NANOPOWDERS BY RADIATION-CHEMICAL METHOD M.E. Balezin, S.Yu. Sokovnin, M.A. Uimin	169
INVESTIGATION OF BIOLOGICAL ACTIVITY OF NANOPOWDER DOPED WITH SILVER O.A. Svetlova, V.G. Ilves, M.V. Ulitko, S.Yu. Sokovnin, T.R. Sultanova	170
MORPHOLOGY HIGHLY DISPERSED SiO ₂ OBTAINED IN THERMAL PLASMA ENVIRONMENT V.V. Shekhovtsov, O.G. Volokitin, N.K. Skripnikova, R.Yu. Bakshanskiy	171
APPLICATION OF A NANOSECOND CORONA DISCHARGE GENERATOR FOR ELECTRICAL SEPARATION OF ORES S.R. Korzhenevskiy, A.A. Komarskiy, A.V. Ponomarev, A.S. Chepusov, O.D. Krasniy	172
MECHANICAL PROPERTIES AND COMPOSITION OF TiSiCN COATINGS OBTAINED BY DECOMPOSITION OF HEXAMETHYLDISILAZANE AND ANODIC EVAPORATION OF TITANIUM IN A LOW PRESSURE ARC DISCHARGE A.I. Men'shakov, Yu.A. Bryuhanova, I.S. Zhidkov, P.A. Skorynina	173
SYNTHESIS OF METASTABLE CUBIC TUNGSTEN CARBIDE WITH A HIGH PURITY IN DISPERSED AND BULK FORMS BY THE PLASMA DYNAMIC METHOD A.A. Sivkov, I.I. Shanenkov, D.S. Nikitin, A. Nassyrbayev	174
INFLUENCE OF THE SUPPLIED ENERGY ON THE PHASE CONTENT OF CRYSTALLINE DISPERSED TITANIUM DIOXIDE OBTAINED BY THE PLASMA DYNAMIC METHOD A.A. Sivkov, Y.N. Vympina, I.A. Rakhmatullin, A.S. Ivashutenko, Y.L. Shanenkova	175

SiAlON SYNTHESIZED BY DC ARC PLASMA V.A. Vlasov, A.A. Klopotov, K.A. Bezukhov, Yu.A. Abzaev, N.N. Golobokov, G.G. Volokitin, V.V. Shekhovtsov, N.A. Tsvetkov	176
EFFECT OF PULSED SOFT X-RAY RADIATION ON THE SURFACE TOPOGRAPHY OF SOME METALS A.E. Ligachev, M.V. Zhidkov, S.A. Sorokin, G.V. Potemkin, Yu.R. Kolobov	177
STUDY OF METHANE STEAM REFORMING IN THE PLASMA OF A NANOSECOND SURFACE GAS DISCHARGE I.E. Filatov, D.L. Kuznetsov, V.V. Uvarin	178
INVESTIGATION OF THE RELATIVE REACTIVITY OF VOLATILE ORGANIC COMPOUNDS IN THE AIR PLASMA OF A PULSED CORONA DISCHARGE BY THE METHOD OF COMPETING REACTIONS I.E. Filatov, V.V. Uvarin, D.L. Kuznetsov	179
SYNTHESIS OF MULLITE FROM ALUMINOSILICATE RAW MATERIALS IN A THERMAL PLASMA FLOW R.E. Gafarov, V.V. Shekhovtsov, O.G. Volokitin	180
SYNTHESIS OF MAX-PHASES, STRUCTURE AND PHASE COMPOSITION OF MODIFIED LAYERS ON TITANIUM ALLOY VT-1 AS A RESULT OF ELECTRON-BEAM TREATMENT A.E. Lapina, N.N. Smirnyagina, V.M. Khaltanova	181
PLASMA-SOLUTION SYNTHESIS OF TRANSITION METAL OXIDES K.V. Smirnova, V.V. Rybkin, D.A. Shutov, A.N. Ivanov	182
DROPLETS GENERATION CONDUCTING DURING LASER-PLASMA TREATING OF METALS IN ELECTRIC FIELD A.Yu. Ivanov, A.L. Sitkevich, S.V. Vasiliev	183
MODIFICATION OF THE SURFACE OF COPPER AND ITS ALLOYS DUE TO NANOSECOND ULTRAVIOLET LASER PULSES IMPACT T.V. Malinskiy, V.E. Rogalin, I.A. Kaplunov	184
THE STUDY OF AN INSTABILITIES ROLE OF PLASMA IN THE HIGH-VOLTAGE DISCHARGE FORMATION INITIATED BY OPTICAL RADIATION AT HIGH PRESSURES IN HIGH-VOLTAGE OPTICALLY TRIGGERED SWITCHES A.I. Lipchak, S.V. Barakhvostov, N.B. Volkov, E.A. Chingina, I.S. Turmyshev	185
FEATURES OF THE GAS-PHASE SYNTHESIS OF OXIDE NANOPOWDERS USING HIGH-POWER LASERS V.V. Osipov, V.V. Lisenkov, V.V. Platonov, E.V. Tikhonov	186
THE POSSIBLE CHEMICAL PATHWAYS IN NRP PLASMA-ASSISTED AMMONIA SYNTHESIS AND NITROGEN FIXATION Shuai Zhang, Xin Zeng, Lijun Zong, Xiucui Hu, Tao Shao	187
INVESTIGATION OF THE EFFECT OF WATER VAPOR AND CONDENSED PHASE ON THE ENERGY CONDITIONS FOR THE INITIATION OF THE PLASMA-CHEMICAL PROCESS OF FLUE GAS PURIFICATION BY A PULSED ELECTRON BEAM R. Sazonov, G. Kholodnaya, D. Ponomarev, I. Egorov, A. Poloskov, M. Serebrennikov	188
CREATING NANOSCALE LUMINESCENCE CENTRES IN SILVER HALIDES SUITABLE FOR INFRARED APPLICATION E.A. Korsakova, V.V. Lisenkov, L.V. Zhukova, A.N. Orlov, A.S. Korsakov, V.V. Osipov, A.E. Lvov, V.V. Platonov, D.D. Salimgareev	189
EVALUATION OF THE EFFECT OF PRE-SOWING ELECTRON IRRADIATION OF BARLEY SEEDS ON PLANT DEVELOPMENT AND DISEASE INCIDENCE N.N. Loy, N.I. Sanzharova, S.N. Gulina, O.V. Suslova, T.V. Chizh, M.S. Vorobyov, S.Yu. Doroshkevich	190

INVESTIGATION OF HYDROXYL GROUP RADICALS GENERATION AT INTERACTION OF A COLD ATMOSPHERIC PLASMA JET WITH AN ENVIRONMENT P.P. Gugin, D.E. Zakrevsky, E.V. Milakhina	191
IMPULSE LASER APPLICATION FOR SURFACE MODIFICATION OF TOOL STEEL WITH B ₄ C-AI POWDERS U.L. Mishigdorzhijn, N.S. Ulakhanov, A.V. Nomoev	192
THE STUDY OF RADIATION DAMAGE ASSESSMENT ON FUEL CLAD OF MNSR USING COMPUTATIONAL TOOLS A. Samiru, V.N. Nesterov	193
EFFECT OF PLASMA ON PROLIFIRATION RATE OF HUMAN CELLS E.A. Shershunova, S.I. Moshkunov, S.V. Nebogatkin, O.S. Rogovaya	194
THE DC PULSE CURRENT PATTERN INFLUENCE DURING SPARK PLASMA SINTERING Thet Naing Soe, I.M. Makhadilov, N.W. Solis Pinargote	195
CARBON NANOPARTICLES (CNP) COATED COPPER OXIDE (CuO) BY ELECTROPHORETIC SYNTHESIS Nay Win Aung, V.A. Mamontov, Myo Min Than, M.A. Pugachevskii, Thet Phyo Naing	196
INFLUENCE OF THE CATALYST PACKING CONFIGURATION ON THE DISCHARGE CHARACTERISTICS AND CO ₂ REDUCTION IN A PACKED BED PLASMA REACTOR M. Zhu, F.F. Wu, H. Ma, S.Y. Xie, C.H. Zhang	197
INVESTIGATION OF PHOTOCALYTIC ACTIVITY OF NANOPOWDER DOPED WITH SILVER OBTAINED BY PULSED ELECTRON BEAM EVAPORATION IN VACUUM O.A. Svetlova, V.G. Ilves, S.Yu. Sokovnin	198
PLASMA SYSTEMS FOR FORMATION OF ELECTROHYDRODYNAMIC FLOWS V.A. Yamshchikov, V.Yu. Khomich	199
PRODUCTION OF NANOPOWDERS OF BISMUTH OXIDE DOPED WITH SILVER BY PULSED ELECTRON BEAM EVAPORATION IN VACUUM V.G. Ilves, S.Yu. Sokovnin, M.A. Uimin	200
INFLUENCE OF RESIDUAL GAS ON THE FIELD ELECTRON EMISSION CHARACTERISTICS OF GRAINED STRUCTURAL GRAPHITE A.S. Chepusov, A.A. Komarskiy, S.R. Korzhenevskiy	201
PHOTOCHEMICAL CONVERSION PROCESSES IN PETROLEUM U.J. Yolchueva, R.A. Jafarova, S.Y. Rashidova, Z.F. Hashimzade Seyid, S.A. Suleymanova	202
INVESTIGATION OF THE ROLE OF CHEMICALLY ACTIVE RADICALS IN THE ANTIBACTERIAL PROPERTIES OF A LOW-TEMPERATURE PLASMA JET AT AMBIENT PRESSURE MIXED WITH ARGON AND AIR N.A. Ashurbekov, Z.M. Isaeva, G.S. Shakhshinov, K.M. Rabadanov, A.A. Murtazaeva, E.Kh. Israpov	203
ELECTRIC ARC IN PLASMA FLOW OF GAS DISCHARGE WITH A LIQUID ELECTROLYTE CATHODE G.K. Tazmeev, A.K. Tazmeev, B.K. Tazmeev	204
PECULIARITIES OF ELECTROPHORETIC DEPOSITION OF NANOPOWDERS OF VARIOUS MORPHOLOGIES USED FOR OPTICAL CERAMICS FABRICATION E.G. Kalinina, M.G. Ivanov, D.S. Rusakova	205
ONE OF THE METHODS OF NUMERICAL OPTIMIZATION IN CHEMICAL KINETICS PROBLEMS L.N. Kashapov, N.F.Kashapov, V.Yu. Chebakova	206
LASER PLUME GLOW ON A SURFACE OF NON-ROTATING AND FAST-ROTATING TARGET V.A. Shitov	207

SYNTHESIS OF CEMENT CLINKER USING PLASMA TECHNOLOGY N.K. Skripnikova, V.V. Shekhovtsov, M.A. Semenovikh, R.Yu. Bakshanskiy.....	208
OBTAINING GLASS-CRYSTALLINE MATERIALS USING ARC PLASMA G.G. Volokitin, N.K. Skripnikova, V.V. Shekhovtsov, M.A. Semenovikh, R.Yu. Bakshanskiy.....	209
Section 4. SOURCES OF LOW-TEMPERATURE PLASMA: generators of continuous, pulse-periodic and pulsed action, gas switches, power supply	210
THE 40 YEARS TO RADAN – COMPACT MULTI-PURPOSED SOURCES FOR VARIOUS PULSE POWER INVESTIGATIONS V.G. Shpak, S.A. Shunailov, M.I. Yalandin.....	211
COMBINED ELECTRIC DISCHARGE "ARC + DISCHARGE WITH LIQUID ELECTROLYTE CATHODE" G.K. Tazmeev, B.A. Timerkaev, K.K. Tazmeev	212
SIMULATION OF CHARGED PARTICLE BEAM DYNAMICS EXTRACTED FROM A PLASMA SOURCE I.A. Kanshin	213
THRUST CHARACTERISTICS OF COMPACT HIGH-VOLTAGE PULSED PLASMA THRUSTER UTILIZING LIQUID PROPELLANT S.A. Buldashev, R.V. Emlin, P.A. Morozov, I.F. Punanov, Y.N. Shcherbakov, L.Y. Yashnov	214
MEASUREMENT OF THE ELECTRON BEAM ENERGY IN A SOURCE WITH A PLASMA ANODE AND THE BEAM EXTRACTION INTO THE ATMOSPHERE THROUGH A FOIL WINDOW E.N. Abdullin, G.F. Basov.....	215
SUPPRESSION OF THE GENERATION OF HEAVY IONS IN VACUUM DIODE WITH PASSIVE ANODE A.I. Pushkarev, A.I. Prima, X.P. Zhu, C.C. Zhang, Y. Li, Yu. Egorova, M.K. Lei.....	216
CATHODIC ARC DISCHARGE SYSTEM WITH LANTHANUM HEXABORIDE CATHODE FOR BORON-CONTAINING PLASMA GENERATION A.S. Bugaev, V.I. Gushenets, E.M. Oks, V.P. Frolova	217
EFFICIENCY OF ELECTRON BEAM EXTRACTION TO THE AMBIENT ATMOSPHERE IN AN ELECTRON ACCELERATOR BASED ON ION-ELECTRON EMISSION S.Yu. Doroshkevich, M.S. Vorobyov, M.S. Torba, N.N. Koval, S.A. Sulakshin, V.A. Levanisov	218
INVESTIGATION OF SEPARATE DISCHARGE PROCESSES IN A HIGH-VOLTAGE NANOSECOND COMBINED SWITCH P.A. Bokhan, N.A. Glubokov, P.P. Gugin, D.E. Zakrevsky.....	219
THE MEASUREMENTS OF PLASMA EXPANSION PROCESSES OF HIGH CURRENT VACUUM ARC I.L. Muzyukin, P.S. Mikhailov, S.A. Chaikovsky, I.V. Uimanov, D.L. Shmelev, Yu.A. Zemskov.....	220
EXPERIMENTAL STUDY OF MICRO PULSED PLASMA THRUSTER I.L. Muzyukin, P.S. Mikhailov	221
EFFECT OF EXTINCTION BEAM-PLASMA DISCHARGE WHILE THE INJECTION THERMOELECTRONS DURING TRANSPORTATION OF THE ELECTRON BEAM IN THE FOREVACUUM PRESSURE RANGE A.A. Zenin, I.Yu. Bakeev, A.S. Klimov.....	222
FEATURES OF GLOW DISCHARGE IGNITION THROUGH A SMALL HOLE IN THE HOLLOW CATHODE OF A LARGE VOLUME A.S. Klimov, I.Yu. Bakeev, V.T. Tran, E.M. Oks, A.A. Zenin	223

HIGH VOLTAGE CAPACITOR FOR POWER SUPPLY SYSTEM A.D. Lenskiy, D.V. Molchanov, D.V. Rybka	224
METHODS FOR INCREASING THE ELECTRICAL BREAKDOWN STRENGTH OF THE ACCELERATING GAP IN AN ELECTRON SOURCE WITH A PLASMA CATHODE P.V. Moskvina, V.N. Devyatkov, I.V. Lopatin, V.I. Shin	225
SUBNANOSECOND SWITCHING OF STANDARD THYRISTORS TRIGGERED IN IMPACT-IONIZATION WAVE MODE BY A HIGH-VOLTAGE PCSS DRIVER A. Gusev, I. Prudaev, I. Lavrinovich, A. De Ferron, B. Novac, L. Pecastaing	226
HIGH-POWER RADIO FREQUENCY GENERATOR FOR PLASMA APPLICATIONS V.E. Patrakov, D.A. Lisovsky	227
WIDE RADIATION BANDS OF SUB-NANOSECOND DISCHARGE IN XENON AND INACCURACIES IN THEIR MEASUREMENTS V.F. Tarasenko, A.N. Panchenko, D.V. Beloplotov, D.A. Sorokin, M.I. Lomaev, V.V. Kozevnikov	228
INFLUENCE OF PLANAR MAGNETRON DISCHARGE PARAMETERS ON SPATIAL DISTRIBUTION OF ION CURRENT DENSITY AND SUBSTRATE TEMPERATURE M.V. Shandrikov, E.M. Oks, A.V. Vizir, G.Yu. Yushkov	229
INFLUENCE OF WORKING PRESSURE ON MASS-TO-CHARGE ION STATE IN A HIGH- CURRENT PULSED PLANAR MAGNETRON DISCHARGE PLASMA M.V. Shandrikov, E.M. Oks, A.V. Vizir, G.Yu. Yushkov	230
INCREASING THE OPERATION STABILITY OF THE ELECTRON ACCELERATOR BASED ON ION-ELECTRON EMISSION M.S. Torba, S.Yu. Doroshkevich, M.S. Vorobyov, N.N. Koval, S.A. Sulakshin, V.A. Levanisov	231
NON-SELF-SUSTAINING HIGH-VOLTAGE DISCHARGE WITH HOLLOW CATHODE AND PLASMA ANODE V.I. Gushenets, E.M. Oks, A.S. Bugaev	232
INFLUENCE OF ACCELERATING GAP CONFIGURATION ON PARAMETERS OF A FOREVACUUM PLASMA-CATHODE SOURCE OF PULSED ELECTRON BEAM A.V. Kazakov, A.V. Medovnik, E.M. Oks, N.A. Panchenko	233
INFLUENCE OF ELECTRON EMISSION ON OPERATION OF A CONSTRICTED ARC DISCHARGE IN A PULSED FOREVACUUM PLASMA-CATHODE ELECTRON SOURCE A.V. Kazakov, E.M. Oks, N.A. Panchenko	234
PROPERTIES OF PULSED MAGNETRON DISCHARGE PLASMA IN HELIUM A.V. Kaziev, D.V. Kolodko, G.I. Rykunov, N.S. Sergeev	235
OPERATING PARAMETERS OF HIGH PULSE REPETITION FREQUENCY CAPILLARY GAS DISCHARGE SWITCH AND ITS APPLICATION FOR ION SELF-TERMINATING LASERS PUMPING P.A. Bokhan, P.P. Gugin, M.A. Lavrukhin, D.E. Zakrevsky	236
INFLUENCE OF THE CATHODE REGION PREIONIZATION ON THE OPERATING PARAMETERS OF THE EPTRON P.A. Bokhan, P.P. Gugin, M.A. Lavrukhin, D.E. Zakrevsky	237
FORMATION OF THE VOLTAGE PULSES UP TO 400 KILOVOLTS WITH FRONT PULSE LESS THAN 10 NANOSECONDS B.A. Kozlov, D.S. Makhanko	238
GENERATION OF A COLD ATMOSPHERIC PLASMA JET IN A PLANAR MULTICHANNEL DEVICE P.P. Gugin, D.E. Zakrevsky, E.V. Milakhina	239
PICOSECOND SEMICONDUCTOR GENERATOR FOR CAPACITIVE SENSORS CALIBRATION V.E. Patrakov, M.S. Pedos, S.N. Rukin	240

SPATIAL DISTRIBUTION AND TIME EVOLUTION OF A METAL-CONTAINING PLASMA OF A LOW-CURRENT ATMOSPHERIC PRESSURE DISCHARGE K.P. Savkin, D.A. Sorokin, G.Yu. Yushkov	241
MINICP DEVICE FOR INVESTIGATION OF THE PLASMA-SURFACE INTERACTIONS N.S. Sergeev, A.V. Kaziev, M.M. Kharkov, Yu.M. Gasparyan, A.Yu. Khomyakov	242
COLD PLASMA SOURCE BASED ON THE APOKAMPIC DISCHARGE IN ATMOSPHERIC-PRESSURE AIR D.A. Sorokin, V.A. Panarin, E.A. Sosnin, V.S. Kuznetsov, V.S. Skakun	243
OPTIMUM TRANSFER CHARACTERISTICS OF THE TESLA TRANSFORMER ON THE FIRST AND SECOND HALF-WAVES OF OUTPUT VOLTAGE V.V. Kladukhin, S.P. Khramtsov	244
INVESTIGATION OF COLD ATMOSPHERIC PLASMA JET GENERATION EXCITED BY SQUARE-WAVE PULSE P.P. Gugin, D.E. Zakrevsky, E.V. Milakhina	245
DYNAMICS OF THE TARGET TEMPERATURE CHANGE UNDER DIRECT IMPACT OF A COLD ATMOSPHERIC PLASMA JET P.P. Gugin, D.E. Zakrevsky, E.V. Milakhina	246
PLASMA GENERATION IN A HIGH-CURRENT GLOW DISCHARGE WITH A HOLLOW CATHODE IN AN AXIALLY SYMMETRICAL SYSTEM USING TWO ELECTRON SOURCES E.V. Ostroverkhov, V.V. Denisov	247
ATMOSPHERIC COLD PLASMA JET GENERATED BY MICROWAVE ELECTRODE DISCHARGE: SOME DIAGNOSTIC TECHNIQUES S.N. Antipov, V.M. Chepelev, M.A. Sargsyan, M.Kh. Gadzhiev	248
FEATURES OF PLASMA GENERATION IN A PULSED MODE OF A NON-SELF-SUSTAINED ARC DISCHARGE S.S. Kovalsky, V.V. Denisov, E.V. Ostroverkhov, V.E. Prokop'ev	249
GENERATION OF ION AND ELECTRON BEAMS AND PLASMA FLOWS IN SPECIAL CONDITIONS WITH "EXTREME" PARAMETERS AND SOME EXAMPLES OF ITS APPLICATIONS E.M. Oks	250
FPGA BASED DEVELOPMENTS FOR HIGH SWITCHING FREQUENCY POWER MODULES BASED ON WIDE BAND GAP SEMICONDUCTORS R. Ruscassie, J.M. Larbaig, R. Leduc, J.M. Dienot	251
A NEW TYPE OF NON-THERMAL ATMOSPHERIC PRESSURE PLASMA SOURCE BASED ON A WAVEGUIDE BRIDGE V.N. Tikhonov, S.A. Gorbatov, I.A. Ivanov, A.V. Tikhonov	252
"OVERHEATING" INSTABILITY FOR AN HF ARC DISCHARGE IN AIR AT ELEVATED PRESSURES A.F. Kokorin	253
AUTHOR INDEX	254

Section 1

FUNDAMENTAL PROCESSES IN LOW-TEMPERATURE PLASMA:

low and high pressure discharges,
near-electrode phenomena,
radiation, ultrafast processes,
diagnostics

DIFFERENT MODES OF RUNAWAY ELECTRON BEAMS IN HIGH-PRESSURE GASES*

V.F. TARASENKO, D.V. BELOPLOTOV, D.A. SOROKIN, M.I. LOMAEV, E.KH. BAKSH, A.G. BURACHENKO

Institute of High Current Electronics, SB, RAS, Tomsk, Russia
e-mail: VFT@loi.hcei.tsc.ru

The generation of runaway electron beams (RAEBs) in high-pressure gases is a fundamental physical phenomenon that began to be investigated in the last century, see review [1] and references in [1]. The research of RAEBs are ongoing, see, for example, papers [2-4]. Due to RAEBs, diffuse discharges are formed in various gases without a source of additional preionization. They are used in different fields, including for pumping lasers [5] and exciting excilamps [6, 7]. To obtain runaway beams that can be recorded at atmospheric pressure and more behind the anode foil, cathodes with a small radius of curvature and voltage pulses with an amplitude of about 100 kV and higher with a subnanosecond rise time are usually used.

This report will present the results of experimental studies of various modes of generation of runaway electron beams and X-ray under the action of RAEBs. In particular, a mode in which the greatest amplitudes of the beam current are achieved, a mode in which two pulses of the beam current are recorded, a mode in which beam current generation in the direction opposite to the anode, see Fig. 1, a mode with x-ray pulses of hundreds of nanoseconds duration and other modes will be described.

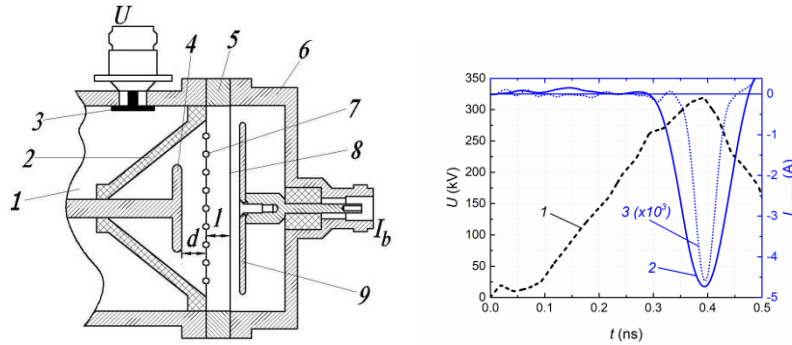


Fig. 1. The gas diode [8] in what beam current generated in the direction opposite to high voltage anode (on the left) with 1 – coaxial line, 2 – insulator, 3 – capacitive voltage divider, 4 – anode, 5 – steel ring, 6 – collector box, 7 – wire grid, 8 – foil, 9 – collector with diameter of receiving part 56 mm. The pulses (on the right) of high voltage on gas diode (1) and runaway beam current from collectors with accepted part 20 (2) and 3 mm (3).

In air at atmospheric pressure, the effect of the cathode design and material on the amplitude and duration of the beam current pulse will be shown.

REFERENCES

- [1] V.F. Tarasenko, “Runaway electrons in diffuse gas discharges (A Review)”, *Plasma Sources Science and Technology*, vol. 29, is. 3, 034001 (21 pp.), 2020.
- [2] N.M. Zubarev, V.Y. Kozhevnikov, A.V. Kozlyev, G.A. Mesyats, N.S. Semeniuk, K.A. Sharypov, S.A. Shunailov, M.I. Yalandin, “Mechanism and dynamics of picosecond radial breakdown of a gas-filled coaxial line.” *Plasma Sources Science and Technology*, vol. 29, is. 12, 125008 (15 pp.), 2020.
- [3] D.V. Beloplotov, V.F. Tarasenko, V.A. Shklyayev, D.A. Sorokin, “Conditions for runaway electrons in a gas diode with a strongly nonuniform electric field,” *JETP Lett.*, vol. 113, is. 2, pp. 133–139, 2021. [In Russian].
- [4] D.V. Beloplotov, V.F. Tarasenko, D.A. Sorokin, V.A. Shklyayev, “Formation of two runaway electron beam current pulses,” *Technical Physics*, vol. 91, is. 4, pp. 589–599, 2021. [In Russian].
- [5] A.N. Panchenko, D.A. Sorokin, V.F. Tarasenko, “Gas lasers pumped by runaway electron preionized diffuse discharge (A Review)”, *Progress in Quantum Electronics*, vol. 76C, 100314, (36 pp.), 2021.
- [6] M.V. Erofeev, V.F. Tarasenko, “XeCl-, KrCl-, XeBr- and KrBr-excilamps of the barrier discharge with the nanosecond pulse duration of radiation”, *Journal of Physics D: Applied Physics*, vol. 39, is. 16, pp. 3609-3614, 2006.
- [7] M.I. Lomaev, G.A. Mesyats, D.V. Rybka, V.F. Tarasenko, E.Kh. Baksht, “High-power short-pulse xenon dimer spontaneous radiation source”, *Quantum Electronics*, vol., 37, is. 6, pp. 595-596, 2007.
- [8] V.F. Tarasenko, I.D. Kostyrya, D.V. Beloplotov, “Backward runaway electrons in a subnanosecond air discharge at atmospheric pressure”, *Laser and Particle Beams*, vol. 34, is. 1, pp. 23-30, 2016.

* The work is performed in the framework of the State task FWRM-2021-0014 for HCEI SB RAS.

FEATURES OF THE LOW-PRESSURE HOLLOW-CATHODE GLOW DISCHARGE SUSTAINING FOR THE CONDITIONS OF ENHANCED EMISSIVITY OF THE CATHODE SURFACE*

N.V. LANDL, Y.D. KOROLEV, O.B. FRANTS, G.A. ARGUNOV, V.G. GEYMAN, V.O. NEKHOROSHEV

Institute of High Current Electronics, SB, RAS, Tomsk, Russia

e-mail: landl@lnp.hcei.tsc.ru

Hollow-cathode low-pressure glow-type discharges are widely used for different applications [1-7]. In particular, such discharges are used for generation of charged particle beams, for surface modification, for generation of extreme ultraviolet radiation, for generation of large volume plasmas and so on. A range of operating pressures of the discharges under consideration corresponds to the left branch of Paschen's curve. Under these conditions the electron free path for ionization is much in excess of the electrode separation and plasma generation is provided due to hollow cathode effect.

In our previous papers we presented the model allows explaining the current passage mechanisms for the high-current pulsed glow discharge in the main gap and for the low-current steady-state glow discharge in the trigger units of the cold-cathode thyratrons [3, 4, 7, 8]. The main idea of the model is that the main component of discharge current on the cathode surface is an ion current and electrons from the cathode are emitted not only due to the ion bombardment, but also as an external emission current due to photoeffect, field emission and explosive emission.

Model was also used to interpret the current-voltage characteristics of the glow discharge with a hollow cathode and hot filament (thermionic cathode) inside the cavity [9], which is used for large-volume plasma generation in the installations for the modification of properties of material surfaces. In such installations, the role of external emission current is played by the thermionic current from the hot filament that is set and changed artificially. Note, that the values of the total discharge currents in this case were at a level of 100 A.

From the other hand, for the low-current hollow-cathode glow discharge we can realize the conditions in which the external emission current from the cathode surface is artificially increased. One of the ways is to use the special high-emissivity tablet [8] that is served for the reduction of discharge ignition and burning voltages of auxiliary glow discharge in the trigger units of commercially produced sealed-off thyratrons.

In this work we present the results of investigation of steady-state hollow-cathode low-current glow discharge for the conditions when the external emission current from the cathode is provided due to special high-emissivity tablet, located at the bottom of cathode cavity. The current-voltage characteristics were obtained and interpreted with the use of model.

REFERENCES

- [1] E. Dewald, K. Frank, D. H. H. Hoffman et al., "Experimental Analysis of Pseudospark Sourced Electron Beam," *IEEE Trans. Plasma Sci.*, vol.25, p. 272, 1997.
- [2] V.N. Devyatkov, Y.F. Ivanov, O.V. Krysinina, N.N. Koval et al., "Equipment and processes of vacuum electron-ion plasma surface engineering," *Vacuum*, vol.143, p.464, 2017.
- [3] Y.D. Korolev and N.N. Koval, "Low-pressure discharges with hollow cathode and hollow anode and their applications," *J. Phys. D: Appl. Phys.*, vol.51, Article Number 323001, 2018.
- [4] Y.D. Korolev, O.B. Frants, N.V. Landl, I.A. Shemyakin, V.G. Geyman, "High-current stages in a low-pressure glow discharge with hollow cathode," *IEEE Trans. Plasma Sci.* vol. 41, pp. 2087–2096, 2013.
- [5] V.D. Bochkov, V.M. Dyagilev, V.G. Ushich, O.B. Frants, Y.D. Korolev, I.A. Shemyakin, K. Frank, "Sealed-off pseudospark switches for pulsed power applications (current status and prospects)," *IEEE Trans. Plasma Sci.*, vol.29, no.5, pp. 802-808, 2001.
- [6] Y.D. Korolev, N.V. Landl, V.G. Geyman, A.V. Bolotov, V.S. Kasyanov, V.O. Nekhoroshev, S.S. Kovalsky, "Nanosecond Triggering for Sealed-Off Cold Cathode Thyratrons With a Trigger Unit Based on an Auxiliary Glow Discharge," *IEEE Trans. Plasma Sci.*, vol.43, no.8, pp.2349-2353, 2015.
- [7] Y.D. Korolev, N.V. Landl, V.G. Geyman, O.B. Frants, "Hollow-cathode glow discharge in a trigger unit of pseudospark switch," *Phys. Plasmas*, vol.25, no.11, 13510, 2018.
- [8] N.V. Landl, Y.D. Korolev, V.G. Geyman, O.B. Frants, G.A. Argunov, A.V. Bolotov, A.V. Akiyov, P.A. Bak, "Special Features of Parasitic Current Formation in a Sealed-Off Cold-Cathode Thyatron with Trigger Unit Based On an Auxiliary Glow Discharge" // *Rus. Phys. J.*, vol.62, no.7, pp. 1279-1288, 2019.
- [9] N.V. Landl, Y.D. Korolev, V.G. Geyman et al., "The Regimes for Sustaining a Hollow-Cathode Glow Discharge with a Hot Filament Inside the Cavity", *Russ Phys J*, vol.62, no.11, pp. 2024-2032, 2020.

* This work was funded by RFBR according to the research project № 19-08-00326a.

INVESTIGATION OF DISCHARGES WITH THE EMISSION OF ELECTRONS FROM COLD CATHODES IN PURE GASES FEATURES*

E.V. BELSKAYA^{1,2}, P.A. BOKHAN¹, P.P. GUGIN¹, V.A. KIM¹, G.V. SHEVCHENKO², D.E. ZAKREVSKY^{1,2}

¹A.V. Rzhzanov Institute of Semiconductor Physics, SB, RAS, Novosibirsk, Russia

²Novosibirsk State Technical University, Novosibirsk, Russia

e-mail: bokhan@isp.nsc.ru

Despite the long history of research and a huge number of publications, so far, there are no appropriate models of abnormal glow discharge, especially at increased (more than 1 kV) operating voltages. Primarily, the problem of cold cathodes emission properties in a gas discharge remains unsolved. For example, applying of generalized emission coefficients under the impact of argon fast atoms and ions $\gamma_{a,i}$ [1] leads to physically meaningless results [2]. Therefore, the coefficients $\gamma_{a,i}$, as well as the photoemission coefficient γ_{ph} , should be taken in the models as unknown quantities and should be acquired from the corresponding specific experimental data, in particular from the current-voltage characteristics (I-V characteristics). Even for the simplest gas helium, usage of predetermined γ is limited and obtaining experiment-consistent I-V characteristics demands of fitting not only $\gamma_{a,i}$, γ_{ph} , but also the coefficient of potential emission γ_p [3]. An additional uncertainty is caused by the uncontrolled purity of operating gases [4].

The recent studies of discharge properties under relatively pure conditions (initial vacuum in cells is not worse than 10^{-5} Torr, purity of working gas is not lower than 10^{-3} %) [5-7] demonstrated significant differences of I-V characteristics from those obtained earlier. In particular, it was found that the I-V characteristics can take Z-shaped form, and the current at increased voltages, for example, 2 kV, is more than 2 orders of magnitude lower than in the previously performed studies.

Present research was carried out in conditions cleaner than in [4-7] experiments. In particular, the initial vacuum in the cells was better than 10^{-7} Torr, the initial purity of helium was 10^{-4} %. Molybdenum was used as the cathode material, its oxides are much easier to remove from the discharge region than Al_2O_3 in [4-6] and SiO_2 in [7]. Molybdenum oxides are the supplier of O_2 to the discharge. Abnormal discharge and open discharge (a 1.5 mm long discharge between a solid cathode and a grid anode with a geometric transparency of $\sim 90\%$, behind which there was a 30 mm long drift space, dimensions were intermediate between those used in [4-7]), were investigated.

Investigations of I-V characteristics and electron beams generation efficiency were carried out in a wide range of conditions both in abnormal and open discharges. In general, the I-V characteristics under the conditions of the present work have even more pronounced Z-shaped characteristics in comparison with [3-6], and a higher efficiency of electron beam generation was achieved. The simulation of discharges is carried out. The obtained results are explained in terms of the dominant influence of cathode surface modification by the operating gas, which determine its emission properties [8].

REFERENCES

- [1] A.V. Phelps, "Role of molecular ions, metastable molecules, and resonance radiation in the breakdown of rare gases", Phys. Rev., vol. 117, №3, pp. 620-632, 1960.
- [2] D. Marić, K. Kutasi, G. Malović, Z. Donkó, Z. Petrović, "Axial emission profiles and apparent secondary electron yield in abnormal glow discharges in argon", Eur. Phys. J. D, vol. 21, pp. 73-81, 2002.
- [3] A. Fierro, Ch. Moore, B. Scheiner, B.T. Yee, M.M. Hopkins, "Radiation transport in kinetic simulations and the influence of photoemission on electron current in self-sustaining discharges", J. Phys. D: Appl. Phys., vol. 50, p. 065202, 2017.
- [4] P.A. Bokhan, P.P. Gugin, D.E. Zakrevsky, M.A. Lavrukhin, "Study of the Properties of an Anomalous Glow Discharge Generating Electron Beams in Helium, Oxygen, and Nitrogen", Plasma Phys. Rep., vol. 45, № 11, pp. 1035-1052, 2019.
- [5] P.A. Bokhan, "On physical processes in an "open" discharge", Physics-Uspexhi, vol. 61, № 12, pp. 1241-1247, 2018.
- [6] P.A. Bokhan, P.P. Gugin, Dm. E. Zakrevskii, "Specific Features of the I-V Characteristics and High-Efficiency Electron-Beam Generation in a Continuous Open Discharge", Tech. Phys. Lett., vol. 44, № 12, pp. 1092-1095, 2018.
- [7] P.A. Bokhan, P.P. Gugin, M.A. Lavrukhin, D.E. Zakrevsky, I.V. Schweigert, A.L. Alexandrov, "Investigation of the characteristics and mechanism of subnanosecond switching of a new type of plasma switches. I. Devices with counter-propagating electron beams—kivotrons", Plasma Sources Sci. Technol., Vol. 29, № 8, p. 084002, 2020.
- [8] P.A. Bokhan, D.E. Zakrevsky, "Adsorption Activated Resonant Photoemission", J. Exp. Theor. Phys. Lett., vol. 96, № 2, pp. 133-137, 2012.

* The work was supported by the RSF Grants No. 19-19-00069

INVESTIGATION OF THE CHARGE STATE VARIATION OF THE CATHODE MATERIAL IONS IN THE LOW CURRENT VACUUM ARC PLASMA

YU.A. ZEMSKOV, I.V. UIMANOV

Institute of Electrophysics, UB, RAS, Yekaterinburg, Russia
e-mail: zemskov@iep.uran.ru

Investigations of variation of the ion charge composition in low current vacuum arc plasma have both theoretical and practical importance. In a fundamental physics area, data of the investigations help to develop a model of plasma generation by cathode explosive emission centers in vacuum discharges. And for practical applications, it is useful to find a range of applicability for the classical data [1] about the charge composition of ions in the vacuum arc plasma, which were obtained in current ranges of tens and hundreds of amperes

Decreasing of the average charge of cathode material ions in vacuum arc plasma with the discharge current was observed in the course of several investigations. This suggests that the number of cells in the low current vacuum arc cathode spot influences the charge state of cathode material ions.

The previously investigated cathode materials were copper and CuCr alloy. To prove the effect of the average charge state variation for other cathode materials the study of the microsecond arc on the refractory cathode materials was also carried out.

Molybdenum samples were used as the vacuum arc cathodes in the 3.5 microsecond vacuum arc discharge. Pulse source was an LC-line with a quasi-rectangular pulse shape. Arc current varied from threshold current of units of ampere to 100 A. Charge state distribution and the average charge state of the cathode material ions were measured via the Thomson spectrometer with automated image recording and digital data processing. It was found that the ion charge state distributions were close to the classical data [1] at the hundred-ampere currents, and the average charge state significantly decreased with the arc current decrease. All the ion signals increase with current, and the average charge variation with an increase in the arc current is determined by a remarkable difference between the growth rate of the quantity of the differently charged ions. The quantity of the multiply charged ions increased with the current considerably faster. It led to decrease of the +1 and +2 ion fractions and increase fractions of ions with the +3 charge and higher with the discharge current.

Therefore the found dependence could be observed not only for copper and CuCr cathodes investigated earlier.

REFERENCES

- [1] W.D. Davis, and H.C. Miller, "Analysis of the electrode products emitted by dc arcs in a vacuum ambient", J. Appl. Phys., vol. 40, pp. 2212–2221, 1969.

SUBNANOSECOND BREAKDOWN OF AIR-INSULATED COAXIAL LINE INITIATED BY RUNAWAY ELECTRONS IN THE PRESENCE OF STRONG AXIAL MAGNETIC FIELD *

G.A. MESYATS¹, E.A. OSIPENKO², K.A. SHARYPOV², V.G. SHPAK², S.A. SHUNAILOV², M.I. YALANDIN^{1,2}, N.M. ZUBAREV^{1,2}

¹Lebedev Physical Institute, RAS, Moscow, Russia
²Institute of Electrophysics, UB, RAS, Yekaterinburg, Russia
e-mail: ssh@iep.uran.ru

Emission of radial runaway electron flow (REF) changes the dynamics and characteristics of subnanosecond air breakdown in the gap of coaxial line (CL) [1]. However, despite the presence of REF, there is no breakdown if the voltage is less in duration and amplitude than the threshold values. We assumed that these values can be increased if the gas ionization is localized near the REF emission zone - at the central CL electrode. An analogy with vacuum CLs with magnetic self-isolation due to a strong azimuthal magnetic field (H_θ) at submegaampere currents is appropriate here. In our case, at a current of 2-4 kA, this mode is unrealizable, because field $H_\theta < 1$ kOe. As an alternative to H_θ field in CL we use an external longitudinal field H_z with a strength of up to 10 kOe created by a pulsed solenoid. In the experiment, the REF was emitted from the boundary of the gas plasma which arises after the exit of field-emission electrons from the metal of electric field (E) enhancer - a thin disk insert into the central electrode of CL. Voltage pulses with an amplitude (modulo) $U_{in}^{max} = 160-190$ kV provided E -field near enhancer required for the REF emission, and had a duration of ≈ 300 ps (FWHM) sufficient for its acceleration in the entire radial gap. The current and resistance of a subsequent discharge were determined by comparing an incident pulse U_{in} and reflected one (U_{ref}) from the breakdown zone. It was revealed that in the absence of H_z , the early emission of REF at the front of U_{in} leads to a higher discharge current (I , Fig. 1a), despite the reduced current (and energy) of fast electrons at the anode. Delay in the field emission initiation and the rise in the REF energy at a higher (modulo) voltage at the front determine, apparently, a lower degree of gas ionization in the gap due to a drop in the impact ionization cross section. As a result, REF current at the anode increases, and discharge current (I in Fig. 1b) turns out to be less than in the case I in Fig. 1a. The presence of $H_z \approx 10$ kOe leads to the absence of REF at the anode in both variants, but relative decrease in U_{ref} and discharge current ($1 \rightarrow 2 \rightarrow 3$) is more pronounced in Fig. 1b. The question arises about the reason for a relatively weak decrease in U_{ref} in a strong field H_z and the nature of the pulses 2 and 3. Analysis of the trajectories of magnetized electrons in the vacuum approach (KARAT code) shows (Fig. 1c) that already at $H_z \approx 2$ kOe the region of the gas ionized by "REF" particles will not reach the anode, and at $H_z \approx 10$ kOe it represents a thin plasma layer expanding "along z ". It can be assumed that the presence of this conducting region and its radial size determine appearance of U_{ref} (and "analogue of the discharge current") in a strong field H_z .

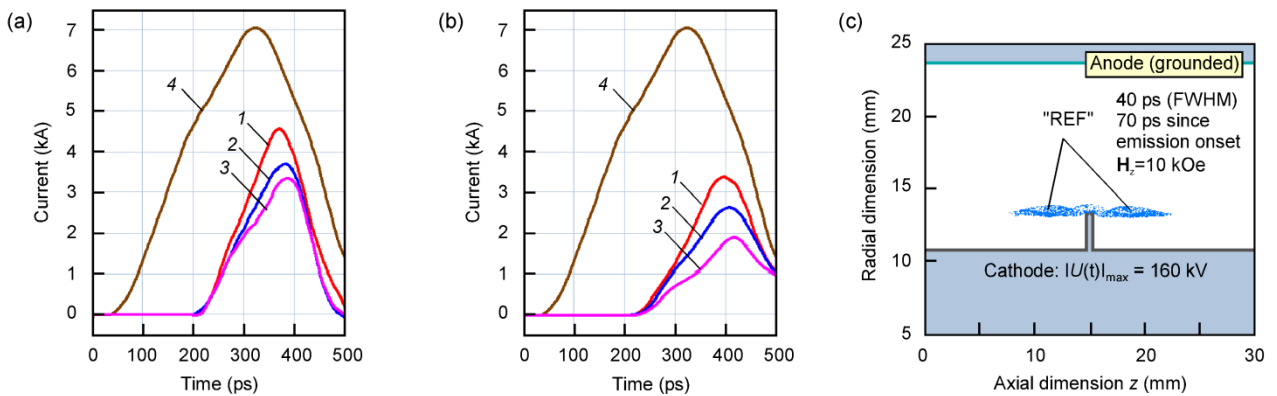


Fig. 1. (a,b) Discharge currents in the CL radial gap. For (b) REF emission occurs 50 ps later. $1-H_z=0$; $2-H_z=5$ kOe; $3-H_z=10$ kOe; $4-H_z=0$, CL is closed radially. (c) Particle-in-cell "vacuum" modeling of electrons motion at (b)-3 mode.

REFERENCES

- [1] N.M. Zubarev, V.Yu. Kozhevnikov, A.V. Kozyrev, G.A. Mesyats, N.S. Semeniuk, K.A. Sharypov, S.A. Shunailov, and M.I. Yalandin, "Mechanism and dynamics of picosecond radial breakdown of a gas-filled coaxial line," Plasma Sources Sci. Technol. vol. 29, p. 125008, 2020.

* The work was supported in part by the RFBR Grants Nos. 20-08-00172 and 20-08-00249

ELECTRICAL PROPERTIES OF HE-INDUCED W "FUZZ" WITHIN THE PRE-BREAKDOWN AND BREAKDOWN REGIMES

YU.A. ZEMSKOV, YU.I. MAMONTOV, I.V. UIMANOV

Institute of Electrophysics UB RAS, Yekaterinburg, Russia
e-mail: zemskov@iep.uran.ru

In the work presented, the investigation of the He-induced W "fuzz" electrical properties was carried out. The W "fuzz" sample was manufactured in an analogous way as the one described in [1]. For this research, an automated experimental setup was designed. The setup was based on a vacuum chamber operated under high vacuum condition ($\sim 10^{-7}$ Pa). The vacuum diode under investigation comprised of a flat W "fuzz" field-emissive cathode with an area of about 1 cm² and a 2 mm radius cylindrical copper anode rounded with a 2 mm radius hemisphere. The cathode-anode distance was about 200 μ m. A voltage applied to the diode was up to 10 kV. An HV power supply was controlled employing the DAC/ADC module "L Card E20-10" (<https://en.lcard.ru/products/external/e20-10>). This module allowed one to register automatically currents and voltages of interest also. As a result of the investigation, the data on the dielectrical strength of the vacuum diode with the W "fuzz" cathode were obtained. The effect of the cathode conditioning was demonstrated after the number of breakdowns. An increase in the breakdown electric field strength from about $4 \cdot 10^5$ V/cm for the very first breakdown up to $9 \cdot 10^5$ V/cm for the 20th breakdown was registered. In addition, the emissive characteristics of the W "fuzz" cathode were studied in accordance with the Fowler-Nordheim theory. Under the conditions described, the field-emissive current didn't exceed several microamperes. The estimated value of the electric field enhancement factor β was found to be about 40 before the breakdown and about 70 after the breakdown. The obtained β values are somewhat smaller than the ones obtained by other research groups for the nanostructured W cathodes [2, 3]. This fact should be investigated additionally.

REFERENCES

- [1] O.V. Ogorodnikova, et.al. "Deuterium and helium retention in W with and without He-induced W 'fuzz' exposed to pulsed high-temperature deuterium plasma," J. of Nuclear Materials, vol. 515, pp. 150-159, 2019.
- [2] D.Hwangbo, Sh.Kajita, N. Ohno, and D.Sinelnikov, "Field Emission From Metal Surfaces Irradiated With Helium Plasmas," IEEE Trans. Plasma Sci., vol. 45, pp. 2080-2086, 2017.
- [3] D.Sinelnikov, et.al. "Arc tracks on nanostructured surfaces after microbreakdowns," J. of Phys.: Conf. Ser., vol. 748, 012012, 2016.

MEASUREMENT OF THE EXPANSION VELOCITY OF THE PLASMA HIGH-CURRENT VACUUM ARC DISCHARGE*

A. S. ZHIGALIN¹, A. G. ROUSSKIKH¹, V. I. ORESHKIN^{1,2}, A.P. ARTYOMOV¹

¹Institute of High Current Electronics, SB, RAS, Tomsk, Russia

²National Research Tomsk Polytechnic University, Tomsk, Russia

e-mail: Zhigalin@ovpe2.hcei.tsc.ru

In this work, we present experimental results on measuring the velocity of vacuum arc discharge plasma expansion. The experiments were carried out on an IMRI-5 pulse power generator (500 kA, 500 ns). All electrodes of the plasma gun were made of aluminum. The cathode diameter varied from 3 to 6 mm. In the experiments, two designs of plasma guns were used. In the first version, the end of the arc discharge cathode was located below the plane of the anode, and the surface of the insulator separating them was parallel to the axis of symmetry of the plasma gun. In this design, the arc discharge plasma escapes the anode through a hole, the diameter of which coincides with the diameter of the cathode. In the second variant, the plane of the end face of the arc discharge cathode coincided with the plane of the anode, and the surface of the insulator separating them was located perpendicular to the axis of symmetry of the plasma gun.

A Rogowski coil, an active voltage divider, and an inductive loop were used to register the main electrophysical characteristics. To obtain an image of plasma in the optical range, an FER-7 optical streak camera was used [1]. The plasma glow registration on the chronograph was carried out with a time base of 750 ns/cm. The slit width was 200 μm . Given that the chronograph slit was located along the axis of the plasma gun, the plasma movement speed was determined in the same direction - from the plasma gun along its axis. At a given time base and a known image scale the plasma movement velocity was calculated from the inclination angle of plasma image relative to the time axis.

REFERENCES

- [1] R.B.Baksht, I.M.Datsko, A.V.Fedunin, A.A.Kim, A.Yu.Labetsky, S.V.Loginov, A.V.Shishlov, and V.I.Oreshkin, "The Rayleigh-Taylor Instabilities and K-radiation Yield for Imploding Gas Liners," *Plasma Phys. Rep.*, vol. 21, No.11, pp. 907-912, 1995.

* The work was supported in part by the Russian Science Foundation Grant No. 19-19-00127.

RUNAWAY ELECTRON FLOWS IN MAGNETIZED COAXIAL GAS DIODES*

G.A. MESYATS¹, K.A. SHARYPOV², V.G. SHPAK², S.A. SHUNAILOV², M.I. YALANDIN^{1,2}, N.M. ZUBAREV^{1,2}

¹Lebedev Physical Institute, RAS, Moscow, Russia

²Institute of Electrophysics, UB, RAS, Yekaterinburg, Russia

e-mail: yalandin@iep.uran.ru

According to numerous natural and numerical experiments, picosecond runaway electron flows (REFs) in elongated gas electrode gaps with a sharply inhomogeneous electric field are described as a strongly diverging layer. Therefore, they are of practical interest when the interaction with an interelectrode medium of a large volume or area (at the anode) is required. For a number of applications, increased uniformity of REF, current/charge density of a particle bunch can be provided by the method of confinement/focusing in a magnetic field. The case with a uniform longitudinal field B_z (Fig. 1a) has already been applied [1] and has an obvious analogy with vacuum magnetically insulated coaxial diodes (MICDs), which generate high-current beams in the explosive electron emission (EEE) mode. Note that the REF duration in gas (tens of ps) is shorter than the time of its acceleration in the gap $d = 30$ mm. That is, the calculation of the electron flow structure by the particle-in-cell method (KARAT code) in a vacuum approach (Fig. 1a) gives an “an open-shutter” image of the REF path. Nevertheless, it can be seen that, in the transversal cross section, calculated vacuum particle flux from a tubular 22 mm-diameter cathode (I) has at $B_z = 0.36$ T approximately the same radial size as we observe in air by the luminescence of the phosphor (Fig. 1b). With an increase in the field up to $B_z = 4.3$ T, the flow becomes a thin tube consisting of many discrete jets. In a weak field, $B_z = 0.36$ T, the discreteness is more pronounced, which resembles the screening effect of the cathode EEE emitters in vacuum MICDs. All the noted features take place for a cathode with diameter of 8 mm (2 in Fig. 1a; b) where a 50-ps REF current with an amplitude of ≈ 10 A was recorded at $B_z \approx 3-4$ T, and its current density reached 40 A/cm². The current density can be significantly increased by applying a magnetic field with converging lines of force (Fig. 1c) [2]. Depending on the length of acceleration section (d_2 or d_1) and the cathode diameter (3 or 4), enhancement (difference) of B -field from emitter to the registration area reaches 10-20 times, respectively. With that, in the region of maximum compression $B_z = 5$ T. As a result, radial compression of the tubular REF reaches 3-4 (Fig. 1d), and from the cathode with diameter of 8 mm we obtain a current of ≈ 7 A with a density of up to 100 A/cm². In the described mode, one should consider the loss of a part of electrons due to reflection by a magnetic mirror. In fact, we observe only those particles that have passed through so-called loss cone - by analogy with processes in open plasma traps. Due to reflections increase with the rise in the B_z difference, an increase in the emission edge length for a cathode with diameter of 22 mm (4 in Fig. 1c) does not lead to an increase in the REF current in comparison with the cathode of a smaller diameter (3 *ibid*). The report will provide a comparison of the characteristics of magnetized REFs in the case of using not only steel, but also graphite cathodes, their time and energy characteristics.

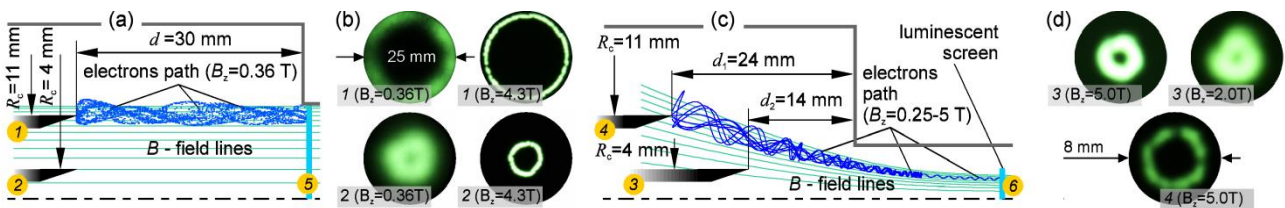


Fig. 1. (a,c) Experiment layouts for REF emission at a homogeneous and convergent magnetic field, respectively. 1,2 and 3,4 – cathodes sizes/positions; 5,6 – locations of luminophor. Reprints of REF for the cases: 1, 2 (b) and 3, 4 (d).

REFERENCES

- [1] G.A. Mesyats, M.I. Yalandin, K.A. Sharypov, V.G. Shpak, and S.A. Shunailov, “Generation of a Picosecond Runaway Electron Beam in a Gas Gap with a Nonuniform Field,” *IEEE Trans. Plasma Sci.* vol. 36, pp. 2497-2504, 2008.
- [2] M.A. Gashkov, N.M. Zubarev, O.V. Zubareva, G.A. Mesyats, K.A. Sharypov, V.G. Shpak, S.A. Shunailov, M.I. Yalandin, “Compression of runaway electron flux in an air gap with an inhomogeneous magnetic field”, *Pis'ma v ZhETF*, vol. 113, no. 6, pp. 370 - 377, 2021. <https://doi.org/10.31857/S1234567821060033>.

* The work was supported in part by the RFBR Grants Nos. 20-08-00172 and 19-08-00292.

METHODS TO ACHIEVE A BETTER EFFECT OF SYNTHETIC SOUND GENERATED BY REPETITIVE NANOSECOND PULSE DISCHARGE*

HANDONG LI, YUTAI LI, XINXIN WANG, HAIYUN LUO

Tsinghua University, Beijing, China
e-mail: lhd941224@163.com

Low-frequency sound can be generated by modulating repetitive nanosecond pulse discharge [1]. In this paper, the experimental studies on repetitive nanosecond pulse discharges at different experimental parameters were carried out, and the time-domain waveforms of voltage, current and corresponding sound were obtained. It is shown that the amplitude and harmonic components of the synthetic sound are influenced by four main factors, which are discharge deposition energy, channel length, gas recovery characteristics, and space environment. The main source of sound generation by gas discharge is the internal energy injected into the discharge channel [2, 3]. As the deposition energy and air gap distance increase, the amplitude of the synthetic sound increases, and shows certain patterns. In addition, due to gas recovery, the energy injected into the discharge channel by repetitive frequency pulse discharge is much smaller than that of a single pulse discharge [4]. Several ways were applied to accelerating the gas recovery to enhance the synthetic sound effect.

REFERENCES

- [1] Olaf B., Lacoste D.A , Moeck J.P. "Low-frequency sound generation by modulated repetitively pulsed nanosecond plasma discharges." *Journal of Physics D Applied Physics* 51(2018).
- [2] Ingard, Uno . "Acoustic Wave Generation and Amplification in a Plasma." *Physical Review* 145.1(1966):41-46.
- [3] Zhang, Bo, Z. Li, and J. He, "A numerical model of acoustic wave caused by a single positive corona source." *Physics of Plasmas* 24.10(2017):103521.
- [4] Xinjing Cai, Xiaobing Zou, Xinxin Wang, Liming Wang,Zhicheng Guan and Weihua Jiang. "Recovery of gas density in a nitrogen gap after breakdown." *Applied Physics Letters* 97.10(2010):726.

* The work was supported by the National Natural Science Foundation of China (Grant No. 52077117 and No. 51877118).

THE INFLUENCE OF BOTH AN EXTERNAL ELECTRODE SECTIONING AND THE PRESENCE OF PLASMA INSIDE A LONG CAPILLARY TUBE ON THE IONIZATION WAVE PROPAGATION IN IT

YU.S. AKISHEV^{1,2}, V.B. KARALNIK¹, A.V. PETRYAKOV¹

¹ SRC RF TRINITY, 108840, Moscow, Troitsk, Pushkovykh street, vladenie 12, Russia

² NRNU MEPhI, 115409, Moscow, Kashirskoe shosse, 31, Russia

e-mail: akishev@trinity.ru

The results of the experimental study on a slow ionization wave propagation in a long dielectric capillary tube filled with helium at a low (1-10 Torr) pressure will be presented. The external electrode is multiple sectioned. Each small section is grounded by an individual resistance to measure the radial current generated by the ionization wave propagation. The images of the ionization wave will be correlated with the individual currents of the sections, which provides information about the dynamics and spatial distribution of the radial current of the wave. The propagation velocity of a slow ionization wave in a dielectric tube is usually determined by both the rate of the dielectric wall charging and the rate of ionization processes at the wavefront. At the same time, the rate of ionization processes depends on the number of seed electrons in front of the wavefront. Therefore, the report will present the results on the influence of a low-current glow discharge in a capillary tube on the propagation velocity of an ionization wave.

METHOD OF TRIGGERING A COLD CATHODE THYRATRON WITH NANOSECOND STABILITY*

G.A. ARGUNOV, N.V. LANDL, Y.D. KOROLEV, O.B. FRANTS, V.G. GEYMAN, V.O. NEKHOROSHEV

Institute of High Current Electronics, SB, RAS, Tomsk, Russia

e-mail: argunov.grigory@yandex.ru

The cold-cathode thyatron under investigation has a trigger unit based on auxiliary glow discharge. Sustaining the auxiliary glow discharge powered by $+V_1$ means that there is not only a glow discharge between the electrodes A_1 and C_1 , but also a parasitic current to the main cathode cavity C [1]. The parasitic current may decrease breakdown voltage of the main gap of the thyatron [1].

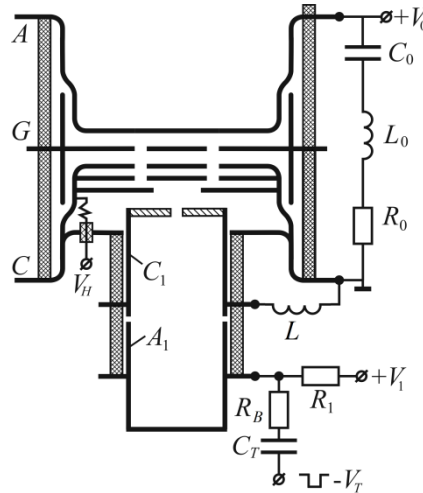


Fig. 1. Sketch design of the thyatron under investigation along with the electric circuit.

A common element of many electric circuits employed for triggering the thyatron is a few kOhm resistor between the electrodes C and C_1 . It helps initiating a pulse discharge between the electrodes A_1 and C , facilitating a faster breakdown of the main gap of the thyatron [2]. At the same time, usage of the resistor increases the parasitic current. One of the ways to decrease parasitic current is to ground both the electrodes C and C_1 . Though this method of triggering still provides nanosecond jitter, the delay time to breakdown increases [3].

In this work we propose a method of triggering the cold-cathode thyatron where an inductance L connects the electrode C_1 with the ground cathode C instead of a resistor. On the one hand it decreases the parasitic current to the electrode C , and on the other hand it leads to igniting the trigger discharge mainly on the electrode C , which decreases delay time to thyatron triggering.

REFERENCES

- [1] Y.D. Korolev, N.V. Landl, V.G. Geyman, O.B. Frants, I.A. Shemyakin, V.S. Kasyanov, and A.V. Bolotov, "Study of cold-cathode thyatron triggering stability at high anode voltages," *Plasma Phys. Rep.*, vol. 44, pp. 112–120, 2018.
- [2] Y.D. Korolev, N.V. Landl, V.G. Geyman, G.A. Argunov, O.B. Frants, and A.V. Bolotov, "Methods of triggering for the cold-cathode thyatrons with a trigger system based on an auxiliary glow discharge," *AIP Advances*, vol. 9, 085326, 2019.
- [3] G.A. Argunov, N.V. Landl, Y.D. Korolev, O.B. Frants, V.G. Geyman, V.O. Nekhoroshev, "Cold-Cathode Thyatron Triggering Method in the Electric Circuit with Grounded Cathode and Grid", 2020 7th International Congress on Energy Fluxes and Radiation Effects (EFRE)

* The work was supported in part by the RFBR Grants Nos. 20-08-00172 (theory) and 20-08-00249 (experiment).

A SOURCE OF POWERFUL SUBNANOSECOND VUV-UV RADIATION PULSES BASED ON A HIGH-PRESSURE GAS DISCHARGE

V.I. BARYSHNIKOV AND V.L. PAPERNY

Irkutsk State University, Irkutsk, Russia

e-mail: paperny@math.isu.runnet.ru

The parameters of the radiation of discharges with a duration of 200 ps with a voltage amplitude of 280 kV, a current of about 5 kA, and a storage energy of 0.3 J in xenon and nitrogen in a pressure range of 0.1 - 3 atm. were studied. It is shown that the duration of a radiation pulse in xenon is ≤ 1 ns, at a power of about 12 MW, and the radiation spectrum in the wavelength range of 110-440 nm can be fitted with satisfactory accuracy by the Planck distribution with a temperature of about 10 eV. The emission spectrum of a discharge in nitrogen at a pressure of 3 atm. in addition to a similar thermal continuum, also contains an intense laser line with a wavelength $\lambda = 337$ nm. The duration of the laser pulse is 200 ps, the intensity is 1.2 MW.

STUDY OF THE GENERATION OF RUNAWAY ELECTRONS WITH REFERENCE TO THE FORMATION OF A STREAMER IN A SHARPLY INHOMOGENEOUS ELECTRIC FIELD*

D.V. BELOPLOTOV, V.F. TARASENKO, V.A. SHKLYAEV, D.A. SOROKIN

Institute of High Current Electronics, SB, RAS, Tomsk, Russia
e-mail: rff.qep.bdim@gmail.com

The report is devoted to the study of the generation of runaway electrons with reference to the formation of a negative streamer in a sharply inhomogeneous electric field in air and helium at atmospheric pressure and below. Nanosecond voltage pulses of negative polarity with an amplitude of 18 kV were applied across a point-to-plane gap 8.5 mm long. Our previously studies have shown that a large-diameter streamer develops when applying voltage pulse across the gap [1, 2]. The propagation of the streamer in the gap is accompanied by the flow of current, the magnitude of which directly depends on the streamer velocity. In the non-ionized part of the gap in front of the streamer, this current is the sum of the displacement currents caused by a change in voltage across the gap and redistribution of the electric field strength during plasma formation (dynamic displacement current - DDC). It is possible to determine with high accuracy the moment when the streamer appears and the moment when it arrives at the opposite electrode by measuring DDC (Fig. 1a). In addition, DDC and current of runaway electrons can be measured together (Fig. 1b). As a result, we can determine exactly when runaway electrons appear. It was found that runaway electrons are generated not only during the breakdown of the gap, but also after that. It has been found that the formation time of explosive emission centers affects the generation of runaway electrons after breakdown.

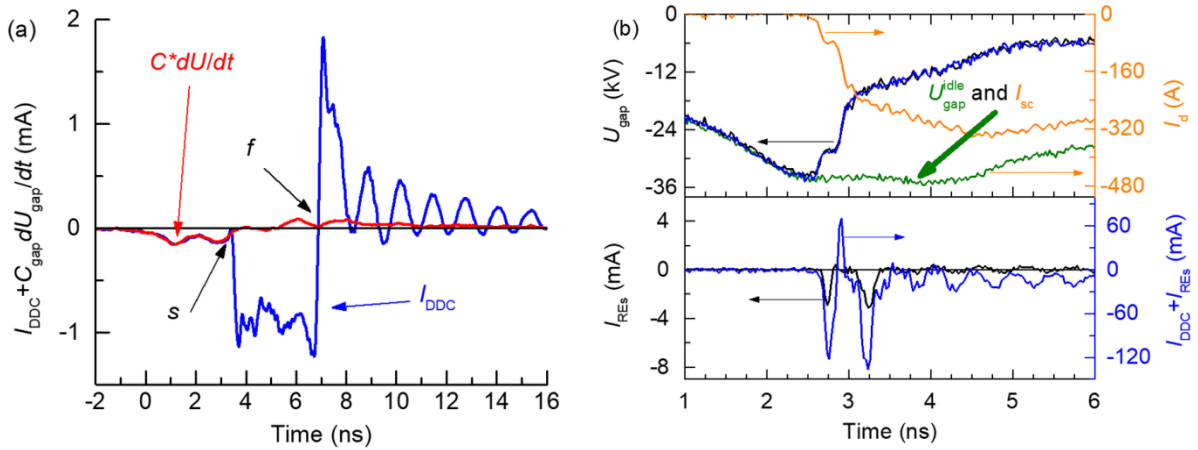


Fig. 1. (a) Waveforms of the dynamic displacement current I_{DDC} and $C_{gap}dU_{gap}/dt$, measured using a collector downstream a grid anode under conditions close to the threshold for breakdown ($U_{max}=26$ kV): s – streamer appears, f – streamer arrives at the opposite electrode. Air at a pressure of 100 kPa.

(b) Waveforms of voltage across the gap U_{gap} , discharge current I_d and RE current I_{REs} as well as waveforms of voltage across the gap U_{gap} and the sum of the dynamic displacement current and RE current ($I_{DDC} + I_{REs}$) recorded in a separate experiment. Air at a pressure of 25 kPa.

REFERENCES

- [1] D.A. Sorokin, V.F. Tarasenko, D.V. Beloplotov, and M.I. Lomaev, “Features of streamer formation in a sharply non-uniform electric field,” J. Appl Phys., vol. 125, 143301, 2019.
- [2] V.F. Tarasenko, G.V. Naidis, D.V. Beloplotov, D.A. Sorokin, M.I. Lomaev, and N.Yu. Babaeva, “Measuring and Modeling Streamer Velocity at an Air Discharge in a Highly Inhomogeneous Electric Field,” Plasma Phys. Rep., vol. 46, pp. 320–327, 2020.

* The reported study was performed within the framework of the State assignment of the IHCE SB RAS, project No. 0291-2021-0014 (FWRM-2021-0014) as well as was funded by RFBR, project number 20-02-00733

DYNAMICS AND FEATURES OF STREAMER FORMATION IN A SHARPLY INHOMOGENEOUS ELECTRIC FIELD*

D.V. BELOPLOTOV, M.I. LOMAEV, D.A. SOROKIN, V.F. TARASENKO

Institute of High Current Electronics, SB, RAS, Tomsk, Russia
e-mail: rff.qep.bdim@gmail.com

Nanosecond gas discharge in atmospheric pressure gases is a source of low-temperature nonequilibrium plasma. It can be used to inactivate microorganisms, destroy organic and inorganic pollutants in gases and liquids, sterilize medical instruments, food, packaging products [1]. Diffuse discharges are formed in the gaps with a highly inhomogeneous electric field. In this case, there is no need to use external sources of ionizing radiation. Experimentally and in simulations it was shown that a large-diameter streamer develops in the gaps [2]. This report presents the results of studies of the streamer formation in the highly inhomogeneous electric fields in air with using a streak camera and a four-channel ICCD camera with simultaneously recording waveforms of voltage and runaway electron current pulses. A large diameter streamer was observed at various amplitudes of nanosecond voltage pulses. The instantaneous streamer velocity was measured using the streak camera. It was found that the streamer has a high velocity at the initial stage of the development, but it rapidly decreases. The minimum streamer velocity corresponds to the maximum diameter. The streamer velocity increases again by an order of magnitude when it approaches the opposite electrode. It was found that the streamer velocity correlates with the value of a displacement current induced by its propagation. At the initial stage of the streamer development during subnanosecond breakdown, the displacement current can reach several kiloamperes that is comparable to the conduction current after the breakdown.

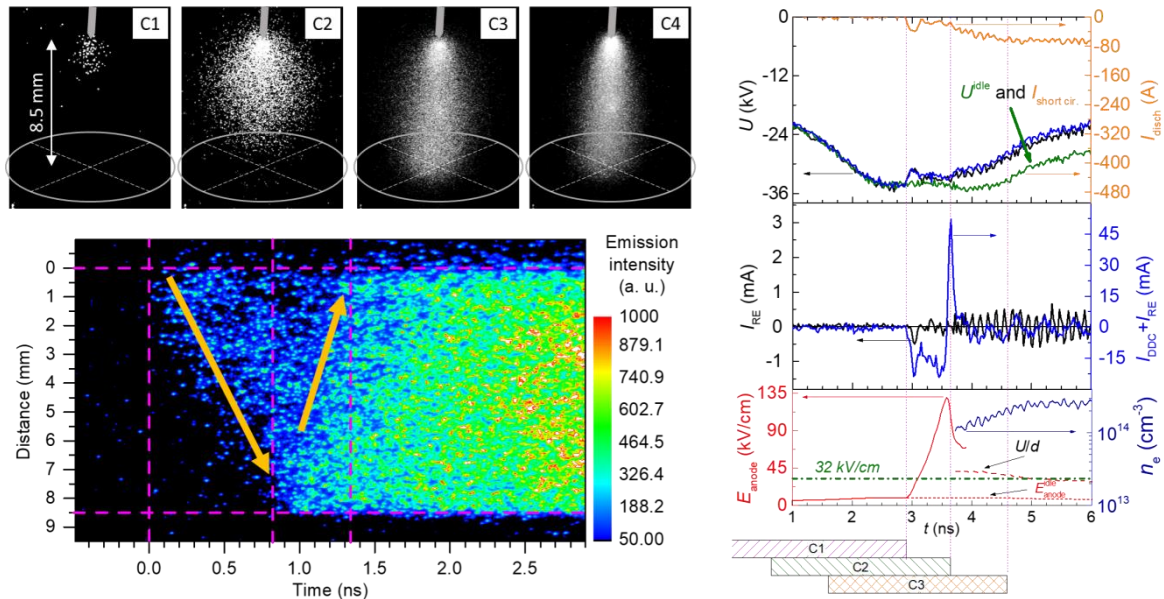


Fig. 1. ICCD and streak images of discharge formation in air at a pressure of 100 kPa. Corresponding waveforms of voltage across the gap U_{gap} , discharge current I_d and RE current I_{REs} as well as waveforms of voltage across the gap U_{gap} and the sum of the dynamic displacement current and RE current ($I_{\text{DDC}} + I_{\text{REs}}$) recorded in a separate experiment. The rectangles show the moments of switching on channels C1–C3 of the ICCD camera. The length of the rectangles corresponds to the duration of the exposure. The exposure time of channel C4 was 20 ns. The corresponding time dependences of the electric field strength near the anode $E_{\text{anode}}(t)$ and electron concentration $n_e(t)$ are also presented.

REFERENCES

- [1] K.-D. Weltmann, J.F. Kolb, M. Holub, D. Uhrlandt, M. Šimek, M. K. Ostrikov, S. Hamaguchi, U. Cvelbar, M. Černák, B. Locke, A. Fridman, P. Favia, and K. Becker, "The future for plasma science and technology," *Plasma Process. Polym.*, vol. 16, 1800118, 2018.
- [2] V.F. Tarasenko, G.V. Naidis, D.V. Beloplotov, D.A. Sorokin, M.I. Lomaev, and N.Yu. Babaeva, "Measuring and Modeling Streamer Velocity at an Air Discharge in a Highly Inhomogeneous Electric Field," *Plasma Phys. Rep.*, vol. 46, pp. 320–327, 2020.

* The reported study was performed within the framework of the State assignment of the IHCE SB RAS, project No. 0291-2021-0014 (FWRM-2021-0014) as well as was funded by RFBR, project number 20-02-00733

NANOSECOND BREAKDOWN IN A PULSED OPEN DISCHARGE *

P.A. BOKHAN¹, N.A. GLUBOKOV², P.P. GUGIN¹, D.E. ZAKREVSKY^{1,2}

¹Rzhanov Institute of Semiconductor Physics, SB, RAS, Novosibirsk, Russia

²Novosibirsk State Technical University, Novosibirsk, Russia

e-mail: gugin@isp.nsc.ru

Similarity laws for a nanosecond pulse breakdown for a system of two flat electrodes under various conditions $E/p = f(p\tau)$, where τ is the discharge formation time, are known [1, 2]. These works deal mainly with the discharge development due to Townsend electron multiplication, including discharges with runaway electrons. There are discharges in which the breakdown development is determined by other sufficiently intense mechanisms to apply the similarity laws to them. In particular, in the open discharge (OD) [3], the main mechanism of discharge development is adsorption-activated resonance photoemission.

In this work the existence of the similarity law $E/p = f(p\tau)$ in OD and in OD with generation of counter propagating electron beams (CPEB) is investigated. In these discharges, the photoemission mechanism is realized in a wide range of conditions. Electron emission occurs under the action of resonant VUV radiation of fast heavy particles; therefore, the current rising rate is determined by the type and particles concentration of the working gas. Under typical conditions of OD existence (helium pressure 3 - 100 Torr, reduced field strength $\sim 10^3$ Td), the Townsend electron multiplication coefficient is low and it is insufficient to maintain the discharge and the electrons go into the runaway mode and either go into the drift space through the anode grid with a geometric transparency of $> 80\%$, or, in the case of the CPEB mode, begin to oscillate between the accelerating gaps. The latter is used to implement high-voltage subnanosecond switches.

The cell design is shown in the figure 1(a). It consists of two identical counter-spaced accelerating gaps with 7 mm long. There is a 12 mm drift space (3) between the anode grids (2) grounded through the current-measuring shunt. The cathodes (1) are made of reaction sintered silicon carbide. Experiments were carried out with working gases He, Ne, Ar in two modes: with one accelerating gap and two. In the second case, an OD with the generation of CPEB was realized. This led to a much faster discharge formation. The excitation pulses had a front of 7 ns with an amplitude of 3.5 to 43 kV. Working gases were in the range of $p_{\text{He}} = 20 - 100$ Torr, $p_{\text{Ne}} = 5-25$ Topp, $p_{\text{Ar}} = 1-15$ Topp. In all cases, similarity curves were obtained. It turned out that the similarity exists both for the discharge development delay (Fig. 1(b), curves 2, 4), and for the breakdown process itself (Fig. 1(b), curves 1, 3), determined by the level of 0.9 - 0.1 of the voltage drop at the cathode. The data obtained on the dependences $E/p = f(p\tau)$ differ significantly from the results [1, 2]. The mechanisms leading to this difference are discussed.

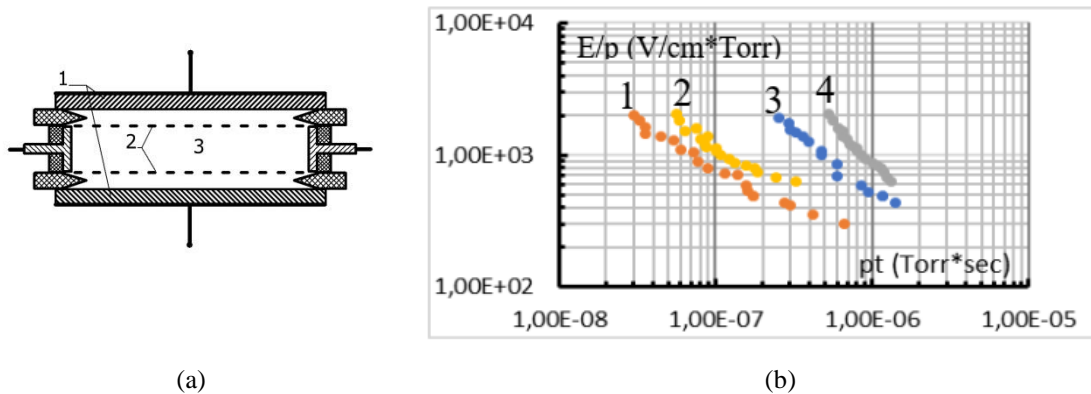


Fig. 1. (a) Cell design, and (b) breakdown time in ODCPEB (1), OD (2), breakdown delay in ODCPEB (3), OD (4) at $p_{\text{He}} = 30$ Torr .

REFERENCES

- [1] G.A. Mesyats "Similarity laws for pulsed gas discharges", Physics-Uspokhi, vol. 49 n. 10, pp. 1045, 2006.
- [2] P. Felsenthal, J.M. Proud "Nanosecond-pulse breakdown in gases", Physical Review, vol. 139 n. 6A, pp. A1796, 1965
- [3] P.A. Bokhan, Dm. E. Zakrevsky. "Adsorption-activated resonant photoemission." JETP letters vol. 96, n. 2, pp. 133-137, 2012.

* The work was supported in part by the RSF Grants No. 19-19-00069 (experiment) and State Assignment ISP SB (theory).

INVESTIGATION OF THE RADIAL DENSITY DISTRIBUTION OF THE NEAR-SURFACE MATTER IN THE CYLINDRICAL CONDUCTORS SKIN EXPLOSION*

L.M. DATSKO, N.A. LABETSKAYA, V.A. VAN'KEVICH

Institute of High Current Electronics SB RAS, Tomsk, Russia

e-mail: datsko@ovpe.hcei.tsc.ru

Investigations of the process of near-surface plasma formation during skin explosion of cylindrical copper and duralumin conductors in rapidly increasing magnetic fields with their induction on the surface up to 500 T were conducted. The experiments were carried out on a high-current MIG generator with a current amplitude of up to 2.5 MA and a rise time of 100 ns. The plasma formation on the conductor surface was recorded by its glow in the visible range using a four-frame optical camera with an exposure time of each frame of 3 ns. In addition, vacuum photoemission diodes recorded the surface plasma reaching a temperature of more than 1 eV in the blackbody approximation. The internal structure of the surface plasma, the density assessment of the matter in it and of its radial distribution were investigated using shadowgrams obtained by X-ray transmission with $h\nu > 0.8$ keV, which is formed at the "hot point" of the X - pinch. This optimization of the X-pinch configuration in order to realize no more than two emitting hot spots made it possible to obtain sufficiently clear images of shadowgrams with a magnification factor of more than three. In addition to obtaining shadow images of the exploded conductor, the density of the expanding surface plasma was estimated using step attenuators from the materials of the conductor under study. A stepped filter was applied to a polypropylene film 6 μm thick.

A calculation code was developed for the numerical solution of the task of reconstructing the distribution profile of a substance from the data of X-ray studies on the conductors electrical explosion in a vacuum, that allows using shadow images (X-ray patterns) of the conductors explosion at certain points in time as initial data. The spatial characteristics $\mu\rho(r)$ (μ - the absorption coefficient of the substance, ρ is its density) of the exploded conductor of cylindrical geometry were determined in the selected section by measuring the integral ratios $I_0/I(r)$ (I_0 is the intensity of the probing radiation, I is the intensity of the substance of the radiation conductor) directly from the X-ray diffraction patterns. Additionally, the code implements the possibility of determining (calibrating) the absorption coefficient $\mu(\nu)$ from the measurements data of the probing radiation flux passage through a step attenuator (since the exact value of $\mu(\nu)$ may be unknown in the experiment). In this case, the calibration results were used as normalization ones directly when calculating the dependence $\rho(r)$.

The dependences of $\mu\rho$ on the radius of the conductor in the selected section of the X-ray diffraction pattern of its explosion are obtained. The value of the mass absorption coefficient of radiation μ was determined from the transmission X-ray diffraction patterns of the step filters. The dependences of the load substance density on its radius were determined and constructed from the obtained X-ray diffraction patterns at different times from the beginning of the current. So at 216 ns at a radius of 1.8 mm of a duralumin conductor with an initial diameter of 2.97 mm, the density of the substance is estimated to be 0.008 g/cm^3 .

* This work was supported by the RFBR Grant № 19-08-00479 and was partially carried out within the framework of the state assignment of the Ministry of Science and Higher Education of the Russian Federation on the topic № FWRM-2021-0001.

THE INITIAL STAGE OF THE PLASMA FORMATION AT THE SKIN EXPLOSION OF CYLINDRICAL CONDUCTORS*

L.M. DATSKO¹, N.A. LABETSKAYA¹, S.A. CHAIKOVSKY^{1,2}, V.A. VAN'KEVICH¹ AND V.I. ORESHKIN¹

¹*Institute of High Current Electronics, SB, RAS, Tomsk, Russia*

²*Institute of Electrophysics, UB, RAS, Yekaterinburg, Russia*

e-mail: datsko@ovpe.hcei.tsc.ru

The formation of plasma on the surface of the electrically exploded conductor is a key issue in terms of the energy introduced into the metal substance. For the rising rates of magnetic field induction typical for magnetically isolated transmission lines of multi-megaampere generators, this question remains insufficiently studied. The purpose of this work was to study the dynamics of dense plasma formation on the metal surface at magnetic induction values of 2-6 MGs and the rising rates of $(2-5) \cdot 10^{13}$ G/s. The experiments were carried out on a terawatt MIG generator with current amplitude up to 2.5 MA and a rise time of 100 ns. In experiments, the skin electrical explosion of cylindrical conductors made of different materials and with different diameters was studied. The formation of plasma on the surface of the conductor was recorded using a four-frame optical camera with an exposure time of 3 ns for each frame. It was shown that when the current increases, "spots" appear on the surface of a cylindrical conductor. These spots are the centers of plasma formation. Later, current channels develop in this surface plasma, as shown in Fig. 1(a). The paper discusses the features of the dynamics of plasma formation as a function of the rising rate of the magnetic field induction.

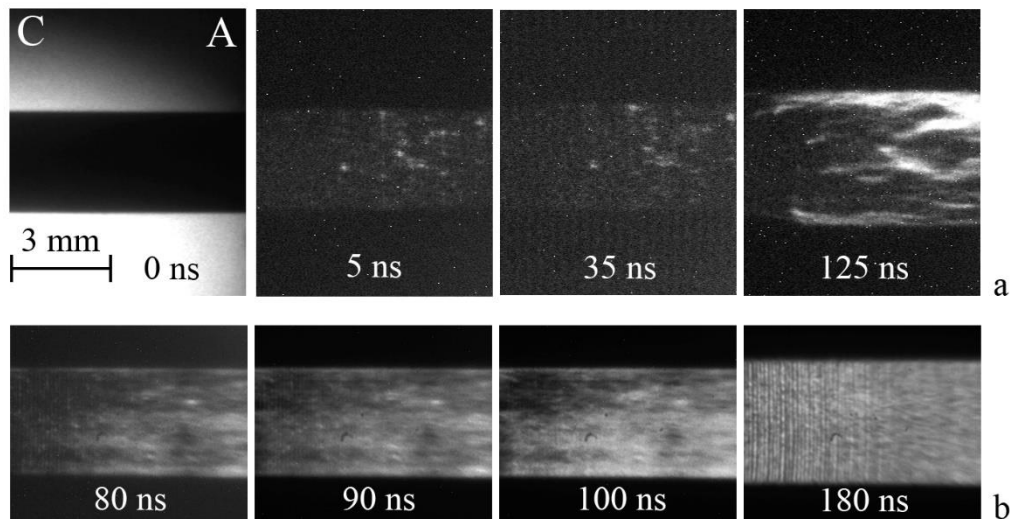


Fig. 1. Images of an exploding duralumin conductor of initial diameter 3 mm taken at different times from the beginning of the current flow for peak current of 1.3 MA (a) and 2.0 MA (b).

* The work was supported by the Russian Science Foundation (grant No. 20-19-00364).

FORMATION OF THE SPATIAL STRUCTURE OF A DIFFUSE DISCHARGE IN EXCIMER LASERS*

YU. N. PANCHENKO¹, A.V. PUCHIKIN¹, M.V. ANDREEV¹, E.V. GORLOV², V.I. ZHARKOV²

¹Institute of High Current Electronic, SB, RAS, Tomsk, Russia,

²V. E. Zuev Institute of Atmospheric Optics, SB, RAS, Tomsk, Russia.

e-mail: ypanchenko@sibmail.com

The studies were carried out on discharge XeCl and KrF lasers developed at the HCEI SB RAS, Tomsk. It is shown in this work that the formation of the spatial structure of a diffuse plasma through which further pumping energy is provided occurs from the moment of breakdown to a decrease in the voltage across the discharge gap. In this case, the fraction of the energy deposited during this time period does not exceed 10% of the total pump energy.

The use of this discharge in dense excimer media made it possible to expand the range of stable existence of diffuse plasma with an electron concentration up to $\sim 8 \times 10^{15} \text{ cm}^{-3}$, while maintaining the properties of the active medium during the entire duration of the pump pulse. The formation of multiple equilibrium diffuse channels was ensured due to the growth rate of the current density dj/dt more than $6 \times 10^{10} \text{ A/cm}^2 \text{ s}$ and the reduced field strength at the moment of the discharge gap breakdown not less than $E/P \sim 3 \text{ kV/cm} \times \text{atm}$. The choice of the ratio of the electron donor and acceptor in the composition of the as mixture makes it possible to implement the completed or incomplete stage of the development of multiple diffuse channels in the discharge.

* This work was supported by the project of the Russian Science Foundation No. 20-79-10297.

PLASMA CHANNEL DYNAMICS IN SUB- AND MICROSECOND DISCHARGES IN WATER*

N.S. SEMENIUK, A.V. KOZYREV, A.A. ZHERLITSYN, S.S. KONDRATIEV, V.M. ALEXEENKO

*Institute of High Current Electronics, SB, RAS, Tomsk, Russia
e-mail: viliiskoezero@yandex.ru*

Pulsed high-current discharges in liquids and their associated shock waves have a high potential for practical application. Research on the use of shock waves in water are carried out for the processing of both primary and secondary raw materials [1, 2].

One of the main limitations of the extensive use of technologies based on shock waves is the low efficiency of transformation of the electrical energy in the capacitive storage of the supply generator into the mechanical energy of an acoustic wave, which in many cases does not exceed a few percent [3]. The electrical parameters of the generators can be varied over a wide range and optimized in order to increase the efficiency. The effect of different discharge durations on the efficiency of acoustic wave generation was investigated.

A mathematical model of a plasma channel in a liquid medium is formulated in relation to the technical parameters of the experiment. The model is based on the hypothesis of an isothermal state of the plasma in the channel of a pulsed high-current discharge. We assumed the presence of three kinds of particles (free electrons, positive ions, and neutral molecules of the same type), as well as the spatial homogeneity of the plasma channel along its cross-section and length. A calculation of the dynamics of an acoustic wave is made on the basis of a theoretical description of the plasma channel. The model of the dynamics of the expanding channel makes it possible to calculate the intensity of the acoustic wave under experimental conditions.

The model has been tested in relation to experiments carried out on the generators with a submicrosecond and microsecond discharge time that allowed us to change the duration of the mode of energy output to the plasma channel while maintaining the initial energy storage. The experiments in which an electric energy of ~ 70 J is introduced into the channel from an electric pulse generator for 0.4 and 2 μ s are described. It was shown that plasma in a high-current channel of a pulsed discharge in water is a strongly ionized state of a gaseous medium with a number density of neutral particles of $\sim 4 \cdot 10^{21}$ cm $^{-3}$. The expansion of this hot channel occurs at a subsonic velocity of about 400-500 m/s, generating a strong diverging acoustic wave in liquid water with initial pressure amplitude in the pulse above 100 MPa.

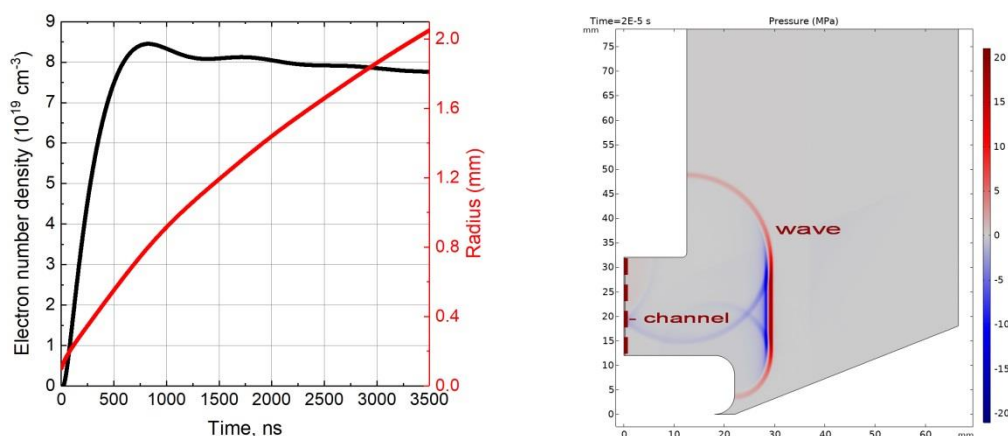


Fig. 1. Time dynamics of the radius and plasma number density in the discharge channel (left) and instant picture of an acoustic wave in discharge chamber (right) 20 μ s after the start of the discharge.

REFERENCES

- [1] H. Bluhm, W. Frey, H. Giese, P. Hoppe, C. Schultheiss, and R. Strassner, "Application of pulsed HV discharges to material fragmentation and recycling," *IEEE Transactions on Dielectrics and Electrical Insulation*, vol. 7, no. 5, p. 625–636, 2000.
- [2] E. Dal Martello, S. Bernardis, R. B. Larsen, G. Tranell, M. Di Sabatino, and L. Arnborg, "Electrical fragmentation as a novel route for the refinement of quartz raw materials for trace mineral impurities," *Powder Technology*, vol. 224, p. 209–216, 2012.
- [3] A. Grinenko, S. Efimov, A. Fedotov, Y. E. Krasik, and I. Schnitzer, "Efficiency of the shock wave generation caused by underwater electrical wire explosion," *Journal of Applied Physics*, vol. 100, no. 11, p. 113509, 2006.

* The work was carried out within the framework of the state assignment of the Ministry of Science and Higher Education of the Russian Federation on the topic No. FWRM-2021-0001 and the grant of the Russian Foundation for Basic Research (RFBR), project number 18-29-24079 mk.

THE DYNAMICS OF THE FORMATION OF INITIAL STAGES OF A TRANSVERSE NANOSECOND DISCHARGE WITH AN EXTENDED SLOT CATHODE IN ARGON*

N.A. ASHURBEKOV¹, K.O. IMINOV¹, M.Z. ZAKARYAEVA^{1,2}, G.S. SHAKHSINOV¹, K.M. RABADANOV¹

¹*Dagestan State University, Makhachkala, Russia*

²*Institute of Physics, DFRC of RAS, Makhachkala, Russia*

e-mail: nashurb@mail.ru

The work presents the results of an experimental study and numerical modelling of the spatio-temporal dynamics of initial stages of discharge in argon at gas pressures up to 10 Torr and the voltage applied to the electrodes of 1.5 kV.

The discharge occurred between a cylindrical cathode with a rectangular slot 0.2 cm wide and 0.6 cm deep, located at a distance of 0.6 cm from the flat anode. The discharge area between the cathode and the anode is confined on both sides by fiberglass dielectric plates [1]. The numerical simulation was carried out with Comsol Multiphysics software using the built-in Plasma Module [2]. A self-consistent system of plasma kinetics equations was solved, supplemented by the electron energy distribution function for conditions corresponding to the experimental studies performed.

The results of the numerical simulations show that the electron density n_e increases at the initial stages in the entire discharge gap. In about 50 ns, n_e in the center of the discharge gap becomes significantly (almost five times) larger than near the anode. In about 100 ns, n_e in the discharge gap reaches 10^{11} cm^{-3} and an ionization wave starts from the anode side and propagates to the cathode at a speed of about $\sim 5 \cdot 10^7 \text{ cm/s}$ (Fig. 1a). It was established that at the entrance to the cathode cavity, the front of the ionization wave is divided into two parts, and two ionization waves propagate in the cavity, sliding along its surfaces (Fig. 1b). After reaching the base of the cavity ($\sim 130 \text{ ns}$), a backward ionization wave is formed and the cavity and the discharge gap between the electrodes are filled with plasma. The maximum values of n_e reach $\sim 5 \cdot 10^{14} \text{ cm}^{-3}$ (Fig. 1c), and further, due to the recombination processes and diffusion, the value of n_e decreases, and the discharge passes into the final stage.

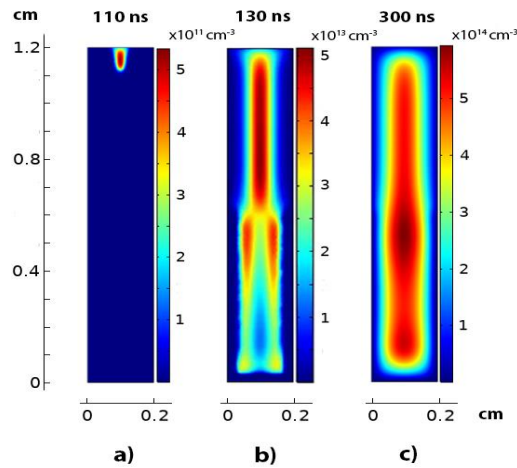


Fig. 1. Typical spatio-temporal dynamics of electron density distribution in the discharge gap.

The paper discusses the regularities of the formation and development of a limited discharge in argon, its features and possible physical processes that affect the dynamics of the discharge development and the formation of its structure. Special attention is paid to the study of the influence of the amount of charge accumulated on the surface of the dielectric plate on the discharge dynamics.

REFERENCES

- [1] N.A. Ashurbekov, K.O. Iminov, O.V. Kobzev, and V.S. Kobzeva, "Periodic plasma structures in nanosecond discharge with a slit cathode," *Technical Physics Letters*, vol. 36, no. 8, pp. 766–769, 2010.
- [2] N.A. Ashurbekov, K.O. Iminov, G.S. Shakhshinov, M.Z. Zakaryaeva, and K.M. Rabadanov, "The dynamics of a nanosecond gas discharge development with an extended slot cathode in argon," *Plasma Science and Technology*, vol. 22, no. 12, p. 125403, 2020.

* This work was supported by a grant from the Russian Foundation for Basic Research No. 19-32-90179 and state assignment FZNZ–2020–0002.

THE MEASUREMENTS OF VACUUM ARC BEHAVIOR AT THRESHOLD CURRENTS

I.L. MUZYUKIN, P.S. MIKHAILOV

*Institute of Electrophysics, UB, RAS, Yekaterinburg, Russia
e-mail: plasmon@mail.ru*

The measurements of vacuum arc current parameters at the threshold current were made. The threshold currents for Cu, Mo, graphite sand tungsten FUSE cathodes were measured. It was shown that the current that vacuum arc chops with has a statistical distribution. The vacuum arc current chopping is accompanied with significant ion current burst. The ion current of Mo and Cu cathodes contains intensive peaks with 10-50 ns durations (see Fig. 1). It was shown that the cathode materials that have intense peaks have significant threshold current.

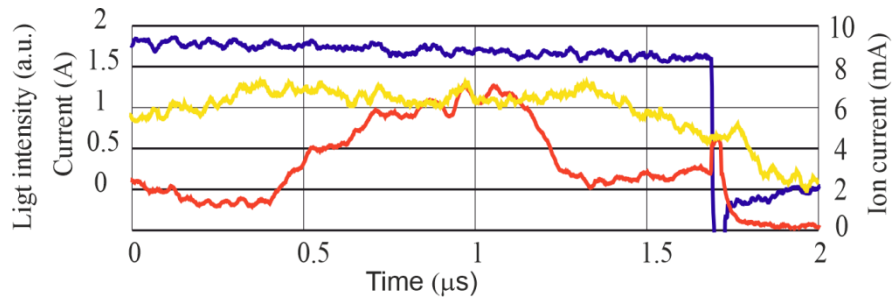


Fig. 1. The waveforms of discharge current, ion current and light emission at a chopping process.

IONIC WIND PRODUCED BY POINT-TO-PLATE DIELECTRIC BARRIER DISCHARGES

E. MOREAU, E. DEFOORT

University of Poitiers, CNRS, PPRIME Institute, Poitiers, France
e-mail: eric.moreau@univ-poitiers.fr

Although corona discharges in atmospheric air involve complex electrical, chemical and mechanical phenomena, they are easy to enforce. Therefore, they are used in numerous engineering applications, such as ozone production, reduction of gaseous pollutants, surface treatment, electrostatic precipitation and more recently thrust production for instance. Indeed, when a high potential difference is applied at a thin electrode (such as a needle or a wire), air molecules are ionized and a corona discharge is induced. Due to the electric field, the produced ions are submitted to Coulomb force, resulting in their motion from the high voltage electrode toward the grounded collecting one. The set of all these Coulomb forces results in a volume electrohydrodynamic (EHD) force occurring inside the discharge. Hence, in the electrode gap, many collisions between ions in motion and neutral air molecules take place, resulting in a momentum transfer that produces a gas flow, which is usually called “ionic wind”.

In this experimental study, we aimed at better understanding the electrohydrodynamic phenomena occurring in a 15-mm gap point-to-plate dielectric barrier discharge. For that, current measurements have been carried out and the produced ionic wind by the discharge has been precisely characterized with the help of a 20 kHz Particle Image Velocimetry system. The influence of several input parameters has been studied (voltage, frequency, HV waveform) and will be presented.

As an example, Fig. 1a presents the discharge current versus time for $V = 12$ kV and $f = 200$ Hz. We can see that one voltage cycle is composed of a positive streamer discharge and a negative Trichel one. In Fig. 1b, we can see that time-averaged ionic wind results in jet starting from the needle and impacting the plate perpendicularly, with a maximum velocity of about 5 m/s at the center of the jet. Finally, Fig. 1c shows the ionic wind velocity at 1.5 mm far from the needle tip; this highlights that the ionic wind produced during the positive discharge is faster than the one during the negative discharge.

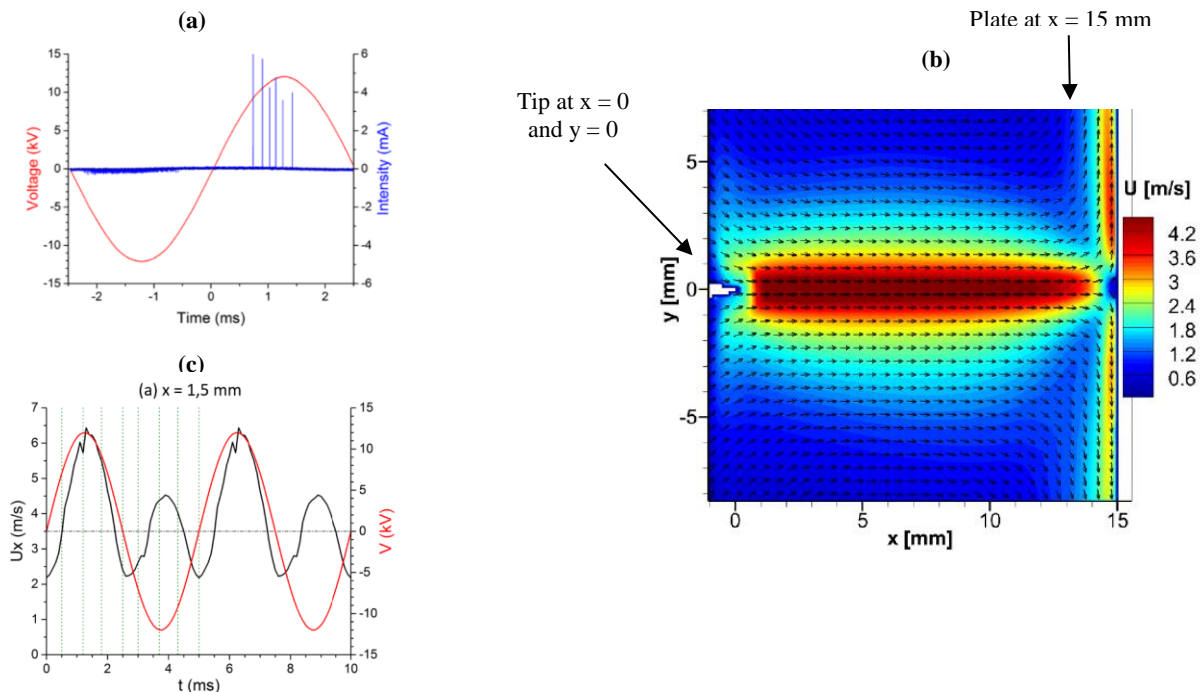


Fig. 1. Current vs time (a), velocity map of the time-averaged ionic wind (b) and velocity vs time (c).

ROLE OF THE SURFACE FINISH ON THE DIFFERENT DISCHARGE REGIMES OF POINT-TO-PLATE DC CORONAS

H. YAN^{1,2}, N. BENARD², E. MOREAU²

¹Dalian University of Technology, Dalian, Republic of China

²University of Poitiers, CNRS, PPRIME Institute, Poitiers, France

e-mail: eric.moreau@univ-poitiers.fr

This experimental study aimed at better understand the electrical and optical properties of corona discharges. As we will see, they depend highly on several input parameters, such as the electrode gap, the value of the applied voltage and also the surface state of the needle tip. Indeed, when the needle is a brand-new tungsten one, the current is pulseless and the discharge regime is always glow, whatever the gap and the voltage are. On the contrary, when the tungsten needle has been used during a few minutes (in absence of spark), its surface becomes lightly oxidized and the discharge regimes are fully different. In this last case, three successive regimes can be observed, including one that has never been reported in the literature to our knowledge. In fact, after the ignition voltage, the current is slowly increasing and the current raise follows perfectly the theoretical Townsend's law; this is the glow regime (Figure 1a). When the voltage reaches a first threshold (8 kV here), some small current pulses appear. However, it is not the breakdown streamer regime as the ionized channels do not cross the entire electrode gap since photographs and iCCD visualizations highlighted that the propagation of the streamers toward the grounded plate was limited to an half of the gap (Figure 1c). In this regime, the time-averaged current becomes higher than the Townsend's law, each current pulse is composed of only one bump and the pulse frequency is higher than the one of breakdown streamer. When the voltage reaches a second threshold (15.6 kV here), the magnitude of the current pulses suddenly increases but their frequency decreases; it is the transition toward the breakdown streamer regime (Figure 1b). In this regime, each current pulse is composed of two bumps, the first one corresponding to the arrival of a primary streamer at the plate and the second one corresponding to a secondary streamer. Finally, we investigated the effect of the electrode gap. We observed that the magnitude of the current pulses decreases when the gap increases whereas the frequency of the breakdown streamers is higher when the gap is smaller.

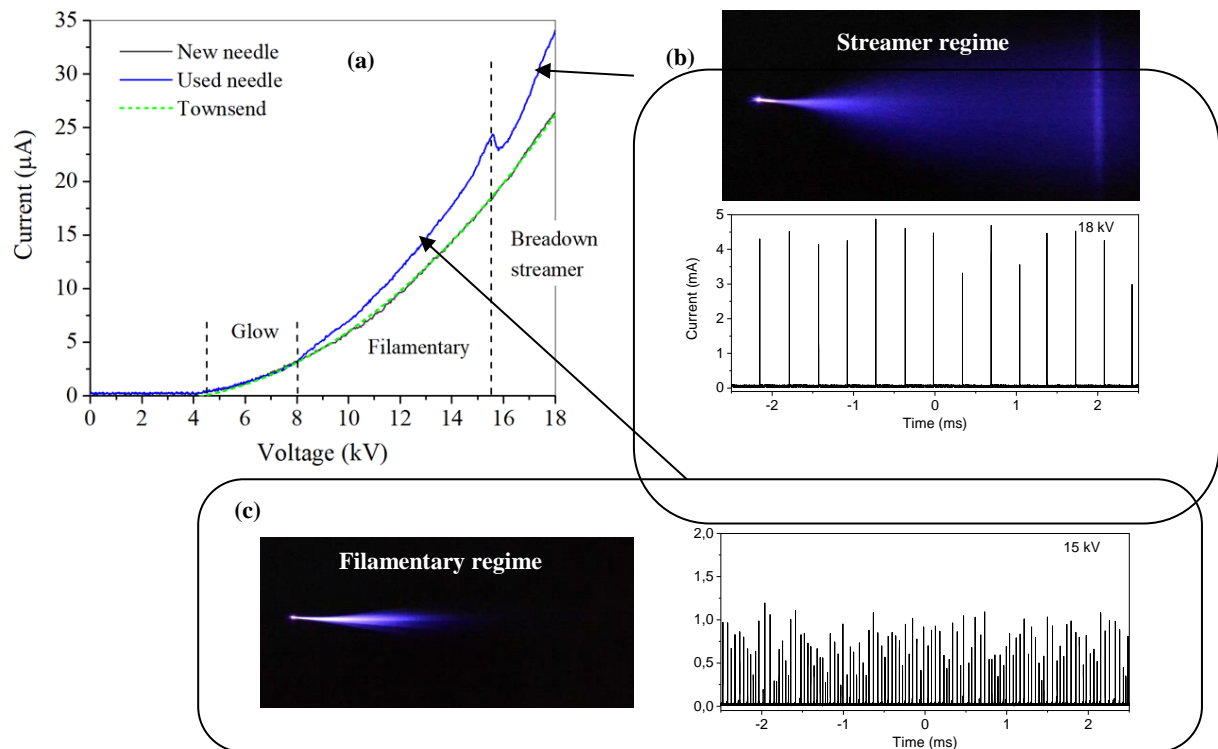


Fig. 1. I-V characteristics of a 30 mm point-to-plate positive corona discharge (a) and current versus time of a streamer corona (b) and a filamentary corona (c).

INVESTIGATION OF THE ALUMINUM ELECTRODES EROSION OF A PLASMA GUN DURING THE OPERATION OF A HIGH-CURRENT VACUUM ARC DISCHARGE

A.P. ARTYOMOV¹, A.G. ROUSSKIKH¹, A.S. ZHIGALIN¹, I.A. ROUSSKIKH¹, A.G. TYUKAVKIN¹, V.I. ORESHKIN^{1,2}

¹*Institute of High Current Electronics, SB, RAS, Tomsk, Russia*
²*National Research Tomsk Polytechnic University, Tomsk, Russia*
e-mail: artyomov@ovpe.hcei.tsc.ru

Currently, we are actively studying the possibility of using high-current vacuum arc discharges as a source of ionized matter for cylindrical Z-pinch shells [1, 2]. The aim of this work was to obtain magnitude quantitative estimates of the plasma gun aluminum electrodes erosion that occurs during the course of a high-current vacuum arc discharge.

The experimental setup consisted of two current generators. The first generator (IMRI-5, capable of generating a current with an amplitude of up to 450 kA and a rise time of 500 ns in a short-circuited load mode) was used as a current source for a plasma gun. In other words, the load of the IMRI-5 pulse power generator was a plasma gun with aluminum electrodes (Fig. 1). The second generator (XPG, 250 kA, 220 ns) was used as an X-ray radiograph to visualize the object under study in the soft X-ray range ($h\nu \approx 0.5\text{--}3$ keV).

A high-current vacuum arc discharge was initiated during self-breakdown along the lateral surface of a polyethylene insulator 3 mm long separating the cathode and anode of the arc. When a high-current arc discharge flowed from the cathode along the insulator to the anode, it formed a plasma jet, which spread from the cathode to the grounded anode. The plasma jet, forming in the interelectrode gap of the plasma gun, flows into the vacuum chamber of the IMRI-5 generator through a cylindrical channel (in anode) with a diameter and length of 4 mm and 2 mm, respectively. The main results and conclusions obtained in the course of these investigations are based on the analysis of experimental data obtained by both electrophysical and radiographic methods. A functional dependence was obtained between the amount of the evaporated cathode substance and the current density of the vacuum arc discharge.

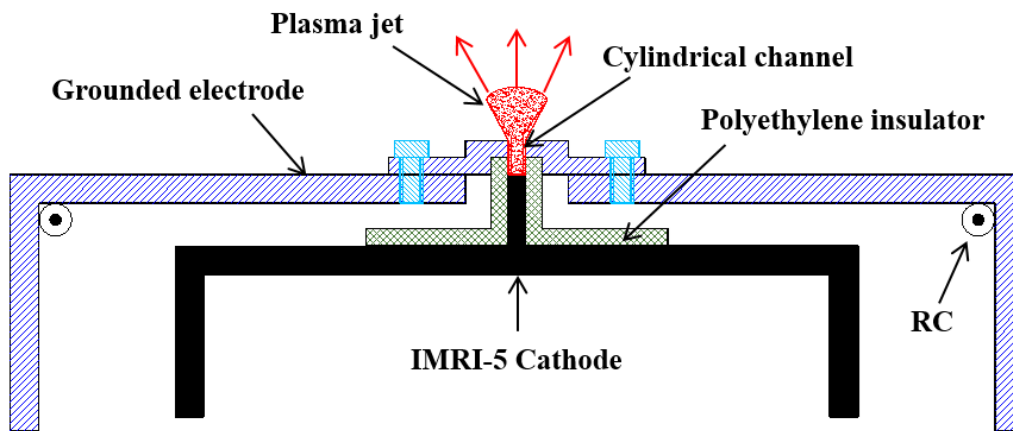


Fig. 1. Experimental arrangement. RC is a Rogowski coil.

REFERENCES

- [1] A.G. Rousskikh, A.V. Shishlov, A.S. Zhigalin, *et al*, "Small-sized vacuum-arc-discharge x-ray radiograph," *Plasma Sources Sci. Technol.*, vol. 20, 035011, 2011.
- [2] A.G. Rousskikh, A.S. Zhigalin, V.I. Oreshkin, *et al*, "Effect of the axial magnetic field on a metallic gas-puff pinch implosion," *Phys. Plasmas.*, vol. 23, 063502, 2016.

DETERMINATION OF THE CONDUCTOR RESISTANCE DURING THEIR EXPLOSION IN VACUUM UNDER CONDITIONS OF SKINNING THE CURRENT*

A.G. ROUSSKIKH, A.S. ZHIGALIN, V.I. ORESHKIN

Institute of High Current Electronics, SB, RAS, Tomsk, Russia

e-mail: russ@ovpe2.hcei.tsc.ru

The work is devoted to the investigation of the features of the conductor explosion in a vacuum under the conditions of skinning the current, and specifically, the effect of the magnetic field nonlinear diffusion wave spreading over the exploded conductor on its electrical properties [1]. Experiments on the explosion of conductors were carried out on the IMRI-5 pulse power generator [2]. The geometry of the load and a typical current oscillogram in the short circuit mode are shown in Fig. 1. The exploded conductor was soldered to the cathode and mechanically clamped between the plates on the anode.

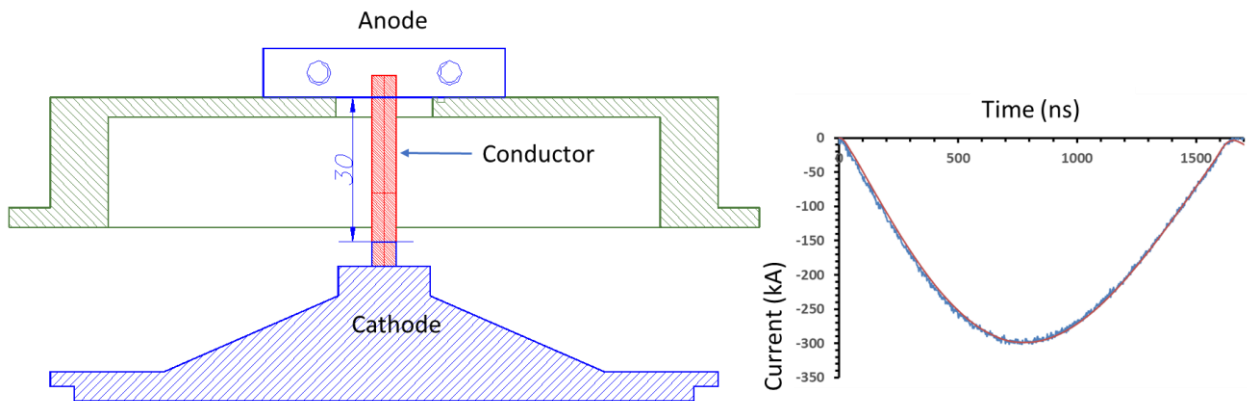


Fig. 1. Load geometry and current oscillogram in short circuit mode.

In the experiments, we used two types of conductors, cylindrical and flat (foils). Cylindrical conductors were of two types: copper (0.5 mm in diameter) and aluminum (0.44 mm in diameter). Foils were also of two types: copper with a thickness of 300 microns and aluminum with a thickness of 200 microns. The foil width varied from 1 to 3 mm. The length always remained 30 mm.

To calculate the circuit inductance and calculate the corrections for the real conductor inductance, we used a load that was either a copper foil 600 μm thick and 1 cm wide, or a copper conductor with a diameter of 2 mm (short circuit mode).

REFERENCES

- [1] V.I. Oreshkin, and S.A. Chaikovsky, "Stability of a nonlinear magnetic field diffusion wave", *Physics of Plasmas*, Vol. 19., p. 022706, 2012.
- [2] A.G. Rousskikh, A.S. Zhigalin, V.I. Oreshkin, N.A. Labetskaya, S.A. Chaikovsky, A.V. Batrakov, G.Yu. Yushkov, and R.B. Baksht, "Study of the stability of Z-pinch implosions with different initial density profiles", *Physics of Plasmas*, Vol. 21., p. 052701, 2014.

* The work was supported by this work was supported by Russian foundation for basic research, grants no. 20-21-00036.

METHODS FOR INTRODUCING NEGATIVE FEEDBACK FOR BEAM CURRENT CONTROL IN SOURCES WITH A PLASMA CATHODE BASED ON A LOW PRESSURE ARC*

M.S. VOROBYOV, V.I. SHIN, V.N. DEVYATKOV, P.V. MOSKVIN, N.N. KOVAL

Institute of High Current Electronics, SB, RAS, Tomsk, Russia

e-mail: vorobyovms@yandex.ru

Electron sources with plasma cathodes [1], in which the plasma boundary is stabilized, for example, by a metal fine-structured grid, have a unique possibility of mutually independent control of the parameters of the electron beam. Thus, such sources make it possible to independently control the energy, amplitude and duration of the beam, as well as the pulse repetition rate of the beam current. In particular, this makes it possible to control the power of a megawatt-level beam during pulses of submillisecond duration [2].

However, in any energy system, that is, in a system in which there is any energy effect of the level of units of kilojoules, there are necessarily instabilities associated with a change in the operating conditions of the electron source directly during the beam current pulse [3]. Such changes, for example, may include a change in the gas conditions during a pulse of the beam current due to the intense bombardment of the electrodes in the system by this beam. In particular, bombardment of the collector surface with an intense electron beam can lead not only to gas desorption from its surface, but also to melting of its surface. Separately, it is worth noting the processes associated with the ionization of the desorbed gas and vapors of the collector material, which leads to the appearance of the so-called collector plasma. The plasma velocity ($\sim 10^6$ cm/s) [1] is two orders of magnitude higher than the gas velocity; therefore, these effects can manifest themselves even when the beam current pulse duration is equal to several tens of microseconds.

This paper presents the results on the introduction of negative feedback in the control of an electron source with a plasma cathode based on a low pressure arc discharge. The negative feedback is as follows: when any instability of the beam current appears, associated with the appearance of a large fraction of accelerated ions in the total current in the accelerating gap I_0 and the corresponding uncontrolled increase in this current I_0 , the number of electrons extracted from the plasma cathode decreases proportionally. The ways and possibilities of introducing such a negative connection are discussed (Fig. 1).

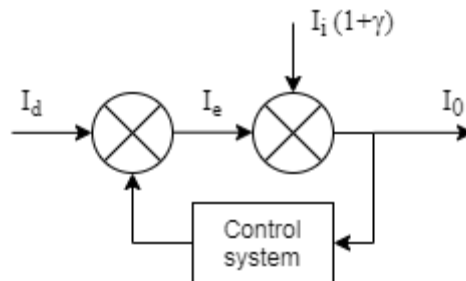


Fig. 1. Scheme for controlling the common current I_0 in the acceleration gap in a source with a plasma cathode: I_d - discharge current, I_e - emission current, I_d - discharge current, I_i - ion current, γ - ion-electron emission factor

First of all, the introduction of negative feedback is necessary for better control of the parameters of the beam current, and, in particular, for a controlled change in its power during pulses of submillisecond duration, which makes it possible to organize a higher repeatability of the process of materials irradiation.

REFERENCES

- [1] E. Oks. Plasma Cathode Electron Sources: Physics, Technology, Applications. WILEY-VCH. (2006). 171 p.
- [2] M.S. Vorobyov, N.N. Koval, P.V. Moskvina, A.D. Teresov, S.Yu. Doroshkevich, V.V. Yakovlev, V.I. Shin. Electron beam generation with variable current amplitude during its pulse in a source with a grid plasma cathode. Journal of Physics: Conference Series 1393 (2019) 012064, doi:10.1088/1742-6596/1393/1/012064
- [3] S.V. Grigoryev, V.T. Astrelin, V.N. Devyatkov, I.V. Kandaurov, N.N. Koval, A.V. Kozyrev, P.V. Moskvina, A.D. Teresov. Generation of submillisecond electron beam in the diode with the grid plasma cathode and the plasma anode generated by the asymmetrical reflective discharge. Proc. of 16th international symposium on high current electronics, 2010, PP. 19-22.

*This work was supported by the Russian Science Foundation (project No. 20-79-10015).

OES OF NITROGEN ATOMS CONCENTRATION DURING PLASMA PROCESSING

S.V. AVTAEVA

Institute of Laser Physics, SB, RAS, Novosibirsk, Russia

e-mail: s_avtaeva@mail.ru

Plasma processing includes various plasma technology such as plasma deposition, etching, nitriding etc. This plasma processes use different low-pressure discharges providing interaction of active plasma species with surface. The quality of the plasma processing depends on comprehending interaction physics and on possibility to control the active plasma species concentration during the process.

Here the OES technique for measuring densities of N atoms is discussed. A control of the N atom density is of important for plasma nitriding. OES gives useful information on the densities of electronically excited states of the emitting species, which, however, are related to the densities in the ground state. The method of the optical emission actinometry makes it possible, in a number of cases, to determine the concentrations of molecules, atoms, or radicals in the ground electronic states from the emission spectra of these particles [1]. In low-pressure (LP) argon-nitrogen discharges, such as glow discharge and arc discharge, N density, it is shown, can be found as [2]

$$[N] = \text{const} \frac{I_N}{I_{Ar}} \frac{k_{Ar}^{dir}}{k_N^{dir}} \frac{x_{Ar}}{x_{N_2}} [N_2], \quad (1)$$

where x_{Ar} , x_{N_2} are the percentage of argon and nitrogen in the gas mixture with the discharge off and $[N_2]$ is the input number density of nitrogen molecules, respectively.

The N_2 dissociation degree in the LP glow discharge operating in pressures ranging from 10 to 100 mTorr and cathode bias of 600-1000 V was measured using I_{NI}/I_{ArI} intensity ratio (Fig. 1). It was shown that in the glow discharge, N_2 dissociation degree reaches about 7% with the argon fraction in the Ar- N_2 mixture < 10% and decreases afterwards approaching to ~ 1-2% when the argon percentage becomes 90% and higher. The atomic nitrogen species is produced by electron-impact processes such as, collisions between electrons and nitrogen molecules or between electrons and N_2^+ ions. At small Ar fraction in Ar- N_2 mixtures, the atomic nitrogen species is most likely produced by the collisions between electrons and N_2^+ ions.

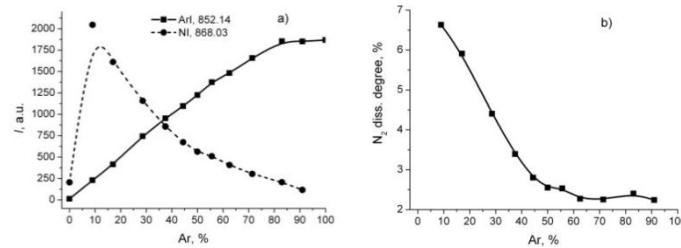


Fig. 1. Intensities of spectral lines NI and ArI (a) and the N_2 dissociation degree (b) for the low-pressure glow discharge in Ar- N_2 mixture as functions of the Ar percentage in the mixture. The discharge voltage is 1000 V and the pressure is 25 mTorr.

The N_2 dissociation degree was also measured in the Ar- N_2 plasma of a cascaded large area LP arc discharge, where a remote anode was used together with a primary anode [3]. A primary arc current was of 75 A while the anode current for remote anode was varied from 5 to 200 A. Gas pressure was varied from 2 to 25 mTorr. The n_e increased from 2.5×10^9 up to 2.5×10^{10} cm^{-3} when the remote anode current was increased from 5 up to 75 A. T_e was in the range of 1.8-3.0 eV. In opposite to the case of the large-area LP glow discharge the N_2 dissociation degree in the cascaded large area LP arc discharge increased with the Ar fraction. The difference is because of 2-3 eV higher T_e in the LP arc as compared with the LP glow discharge. Estimations show, provided that T_e and n_e change a little with Ar fraction, the Ar_m number density rises with increasing Ar fraction, and the most probable mechanism of N_2 dissociation under LP arc conditions is excitation transfer from Ar_m to N_2 .

REFERENCES

- [1] V. M. Donnelly, "Review Article: Reactions of fluorine atoms with silicon, revisited, again", *J. Vac. Sci. Technol. A*, vol. 35, 05C202, 2017.
- [2] S. Avtaeva, V. Gorokhovskiy, S. Myers, S. Robertson, E. Shunko, Z. Zembower, "Characterization of the large area plane-symmetric low-pressure DC glow discharge", *Spectrochimica Acta Part B*, vol. 124, pp. 25-39, 2016.
- [3] S. Avtaeva, V. Gorokhovskiy, S. Robertson, E. Shunko, "Characterization of low-pressure high-current cascaded arc plasma in large volumes", *Spectrochimica Acta Part B: Atomic Spectroscopy*, vol. 165, 105785, 2020.

THE DEVELOPMENT OF HYDRODYNAMIC AND THERMAL INSTABILITIES IN A LIQUID METAL JETS IN THE CATHODE SPOT OF A VACUUM ARC*

I.V. UIMANOV¹, G.A. MESYATS^{1,2}

¹Institute of Electrophysics, UB, RAS, Yekaterinburg, Russia

²Lebedev Physical Institute, RAS, Moscow, Russia

e-mail: uimanov@iep.uran.ru

The explosion of the liquid metal jets is considered to be the basic mechanism of the birth of new cathode spot cells [1-4]. In this work a two-dimensional axisymmetric model has been developed to describe the formation of a liquid metal jet, the droplet pinch-off and temperature runaway in the droplet-jet neck during melt splashing from the cathode crater in a vacuum arc. The development of hydrodynamic and thermal instabilities has been self-consistent simulated in a copper current-carrying liquid metal jet in the “inertial” mode of the melt splashing (see Fig. 1). In this case, a jet with a longitudinal velocity gradient is formed and the droplet-jet neck becomes unstable due to the action of capillary forces (Rayleigh–Plateau instability). As a result, the neck radius decreases rapidly and the droplet splits off. In a current-carrying jet, this process is accompanied by a strong increase in the current density in the neck and its rapid heating due to the Joule effect to a critical temperature at certain values of current from the cathode spot plasma. It is shown that the heating process has the nature of a temperature runaway and, accordingly, can lead to its electric explosion. Assuming a constant current density on the jet surface, its minimum “explosion” value was calculated depending on the diameter, velocity and initial temperature of the jet. It is shown that for craters and jets of low-current arcs this density does not exceed 10^7 A/cm² and, accordingly, can be provided by the ion current from the plasma of the cathode spot.

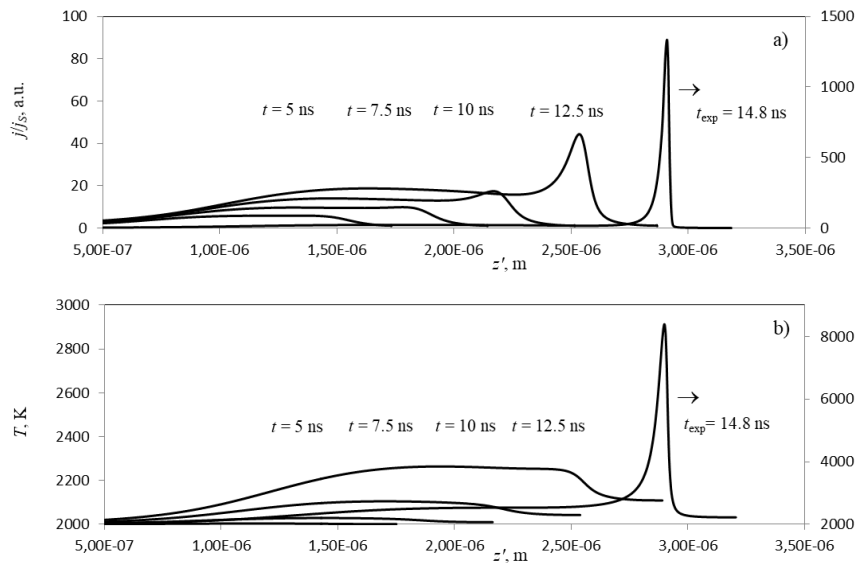


Fig. 1. Temporal evolution of the current density a) and temperature b) distributions along the jet.

REFERENCES

- [1] G A Mesyats and D I Proskurovsky, Pulsed Electrical Discharge in Vacuum, Berlin: Springer, 1989, pp. 110–114.
- [2] G A Mesyats, Cathode Phenomena in a Vacuum Discharge: The Breakdown, the Spark and the Arc, Nauka, Moscow, 2000. pp. 167–170.
- [3] G A Mesyats, JETP Lett., vol. 60, pp. 593–596, April 1994.
- [4] E A Litvinov, G A Mesyats, A G Parfenov and A I Fedosov, Zh. Tekh. Fiz., vol. 55, p. 2270, May 1985.

*This work was supported in part by RFBR Grant Nos. 19-08-00783.

SURFACE DISCHARGE DURING ELECTRICAL EXPLOSION OF CONDUCTORS IN STRONG MAGNETIC FIELDS*

V.I. ORESHKIN^{1,2}, S.A. CHAIKOVSKY³, E.V. ORESHKIN⁴

¹*Institute of High Current Electronics, RAS, Tomsk, Russia*

²*National Research Tomsk Polytechnic University, Tomsk, Russia*

³*Institute of Electrophysics UB RAS, Ekaterinburg, Russia*

⁴*P. N. Lebedev Physical Institute, RAS, Moscow, Russia*

e-mail: oreshkin@ovpe.hcei.tsc.ru

The article [1] studied the initial stage of explosion of aluminum rods with a diameter of 1 mm at a current amplitude of about 1 MA. At the initial stage of the explosion, “hot spots” of up to 500 pcs/mm² were recorded on the surface. At a later stage, a plasma layer was formed on the surface of the conductor, in which filaments, that is, current channels, were formed. In this work, on the basis of the ecton theory [2], a model of the development of a surface discharge is constructed. The model makes it possible to estimate, firstly, the magnitude of the current flowing through the surface plasma, and secondly, the thickness of the plasma layer.

REFERENCES

- [1] Awe, T. J., Yu, E. P., Yates, K. C., Yelton, W. G., Bauer, B. S., Hutchinson, T. M., Fuelling, S., McKenzie, B. B. “On the evolution from micrometer-scale inhomogeneity to global overheated structure during the intense joule heating of a Z-pinch rod”. *IEEE Transactions on Plasma Science*, 45(4), 584-589, 2017.
- [2] Mesyats, G. A. “Cathode Phenomena in a Vacuum Discharge: The breakdown, the spark, and the arc.” Nauka Publishers, 2000.

* The work was supported by the Russian Science Foundation (grant No. 20-19-00364).

RESEARCH OF THE LIFE CHARACTERISTICS OF THERMOCATODES IN ARC PLASMA TORCH*

A.S. ANSHAKOV, P.V. DOMAROV

Kutateladze Institute of Thermophysics SB RAS, Novosibirsk, Russia
e-mail: Domaroff@yandex.ru

Among the technological problems of using electric arc plasma, the most urgent is the erosion of electrodes in plasmatrons, which determine the continuous operation life of the plasma device and the duration of the technological process as a whole. The object of the study is thermionic tungsten cathodes and thermochemical cathodes (hafnium, zirconium) when operated in an oxygen-free environment and in air, respectively. In fig. 1 shows the diagrams of cylindrical W-cathodes.

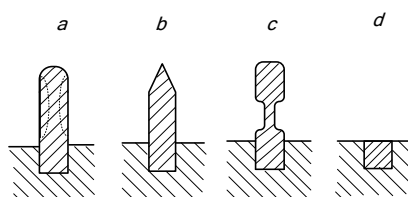


Fig. 1. Schemes solid cathodes (a, b, c, e).

Specific erosion of the electrode \bar{G} is defined as the ablation of the material mass Δm , referred to the value of the current I per unit time t , i.e. $\bar{G} = \Delta m / (It)$, kg/C. Knowing the values of \bar{G} and Δm , it is quite simple to estimate the continuous operation of the electrode at a given arc discharge current. Erosion of electrodes is a consequence of complex thermal, electrical, chemical and other processes in the near-electrode region, on the surface and inside the crystal lattice. The fundamental phenomenon discovered in the 70s - the recycling of tungsten atoms - made it possible to explain many experimental results on the resource of W-cathodes. The essence of the phenomenon is that tungsten atoms, falling into the electric field of the arc, are ionized and return in the form of ions to the end surface of the cathode. Under the influence of a powerful heat source from the side of the near-electrode area, the processes of explosive destruction, intense melting, evaporation and boiling take place, which actually determine the life of the electrodes. Therefore, the desire of researchers to reduce the thermal load on the cathode, to reduce the temperature of the working surface of the cathode by expanding the contact zone between the arc and the electrode by increasing the length of the cathode (Fig. 1, a, b) or thermal decoupling (Fig. 1, c) is understandable. However, it should be taken into account that at the same time the emitting area grows, from which intensive evaporation of the material occurs and the erosion of the cathode grows. An effective way to reduce the erosion of the W-cathode is to reduce the surface from which the tungsten evaporates. Experiments have shown [1] that a decrease in the length of the rod electrode ($l_c > 0$) leads to a decrease in cathode erosion and its minimum value is reached at $l_c = 0$ (Fig. 1, d).

The paper presents the calculated and experimental results of studies of the specific erosion of tungsten electrodes depending on the length l_c , the diameter of the cathode and the arc discharge current. The possibility is shown and the long-term operation of W-cathodes in argon, nitrogen, helium, hydrogen is realized and implemented in practice [2]. In an oxygen-containing environment, thermochemical cathodes (TCC) based on hafnium and zirconium have been recommended as highly efficient cathodes. In air, the high-temperature surface of zirconium (hafnium) chemically interacts with nitrogen and oxygen, forming an oxonitride film with good emission properties and heat resistance. The formed film reliably protects the cathode from further oxidation. The main regularities of TCA erosion from current and operating time have been established, which are successfully used in production. Taking into account their limited operation at currents of 50-400 A, thermochemical cathodes are widely used in plasmatrons for cutting metals, powder metallurgy, spraying, etc.

REFERENCES

- [1] M.F. Zhukov, N.P. Kozlov, A.V. Pustogarov, et al., Near-electrode processes in arc discharges. Novosibirsk: Nauka, 1982.
- [2] V.S. Cherednichenko, A.S. Anshakov and M.G. Kuzmin, Plasma Electrotechnical Installations. Novosibirsk: NGTU, 2011.

* The work was supported in part by the RFBR Grants Nos. 20-08-00172 (theory) and 20-08-00249 (experiment).

DETERMINATION OF THE VOLTAGE DROP ON A HIGH-CURRENT VACUUM ARC DISCHARGE UNDER CONDITIONS OF A LIMITED CROSS-SECTION OF THE PLASMA FLOW*

A.G. ROUSSKIKH¹, A.S. ZHIGALIN¹, V.I. ORESHKIN^{1,2}, A.P. ARTYOMOV¹

¹ *Institute of High Current Electronics, SB, RAS, Tomsk, Russia*

² *National Research Tomsk Polytechnic University, Tomsk, Russia*

e-mail: russ@ovpe2.hcei.tsc.ru

The work is devoted to the study of the high-current vacuum arc discharge characteristics under conditions of a limited cross-section of the plasma flow. The experiments were carried out on the IMRI-5 setup [1] with a sinusoidal arc current amplitude of 300–350 kA and a rise time of 500 ns. Aluminum rods with diameters from 3 to 7 mm were used as a cathode. The plasma flow was formed in a channel whose diameter was equal to that of the cathode. The features of the formation of a plasma jet with various configurations of the used plasma gun are described. The electrophysical parameters of the arc discharge are presented. Theoretical estimates of the voltage drop across the high-current arc during the outflow of a plasma flow through holes with a limited diameter are provided.

REFERENCES

- [1] A.G. Rousskikh, A.S. Zhigalin, V.I. Oreshkin, N.A. Labetskaya, S.A. Chaikovsky, A.V. Batrakov, G.Yu. Yushkov, and R.B. Baksht, “Study of the stability of Z-pinch implosions with different initial density profiles”, *Physics of Plasmas*, Vol. 21, 052701, 2014.

* The work was supported by Russian Science Foundation, grant no. 19-19-00127.

COMPARATIVE CHARACTERISTICS OF A GLOWING ANOMALOUS, AN OPEN AND A HOLLOW CATHODE DISCHARGES*

E.V. BELSKAYA^{1,2}, *P.A. BOKHAN*¹, *P.P. GUGIN*¹, *A.A. KVASHNINA*², *D.E. ZAKREVSKY*^{1,2}

¹*A. V. Rzhzanov Institute of Semiconductor Physics, SB, RAS, Novosibirsk, Russia*

²*Novosibirsk State Technical University, Novosibirsk, Russia*

e-mail: zakrdm@isp.nsc.ru

Gas-discharge and electron-beam excitation is applied for gas lasers active medium pumping. There are two types of discharges which allow to generate electron beams at the operating gas pressure in the active volume: a hollow cathode discharge and an open discharge. In the present work the operating parameters of these two discharge types in similar geometries were investigated and compared in the scope of their application for lasers on self-terminating transitions excitation. Observed discharges are also compared with an anomalous glow discharge.

The hollow cathode discharge and the open discharge were realized in a coaxial geometry with silicon carbide cathodes with an inner diameter $D_c = 33$ mm and a length $L = 60$ mm. The anode of the open discharge cell was a metal grid cylinder 27 mm in diameter, 97% transparency, and a distance between the grid wires of 1 mm. The anode of the hollow cathode discharge cell consisted from two metal rings with a diameter D_c , located at a distance of 12 mm from both sides of the cathode. The anomalous glow discharge was realized between two metal coaxial electrodes with an inner diameter D_c located at a distance L .

Current-voltage characteristics were investigated at different helium pressures. The open discharge in a pulsed mode operates in a wide range of pressures: e.g., 5-50 Torr in helium. In the case of hollow cathode and anomalous discharges in the pulsed mode the optimal pressures are significantly lower: up to 7 Torr of helium.

The nature of the excitation of atomic states transitions depends on the excitation cross section and the electron energy distribution function (EEDF), which are different for different types of discharges. In the hollow-cathode discharge the electron energy distribution differs from the Maxwellian one because the region where the electrons gain energy and the region of electron beam deceleration are spatially separated. In open discharge almost monoenergetic electron beam is generated due to small length of cathode potential drop. The shape of the EEDF determines the relative fraction of the operating atoms or ions levels excitation.

The effect of differences in EEDF, which occurred in the investigated discharges, was studied on the example of population behavior of the helium self-terminating transition $2^1P_1^0 - 2^1S_0$ lower operating level. The population of the He(2^1S_0) metastable state was measured in the afterglow by resonant light absorption on the helium self-terminating transition $2^1P_1^0 - 2^1S_0$. Laser radiation on the same transition was used as probing radiation. The probing laser radiation passed through the investigated device and its absorption was measured after the end of the excitation pulse applied to the investigated device. From the absorption data, the metastable level population was calculated:

$$I = I_0 \exp(-\varkappa N_m l), \quad (1)$$

where I_0 , I are the intensities of reflected and passed through the active medium radiation; \varkappa is the absorption cross section for Doppler broadening, N_m is the absorbing particles concentration (in this case He(2^1S_0)); l is the absorbing layer length.

The amplifying properties of the active medium, excited by different types of discharges, were investigated in the master oscillator power amplifier mode. Same open-discharge device with cathode internal diameter of 5 cm and length of 15 cm was used as a master oscillator. Studied devices with different types of discharges were successively installed as power amplifier. Gain was measured by changing the delay between the voltage pulses applied to the master oscillator and to the electrodes of the investigated device. Significant differences in the temporal behavior of \varkappa and its maximum value for open and hollow-cathode discharges are demonstrated.

* The work was supported by the State Assignment ISP SB.

FEATURES OF THE ELECTRON AVALANCHE FORMATION PROCESS IN A STRONGLY INHOMOGENEOUS ELECTRIC FIELD UNDER HIGH OVERVOLTAGES*

Y.I. MAMONTOV¹, V.V. LISEKOV^{1,2}

¹*Institute of Electrophysics, UB, RAS, Yekaterinburg, Russia*

²*Ural Federal University, Yekaterinburg, Russia*

e-mail: mamontov@iep.uran.ru

In gas discharge physics, this is an electron avalanche development process that determines largely the dynamics of the discharge formation. Under given conditions (a gas type and pressure, a voltage applied to the discharge gap, etc.), the rate of the electron number exponential growth and the critical number of electrons comprising the avalanche have a strong effect on the distribution of an electric field across a discharge gap, as well as on plasma processes taking place, and, eventually, on a gas discharge type. So, the Townsend and streamer mechanisms of the discharge development are usually distinguished. However, in subnanosecond discharges of high pressure, the explanation of the discharge dynamics using these mechanisms may be inapplicable. In particular, in [1], it was shown that the subnanosecond discharge in nitrogen of 6 atm pressure developed in a way that differed substantially from the streamer discharge theory commonly used for the description of similar discharges.

In the present paper, the simulation of the electron avalanche formation process in subnanosecond discharges of high pressure was carried out by means of the Monte-Carlo approach. The Monte-Carlo code used is described in details in [2]. The discharge gap under consideration in the configuration “the finger-shaped cathode – the hemispherical anode” generating the inhomogeneous distribution of an electric field was the same as the one described in [1]. A gas simulated was nitrogen under a pressure in the range from 1 atm up to 10 atm. An average electric field strength across the discharge gap was about 200 kV/cm. As a result, the critical size of the electron avalanche was determined for various nitrogen pressures and voltages applied to the discharge gap. In addition, the probabilities of the electron transition into runaway regime under various conditions were determined. Pre-ionization of the gas medium by runaway electrons was estimated. Special attention was paid to the problem of the electron and ion space charge consideration in the investigation of a runaway electron beam propagation process.

The paper is of importance for the fundamentals of subnanosecond gas discharge physics. Also, it is believed that pre-ionization of a gas medium by a beam of fast electrons at the breakdown delay stage influences significantly on the commutation time of a high-pressure discharge gap [3]. Also, the pre-ionization may lead to the initial formation of the subnanosecond high-pressure discharge in a volume form before the development of a highly conductive spark channel [4, 5]. Therefore, the results obtained can be used in pulsed-power technologies.

REFERENCES

- [1] S.N. Ivanov, V.V. Lisenkov, and Y.I. Mamontov. “Streak investigations of the dynamics of subnanosecond discharge developing in nitrogen at a pressure of 6 atmospheres with the participation of runaway electrons,” *Plasma Sourc. Sci. Tech.*, IN PRINT, doi: <https://doi.org/10.1088/1361-6595/abf31f>, 2021.
- [2] Y.I. Mamontov, I.V. Uimanov, A.V. Kozyrev, N.M. Zubarev, and N.S. Semeniuk, “Influence of Inhomogeneous Electric Field Geometry Factors on Runaway Electrons Generation Conditions,” *Proc. 7th Int. Congress on Energy Flux. and Rad. Effects (EFRE)*, Tomsk, Russia, pp. 140–146, 2020.
- [3] G.A. Mesyats and M.I. Yalandin, “On the nature of picosecond runaway electron beams in air,” *IEEE Trans. on Plasma Sci.*, vol. 37, no. 6, pp. 785–789, 2009.
- [4] G.A. Mesyats and M.I. Yalandin, “Nanosecond volume discharge in air initiated by a picosecond runaway electron beam,” *Phys. Usp.*, vol. 62, pp. 699–703, 2019.
- [5] N.Yu. Babaeva, Ch. Zhang, J. Qiu, X. Hou, V.F. Tarasenko, and T. Shao, “The role of fast electrons in diffuse discharge formation: Monte Carlo simulation,” *Plasma Sources Sci. Technol.*, vol. 26, no. 8, 085008, 2017.

* The work was supported in part by the RFBR Grants Nos. 20-38-90147 and 20-08-00172.

ELECTRON EMISSION FROM AN EXPANDING PLASMA FRONT WITHIN THE FOREVACUUM PRESSURE RANGE IN SPHERICAL GEOMETRY*

Y.I. MAMONTOV, I.V. UIMANOV

*Institute of Electrophysics, UB, RAS, Yekaterinburg, Russia
e-mail: mamontov@iep.uran.ru*

It is commonly accepted that under the high vacuum conditions, the only factor determining the electron current flow in the vacuum diode with an explosive-emission plasma cathode is the throughput of a vacuum gap [1, 2]. The throughput is determined by the Child-Langmuir law (which is also known as the law of three second degree). However, nowadays, there are a lot of technical applications of electron beams travelling through the vacuum of low quality [3, 4]. If the diode is operated under pressure about 10^{-1} Pa and higher (forevacuum), there are a lot of residual gas particles in an accelerating gap and in a drift space. These particles may be ionized by the emitted electrons. Earlier [5], the expansion of explosive-emission plasma front with the constant velocity of $2 \cdot 10^6$ cm/s and the initial radius of 10 μ m was considered in the hemispherical forevacuum diode within the zero initial electron velocity assumption using the 1D-3V PIC-MCC technique. It was shown that the presence of the residual gas at the pressure of more than 1 Pa led to significant growth of the plasma-emission electron current for a constant diode voltage of 50 kV. But in [5] it was noted that the zero initial electron velocity assumption was rather crude since electrons were emitted from the plasma front with the velocity corresponding to the plasma temperature (several eV). Within the present work, the numerical model developed has been improved to take into account the finite velocities of plasma-emitted electrons. As a result of the simulation, volt-ampere characteristics of the explosive emission plasma cathode are presented for the plasma temperature range from 1 eV up to 5 eV. These data have been used in the model of the plasma expansion with the constant velocity in the hemispherical forevacuum diode. The comparison of new results with the ones obtained within the zero initial electron velocity assumption [5] is given. The dynamics of the plasma emission electron current is investigated within the residual gas pressure range from 10^{-1} Pa up to 10 Pa. The voltage applied to the forevacuum diode is varied from 10 kV up to 100 kV. The determination of the pressure and applied voltage magnitude ranges for which significant influence of residual gas ionization on the vacuum spark current was observed was carried out.

REFERENCES

- [1] G.A. Mesyats and D.I. Proskurovsky, *Pulsed Electrical Discharge in Vacuum*. Berlin: Springer, 1989.
- [2] G.A. Mesyats, *Cathode Phenomena in a Vacuum Discharge: The Breakdown, the Spark and the Arc*. Moscow: Nauka, 2000.
- [3] G.E. Ozur, D.I. Proskurovsky, V.P. Rotshtein, and A.B. Markov, "Production and application of low-energy, high-current electron beams," *Laser and Particle Beams*, vol. 21, no. 2, pp. 157–174, 2003.
- [4] I.Yu. Bakeev, A.S. Klimov, E.M. Oks, and A.A. Zenin, "Generation of high-power-density electron beams by a forevacuum-pressure plasma-cathode electron source," *Plasma Sourc. Sci. Tech.*, vol. 27, no. 7, 075002, 2018.
- [5] Y.I. Mamontov and I.V. Uimanov, "Dynamics of Forevacuum Spark Plasma Emitted Electrons and Influence of Residual Gas Ionization on a Forevacuum Spark Current," *Proc. 7th Int. Congress on Energy Flux. and Rad. Effects (EFRE)*, Tomsk, Russia, pp. 412–416, 2020.

* The work was supported in part by the RFBR Grants Nos. 20-38-90147 (Y.I. Mamontov), 19-08-00783 and 19-58-53006 (I.V. Uimanov).

NUMERICAL INVESTIGATION OF A HIGH-PRESSURE GAS MEDIUM PRE-IONIZATION BY RUNAWAY ELECTRONS*

V.V. LISEKOV^{1,2}, Y.I. MAMONTOV¹,

¹Institute of Electrophysics, UB, RAS, Yekaterinburg, Russia

²Ural Federal University, Yekaterinburg, Russia

e-mail: lisenkov@iep.uran.ru

The generation of runaway electron beams in high pressure gases, in particular, air, is one of the most interesting problems in gas discharge physics. The greatest success in the generation of runaway electrons at high pressure was achieved using nano- and subnanosecond accelerators [1]. In such a situation, the generation of runaway electrons and the formation of a gas discharge occur simultaneously in many cases. If the electrons transfer into the runaway mode in the near-cathode region, they can pre-ionize the interelectrode gap and convert the discharge into a multi-avalanche or volume form [2].

In this paper, a comparative simulation of the generation and acceleration of runaway electrons in the discharge gap during the initiation of the discharge by nanosecond and subnanosecond pulses is carried out. We used a numerical model based on the PIC-MCC method, described in detail in [2] and in the references in this paper. Calculations were carried out for N₂ 6 atm. pressure.

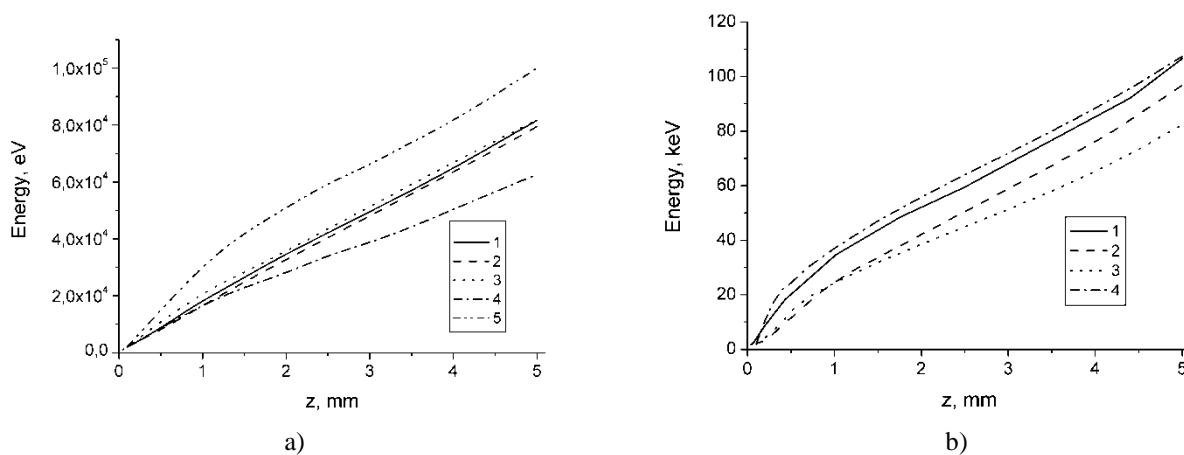


Fig. 1. Energy of runaway electrons vs distance from the cathode ($z=0$) ($z=5$ – anode) for nanosecond (a) and subnanosecond (b) pulses. Curves 1-3 in (a) and 1-2 in (b) – corresponds of different trajectories of runaway electrons calculated by PIC-MCC method. Curves 4 in (a) and 3 in (b) – trajectories calculated using equation in [3] with Bethe formula. Curves 5 in (a) and 4 in (b) – trajectories calculated using equation in [3] with real ionization cross section.

Fig. 1 shows the results of runaway electron acceleration modeling by PIC-MCC method. Fig. 1 (a) corresponds to nanosecond pulse [2]. Fig. 1 (b) corresponds to subnanosecond pulse [4]. Curves 1-3 in (a) and 1-2 in (b) – corresponds of different trajectories of runaway electrons. We compared our results with calculations using “traditional” differential equation of electron acceleration using braking force in Bethe approximation [3] (curves 4 in (a) and 3 in (b)). We solved this equation also for braking force based on real (experimental) ionization cross section (curves 5 in (a) and 4 in (b)).

The reasons for the discrepancy in the calculation results are discussed.

REFERENCES

- [1] G.A. Mesyats, M.I. Yalandin, A.G. Reutova, K.A. Sharypov, V.G. Shpak, and S.A. Shunailov. “Picosecond runaway electron beams in air” *Plasma Phys. Rep.*, vol. 38, pp. 29–45, 2012
- [2] S.N. Ivanov, V.V. Lisenkov, and Y.I. Mamontov. “Streak investigations of the dynamics of subnanosecond discharge developing in nitrogen at a pressure of 6 atmospheres with the participation of runaway electrons,” *Plasma Sourc. Sci. Tech.*, IN PRINT, doi: <https://doi.org/10.1088/1361-6595/abf31f>, 2021.
- [3] A.V. Gurevich, K.P. Zybin, “Runaway breakdown and electric discharges in thunderstorms,” *Phys. Usp.*, vol. 44, pp. 1119–1140, 2001.
- [4] S.N. Ivanov and V.V. Lisenkov, “Investigation of the prebreakdown stage of the self-sustained subnanosecond discharge in high pressure nitrogen,” *Journal of Applied Physics*, vol. 124, p. 103304, 2018.

* The work was supported in part by the RFBR Grant No. 20-08-00172.

SOME ISSUES OF THE OPERATION OF PLASMA OPENING SWITCHES*

S.V. LOGINOV

Institute of High Current Electronics, SB, RAS, Tomsk, Russia

e-mail: loginov@oit.hcei.tsc.ru

The main process that accompanies the penetration of a fast-rising magnetic field in a fully ionized plasma is the magnetization of electrons during the field rise. The magnetization time depends on the plasma resistivity. If the magnetization of electrons is faster than their collisions with ions, the plasma is collisionless and the depth of field penetration is limited by a value of the order of the collisionless electron skin layer [1]. In a collisional plasma, the depth of magnetic field penetration is determined by diffusion.

The conduction phase of a low-density plasma opening switch lasts for no more than ~100 ns. For such a switch, the magnetic field velocity is proportional to the square root of the field rise rate to plasma density ratio [2]. As the plasma density increases, the plasma gains substantial acceleration in the direction of field penetration. However, irrespective of the plasma density, the motion of electrons across a strong magnetic field occurs by their drift in crossed magnetic and polarization electric fields, which suppresses the current channel conductivity and makes it inversely proportional to the Hall parameter raised to the first or second power.

The motion of electrons off the cathode uncovers an ion sheath whose evolution to a space charge-limited ion flow needs a separate study at least for determining the actual ion to electron current ratio. In the analysis presented, the evolution of such a sheath is studied showing what extreme values of the ion current are possible at one or another plasma density and field rise rate. It is also shown that the ion sheath turns to the state of space charge-limited flow before its width becomes equal to the Larmor radius of electrons and that the charge transfer by ions is no greater than 5% of the total charge transfer.

The analysis demonstrates that for suppressed current channel conductivity with neglect of plasma acceleration, the energies expended in ohmic heating and magnetic field induction in the plasma volume are equal. Another outcome of the analysis is the possibility of estimating the electron temperature.

The applicability domain of estimates derived in the analysis is discussed. Their comparison with experimental data is presented.

REFERENCES

- [1] N.A. Krall and A.W. Trivelpiece, *Principles of Plasma Physics*. New York: McGraw-Hill, 1973.
- [2] S.V. Loginov, "Self-magnetic insulation in plasma opening switches," *J. Plasma Phys.*, vol. 86, p. 905860609 (11 pp.), 2020.

* The work was performed under State Assignment of the Ministry of Science and Higher Education of the Russian Federation (project No. FWRM-2021-0001).

INTERRELATION FORMS THE CHANNEL THE HIGH FREQUENCY TORCH DISCHARGE TO THE CHARACTERISTICS OF ITS ELEMENTS TO THE ELECTROMAGNETIC FIELD

Y.Y. LUTSENKO, A.E. MYUSOVA

Tomsk Polytechnic University, Tomsk, Russia

e-mail: aidanamyusova@yandex.ru

High-frequency torch discharge, excited at atmospheric pressure, is a plasma channel, surrounded by a low-luminous diffusion sheath. Burning of a torch discharge is carried out due to the dissipation of the energy of an electromagnetic wave propagating along the discharge channel. Therefore, the physical characteristics of the discharge substantially depend on the geometry of its channel. When a discharge is excited in different media, the shape of its channel changes, which in turn causes changes in the characteristics of electromagnetic field.

In the present study measured the axial distribution of the radial component amplitude of the intensity of the electric field torch discharge, burning of gases of different densities, and also analyzed the interaction bond forms a discharge channel with its electromagnetic field characteristics.

As a result of measurements it was found that in relatively heavy gases, such as nitrogen and argon, the attenuation of the electromagnetic field along the discharge channel is practically absent. Deficiency of attenuation of the electromagnetic field can be explained by the presence in the discharge channel [1] of the reflected electromagnetic wave. In this case, the shape of the discharge channel is close to conical. At the same time, when a discharge burns in light gases, a significant attenuation of the electromagnetic field is observed. The obtained results of measurements of the axial distribution of the electric field strength for helium and mixtures of helium with air and argon are shown in fig. 1.

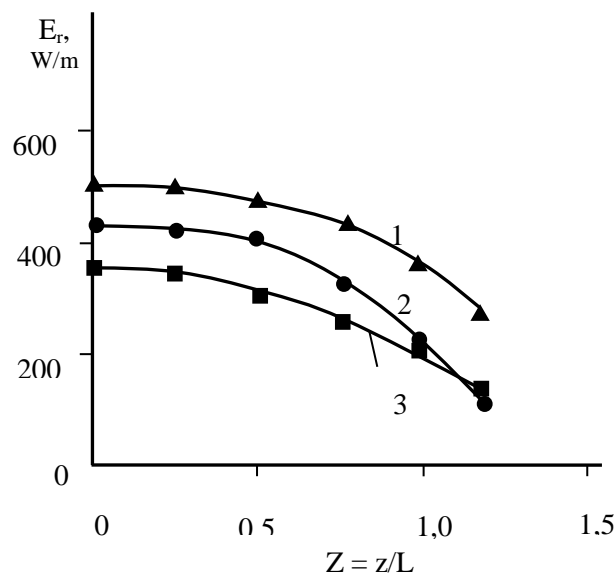


Fig. 1. The axial distribution of the electric field torch discharge channel with a length L. 1 - a mixture of air with helium; 2 - helium; 3 - a mixture of argon with helium.

As can be seen from the figure, the electric field strength of a torch discharge burning in helium decreases by half along its channel. The results indicate deficiency reflection of electromagnetic wave us in a helium discharge plasma, which in turn is due to a change in its shape of the channel.

REFERENCES

- [1] I.A. Tikhomirov, Yu.Yu. Lutsenko, "Interrelation characteristics of the geometry of the high frequency jet discharge and its electromagnetic field," Journal of Technical Physics, vol. 59, no. 11, pp. 128-130, 1989.

FEATURES OF THE IONIZATION WAVE DEVELOPMENT PRECEDING THE BREAKDOWN IN A LONG CAPILLARY TUBE SURROUNDED BY A CONTINUOUS OR SECTIONED ELECTRODE*

YU.S. AKISHEV^{1,2}, V.B. KARALNIK¹, A.V. PETRYAKOV¹

¹SRC RF TRINITI, Troitsk, Moscow, Russia

²NRNU MEPhI, Moscow, Russia

e-mail: petryakov@triniti.ru

The report presents the results on studies of the ionization wave propagation in a long capillary tube (length 250 mm, inner diameter 2.5 mm) filled with helium at a pressure of 10 Torr. A high-voltage electrode in the form of a hollow cylinder is placed inside the tube (Fig. 1), a grounded electrode (continuous or sectioned) is located on the outer surface of the tube. The sectioned electrode consists of 16 sections, each is grounded through a shunt resistor. Shunts are used to measure the ionization wave current collected by a single section. Figure 1 shows a sketch of the discharge tube with a sectioned external electrode.

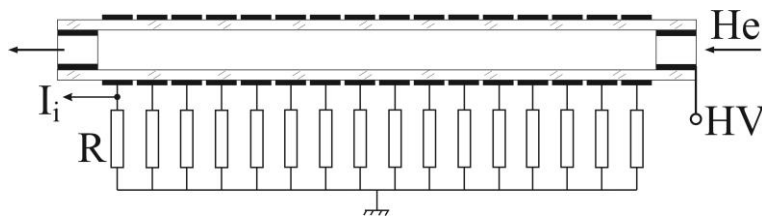


Fig. 1. Sketch of the experimental setup with a long capillary quartz tube. High Voltage electrode is located inside, sectioned grounded electrode outside (16 sections). R – current shunts.

Fig. 2a shows photographs of the ionization wave (IW) propagating along the tube with sectioned external electrode. Images were taken with high-speed ICCD camera PCO.dicam C4. The exposure time of each frame is 60 ns, the time delay between frames is 20 ns. Unlike the case with continuous outer electrode when the outer electrode is sectioned IW propagates in jumps with a noticeable deceleration before each gap between sections as can be seen in Fig. 2a. This effect is illustrated in Fig. 2b, which shows the glow profiles of the IW leading edge before and after passing the gap between adjacent sections. At the same time, the voltage at the high-voltage electrode remains practically constant (Fig. 2c), however, current oscillograms synchronized with the images show that before the IW jumps to the next section, the current in the previous section for a short time increases noticeably (Fig. 2.c). This effect is associated with an increase in conductivity at the front edge of the IW, leading to an increase in the potential difference between the preceding and subsequent sections and the acceleration of the IW (it "jumps" through the gap between the sections).

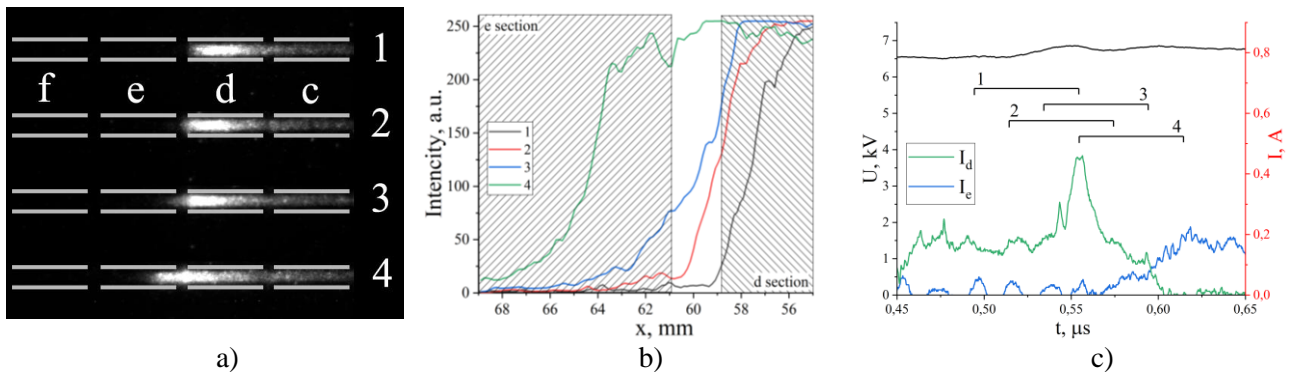


Fig. 2. a) Photographs of the ionization wave propagating along the tube, 1 – 4 – frame numbers, c – f – serial numbers of sections of the external electrode, b) propagation along the x-axis (measured from the high-voltage electrode) of the leading edge of the IW glow profile, 1 – 4 frame numbers, c) oscillograms of the voltage at the HV electrode and the current on the sections of the external electrode when the IW passes them 1 – 4 frame numbers.

* The work was supported in part by the RFBR Grant No 19-02-00288.

SPATIAL SPECTROSCOPY OF MAGNETRON DISCHARGE ARGON PLASMA USING A RADIATIVE-COLLISIONAL MODEL*

S.V. SERUSHKIN

Bauman Moscow State Technical University, Moscow, Russia

e-mail: ssv1988@mail.ru

The report presents a technique and results of an experimental study of a magnetron discharge based on argon plasma emission spectra. A hardware-software measuring complex for recording discharge plasma radiation with a high resolution is described.

For studies of magnetron plasma, a diagnostic complex based on the AvaSpec-2048 spectrophotometer is used, which allows automatic registration of radiation from various areas of the discharge, as well as its computer processing and analysis [1]. The spectral diagnostics technique is based on the registration of spectra with two-coordinate movement of the optical collimator in the plane perpendicular to the magnetron axis (see Fig. 1). In the experiment, the following parameters of the magnetron discharge were maintained: current $I = 0.32$ A, voltage $U = 400$ V, argon pressure in the vacuum chamber $P = 2$ Pa.

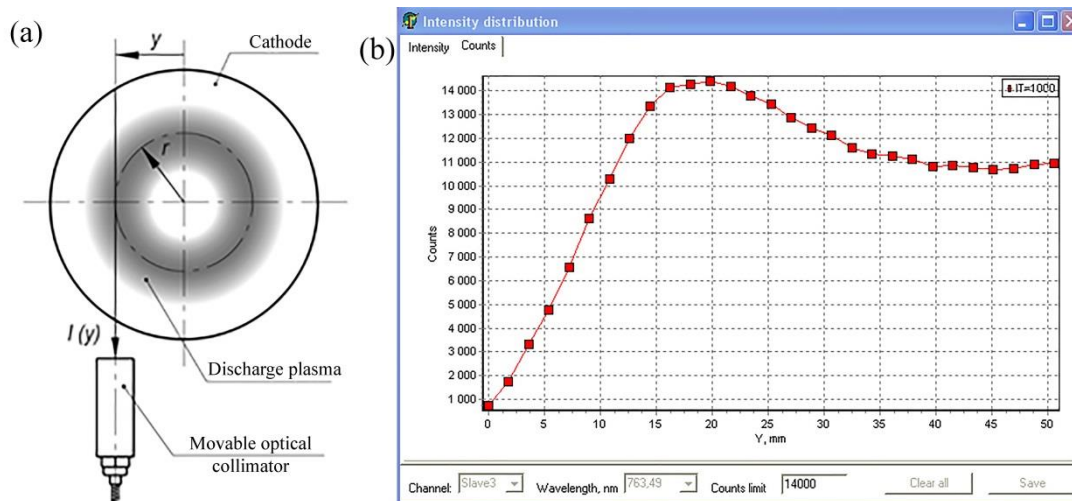


Fig. 1. (a) Schematic for capturing plasma radiation by collimator, and (b) spatial distribution of the spectral line emission intensity along the observation chords.

The obtained distributions of the spectral lines intensities of Ar atoms in the near-infrared spectral range were used to calculate the electron temperatures in different regions of the discharge. For this, an analysis of electron-impact excitation processes and spontaneous emitting transitions was applied according to the plasma radiative-collisional model with allowance for metastable levels [2, 3]. Electron energy distribution function was considered to be both Maxwellian and non-Maxwellian [4]. As a result, the electron temperature chordal distributions were determined, which, due to the cylindrical symmetry, can be recalculated into radial distributions in various discharge cross sections using the integral Abel transform.

REFERENCES

- [1] V.M. Gradov, A.M. Zimin, S.V. Serushkin, I.A. Zemtsov, "Determination of spatial distributions of plasma parameters of a compact magnetron discharge," *Physics of Atomic Nuclei*, vol. 82, pp. 1376-1381, 2019.
- [2] K.E. Evdokimov, M.E. Konischev, V.F. Pichugin, Z. Sun, "Study of argon ions density and electron temperature and density in magnetron plasma by optical emission spectroscopy and collisional-radiative model," *Resource-Efficient Technologies*, vol. 3, pp. 187-193, 2017.
- [3] X.-M. Zhu, Y.-K. Pu, "Optical emission spectroscopy in low-temperature plasmas containing argon and nitrogen: determination of the electron temperature and density by the line-ratio method," *J. Phys. D*, vol. 43, 403001 (24 pp), 2010.
- [4] X.-M. Zhu, Y.-K. Pu, Y. Celik, S. Siepa, E. Schungel, D. Luggenholcher, U. Czarnetzki, "Possibilities of determining non-Maxwellian EEDFs from the OES line-ratios in low-pressure capacitive and inductive plasmas containing argon and krypton," *Plasma Sources Sci. Technol.*, vol. 21, 024003 (11 pp), 2012.

* The work was supported by the RFBR Grant № 18-29-21039.

FEATURES OF PLASMA SUSTAINING IN A LARGE-VOLUME HOLLOW ANODE*

N.V. LANDL, Y.D. KOROLEV, I.V. LOPATIN, S.S. KOVALSKY, V.S. KASYANOV, V.O. NEKHOROSHEV

Institute of High Current Electronics, SB, RAS, Tomsk, Russia

e-mail: landl@inp.hcei.tsc.ru

Nowadays, glow discharge plasma sustained in large-volume hollow electrodes is widely used for material surface modification [1-5]. Depending on the composition of the modified layer, the plasma in the cavity can be either a plasma of negative glow or a plasma of a positive column. In a later case for plasma sustaining in the hollow anode the "PINK" plasma generator with combined hollow and thermionic cathode is often used [1, 2, 4].

One of the problems arising during the processing of a part with large dimensions or several parts of a small size is the non-uniformity of surface modification over the part area. This is because most plasma generators have cylindrical or conical cathodes with a diameter of 50-150 mm. As a result, the plasma in the anode cavity has a large density gradient in the direction from the outlet of the plasma generator to the chamber walls [6]. Usually this problem is solved by planetary rotation of parts and installation of several plasma generators.

On the other hand, the efficiency and uniformity of the surface treatment is usually estimated by the plasma density distribution within the chamber. In this case, the required plasma density determines the discharge parameters, such as the heating current of the thermionic cathode, the discharge burning voltage and discharge current. Therefore, the estimation of the plasma density in a large-volume cavity is an important task.

In our recent work [7], a model was proposed that describes the mechanisms of current passage in a glow discharge with a combined hollow and thermionic cathode and a large-volume hollow anode. The main idea of the approach was that the discharge current at the anode is carried not only by electrons, but also by ions from the plasma of the positive column. Despite the good agreement between the estimates of the plasma parameters of the positive column and experiment, this approach had a serious drawback. It was assumed that the plasma density inside the hollow anode is uniformly distributed.

The aim of this work is to develop the approach that we proposed earlier for describing the mechanisms of maintaining plasma in a large-volume hollow anode, taking into account the non-uniform distribution of the plasma density in it. Based on the model, the parameters of the plasma in the anode cavity are estimated and the data obtained are compared with the experiment.

REFERENCES

- [1] Y.D. Korolev and N.N. Koval, "Low-pressure discharges with hollow cathode and hollow anode and their applications," *J. Phys. D: Appl. Phys.*, vol.51, Article Number 323001, 2018.
- [2] I.V. Lopatin, Y.H. Akhmadeev, N.N. Koval, "Effect of thermionic cathode heating current self-magnetic field on gaseous plasma generator characteristics", *Rev. Sci. Instrum.* vol. 86, 103301, 2015
- [3] N.N. Koval, Y.F. Ivanov, I.V. Lopatin, Y.H. Akhmadeev, V.V. Shugurov, O.V. Krysina, V.V. Denisov, "Generation of low-temperature gas discharge plasma in large vacuum volumes for plasma chemical processes", *Russian Journal of General Chemistry*, vol. 85, p. 1326, 2015
- [4] N.V. Landl, Y.D. Korolev, V.G. Geyman et al., "The Regimes for Sustaining a Hollow-Cathode Glow Discharge with a Hot Filament Inside the Cavity", *Russ Phys J*, vol.62, no.11, pp. 2024-2032, 2020
- [5] V.V. Denisov, Yu.H. Akhmadeev, N.N. Koval, S.S. Kovalsky, I.V. Lopatin et.al, "The source of volume beam-plasma formations based on a high-current non-self-sustained glow discharge with a large hollow cathode, *Physics of Plasmas*, vol. 26, no. 12, Article Number 123510, 2019
- [6] L.G. Vintzenko, S.V. Grigoriev, N.N. Koval, V.S. Tolkachev, I.V. Lopatin, and P.M. Schanin, "Hollow-cathode low-pressure arc discharges and their application in plasma generators and chargedparticle sources", *Russ Phys J*, vol. 44, no. 9, pp. 927-936, 2001
- [7] N.V. Landl, Y.D. Korolev, V.G. Geyman, I.V. Lopatin, O.V. Krysina, O.B. Frans, G.A. Argunov, "Plasma maintenance mechanisms in large-volume hollow anode", *Russ Phys J*, vol.63, no.10, pp. 1766-1772, 2021

* This work was funded by RFBR according to the research project № 19-08-0032

GENERATION OF A PLASMA OF A NON-SELF-SUSTAINING GLOW DISCHARGE AT LOW PRESSURE INSIDE LONG CAVITIES*

D.Y. IGNATOV, S.S. KOVALSKY, I.V. LOPATIN

Institute of High Current Electronics, SB, RAS, Tomsk, Russia

e-mail: danilabay29@ya.ru

Plasma generation at low pressure (up to 1000 Pa) along the entire cavity of long metal products is the most difficult technological problem. A method was proposed for generating plasma in a metal tube [1] using a non-self-sustaining glow discharge with additional external injection of electrons from the auxiliary discharge plasma at a pressure of 1 Pa. The research results showed the possibility of such a system to heat the walls of pipelines of various shapes with a uniformity of up to $\pm 5\%$ and to perform their ion-plasma treatment with a uniformity of the nitrated layer thickness along the entire length up to $\pm 10\%$ of the average value.

This paper [2] presents the results of studying the effect of the parameters of a non-self-sustaining glow discharge on the degree of inhomogeneity of the generated plasma inside a hollow cathode, at a glow discharge voltage of up to 250 V. Inside a tube with a length of 300 mm and an inner diameter of 25 mm, a degree of inhomogeneity of the generated plasma of 11.5% can be achieved. at an average ion current density of 13 mA/m^2 due to multiple oscillations in the hollow cathode, mainly due to electrons injected from the auxiliary discharge plasma.

This work is a continuation of the study of a non-self-sustaining glow discharge plasma generated in a long metal cavity. Plasma parameters were investigated using five double probes installed along the cavity. An automatic system for measuring the probe parameters was used to measure the VAC characteristic of the double probe.

REFERENCES

- [1] D. Y. Ignatov, I. V. Lopatin, V. V. Denisov, N. N. Koval and Y. H. Ahmadeev, "Generation of Plasma in Non-Self-Sustained Glow Discharge With Hollow Cathode for Nitriding Inner Surfaces of Elongated and Complex Shaped Cavities", *IEEE Trans. Plasma Sci.*, vol. 48, no. 6, pp. 2050-2059, 2020.
- [2] D. Y. Ignatov, I. V. Lopatin, N. N. Koval, V. V. Denisov "Influence of Parameters of a Non-self-sustaining Glow Discharge with an Elongated Hollow Cathode on the Degree of Inhomogeneity of the Generated Plasma", *IEEE: 2020 7th International Congress on Energy Fluxes and Radiation Effects (EFRE)*, 2020.

* The work was supported by the Basic Research Project of State Assignments of the Ministry of Science and Higher Education of the Russian Federation № 0291-2019-0002.

INFLUENCE OF MOLECULAR OXYGEN ON ENERGY CHARACTERISTICS OF A GAS DISCHARGE OF ATMOSPHERIC PRESSURE IN AIR WITH ADDITION OF CARBON OXIDE

V.V. OSIPOV, A.N. ORLOV, V.V. LISENKOV, S.M. ARMYNINOV

Institute of Electrophysics, UB, RAS, Yekaterinburg, Russia

e-mail: orlov@iep.uran.ru

When atmospheric air is used as a gas mixture of a TEA CO₂ laser, a very serious problem associated with the difficulty of igniting a glow discharge in atmospheric air due to the presence of oxygen in it arises. In addition, the absence of helium in the gas mixture by more than an order of magnitude reduces the relaxation rate of the CO₂ (010) level, which ultimately leads to an additional population of the lower laser level and a decrease in the CO₂ laser efficiency. However, as shown in [1], even in the absence of helium and the presence of a large amount of molecular oxygen, a glow gas discharge can be ignited at atmospheric pressure. With an efficiency of 0.4%, the output energy of the LVS-1 laser was 400 mJ.



Fig. 1. TEA CO₂ laser LVS-2.

This paper presents theoretical calculations and experimental data on the effect of different concentrations of molecular oxygen on the uniformity of a glow discharge and changes in its parameters in a repetitively pulsed mode of operation. Experimental studies of the characteristics of a glow discharge in atmospheric air with the addition of carbon dioxide were carried out using an LVS-2 pulse-periodic gas-discharge laser [see Fig. 1].

The necessary data for calculating the energy characteristics of the discharge are the constants of plasma-chemical reactions with the participation of electrons, such as excitation, ionization, and dissociative attachment. Their values depend on the electric field in the discharge gap. We calculated these dependencies using the Monte Carlo method. The calculation results show that the curves of the dissociative attachment frequencies depending on the electric field strength are practically similar when the CO₂ fraction changes from 0.1 to 0.45. This is because of dissociative attachment to oxygen is significantly higher than to CO₂. Therefore, an increase in the CO₂ fraction from 0.1 to 0.45 almost exactly compensates for a decrease in the O₂ fraction, respectively, from 0.18 to 0.11. This creates practically equal conditions for energy input in a wide range of CO₂ concentrations.

REFERENCES

- [1] V.V. Osipov, A.N. Orlov, S.M. Belkov, I.I. Belyakov, A.V. Bochkov, L.E. Magda, I.V. Kasyanov, "Electric-discharge laser on an air mixture with carbon dioxide", *Instruments and experimental techniques*, No. 6, pp. 132-133, 2019

SIMULATION OF NEGATIVE CORONA DISCHARGE IN ATMOSPHERIC AIR: FROM MODE OF TRICHEL PULSES TO STATIONARY DISCHARGE*

A.O. KOKOVIN, A.V. KOZYREV, V.Y. KOZHEVNIKOV

Institute of High Current Electronics, SB, RAS, Tomsk, Russia
e-mail: alexander.kokovin.desch@gmail.com

Corona discharge in atmospheric-pressure air is a specific type of self-sustained stable discharge. The specific feature of the corona discharge is that, for its formation, it sufficient to apply high voltage to the electrode with a small radius of curvature. However, there is a range of applied voltage value, at which the corona discharge has an unstable mode [1]. The Trichel pulse mode was studied both experimentally [2] and theoretically [3], but there is still no complete understanding of the process. In this paper, a new two-dimensional numerical model of negative corona discharge in atmospheric air is presented.

We use a gas discharge model, based on the two-moment drift-diffusion hydrodynamic time-dependent model including two continuity equations for the electron component (density & mean energy) and a number of ion continuity equations. The transport equations are coupled to the Poisson's equation in order to take into account the electric field self-consistently. The gas discharge diode represents the tip-to-plate structure with small radius of curvature. To consider the most important reactions in the atmospheric air (production of single charged ions including photoionization, ions recharging, important conversion reactions, various electron energy losses) the simplified plasma-chemical reaction set is implemented in the model. The calculations are performed using the COMSOL Multiphysics software.

We investigated the modes of corona discharge for a pin-to-plane gap of 1 cm, the radius of the tip apex was 12, 30 or 100 μm , the gap voltage was from 8 to 100 kV.

Numerical calculations have been shown that the negative ion cloud triggers the Trichel pulse process. Photoionization and detachment processes play important roles in formation of the pulses. The results confirm that the amplitude of the first Trichel pulse is several times larger than that of subsequent pulses and the frequency of the Trichel pulses increases as the applied voltage is increased.

The study showed that the Trichel pulse sequence over time builds up a plasma background leading to the formation of a stationary discharge.

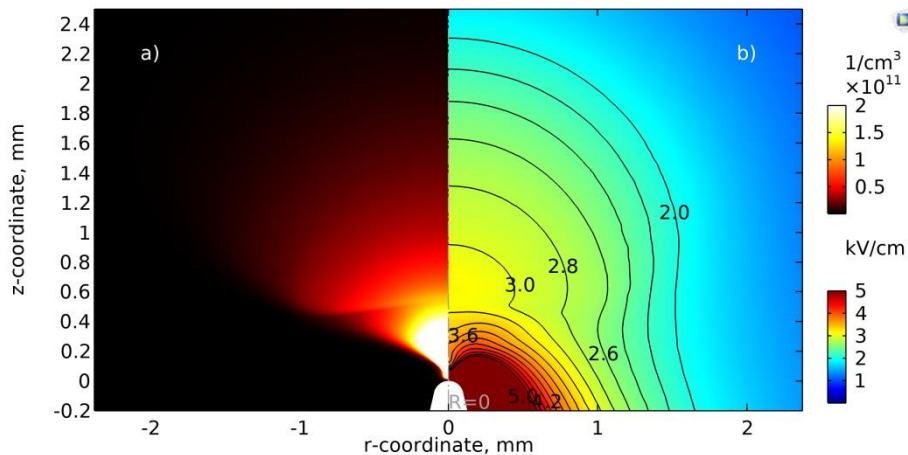


Fig. 1. Spatial distributions of negative number density ions (left), and electric field strength (right).

REFERENCES

- [1] G.W. Trichel, "The mechanism of the negative point to plane corona near onset," *Phys. Rev.*, vol. 54, pp. 1078, 1938.
- [2] V.F. Tarasenko, E.K. Baksht, E.A. Sosnin, et al. "Characteristics of a Pulse-Periodic Corona Discharge in Atmospheric Air," *Plasma Phys. Rep.* vol. 44, pp. 520–532, 2018.
- [3] P. Sattari, G.S.P. Castle and K. Adamiak, "Numerical Simulation of Trichel Pulses in a Negative Corona Discharge in Air," in *IEEE Transactions on Industry Applications*, vol. 47, no. 4, pp. 1935-1943, 2011.

* The work was carried out within the framework of the state assignment of the Ministry of Science and Higher Education of the Russian Federation on the topics FWRM-2021-0007, FWRM-2021-0014.

THE PROBLEM OF "ANOMALOUS" ION TRANSPORT IN HIGH-CURRENT VACUUM DISCHARGES*

V.Y. KOZHEVNIKOV, A.V. KOZYREV, A.O. KOKOVIN

Institute of High Current Electronics, SB, RAS, Tomsk, Russia

e-mail: Vasily.Y.Kozhevnikov@ieec.org

The studying of vacuum arcs and vacuum discharges cover wide areas of applied physics from the development of vacuum interrupters to the arcing in fusion devices and onboard satellite systems [1]. In high-current vacuum diodes, the discharge's initial phase is the formation of a vacuum breakdown due to the plasma inflow to the gap. Ions are mainly originating from metal electrodes and the dominating physical mechanism here is an explosive emission from cathode [2]. Further dynamics of the vacuum discharge is determined by the dense plasma extension into interelectrode gap. According to the available experimental data, the plasma flow from cathode to anode is sufficiently fast. Such motion is possible when metal ions move towards anode. We conventionally call this form of ion transport "anomalous". In this paper, the phenomenon of "anomalous" ion transport is investigated from a standpoint of physical kinetics.

We use an original theoretical model of a planar one-dimensional vacuum diode with boundary conditions simulating continuous emission of ions and electrons from the cathode surface into the initially empty interelectrode gap. For simplicity reasons we consider only electrons and single-charged ions are considered. Their dynamics is described by two collisionless kinetic equations, respectively. The mathematical model is complemented by the Poisson's equation in order to account the electrostatic field change self-consistently [3].

Numerical calculations have been shown that on the initial stage, due to steady emission the anode-directed quasineutral plasma flow forms the negative potential region (virtual cathode) near the cathode. Due to the virtual cathode voltage drop ions accelerate to anode. Plasma fills the gap between real and virtual cathode by forming there a quasi-neutral plasma region. Since electrons are still moving to anode, this leads to the displacement of virtual cathode. This, in turn, leads to further ions advancement towards anode and to corresponding prolongation of quasineutral dense plasma region. It is important that the effect of "anomalous" ion transport is theoretically shown regardless of the discharge gap geometrical peculiarities or the ionization of cathode metal atoms.

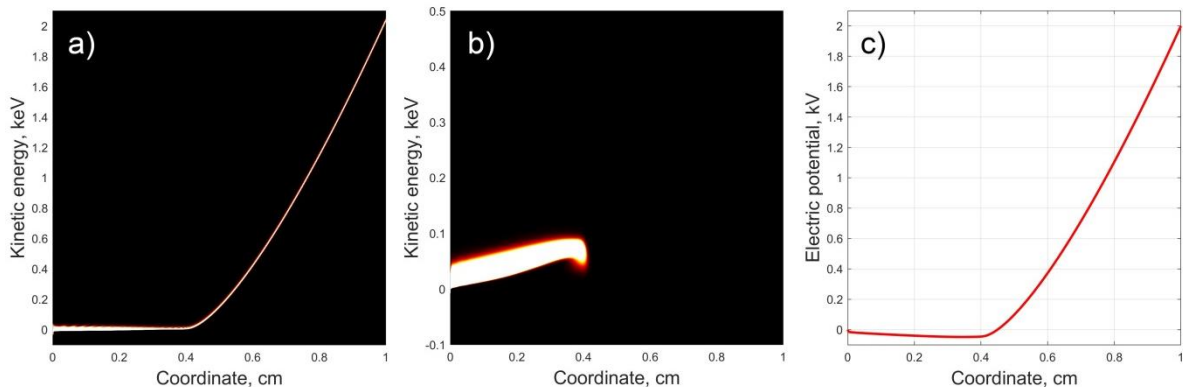


Fig. 1. Density plots of the electron a) and ion b) distribution functions and corresponding electrostatic potential distribution c).

REFERENCES

- [1] S. Anders, A. Anders, and I. Brown, "Vacuum arc ion sources: Some vacuum arc basics and recent results (invited)," *Review of Scientific Instruments*, vol. 65, no. 4, pp. 1253–1258, 1994.
- [2] G.A. Mesyats, *Pulsed Power and Electronics*, Moscow: Nauka, 2004.
- [3] A. Kozyrev, V. Kozhevnikov, and N. Semeniuk, "Kinetic theory of high-voltage low-pressure gas discharge with electron initiation on a cathode in a planar gap," *Plasma Sources Science and Technology*, vol. 29, no. 12, p. 125023, 2020.

* The work was carried out within the framework of the state assignment of the Ministry of Science and Higher Education of the Russian Federation on the topics FWRM-2021-0007, FWRM-2021-0014.

“ELECTRICAL WIND” IN CO₂-LASER MIXTURES AT SUPERATMOSPHERIC PRESSURES

B.A. KOZLOV¹, D.S. MAKHANKO²

¹*Ryazan State Radio Engineering University, Ryazan, Russia*

²*PLASMA, JSC Research Institute of Gas-Discharge Devices, Ryazan, Russia*
e-mail: kozlov.qe.ryazan@mail.ru

The problem of creating small-sized sealed-off CO₂ lasers of superatmospheric pressure operating in the pulse-periodical regime is largely related to the method used for pumping gas mixtures through the discharge gap. The most acceptable method of pumping gases in small volumes is "electrical wind". At atmospheric pressure the "electrical wind" provides pulse repetition rates of 20-50 Hz in TEA-CO₂ lasers [1, 2].

The properties of the "electrical wind" at pressures of 1 atmosphere have been studied quite fully to date. For superatmospheric pressures such information is completely absent.

The aim of this work is to investigate the current-voltage characteristics of unipolar corona discharges and the dependences of the "electrical wind" velocities on the corona discharge currents in CO₂-laser mixtures in the pressure range of 1-12 atmospheres.

Experimental investigations were carried out in a cylindrical chamber (diameter 100 mm, length 300 mm) made of stainless steel. In the discharge chamber electrode systems were installed to ignite corona discharges of positive and negative polarities. We used the electrode systems such as "a set of needles – grid", "thread – grid", "blade - grid", "thread – two cylinders", "tip – ring". The size of the "anode-cathode" gap varied from 2 to 8 mm. The dynamic pressure sensor was located at a distance of 2 cm behind the non-crowning electrode. "Electrical wind" velocity was determined according to the measured values of dynamic pressure in the gas flow. To determine the velocity the next formula was used:

$$V_{EW} = \sqrt{\frac{2 \cdot \rho_1 \cdot g \cdot \Delta H}{\rho_2}}, \quad (1)$$

where ρ_1 – liquid density of vacuum oil in gas-dynamic sensor; ρ_2 – density of gas mixture; g - free fall acceleration; ΔH – pressure drop in gas-dynamic sensor.

CO₂:N₂:He mixtures were used in the ratios from 1:1:1 to 1:1:8. Measurements of the current-voltage characteristics of the corona discharge in these mixtures showed a linear increase in the corona discharge voltages with pressure.

The dependencies of the corona discharge current on the voltage increases as the voltage across the gap increases and there is a clear tendency for the current to decrease with increasing pressure.

Measurements of the "electrical wind" velocity showed that its value does not depend on the pressure and the maximum velocity at total pressures up to 12 atmospheres reach 3-3.5 m•s⁻¹.

REFERENCES

- [1] B.A. Kozlov, V.I. Solovyov, "Formation of gas flows in a active media of small-sized sealed-off TEA-lasers by an "electrical wind",” Proceedings of SPIE, Vol. 3574, pp. 519–525, 1998.
- [2] Quang Manh Do, B.A. Kozlov, The Nguyen Mai, A. Ya. Payurov, A. B. Yastrebkov, "Super-atmospheric pressure CO₂-lasers with duration of radiation pulses less than 10 nanoseconds and pulse repetition rates up to 20 Hz", Proceedings of SPIE, Vol. 11322 113220I-1, pp. 1-11, 2019.

FORMATION OF VOLUME DISCHARGES IN DENSE GASES AT PULSE REPETITION RATES UP TO 10 kHz

B.A. KOZLOV

Ryazan State Radio Engineering University, Ryazan, Russia
e-mail: kozlov.qe.ryazan@mail.ru

This work is devoted to determining of the conditions for the formation of volume discharges in CO₂:N₂:He -, N₂:He - and Xe-He - laser mixtures at atmospheric pressure at pulse repetition frequencies from 1 to 10 kHz.

Knowledge of the regularities self- sustained volume discharges ignition at pulse repetition rates of more than 1 kHz (up to 20 kHz) makes it possible to create TEA-lasers with an increased level of average radiation power. TEA lasers with a high pulse repetition rates with a relatively small values of radiation energy per pulse and radiation pulse durations of 10-20 nanoseconds are a new technological tool.

The main constraining factor to the creation of TEA-lasers with an increased pulse repetition rate is the localization of the volume discharge under the influence of many factors [1]. The analytical expression obtained in [2] for the limit value of the ignition frequency of the volume discharges in dense gases indicates the feasibility of partitioning the discharge gap and exciting the volume discharges in each section from an autonomous pulse generator.

Natural partitioning of the gas-discharge gap takes place in electrode structures of the "tip-plane" type (a set of tips – plane) with individual decoupling using resistors or capacitors. In this case it is possible to use only one pulse generator.

Experimental investigates were carried out on a gas-discharge structure formed by a set of tungsten rods with a diameter of 1 mm and a profiled monolithic copper anode. The rods were installed at intervals of 1 cm at a length of 24 cm. The gas-discharge with interelectrode gap 1.2-2 cm was blown by a gas stream at a velocity of up to 50 m•s⁻¹.

High-voltage pulses were generated using a two-stage Marx generator with thyratrons TGI1-1000/25 as switches.

The main results of the research:

- to stabilize of the discharge current parameters it is necessary to carry out preliminary ionization of gases;
- volume discharges with the energy density of 100-120 mJ•cm⁻³ at pulse repetition frequencies up to 8 kHz are implemented in CO₂-laser mixtures;
- volume discharges in N₂:He - and Xe-He - laser mixtures with energy densities of 80 and 60 mJ•cm⁻³ are implemented at pulse repetition frequencies up to 10 kHz.

REFERENCES

- [1] V.Yu. Khomich, V.A. Yamschikov, Foundations of electro-discharge excitation systems for CO₂-, N₂- and F₂-lasers. Moscow: Fizmatlit, 2015.
- [2] B.A. Kozlov, A limit value of the volume discharge ignition frequency in dense gases, Journal of Physics: Conference Series 1393 012009 pp. 1-8, 2019.

ELECTRIC EXPLOSION OF FLAT COPPER CONDUCTORS IN ASYMMETRIC AND SYMMETRIC CONFIGURATIONS IN THE CURRENT SKINNING MODE*

N.A. LABETSKAYA¹, I.M. DATSKO¹, S.A. CHAIKOVSKY^{1,2}, V.A. VAN'KEVICH¹, E.V. ORESHKIN³, V.I. ORESHKIN¹

¹Institute of High Current Electronics, SB, RAS, Tomsk, Russia

²Institute of Electrophysics, UB, RAS, Yekaterinburg, Russia

³Lebedev Physical Institute, RAS, Moscow, Russia

e-mail: natalia@ovpe2.hcei.tsc.ru

Plasma formation on the surface of conductors as a result of a skin explosion is one of the key issues of the efficiency of energy transportation along the vacuum lines of powerful terawatt-level pulse generators. Non-thermal processes, such as gas-discharge phenomena in desorbed gas or metal vapors, can significantly reduce the magnitude of the magnetic field at which a low-temperature plasma is formed on the surface of the conductor. Experimental studies of plasma formation on the surface of flat conductors were carried out on the MIG generator at a current level of up to 2.5 MA and a rise time of 100 ns. The magnitude of the peak magnetic field induction exceeded the values required for the explosion of the conductor surface facing the magnetic field in an asymmetric configuration or both surfaces of the conductor in a symmetric configuration. The formation of plasma on the surface of the conductor was recorded by its self-emission in the visible range using a four-frame optical camera with an exposure time of 3 ns. It was shown that in both configurations, a plasma channel is formed on the surface of a copper foil with a thickness of 100 microns along its longitudinal axis about 75 ns from the beginning of the current. The features of the formation of this channel on the parameters of the foil have been investigated. Experimental data on the dynamics of plasma formation at the edges of a flat conductor have been obtained. Magnetohydrodynamic simulations of the explosion of flat conductors in a symmetric configuration and their comparison with the experimental results have been performed.

* The work was supported by the Russian Science Foundation (grant No. 20-19-00364)

ARC DISCHARGES OPERATION IN "ELION" MODE*

I.V. LOPATIN, YU.H. AKHMADEEV, S.S. KOVALSKY, D.YU. IGNATOV

*Institute of High Current Electronics, SB, RAS, Tomsk, Russia
e-mail: lopatin@opee.hcei.tsc.ru*

The article presents the results of a study of the operation of a system for electron-ion-plasma alitization using two arc plasma generators: a gas plasma generator based on a non-self-sustaining arc discharge with a thermionic cathode and a gas-metal plasma generator based on an arc discharge with a cathode spot. The discharge power supply system and samples bias supply (Fig. 1) implies two modes of operation: the mode of ion samples cleaning (ion mode) and the mode of electron samples heating (electron mode). The sequential switching of power supplies (discharges and bias) to the main one anode (vacuum chamber walls) with a surface area of $\approx 20 \times 10^3 \text{ cm}^2$, or an auxiliary anode (sample holder) with a surface area of $\approx 200 \text{ cm}^2$ was performed for this. Thus, the "Elion" system operation mode was realized. In the course of the experiments, both the dependence of the discharges burning average values of currents and voltages on the conditions of discharge sustaining and probe measurements of plasma parameters instantaneous values in both system operating modes were investigated. It is shown that the electron mode of the system operation is characterized by an increased burning voltage, which is caused by the formation of a positive anodic drop in the plasma of more than 10 V. Such potential distribution in the discharges ensures the effective heating of the samples by the electron component of the discharge plasmas.

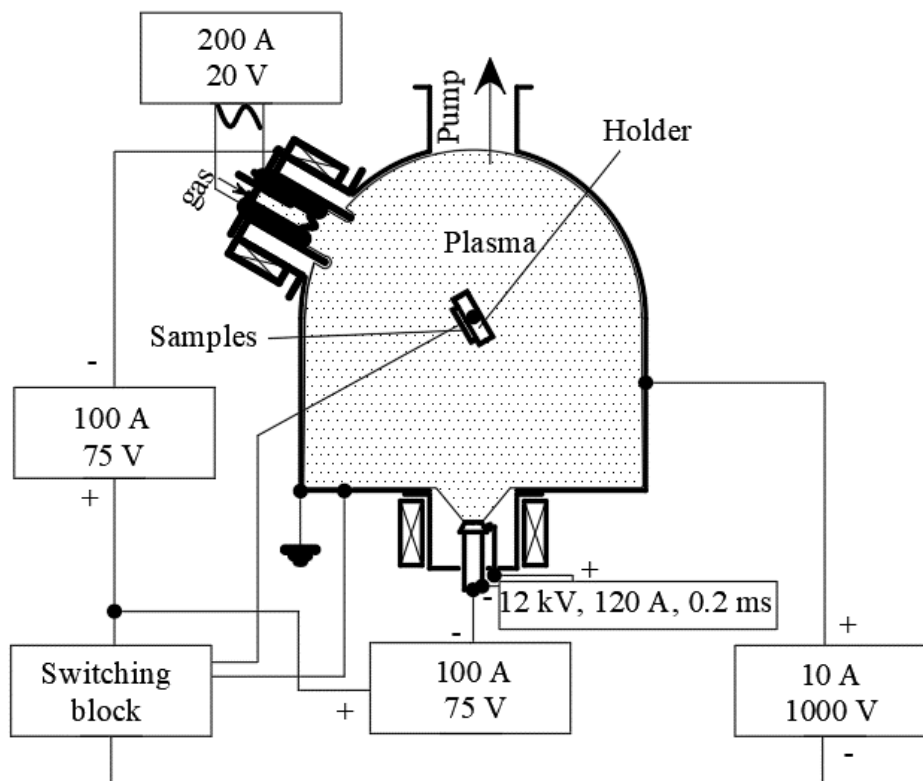


Fig. 1. Experiment scheme

* The work was supported by RSF project No. 20-21-00111.

TRAPPED RUNAWAY MODE OF ELECTRONS ACCELERATION AND IONIZATION PROCESSES IN PULSED DISCHARGE

M.M. TSVENOUKH

Lebedev Physical Institute, RAS, Moscow, Russia
e-mail: elley@list.ru, mmtsv@lebedev.ru

There are extensive studies of runaway electron beam (REB) generation in pulsed discharge, see Refs. 1-3. It is widely accepted that REB appearance could drastically change the discharge properties providing a tool for pulsed power devices [4, 5].

It was proposed that in non-uniform electric field enhanced by a plasma in streamer phase there are two groups of runaway electrons – passing and trapped ones [6], named similarly to particle moving in magnetic fields with mirrors. Passing electrons (of energy above several 100 s of eV [6,7]) can be continuously accelerated in runaway mode throughout whole gap and finally producing x-rays from the anode, whereas trapped ones are being absorbed in front of streamer head. (See recent detailed study in Ref. 8.)

However, the ionization cross section has a maximum at about the same electron energy $T \sim 100$ eV. This means that the acceleration of electrons up to a significantly higher kinetic energy T , including in the continuous runaway mode, is less favorable for ionization. Also at a weak field – electron impact ionization occurs only by electrons of sufficient energy – from the high-energy tail of their distribution function.

For the ionization cross-section for nitrogen taken as $\sigma(T) = \sigma_0 * 270 T \text{ eV} / [(T + 30 \text{ eV}) * (T + 120 \text{ eV})]$ (where $\sigma_0 \approx 3 * 10^{-16} \text{ cm}^2$ [9]) by Poisson equation one may estimate the plasma density $n_e(T)$ providing enhancement of electric field accelerating electrons up to energy T at the mean free path $\lambda(T) = 1/n\sigma(T)$:

$$n_e = T n^2 \sigma^2(T) / 4\pi e^2.$$

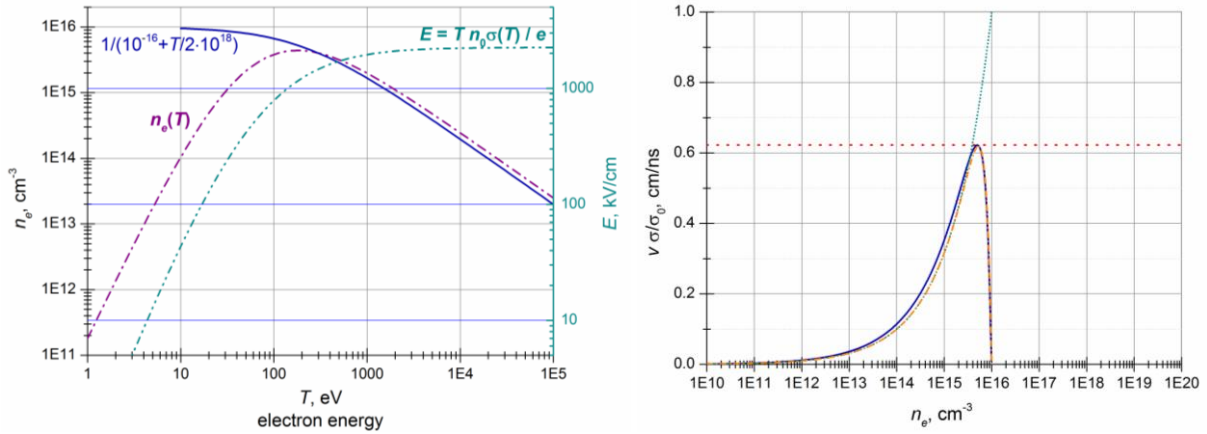


Fig. 1. (left) Plasma density n_e , providing the acceleration of electrons to the energy T at the mean free path length $\lambda(T)$, and the induced electric field, and (right) ionization rate $v\sigma$ versus plasma density n_e .

The ionization rate $v\sigma$ can be then estimated using approximate dependence of the electron energy from produced plasma density $T(n_e)$, see fig. 1. One may propose a simple estimation $v\sigma \approx 10 \sigma_0 n_e^{1/2} [1 - (n_e/10^{16} \text{ cm}^{-3})^3]$, which demonstrates that there is a maximum in the ionization rate at a certain density level (near plasma-oscillations dominated regime, see [10]), which provides acceleration of the electrons in trapped-runaway mode. This supports our proposition on importance of trapped-runaway electrons in gas discharge.

REFERENCES

- [1] Mesyats G.A. et al, 2020, Appl. Phys. Lett., 116, 063501.
- [2] Zubarev N.M. et al, 2020, Plasma Sources Sci. Technol., 29, 125008 .
- [3] Yalandin M.I. et al, 2020, Phys. Plasmas, 27, 103505.
- [4] Korolev Yu.D. and Mesyats G.A., Physics of Pulsed Breakdown in Gases. Ekaterinburg (URO-Press, 1998).
- [5] Mesyats G.A., Bychkov Yu.I., Kremnev V.V., 1972, Sov. Phys. Usp., 15, 282–297.
- [6] Kunhardt E.E. and Byszewsky W.W., 1980, Phys. Rev. A, 21, 2069.
- [7] Byszewski W.W. and Reinhold G., 1982, Phys. Rev. A, 26, 2826.
- [8] Zubarev N.M. et al., 2018, J. Phys. D: Appl. Phys., 51, 284003.
- [9] Smirnov B.M. "Physics of a weakly ionized gas" Nauka, Moscow, 1972.
- [10] Barengolts S.A., Mesyats G.A., Tsventoukh M.M. and Uimanov I.V., 2012, Appl. Phys. Lett., 100, 134102.

AVERAGE ION-CHARGE STATE AND EXPLOSIVE EMISSION PLASMA MOMENTUM DERIVATION FROM CRITICAL TEMPERATURE OF METAL*

M.M. TSVENOUKH

Lebedev Physical Institute, RAS, Moscow, Russia
e-mail: elley@list.ru, mmtsv@lebedev.ru

The parameters of the cathode spot plasma produced by explosive electron emission pulses [1, 2] have been estimated from the critical state properties for various materials [3]. The kinetic energy of the cathode plasma flare has been estimated as $100 T_{cr}$, where T_{cr} is the critical temperature of the cathode material [4]. Based on a Saha-like equation [5] and a two-temperature simulation of the explosion of a liquid-metal micro jet [2, 3], an estimation formula for the average ion charge has been derived, $Z_{av} = 1 + T_{cr}/eV$, which fits the available experimental data. This has made it possible to explain the linear relationship between average charge and kinetic energy obtained experimentally for the cathode plasma ions [6]. Using this formula, the previously derived expression for the plasma momentum per transferred charge μ [2] has been simplified to become $\mu \sim 5 (M_i/M_p)^{1/2} \text{ g cm}/(\text{s C})$, where M_i/M_p is the ion-to-proton mass ratio.

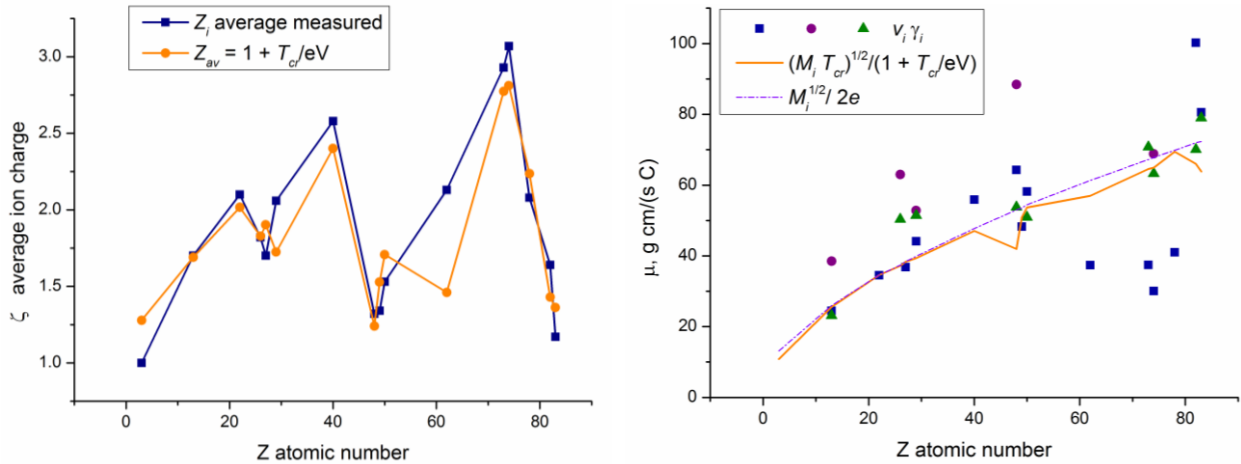


Fig. 1. Average ion charge measurements and estimates (left), and EEE plasma momentum per transferred charge: experimental values of $v_i \gamma_i$ and estimates by formulas $\mu = (M_i T_{cr})^{1/2} / e(1 + T_{cr}/eV)$ and $\mu = M_i^{1/2} / 2e$ (right).

The critical temperature values used here have been obtained by Acad. Prof. Vladimir E. Fortov [7] who left a legacy in physics of plasmas.

It is noteworthy that the charge state of plasma ions in a vacuum arc can be measured in detail, in contrast to the critical temperatures measured only for several metals, see [8]. This is due to the high energy density in such an extreme state of matter (temperature $\sim 1 \text{ eV}$, density $\sim 10^{22} \text{ cm}^{-3}$).

Thus, we can propose on contrary – to estimate the critical temperature for materials from the measured average charge of ions in vacuum arc cathode spot as $T_{cr} = 11594^\circ\text{K} \times (Z_{av} - 1)$.

REFERENCES

- [1] Mesyats G.A. and Tsvetoukh M.M., 2015, IEEE Trans. Plasma Sci. 43, 3320.
- [2] Tsvetoukh M.M., 2018, Phys Plasmas, 25, 053504.
- [3] Tsvetoukh M.M., 2021, Phys Plasmas, 28, 054501.
- [4] Fortov V.E., Yakubov I.T. and Khrapak A.G., Physics of Strongly Coupled Plasma (Oxford University Press, Oxford, UK, 2006).
- [5] Zeldovich Y.B. and Rayzer Y.P., 1967, Physics of Shock Waves and High Temperature Hydrodynamic Phenomena (New York: Academic).
- [6] Zhirkov I., Oks E. and Rosen J., 2015, J. Appl. Phys., 117, 093301.
- [7] Fortov V.E., Dreminev A.N., and Leont'ev A.A., 1975, Teplofiz. Vys. Temp., 13(5), 1072.
- [8] <https://rg.ru/2006/09/27/fortov.html>.

* The work was supported in part by the RFBR Grant No. 19-08-01249.

MODELING DC DISCHARGES: FROM TOWNSEND TO ARC MODE IN ATOMIC AND MOLECULAR GASES*

A.I. SAIFUTDINOV, B.A.TIMERKAEV, A.R.SOROKINA, A.A.SAIFUTDINOVA

Kazan National Research Technical University named after A.N.Tupolev, Kazan, Russia

e-mail: as.uav@bk.ru

The paper presents unified self-consistent discharge models based on an extended fluid description of plasma taking into account heating of electrodes, secondary electron emission, thermionic emission, and ablation of electrodes [1-4]. On the basis of the formulated models, numerical studies of atmospheric pressure discharges in atomic and molecular gases in one-dimensional [1, 2] and two-dimensional geometries [3] are carried out.

Various scenarios of the dependences of the voltage on the discharge on the current density for a one-dimensional geometry of the discharge and the current-voltage characteristics of the discharge for a two-dimensional geometry are presented, demonstrating the transition of the discharge from the Townsend mode through a normal glow discharge to the arc. The fundamental dependence of the plasma parameters on the cooling conditions of the electrodes is shown.

For the mode corresponding to the transition from the Townsend to a subnormal glow discharge, oscillations of current and voltage are analyzed depending on the electro-physical parameters of the discharge and the circuit.

For the transition from a glow discharge to an arc, two scenarios are presented: with the formation of a contracted current spot and with the formation of a diffuse current spot. In addition, the possibility of forming an arc discharge with a free cathode mode is shown for molecular gases.

For normal, anomalous, and arc discharges, the effect of ablation of metal electrodes [5] on the parameters of the discharge plasma is investigated.

Additional research has been carried out on the ablation of a germanium anode in an arc discharge.

REFERENCES

- [1] Saifutdinov A.I., "Unified simulation of different modes in atmospheric pressure DC discharges in nitrogen", *Journal of Applied Physics*, 129, 9, № 093302, 2021.
- [2] Saifutdinov A.I., Timerkaev B.A., Saifutdinova A.A., "Features of Transient Processes in DC Microdischarges in Molecular Gases: From a Glow Discharge to an Arc Discharge with a Unfree or Free Cathode Regime", *JETP Letters*, 112, 7, pp. 405-412, 2020.
- [3] Saifutdinov A.I., Fairushin I.I., Kashapov N.F., "Analysis of various scenarios of the behavior of voltage-current characteristics of direct-current microdischarges at atmospheric pressure", *JETP Letters*, 104, 2016.
- [4] Benilov M.S. "Modeling the physics of interaction of high-pressure arcs with their electrodes: advances and challenges", *J. Phys. D: Appl. Phys.*, 53, 013002, 2020.
- [5] Nielsen T., Kadani A. and Benilov M.S. "Model for arc cathode region in a wide pressure range", *J. Phys. D: Appl. Phys.*, 34, 2016-21, 2001.

* The study is supported by Russian Federation President's scholarship for young scientist's CII239.2021.1 and by the Russian Foundation for Basic Research, project 18-43-160005

DYNAMICS OF THE FORMATION AND CONTRACTION OF A MICROWAVE DISCHARGE AND FAST GAS HEATING IN NITROGEN

A.I. SAIFUTDINOV¹, E.V. KUSTOVA²

¹ *Kazan National Research Technical University named after A.N.Tupolev, Kazan, Russia*

² *Saint-Petersburg university, Saint-Petersburg, Russia*

e-mail: as.uav@bk.ru

The presented work is a development of research on the dynamics of the formation of a microwave discharge in a focusing device which demonstrates an efficient way of energy supplying to supersonic gas flows [1-3].

On the basis of the extended fluid-dynamic model, numerical experiments have been carried out in the two-dimensional approximation; plasma formation and growth in the active phase and the afterglow phase of the microwave discharge in nitrogen is studied for extended set of plasma-chemical reactions [3, 4, 5].

The dynamics of the constriction of a microwave discharge is investigated depending on the duration of the microwave pulse, as well as on the presence of small oxygen impurities in the buffer nitrogen.

The main channels of gas heating in the active phase and in the afterglow phase of the discharge are analyzed.

The developed self-consistent model and performed numerical experiments make it possible to describe in detail the dynamics of plasma formation in focused pulsed microwave discharges in real devices and facilities. The results represent an important stage in understanding the physics and mechanics of focused microwave discharges and can be used to simulate the interaction of a discharge with supersonic gas flows [1].

REFERENCES

- [1] V. A. Lashkov, A. G.Karpenko, R. S.Khoronzhuk, and I. Ch.Mashek, "Effect of Mach number on the efficiency of microwave energy deposition in supersonic Flow", *Physics of Plasmas*. 23, 052305, 2016.
- [2] A. I. Saifutdinov, E. V. Kustova, A. G. Karpenko , & V. A. Lashkov, "Dynamics of Focused Pulsed Microwave Discharge in Air", *Plasma Physics Reports*. 45, 6, 602-609, 2019.
- [3] A. I. Saifutdinov, E. V. Kustova, "Dynamics of plasma formation and gas heating in a focused-microwave discharge in nitrogen", *Journal of Applied Physics* 129, 023301, 2021.
- [4] N. A. Popov, "Investigation of the Mechanism for Rapid Heating of Nitrogen and Air in Gas Discharges", *Plasma Physics Reports*. 27, 886, 2001.
- [5] N. Popov, "Fast gas heating in a nitrogen–oxygen discharge plasma: I. kinetic mechanism", *Journal of Physics D: Applied Physics*. 44, 285201, 2011.

NUMERICAL STUDIES OF THE DYNAMICS OF A SURFACE BARRIER DISCHARGE IN MOLECULAR GASES AND GAS HEATING IN THE REGION OF THE DISCHARGE FORMATION*

A.A. SAIFUTDINOVA, B.A. TIMERKAEV, A.I. SAIFUTDINOV

Kazan National Research Technical University named after A.N. Tupolev, Kazan, Russia

e-mail: aliya_2007@list.ru

A self-consistent extended fluid-dynamic model describing a surface barrier discharge in a molecular gas is developed [1]. Extended fluid-dynamic model [2] includes k equations of chemical kinetics for the number densities of all mixture species (neutral, excited particles, electrons and ions), the equation for the electron energy density, the Poisson equation for self-consistent space-charge electric field in plasma, which in turn is related to the electric potential. To describe gas dynamic effects and gas heating, the model is supplemented by the Navier-Stokes equations, equation of the energy balance for heavy particles, and vibrational energy relaxation equation for molecules.

$$\frac{\partial n_k}{\partial t} + \nabla \cdot (-D_k \nabla n_k + z_k \mu_k \mathbf{E}_s n_k) + (\mathbf{u} \cdot \nabla) n_k = S_k \quad (1)$$

$$\frac{3}{2} \frac{\partial n_e}{\partial t} + \nabla \cdot (-D_e \nabla n_e + \mu_e \mathbf{E}_s n_e) + (\mathbf{u} \cdot \nabla) n_e = -e \mathbf{E}_s \cdot \Gamma_e + Q_{rh} - Q_{el} - Q_{in} - Q_{eV} \quad (2)$$

$$\Delta \varphi = -\frac{q_e}{\varepsilon_0} \left(\sum_{k=1}^N z_k n_k - n_e \right), \quad \mathbf{E}_s = -\nabla \varphi, \quad (3)$$

$$\frac{\partial(\rho h_h)}{\partial t} + \nabla \cdot (\rho h_h \mathbf{u}) - \nabla \cdot \left(\lambda \nabla T + \sum_k h_k \Gamma_k \right) - \frac{\partial p}{\partial t} - \hat{\tau} : \nabla \mathbf{u} = Q_{el} + Q_{electronic} + Q_{rec} + Q_{VT}, \quad (4)$$

$$\frac{\partial E_v}{\partial t} + \nabla \cdot (E_v \mathbf{u}) = Q_{eV} - Q_{VT}, \quad (5)$$

$$\frac{\partial \rho}{\partial t} + \nabla \cdot (\rho \mathbf{u}) = 0 \quad (6)$$

$$\frac{\partial(\rho \mathbf{u})}{\partial t} + (\rho \mathbf{u} \cdot \nabla) \mathbf{u} = -\nabla p + \nabla \cdot \hat{\tau} \quad \hat{\tau} = \mu \left(\nabla \mathbf{u} + (\nabla \mathbf{u})^T \right) - \frac{2}{3} \mu (\nabla \cdot \mathbf{u}) \hat{\mathbf{I}} \quad (7)$$

A detailed description of the model, functions and notation in the equations can be found in [1, 2].

Based on formulated model numerical simulations of the formation of surface barrier discharge in pure nitrogen [2] and air (for reduced and extended plasma-chemical sets) [1, 3, 4].

The effect of fast gas heating has been demonstrated, which can be used in aerodynamic applications, including for UAVs.

REFERENCES

- [1] A.A. Saifutdinova, B.A. Timerkaev, A.I. Saifutdinov, "Numerical Investigation of a Surface Barrier Discharge in Air at Atmospheric Pressure", Russian Physics Journal, 62 (11), pp. 2015-2019, 2020.
- [2] A.I. Saifutdinov, E.V. Kustova, "Dynamics of plasma formation and gas heating in a focused-microwave discharge in nitrogen", Journal of Applied Physics 129, 023301, 2021.
- [3] N.A. Popov, "Investigation of the Mechanism for Rapid Heating of Nitrogen and Air in Gas Discharges", Plasma Physics Reports. 27, 886, 2001.
- [4] N. Popov, "Fast gas heating in a nitrogen–oxygen discharge plasma: I. kinetic mechanism", Journal of Physics D: Applied Physics. 44, 285201, 2011.

* The study is supported by by the Russian Foundation for Basic Research, project [19-31-90101](#).

ON HYBRID TYPE OF CATHODE ATTACHMENT IN HIGH CURRENT VACUUM ARCS

D.L. SHMELEV, S.A. CHAIKOVSKY, I.V. UIMANOV

Institute of Electrophysics, UB, RAS, Ekaterinburg, Russia
 e-mail: shmelev@iep.uran.ru

This paper discusses the issues of a possible change of the type of cathode attachment of high-current vacuum arcs (HCVA) with an average cathode current density of more than 10^5 A/cm². This type of HCVA is used as pumping plasma gun in experiments with plasma puff z-pinches ([1] for example). These experiments showed that the measured linear mass of the HCVA plasma jet is much higher (by a factor of 10 or more) than the expected mass, which can be obtained from the assumption that cathode attachment occurs only through a multitude of cathode spots emitting supersonic plasma jets. A simple explanation for this discrepancy is the assumption that cathode spots are not the only type of cathode attachment in this case. Indeed, at an average current density at the cathode $> 10^5$ A/cm², less than 1% of the cathode surface is occupied by the cathode spots. But in HCVA, the cathode surface is heated under the influence of various heat fluxes, such as: the flux of ions from the plasma of the vacuum arc column, the flux of radiant energy from the plasma and heating from moving cathode spots. Under the influence of these heat fluxes in a discharge of sufficient duration, the cathode surface temperature can exceed the boiling point. After that, the cathode surface, not occupied by cathode spots, becomes an additional source of erosion for the HCVA jet. In addition, a thermionic current arises, which has a relatively low density, but due to the large cathode surface area makes a significant contribution to the total arc current (Fig. 1 a). Thus, in HCVA of the type under consideration, at some time instant there are two types of cathode attachments - cathode spots and thermionic erosion attachment (TEA). It can be said that HCVA of this type have a hybrid cathodic attachment. Unlike cathode spots, TEA produces a subsonic plasma flow, which contributes to an increase in the linear mass of the HCVA plasma jet.

In this paper, we discuss the emergence of a hybrid cathode attachment and carry out a self-consistent calculation of HCVA using the previously developed hybrid method [2].

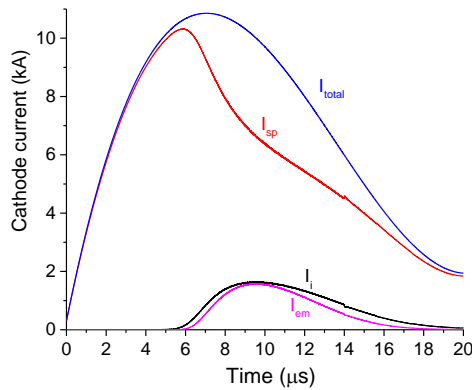


Fig. 1a. Current components at HCVA cathode. Total current (I_{total}), cathode spot current (I_{sp}), TEA ion current (I_i), TEA electron emission current (I_{em}). Cathode radius – 0.75 mm.

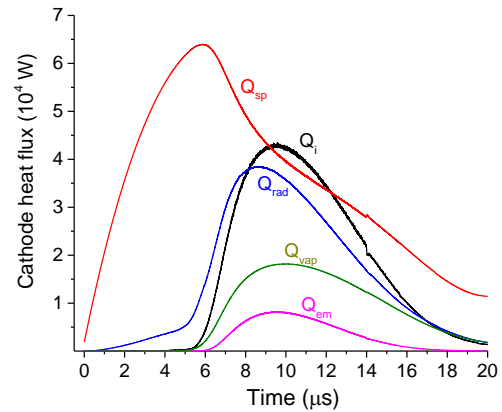


Fig. 1b. Heat flux components at HCVA cathode. Cathode spot heating (Q_{sp}), TEA ion heating (Q_i), TEA emission cooling ($-Q_{em}$), TEA evaporation cooling ($-Q_{vap}$), radiative heating (Q_{rad}).

REFERENCES

- [1] A.G. Rousskikh, A. S. Zhigalin, V. I. Oreshkin, R. B. Baksht, “Measuring the compression velocity of a Z pinch in an axial magnetic field”, *Phys. Plasmas*, vol. 24, 063519, 2017; doi: 10.1063/1.4986096
- [2] D.L. Shmelev, V.I. Oreshkin, I.V. Uimanov, “Hybrid numerical simulation of high-current vacuum arc taking into account secondary plasma generation”, *IEEE Trans. Plasma Sci.*, vol. 47, pp. 3478- 3483, 2019.

2D KINETIC SIMULATION OF CATHODE SPOT PLASMA EXPANSION

D.L. SHMELEV¹, S.A. BARENGOLTS², M.M. TSVENOUKH³, I.V. UIMANOV¹

¹*Institute of Electrophysics, UB, RAS, Ekaterinburg, Russia*

²*Prokhorov General Physics Institute, RAS, Moscow, Russia*

³*Lebedev Physical Institute, RAS, Moscow, Russia*

e-mail: shmelev@iep.uran.ru

A two-dimensional kinetic simulation of the expansion of the current-carrying plasma of the cathode spot of a vacuum arc is carried out. The modeling was performed by Particle-in-Cell and Direct Simulation Monte Carlo methods. The processes of ionization and recombination and Coulomb scattering were taken into account. Two fundamentally different solutions are demonstrated for an expanding plasma in an external electric field, but in contrast to [1] in a two-dimensional version. The first solution is a “quiet” expansion of the plasma at a relatively low current. At low current only ion-acoustic current instabilities arise (Fig. 1 a), which do not lead to catastrophic consequences. In this regime, the plasma expands at a speed of $\sim 10^6$ cm/s, the electron temperature of the plasma reaches 3 eV, and the average charge state of ions (Cu) is ~ 2 (Typical distributions of the plasma parameters are shown in Figs below.). In the second case, the current is large enough to excite the Buneman instability, after which the plasma plume decays and ions with relatively high energies scatter towards the anode and cathode.

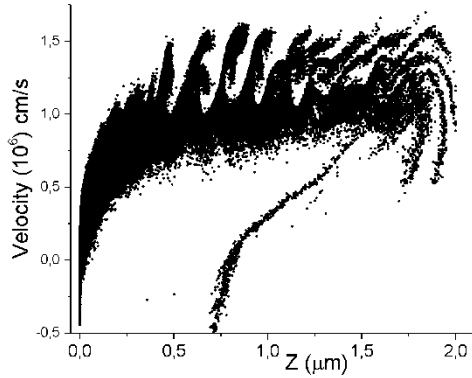


Fig. 1a. Ion phase plot along the plasma plume axis.

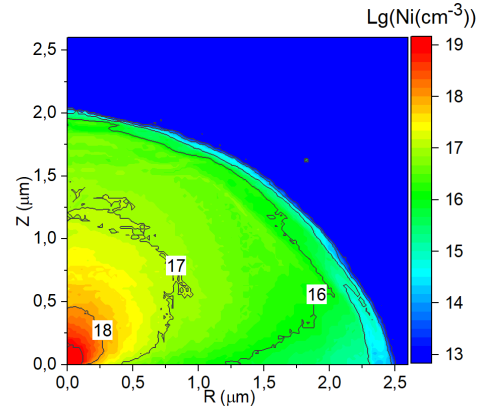


Fig. 1b. Ion plasma density at $t=21$ ps.

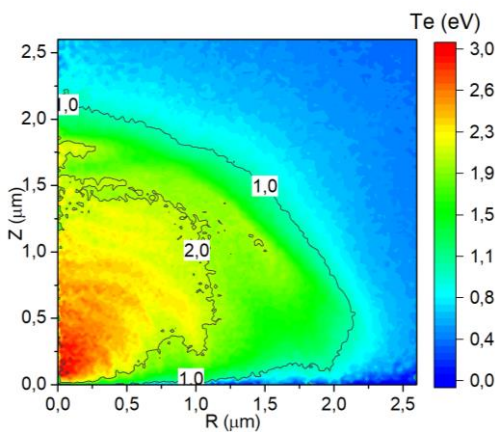


Fig. 1c. Electron temperature at $t=21$ ps.

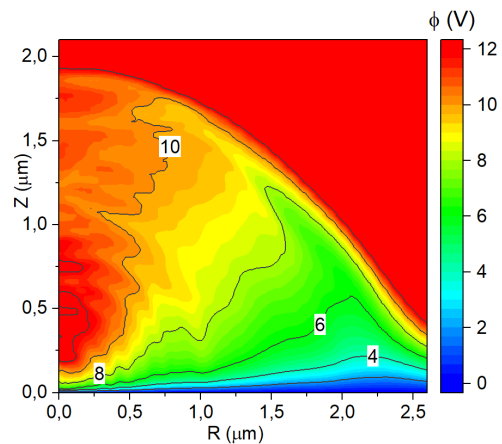


Fig. 1d. Electric potential at $t=21$ ps.

REFERENCES

- [1] D.L. Shmelev, S.A. Barengolts and M.M. Tsvetoukh, "Numerical Simulation of Plasma Near the Cathode Spot of Vacuum Arc," IEEE Trans. Plasma Sci., vol. 45, pp. 3046-3053, 2017.

MECHANISM OF ADDITIONAL SELF-FOCUSING OF AN ELECTRON BEAM GENERATED DURING A HIGH-VOLTAGE NANOSECOND DISCHARGE IN A GAS-FILLED DIODE*

M.I. LOMAEV^{1,2}, A.V. DYATLOV², V.F. TARASENKO¹, D.A. SOROKIN¹

¹Institute of High Current Electronics, SB, RAS, Tomsk, Russia

²National Research Tomsk State University, Tomsk, Russia

e-mail: SDmA-70@loi.hcei.tsc.ru

From a practical point of view, the effect of self-focusing (cumulation) of an electron beam [1, 2] is attractive, first of all, by the possibility of increasing the beam current density and, accordingly, increasing the power density in the cumulation zone. This effect can be used to generate highly ionized plasma and powerful X-ray radiation, in the study of matter at elevated pressure and thermonuclear research, in the fields of radiation chemistry and solid state physics, to generate powerful radiation in the terahertz frequency range, excitation of luminescence of artificial and synthetic crystals and in a number of other applications [3–5].

The effect of cumulation of an electron beam was studied during the formation of a high-voltage nanosecond discharge in gas-filled (air) and vacuum diodes (Figs. 1*ab*). It was established that in both cases the distribution of the beam current density in the plane of a grounded anode is non-uniform (Figs. 1*cd*). The highest beam current density occurs in the axial part of the anode. It was found that in the case of a gas diode (pressure 0.2 Torr), ~ 2 ns after the onset of the beam current pulse, the self-focusing effect is enhanced.

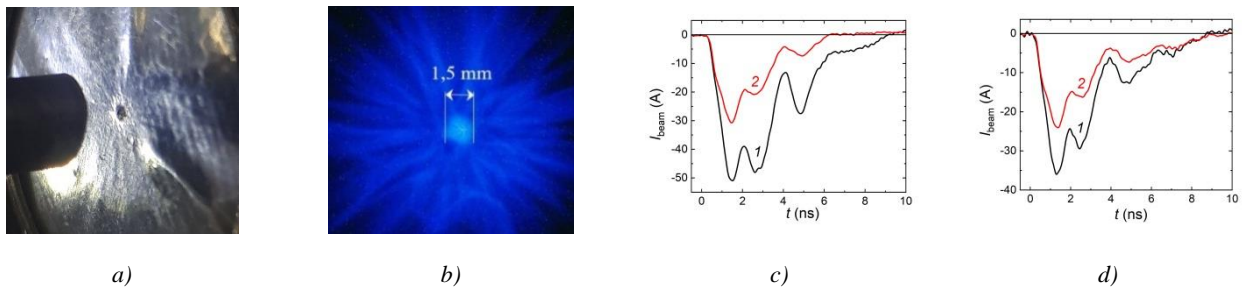


Fig. 1. (a) Photo of a discharge gap with a hole formed in a 30- μ m-thickness aluminum foil. (b) Glow of a plexiglass plate installed behind an anode made of a 15- μ m-thickness aluminum foil. $p_{air} \approx 0.2$ Torr. (c, d) Waveforms of the current pulses of the electron beam passing through holes in the anode (one hole on the diode axis (curve 1) and four holes on the periphery (curve 2)) at pressures of 0.2 Torr (c) and 10^{-5} Torr (d).

The results of studies indicate that in a gas diode, in addition to the effect of self-focusing of the beam, a few nanoseconds after the onset of the beam current pulse, an additional self-focusing mechanism is activated. The most probable reason for the additional self-focusing of the electron beam in the gas-filled diode is the effect of compensation of the electron charge by the charge of positive ions arising as a result of gas ionization by electrons of the beam. The values of the characteristic ionization time τ_i required for the manifestation of the charge compensation effect at a pressure of 0.2 Torr obtained on the basis of experimental data and as a result of estimates are close to each other (~ 2 ns). Their real difference may be smaller if we take into account the possibility of forming at the initial stage a beam of electrons with an energy of less than 40 keV.

REFERENCES

- [1] S.A. Goldstein, R.C. Davidson, J.G. Siambis, L. Roswell, "Focused-Flow Model of Relativistic Diodes," Phys. Rev. Lett., Vol. 33, no. 25, pp. 1471–1474, 1974.
- [2] G.A. Mesyats, Pulsed Power and Electronics, Moscow: Nauka, 2004.
- [3] A.C. Kolb, "Uses of intense electron beams," IEEE Trans. Nucl. Sci., Vol. 22, no. 3, pp. 956–961, 1967.
- [4] S.V. Anishchenko, V.G. Baryshevsky, A.A. Gurinovich, "Electrostatic cumulation of high-current electron beams for terahertz sources", Phys. Rev. Accel. Beams, Vol. 22, art. no. 043403, 2019.
- [5] D.A. Sorokin, A.G. Burachenko, D.V. Beloplotov, V.F. Tarasenko, E.Kh. Baksht, E.I. Lipatov, M.I. Lomaev, "Luminescence of crystals excited by a runaway electron beam and by excilamp radiation with a peak wavelength of 222nm," J. Appl. Phys., Vol. 122, art. no. 154902, 2017.

* The work was performed in the framework of the State Task for IHCE SB RAS, # FWRM-2021-0014.

SPLITTING OF THE IONIZATION WAVE DURING THE DEVELOPMENT OF GAS BREAKDOWN IN A MULTICHANNEL DISCHARGE SYSTEM

A.I. SHISHPANOV, P.S. BAZHIN, A.V. MESCHANOV

Saint Petersburg State University, Saint Petersburg, Russia

e-mail: a.shishpanov@spbu.ru

We investigate splitting of the ionization wave [1] (IW) that occurs during a pulsed single-electrode breakdown [2, 3] in one of the channels of an Y-shaped discharge system (DS) in the experiment with neon at a pressure of 1 Torr. The DS consists of three tubes equipped with electrodes on one edge and welded together by other edges at the branch point (x_0) of the system. Its geometry made it possible to study the split at 45° and 90° angles relative to the initial direction of IW motion. The IW x - t diagrams (Fig. 1) before and after the branch point were obtained by recording the wave optical signals in different points of DS and then analyzed.

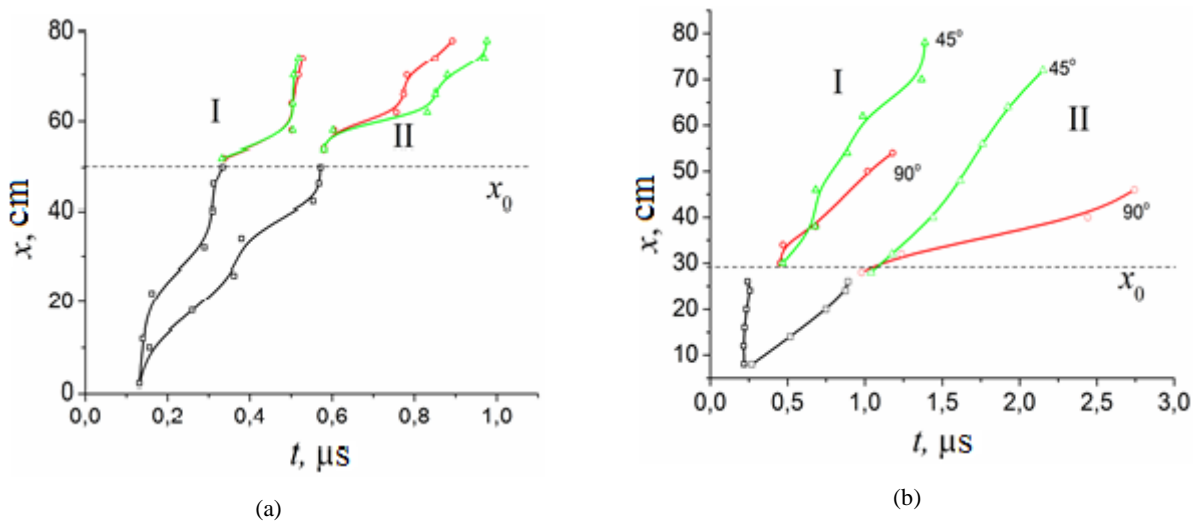


Fig. 1. x - t diagrams of IW splitting in x_0 point for (I) positive, and (II) negative polarity. a) Symmetrical split at the angle 45° , b) asymmetric split at the angles: 45° and 90° . Ne 1 Torr, $U = 2.5$ kV, voltage pulse repetition rate 500 Hz.

The black curves of the diagrams correspond to the IW propagation in the central channel, and the colored curves show the IW propagation along the branching channels. Fig. 1a illustrates the IW symmetric splitting into two waves diverging at 45° angle to the initial direction of propagation while Fig. 1b shows asymmetric IW splitting at 45° and 90° angles. In both cases we observed a sharp drop in the IW velocity at the moment of its splitting in x_0 (horizontal shift of the diagrams). In the case of symmetric split, two identical IWs appear with velocities restoring to the initial IW velocity during their propagation. But the negative IWs may appear with significant time shift. In case of asymmetric split, the smaller the splitting angle the higher the speed of the resulting IW. This pattern was found for both polarities. In case of positive polarity we observed almost complete stop of initial IW in branch point prior to splitting, while the negative IW split without considerable time shift.

REFERENCES

- [1] Vasilyak L.M., Kostyuchenko S.V., Kudryavtsev N.N. and Filyugin I.V., "Fast ionization waves under electrical breakdown conditions", Phys.-Usp., V.37, p. 247, 1994.
- [2] Shishpanov A.I., Ivanov D.O., Kalinin S.A. "Collision of ionization waves in long discharge tubes." Plasma Research Express, V. 1 N2. P. 025004, 2019.
- [3] Shishpanov A.I., Bazhin P.S., Ivanov D.O., Meschanov A.V., "Low-frequency one-electrode discharge in long tubes at low gas pressure", Plasma Research Express, V.2. p.015012, 2020.

HOLE SIZE EFFECT ON MICROHOLLOW CATHODE DISCHARGE IN AIR*

S.I. MOSHKUNOV, S.V. NEBOGATKIN, K.I. ROMANOV, E.A. SHERSHUNOVA

Institute for Electrophysics and Electric Power, RAS, Moscow, Russia
e-mail: eshershunova@ieeras.ru

Microhollow cathode discharge is realized in a gas region with micron dimensions, where an anode and a cathode are separated by a dielectric of micron thickness. Due to a small micron size of the gap the Pendel effect, a vibrational motion of electrons near the hollow cathode, leading to a strong ionization of the gap, is observed [1].

Discharges in plasma cell with diameters of the microhole d from 200 to 500 μm were studied. Cuprum served as a material of electrodes, ceramic laminate Rogers RO4000 served as a dielectric material. Negative DC voltage V_{in} with amplitude from 600 V to 1400 V was applied to the electrodes. The input current in the discharge cell I_{in} was limited by 200 k Ω ballast resistor. The voltage across the discharge gap V was measured with a high-voltage probe, and the current through the cell I was measured by a resistive sensor connected in series with the cell. Typical waveforms of voltage at the gap and discharge current at input voltage $V_{in} = -600$ V for $d = 400$ μm are presented in Fig. 1a.

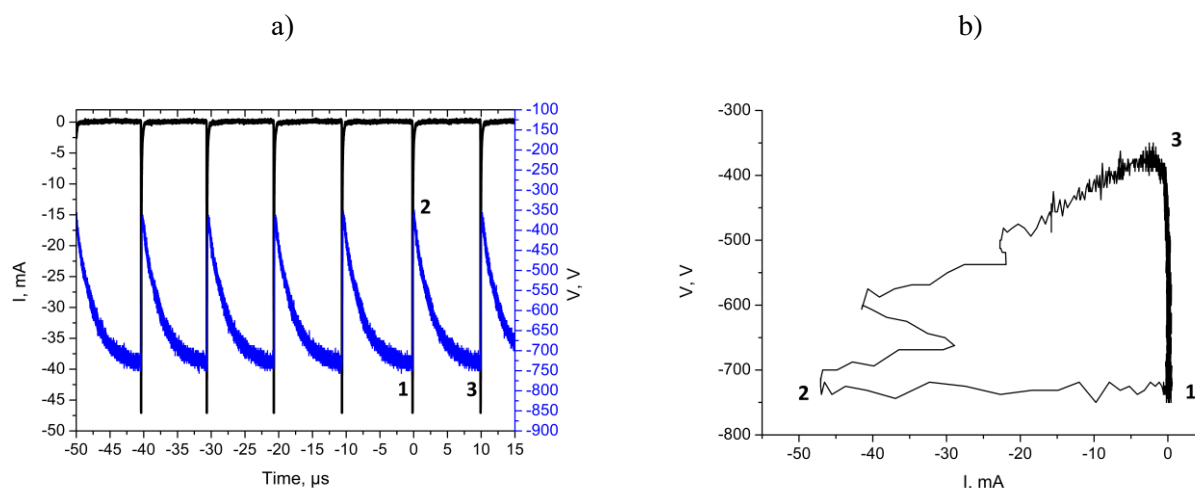


Fig. 1. Waveforms of the discharge current I and voltage across the discharge gap V at input voltage $V_{dc} = -600$ V and input current $I_{in} = 5$ mA for $d = 400$ μm

According to the Volt-Ampere Curve (Fig. 1b) there were made conclusions about a self-pulsing mode of the discharge [2]. There were plotted dependencies of the peak current value I_{pk} and the discharge ignition voltage V_{dg} on the input current I_{in} for the cathode holes from 200 to 500 μm .

It was found that with an increase in the input current I_{in} , the peak value of the discharge current I_{pk} increases and the discharge ignition voltage V_{dg} decreases. It should be noted that the ignition voltage was at $600 \text{ V} \pm 50 \text{ V}$ in all cases when the input current was more than 2 mA. Besides, with an increase in the input current, the discharge becomes unstable, it is realized in the train of pulses with different time intervals between them.

REFERENCES

- [1] Schoenbach K. H. et al. High-pressure hollow cathode discharges //Plasma Sources Science and Technology. – 1997. – T. 6. – №. 4. – C. 468.
- [2] Lazzaroni C., Chabert P. Discharge resistance and power dissipation in the self-pulsing regime of micro-hollow cathode discharges //Plasma Sources Science and Technology. – 2011. – T. 20. – №. 5. – C. 055004.

*This work was supported by the Russian Foundation for Basic Research, grant 19-08-00069a

FORMATION OF PLASMA JETS BY A HIGH-CURRENT DISCHARGE IN METAL VAPOR*

V.A. KOKSHENEV, N.E. KURMAEV

Institute of High Current Electronics, SB, RAS, Tomsk, Russia

e-mail: yak@oit.hcei.tsc.ru

High-current discharges with initiation of a vacuum arc on the surface of a hydrogen-containing dielectric form a plasma flow with a pronounced precursor. This plasma precursor (prepulse) consists of hydrogen ions and has a velocity of ≥ 10 cm/ μ s. Ceramics were used to suppress the precursor amplitude and form a plasma flow of heavy ions to initiate the arc. The paper presents the results of experiments on the study of a plasma flow formed by a high-current discharge with a current of up to 20 kA in vapors of the electrode material (copper, aluminum), initiated by breakdown along the corundum surface.

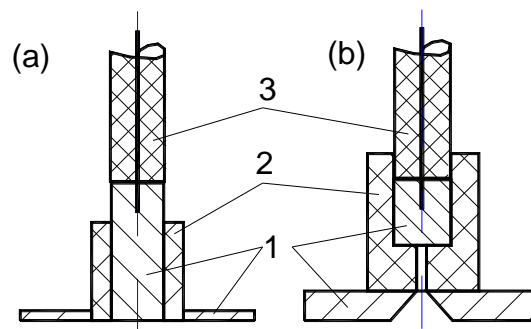


Fig. 1. Types of electrode systems for initiating a vacuum arc discharge over the ceramic surface: (a) end-face, (b) capillary. 1 - aluminum electrodes, 2 - ceramics, 3 - cable RK 75-9.

The motion of plasma jets in the interelectrode gap of a magnetically insulated transmission line (MITL) is investigated. It is shown that at equal amplitudes of the discharge current, the capillary source has a higher penetration rate into the transverse magnetic field. Probe measurements of the velocity of free expansion of plasma bunches showed that for the electrode system in Fig. 1 (a) the maximum concentration of the plasma flow moves at a speed of ~ 6 cm / μ s, and for the electrode system (b) - (8-9) cm / μ s. This may be due to an increase in the electron temperature T_e in the discharge in a capillary, which leads to an increase in the electric field of the space charge and, accordingly, to an increase in the ion velocity: $v \sim [(kT_e/m_i) \cdot \ln(T_e m_i / T_i m_e)]^{1/2}$ [1].

The design of the anode unit of a crowbar spark gap based on a plasma switch built into the MITL is presented. The installation of arc plasma sources (8 or 16) along the perimeter of the anode unit made it possible to controllably bridge the interelectrode gap of the MITL with a long cutoff of the generator from the load circuit.

REFERENCES

- [1] V.A. Kokshenev, N.E. Kurmaev, and R.K. Cherdizov, "Plasma flows of high-current discharge in a capillary and their propagation across a magnetically insulated line", *Izv. VUZov, Fizika*, vol. 62, No. 7, pp. 116–123, 2019.

* The work was performed under State Assignment of the Ministry of Science and Higher Education of the Russian Federation (project No. FWRM-2021-0001).

DENSE PLASMA FORMATION ON THE SURFACE OF A STAINLESS STEEL CONDUCTOR IN ULTRAHIGH MAGNETIC FIELDS*

V.A. KOKSHENEV, N.E. KURMAEV

Institute of High Current Electronics, SB, RAS, Tomsk, Russia

e-mail: yak@oit.hcei.tsc.ru

In experiments on the GIT-12 generator, the critical parameters of 12X18N10T stainless steel (SS) were measured for the microsecond growth mode of ultrahigh magnetic fields, in which a skin explosion of the conductor material takes place with the formation of a dense plasma and its expansion into the interelectrode gap of the vacuum transmission line. The experiments were carried out with stainless steel samples in the form of rods or tubes with an outer diameter of 3, 4, 6 mm and a wall thickness of 0.25, 0.5, 0.9, 1 mm. In addition, we investigated two-layer conductors with an outer layer of stainless steel with a wall thickness of 0.25, 0.5, 1 mm, and a tightly inserted copper conductor with diameters of 2, 3, and 3.5 mm inside. The samples either had a uniform structure along their entire length, or were composite. The upper anode half of the cylinder remained solid, while the lower half was a stainless steel layer with a copper insert. The experimental technique is described in detail in [1].

Analysis of experiments with a current amplitude in the samples of 4.3 MA with a rise time of $\sim 1.8 \mu\text{s}$ made it possible to establish the following characteristics for stainless steel 12X18N10T. The value of the characteristic magnetic field $B_0 \cong 100 \pm 10 \text{ T}$ was determined, above which the effect of nonlinear diffusion of the magnetic field into the conductor takes place. The values of the integral of the specific action $h_{SS} \cong 1.2 \pm 0.1 \cdot 10^9 \text{ A}^2\text{s} / \text{cm}^4$ and the temperature coefficient of resistance $\alpha_{SS} \sim 7.8 \pm 0.1 \cdot 10^{-4} \text{ 1/K}$ are estimated. The critical magnetic field is found to be $B_{cr} \cong 260 \text{ T}$, exceeding which leads to the formation of a dense plasma on the surface of a massive conductor. A method is proposed for increasing the critical magnetic field on the surface of a conductor up to 1.5 times by choosing the optimal thickness of the conducting surface, and criteria for its determination are given. In our experiments on the GIT-12 generator, the average rate of rise of the magnetic field is $k \cong 3 \cdot 10^8 \text{ T/s}$ and the optimal thickness is $\Delta \cong 1 \text{ mm}$ (see Fig. 1, frame 2). The effect of an increase in the critical magnetic field on the surface of a two-layer sample and the creation of a pressure in the megabar range until the moment of expansion of the explosion products of an inner conductor with high conductivity has been tested. The increase in critical parameters is due to the non-monotonic distribution of the current in the sample volume due to the interaction of competing skin-effect processes and nonlinear diffusion of the magnetic field into the conductor.

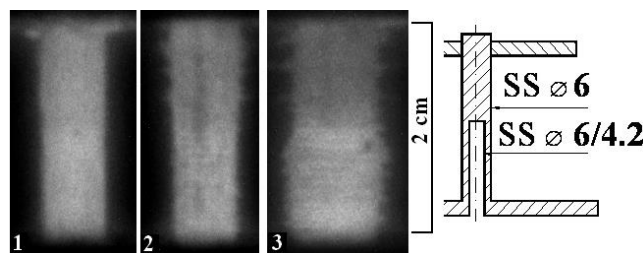


Fig. 1. Images obtained with optical cameras "Nanogate Frame-9" with a frame exposure time of 10 ns at different times from the beginning of the current: 1 - 1280 ns, 2 - 1500 ns, 3 - 1900 ns. On the right, the structure of a stainless steel sample is shown.

REFERENCES

- [1] V.A. Kokshenev, N.E. Kurmaev, and F.I. Fursov, "Surface explosion of conductors in a megagauss magnetic field", *Izv. VUZov, Fizika*, vol. 61, No. 9/2, pp. 171–175, 2018.

* The work was performed under State Assignment of the Ministry of Science and Higher Education of the Russian Federation (project No. FWRM-2021-0001).

MECHANISMS FOR INCREASING THE DIFFUSE CHANNELS DENSITY IN PUMP DISCHARGES OF EXCIMER LASERS*

A.G. YASTREMSKII, S.A. YAMPOLSKAYA

Institute of High Current Electronics, SB, RAS, Tomsk, Russia

e-mail: s_yampolskaya@yahoo.com

Despite the progress in the development of semiconductor lasers, atmospheric pressure gas lasers reliably occupy their own place as powerful laser sources. The main problem that limits their capabilities is the instability of pump discharges with increasing pump power and discharges themselves are fundamentally inhomogeneous. With sufficient preionization of the discharge gap, the inhomogeneity of the discharge is associated with the appearance of plasma spots on the cathode surface. The discharge is represented by overlapping diffuse channels, which are attached to these spots. The more cathode spots appear on the cathode surface, the longer the discharge retains glow form.

In this work, we present the results of a numerical study of the development of a discharge with several cathode spots. A detailed model of an inhomogeneous discharge is presented in [1]. The emitting centers on the cathode were modeled by the regular structure of the tips on its surface. It was found that with a geometric difference in the sizes of the tips, the oppression of smaller cathode spots by larger neighbors occurs. An analysis of the mechanism for intercepting the discharge current by larger channels showed that in most cases, the number of emitting centers on the cathode surface, which are the nuclei of cathode spots, is greater than the number of observed cathode spots at the maximum of the discharge current (see Fig. 1).

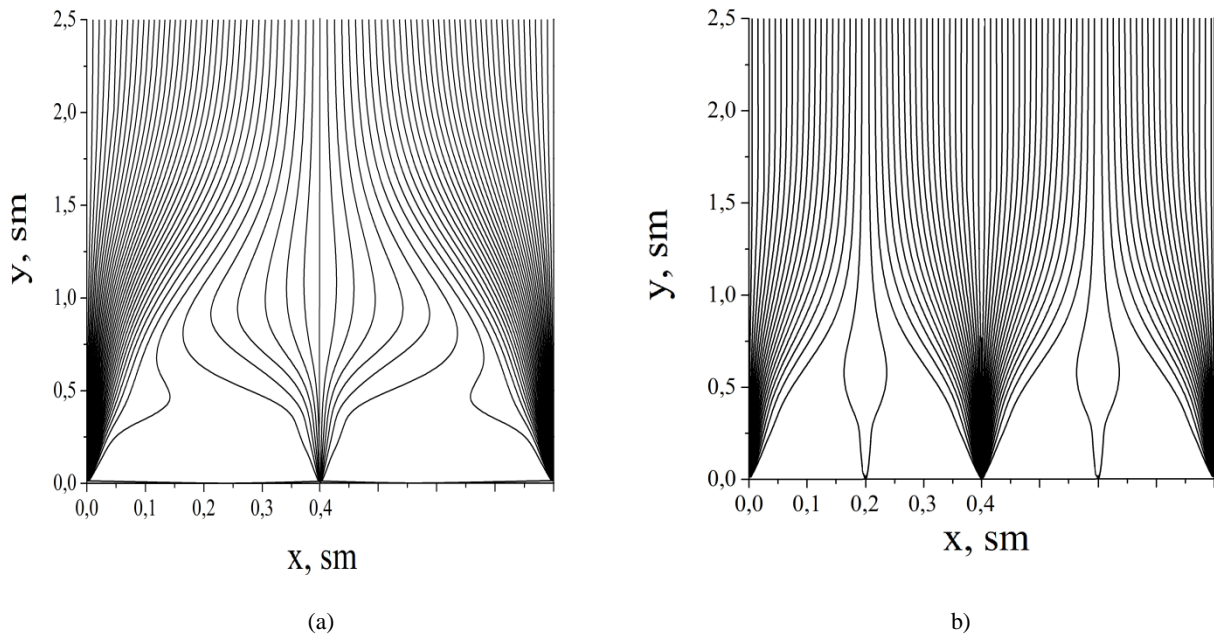


Fig. 1. Isolines of the discharge current density: (a) the distance between adjacent tips $dx = 4$ mm, and (b) $dx = 2$ mm. Height difference between adjacent tips is 0.01mm. Total cathode width 2 cm.

REFERENCES

- [1] S.A. Yampolskaya, A.G. Yastremskii, Yu.N. Panchenko, A.V. Puchikin, and S.M. Bobrovnikov, "Numerical study of the discharge spatial characteristics influence on the KrF laser generation," IEEE J. of Quant. Electr., vol. 56, pp. 1–9, 2020.

* The work was supported in part by the RFBR Grants Nos. 20-08-00371 and 20-58-00008.

RUNAWAY OF ELECTRONS AND INITIATION OF EXPLOSIVE ELECTRON EMISSION DURING PULSE BREAKDOWN OF DENSE GASES *

G.A. MESYATS¹, N.M. ZUBAREV^{1,2}

¹*Lebedev Physical Institute, RAS, Moscow, Russia*

²*Institute of Electrophysics, UB, RAS, Yekaterinburg, Russia*

e-mail: nick@iep.uran.ru

Runaway (continuously accelerated in a gas or plasma medium in a sufficiently strong electric field) electrons play an important role in the pulsed gas breakdown [1, 2]. Crossing the gap in times comparable with the propagation time of light, they ionize it, providing conditions for the ignition of a volume discharge [3, 4]. Recent active experimental and theoretical studies have provided an explanation for many important phenomena associated with runaway electrons. However, no satisfactory explanation has yet been given for the reasons for generation of runaway electrons in gases of high – tens of atmospheres – pressure under conditions of the uniform field in the gap when the reduced field (i.e., the ratio of its strength to pressure), firstly, is an order of magnitude lower than that required for the transition of thermal electrons into the runaway regime and, secondly, so low that the characteristic time of the avalanche multiplication of thermal electrons is longer than the duration of the voltage pulse (see the experimental work [5]).

In the present work (see also our recent paper [7]), a mechanism for the initiation of explosive electron emission [6] at the interface between the cathode and a dense gas is proposed, based on the accumulation of positive ions near natural protrusions of micron size, which are formed as a result of gas ionization by field-emission electrons. The distance at which ions are born decreases with increasing gas density, which leads to an increase in their Coulomb field on the emitting surface. As a result, an explosive increase in the emission current density occurs for a high-pressure (tens of atmospheres) gas leading to the formation of many explosive-emission centers in tens of picoseconds. They give a start to the development of plasma channels growing towards the anode. Runaway electrons are generated at the tops of the plasma tips, which ionize the gas, providing its subnanosecond breakdown. This scenario of the breakdown development can be implemented under conditions of a critically low reduced electric field, as, for example, in Ref. [5].

REFERENCES

- [1] G.A. Mesyats, Y.I. Bychkov, and V.V. Kremnev, “Pulsed nanosecond electric discharges in gases,” *Sov. Phys.-Usp.*, vol. 15, pp. 282–297, 1972.
- [2] L.P. Babich, T.V. Loiko, and V.A. Tsukerman, “High-voltage nanosecond discharge in a dense gas at a high overvoltage with runaway electrons,” *Sov. Phys.-Usp.*, vol. 33, pp. 521–540, 1990.
- [3] G.A. Mesyats and M.I. Yalandin, “Nanosecond volume discharge in air initiated by a picosecond runaway electron beam,” *Phys.-Usp.*, vol. 62, pp. 699–703, 2019.
- [4] V. Tarasenko, “Runaway electrons in diffuse gas discharges,” *Plasma Sources Sci. Technol.*, vol. 29, p. 034001, 2020.
- [5] S.N. Ivanov, “The transition of electrons to continuous acceleration mode at subnanosecond pulsed electric breakdown in high-pressure gases,” *J. Phys. D: Appl. Phys.*, vol. 46, p. 285201, 2013.
- [6] Yu.D. Korolev and G.A. Mesyats, *Field Emission and Explosion Processes in Gas Discharge*. Novosibirsk: Nauka, 1982.
- [7] N.M. Zubarev and G.A. Mesyats, “Initiation of explosive electron emission and runaway of electrons during pulse breakdown of dense gases,” *JETP Lett.*, vol. 113 (in production), 2021.

* The work was supported in part by the RFBR Grant No. 20-08-00172.

EXPERIMENTAL INSTALLATION FOR STUDYING CATHODE PLASMA PROCESSES IN VACUUM GAP OF PULSED ELECTRON ACCELERATOR WITH GAS OR LIQUIDE INJECTION*

I.S. EGOROV¹, A.V. KLIMKIN², A.V. POLOSKOV¹, M.A. SEREBRENNIKOV¹, M.V. TRIGUB²

¹Tomsk Polytechnic University, Tomsk, Russia

²V.E. Zuev Institute of Atmospheric Optics, SB, RAS, Tomsk, Russia

e-mail: egoris@tpu.ru

One of the directions of using plasma sources is the formation of plasma emitters for electron beams as part of direct-action charged particle accelerators. The parameters of the accelerator generators require mutual matching with the characteristics of the plasma emitters. The paper describes the design, composition and diagnostic equipment of an experimental stand based on a vacuum chamber of a pulsed electron accelerator for testing plasma sources of pulsed electron beams. The stand includes a vacuum volume with a high-voltage bushing, pumping out pipes, diagnostic windows along the perimeter and a mounting flange of a complex device for diagnosing the characteristics of pulsed electron beams [1]. The stand provides the possibility of controlled supply of gas and liquid to the formation region of the plasma emitter of electrons under the influence of an accelerating voltage pulse [2]. The location of the diagnostic windows and flanges of the stand allows direct optical observations of the plasma formation region in the frontal and profile directions. The use of the stand will make it possible to determine the characteristics of the tested plasma emitters for their operation as part of a vacuum electron diode of a pulse accelerator.

REFERENCES

- [1] Egorov, I., Poloskov, A., "Combined device for vacuum electron diode adjustment," NIMA, vol. 911, pp. 10–14, 2018.
- [2] Egorov, I., Poloskov, A., Serebrennikov, M., Remnev, G., "Experimental demonstration of a single capillary, water-activated cathode for a sub-microsecond electron accelerator," JETP Lett., vol. 943, art. 162459, 2019.

* The work was supported in part by the RFBR Grant No. 20-02-00870.

OES INVESTIGATION OF A LOW-PREASSURE NON-SELF-SUSTAINED GLOW DISCHARGE PLASMA IN Ar:N₂ GAS MIXTURE*

S.S. KOVALSKY, V.V. DENISOV, E.V. OSTROVERKHOV, V.E. PROKOP'EV

Institute of High Current Electronics, SB, RAS, Tomsk, Russia

e-mail: kovalsky@opee.hcei.tsc.ru

A high-current non-self-sustained low-pressure glow discharge with a hollow cathode provides a high degree of homogeneity in the distribution of plasma parameters over the volume of a vacuum chamber [1] and it is promising for surface treatment of large-sized items, including for an ion-plasma nitriding processes [2].

For some steel grades it is necessary to avoid the appearance a compound layer consisting of brittle phases on the surface. The solution to this problem is using a nitrogen-argon gas mixture with a high argon content, which makes it possible to reduce the nitrogen flow at the plasma-solid boundary.

In this work, we measured the emission spectra of a glow discharge plasma with a change in the nitrogen content in a nitrogen-argon gas mixture from 100 to 0% with a step of decreasing the nitrogen fraction of 25%, and also considered in more detail the region with a nitrogen content of less than 25% (10% and 15%) at a total pressure $p = 1$ Pa with maintaining the same values of the voltage and discharge current due to a change in the electron emission current from the auxiliary discharge plasma. An increase in the intensity of the emission lines of argon ions at small fractions of the volumetric nitrogen content is observed. Possible reasons for the manifestation of this effect are given. It is also shown that argon has a significant effect on the generation of molecular nitrogen ions and atomic nitrogen when the volumetric nitrogen content changes from 50% to 75%.

REFERENCES

- [1] Denisov V.V., Akhmadeev Yu.H., Koval N.N., Kovalsky S.S., Lopatin I.V., Ostroverkhov E.V., Pedin N.N., Yakovlev V.V., Schanin P.M., "The source of volume beam-plasma formations based on a high current non-self-sustained glow discharge with a large hollow cathode", *Phys. Plasmas*, 26, 123510 (2019).
- [2] Ostroverkhov E.V., Denisov V.V., Denisova Yu A., Koval N.N., Lopatin I.V., "Non-self-sustained low-pressure glow discharge for nitriding steels and alloys", *IOP Conf. Ser.: Mater. Sci. Eng.*, 387, 012056 (2018).

* The work was performed under State Assignment of the Ministry of Science and Higher Education of the Russian Federation (project No. FWRM-2019-0002).

PRELIMINARY EXPERIMENTAL STUDY ON HIGH REPETITIVE AND SHORT NANOSECOND PULSED DISCHARGE IN AIR AT ATMOSPHERIC PRESSURE*

YUTALI, HANDONG LI, ZHIGANG LIU, YANGYANG FU, XIAOBING ZOU, XINXIN WANG

Tsinghua University, Beijing, China

email: 923530913@qq.com

High repetitive (≤ 100 kHz) and short nanosecond (~ 10 ns) pulsed discharge was investigated. With a voltage of 40 kV in amplitude, if only one pulse is applied, the length of the gap is only 1 mm for the reliable breakdown. However, if 1000 repetitive pulses are applied, the longest gap that can be broken down dramatically increases with the repetitive rate and reaches to 90 mm at 100 kHz. The voltage recovery was determined with two-pulse method. The similarities between the gas recovery after the short nanosecond pulsed breakdown and that after the microsecond pulsed breakdown were found and the reason for this similarities was given. The evolution in the discharge mode with the applied voltage and the repetitive rate was observed. The existence of the multichannel spark discharge was confirmed with 10ns time-resolved photo. The reason for the formation of the multichannel spark was given.

* The work was supported by the National Natural Science Foundation of China (Grant No. 52077117).

CURRENT AND VOLTAGE IN PLANAR DIODE WITH A MOVING CONDUCTING CHANNEL

V.A. SHKLYAEV, S.YA. BELOMYTTSEV, A.A. GRISHKOV

Institute of High Current Electronics, SB, RAS, Tomsk, Russia
e-mail: shklyaev@to.hcei.tsc.ru

In this work, based on the current continuity equation and the Gauss theorem, we analyze the currents and voltages in the diode when the boundary of the conductive channel moves at a constant speed in the gap bounded by two parallel electrodes. It is shown that the high speed of movement of the boundary of the conducting channel leads to the fact that at the moment when it completely overlaps the interelectrode gap, the current flowing in the gap differs from the current determined by Ohm's law.

ON THE SCALING LAWS FOR LOW-TEMPERATURE PLASMAS AT MACRO AND MICRO SCALES

YANGYANG FU¹, XINXIN WANG¹, BOCONG ZHENG², PENG ZHANG³, QI HUA FAN³, AND JOHN P. VERBONCOEUR³

¹Tsinghua University, Beijing, China

²Michigan State University, Michigan, United States of America

³Michigan State University, Michigan, United States of America

e-mail: fuyangyang@tsinghua.edu.cn

The theoretical background and historical development of the similarity theory during the past decades are reviewed. We demonstrate similar discharges in local and nonlocal kinetic regimes, taking the low-pressure capacitive radio frequency (rf) discharges and microdischarges as examples. By using fully kinetic particle-in-cell simulations, we verify the similarity law (SL) and show a violation of frequency scaling (f-scaling) in the low-pressure capacitive rf plasmas [1, 2]. The SL scaling relations for electron density and electron power absorption are confirmed in similar rf discharges. With only the driving frequency varied, the f-scaling for electron density is also validated, showing almost the same trend as the SL scaling, across most of the frequency regime. However, violations of the f-scaling are observed at lower frequencies, which are found to be relevant to the electron heating mode transition from stochastic to Ohmic heating. The scaling characteristics have also been comprehensively studied for microdischarges with dimensions from hundreds to several microns, with transition from secondary electron dominated regime to field emission regime [3, 4]. Finally, practical applications of the similarity and scaling laws are summarized.

REFERENCES

- [1] Y. Fu, B. Zheng, D.-Q. Wen, P. Zhang, Q. H. Fan, and J. P. Verboncoeur, *Appl. Phys. Lett.* 117, 204101 (2020).
- [2] Y. Fu, B. Zheng, P. Zhang, Q. H. Fan, J. P. Verboncoeur, and X. Wang, *Phys. Plasmas* 27, 113501 (2020).
- [3] Y. Fu, P. Zhang, J. Krek, and J. P. Verboncoeur, *Appl. Phys. Lett.* 114, 014102 (2019).
- [4] Y. Fu, P. Zhang, J. P. Verboncoeur, and X. Wang, *Plasma Res. Express* 2, 013001 (2020).

INITIATION MECHANISMS AND DYNAMICS OF DEVELOPMENT AT THE PREBREAKDOWN STAGE OF A SELF-SUSTAINED SUBNANOSECOND DISCHARGE IN HIGH-PRESSURE NITROGEN*

S.N. IVANOV, V.V. LISEKOV, Y.I. MAMONTOV

Institute of Electrophysics, UB, RAS, Ekaterinburg, Russia

e-mail: stivan@iep.uran.ru

The results of an investigation of a self-sustained subnanosecond discharge in nitrogen at a pressure of 6 atm are presented. For our investigations, we chose the experimental condition range for which, according to the classical concepts, both in an average electric field across the discharge gap and in the enhanced electric field domain determined by the cathode geometry generation of runaway electrons (RAEs) didn't have to occur, but the electric field was sufficient for the discharge initiation through the field emission of electrons from microprotrusions on the cathode surface. A high voltage pulse with front of 770 ps was applied to the studied gas gap. In this case, the voltage rise rate in the discharge gap at the prebreakdown stage was 1.45×10^{14} V/s. A breakdown occurs at the end of the front of the voltage pulse. The cathode geometry used provided a 3.3 fold enhancement of an electric field in the near-cathode spatial domain. It is shown that at the initial stage the discharge is of a volumetric form which turns into a spark form further. The discharge contraction starts from a cathode and an anode almost simultaneously. The propagation rate of ionization waves accompanying the spark channel development is 4.2×10^8 cm/s. The initial volumetric form of the discharge is provided by preliminary ionization of a gas medium by RAEs. Generation of RAEs takes place in the enhanced electric field area formed near a microprotrusion on the cathode surface, while the macro-geometry of the discharge gap doesn't ensure enhancing of the electric field up to the value which is sufficient to implementation of the RAE generation criterion. Numerical simulation of a formation process of the electron avalanche initiated by an electron field-emitted from the top of the cathode microprotrusion was carried out taking into account the motion of each electron in the avalanche. To simulate electron motion through the discharge gap, the 3D Monte-Carlo technique was employed. The following runaway electron parameters were calculated: characteristic RAE trajectories; RAE energy gained during the motion through the discharge gap; times required for RAEs to reach the anode.

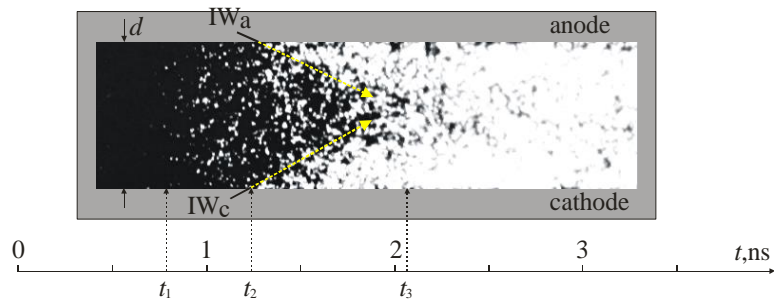


Fig. 1. A typical streak image of the discharge glow (nitrogen, $p = 6$ atm, $d = 5$ mm). The time moment corresponding to the voltage rise onset across the discharge gap is set to be the zero time scale point. IW_c and IW_a are, correspondingly, the cathode and anode ionization waves accompanying the spark channel development. t_1 is the beginning of the volumetric phase of the discharge, t_2 is the beginning of the contraction, t_3 is the moment of time corresponding to the overlap of the discharge gap by the conducting channel.

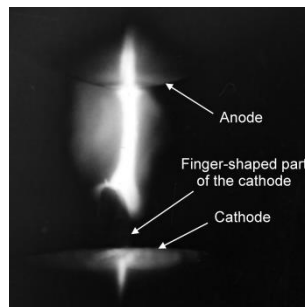


Fig. 2. The integral glow of the discharge (nitrogen, $p = 6$ atm, $d = 5$ mm).

* The work was supported by the Russian Foundation for Basic Research, grants 20-08-00172 and 20-38-90147

STUDY OF RADIATIVE CHARACTERISTICS OF A COMPLETED PARTIAL DISCHARGE

E.A.YAKOVLEV¹, V.V. YUGAY¹, L.A. ZINOVYEV², A.R.KASHLEV¹, V.O.BEZRUKOV¹

¹Karaganda technical university, Karaganda, Kazakhstan

² Karaganda university named after E.A. Buketov, Karaganda, Kazakhstan

e-mail: jenia2001@mail.ru

The object of research in this work is a completed partial discharge burning in a pulsed plasmatron [1].

Investigations, in particular, high-speed photographing of a partial discharge (PD) in the presence of an electrolyte, have shown that with a completed partial discharge, a bright flash occurs with a lifetime of 0.001 s. In contrast to the classical partial discharge, i.e. without electrolyte, the brightness of the discharge is comparable to the brightness of the welding arc.

To characterize the radiation intensity of a completed partial discharge, the illumination created by this discharge at a certain distance was used.

The illumination was measured using the TMD 4903 optical sensor, which is part of the equipment of the Xiaomi smartphone. Data on the characteristics of the radiation detector were taken from [2]. Based on the characteristics of the radiation detector, the parameters of radiation in the visible region of the spectrum were measured in the course of the experiments.

A pulsed RC generator described in [3] was used to power the plasmatron.

Due to the discrepancy between the discharge lifetime and the time constant of the radiation receiver (about 1 s), to obtain real values of illumination, the readings of the illumination sensor were recalculated according to the formula $E_{\text{calc}} = E_{\text{meas}} * (t_2 / t_1)$, where t_2 is twice the time constant (the reaction time to the appearance of a flash and its extinction), t_1 is the lifetime of the discharge.

Illumination measurements were carried out for discharges that occurred in the absence and in the presence of ballast resistance R_b in the discharge circuit.

The data obtained during the experiments are shown in table 1.

Table 1 - The results of measuring the illumination created by the completed PD in the presence of an electrolyte (discharge gap 3 mm).

№	U, V	R_b , Ohm	r, mm	E (measured), lx	E (calculated), Mlx
1	950	0	150	354	0.7
2			850	14	0.028
3		68	150	19	0.038
4			850	4	0.008

A very high value of the calculated illumination at small distances from the discharge significantly exceeds the range of illumination measurement by the TMD 4903 sensor, in which the linearity of the sensitivity characteristic remains (up to 60000 lx).

In this regard, the distance from the discharge during measurements should exceed 400 mm (based on the data in Table 1).

The sensitivity of the radiation detector used did not make it possible to determine the radiation parameters of an incomplete partial discharge due to its significantly lower brightness.

REFERENCES

- [1] Yakovlev E.A., Zinovyev L.A., Kashlev A.R., Bezrukov V.O., Danko I.A. Partial discharge gas dynamics in a plasma-chemical reactor. Proceedings of the University, Karaganda, KTU, vol.3(80). pp.129–134, 2020.
- [2] <https://ams.com/tmd4903#tab/features>.
- [3] Yakovlev E.A., Mekhtiyev A.D., Yugay V.V., Zinovyev L.A. Research of generators of impulses for electrotechnological installations with solutions of electrolytes. Bulletin of the Karaganda university. Physics series, vol.90, pp.65-70, 2018.

MAGNETIC FIELD INFLUENCE ON THE PENNING DISCHARGE CHARACTERISTICS

N.V. MAMEDOV^{1,2}, A.S. ROHMANENKOV¹, A.A. SOLODOVNIKOV¹

¹*Dukhov Research Institute of Automatics (VNIIA), Moscow, Russia*

²*National Research Nuclear University MEPhI, Moscow, Russia,*

e-mail: M_nikitos@mail.ru

A pulsed gas discharge in crossed ExH fields (Penning discharge) was studied in this paper. It is worth noting the relevance of these studies. The Penning discharge is widely used in ion sources (PIS) for miniature linear accelerators (MLA) of a neutron generator [1]. For the stable PIS operation, it is necessary that the extracted pulsed ion current must be square type with short leading and trailing edges. In this case, the discharge current (and the extracted ion current) should linearly depend on the pressure and the extraction coefficient (the ratio of the extracted ion current to the discharge current) should be the maximum.

In this paper, experimental and numerical studies of the current pulses depending on the magnitude and configuration of the magnetic field and pressure were done. We used deuterium as a working gas. The details of the physical measurements are published in the article [2]. The simulation was carried out using a three-dimensional PIC code (in combination with the Monte Carlo method for modeling gas kinetics). The obtained results indicate the existence of various (stable and unstable) discharge modes, which are realized depending on the magnetic field and pressure.

For an unstable discharge mode, the following stages can be detected:

1. gradual accumulation of volume charge. The electrons are distributed fairly evenly. Electron concentration slight increases in the anode central part. The ions are distributed mainly in the anode center in the cylinder form with rather vague edges.

2. the rapid growth of the particle number and the sharp accumulation of the volume charge. The electrons occupy almost the entire anode volume. In this case, the electron concentration increases in the cylinder at a small radius from the system axis. The electron distribution in this cylinder is uneven and constantly changes. Almost all ions are located in the same cylinder with clear boundaries.

3. chaotic mixing of plasma. The electron-neutral plasma spots fall on the anode. After that, the particle concentration drops rapidly.

4. redistribution of the remaining charged particles by the PIS volume. In this case, the distribution of charged particles returns to the case of gradual volume charge accumulation. The process is then repeated.

This discharge process has a strict periodicity. In this case, the period may vary depending on the geometry and physical parameters of the penning discharge. Also, conditionally, the "stationary" discharge mode stages can be described:

1. the charge accumulation stage. The electrons are not evenly distributed and occupy only part of the anode. In this case, the rotation of the electron cloud around the anode axis is observed over time. The ions are distributed mainly in the anode center in the cylinder form with rather vague edges.

2. the stage of establishing a stationary mode. Due to the particle concentration increase, their redistribution occurs. Part of the charged particles goes to the anode. The electronic cloud becomes more concentrated with fairly clear boundaries, but smaller in volume. Almost all the ions are evenly distributed over a cylinder with clear boundaries.

3. the stationary mode stage. Here, the main part of the electrons forms a stable cloud rotating around the PIS axis. The ions are evenly distributed throughout the cylinder. This charge distribution picture does not change over time in the future.

REFERENCES

- [1] V. Valkovic // 14 MeV Neutrons. Physics and Applications. CRC Press Taylor&Francis Group, Boca Raton, London, New York, 2016, 500 p.
- [2] N.V. Mamedov, A.V. Gubarev, et al, Plasma Sources Sci. Technol. 29 (2020) 025001 (9 pp)., DOI: 10.1088/1361-6595/ab6758.

STUDY OF ANODE AND CATHODE PLASMAS FORMATION IN AN ELECTRON DIODE WITH AN EXPLOSIVE EMISSION CATHODE*

A.I. PUSHKAREV, A.I. PRIMA

Tomsk Polytechnic University, Tomsk, Russia

e-mail: aipush@mail.ru

We presents the results of simulation and experimental study of anode and cathode plasmas formation in a vacuum diode with an explosive emission cathode during generation of a pulsed electron beam with a current density of 0.3-0.4 kA/cm², an accelerating voltage of 300-500 kV and pulse duration 80 ns. The studies were carried out on accelerator TEU-500 [1]. We used a diode with a flat cylindrical cathode with a diameter of 60 mm, made of different materials, anode-cathode (A-K) gap spacing of 12 mm. A 92 mm in diameter flat copper collector of a Faraday cup was used as the anode.

The performed analysis showed that during the generation of an electron beam in a vacuum diode with a passive cathode, in the A-K gap, in addition to the explosive-emission plasma, the anode and cathode gas plasmas are present. These plasma regions are formed during desorption of molecules from the surface of the diode electrodes, dissociation of desorbed molecules, and ionization of atoms by electrons. The plasma concentration was calculated from the linear energy losses of electrons. Low efficiency of electron-stimulated desorption of molecules from the working surface of the anode (\approx one molecule per electron) and insignificant linear energy losses of electrons (less than 20 eV/cm) in the anode gas layer provide a low concentration of the anode plasma, which does not exceed 10¹² cm⁻³ (see Fig. 1a), the degree ionization of the anode plasma is equal to $\approx 10^{-4}$.

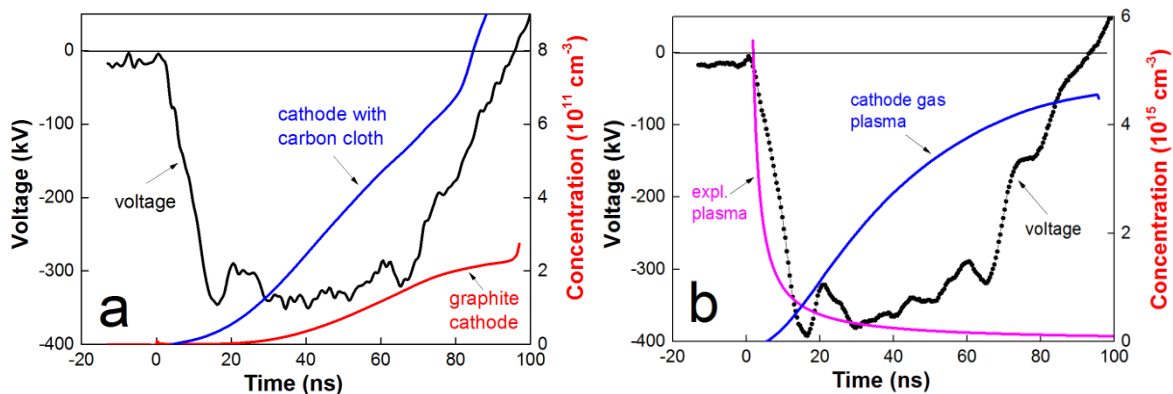


Fig. 1. Waveforms of the accelerating voltage and the change in the concentration of the anode plasma (a), cathode gas and explosive-emission plasmas (b)

The expansion rate of the anode plasma is ≈ 0.17 cm/ μ s, the thickness of the plasma layer is 0.14 mm at an A-K gap of 10-18 mm. Therefore, the anode plasma does not make a significant contribution to the operation of a vacuum diode with a passive cathode at a pulse duration of less than 0.1 μ s.

The complete desorption of molecules from the working surface of the cathode (during explosive-emission plasma formation), and the high efficiency of ionization of atoms in the cathode gas layer provide a high plasma concentration $\approx 10^{15}$ cm⁻³ (see Fig. 1b) and a high degree of ionization $\approx 10^{-2}$.

The charge of the explosive-emission plasma layer is much less, than the charge of the electron beam, and the main source of electrons is not the explosive-emission plasma, but the cathode gas plasma. In this case, the electron current is limited by the concentration of the cathode plasma. The use of a cathode with a developed surface (a cathode with a carbon cloth coating, multipoint copper or tungsten cathodes) makes it possible to increase the total charge of the electron beam by more than 1.5 times without changing the cathode diameter and A-K gap spacing.

REFERENCES

- [1] Pushkarev A.I., Novoselov Yu.N., and Sazonov R.V. Losses in a Pulsed Electron Beam during its Formation and Extraction from the Diode Chamber of an Accelerator // Instruments and Experimental Techniques, 2007, Vol. 50, No. 5, p. 687-694.

* The work was supported by the Russian Foundation for Basic Research, projects no. 19-38-90001.

DYNAMICS OF CHARGE SYSTEM IN OWN FIELD

A.S. CHIKHACHEV

VEI, Moscow, Russia
e-mail: churchev@male.ru

The work examines the transient dynamics of single-component systems. The problem on dynamics of flat layer and spherical symmetric configuration is considered. A classical clash-free system is considered, described using the "Meshchersky integral" and the "conjugate" integral of motion. States characterized by constant charge in non-stationary coordinates are obtained.

The study of non-stationary systems that interact intensively with their own field is of great interest both from an experimental and theoretical point of view. In this work, a non-stationary Hamiltonian will be used, the next of Meshchersky's works [1]. A similar Hamiltonian was used in work [2], in which, apparently, for the first time, the problem of accurately accounting for one's own field was solved.

It should be noted that the model Hamiltonian of a non-stationary system can be used both for the quantum mechanical system and for the classical one.

REFERENCES

- [1] Meshchersky J. Uber die Integration der Bewegungsgleichungen im Probleme zweier Korper von verandlicher Masse // Astron.Nachr., 1902, v.159, p.229.
- [2] Chikhachev A.S. Non-stationary self-consistent model of the ensemble in its own field // Technical Physics, 2014, V.59, No. 4, p.474.

GENERATION OF PLASMA IN LOW-PRESSURE DISCHARGE

S.P. NIKULIN^{1,2}

¹*Institute of Electrophysics, UB, RAS, Yekaterinburg, Russia*

²*Ural Federal University, Yekaterinburg, Russia*

e-mail: nikulin@iep.uran.ru

Tonks-Langmuir free-fall theory [1] and different hydrodynamic models of plasma [2] use the Boltzmann's law to describe electron space distribution. This assumption is valid if plasma potential is higher significantly than anode potential. At the same time a positive anode fall was observed in many experiments. In our opinion, the reason of the discrepancy is the unjustified neglect of the contribution made by the primary electrons to the plasma concentration.

We have developed a hydrodynamic model of plasma, which takes into account both secondary and primary electrons. The quasi-neutrality condition was written in the following form

$$n = n_i = n_e + n_1, \quad (1)$$

where n is the plasma concentration, which coincides with the concentration of ions n_i , n_1 and n_e are the concentrations of primary and secondary electrons, respectively.

It was believed that the primary electrons are uniformly distributed in the plasma, and the ionization of atoms is carried out only by the primary electrons. For secondary electrons and ions, the equations of continuity and motion were used in the following form

$$\frac{d}{dx}(n_i v_i) = \nu_i n_1, \quad (2)$$

$$\frac{d}{dx}(n_e v_e) = \nu_i n_1 \quad (3)$$

$$M n_i v_i \frac{dv_i}{dx} + \nu_i n_1 M v_i = -e n_i \frac{d\varphi}{dx}, \quad (4)$$

$$M n_e v_e \frac{dv_e}{dx} + \nu_i n_1 M v_e = e n_e \frac{d\varphi}{dx} - k T_e \frac{dn_e}{dx} \quad (5)$$

where M and m are masses of ion and electron, respectively, v_i and v_e are the average velocities of ions and secondary electrons, T_e is the electron temperature, ν_i is the ionization frequency, φ is the potential.

It turned out that a solution of the system (1-5) with a plasma potential higher than the anode potential is possible if the ionization frequency is higher than some critical value. At lower ionization frequencies, it is possible to obtain a solution with a plasma potential below the anode potential.

REFERENCES

- [1] L. Tonks and I. Langmuir, "General Theory of the Plasma of an Arc", Phys. Rev. 34, 876, 1929.
- [2] R.C. Bissell, P.C. Johnson, and P.C. Stangeby, "A review of models for collisionless one-dimensional plasma flow to a boundary", Phys. Fluids. B 1(5) 1133-1140, 1989.

EFFECT OF BREMSSTRAHLUNG ON THE CHARACTERISTIC GROWTH LENGTH OF AN AVALANCHE OF RUNAWAY ELECTRONS *

E. V. ORESHKIN

P. N. Lebedev Physical Institute, RAS, Moscow, Russia

e-mail: Oreshkin@lebedev.ru

In avalanches of runaway electrons, which are formed in high-altitude atmospheric discharges, the average electron energy is several megaelectronvolts [1]. For such high-energy electrons, the loss of energy by bremsstrahlung is significant when they collide with gas atoms [2]. The aim of this study was to evaluate the effect of bremsstrahlung on the exponential growth length of a runaway electron avalanche. It has been shown that taking account of the bremsstrahlung produced by the electrons of an avalanche gives corrections of no more than a few percent to the avalanche exponential growth length. The corrections are maximum for electric field strengths close to the threshold below which the avalanche electrons fail to become continuously accelerated. The effect of bremsstrahlung decreases with increasing electric field strength. The higher the atomic number of the gas in which an avalanche of runaway electrons propagates, the greater the corrections.

REFERENCES

- [1] Gurevich, A. V., & Zybin, K. P. "Runaway breakdown and electric discharges in thunderstorms." *Physics-Uspekhi*, 44(11), 1119, 2001.
- [2] Oreshkin, E. V., Barenholts, S. A., Chaikovsky, S. A., Oginov, A. V., Shpakov, K. V., & Bogachenkov, V. A. "Bremsstrahlung of fast electrons in long air gaps." *Physics of plasmas*, 19(1), 013108, 2012.

* The work was supported by the Russian Science Foundation (grant No. 19-79-00280).

Section 2

GAS-DISCHARGE METHODS FOR SURFACE MODIFICATION AND COATING DEPOSITION:

surface modification,
ion implantation,
combined methods
of surface treatment

MULTI-CYCLE MODIFICATION OF 40CR STEEL BY IRRADIATING THE "FILM (Si (0.2 μM) + Nb (0.2 μM)) / SUBSTRATE (40CR STEEL)" SYSTEM BY AN INTENSIVE PULSED ELECTRON BEAM*

N.N. KOVAL, YU.F. IVANOV, V.V. SHUGUROV, A.D. TERESOV, E.A. PETRIKOVA

Institute of High Current Electronics, SB RAS, Tomsk, Russia

e-mail: yufi55@mail.ru

The modification of the surface layer of 40Cr steel, performed by multi-cycle high-speed melting of the "film (Si + Nb) / substrate (40Cr steel)" system with an intense pulsed electron beam with an impact area of several square centimeters was implemented in a single vacuum space on COMPLEX setup [1]. For this purpose, thin (0.2 μm each) films of silicon and niobium were successively deposited to the polished surface of the specimens. The deposition of a silicon film was carried out by the magnetron method, and niobium films - by an arc discharge method with plasma assistance. Next, the resulting "film / substrate" system was irradiated with a pulsed electron beam in the selected mode. A similar procedure was repeated up to five times (1, 2, 3, 4, and 5 cycles of modification of the steel surface layer).

The mode of irradiation of the "film (Si (0.2 μm) + Nb (0.2 μm)) / substrate (40Cr steel)" system with an intense pulsed electron beam (20 J/cm², 200 μs , 3 pulses, 3 cycles), which makes it possible to form a surface layer characterized by high hardness, more than 3 times higher than the hardness of 40Cr steel in the initial (ferrite-pearlite structure) state, and wear resistance, more than 90 times higher than the wear resistance of the original 40Cr steel, was revealed. It is shown that high strength and tribological properties of steel are due to the formation of particles of the hardening phase (niobium silicides of Nb₅Si₃ composition). It has been established that the multi-cycle mode of modification of 40Cr steel makes it possible to form a thermally stable state in the surface layer of the material, the hardness of which exceeds hardness of the initial state of 40Cr steel by more than 20%, wear resistance - more than 20 times after annealing for 3 hours at a temperature of 650°C.

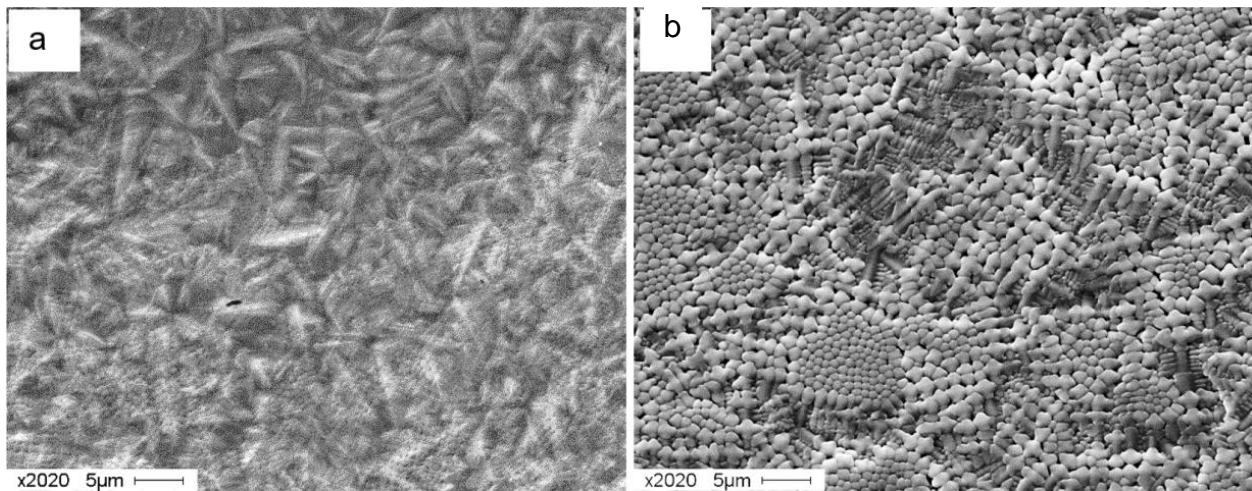


Fig. 1. SEM image of the surface structure of specimen of 40Cr steel, formed as a result of irradiation of the "film (Si (0.2 μm) + Nb (0.2 μm)) / substrate (40Cr steel)" system by a pulsed electron beam with parameters 20 J/cm², 3 pulses (a) and 30 pulses (b). Three-cycle processing.

The results obtained can be recommended for use in industry in surface treatment of parts operating in friction pairs under increased temperature-power operating conditions.

REFERENCES

- [1] Koval N.N., Ivanov Yu.F. // Russian Physics Journal. - 2019. - V. 62. - pp. 1161-1170.

* The work was supported by RFBR project No. 19-08-00248.

CHARGE AND ELEMENTAL COMPOSITION OF PLASMA GENERATED BY SPUTTERING OF POWDER TARGET FROM AMORPHOUS BORON*

YU.F. IVANOV, V.V. SHUGUROV, O.V. KRYSINA, V.E. PROKOP'EV

Institute of High Current Electronics, SB RAS, Tomsk, Russia

e-mail: yufi55@mail.ru

The purpose of the present studies is to develop a method for the formation and study of parameters (electron temperature, plasma potential and concentration), elemental and charge composition of plasma generated by sputtering of a boron powder target. The target was amorphous boron, powder with "A" grade (TU 2112-001-49534204-2003) of the following composition (wt.%): B – 96.2, Fe – 0.3, Si – 0.2, H₂O – 0.3.

Experiments were carried out in a COMPLEX equipment [1]. The scheme of the experiment is shown in Fig. 1, a. Input of high-frequency (HF) radiation 6 with electrode-holder of boron powder 8 is installed in sputtering chamber 9. On the upper flanges of the vacuum chamber there is a window from quartz glass 2 for spectroscopic measurements and a flange with a cylindrical Langmuir probe 4 for probe measurements of plasma parameters. Gas plasma was created using a PINK plasma source with thermionic and hollow cathodes. Argon was used as a working gas at a pressure of (0.5-0.6) Pa.

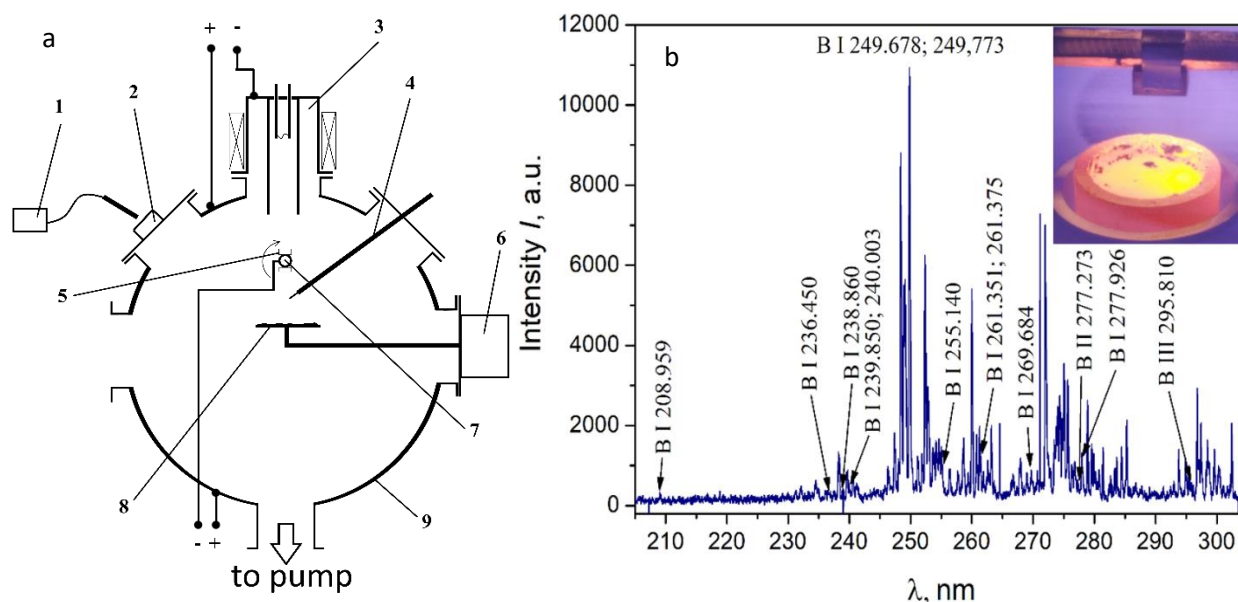


Fig. 1. Scheme of experiment (a): 1 – spectrometer with light guide; 2 – window with quartz glass; 3 – PINK gas plasma generator; 4 – Langmuir cylindrical probe; 5 – treated samples; 6 – RF generator with matching device; 7 – thermocouple; 8 – RF electrode with boron powder suspension; 9 - working vacuum chamber; an optical radiation spectrum of plasma (b) generated during sputtering of a powder target from amorphous boron in the wavelength range of (205-305) nm (parameters: gas – Ar, $p = 0.2$ Pa, $W = 600$ W). On insert (b) there is a fully heated anode-crucible with boron powder.

The optimization was carried out and the samples of sintered boron powder in graphite crucibles with a diameter of 35 mm and a powder filling thickness of up to 8 mm were obtained (Fig. 1, b, insert). This system is used to obtain sintered cathodes from boron powder for an arc evaporator with a hot cathode. A pulsed arc evaporator with a hot cathode made of sintered boron powder was developed, designed, produced and tested. Charge and elemental composition of boron-containing plasma generated during powder target sputtering from amorphous boron are determined by spectrometry method. It was shown that the generated plasma contains mainly neutral atoms and single-charge boron ions, as well as iron, silicon, copper and argon (Fig. 1, b).

REFERENCES

- [1] Koval N. N., Ivanov Yu. F. // Russian Physics Journal. - 2019. – V. 62. - pp. 1161-1170.

* The work was supported by RSF project No. 19-19-00183.

STRUCTURE AND PROPERTIES OF HIGH-CHROMIUM STEEL IRRADIATED WITH A PULSED ELECTRON BEAM AND NITRIDED IN A LOW-PRESSURE GAS DISCHARGE PLASMA*

YU.F. IVANOV, E.A. PETRIKOVA, A.D. TERESOV, S.V. LYKOV, M.E. RYGINA

Institute of High Current Electronics, SB RAS, Tomsk, Russia

e-mail: yufi55@mail.ru

The aim of this work is to establish the regularities of the formation of the structure and properties of AISI 310 steel, subjected to complex processing, combining irradiation with an intense pulsed electron beam and subsequent nitriding in the plasma of a low-pressure gas discharge using a PINK plasma generator. Irradiation of steel was carried out on an SOLO electron-beam setup with an electron source based on a pulsed low-pressure arc discharge with grid stabilization of the cathode plasma boundary and an open anode plasma boundary [1]. Irradiation was carried out with the following parameters: the energy of accelerated electrons $eV = 18$ keV; electron beam energy density E_S (J/cm^2) = 10, 20 and 30; pulse duration τ (μs) = 50 and 200; the number of pulses of exposure $N = 3$; pulse repetition rate $f = 0.3$ s^{-1} ; residual gas pressure (argon) in the working chamber ~ 0.02 Pa. Steel nitriding was carried out on a modernized unit of NNV-6.6-II type, equipped with a PINK plasma generator. The nitriding temperature was 723 K, 793 K and 873 K, the nitriding time - 1, 3, 5 hours. The structure and phase composition of the material was studied by scanning and transmission diffraction electron microscopy and X-ray diffraction analysis. The properties of the modified layer were characterized by microhardness and wear resistance.

It has been established that AISI 310 steel in the initial state is a polycrystalline material. Globular particles of the second phase (chromium and iron carbides) of submicron sizes are located in the bulk and along the grain boundaries. It has been shown that electron-beam processing of steel leads to the dissolution of globular particles of the carbide phase and the formation of a cellular crystallization structure [2]. Along the boundaries of the cells, nanosized (≈ 25 nm) particles of chromium and iron carbides are located, which stabilize the defective substructure of the material. Subsequent nitriding of steel is accompanied by the formation of chromium and iron nitrides and carbonitrides in the surface layer, the relative content of which depends on the parameters of combined processing. It was found that the highest tribological properties are possessed by steel samples, the complex processing of which was carried out with the following parameters: irradiation with a pulsed electron beam of 30 J/cm^2 , 200 μs , 3 pulses; subsequent nitriding at a temperature of 973 K for 3 hours. In this case, the wear resistance of the steel exceeds the wear resistance of the initial material by more than 100 times. The hardness of the surface layer of steel modified with these parameters exceeds the hardness of the original material by more than 12 times. The performed studies of the structure and phase composition of the modified steel made it possible to make assumptions about the physical mechanisms that make it possible to multiply the tribological and strength properties of AISI 310 high-chromium steel.

REFERENCES

- [1] Koval N.N., Ivanov Yu.F. // *Izvestiya VUZov. Fizika.* - 2008. - №5. - pp. 60-70 [in Russian].
- [2] Ivanov Yu.F., Petrikova E.A., Teresov A.D., Ivanova O.V. // *Izvestiya VUZov. Fizika.* - 2019. -V. 62. - №11. - pp. 112-116 [in Russian].

* The work was supported by RFBR project No. 19-48-700010.

NUMERICAL ESTIMATION OF THE SPUTTERING COEFFICIENT OF COPPER ANODE OF A PLANAR MAGNETRON BY A BEAM OF ACCELERATED ARGON IONS WITH ENERGY OF 1-10 keV*

A.P. SEMENOV, I.A. SEMENOVA, D.B-D. TSYRENOV, E.O. NIKOLAEV

Institute of Physical Materials Science, SB, RAS, Ulan-Ude, Russia

e-mail: alexandersemenov2018@mail.ru

In the approximation of kinetic energy transfer in collision cascades [1, 2], a numerical estimate of the coefficient of sputtering of the central copper anode of a planar magnetron by an accelerated beam of argon ions in the design of a sputtering gas-discharge device is considered [3].

Based on the solution of the equations of the cascade theory [1], the formula for calculating the copper sputtering coefficient $Y_{Cu}(0)$ for kiloelectron-volt energies and average masses of sputtering ions can be led to the form

$$Y_{Cu}(0) = \frac{0,467\alpha e^2 \alpha_o s_n(\varepsilon)}{U_o} \cdot \frac{Z_{Ar} Z_{Cu}}{\left(Z_{Ar}^2 + Z_{Cu}^2 \right)^{\frac{2}{3}}} \cdot \frac{M_{Ar}}{(M_{Ar} + M_{Cu})}, \quad (1)$$

where α - dimensionless ratio function M_{Cu}/M_{Ar} sputtered atom mass to atomizing ion mass; α_o - Bohr radius; Z_{Ar} , Z_{Cu} – atomic numbers; e^2 - electron charge square; $s_n(\varepsilon)$ - reduced nuclear deceleration cross section for the Thomas-Fermi interaction; U_o – sublimation energy Cu.

Calculated dependence of the sputtering coefficient at normal incidence of ions $\theta = 0$ (θ – angle of incidence of ions) on the ion energy is shown in Fig. 1, which is in good agreement with the experimental values of the sputtering coefficients of Cu by the Ar^+ ions in the energy range of 1-10 keV [2].

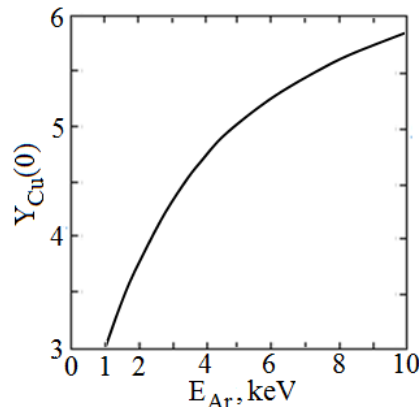


Fig. 1. Calculated energy dependence of the copper sputtering coefficient on energy of sputtering argon ions.

It is shown that when a 1-10 keV and 4 mA ion beam is injected into a magnetron, the sputtering coefficient of the copper anode of the magnetron is 3-6 atoms (Fig. 1) per incident ion. Which makes it possible to introduce and control with high accuracy and in small fractional ratios (units at.%) an impurity, in particular, copper in the conditions of synthesis of superhard TiN-Cu coatings by reactive sputtering in a magnetron discharge and to affect directly to the nanocrystalline structure of the coatings.

REFERENCES

- [1] P. Sigmund, "Theory of sputtering. 1. Sputtering yield of amorphous and polycrystalline targets," *Phys. Rev.*, vol.184, No. 2, pp. 383-416, 1969.
- [2] M.D. Gabovich, N.V. Pleshivtsev, N.N. Semashko, *Ion and atom beams for controlled thermonuclear fusion and technological purposes*. Moscow: Energoatomizdat, 1986.
- [3] A.P. Semenov, I.A. Semenova, D.B-D. Tsyrenov, E.O. Nikolaev, "A gas-discharge sputtering device based on a planar magnetron with an ion source," *Instruments and Experimental Techniques*, vol. 63. No. 5, pp. 782–786, 2020.

* This study was supported by the Russian Foundation for Basic Research (project no. 20-08-00207_a) and the State Job of the Ministry of Science and Education of the Russian Federation (topic no. 0270-2021-0001).

FEATURES OF THE DISCHARGE AND DEPOSITION OF THE CrN_x COATINGS WHEN USING MAGNETRON WITH A HOT TARGET

G.A. BLEYKHER, V.A. GRUDININ, D.V. SIDELEV, V.P. KRIVOBOKOV

Tomsk Polytechnic University, Tomsk, Russia
e-mail: bga@tpu.ru

Our previous studies have shown that the use of a hot chromium target undergoing sublimation can significantly increase the deposition rate of chromium coatings during the operation of magnetron sputtering systems [1, 2]. This circumstance was used for the synthesis of coatings based on chromium-nitrogen compounds, which are of great interest for various industries. It seems that in this case it will be possible to significantly increase the productivity of applying such coatings to the surface of products.

A new scheme for the synthesis of CrN_x films in an atmosphere of argon and nitrogen during the operation of a magnetron sputtering system has been developed and implemented in experiments. Its specifics are as follows. The inlet of argon and nitrogen is carried out separately in the space of the vacuum chamber. A magnetron with a hot chromium target operates in a metallic mode and creates a flow of atomic chromium particles on the substrate. To increase the reactivity of nitrogen, an assisting radio-frequency inductively coupled plasma (RF-ICP) source is used. The regions of the RF-ICP discharge and the nitrogen flow into the chamber are combined and are significantly distant from the region of the magnetron discharge localization. Experiments have shown that this technique reduces the flow of nitrogen particles to the surface of the magnetron target (i.e., prevents its "poisoning") and provides conditions for intensive dissociation and ionization of nitrogen, which are necessary for the synthesis of chromium nitride on the substrate surface.

The effect of target heating on the functioning of the magnetron discharge is investigated. It is shown that under these conditions there is practically no hysteresis in the behavior of current and voltage depending on the rate of nitrogen flow into the chamber. Analysis of the target substance after a series of experiments showed the absence of chromium and nitrogen compounds in it. The contribution of the sublimation of the chromium target to the increase in the deposition rate of the chromium and CrN_x coating with the increase in the magnetron power is revealed experimentally and by calculations. The kinetics of the particles entering the substrate during the coating formation is studied. The balance of the fluxes of various types of particles and energy on the substrate is constructed, and its heating is analyzed depending on the power of the magnetron, the RF-ICP source, and the nitrogen input into the chamber. It is shown that for this deposition scheme, an increase in the rate of nitrogen flow into the chamber leads to an increase in the growth rate of the CrN_x-based coating. The elemental composition and structure of the formed coatings are studied depending on various parameters that control the deposition.

REFERENCES

- [1] D.V. Sidelev, G.A. Bleykher, V.P. Krivobokov, Z. Koishybayeva, "High-rate magnetron sputtering with hot target", *Surf. Coat. Technol.*, vol. 308, pp. 168-173, 2016.
- [2] G.A. Bleykher, D.V. Sidelev, V.A. Grudin, V.P. Krivobokov, M. Bestetti, "Surface erosion of hot Cr target and deposition rates of Cr coatings in high power pulsed magnetron sputtering", *Surf. Coat. Technol.*, vol. 354, pp. 161-169, 2018.

DEVELOPMENT OF THE COMPUTER MODEL OF THE PLASMA INSTALLATION*

R.A. OKULOV^{1,2}, E.V. POPOV¹, B.R. GELCHINSKI¹, A.A. REMPEL¹

¹*Institute of Metallurgy, UB, RAS, Yekaterinburg, Russia*

²*Ural Federal University named after the first President of Russia B.N. Yeltsin, Yekaterinburg, Russia*

e-mail: okulov.roman@gmail.com

Improvement of technology and equipment, allowing to create protective coatings, is an urgent scientific and technical task [1]. Plasma installations are widely used in the creation of functional coatings [2]. The plasma method is also used to produce nanodispersed powders, including those used in additive technologies [3].

In the coating process, powder materials are used as raw materials, which are fed into the plasma flow. The degree of heating depends on the point of introduction of powder raw materials, which affects the quality of the applied coatings. The result of coating and powder production is influenced by several factors. The temperature of the plasma jet plays a special role. Developers and consumers of technological equipment need to consider the temperature distribution in the space of the plasma jet to select a rational area for inputting raw materials. Therefore, the determination of the temperature of the flow of a plasma jet is an urgent task and determines the scientific significance. The purpose of the article is to create an objective computer model of a plasma installation that allows an adequate description of the plasma jet flow. The problem is solved numerically using the ANSYS software package, which implements the finite element method.

In the literature, the use of finite element analysis for solving such problems is described quite fully [4]. As a prototype for creating a computer model, a laboratory plasma installation in IMET UB RAS was adopted, which is used both for coating and to produce powders.

To verify the results of the computer experiment, a full-scale experiment was carried out to establish the temperature value at a characteristic point. The results were averaged and compared with the results of a numerical experiment. Comparative analysis of the results of numerical and field experiments showed satisfactory convergence. To assess the statistical error, a few parallel experiments were carried out and methods of statistical data processing were used. A histogram of the distributions of the results of measurements of the numerical experiment was constructed and it was demonstrated that the distribution of the investigated quantity at the characteristic point obeys the normal Gaussian distribution law.

The presented results are of practical use for manufacturers and consumers of technological equipment. The presented computer model makes it possible to predict the parameters of the plasma jet.

REFERENCES

- [1] S.V. Anakhov, Yu.A. Pykin, and A.V. Matushkin, "Gas vortex stabilization in plasma torches: new solutions", *Welding International.*, vol. 30, iss. 5, pp. 408-412, 2016.
- [2] P. Wei, Z. Wei, G. Zhao, J. Du, and Y. Bai, "The analysis of melting and refining process for in-flight particles in supersonic plasma spraying", *Computational Materials Science.*, vol. 103, pp. 8-19, 2015.
- [3] S. Sunpreet, R. Seeram, and S. Rupinder "Material issues in additive manufacturing: A review", *Journal of Manufacturing Processes.*, vol. 25, pp. 185-200, 2017.
- [4] S. Masaya and W. Takayuki, "Effect of precursor fraction on silicide nanopowder growth under thermal plasma conditions: A computational study", *Powder Technology.*, vol. 288, pp. 191-201, 2016.

* The work was supported in part by the RFBR Grant Nos. 20- 21-00063.

BALANCED CONTROL OF THERMAL IMPACT ON METAL MATERIALS IN ELECTRON SOURCE WITH A PLASMA CATHODE*

K.T. ASHUROVA¹, T.V. KOVAL², M.S. VOROBYOV¹, MY KIM AN TRAN³, V.I. SHIN¹, P.V. MOSKVIN¹, N.N. KOVAL¹

¹*Institute of High Current Electronics SB RAS, Tomsk, Russia*

²*Tomsk Polytechnic University, Tomsk, Russia*

³*Ton Duc Thang University, Ho Chi Minh, Vietnam*

e-mail: 11k.ashurovak@gmail.com

The main objective of this work is a theoretically and experimentally demonstrate the possibility of holding the surface temperature when exposed to a submillisecond modulated megawatt electron beam with a controlled variable power, as well as numerical simulation and comparison with experiment. To study the possibility of controlling the temperature field and depth of the sample melted layer by the numerical simulation.

The mathematical formulation of the problem of the temperature field dynamics under the high-energy action of the electron beam on the sample consists of writing the heat transfer equation taking into account the assumed assumptions of the mathematical model, boundary and initial conditions. In the experiment, the electron beam is low-energy (the electron beam energy is < 15 keV), the beam diameter is much greater than the heating depth per irradiation pulse. Therefore, it is possible to consider the source of energy impact as surface, and consider the thermal processes in the sample in a one-dimensional approximation.

The mathematical model includes the presence of a two-phase zone, which in the solid-liquid system is characterized by the average volume fraction of the liquid phase θ [1, 2]. The phase transition occurs in the temperature range ΔT , in which the material phase, is modelled by a smoothed function θ , varying from 1 to 0. The effective thermal conductivity of the solid-liquid system λ is related to the conductivity of the solid λ_s and the conductivity of the liquid λ_l : $\lambda = (1 - \theta)\lambda_s + \theta\lambda_l$, the density of the two-phase region and the heat capacity were considered, the latent heat of fusion L is included as an additional term in the heat capacity: $c = c_s + L/\Delta T$:

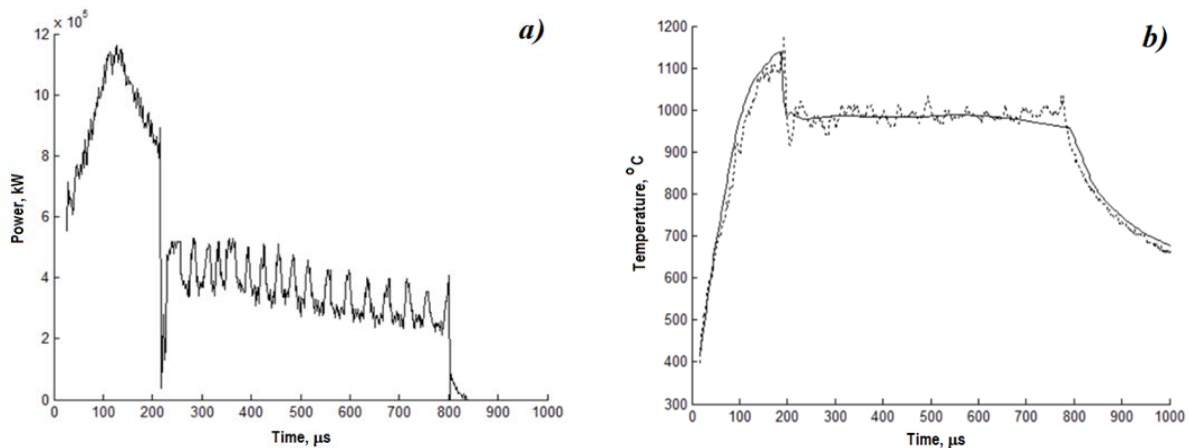


Fig. 1. (a) Change of the power of the heat source, and (b) calculated (—) and experimental surface temperature (---).

Fig. 1a shows the power of the heat source. The calculated surface temperature $T(t)$ (Fig. 1b) obtained for experimental current and voltage pulses is in good agreement with experimental temperature measurements. The pulsed character of the $T(t)$ dependence while maintaining the surface temperature is associated with oscillations of the beam current.

REFERENCES

- [1] S.H. Chen, D.H. Cho, G. Kocamustafaogullary, "Melting and Solidification with Internal Radiative Transfer – A Generalized Phase Change Model," Intern. J. Heat Mass Transfer, 1983, vol. 26, pp. 621.
- [2] A.Yu. Vorob'ev, V.A. Petrov, V.E. Titov, "Fast heating and melting of alumina under the effect of concentrated laser radiation," High Temperature, 2007, vol. 45, pp.478–487. (in Russian)

*This work was supported by the Russian Science Foundation (project No. 20-79-10015).

PLASMA MODIFICATION OF THE SURFACE OF A STEEL PRODUCT USING THE MAK-10 INSTALLATION*

S.A. IL'INYH, S.A. AHMETSHIN, V.A. KRASHANININ, B.R. GELCHINSKI, A.A. REMPEL

Institute of Metallurgy, UB, RAS, Yekaterinburg, Russia
e-mail: b.gelchiski@gmail.com

This paper presents the results of surface modification of steel samples used in drilling equipment. Samples with high tribological characteristics were obtained. The work was carried out using a plasma modification unit UPM MAK-10, created by us at IMET UB RAS. The installation works with arc plasmatrons of direct (direct and reverse polarity) and indirect action with power up to 10 kW. The versatility of UPM MAK-10 lies in its mobility, both when moving in space, and when reconfiguring the power module for various technological operations: finishing plasma hardening, plasma surfacing using filler materials, argon-arc welding in an inert gas environment with direct and alternating current.

Samples of tool steel ($40 \times 20 \times 15$ mm) were used as the material for the modification. Strengthening was carried out with the following characteristics: anode nozzle diameter 10 mm; the distance from the nozzle exit to the sample surface is 15 mm; the speed of movement of the plasmatron along the sample was chosen such as to prevent fusion. The width of the heat-affected zone in this case reached 12-15 mm per 1 pass.

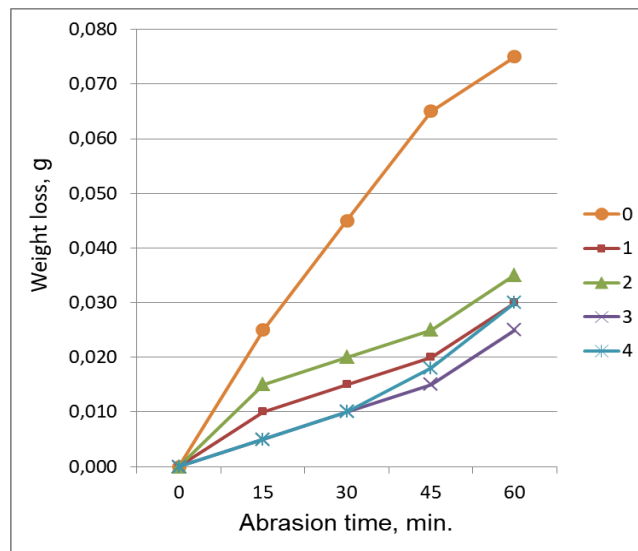


Fig. 1. Wear resistance of samples of tool steel with surface modification.

The studies of the wear resistance of the samples were carried out at IMET UB RAS on an upgraded SMT-1M friction machine with a digital unit for measuring parameters according to the stationary shoe scheme tool steel sample ($40 \times 20 \times 15$ mm) - a hard rotating disk (counterbody). The weight of the samples was measured on a high-precision balance MWP-150 with an accuracy of 0.005 g. Proceeding from this, it can be argued that the measurement error is not more than 3%.

For a comparative analysis of the degree of wear of steel samples after plasma surface modification, the constancy of the parameters characterizing the operation of the friction machine was observed: the rotation speed of the counterbody $v = 200$ rpm, the load on the sample $P = 200$ N. Each of the samples was worn out for 1 hour. Every 15 minutes the machine was stopped and the sample was weighed.

From the experimental results for five samples (Fig. 1), it follows that the wear of plasma-hardened samples (samples 1 to 4) of tool steel is much lower (2-2.5 times) than that of an unmodified sample (0 sample). Samples (1-4) differ in the operating modes of the plasma installation for a current from 100 to 200 A. In this case, the best (curves 3 and 4) are observed at a higher current.

* The work was supported in part by the RFBR Grant Nos. 20- 21-00063.

DEPOSITION OF TiSiCN COATINGS BY DECOMPOSITION OF HEXAMETHYLDISILAZANE AND ANODIC EVAPORATION OF TITANIUM IN A LOW-PRESSURE ARC DISCHARGE *

A.I. MEN'SHAKOV^{1,2}, YU.A. BRYUHANOVA¹, YU.S. SURKOV¹, A.V. CHUKIN²

¹ Institute of Electrophysics UB RAS, Yekaterinburg, Russia

² Ural Federal University named after the first President of Russia B.N. Yeltsin, Yekaterinburg, Russia

e-mail: aim@iep.uran.ru

Method of deposition of TiSiCN-coatings by anodic evaporation of Ti and decomposition of organosilicon precursor (hexamethyldisilazane, HMDS) in nitrogen-argon low-pressure (~1 mTorr) hollow cathode arc discharge was investigated (Fig. 1). The analysis of plasma composition by optical emission spectroscopy was carried out. The influence of discharge current (10-50 A), flow of HMDS (1-10 g/h) and Ti-vapors flow on plasma composition and HMDS decomposition degree was investigated. It is shown that the proposed method provides both an intense flow and a high activation degree of metal vapors, and a sufficient degree of decomposition of precursor vapors for the formation of solid TiSiCN coatings at a high deposition rate. On the surface of samples made of stainless steel TiSiCN-coatings up to 6 μm thick with hardness up to 31 GPa were obtained during 1 hour at 400°C. Coatings composition was analyzed by FTIR and XRD methods, the influence of the deposition conditions on the hardness of the resulting coatings has been studied.

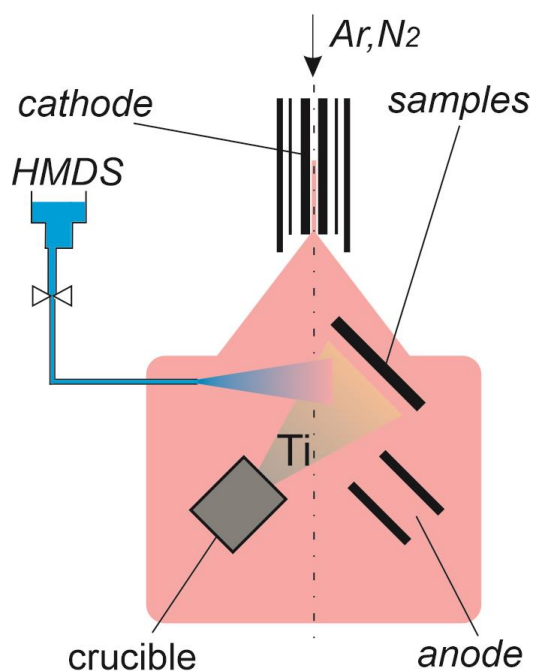


Fig. 1. Experimental scheme of discharge system.

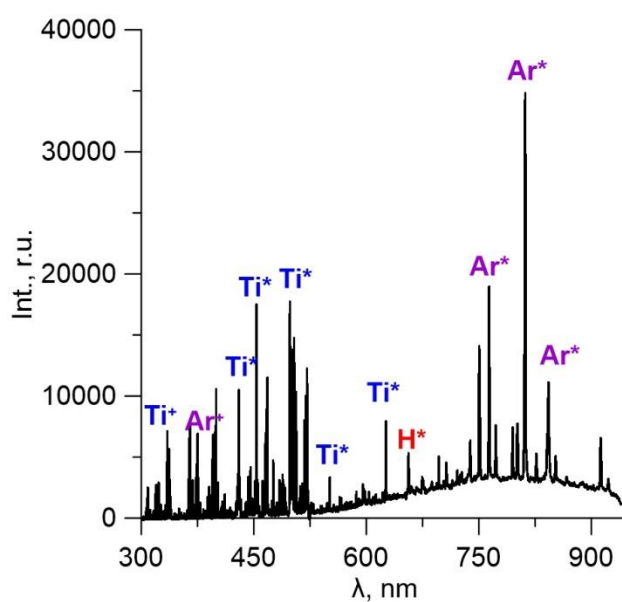


Fig. 2. The optical spectrum of discharge plasma in a mixture of Ar+N₂+Ti+HMDS. P_{Total}=0.7 mTorr, discharge current 20 A, Q_{HMDS}=4 g/h.

* The study was financially supported by the Russian Science Fund, grant No. 20-79-10059.

EFFECT OF 3d IONS IMPLANTATION ON ELECTRONIC STRUCTURE OF V₂O₅ BASED CATHODE FOR LITHIUM-ION BATTERIES*

L.S. ZHIDKOV^{1,2}, A.I. KUKHARENKO¹, D.A. ERZUNOV¹, S.O. CHOLAKH¹, N.V. GAVRILOV³, E.Z. KURMAEV^{1,2}

¹*Ural Federal University, Yekaterinburg, Russia*

²*Institute of Metal Physics, UB, RAS, Yekaterinburg, Russia*

³*Institute of Electrophysics, UB, RAS, Yekaterinburg, Russia*

e-mail: i.s.zhidkov@urfu.ru

The need for energy storage devices of elevated efficiency becomes obvious under the actual conditions of rising demand in various application fields of highly energy-consuming applications, such as electric and hybrid vehicles. Among the present-date devices, the lithium-ion batteries (LIB) enjoy a considerable success on the market, due to a broad range of applications they may serve, from portable or implantable medical devices to the electric transport vehicles and electric networks. To match the rising demands by new technologies, the next-generation LIB must possess elevated energy density and combine good performance parameters with high safety standards and low cost. In the contents of properties of the materials involved, the capacity and disposability of LIB are usually conditioned by the development of cheap and highly efficient cathode materials. Layered lithium-cobalt mixed oxide (LiCoO₂) was the first cathode material which found use in commercial LIB. If a total removal of lithium would, in theory, yield as high capacity as about 274 mAh/g, the Li_{1-x}CoO₂ structure turned out to be unstable at low lithium content (x>0.5); therefore, the useful specific capacity of LiCoO₂ is lower than 150 mAh/g. Moreover, LiCoO₂ is expensive and highly toxic material, that, on one hand, boosts its production costs, and, on the other hand, is damaging for environment. Under this perspective, the use of LiNiO₂ might look preferential, due to its lower cost per given energy density, yet the synthesis of LiNiO₂ is much more complex than that of LiCoO₂.

Among other materials under discussion for the use as LIB cathodes, vanadium pentoxide (V₂O₅) attracted attention due to its high attainable energy density, low cost, broad availability and easy conditions of synthesis, combined with acceptable safety properties [1]. The theoretical capacity of V₂O₅ reaches about 294 mAh/g, by far higher than in other conventionally used cathode materials (150 mAh/g for LiCoO₂, 170 mAh/g for LiFePO₄, 148 mAh/g for LiMn₂O₄), that makes V₂O₅ a promising candidate for next-generation LIB. Unfortunately, low diffusion coefficient of Li⁺ ions and moderate electrical conductivity are obstacles for a broad use of V₂O₅. These shortcomings can be hopefully healed via cation doping, which is considered an efficient way to improve the intercalation of lithium ions. Indeed, V₂O₅ doped with Ni²⁺ exhibited reversible capacitance of 262 mAh/g at 1C [2]. The doping with Mn²⁺ brings about the formation of oxygen vacancies, that facilitates the diffusion of Li⁺ ions and improves the electron conductivity [3]. Similarly, V₂O₅ doped with Cu⁺ ions delivered higher reversible specific capacities, better cycling stabilities and excellent rate capabilities [4].

The abovementioned improvements of the V₂O₅ performance are largely based on empirical studies. A deep understanding of underlying physics, which would facilitate intentional optimization of certain target properties, is largely absent. This concerns the microstructure of doping (substitution or interstitial sites, creation of vacancies or other secondary defects etc.) as well as the related electronic structure (formation of localized states, charge transfers and charge states of different atoms). Both these aspects would affect the placement and drift of lithium ions, as well as electron transport. The aim of the present study is to contribute to elucidating these issues, by combined efforts from experiment and theory. We provide the XPS and DFT results for the V₂O₅ cathode materials implanted with 3d ions (Cu, Ni etc.).

REFERENCES

- [1] Y. Wang, K. Takahashi, K.H. Lee, G.Z. Cao, Nanostructured vanadium oxide electrodes for enhanced lithium-ion intercalation, *Adv. Funct. Mater.*, 16, 1133–1144, 2006.
- [2] F. Ding, W. Xu, G.L. Graff, J. Zhang, M.L. Sushko, X. Chen, Y. Shao, M.H. Engelhard, Z. Nie, J. Xiao, X. Liu, P.V. Sushko, J. Liu, J.G. Zhang, Dendritefree lithium deposition via self-healing electrostatic shield mechanism, *J. Am. Chem. Soc.*, 135, 4450–4456, 2013.
- [3] J.M. Cocciantelli, J.P. Doumerc, M. Pouchard, M. Broussely, J. Labat, Crystal chemistry of electrochemically inserted Li_xV₂O₅, *J. Power Sources*, 34, 103–111, 1991.
- [4] H. Yu, X. Rui, H. Tan, J. Chen, X. Huang, C. Xu, W. Liu, D.Y.W. Yu, H.H. Hng, H.E. Hoster, Q. Yan, Cu doped V₂O₅ flowers as cathode material for high-performance lithium ion batteries, *Nanoscale*, 5, 4937–4943, 2013.

* The work was supported by the grant program of the President of Russian Federation (grant No. MK-989.2020.2).

DEPOSITION OF Al_2O_3 COATINGS IN Ar- O_2 LOW-PRESSURE DISCHARGE PLASMA UNDER HIGH DISSOCIATION DEGREE OF O_2^*

P.V. TRETIKOV¹, N.V. GAVRILOV¹, A.S. KAMENETSKIKH¹, S.V. KRIVOSHAPKO¹, A.V. CHUKIN²

¹Institute of Electrophysics, UB, RAS, Yekaterinburg, Russia

²Ural Federal University, Yekaterinburg, Russia

e-mail: tpetr@iep.uran.ru

The Al_2O_3 coating with a corundum structure was deposited by anodic evaporation in a low-pressure arc with a self-heated hollow cathode. The conditions were created for increasing the energy of plasma electrons and a corresponding increase in the frequency of O_2 dissociation by contraction of the discharge in the anode region [1]. The discharge was maintained in a combined mode with a constant current level (70-100 A), on which pulses (100 μs , 1 kHz) with an amplitude adjustable to 220 A were superimposed. This mode ensured a change in the degree of O_2 dissociation ($n_{\text{O}} / 2n_{\text{O}_2}$, there n – concentration of atomic O and molecular O_2 particles) in the range of 0.3 - 0.5 (Fig. 1) at constant average discharge current and Al evaporation rate. It is shown that an increase in the degree of O_2 dissociation in the indicated range leads to an increase in the rate of coating deposition by a factor of 1.3 (Fig. 1) and an promotion of the preferred (300) orientation of crystallites (Fig. 2). The effect is due to the difference in the features of the adsorption of molecular and atomic oxygen on the Al_2O_3 surface, and is consistent with the results of molecular dynamics modeling [2].

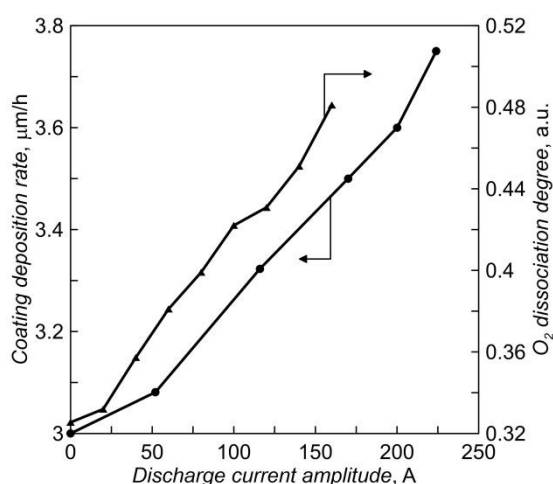


Fig. 1. The dependences of coating deposition rate and O_2 dissociation degree vs discharge current amplitude. The average discharge current 100 A.

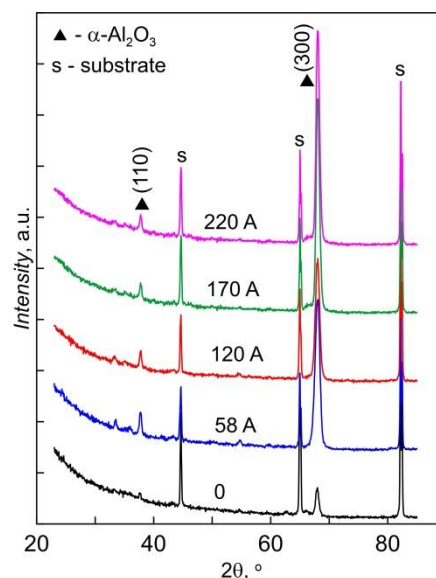


Fig. 2. XRD patterns of the Al_2O_3 coatings deposited under different discharge current amplitude. The average discharge current 100 A.

REFERENCES

- [1] N.V. Gavrilov, A.S. Kamenetskikh, P.V. Tretnikov and A.V. Chukin, "Ion assisted deposition of $\alpha\text{-Al}_2\text{O}_3$ coatings by anodic evaporation in the arc discharge," *Surf. Coat. Technol.*, vol. 337, pp. 453–460, 2018.
- [2] E. Wallin, J.M. Andersson, E.P. Munger, V. Chirita and U. Helmersson, "Ab initio studies of Al, O, and O_2 adsorption on $\alpha\text{-Al}_2\text{O}_3$ (0001) surfaces", *Phys. Rev. B*, vol. 74, p. 125409, 2006.

* The work was supported in part by RFBR, project number 20-08-00169.

IMPROVEMENT OF VACUUM SURFACE FLASHOVER VOLTAGE FOR POLYMER BY ATMOSPHERIC PRESSURE PLASMA JET*

CHENGYAN REN^{1,2}, CHUANSHENG ZHANG^{1,2}, KUN XIE¹, CHENG ZHANG^{1,2}, TAO SHAO^{1,2}

¹Beijing International S&T Cooperation Base for Plasma Science and Energy Conversion, Institute of Electrical Engineering, Chinese Academy of Sciences, Beijing, China

²University of Chinese Academy of Sciences, Beijing, China
e-mail: rcy@mail.iee.ac.cn

The surface flashover across the vacuum-insulator interface is a key factor to restrict the development of vacuum devices [1]. The surface modification of insulating materials is one of important applications for low temperature plasma. In this paper, the polytetrafluoroethylene (PTFE) film was treated by atmospheric pressure plasma jet (APPJ), and the SiO_x thin film was deposited on the PTFE surface. The effect of different processing conditions on the surface insulation properties was studied. Then the surface chemical composition and crystalline state were measured by Fourier Transform Infrared Spectrum (FTIR) and X-Ray Diffraction (XRD). The surface trap parameters and space charge distribution in PTFE film were obtained by means of isothermal surface potential decay (ISPD) and pulsed electro-acoustic (PEA). The surface resistance was also measured by high resistance meter to analyze the relationship between the surface charge and surface withstand voltage. At last the experiment of vacuum surface flashover was developed under DC and microsecond pulsed voltages. The results show that some inorganic groups (Si-O-Si and Si-OH) are introduced on the PTFE surface. After APPJ treatment, the trap density increases, the trap energy level is deeper first, and then shallower with increase of treatment time. Moreover, the space charge in PTFE shows a positive correlation with the shallow trap density. The vacuum flashover voltage of PTFE film decreases first and then increases with the treatment time. The introduced shallow trap and low surface resistance after APPJ treatment are main reasons for the enhancement of vacuum flashover voltage [2, 3].

REFERENCES

- [1] H.C. Miller, "Flashover of insulators in vacuum: the last twenty years," *IEEE Trans. Dielectr. Electr. Insul.*, vol. 22, pp. 3641-3657, 2015.
- [2] Q. Xie, H. Lin, S. Zhang, R. Wang, F. Kong, T. Shao, "Deposition of SiC_xH_yO_z thin film on epoxy resin by nanosecond pulsed APPJ for improving the surface insulating performance," *Plasma Sci. Technol.*, vol. 20, pp. 025504, 2018.
- [3] R. Wang, H. Lin, Y. Gao, C. Ren, K. Ostrikov, T. Shao, "Inorganic nanofilms for surface charge control on polymer surfaces by atmospheric pressure plasma deposition," *J. Appl. Phys.*, vol.122, pp. 233302, 2017.

* The work was supported in part by the National Natural Science Foundation of China (51977202, U1830135, 51807189).

THE EFFECT OF O₂ DISSOCIATION DEGREE ON THE RATE OF ANODIC EVAPORATION OF Al IN LOW-PRESSURE ARC*

S.V. KRIVOSHAPKO¹, N.V. GAVRILOV¹, A.S. KAMENETSKIKH¹, P.V. TRETIKOV¹, A.V. CHUKIN²

¹*Institute of Electrophysics, UB, RAS, Yekaterinburg, Russia*

²*Ural Federal University, Yekaterinburg, Russia*

e-mail: alx@iep.uran.ru

In a gas-discharge system with a self-heated hollow cathode and an anode-crucible, the use of an additional anode which collected the main fraction of the electron discharge current (up to 100 A) through the contraction channel, the degree of O₂ dissociation reaches ~ 0.25 [1]. By imposing the pulses with a duration of 100 μs, a frequency of 1 kHz on the DC discharge current, the increasing of O₂ dissociation degree and its regulation by changing the current amplitude (up to 200 A) provided [2]. The paper presents the results of probe diagnostics and emission optical spectroscopy of Ar-O₂ plasma generated under evaporation of Al and an increased (0.32 - 0.48) degree of O₂ dissociation. It is shown that an increase in the degree of O₂ dissociation at a constant gas flow into the discharge gap leads to a significant (more than 1.5 times) decrease in the density of evaporated atoms flux and a corresponding decrease in the coating deposition rate (Fig. 1). The observed effect is due to the accelerated growth of the oxide film on the melt surface, which leads to the limitation of the flow of evaporated Al atoms by the rate of diffusion through the alumina. Pulsed (1 kHz, 100 μs, 20-100 A) heating of the crucible provides an increase in the evaporation rate at low current values in the crucible circuit 3 times less than in DC mode.

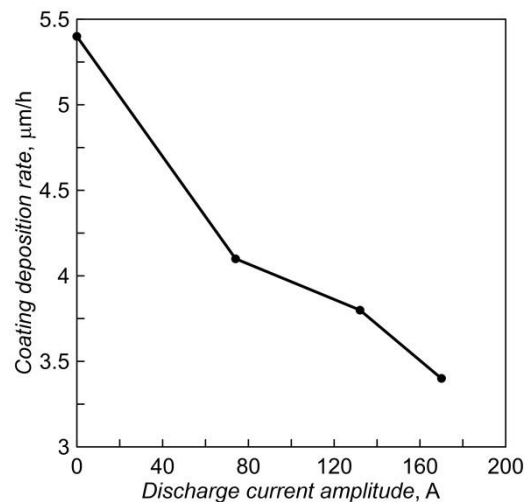


Fig. 1. Al₂O₃ coating deposition rate vs discharge current amplitude.

REFERENCES

- [1] A. Kamenetskikh, N. Gavrilov, S. Krivoshapko, and P.V. Tretnikov, "Application of the catalytic probe method for measuring the concentration of oxygen atoms in Ar/O₂ plasma of a low-pressure arc," *Plasma Sources Sci. Technol.*, vol. 30, p. 015004, 2021.
- [2] N. Gavrilov, A. Kamenetskikh, S. Krivoshapko, and P.V. Tretnikov, "Increasing the oxygen dissociation degree in the plasma of a pulse-periodic Ar/O₂ low-pressure arc," *Plasma Sources Sci. Technol.*, in press.

* The work was supported in part by RFBR, project number 20-08-00169.

INFLUENCE OF ELECTRON-BEAM HEATING MODES ON THE STRUCTURE OF COMPOSITE ZrO_2 - Al_2O_3 CERAMICS*

A.S. KLIMOV, I.Yu. BAKEEV, A.A. ZENIN

Tomsk State University of Control Systems and Radioelectronics, Tomsk, Russia

e-mail: klimov680@gmail.com

Ceramics are characterized by a set of unique physical and chemical properties, such as hardness, compressive strength, bending strength, increased corrosion resistance, resistance to aggressive environments, and many others [1]. Gradient ceramics, and in particular the system based on Al_2O_3 - ZrO_2 , currently displaces a number of metals and alloys for structural purposes [2]. Earlier, the prospects of using an electron beam formed by a forevacuum plasma electron source for sintering ceramic compacts were shown [3].

In this paper, the influence of electron-beam irradiation modes of gradient ceramics on its structure is presented.

A forevacuum plasma electron source was used for sintering [4]. The source formed a narrowly focused electron beam with a diameter of 0.5 mm. Disks consisting of several layers of zirconium oxide and aluminum powders were used as sintered samples. The percentages of zirconium oxide and aluminum oxide varied with the depth of the sample.

As a result of irradiation for 10 minutes at different heating temperatures, a set of samples with different structure and mechanical properties was obtained. The most dense samples were obtained when heated to 1450 degrees. Further research will be aimed at improving the strength properties of the samples.

REFERENCES

- [1] P. Edwards, A. O'Conner, M. Ramulu, "Electron Beam Additive Manufacturing of Titanium Components: Properties and Performance," *J. Manuf. Sci.*, vol. 135., Iss. 6. pp. 061016(7), 2013.
- [2] O. Guillon, J. Gonzalez-Julian, B. Dargatz, T. Kessel, G. Schiering, J. Rathel, M. Herrmann, "Field-Assisted Sintering Technology/Spark Plasma Sintering: Mechanisms, Materials, and Technology Developments," *Advanced engineering materials*, pp. 1-3, 2014.
- [3] A.V. Kazakov, A.S. Klimov, A.A. Zenin, "Electron-beam synthesis of zirconia ceramics," *Reports of TUSUR*, No. 2-2 (26). pp. 186-189, 2012.
- [4] A.S. Klimov, I.Yu. Bakeev, E.M. Oks, A.A. Zenin, "Forevacuum plasma source of continuous electron beam," *Laser and Particle Beams*, vol. 37, Iss. 2, pp. 203-208, 2019.

* The work was supported under the grant from the President of the Russian Federation for doctors of sciences MD-754.2021.4.

ELECTRON BEAM SINTERING OF Mn-Zn FERRITES USING A FOREVACUUM PLASMA ELECTRON SOURCE*

A.S. KLIMOV, I.Yu. BAKEEV, A.A. ZENIN

Tomsk State University of Control Systems and Radioelectronics, Tomsk, Russia

e-mail: klimov680@gmail.com

Ferrites are semiconductor materials of great technological importance. The high resistivity of ferrites makes them suitable for use in microelectronics. The development of communication technologies based on microwave and millimeter waves, the production of dielectric resonators has become one of the fastest growing types of electro-ceramic production. The dielectric properties of ferrites depend on several factors, such as the method of preparation, chemical composition, and structure or grain size [1, 2]. One of the new methods for the synthesis of materials using ceramic technology is electron-beam sintering in the forevacuum pressure range [3]. The purpose of this work is to study the possibility of electron-beam sintering of Mn-Zn ferrites pre-pressed from coarse-grained powders of the same composition, Fig. 1 a.

Electron beam sintering was performed using a forevacuum plasma electron source [4] in a helium atmosphere at a pressure of 30 Pa. The sintering temperature is 1250 degrees. The duration of heating is 20 minutes, the duration of isothermal exposure is 10 minutes. The sample cooling time is 20 minutes.

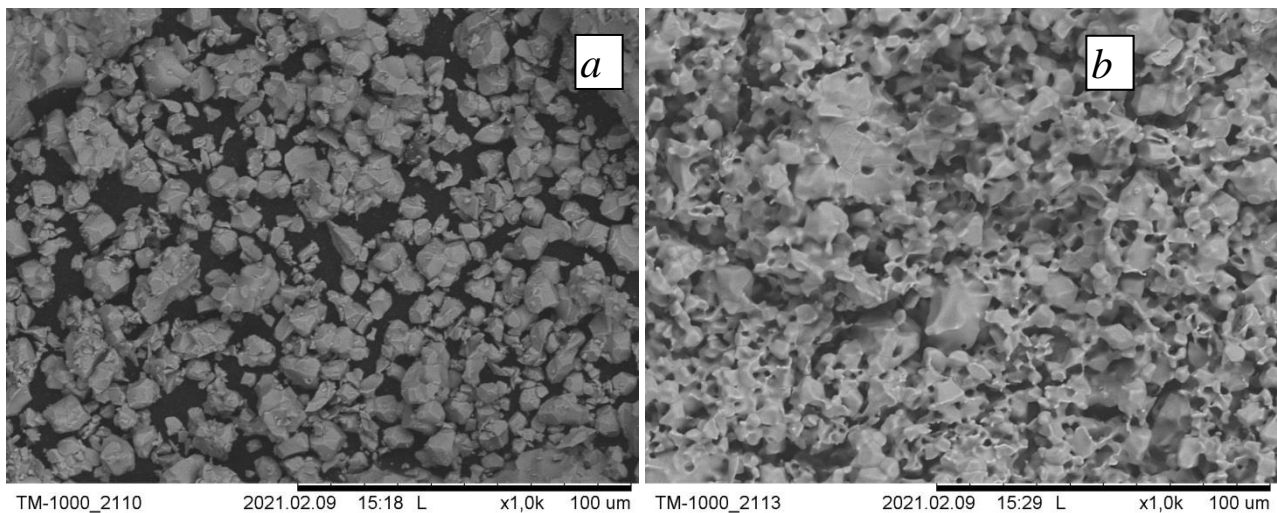


Fig. 1. SEM image of the initial Mn-Zn ferrite powder (a) and after electron beam irradiation (b).

As a result, a sintered sample of manganese-zinc ferrite was obtained. The irradiated side, Fig. 1b, completely lost zinc due to the high temperature. On the non-irradiated side, there is a slight decrease in the content of zinc and oxygen compared to the composition of the initial powder. The latter circumstance indicates the possibility of electron-beam sintering of ferrites, but careful selection of sintering modes is required.

REFERENCES

- [1] M. Hashim, S. Kumar, B.H. Koo, S.E. Shirsath, et. al. *Alloys Compds.* 518, 11, 2012.
- [2] S. Santosh, S. Jadhav, E. Shirsath, B.G. Toksha, D.R. Shen-gule, K.M. Jadhav, *Optoelectron J. Adv. Mater.* 10, 2644, 2008.
- [3] A.V. Kazakov, A.S. Klimov, A.A. Zenin, "Electron-beam synthesis of zirconia ceramics", *Reports of TUSUR*, No. 2-2 (26), pp. 186-189, 2012.
- [4] A.S. Klimov, I.Yu. Bakeev, E.M. Oks, A.A. Zenin, *Laser and Particle Beams*, 37(2), 203-208, 2019.

* The work was supported under the grant from the President of the Russian Federation for doctors of sciences MD-754.2021.4.

FEATURES OF BORIDING DIE STEEL D5 BY ELECTRON BEAMS *

A.S. MILONOV, D.E. DASHEEV, N.N. SMIRNYAGINA, A.E. LAPINA

*Institute of Physical Materials Science SB RAS, Ulan-Ude, Russia
e-mail: terwer81@mail.ru*

Boron saturation of the surface layer of steel is used for a fast-cutting and stamping tool. Boriding technology is made according to various methods, the application of which is dictated by the peculiarities of production and the types of processed products. The process mode depends on the desired coating thickness and steel grade. Usually, boriding steels contain a significant content of carbon and alloying components. In the work, boron saturation of the surface of steel D5 was investigated under the influence of continuous and pulsed electron beams in a vacuum (Fig. 1). The influence of alloying elements on the formation of iron boride layers is considered. Thermophysical processes were simulated using COMSOL Multiphysics software. A study of the distribution of temperatures and their rates of change under the influence of an electron beam was carried out. The obtained calculations showed that the temperature-time conditions of heating and cooling determine the nature of structural transformations.

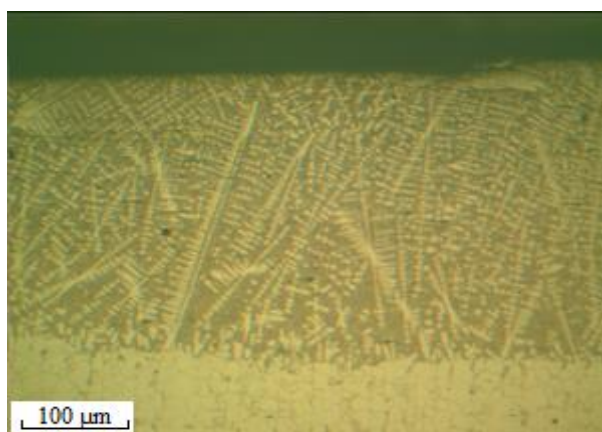


Fig. 1. Boride layer on die steel D5.

The microstructure and microhardness of the obtained Fe_2B layers were also investigated. The thickness of the layer reaches 1 mm. The microhardness of steel D5 is 2560 MPa. It is seen that the microhardness of the boride layer reaches up to 8500 MPa, and of the base up to 4000 MPa (Fig. 2). Hence, we can conclude that the heat tempering of steel with an electron beam.

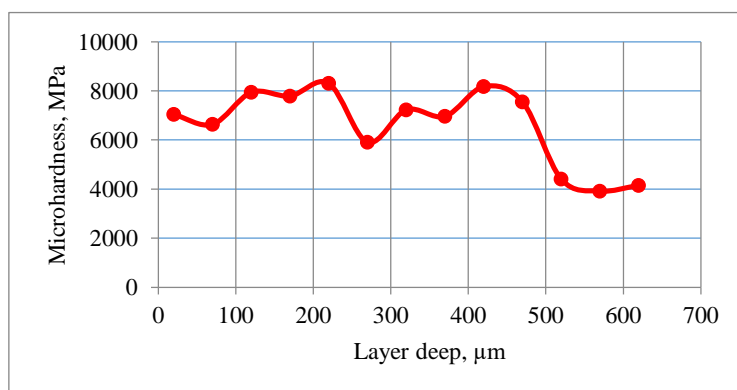


Fig. 2. Microhardness of boride layer on die steel D5.

The results obtained in this investigation give us the opportunity to consider the application of boriding of dies steels with electron beams in industrial production.

* The work was carried out with the financial support of the state task of the Ministry of Science and Higher Education of the Russian Federation, topic No. 0270-2021-0001.

EFFECT OF PLASMA ASSISTANCE ON THE PROPERTIES OF COATINGS BASED ON ALUMINUM OXIDE

A.YU. NAZAROV¹, E.L. VARDANYAN², R.SH. NAGIMOV², A.A. MASLOV²

¹Scientific and Production Association «Technopark of aviation technologies», Ufa, Russia

²Ufa State Aviation Technical University, Ufa, Russia

e-mail: nazarov_almaz15@mail.ru

It is known that oxide coatings (Al_2O_3 , SiO_2 , TiO_2 , ZrO_2 , B_2O_3 , HfO_2 , CeO_2) have a number of properties that are not inherent in metallic and other types of coatings - low thermal conductivity, chemical inertness, and wear resistance. Most oxides have a high melting point, hardness and wear resistance, are the most versatile in operating conditions and can be used as corrosion-resistant, heat-resistant, heat-shielding, electrical insulating and wear-resistant. Aluminum oxide coating is one of the most suitable materials for metal cutting tool applications. Among the various modifications of aluminum oxide, $\alpha\text{-Al}_2\text{O}_3$ is the most preferable due to its better properties compared to other modifications [1, 2]. To obtain coatings from aluminum oxide, the CVD method is often used. This method is not widely used due to the fact that the temperature of coating deposition in these installations is 1050°C , metastable modifications of Al_2O_3 are obtained by the CVD method, since the temperature of the transition of $\theta\text{-Al}_2\text{O}_3$ to a less porous and more solid modification of $\alpha\text{-Al}_2\text{O}_3$ is 1200°C [3].

When applying coatings based on aluminum oxide by the method of cathodic-arc deposition due to the lower temperature of the process, the formation of an amorphous or other phase of aluminum oxide occurs [4, 5].

Figure 1 shows a diagram of the setup for carrying out the experiment. The installation is equipped with two electric arc evaporators and a plasma source with a hollow cathode for plasma assistance for the coating process.

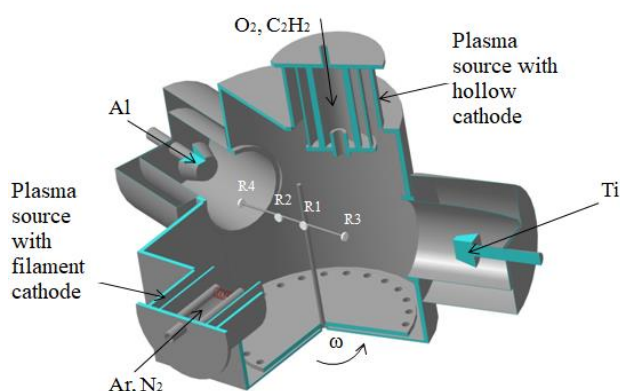


Fig. 1. Experimental installation NNV-6.6 I1.

In [6], the influence of the reference voltage on the phase composition and physical and mechanical properties was considered. This paper will consider the effect of plasma-assisted alumina-based coating on coating properties.

REFERENCES

- [1] B. Lux, C. Colombier, H. Altena "Preparation of alumina coatings by chemical vapour deposition", *Thin Solid Films*. Vol. 138, pp. 49-64, 1986.
- [2] A. L. Drago, J. J. Diamond "Transitions in Vapor Deposited Alumina from 300° to 1200°C ", *Am. Ceram. Soc.* Vol. 50, pp. 568-574. 1967.
- [3] Chaly V.P. "Metal hydroxides." Kiev: Naukova dumka, 1972. p. 160.
- [4] J.M. Schneider, W.D. Sproul "Crystalline alumina deposited at low temperatures by ionized magnetron sputtering", *Journal of Vacuum Science & Technology A15*, pp. 1084, 1997.
- [5] R. Cremer, M. Withaut "Comparative characterization of alumina coatings deposited by RF, DC and pulsed reactive magnetron sputtering", *Surf. Coat. Technol.* Vol. 120/121, pp. 213-218, 1999.
- [6] E. Vardanyan, A. Nazarov, R. Nagimov, K. Ramazanov, A. Maslov, "Deposition of Aluminum Oxides From a Vacuum-Arc Discharge Plasma," 2020 7th International Congress on Energy Fluxes and Radiation Effects (EFRE), pp. 853-855, 2020.

Nb/NbN MULTILAYER COATINGS DEPOSITED BY THE VACUUM-ARC PLASMA-ASSISTED METHOD: SYNTHESIS, PROPERTIES, STRUCTURE*

O.V. KRYSINA, N.A. PROKOPENKO, YU.F. IVANOV, V.V. SHUGUROV, E.A. PETRIKOVA, O.S. TOLKACHEV, M.E. RYGINA

Institute of High Current Electronics SB, RAS, Tomsk, Russia

e-mail: nick08_phantom@mail.ru

Modern research on the production of multilayer coatings is aimed at creating alternating layers of high-strength ceramics and a bonding layer of metal. One of the most common methods for producing such multilayer coatings is the method of condensation with ion bombardment. But it has great inertia when passing between layers, which reduces the strength properties of the resulting coatings. The aim of this work was to develop an original method for applying vacuum-arc multilayer coatings with a sharp boundary between the layers.

The studies were conducted on the vacuum ion-plasma unit "Quinta" [1]. The installation can be used for: cleaning, heating and activating a surface in a low-pressure gas-discharge plasma; nitriding or oxidizing in low pressure arc discharges; vacuum arc plasma-assisted deposition of coatings of different composition and function. For ion-plasma nitriding, final cleaning and activation of the surfaces of materials and products, as well as for plasma assisting in the vacuum electric arc deposition of functional coatings, a plasma generator based on low-pressure non-self-sustaining arc discharge was used. To generate the metal plasma, the electric arc evaporator was used.

Experiments on vacuum-arc plasma-assisted deposition of multilayer coatings have been carried out. In this work, we used a low-inertia method for formation of the coatings with a sharp boundary between the layers. This is achieved by changing the discharge current of the low-pressure non-self-sustaining arc discharge, which changes the proportion of nitrogen ions in the discharge gap. In this case, the discharge current of the arc evaporator, as well as the composition and pressure of the working gas remain unchanged.

In the work, 4 types of coatings were deposited and investigated. The composition was Nb/NbN. Two layer thicknesses were taken: 10 nm and 100 nm. The multilayer coatings were formed by two methods: traditional (by gas type changing) and new low-inertia (by changing arc current of gas plasma source).

REFERENCES

- [1] V V Shugurov, N N Koval, O V Krysinina and N A Prokopenko, "QUINTA equipment for ion-plasma modification of materials and products surface and vacuum arc plasma-assisted deposition of coatings" J. Phys.: Conf. Ser. **1393** 012131, 2019.

* The research was supported by RSF (project No. 18-79-10111)

STRUCTURAL AND PHASE DEPENDENCIES OF COATINGS FORMATION BASED ON INTERMETALLIDES Ti-Al SYSTEMS FOR INCREASING THE DURABILITY OF CUTTING TOOLS

E.L. VARDANYAN, K.N. RAMAZANOV, A.Yu. NAZAROV, R.SH. NAGIMOV, A.A. MASLOV

Ufa State Aviation Technical University, Ufa, Russia

e-mail: Vardanyaned@gmail.com

The results of investigations of multilayer coatings with alternating layers synthesized in nitrogen or argon are presented. The coatings were applied by changing the parameter S (the ratio of the thickness of alternating macro-layers). The first technology consists in the deposition of 3-layer coatings with alternating layers of Ti-TiAl-TiAlN ($h_{TiAlN} = 1.5 * h_{TiAl} = 3 * h_{Ti}$), 2-4 technology is the alternation of TiAl-TiAlN layers with different thickness ratios ($h_{TiAlN} = 0.3 * h_{TiAl}$, $h_{TiAlN} = 1.5 * h_{TiAl}$, $h_{TiAlN} = h_{TiAl}$). The thickness of the macrolayers was varied in the range from 40 to 500 nm. The architecture of the coatings and photos of spherical holes for measuring the thickness of the layers are shown in fig 1.

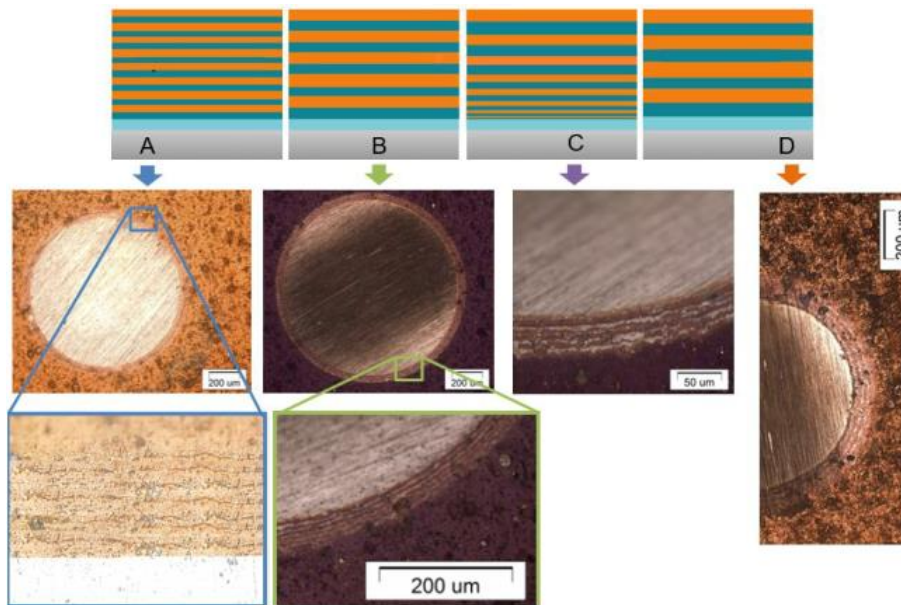


Fig. 1. The architecture of the investigated coatings and spherical sections for determining the thickness of the coatings.

The results of sclerometric tests showed that composite coatings based on the Ti-Al intermetallic compound do not fail under loads up to 30 N. The coating with the number of macrolayers = 60 does not have a region of elastic-plastic deformation and the coefficient of elastic recovery $We = 33\%$, an increase in the thickness of macrolayers to 500 nm and a decrease in their number to 8 leads to an increase in the coefficient of elastic recovery to 75%. According to the results of nanoindenting (Fig. 1), it was found that an increase in the thickness of macrolayers up to 500 nm leads to an increase in nanohardness up to 45 GPa at an elastic modulus = 230 GPa.

REFERENCES

- [1] E.L. Vardanyan, K.N. Ramazanov, R.S. Nagimov, A.Y. Nazarov, *Surface and Coatings Technology*, 389, 125657, (2020).
- [2] A.A. Kalushevich, N.N. Koval, V.V. Denisov, et al., *Izv. Vyssh. Uchebn. Zaved. Fiz.*, 55, No. 12/3, 118–122, (2012).
- [3] O.V. Krysina, V.V. Shugurov, N.A. Prokopenko, et al., *Russ. Phys. J.*, 62, No. 5, 848–853, (2019).

Ti₂AlC MAX PHASE COATINGS MADE BY REACTIVE CATHODIC ARC DEPOSITION (ARC-PVD)

A.A. MASLOV, A.YU. NAZAROV, E.L. VARDANYAN

Ufa State Aviation Technical University, Ufa, Russia

e-mail: alexey.maslov2011@gmail.com

In late 1990s the term MAX phases was coined and determined as new family of nitrides and carbides with chemical formula $M_{n+1}AX_n$, where $n=1\dots3$, M is an early transitional metal, A is an A-group element, and X is carbon or nitrogen. MAX phases have interesting properties both in bulk form and in thin film coating form. One of prospective methods to synthesize MAX phase thin film is a reactive cathodic arc deposition (as well as reactive magnetron sputtering). Ti₃AlC₂ and especially Ti₂AlC are promising MAX phases in terms of high-temperature applications, therefore a technology of these phases synthesis is important for exploration.

In this work Ti₂AlC was a desired MAX phase for thin film deposition. There are 2 ways to evaporate and deposit Ti and Al: using 2 elemental targets made from pure titanium and aluminum and using one Ti-Al target. In some works, it was shown that deposition from 2 different targets are more preferably due to possibility to use optimal evaporation mode for each element. It is also known that the following annealing can significantly improve formation and amount of desired MAX phase in coating. Therefore, in current work reactive Arc-PVD technology with 2 cathodes was used. After deposition some samples were annealed in vacuum at 800°C. Chamber atmosphere consisted of C₂H₂/Ar mixture which was supplied through hollow-cathode plasma generator.

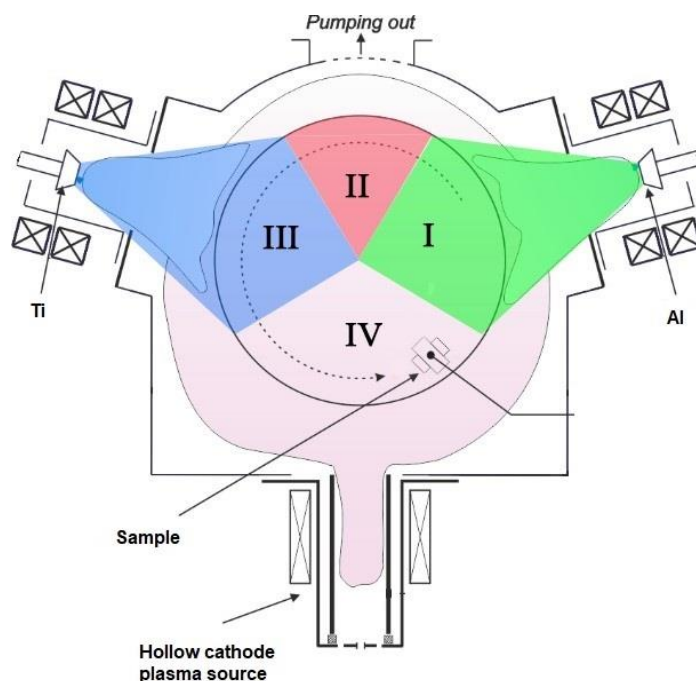


Fig. 1. Deposition scheme

Initial results shown that amount of Ti₂AlC phase in coating is not 100%, but following annealing improves MAX phase formation, as was described before. For further MAX phase formation improvement more significant samples heating during process is required. Current temperature is about 400°C, and planned heating at 700°C should significantly intensify formation of Ti₂AlC.

REFERENCES

- [1] Eklund P. et al. The Mn_{n+1}AlX_n phases: Materials science and thin-film processing // *Thin Solid Films*. – 2010. – V. 518. – No. 8. – P. 1851-1878. Mahmoudi Z. et al. Synthesis of Ti₂AlC & Ti₃AlC₂ MAX phases by Arc-PVD using Ti–Al target in C₂H₂/Ar gas mixture and subsequent annealing // *Ceramics International*. – 2020. – V. 46. – No. 4. – P. 4968-4975.
- [2] Berger O. The correlation between structure, multifunctional properties and application of PVD MAX phase coatings. Part I. Texture and room temperature properties // *Surface Engineering*. – 2020. – V. 36. – No. 3. – P. 225-267.

EFFECT OF ION NITRIDING BY GLOW DISCHARGE ON THE PHYSICOMECHANICAL PROPERTIES OF THE PLASTICALLY DEFORMED TOOL STEEL R6M5

R.K. VAFIN, A.V. ASYLBAEV, D.V. MAMONTOV, I.D. SKLIZKOV, G.I. RAAB, E.F. KHAIRETDINOV, R.S. ESIPOV

*Ufa State Aviation Technical University, USATU, Ufa, Russia
e-mail: vafinrk@mail.ru*

This work is devoted to the study of the effect of the duration of ion nitriding in a glow discharge (see Fig. 1 a) on the physical and mechanical properties of tool steel with different initial structure. We used specimens of R6M5 tool steel with a coarse-grained structure obtained after annealing at a temperature of 850 ° C and with a fine-grained structure obtained after severe plastic deformation by torsion discharge (see Fig. 1 b). With an increase in the duration of ion nitriding, the thickness of the hardened layer and wear resistance increase. The combination of plastic deformation with ion nitriding in a glow discharge increases the diffusion rate of the saturating element due to the creation of a highly fragmented and disoriented fine-grained structure.

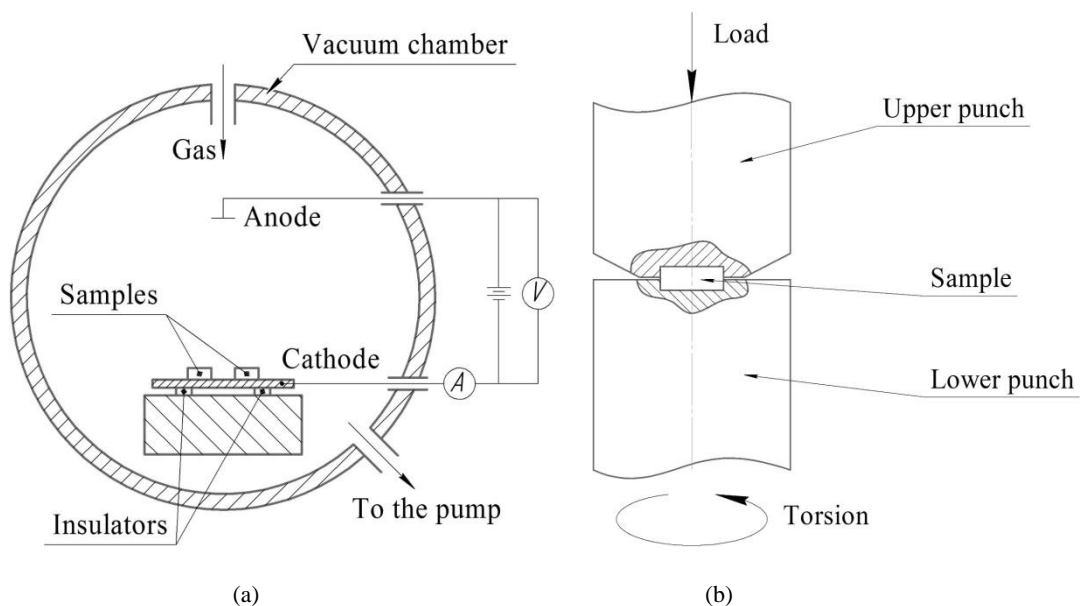


Fig. 1. (a) scheme of the experimental ion nitriding by glow discharge, and (b) scheme of severe plastic deformation of the samples.

REFERENCES

- [1] B.N. Arzamasov, A.G. Bratuhin, Yu.V. Eliseev, T.A. Panajoti, Ion chemical heat treatment of alloys. Moscow: The Bauman Moscow State Technical University, 1999.
- [2] Yu.D. Korolev and G.A. Mesyats, Field Emission and Explosion Processes in Gas Discharge. Novosibirsk: Nauka, 1982.
- [3] R.Z. Valiev, A.P. Zhilyaev, T.G. Langdon, Bulk nanostructured materials. Fundamental and Applications, TMS-Wiley, Hoboken (NJ), 2014.

MODELING OF ION-PLASMA SYNTHESIS OF LINEAR-CHAINED CARBON*

E.A. BUNTOV, A.F. ZATSEPIN, A.I. MATITSEV, V.A. DUTOV, K.P. ARSLANOV

*Ural Federal University, Ekaterinburg, Russia
e-mail: e.a.buntov@urfu.ru*

Low-dimensional, in particular, one-dimensional modifications of carbon (isolated chains of atoms, carbyne, graphidyne, etc.) attract the attention of researchers due to their unique physical properties [1]. Their electronic characteristics are determined by the distribution of the types of covalent bonds and the type of hybridization of the orbitals of carbon atoms. One of the successful methods for the synthesis of such structures is the pulsed deposition from a low-temperature carbon plasma, which can be accompanied by stimulation with an additional ion beam [2]. Changing the synthesis modes (energy and fluence of the stimulating ion beam, the type of substrate and geometry of the experiment, the introduction of dopants) makes it possible to control the band structure of the material, in particular, to carry out the metal-semiconductor transition. A fundamental problem in this area is the lack of detailed studies, and, consequently, understanding of the relationship between the modes of ion-stimulated synthesis, the structure and properties of low-dimensional carbon structures, including doped ones, on metal and semiconductor substrates with different types of conductivity. The lack of an adequate model of the micromechanisms of ion-stimulated plasma synthesis prevents the intentional control of the properties of the synthesized structures. The complexity of describing the complex of phenomena in the course of ion-stimulated formation of nanocarbon is the combination of long time intervals with the need to take into account the excited states of the ions involved. At the same time, examples of successful modeling of the PECVD process with additional irradiation with argon ions by molecular dynamics methods are already known [3]. In order to simulate the low-temperature plasma synthesis of low-dimensional carbon coatings successfully, it is necessary to choose a suitable theoretical method to consider possible charge transfer processes. In our recent work, we studied numerically the breaking of the carbon bond CC under irradiation with slow argon ions for model molecules having sp^3 -, sp^2 and sp -hybridization. Bond cleavage threshold energies were calculated for carbon atoms in three hybridizations at three levels of theory: classical dynamics, Car-Parrinello method and Ehrenfest's approach, the results were compared with experimental data [4]. Based on the accuracy of the results obtained, a combined QM/MM approach to modeling ion-stimulated plasma synthesis is proposed and implemented in the current study to examine the deposition of carbon chains on diamond and silicon substrate (Fig. 1). A set of optimal parameters is elaborated for experimental synthesis enhancement.

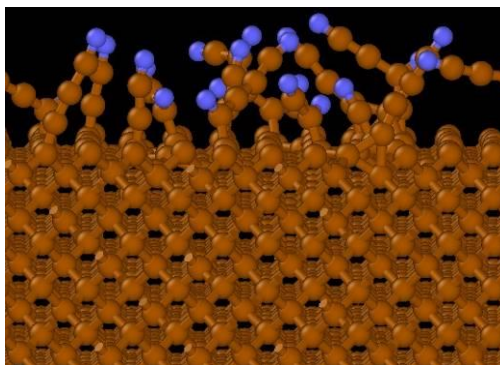


Fig. 1. Structure of a diamond substrate under carbon species deposition in molecular dynamics simulation with ReaxFF force field.

REFERENCES

- [1] C.S. Casari, A. Milani, "Carbyne: from the elusive allotrope to stable carbon atom wires," *MRS Commun*, 2018, vol. 8, pp. 207-219.
- [2] E.A. Buntov, A.F. Zatsepin et al., "Effect of thickness and substrate type on the structure and low vacuum photoemission of carbyne-containing films," *Carbon*, 2019, vol. 152, pp. 388-395.
- [3] E. Neyts, P. Brault, "Molecular dynamics simulations for plasma-surface interactions," *Plasma Process. Polym.* 2017, vol. 14, pp. 1600145.
- [4] E.A. Buntov, A.F. Zatsepin, "Carbon bond breaking under Ar^+ -Ion irradiation in dependence on sp hybridization: car-parrinello, ehrenfest, and classical dynamics study," *Journal of Physical Chemistry A*, 2020, vol. 124 (44), pp. 9128-9132.

* The work was supported by the Russian Scientific Foundation project no. 21-12-00392.

ADVANTAGES OF USING OF PLASMA OF PULSE-PERIODIC LOW-PRESSURE DISCHARGES FOR SURFACE TREATMENT*

V.V. DENISOV, YU.A. DENISOVA, S.S. KOVALSKY, A.A. LEONOV, E.V. OSTROVERKHOV, V.N. TISHCHENKO,
V.V. YAKOVLEV

Institute of High Current Electronics, SB, RAS, Tomsk, Russia

e-mail: denisov@opee.hcei.tsc.ru

In this paper, we consider some technological capabilities of the plasma generated by pulsed-periodic low-pressure discharges [1, 2]. The advantages of using of a pulsed nitrogen-containing plasma of low-pressure discharges in comparison with a plasma of stationary discharges for the processes of ion-plasma nitriding and plasma-assisted cathodic arc deposition of functional coatings on the surface of products of complex shape are justified. Examples of successfully processed products are given.

REFERENCES

- [1] V. V. Yakovlev, V. V. Denisov, N. N. Koval, S. S. Kovalsky, E. V. Ostroverkhov, A. O. Egorov, and M. V. Savchuk "Generation of plasma with increased ionization degree in a pulsed high-current low-pressure hollow cathode discharge," Russian Physics Journal. Vol. 63(10), pp. 1757-1765, 2020.
- [2] V. V. Denisov, Yu. Kh. Akhmadeev, N. N. Koval, S. S. Kovalskiy, N. N. Pedin, and V.V. Yakovlev "Plasma Generation in a Pulsed Mode of a Non-Self-Sustained Arc Discharge with a Hybrid Hot-and-hollow Cathode," Russian Physics Journal. Vol. 62(3), pp. 541-546, 2019.

* The work was performed under State Assignment of the Ministry of Science and Higher Education of the Russian Federation (project No. FWRM-2019-0002).

INVESTIGATION OF TUNGSTEN SURFACE CARBIDIZATION UNDER PLASMA IRRADIATION*

*A.Zh. MINIYAZOV¹, T.R. TULENBERGENOV¹, I.A. SOKOLOV¹, G.K. ZHANBOLATOVA¹, O.S. BUKINA¹,
Ye.A. KOZHAHMETOV¹, M.K. SKAKOV²*

¹*“Institute of Atomic Energy” Branch of the National Nuclear Center of the Republic of Kazakhstan, Kurchatov, Kazakhstan*

²*National Nuclear Center of the Republic of Kazakhstan, Kurchatov, Kazakhstan*

e-mail: gainiya.kaiyrdy@gmail.com

As it is known, W and C are the most suitable as plasma facing materials for the divertor of a thermonuclear reactor [1]. The presence of various materials, as well as impurities, in the installation chamber will lead to the formation of mixed layers in the surfaces facing the plasma, which can affect the interaction with hydrogen isotopes from the boundary plasma. To study diffusion of hydrogen isotopes and their retention in W with mixed layers, in particular with a carbidized surface, co-deposition of W and C in a tokamak divertor are simulated by various methods of surface coating deposition.

To study the surface carbidization of tungsten, a series of experimental works were carried out in a plasma-beam installation (PBI) [2, 3]. Figure 1 presents general scheme of the installation.

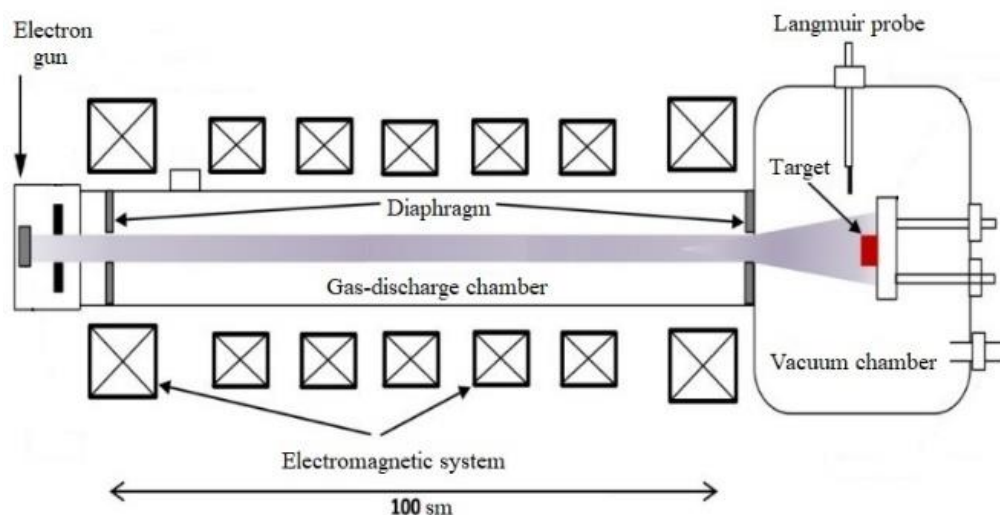


Fig. 1. Schematic diagram of PBI.

Based on the results of X-ray diffraction analysis, it was found that a change in the surface temperature of the tungsten sample and the irradiation time leads to different degrees of carbidization of the tungsten surface. The low intensity peaks of the WC, W₂C crystalline phases were noted at a temperature of 1573 K staying in methane for 600 s. A further increase in temperature at a given irradiation time leads to an increase in the W₂C crystalline phase. An increase exposure time from 300 s to 3600 s at a constant temperature of the sample surface of 1773 K accelerates diffusion and interaction of C, which leads to the transformation of W₂C into WC.

REFERENCES

- [1] H. Bolt, V. Barabash, G. Federici, J. Linke, A. Loarte, J. Roth, K. Sato. “Plasma facing and high heat flux materials-needs for ITER and beyond”, J. Nucl. Mater., vol. 307, pp. 43-52, 2002.
- [2] Patent of the Republic of Kazakhstan for a utility model № 2080. Imitatsionnyy stend s plazmenno-puchkovoy ustanovkoy / Kolodeshnikov A.A., Zuev V.A., Ganovichev D.A., Tulenbergenov T.R., et.al. – publ. 15.03.2017, Bul. no. 5.
- [3] V. Kurnaev, I. Vizgalov, et.al. “Investigation of plasma–surface interaction at plasma beam facilities”, J. Nucl. Mater., vol. 463, pp. 228-232, 2015.

* This paper was prepared due to the “Study of the interaction of plasma with a carbidized tungsten surface” within the framework of the Republican scientific and technical program “Scientific and technical support of experimental research at the Kazakhstan Material Testing tokamak KTM” in the Institute of Atomic Energy Branch of the Republican state enterprise on the economic control right “National Nuclear Center of the Republic of Kazakhstan” of the Ministry of Energy of the Republic of Kazakhstan.

STUDY OF THE TiN-Cu FILMS DEPOSITED ON ALLOY T15K6 BY PLASMA OF LOW PRESSURE VACUUM-ARC AND MAGNETRON DISCHARGES *

D.B-D. TSYRENOV¹, A.P. SEMENOV¹, E.O. NIKOLAEV¹, N.S. ULAKHANOV^{1,2}

¹*Institute of Physical Materials Science, SB, RAS, Ulan-Ude, Russia,*

²*East Siberia State University of Technology and Management, Ulan-Ude, Russia*

e-mail: frjockey@gmail.com

The purpose of this work was to investigate the structure, phase composition and wear resistance of composite TiN-Cu layers on the T16K6 alloy obtained at different values of the arc current, magnetron discharge current, and working gas pressure. The deposition of the composite layers was carried out on a modernized installation with a vacuum arc evaporator and a planar magnetron [1].

TiN-Cu coatings were deposited in copper vapor in the mode of titanium evaporation in argon and nitrogen-containing plasma, dissociation of molecular nitrogen $N_2 - 2N$, and chemical reaction of Ti and N. Samples of alloy T15K6, 18x16 mm in size and 5 mm thick, were used as substrates. For a more efficient sputtering of the magnetron target, a gas mixer was used, in which nitrogen and argon were mixed in different proportions. The proportion of argon ranged from 20% to 50% of the total volume of the working gas. X-ray phase analysis (XRD) was performed on a Phaser 2D Bruker diffractometer (CuK_{α} - radiation). The microstructure of the layers was investigated on a METAM PB-22 microscope. Using a scanning atomic force microscope MultiMode8, the topology and structure of the surface of the TiN-Cu coating were studied. The microhardness of the formed layers was determined using a PMT-3 microhardness meter. X-ray phase analysis was performed according to which the samples contained TiN phases with different crystal lattice and volume fraction. In addition, reflections of copper reflections were recorded, the intensity of which was about 1–2%. The thickness of the TiN layers and the TiN-Cu composite ranged from 2-3 microns to 5-8 microns depending on the deposition time.

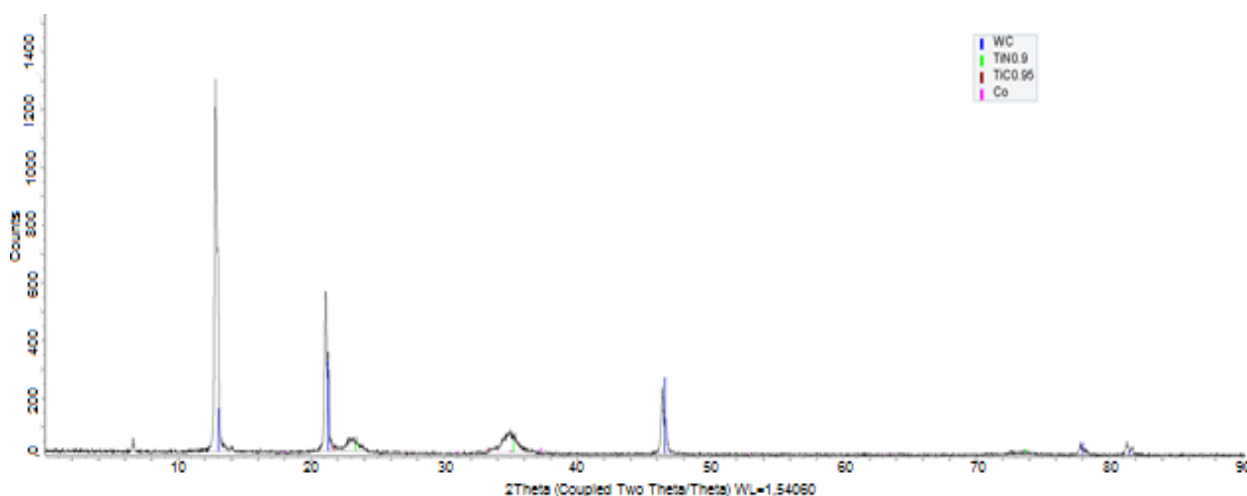


Fig. 1. XRD pattern for coating TiN on alloy T15K6.

REFERENCES

- [1] A.P. Semenov, D.B-D. Tsyrenov, I.A. Semenova // Instruments and Experimental Techniques - 2017. - Volume. 60 – No. 6. Pages 892-895.

* This study was supported by the State Job of the Ministry of Science and Education of the Russian Federation (topic no. 0270-2021-0001).

FORMATION OF CATALYTIC AND CORROSION PROTECTIVE LAYERS WITH USE OF ION BEAM ASSISTED DEPOSITION OF METALS FROM VACUUM ARC DISCHARGE PLASMA *

V.V. POPLAVSKY

Belarusian State Technological University, Minsk, Belarus

e-mail: vasily.poplav@tut.by

Of great interest is the modification with the use of ion-plasma technologies of functional materials, the properties, in particular, catalytic and corrosion-resistant, which are determined primarily by the composition of the surface [1]. The goal of our research is the formation of catalytic also corrosion protective layers with use of ion beam assisted deposition (IBAD) of active or alloying metals from vacuum arc discharge plasma, which is generated in metal vapor. We carried out IBAD mode in which the deposition of the metal and the mixing of deposited layer with the substrate are carried out by accelerated ($U = 10$ or 5 kV) ions of the same metal. Deposition of the metal and mixing of the deposited layer with substrate by accelerated ions of the same metal were performed in an experimental unit, respectively, from a neutral fraction of metal vapor and the vacuum arc discharge plasma of a pulse arc ion source, respectively. The pressure in work chamber was $\sim 10^{-2}$ Pa.

Catalytic surface layers were prepared by IBAD of platinum as basic active metal and one of metals (Ir, Sn, Ce, Gd, Dy, Ho, Yb) as an activating additive. Active layers were formed by IBAD of metals onto substrates from valve metals (Al, Ti, and Ta) and carbon materials (glassy carbon, Toray Carbon Fiber Paper TGP-H-060 T and AVCarb[®] Carbon Fiber Paper P50 carbon fiber catalyst carriers) also on Nafion[™] N115 membrane which are used as material of diffusion layers and electrolyte of membrane electrode assemblies of electrolyzers and low-temperature fuel cells with polymer membrane electrolyte [2–4]. Corrosion protective layers were formed by IBAD of alloying metals (Zn, Cd, Al) onto carbon steel and stainless-steel [5], (Zn, Cd, Zr, Cr) – onto pure aluminum and aluminum alloy [6]. The composition of the layers were studied by energy dispersive electron-probe microanalysis (EDX) with scanning electron microscopy (SEM), wave dispersive X-ray fluorescence analysis (WD-XRF), Rutherford backscattering spectrometry (RBS), and X-ray photoelectron spectroscopy (XPS). The activity of electrocatalysts with prepared layers was studied in reactions of the hydrogen evolution and electrochemical oxidation of methanol and ethanol, which determine the principle of action of low-temperature fuel cells. Corrosion properties of samples with IBAD produced layers were tested with use of electrochemical polarization method. It has been established that the obtained layers are characterized by amorphous atomic structure and contain atoms of the deposited metals, substrate material, as well as impurities of oxygen and carbon; their thickness reaches ~ 50 – 80 nm. The content of each deposited metal is several percent by weight. Inclusions of the deposited metals of about several micrometers occur on the surface which is conditioned by metal drops deposition from the arc source; they cover less than 1% of the surface area. Electrocatalysts with the obtained layers exhibit activity in processes of hydrogen evolution and oxidation of alcohols – methanol and ethanol. Corrosion characteristics of samples with layers formed by IBAD of alloying metals are analogous to those of samples with coatings obtained by electrochemical metal deposition. As compared to electrochemical treatment, vacuum ion-beam assisted deposition is distinguished by the simple preparation of substrate surfaces, single-stage treatment, environmental safety, and cost efficiency.

REFERENCES

- [1] V.V. Poplavsky, "Influence of the implantation of transition metal ions on the electrocatalytic activity of carbon materials", Nucl. Instr. and Meth. Phys. Res., vol. B28, pp. 534–539, 1987.
- [2] V.V. Poplavsky, T.S. Mishchenko, V.G. Matys, "Composition and electrocatalytic properties of the coatings formed by the ion-beam-assisted deposition of platinum from a pulsed arc-discharge plasma onto aluminium", Techn. Phys., vol. 55, pp. 296–302, 2010.
- [3] V.V. Poplavsky, A.V. Dorozhko, V.G. Matys, "On the formation of electrocatalysts for methanol and ethanol oxidation by the ion beam-assisted deposition of rare-earth metals and platinum on carbon carriers", J. Surf. Investig. X-ray, Synchr. and Neutr. Techniq., vol. 13, pp. 1314–1322, 2019.
- [4] V.V. Poplavsky, O.G. Bobrovich, A.V. Dorozhko, "Modification of the surface of polymer electrolyte membrane Nafion by ion beam assisted deposition of catalytic metals", IEEE Book Series: 7th International Congress "Energy Fluxes and Radiation Effects", pp. 347–350, 2020.
- [5] V.V. Poplavsky, A.V. Dorozhko, V.G. Matys, "Study of the composition and properties of protective layers formed by the ion-beam-assisted deposition of cadmium, zinc, and aluminum onto steel surfaces", J. Surf. Investig. X-ray, Synchr. and Neutr. Techniq., vol. 10, pp. 981–988, 2016.
- [6] V.V. Poplavsky, F.F. Komarov, V.G. Luhn, V.V. Pil'ko, J. Partyka, "Composition and microstructure of surface layers produced by the ion beam assisted deposition of metals from a pulsed arc-discharge plasma onto aluminum substrates", Acta Physica Polonica A., vol. 128, pp. 946–948, 2015.

* The work is financially supported by the Republic of Belarus State research program "Materials science, new materials and technologies".

INFLUENCE OF PULSE-PERIODIC LOW-PRESSURE ARC DISCHARGE MODE ON COATING PROPERTIES*

M.V. SAVCHUK, V.V. YAKOVLEV, V.V. DENISOV, A.A. LEONOV, A.O. EGOROV

Institute of High Current Electronics, SB, RAS, Tomsk, Russia
e-mail: mixail96@bk.ru

The cathode spot of a vacuum arc discharge generates a plasma flow consisting of electrons, ions and microdroplets from cathode material. Microdroplets reduce the technological properties of depositing coatings. This problem solved by using magnetic separation systems [1] or improving the cooling system of the cathode [2].

In this paper the pulse-periodic mode of arc discharge burning with cathode spot at low pressure for different cathode materials has been studied. The ways to reduce microdroplets fraction value in the coating obtained in this mode of vacuum arc discharge burning were investigated.

REFERENCES

- [1] P.J. Martin, A. Bendavid "Review of the filtered vacuum arc process and materials deposition," Thin solid films, vol. 394, pp. 1-14, 2001.
- [2] A.A. Andreev, L.P. Sablev, V.M. Shulaev "Vacuum-arc systems and coatings," Kharkov: National Science Center Kharkov Institute of Physics and Technology, pp. 236, 2005.

* The work was carried out with the financial support of the RFBR grant № 19-08-00370 A.

EFFECT OF TEMPERATURE ON THE FORMATION OF TUNGSTEN CARBIDE IN A BEAM-PLASMA DISCHARGE*

G.K. ZHANBOLATOVA¹, V.V. BAKLANOV¹, M.K. SKAKOV², I.A. SOKOLOV¹, O.S. BUKINA¹, YE.A. KOZHAHMETOV¹,
N.A. ORAZGALIEV¹

¹Branch "Institute of Atomic Energy" of National Nuclear Center of the Republic of Kazakhstan, Kurchatov, Kazakhstan

²National Nuclear Center of the Republic of Kazakhstan, Kurchatov, Kazakhstan

e-mail: gainiya.kaiyrdy@gmail.com

Tungsten is known to be considered as a plasma facing material in future fusion reactors [1]. However, to date, either tungsten coatings applied to graphite tile, or uncoated graphite tile, as in the Kazakhstani Material Testing Tokamak KTM [2, 3], are used as the first wall material in the most fusion reactors. Since plasma-facing materials of a fusion reactor will be exposed to intense fluxes of incident particles and thermal stress, changes in their composition and structure should be expected. Consequently, study of tungsten carbide formation is still of great importance.

The tungsten carbide formation in a beam-plasma discharge was studied on an imitation stand with a plasma-beam installation [4, 5]. Methane was used as a plasma-forming gas. The working gas pressure in the chamber was $(1.01-1.06) \cdot 10^{-3}$ Torr. Experiments on the formation of tungsten carbides were carried out in the temperature range from 700°C to 1000°C with a step of 100°C. Figure 1 provides the results of X-ray phase analysis of the sample surface.

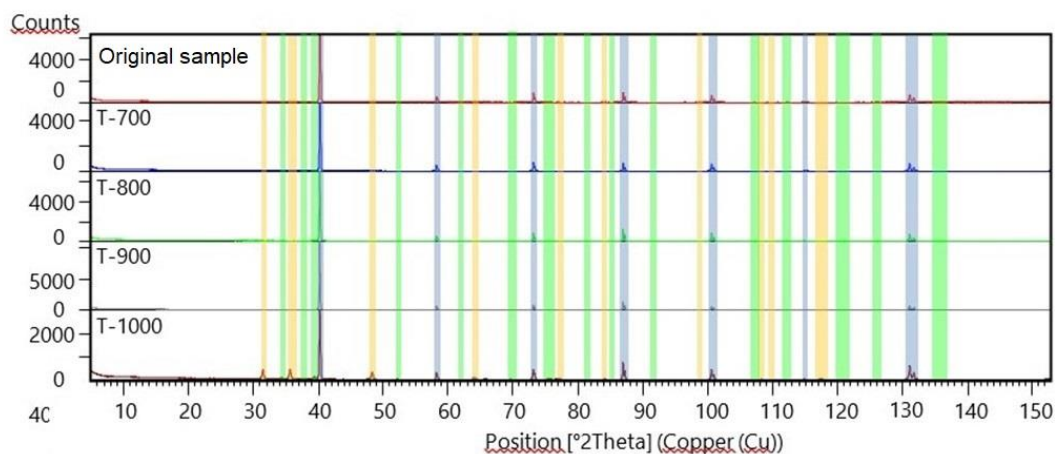


Fig. 1. Diffraction patterns of the initial sample and T-700, T-800, T-900, T-1000 samples (orange indicates locations of the WC phase peaks, green indicates the W_2C phase, and blue indicates the W peaks).

It was found that in the initial state and at temperatures of 700°C and 800°C, the basis of the phase composition of sample surface is metallic tungsten of the BCC structure. After heating the surface to 900°C, the W_2C phase of the orthorhombic system appears in the phase composition with a content of less than 5% according to the data of automatic standardless analysis. In this case, the basis of the phase composition remains metallic W. After heating to 1000°C, in addition to the phase of orthorhombic carbide W_2C (< 5%), the WC phase of the hexagonal system fixes, the quantitative content of which is about 15%.

REFERENCES

- [1] G. Pintsuk., A. Hasegawa, "Tungsten as a plasma-facing material", Reference Module in Materials Science and Materials Engineering, 2019.
- [2] J. Luthin, Ch. Linsmeier, "Carbon films and carbide formation on tungsten", Surface Science, vol. 454–456, pp.78–82, 2000.
- [3] I. L. Tazhibayeva, et al., "KTM Experimental Complex Project Status", Fusion Science and Technology, vol. 47, pp. 746–750, 2005.
- [4] Patent of the Republic of Kazakhstan for a utility model № 2080. Imitatsionnyy stend s plazmenno-puchkovoy ustanovkoy / Kolodeshnikov A.A., Zuev V.A., Ganovichev D.A., Tulenbergenov T.R., et.al. – publ. 15.03.2017, Bul. no. 5.
- [5] V. KurnaeV, I. Vizgalov, et.al., "Investigation of plasma–surface interaction at plasma beam facilities", Journal of Nuclear Materials, vol. 463, pp. 228–232, 2015.

* The work was supported by the Science Committee of the Ministry of Education and Science of the Republic of Kazakhstan (Grant No. AP08955992 "Study of the formation of a carbided layer on the surface of tungsten under plasma irradiation").

TiCrN VACUUM ARC COATING TO INCREASE WEAR RESISTANCE OF DIE STEELS*

A.A. LEONOV, YU.A. DENISOVA, V.V. DENISOV, M.V. SAVCHUK, V.N. TISHCHENKO

Institute of High Current Electronics SB RAS, Tomsk, Russia

e-mail: laa-91@yandex.ru

Vacuum arc nitride coatings based on various systems are used in industry to harden the surface of cut and die tools. Despite significant progress in the development of wear resistant coatings and a large quantity of studies in this area, there are no works in the literature describing complex studies of coatings on die steels for cold deformation. The aim of this work was to study the effect of the composition of TiCrN nitride coatings on their mechanical and tribological characteristics.

The coatings of the TiCrN system were deposited by vacuum arc plasma assisted method on the "QUADRO" device on pre-hardened Cr6WV die steel. To generate a metal plasma flow used two arc evaporators with cylindrical cathodes 80 mm in diameter made of Ti grade VT1-0 and Cr (99.8% pure). A source of gas plasma with a glowing and hollow cathode "PINK" was used for heating steel samples and preliminary cleaning of their surface by ion etching with gas ions, as well as for additional ionization of the gas and assist in the deposition of coatings. Influence of the ratio of Cr and Ti in the coating on its characteristics a series of experiments was carried out with different ratios of the currents of electric arc evaporators I_d (Cr) and I_d (Ti). The current of the arc evaporator with a titanium cathode I_d (Ti) in all processes was equal to 80 A, and with a chromium cathode I_d (Cr) was varied in the range from 100 A to 40 A (Table 1). The deposition of coatings was carried out at a working gas pressure P ($N_2 + Ar$ (10%)) = 0.6 Pa, a substrate bias voltage $U_b = -150$ V, and a substrate temperature $T_{sub} = 400^\circ C$. The elemental composition (Table 1), phase composition, mechanical and tribotechnical characteristics of the obtained TiCrN coatings were studied.

Table 1. Elemental composition of coatings based on the TiCrN system on Cr6WV steel.

№ of coating	Deposition conditions	Cr, at. %	Ti, at. %	N, at. %
№1	$I_d(Cr)/I_d(Ti) = 100/80$	29	27	44
№2	$I_d(Cr)/I_d(Ti) = 80/80$	23	28	49
№3	$I_d(Cr)/I_d(Ti) = 60/80$	19	32	49
№4	$I_d(Cr)/I_d(Ti) = 40/80$	14	38	48

The results of nanohardness measurements showed that the maximum value of hardness is achieved at a certain elemental composition of the TiCrN coating in deposition modes № (2-4) and is 34-36 GPa, which is approximately 2 times higher than the hardness of CrN and 1.5 times higher than for TiN. The H/E ratio for these coatings is 0.09. Tribotechnical tests of coatings were carried out on a TRIBOTechnic tribometer under dry friction conditions with reciprocating movement of the sample relative to the counterbody (Al_2O_3 ball). It was found that TiCrN coatings have a fairly low friction coefficient (about 0.13-0.14). The most wear resistant coating is formed in deposition mode № 2, which has a wear coefficient of $3.75 \cdot 10^{-7} \text{ mm}^3/N \cdot m$. According to the data of XRD analysis, in the TiCrN coating deposited during the simultaneous operation of two arc evaporators, the main phase is (Ti, Cr)N – a phase with a face-centered cubic lattice of the NaCl type.

* The work was carried out with the financial support of the RFBR grant № 19-08-00370 A.

COMPARATIVE STUDY ON HIGH-VOLTAGE NANOSECOND PULSES AND DIELECTRIC BARRIER DISCHARGE EFFECTS ON SURFACE MORPHOLOGY AND PHYSICO-CHEMICAL PROPERTIES OF NATURAL PYRRHOTITE

I.Zh. BUNIN, I.A. KHABAROVA

Institute of Comprehensive Exploitation of Mineral Resources, RAS, Moscow, Russia

e-mail: bunin_i@mail.ru

The use of electromagnetic impulse irradiations as preparatory operations preceding the flotation process makes it possible to increase the efficiency of the flotation separation of sulfide minerals with similar physical and chemical properties due to contrast changes in the phase composition and physicochemical properties of the sulfide surface [1]. The *nonthermal* effect of the high-power nanosecond electromagnetic pulses (HPEMP) on the chemical and phase compositions of mineral surface, electrochemical, physical-chemical, and flotation properties of sulfide minerals (pyrite, arsenopyrite, and other sulfide minerals) was the subject of our previous studies [1]. In this work, using the methods of scanning electron microscopy, potentiometric titration (electrode potential; E , mV), sorption and flotation measurements, we studied the mechanism of the influence of electromagnetic pulsed actions of two types, namely, a high-voltage nanosecond electromagnetic pulses and dielectric barrier discharge (DBD) in air at atmospheric pressure, on the surface morphology, and the physicochemical properties of the natural pyrrhotite. The purpose of our research is to increase the efficiency of the processing of refractory *sulfide copper-nickel ores*.

The nanosecond pulse generator (HPEMP) operates at a frequency of 100 Hz (pulse repetition rate), the output pulse amplitude is ~ 25 kV, the duration of the leading edge of the pulse varies from pulse to pulse within 2-5 ns, and the pulse duration varies within 4-10 ns. Video pulses of a bipolar shape are generated, pulse energy ~ 0.1 J, electric field strength in the interelectrode gap $(0.5-1) \times 10^7$ V/m, time range of the pulsed treatment of the mineral samples $t_{\text{treat}}=10-150$ s. We consider different modes of the existence and development of a dielectric barrier discharge (DBD) upon a change in applied stress and the frequency of pulse repetition. We establish the operating parameters of pulses that initiate a discharge at which the greatest changes in the structural-sensitive properties of minerals are observed: the length of the leading edge of a pulse is 250-300 ns, the length of pulse is 8 μs , the electrode voltage in the barrier discharge cell is 20 kV, and the frequency of pulse repetition is 16 kHz. The range of change in the duration of the DBD-treatment of the samples is $t_{\text{treat}}=10-150$ s. The flow of a discharge current in a discharge cell was limited by one dielectric layer, and the sizes of the electrodes exceeded the length of the inter-electrode space (~ 5 mm).

As a result of exposure to HPEMP ($t_{\text{treat}} = 10-30$ s), new micro- and nano-phases of hydrophobic elemental sulfur (S^0) and polysulfide sulfur (S_n^{2-}), and iron oxides and insoluble polysulfide's of complex morphology were found on the pyrrhotite surface. Under the action of DBD, the effect of the formation of microcracks and electric breakdown channels was established, as well as the removal of microcrystalline fragments of the mineral substance (micro-chips) from the mineral surface, due to mass transfer under the action of an electric field and/or, possibly, ponderomotive forces. During a short-term electric pulse ($t_{\text{treat}} = 10$ s) processing of pyrrhotite, the electrode potential of the mineral shifted in the direction of negative values. The maximum difference in the values of the electrode potential before and after treatment was 73 mV and was achieved in an alkaline medium at pH 10. The minimum sorption of the flotation reagent on the surface of the mineral was also found in the case of a short-term mode of impulse action ($t_{\text{treat}} = 10$ s), it is consistent with the data on the HPEMP effect on the electrode potential of the mineral. A sharp shift in E of pyrrhotite to the region of negative values caused a decrease in the sorption of the anionic collector on the mineral, a decrease in the hydrophobicity of the surface and flotation of the mineral was due to an increase in the content of oxidized ferric iron on the mineral surface. Dielectric barrier discharge processing caused an increase in the positive values of the electrode potential of pyrrhotite by 10-65 mV in the range of pH 5.5-9.6. At pH 9.7-12, the largest changes in the E -values were established for the mode of short-term ($t_{\text{treat}} = 10$ s) treatment of the mineral. The shift of the electrode potential to the region of negative values ($E=-60$ mV) occurred, which causes the effect of a decrease in the sorption and flotation activity of pyrrhotite. Thus, the advantages of using the short-term ($t_{\text{treat}}= 10-30$ s) energy impacts for structural and chemical modification of the surface and physicochemical properties of sulfide minerals of iron and copper are shown.

REFERENCES

- [1] I.Zh. Bunin, M.V. Ryazantseva, A.L. Samusev, and I.A. Khabarova, "Theory and practice of application of combined physicochemical and energy effects on geomaterials and water suspensions," *Gornyi Zhurnal*, No. 11, pp. 77-83, 2017.

EFFECT OF POWER OF ULTRASOUND DURING MICRO-ARC OXIDATION ON PHASE COMPOSITION AND MORPHOLOGY OF CALCIUM PHOSPHATE COATINGS*

E.A. KAZANTSEVA^{1,2}, E.G. KOMAROVA¹, Y.P. SHAKREEV¹

¹Institute of Strength Physics and Materials Science SB, RAS, Tomsk, Russia

²National Research Tomsk State University, Tomsk, Russia

e-mail: kati10_95@mail.ru

The aim of the work was to study the influence of the power magnitude of the ultrasound (US) during the micro-arc oxidation (MAO) on the morphology and phase composition of the formed calcium phosphate (CaP) coatings. The synthesis of the CaP coatings on titanium samples was carried out by the MAO method in the base electrolyte, and in the standard regime [1] with the anode voltage of 200 V, pulse duration of 100 μ s, frequency of 50 Hz, and deposition time of 10 min. The US field with a sinusoidal waveform, a frequency of 35 kHz and varied powers of 20, 60, 100, 160 and 200 W was applied during the MAO process.

The SEM data show that in the control MAO regime (without US), structural elements of a spheroidal shape (spheres) with internal pores and external pores the spaces between the spheres on the surface of the coatings are formed [1]. The action of the US fields during the MAO process lead to the change in the coating surface's morphology: the structural elements are destroyed due to the action of shock waves that occur when cavitation bubbles collapse in the electrolyte, and the pore spaces are filled with fragments. The square percentage of the surface areas containing destroyed spheres and fragments increases from 6 to 26% with an increase in the US power in the range of 20-100 W. However, a further increase of the power from 100 to 200 W does not lead to the changes in the morphology, and the failure areas percentage is 20-25%. The SEM data of the cross-sectional coatings show the internal structure with numerous branched pores, pore channels, and cracks. The US application during the MAO leads to an increase in the average size of internal pores from 2.5 to 4.7 μ m and to the formation of local macropores with the size of 15-30 μ m at the interface "coating/substrate" regardless of the magnitude of the US power [1].

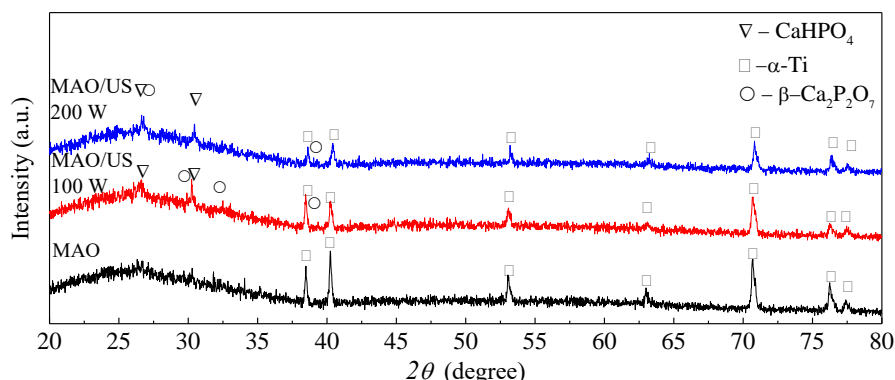


Fig. 1. XRD patterns of the CaP coatings.

XRD analysis shows the presence of diffused halo in the range of $2\theta = 20-35^\circ$ corresponding to the X-ray amorphous CaP phase and weak reflections from the phase α -Ti (ICDD No. 44-1294) corresponding to the substrate material (Fig. 1). In addition, several weak reflexes from the CaHPO_4 (DCPA, monetite) (ICDD No. 09-0080) and β - $\text{Ca}_2\text{P}_2\text{O}_7$ (β -CPP) (ICDD No. 09-0346) are observed on the XRD patterns of the US-assisted CaP coatings (regardless of US power). In this case, the intensity of the reflections from α -Ti phase decreases that may be the result of increasing the thickness of the US-assisted CaP coatings.

Thus, the US power magnitude of 100 W and more affected on the MAO CaP coating phase composition and morphology.

REFERENCES

- [1] Kazantseva E.A., Komarova E.G., Sharkeev Y.P. Structural and morphological features of the ultrasound-assisted micro-arc oxidation coatings, AIP Conf. Proc., 2167, 020156, 2019.

* The work has been financially supported by the Russian Science Foundation (Project No. 21-73-10265).

EFFECT OF BIAS VOLTAGE ON THE PERFORMANCE OF MAGNETRON DEPOSITED MoS₂ COATINGS

M.M. KHARKOV^{1,2}, G.I. RYKUNOV¹, A.V. KAZIEV¹, M.S. KUKUSHKINA¹, D.V. KOLODKO^{1,3}, M.V. PROZHEGA⁴, E.O. RESCHIKOV⁴, I.S. BABINETS^{4,5}, P.P. BESCHAPOV^{4,5}, A.M. STASENKO^{4,5}, S.V. CHERNYSHOV^{4,5}

¹National Research Nuclear University MEPhI (Moscow Engineering Physics Institute), Moscow, Russia

²A.A. Bochvar High-Technology Scientific Research Institute for Inorganic Materials, Moscow, Russia

³Kotelnikov Institute of Radio Engineering and Electronics, RAS, Fryazino, Moscow Region, Russia

⁴Blagonravov Institute of Machine Science, Moscow, Russia

⁵Bauman Moscow State Technical University, Moscow, Russia

e-mail: kharkovmm@ya.ru

Molybdenum disulfide coatings are often used as hard grease. They are also applied to prevent sticking of machine parts experiencing high thermal loads, e. g., the fasteners of the first wall elements in tokamaks [1]. The adhesive properties of such coatings are primarily determined by the surface preparation method and deposition mode.

The composition and parameters of magnetron plasma have been examined for the case of MoS₂ target sputtering in argon. The magnetron discharge was operated in a direct current (DC) and in a mid-frequency pulsed modes with $f = 1\text{--}100$ kHz repetition rate. The argon pressure was kept at $p_{Ar} = 0.5$ Pa, and the discharge power was varied in the range $P_d = 10\text{--}30$ W. Density and temperature of electrons were measured with a Langmuir probe. Coating thickness was measured with a surface profiler after the deposition. Coating density was evaluated by a weighing method. The mass-resolved ion fluxes incident at the substrate were measured by a dedicated mass-analyzer [2].

MoS₂ coatings were deposited in pulsed and DC modes with different bias voltages applied to the sample. Coatings prepared in DC mode exhibited better adhesion. After film thickness measurements, we observed that the effective growth rate of the film deposited at positive bias voltage (+100 V) was $\sim 30\%$ higher than that of the film deposited at negative bias voltage (-20 V).

MoS₂ coatings deposited on AISI316L steel samples with different surface roughness underwent tribological tests in vacuum, at 250°C temperature, with a 3-mm-radius indenter. The testing procedure is described in detail in [3]. Typical results are shown in Fig. 1.

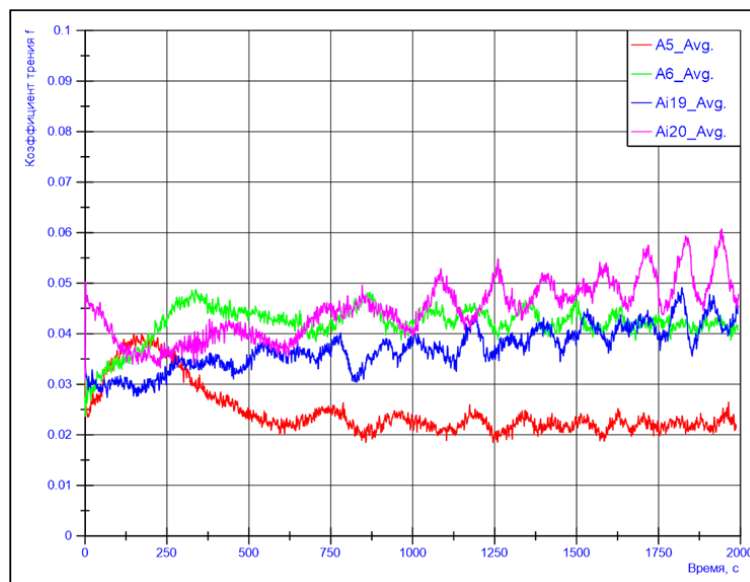


Fig. 1. Averaged results of tribological tests for samples with different surface roughness — A5(Ra0.1), A6(Ra0.05), Ai19(Ra1.5), Ai20(Ra2.3).

REFERENCES

- [1] V. Thompson, R. Eaton, R. Raffray, K. Egorov, Properties of low friction anti-seize coatings for fusion applications // Fusion Engineering and Design 146 (2019) P. 345–348.
- [2] D.V. Kolodko D.V., D.G. Ageychenkov, A.V. Kaziev, K.A. Leonova, M.M. Kharkov, A.V. Tumarkin, Diagnostics of ion fluxes in low-temperature laboratory and industrial plasmas // Journal of Instrumentation 14 (2019) P. 10005.
- [3] M.V. Prozhega, E.O. Reschikov, A.D. Shirshov, N.G. Yakovenko, Frictional properties of 3D printing polymers in vacuum // Journal of Friction and Wear 41 (2020) P. 565–570.

SURFACE ENGINEERING OF TITANIUM: INFLUENCE OF ICP ETCHING AND CALCIUM-PHOSPHATE-BASED COATING DEPOSITION*

*M.M. KHARKOV^{1,2}, A.V. KAZIEV¹, G.I. RYKUNOV¹, M.S. KUKUSHKINA¹,
K.A. PROSOLOV³, M.A. KHIMICH³, YU.P. SHARKEEV^{3,4}*

¹*National Research Nuclear University MEPhI (Moscow Engineering Physics Institute), Moscow, Russia*

²*A.A. Bochvar High-Technology Scientific Research Institute for Inorganic Materials, Moscow, Russia*

³*Institute of Strength Physics and Materials Science of SB RAS, Tomsk, Russia*

⁴*National Research Tomsk Polytechnic University, Tomsk, Russia*

e-mail: kaziev@plasma.mephi.ru

Surface engineering in medical technology is a booming area of research owing to the growing demand for new devices and materials needed in various clinical applications. Surface modifications such as plasma treatment and physical vapor deposition (PVD) directly influence the surface morphology, elemental composition and wetting behavior of materials for medical applications. Currently, titanium (Ti) and its alloys are the most widely used biointerface materials. This is due to their outstanding biocompatibility resulting from bioinert nature of titanium. It has been lately discovered that the surface morphology of bioinert structures could be a governing parameter regulating stem cell fate and bacteria adhesion [1]. It is speculated that the application of cell-specific nanopatterns and high-aspect-ratio surface features in medical devices could have a significant impact on the clinical outcome.

Following the studies of titanium surface modification in inductively coupled argon plasma (ICP) [2] and deposition of functional hydroxyapatite-based coatings [3], we report the progress of examining the combined effect of these two treatment options on the structure, composition, and other surface properties.

The study was carried out with Gr. 1 Ti samples. The first step was ion treatment in the inductively coupled argon plasma (the results are shown in Fig. 1). The samples with porous surface structure and enhanced roughness were selected for the next step. They were used for calcium-phosphate-based coating deposition in custom made vacuum installation equipped with RF magnetron operated at 13.56 MHz. The input RF power was 250 W, while throw distance was kept at 70 mm. The average coating thickness, evaluated by ellipsometry, was from 0.5 to 1 μm . The high-energy ICP treatment resulted in significant change of residual stress and recrystallization of Ti while deposited coatings were found to be X-ray amorphous. The coating deposition significantly changed the wetting behavior of the samples making them more hydrophilic, which is favorable for biomedical applications. Elemental composition determined by energy dispersive spectroscopy confirmed the slight change in Ca/P ratio upon variation in coating thickness and deposition regimes.

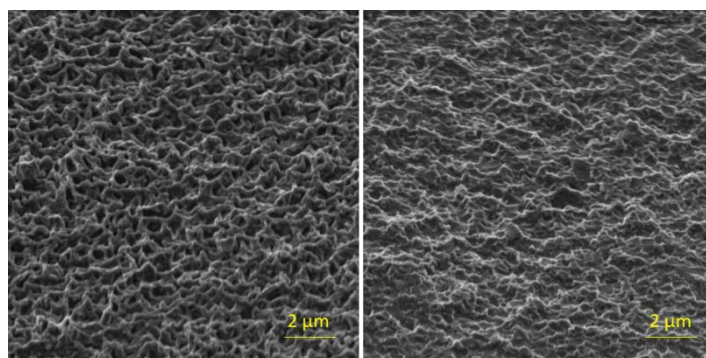


Fig. 1. Structure of the titanium surface after ion-plasma treatment. The figure made at 45°.

REFERENCES

- [1] H. Anderson, V. Llopis-Hernandez, P. Sweeten, H. Donnelly, R. Gurden, W. Orapiriyakul, M. Salmeron-Sanchez, M. J. Dalby, M. P. Tsimbouri, “Nanoscale surface cues and cell behavior”, *Comprehensive Biomaterials*, vol. 2, pp. 163-179, 2017.
- [2] M. M. Kharkov, A. V. Kaziev, D. V. Danilyuk, M. S. Kukushkina, N. A. Chernyh, A. V. Tumarkin, D. V. Kolodko, “Effects of Ar ion irradiation in an ICP discharge on the titanium surface topology”, *Applied Surface Science*, vol. 527, pp 146902, 2020.
- [3] K. A. Prosolov, M. A. Khimich, J. V. Rau, D. V. Lychagin, Yu. P. Sharkeev, “Influence of oblique angle deposition on Cu-substituted hydroxyapatite nano-roughness and morphology”, *Surface and Coatings Technology*, vol. 394, pp. 125883, 2020.

* The work was performed according to the Government research assignment for ISPMS SB RAS, project FWRW-2021-0007

PVD GRADIENT AND MULTILAYER COATINGS DEPOSITED BY VACUUM-ARC PLASMA-ASSISTED METHOD*

O.V. KRYSINA, N.N. KOVAL, YU.F. IVANOV, N.A. PROKOPENKO, V.V. SHUGUROV

Institute of High Current Electronics, SB, RAS, Tomsk, Russia
e-mail: krysina_82@mail.ru

The vacuum-arc synthesis of PVD coatings with multilayer and gradient structure has been described. The feature of deposition method is the use of a gas plasma source based on a non-self-sustained arc discharge with thermionic and hollow cathodes. The coatings were synthesized in the mode with plasma assistance by the vacuum-arc method in a QUINTA ion-plasma facility (IHCE, Tomsk, Russia). Its description is detailed elsewhere [1]. The examples of gradient and multilayered coatings deposited by low-inertia method are presented. The systems of gradient coating are ZrAlNbN and ZrNbN. The system of multilayer coating is Mo/MoN. It is shown that selected method characterized by low inertia, which would make it possible to achieve a high reproducibility of the composition and thickness of multi-layer and gradient coatings, which would naturally improve their functional properties.

REFERENCES

- [1] V.V. Shugurov, N.N. Koval, O.V. Krysina, N.A. Prokopenko, "QUINTA equipment for ion-plasma modification of materials and products surface and vacuum arc plasma-assisted deposition of coatings," IOP Conf. Ser.: J. Phys.: Conf. Ser., vol. 1393, pp. 12131 (1–10), 2019.

* The work was supported by the RSF Grants No. 18-79-10111 (ZrAlNbN gradient coatings) and by RFBR No. 18-48-700016 (Mo/MoN multilayer coatings).

COMPUTER SIMULATION OF TEMPERATURE FIELDS IN THE Cr (FILM) – Zn (SUBSTRATE) SYSTEM DURING PULSED ELECTRON BEAM IRRADIATION

A.B. MARKOV, A.V. SOLOVEV, E.V. YAKOVLEV, E.A. PESTEREV

Tomsk Scientific Centre, SB, RAS, Tomsk, Russia

e-mail: eugenejuk@gmail.com

Currently, the use of zirconium alloy is widespread in medicine and the nuclear power industry. Zirconium alloys are most actively used for fuel element cladding, fuel channel tubes, and various fuel assembly parts. However, zirconium alloys have their disadvantages. For example, Zr actively dissolves hydrogen, which often occurs during corrosion. Because of this, zirconium hydrides are formed, which greatly reduce the ductility of the raw material and make the metal more brittle [1]. This leads to cracks in the zirconium tubes. This problem can be solved by applying a highly corrosive and heat-resistant coating to the zirconium surface [2]. Such a coating can be a Cr-Zr surface alloy [3]. The surface alloy will be synthesized using a low-energy high-current electron beam (LEHCEB) of microsecond duration. It is necessary to establish the optimal parameters of LEHCEB by means of computer modeling of temperature fields in the film/substrate systems.

Calculations of temperature fields for the Cr (film)-Zr (substrate) system were performed. Melting thresholds for pure metals were calculated: Cr - 4.8 J/cm^2 , Zr - 1.85 J/cm^2 . The dependences of melting thresholds for the Cr-Zr system as a function of film thickness were calculated. For film thicknesses from 0.25 to $3.5 \text{ }\mu\text{m}$, the melting threshold for the Cr-Zr system increases linearly from 2.05 to 6.23 J/cm^2 . The dependences of the molten layer thickness on the LEHCEB energy density for the systems Cr(0.25)/Zr, Cr(0.5)/Zr, Cr(1.0)/Zr, and Cr(1.75)/Zr were calculated. The limiting values of the LEHCEB energy density up to which the thickness of the molten layer increases linearly have been established. At LEHCEB energy density values above the limiting values, the thickness of the molten layer increases logarithmically due to the processes of evaporation of the film surface. The calculated limit values of the LEHCEB energy density increase linearly with film thickness. The lifetime dependences of film and substrate melts on the LEHCEB energy density for the systems Cr(0.25)/Zr, Cr(0.5)/Zr, Cr(1.0)/Zr, and Cr(1.75)/Zr were calculated. The lifetimes of the film and substrate melts increase linearly. The values of the LEHCEB energy density above which the lifetime of the film melt is less than that of the substrate melt have been established. The optimal conditions for the synthesis of a Cr-Zr surface alloy without barrier layers have been determined numerically. The optimal value of the LEHCEB energy density is suggested to be the one at which the lifetime of the film and substrate melts will be equal.

REFERENCES

- [1] I.N. Volkova, A.E. Novoselov, G.P. Kobylansky, A.N. Kostyuchenko / Corrosion of the E635 alloy in the conditions of VVER-1000 reactors // VANT. – 2012. No. 2 (78). P. 46-51.
- [2] Z. Karoutas, J. Brown, A. Atwood, L. Hallstadius, E. Lahoda, S. Ray, J. Bradfute / The maturing of nuclear fuel: Past to Accident Tolerant Fuel // Progress in Nuclear Energy. – 2018. V. 102. P. 68-78.
- [3] C.C. Tang, M. Stueber, H.J. Seifert, M. Steinbrueck / Protective coatings on zirconium-based alloys as accident-tolerant fuel (ATF) claddings // Corrosion Reviews. – 2017. V. 35. No. 3. P. 141-165.

FIELD ELECTRON EMISSION FROM NANOSTRUCTURED TUNGSTEN SURFACE

I.L. MUZYUKIN, P.S. MIKHAILOV

Institute of Electrophysics, UB, RAS, Yekaterinburg, Russia
e-mail: gmgm01@mail.ru

The interaction of plasma with the surface is a key factor for the realization of magnetic confinement fusion. Experiments on the interaction of plasma and tungsten walls were carried out on linear accelerators and tokamaks. As a result of the interaction of helium plasma with the walls, thin nanorods are formed, called "fuzz" [1]. This work is devoted to the study of the field emission properties of a tungsten cathode with a nanostructured surface.

To measure the field emission properties of the non-excited tungsten, surface the extremely low current measurement procedure was developed. Point anode was used, with an electrode gap of about 0.4 – 0.8 mm. The slow rising of the electrical field in some cases led to avalanche-like emission current amplification that in turn led to the breakdown. The current amplification waveforms suggest that emission structures are formed on the cathode surface. The field-induced emission structures time was in the range of 10 – 100 μ s. The emission pictures on a phosphor screen and emission current waveforms suggest that during avalanche-like emission current rise several emission structures could be formed.

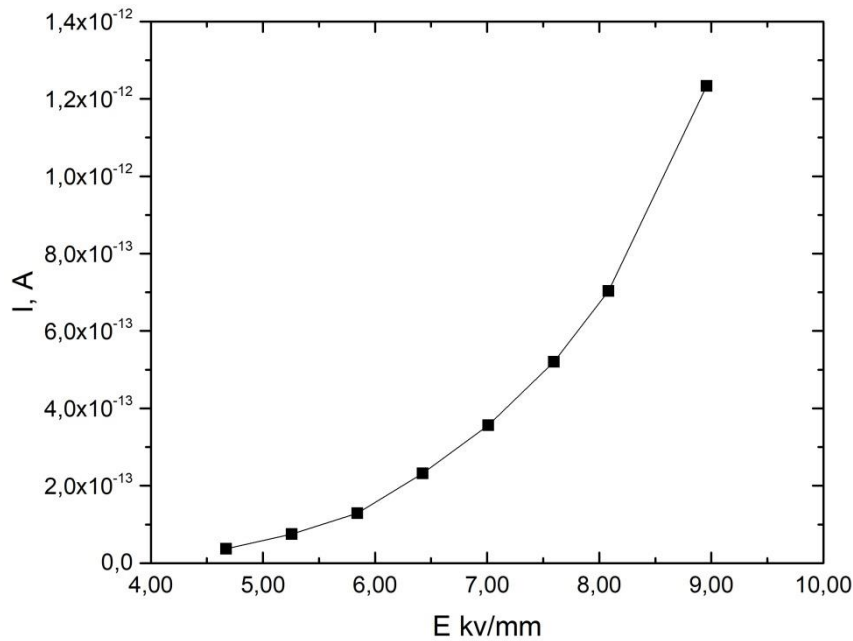


Fig. 1. I-V curve of tungsten cathode with the nanostructured surface.

REFERENCES

- [1] Kajita Shin, Naoaki Yoshida, and Noriyasu Ohno. "Tungsten fuzz: deposition effects and influence to fusion devices." *Nuclear Materials and Energy* (2020): 100828.

EFFECT OF ION IRRADIATION ON THE STRUCTURAL STATE AND MECHANICAL PROPERTIES OF NATURALLY-AGED HOT-PRESSED D16 (Al-Cu-Mg) ALLOY PROFILES*

N.V. GUSHCHINA¹, V.V. OVCHINNIKOV¹, L.I. KAIGORODOVA², D.Y. RASPOSIENKO², D.I. VICHUZHANIN³

¹*Institute of Electrophysics, UB, RAS, Yekaterinburg, Russia*

²*Institute of Metal Physics, UB, RAS, Yekaterinburg, Russia*

³*Institute of Engineering Science, UB, RAS, Yekaterinburg, Russia*

e-mail: guscha@rambler.ru

The effect of 20-keV argon ion irradiation on the mechanical properties, structure, and phase composition of quenched and then naturally-aged hot-pressed profiles (6 mm thick) made of an D16 alloy (Al–Cu–Mg system) has been studied.

The profiles were used to prepare standard flat specimens for tensile testing. The specimens were irradiated with continuous accelerated argon ion beams using an ILM-1 ion beam implanter equipped with a PULSAR-1M ion source based on a glow discharge with a hollow cold cathode [1]. A line-focus ion beam 100×20 mm² in cross section was cut from a cylindrical ion beam using a collimator. The specimens were irradiated on both sides. Irradiation was performed at $E = 20$ keV, $j = 200$ $\mu\text{A}/\text{cm}^2$, and $F = 2 \cdot 10^{15}$ and $1 \cdot 10^{16}$ cm⁻². The maximum temperature to which the specimens were heated during irradiation was below 40–50°C.

The standard mechanical tests for uniaxial tension were conducted on the flat specimens according to the State Standard GOST 14972 [2]. The specimens were tested on an INSTRON-8801 universal servohydraulic tester. The measurement error was ~ 3 %.

The structure and the phase composition of the alloy foils were examined in JEM-200CX and Philips CM 30 Super Twin electron microscopes at the Electron Microscopy Center of Collaborative Access of the Institute of Metal Physics, UB RAS. The microstructure was examined in two sections parallel to the irradiated surface, directly near the surface and at a distance of ~ 150 μm from it.

The initial quenched and naturally-aged D16 alloy has been found to have $\sigma_u = 557$ MPa, $\sigma_{0.2} = 441$ MPa, and $\delta = 9.7\%$. The mechanical properties after ion irradiation at the fluence $F = 2 \cdot 10^{15}$ cm⁻² remain almost the same. Irradiation at a higher fluence $F = 1 \cdot 10^{16}$ cm⁻² increases the relative elongation to $\delta = 12.3\%$, without changing the strength properties.

A developed subgrain structure is shown to be formed in the initial D16 alloy. Al₆ (Fe, Mn) intermetallic compounds of crystallization origin are uniformly distributed throughout subgrains. The intermetallic compounds are mainly lamellar in shape. In addition, Al, Cu, Mg, Fe, Mn, and Si phases of complex composition in the form of round-shaped particles resulted from crystallization are observed along grain boundaries. Fine particles of strengthening phases, such as θ'' (θ'') (CuA₂), and S' (A₂MgCu), form in the alloy due to aging.

Ar⁺ ion irradiations at $F = 1 \cdot 10^{16}$ cm⁻² causes coarsening of the subgrain structure near the specimen surface. In addition, irradiation lead to partial dissolution and fragmentation of complex intermetallic compounds of crystallization origin, which lie along the grain boundaries, both in the surface layer and at a distance of 150 μm from it. Intermetallic Al₆(Fe, Mn) compounds decrease in size and their morphology changes, namely, the density of distribution of lamellar precipitates decreases, and equiaxed precipitates disappear. The irradiation triggers the decomposition of the supersaturated solid solution to form a more stable S' phase. An increase in the volume fraction of the lamellar stable S'-phase precipitates suppresses the nucleation and growth of the metastable aluminium–copper θ'' (θ'') phases.

We found that short-term (during 8 s) Ar⁺ ion irradiation transforms the microstructure and the phase composition of the naturally-aged hot-pressed profiles made of the D16 alloy, and increases their plasticity. This result is interesting, since the improvement of plastic properties while maintaining strength can favorably affect the resource characteristics.

REFERENCES

- [1] N.V. Gavrilov., G.A. Mesyats, S.P. Nikulin, G.V. Radkovskii, A. Eklind and A.J. Perry, "A New Broad Beam Gas Ion Source for Industrial Applications", J. Vac. Sci. Technol., vol. A 14, pp. 1050-1056, 1996.
- [2] GOST (State Standard) 1497-84 Techniques tensile tests, Moscow: Standartinform, 2008.

* This work was supported in part by RFBR grant № 19-08-00802-A.

POSSIBILITY OF ANNEALING OF A DEFORMED Ni–13.9 wt. % W ALLOY WITH A BEAM OF ACCELERATED ARGON IONS*

N.V. GUSHCHINA¹, V.V. OVCHINNIKOV¹, V.I. BOBROVSKII², V.I. VORONIN²

¹*Institute of Electrophysics, UB, RAS, Yekaterinburg, Russia*

²*Institute of Metal Physics, UB, RAS, Yekaterinburg, Russia*

e-mail: guscha@rambler.ru

The Ni–13.9 wt.% W alloy after cold working to a high reduction (99%) and subsequent recrystallization annealing ($T = 1000^{\circ}\text{C}$, 1 h) acquires a particularly sharp cubic texture $\{100\}\langle 001\rangle$. It is a promising material for the manufacture of substrates for HTSC cables [1].

Inert gas ion irradiation of alloys in the metastable state, in particular after cold working in ion energy range 10–50 keV and ion current density range $j = 100\text{--}400 \mu\text{A}/\text{cm}^2$ is known to cause annealing at much lower temperatures and a shorter time as compared to thermal annealing [2]. The aim of this work was to estimate the possibility of annealing Ni–W alloy tapes to form a particularly sharp cubic texture using ion-beam treatment.

The tapes were irradiated on one side with continuous Ar^+ ion beams using an ILM-1 ion beam implanter equipped with a PULSAR-1M ion source based on a low-pressure glow discharge with a hollow cold cathode [3]. The irradiation parameters were chosen to irradiate Ni–13.9 wt.% W samples at two different temperatures. Irradiation at $E = 15 \text{ keV}$ and $j = 100 \mu\text{A}/\text{cm}^2$ heated the samples to $T = 630^{\circ}\text{C}$, and irradiation at $E = 15 \text{ keV}$ and $j = 300 \mu\text{A}/\text{cm}^2$, to $T = 850^{\circ}\text{C}$. Fluences of $3.2 \cdot 10^{16}$ and $1.6 \cdot 10^{17} \text{ cm}^{-2}$ were achieved under the above conditions.

X-ray diffraction (XRD) analysis of the initial and irradiated samples on both sides was carried out on a DRON-UM-1 diffractometer. The XRD data were analyzed by the Rietveld full-profile method using FullProf software.

Argon ion irradiation of the alloy tapes at a fluence of $F = 3.2 \cdot 10^{16} \text{ cm}^{-2}$ and an irradiation time of 51 s resulted in heating the samples to 630°C and a decrease in the microstress level ($\Delta d/d \times 10^4 = 20.7$ and 22.0 on both irradiated and nonirradiated sides instead of 39.0 for the initial sample). The (220) texture characteristic of the initial deformed state retains. Further irradiation of this sample at a fluence of $1.6 \cdot 10^{17} \text{ cm}^{-2}$ (250-s irradiation) results in the disappearance of the preferential grain orientation. The level of microstresses increases slightly to $\Delta d/d \times 10^4 = 26.5$ for the irradiated side and $\Delta d/d \times 10^4 = 18.7$ for the unirradiated side.

Irradiation for heating the deformed tapes to a higher temperature $T = 850^{\circ}\text{C}$ results in a sharp microstress decrease $\Delta d/d \times 10^4 = 8.9$ and 8.3 (irradiated and nonirradiated sides) and a radical change in texture from (220) to (200) already at fluence $F = 3.2 \cdot 10^{16} \text{ cm}^{-2}$ (irradiation time of 17 s). Subsequent irradiation of this sample at a fluence of $1.6 \cdot 10^{17} \text{ cm}^{-2}$ (85-s irradiation) does not cause any important changes. The level of microstresses remains the same. The grain orientation that changed earlier retains. A comparative analysis of the samples irradiated for 17 s and heated in the furnace in a similar way showed that annealing changed the grain orientation as well and reduced the level of microstresses. However, its effect is about three times less than during irradiation.

We plan to continue the search for optimal irradiation conditions for annealing Ni–W films to form the desired texture. We should note that the changes in the microstress level on both the irradiated and nonirradiated sides of the 80- μm -thick sample are approximately the same, although the projective range of argon ions with an energy of 15 keV in nickel, according to the TRIM calculations, is only 7 nm. This result supports the radiation-dynamic nature of the accelerated ion beam effect on the substance due to the generation of powerful elastic shock postcascade waves [2].

REFERENCES

- [1] D.P. Rodionov, I.V. Gervas'eva, and Yu.V. Khlebnikova, *Textured Nickel-Alloy-Based Substrates*. Yekaterinburg: UB of RAS, 2012.
- [2] V.V. Ovchinnikov, "Nanoscale dynamic and long-range effects under cascade-forming irradiation", *Surface and Coating Technology*, vol. 355, pp. 65-83, 2018.
- [3] N.V. Gavrilov, G.A. Mesyats, S.P. Nikulin, G.V. Radkovskii, A. Eklind and A.J. Perry, "A New Broad Beam Gas Ion Source for Industrial Applications", *J. Vac. Sci. Technol.*, vol. A 14, pp. 1050-1056, 1996.

* This work was supported by the Russian Scientific Foundation, project No. 19-79-20173.

ION CURRENT OPTIMIZATION IN A MAGNETRON WITH TUNABLE MAGNETIC FIELD

A.V. KAZIEV¹, D.G. AGEYCHENKOV¹, A.V. TUMARKIN¹, D.V. KOLODKO^{1,2}, N.S. SERGEEV^{1,3}, M.M. KHARKOV^{1,4}

¹*National Research Nuclear University MEPhI (Moscow Engineering Physics Institute), Moscow, Russia*

²*Kotelnikov Institute of Radio Engineering and Electronics, RAS, Fryazino, Moscow Region, Russia*

³*National Research Center “Kurchatov Institute”, Moscow, Russia*

⁴*A.A. Bochvar High-Technology Scientific Research Institute for Inorganic Materials, Moscow, Russia*

e-mail: kaziev@plasma.mephi.ru

One of the methods to improve quality of thin films prepared by magnetron sputtering is to elevate the ionization degree and thus to arrange the ion assistance of coating growth. Generally, it can be done in several ways: by optimizing the magnetic field configuration, by changing the power supply regime (i.e. utilizing high power pulsed sputtering modes —HiPIMS [1], L-HiPIMS [2], MPPS [3], and others), or both.

The response of the ion current in the substrate region to the magnetic system configuration of a circular magnetron (Pinch Magneto series) was studied during direct current sputtering of aluminum target in argon. The unbalancing degree induced by changing the positions of magnets was modelled with finite element methods (COMSOL Multiphysics). The ion saturation current in the substrate region showed more than twofold variation with unbalancing degree in the range 0.6–1.2. The dependence was non-monotonic, and the system was optimized to maximize the substrate ion current. The Langmuir probe diagnostics showed plasma density $\sim 10^{16} \text{ m}^{-3}$ in the optimized magnetic configuration.

The dependence of ion saturation current on the relative position of magnets (Δz) is shown in Fig. 1 along with the unbalancing degree g calculated for a number of magnetic configurations. Discharge power P was fixed at 100 W.

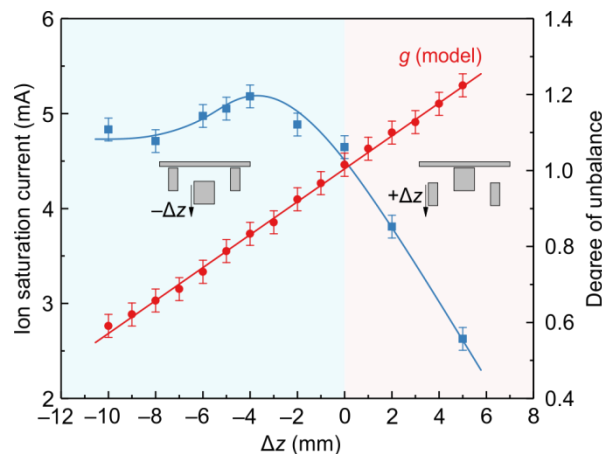


Fig. 1. Ion saturation current and degree of unbalancing (g) for different positions of magnets.

Varying the magnetic field configuration is a convenient tool for tuning the ion content in the substrate region. Having the capabilities of in situ magnet positioning ensures widening of film properties that can be prepared using the magnetron.

REFERENCES

- [1] Gudmundsson J T, Brenning N, Lundin D, Helmersson U 2012 *J. Vac. Sci. Technol. A* 30(3) 030801.
- [2] Mozgrin D V, Fetisov I K, Khodachenko G V 1995 *Plasma Phys. Rep.* 21 422.
- [3] Lin J, Moore J J, Sproul W D, Mishra B, Rees J A, Wu Z, Chistyakov R, Abraham B 2009 *Surf. Coat. Technol.* 203 3676.

APPLICATION OF COMPOSITE SHS-CATHODES IN RECENT PVD TECHNOLOGIES FOR MANUFACTURING OF PROTECTIVE UHTC-BASED COATINGS*

Ph. KIRYUKHANTSEV-KORNEEV, E. LEVASHOV

National University of Science and Technology "MISIS", Moscow, Russia

e-mail: kiruhancev-korneev@yandex.ru

Complex study of multicomponent coatings based on ultra high temperature ceramics (UHTC), including MeNm (Me: Zr, Hf, Ta, Ti, Nm: B, C, N), and SiC was carried out. The development of PVD technologies is often related with creation of new multicomponent materials that are used as precursors in deposition process. Among the methods of composite targets manufacturing the combination of SHS with subsequent hot pressing or SPS is cost effective technology. Self-propagating high-temperature synthesis (SHS) allows obtaining a wide range of composites with unique structure, low porosity, low impurities content. The nanocomposite coatings were obtained in various energy regimes, including rigid, due to the use of functionally graded materials, reinforced materials, and ceramic with hierarchical structure. Coatings were deposited by magnetron sputtering in DC, pulsed DC, and HIPIMS regimes, pulsed cathodic arc evaporation (PCAE), or using ion sputtering [1]. Multiphase MeNm targets were used. Depositions were performed in Ar, N₂, C₂H₄, and gas mixtures. To evaluate the high-temperature oxidation resistance, diffusion-barrier properties, and thermal stability, the as-deposited coatings were isothermally annealed in air atmosphere or in vacuum at temperatures range $T=1000-1700^{\circ}\text{C}$ [2]. The additional thermo-cycling experiments were fulfilled between 25 and 1000°C for 100 cycles. The structure of as-deposited and heat-treated coatings was studied by means of XRD, SEM, TEM, GDOES, XPS, Raman and FTIR spectroscopy. The mechanical properties were measured using indentation and scratch-testing. The tribological properties were evaluated in air using a high-temperature tribometer. Deep knowledge about the influence of parameters and morphological features of coatings structure on mechanical properties was obtained using the investigation of deformation mechanisms by nano- and pico- indentation. In-situ studies of phase transformation, recrystallization and phase segregation in Zr-B-N, Zr-Ta-Si-B-C, Zr-Ta-Si-B-N, and Zr-Mo-Si-B coatings were carried out upon heating in column of TEM.

REFERENCES

- [1] Ph.V. Kiryukhantsev-Korneev et al. *Surface and Coatings Technology*, 403, 2020, 126373.
- [2] Ph.V. Kiryukhantsev-Korneev et al. *Corrosion Science*, 123, 2017, 319-327.

* This work was carried out with financial support from the Ministry of Science and High Education of the Russian Federation under State Assignment (project 0718-2020-0034).

INVESTIGATION OF THE STRUCTURE OF CRATERS ON THE SURFACE OF STEEL 12X18H10T AFTER ITS TREATMENT WITH A HIGH PULSE POWER BEAM OF CARBON IONS*

M.V. ZHIDKOV¹, A.E. LIGACHEV², G.V. POTEKIN³, G.E. REMNEV³

¹Belgorod National Research University, Belgorod, Russia

²Prokhorov General Physics Institute, RAS, Moscow, Russia

³Tomsk Polytechnic University, Tomsk, Russia

e-mail: carbin@yandex.ru

Surface defects in the form of craters are characteristic elements of the surface relief of metals after irradiated by high pulse power ion beam (HPPIB) [1]. Craters also occur after irradiating of 12X18H10T steel at the TEMP-4M ion accelerator (the energy of C⁺ ions is 250 keV, $\tau \sim 100$ ns, the number of pulses 1,5,10,50, the energy density of a single pulse F is 1 and 3 J/cm²). At $F = 1$ J/cm² and a single pulse, small microcraters (up to 10 microns in diameter) are formed on the surface of the steel with an indistinct parapet, traces of material boiling in the central region of the crater, and, as a rule, inclusion in the center. After processing with 10 pulses, spherical microcraters and larger craters with a clear parapet are formed. The average size of the craters increases with the number of pulses. At $F = 3$ J/cm², classical spherical craters appear after 1 impact pulse (Fig. 1). It is established that the morphology of the craters formed at the same processing parameters does not depend on the degree of preliminary deformation of the steel. Also, inclusions of various elemental and phase compositions, such as TiN and MnS, were found in the center of the craters.

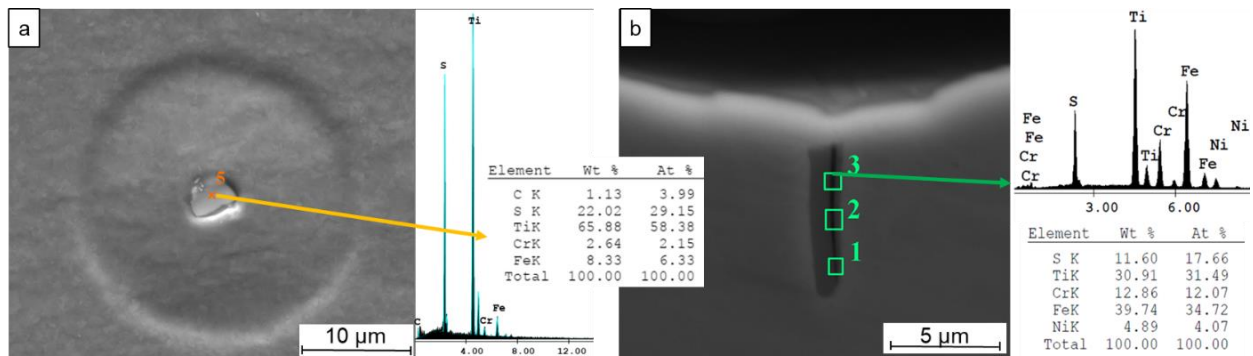


Fig. 1 (a) A crater on the surface of steel after MIP treatment with an energy density of 3 J/cm² (1 pulse); (b) The cross-section of the crater after exposure to 10 HPPIB pulses with a current density of 3 J/cm². To the right of the image are the X-ray microanalysis spectra from the areas indicated by the arrows.

REFERENCES

- [1] Remnev, G.E. and Shulov, V.A., "Application of high-power ion beams for technology", Laser and Particle Beams, 1993, vol. 11, pp. 707–731.

* The work was supported by RFBR, project number 20-08-00907 and Program 11 of Russian Academy of Science.

FORMATION OF A Cr-Zr SURFACE ALLOY USING A LOW-ENERGY HIGH-CURRENT ELECTRON BEAM

A.B. MARKOV, E.V. YAKOVLEV, A.V. SOLOVEV, E.A. PESTEREV, M.S. SLOBODYAN, V.I. PETROV

*Tomsk Scientific Centre, SB, RAS, Tomsk, Russia
e-mail: a.markov@hq.tsc.ru*

Zirconium-based alloys are widely used in modern nuclear power engineering due to a set of exceptional properties, such as high neutron transparency, acceptable mechanical properties, and good corrosion resistance. In regular operation of nuclear power plants, zirconium alloys satisfy the basic requirements for reactor materials. However, under emergency conditions such as a loss of coolant accident (LOCA), zirconium is subject to significant degradation. Temperatures beyond 700°C cause an uncontrolled oxidative reaction of zirconium and water (steam) with the generation of heat and hydrogen gas [1]. Reducing the rate of oxidation of Zr at high temperatures is one of the key problems associated with increasing the accident stability of nuclear power plants. Considerable efforts are directed at improving the operational properties of zirconium alloys through the application of protective coatings [2, 3]. The most likely candidates among them are chromium-containing coating. Nevertheless, there are several problems in the application of coatings, among which the most relevant are their discontinuity, low adhesion, as well as the mutual diffusion of elements between the materials of the substrate and the coating. One of the methods that allow the formation of uniform coatings with good adhesion is the method of forming surface alloys [4].

In the presented work, the regularities of the formation and properties of the Cr-Zr surface alloy use produced by using a low-energy high-current electron beam are investigated. The electron-beam machine “RITM-SP” with an explosive-emission cathode and a plasma-filled diode generating the LEHCEB was employed in the work [5]. This machine is equipped with a magnetron sputtering system which allows forming the surface alloys in a single vacuum cycle. The process of formation of surface alloys consists of the deposition of Cr film on a Zr substrate followed by a liquid-phase mixing of the deposited film and the substrate upper layer with a LEHCEB. These operations can be repeated to obtain a thicker surface alloy. The effect of various modes of formation a surface alloy on its structure, elemental composition and properties is investigated. The formation mode is defined by the thickness of deposited Cr film, the energy density of the electron beam, and the pulse number of LEHCEB treatment. Different techniques like SEM, XRD, EDS have been used for characterization of the surface morphology, phase and elemental composition of the surface alloys. It was found that an important factor in the formation of a defect-free surface alloy is the concentration of chromium in the near-surface layer. Experiments have shown that for surface alloys formed in different modes, but for which the chromium concentration was more than 30 at.%, cracks formed on the surface (Fig. 1).

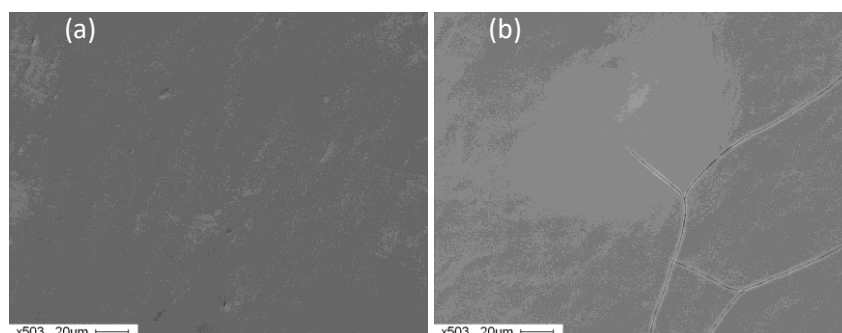


Fig. 1. SEM images of Cr-Zr surface alloy with a thickness of 1 μm and a Cr concentration of (a) 23 and (b) 39 at.%.

REFERENCES

- [1] H.H. Kim, J.H. Kim, J.Y. Moon, H.S. Lee, J.J.Kim, Y.S. Chai, “High-temperature oxidation behavior of Zircaloy-4 and Zirlo in steam ambient”, *J. Mater. Sci. Technol.*, vol. 26, no. 9, pp. 827-832, 2010.
- [2] B.A. Pint, K.A. Terrani, Y. Yamamoto, L.L. Snead, “Material selection for accident tolerant fuel cladding”, *Metall. Mater. Trans. E*, vol. 2, pp. 190-196, 2015.
- [3] B.A. Pint, K.A. Terrani, R.B. Rebak, “Steam oxidation behavior of FeCrAl cladding”, *Metall. Mater. Trans. E*, vol. 2, pp. 1451-1460, 2019.
- [4] A. Markov, E. Yakovlev, D. Shepel', M. Bestetti, “Synthesis of a Cr-Cu surface alloy using a low-energy high-current electron beam”, *Results Phys.*, vol. 12, pp. 1915-1924, 2019.
- [5] A.B. Markov, A.V. Mikov, G.E. Ozur, A.G. Padei, “A РИТМ-СП facility for the surface alloying”, *Instrum. Exp. Tech.*, vol. 54, pp. 862-866, 2011.

MODIFICATION OF STAINLESS STEEL BASED ON SYNERGISTIC OF LOW-ENERGY HIGH-INTENSITY ION IMPLANTATION AND HIGH-CURRENT ELECTRON BEAM IMPACT ON THE SURFACE LAYER*

A.I. RYABCHIKOV¹, O.S. KORNEVA¹, D.O. SIVIN¹, A.I. IVANOVA¹, I.V. LOPATIN², I.A. BOZHKO¹

¹National Research Tomsk Polytechnic University, Tomsk, Russia

²Institute of High Current Electronics, SB, RAS, Tomsk, Russia

e-mail: oskar@tpu.ru

The results of experiments on low-energy implantation of AISI 321 stainless steel by nitrogen ions are presented. The treatment was carried out by a pulsed beam of nitrogen ions obtained using a ballistic ion focusing system. It is shown that such treatment leads to the formation of an etching crater, the depth of which, at a constant energy of incident ions, depends on their current. Simultaneously, the surface modification occurs with the formation of a two-layer structure, which is typical for ion-plasma nitriding processes of stainless steels.

The thickness of the modified layer can reach 33 μm after 1 hour of ion-plasma treatment. The influence of subsequent modification of the ion-doped layer by the action on the surface of the pulsed high-current electron beam of microsecond duration is studied. The work presents the results of the studying the regularities of changes in the depth distribution of dopants, microstructure and phase composition of the modified and matrix layers by optical metallography, diffraction analysis and transmission electron microscopy.

* This work was carried out with the financial support of the Russian Science Foundation (Grant No. 17-19-01169 P).

Ti-W SURFACE ALLOYS SYNTHETIZED BY PVD-LEHCEB AND OXIDIZED BY PEO

F. MORINI¹, A. PALMERI¹, S. FRANZ¹, A. VICENZO¹, M. BESTETTI^{1,2}

¹Politecnico di Milano, Department of Chemistry, Materials and Chemical Engineering “G. Natta”, Milano, Italy

²Tomsk Polytechnic University, Tomsk, Russia

e-mail: federico.morini@polimi.it

An innovative method to produce Ti-W surface alloys consists in the coupling of PVD and LEHCEB techniques. Ti-W alloys were synthesized by depositing W films of 600 nm onto c.p. Ti substrates; the two metals were then alloyed by LEHCEB treatment, carried out at 30 kV for 60 pulses. This treatment led to a W content in the surface alloy of about 10 at.%.

Ti-W surface alloys are an interesting material for the mechanical properties [1]. Indentation tests showed an increase in the Vickers microhardness in respect to titanium.

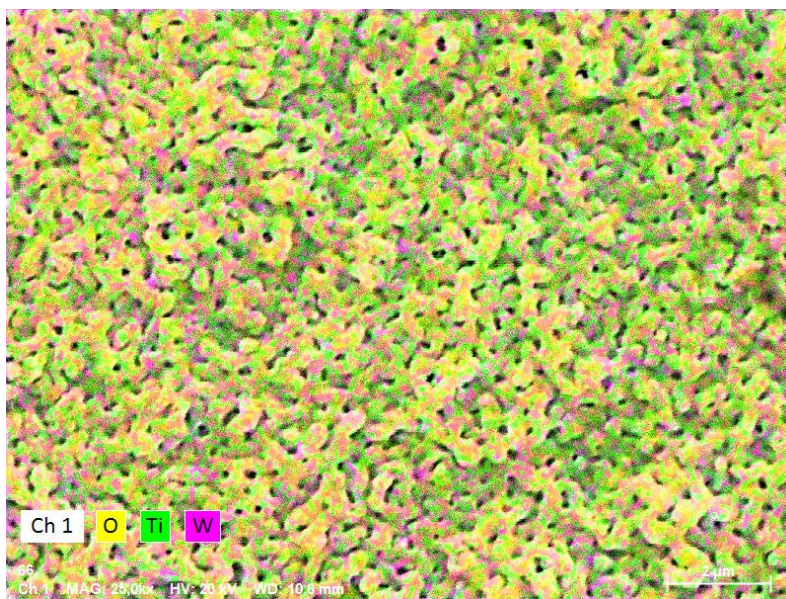


Fig. 1. Surface EDS color map of the sample synthesized at 120 V for 5 min at 25°C in 1.5 M H₂SO₄.

Another useful application of Ti-W alloys is in the synthesis of mixed oxides by plasma electrolytic oxidation (PEO) for photoelectrocatalytic water treatments. In the present work, we obtained a nanoporous oxide by PEO carried out in 1.5 M H₂SO₄ at 25°C and 0°C for 5 minutes, by employing different applied voltages, from 100 to 200 V (Fig.1). Mixed oxides were investigated with XRD, SEM and EDS analysis. Photoelectrochemical properties were examined by LSV under UV and VIS irradiation.

The synthesis of mixed oxides of Ti and W is promising for decreasing the band gap of TiO₂ by addition of W [2, 3]. A possible effect due to the presence of W is the influence on the formation of anatase phase. We observed that an increase in W content stabilizes the presence of anatase even at high PEO voltages.

REFERENCES

- [1] M. Frary, S. Abkowitz, S.M. Abkowitz, D.C. Dunand, “Microstructure and mechanical properties of Ti/W and Ti/6Al/4V/W composites fabricated by powder-metallurgy”, *Mater. Sci. Eng. A*, vol. 344, pp. 103-112, 2003.
- [2] S. Siol, N. Ott, C. Beall, M. Stiefel, Y. Unutulmazsoy, M. Döbeli, S.D. Tilley, P. Schmutz, L.P.H. Jeurgens, C. Cancellieri, “A combinatorial guide to phase formation and surface passivation of tungsten titanium oxide prepared by thermal oxidation”, *Acta Mater.*, vol. 186, pp. 95-104, 2020.
- [3] M. Fernández-García, A. Martínez-Arias, A. Fuerte, J.C. Conesa, “Nanostructured Ti-W mixed-metal oxides: structural and electronic properties”, *J. Phys. Chem. B*, vol. 109, no. 13, pp. 6075-6083, 2005.

INFLUENCE OF ION NITRIDING ON THE PROPERTIES OF DUPLEX SURFACE TREATMENT OF HIGH-SPEED STEEL

R.Sh. NAGIMOV, E.L. VARDANYAN, A.A. NIKOLAEV, A.V. OLEINIK, A.Yu. NAZAROV

Ufa State Aviation Technical University, Ufa, Russia

e-mail: r.sh.nagimov@gmail.ru

Various hardening methods are used to improve the performance of HSS cutting tools. The most common way to harden a tool is to apply wear-resistant coatings [1]. This is the most effective way to ensure the optimal combination of hardness-ductility [2]. Physical Vapor Deposition (PVD) [3, 4] is the most common of the variety of coating options.

Recently, combined processing methods that combine 2 or more hardening methods are gaining popularity. The system “Substrate - Surface alloying - Coating” has a smooth transition of microhardness and improved adhesive strength of the coating [5]. Ion nitriding is often used as an assisting method for surface doping [6]. This method is called duplex surface treatment.

The nitriding depth plays an important role in improving duplex adhesion. According to [7], the optimal depth is 40 μm . Greater depths lead to embrittlement of the steel surface. This depth can be achieved using various mode variations. Also, the optimal ratio of the size of the nitrided layer to the thickness of the coating is in the range of 0.05 - 0.125.

In connection with the above, the purpose of this work is to determine the nitriding modes to identify the optimal nitriding depth for duplex processing. Figure 1 shows a diagram of the setup for carrying out the experiment. The plant is equipped with two electric arc evaporators and a hollow cathode plasma source for ion nitriding of the coating process. Using mathematical modeling, the dependences of nitriding time, gas composition, and technological modes on the properties of duplex machining of tool steel were investigated.

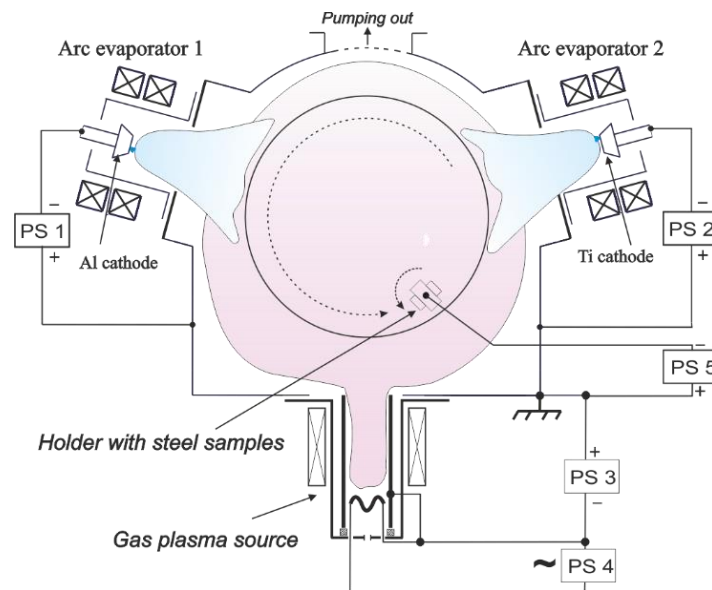


Fig. 1. Experimental installation NNV-6.6 II.

REFERENCES

- [1] Vereschaka A. S., Dacheva A. V., Anikeev A. I. Serviceability increase of a cutting tool at processing of difficult materials by complex application of the nanostructured wearproof covering and a hard alloy of an optimum composition (in Russian) // *Izvestia Moscow State Technical University MAMI*, 2010.
- [2] Grigoriev S. N., Tabakov V. P., Volosova M. A. Technological methods to increase the wear resistance of the cutting tool contact pads (in Russian) // *Stariy Oskol: TNT*, 2011.
- [3] Loktev D., Yamashkin E. Methods and equipment for wearproof coatings application. *Nanoindustriya*, vol. 4, pp 18-25, 2007.
- [4] Vardanyan E. L. et al. Properties of intermetallic TiAl based coatings deposited on ultrafine grained martensitic steel. *Surface and Coatings Technology*, vol. 389, pp 125657, 2020.
- [5] Bell T., Dong H., Sun Y. Realising the potential of duplex surface engineering. *Tribology International*, vol. 31, pp 127-137, 1998.
- [6] Gurevich Ya. L. Modes of cutting of hard-to-machine materials. *Handbook*, 1986.
- [7] Grigoriev S. N., Metel A. S., Fedorov S.V. Modification of the structure and properties of high-speed steel by combined vacuum-plasma processing. *Metal Science and Heat Treatment of Metal*, vol. 1, p. 20, 2012.

FORMATION OF WEAR-RESISTANCE NEAR SURFACE LAYERS IN Al-Si ALLOYS WITH AN ELECTRON-BEAM TREATMENT*

E.A. PETRIKOVA, Yu.F. IVANOV, N.A. PROKOPENKO, A.D. TERESOV

Institute of High Current Electronics, SB, RAS, Tomsk, Russia
e-mail: elizmarkova@yahoo.com

The work is aimed at obtaining fundamental knowledge about the regularities of the formation of the structural-phase state and the physical mechanisms of hardening of the hypereutectic silumin subjected to electron-beam treatment.

Irradiation of hypereutectic silumin with a pulsed electron beam is accompanied by multiple transformations of the structure and phase composition of the surface layer up to 100 μm thick. As a result of the performed studies, it was established that, regardless of the energy density of the electron beam, two types of regions (grains) are formed in the surface layer of silumin, differing in the silicon concentration and the type of substructure. Namely, grains, in the volume of which a structure of high-speed cellular crystallization is formed, and grains, in the volume of which, along with the structure of high-speed cellular crystallization, crystallites of excess silicon are present. It is shown that silicon crystallites (grains) have a polyhedral shape, their sizes vary from 0.5 μm to 1.3 μm . It was found that the volume of crystallization cells was formed by a solid solution based on aluminum. The predominant element of the interlayers separating the crystallization cells is silicon. The interlayers contain atoms of copper, iron and magnesium along with silicon. It was found that the average cell size increases with an increase in the energy density of the electron beam in the range (25-40) J/cm^2 from 290 nm to 500 nm. At the same time, the transverse dimensions of the interlayers of the second phase increase from 80 nm to 110 nm. It is shown that the structure formed in silumin samples upon irradiation with a pulsed electron beam depends on the distance from the irradiation surface. In the surface layer (40-60) microns thick, upon irradiation with a pulsed electron beam, all phases present in the initial silumin melt. There are intermetallic compounds based on cast iron at a greater distance from the irradiation surface. At a depth of (80-90) microns, regardless of the energy density of the electron beam, a structure is observed that is formed as a result of melting of aluminum and partial dissolution of silicon; silicon and intermetallic plates are preserved. A high-speed cellular crystallization structure is formed near the silicon wafers.

* The work was supported by RSF project No. 19-52-04009.

ENERGY DENSITY DISTRIBUTION OF A MODULATED ELECTRON BEAM IN A SOURCE WITH A PLASMA CATHODE BASED ON A LOW PRESSURE ARC*

V.I. SHIN, P.V. MOSKVIN, M.S. VOROBYOV, V.N. DEVYATKOV, N.N. KOVAL

Institute of High Current Electronics, SB, RAS, Tomsk, Russia

e-mail: shin.v.i@yandex.ru

Generation of electron beams from plasma cathodes with grid stabilization of the emission plasma boundary has a number of advantages, in particular, a weak dependence of the parameters of the generated beam on each other [1, 2]. Using of this advantage, the possibility of amplitude modulation of the current of a submillisecond electron beam due to a proportional change in the amplitude of the arc discharge current was demonstrated in [3]. This possibility of modulating the beam current makes it possible to dynamically control its power and provide not only an incident or constant, but also an increasing beam power during a pulse. Power control during a submillisecond pulse provides a controlled change in the temperature of the target surface exposed to irradiation in order to modify its functional properties. Certainly, an important parameter in such processes is the energy density distribution. This work is devoted to the study of the energy density distribution of an electron beam during its modulation. In the course of the work, the processes leading to a change in the distribution of the energy density of the beam were studied. Figure 1 shows the energy density curves for an unmodulated and for 2 cases of a modulated beam.

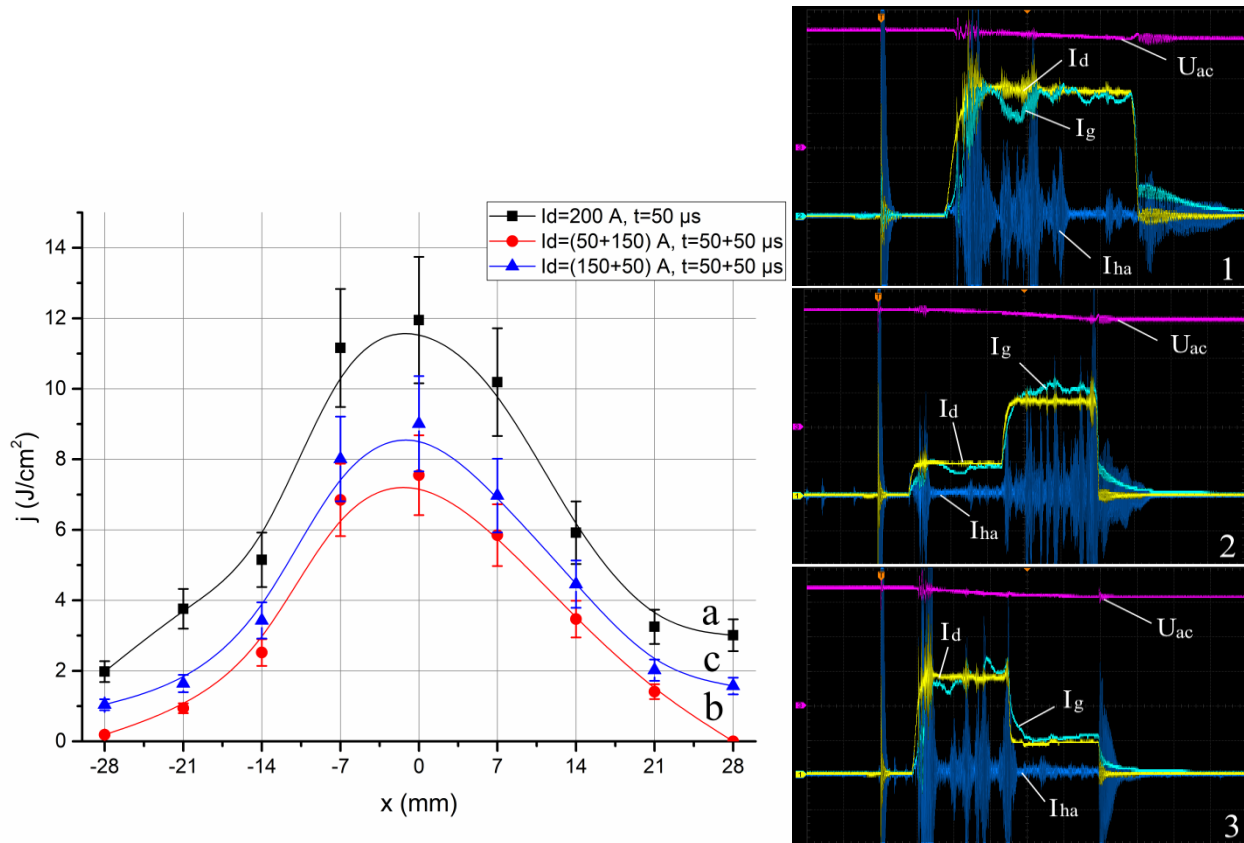


Fig. 1. Electron beam energy density distribution: a - for the beam current on oscillogram 1; b - on oscillogram 2; c - on oscillogram 3.

REFERENCES

- [1] E.M. Oks, Plasma Cathode Electron Sources: Physics, Technology, Applications. Weinheim: WILEY-VCH, 2006.
- [2] D.I. Proskurovsky, Emission electronics. Tomsk: Tomsk state university, 2010.
- [3] M.S. Vorobyov, N.N. Koval, P.V. Moskvina, A.D. Teresov, S.Yu. Doroshkevich, V.V. Yakovlev, V.I. Shin, "Electron beam generation with variable current amplitude during its pulse in a source with a grid plasma cathode", in: J. Phys. Conf. Ser., Institute of Physics Publishing, p. 12064, 2019.

* This work was supported by the Russian Science Foundation (project No. 20-79-10015).

FORMATION OF A SILICON-NIOBIUM-BASED SURFACE ALLOY USING ELECTRON-ION-PLASMA SURFACE ENGINEERING*

V.V. SHUGUROV, N.N. KOVAL, Yu.F. IVANOV, A.D. TERESOV, E.A. PETRIKOVA

Institute of High Current Electronics, SB, RAS, Tomsk, Russia
e-mail: shugurov@inbox.ru

In this work, studies on the formation of a surface alloy based on silicon and niobium on substrates of 40Cr steel were carried out. The method of electron-ion-plasma surface engineering was used to form the surface alloy. Experiments were carried out on the COMPLEX setup [1]. The diagram of the electrode system is shown in Figure 1.

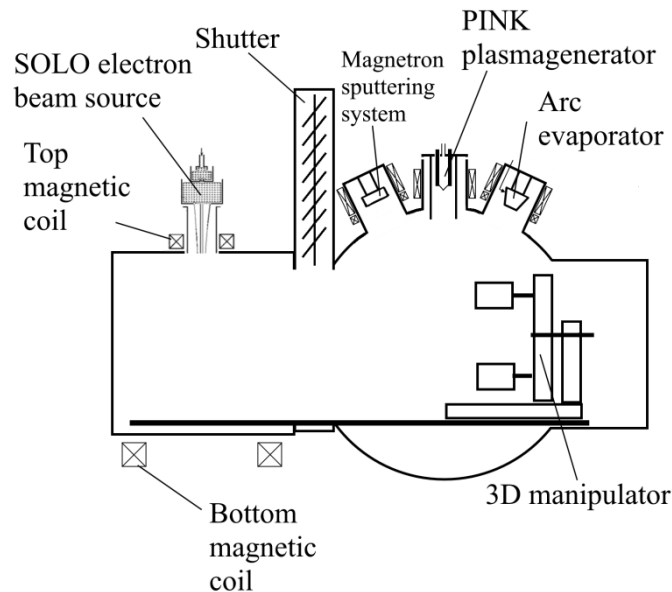


Fig. 1. Scheme of experiment.

To carry out these experiments, the equipment was modernized. A magnetron sputtering system for the deposition of silicon films was installed, and the discharge system of a pulsed electronic source SOLO was optimized.

The experiments were carried out in a single vacuum cycle. The optimal modes of deposition of silicon and niobium films, as well as electron-beam mixing of the film-substrate system, were investigated and selected.

REFERENCES

- [1] Koval N. N., Ivanov Yu. F. // Russian Physics Journal. - 2019. - V. 62. - pp. 1161-1170.

* The work was supported by RFBR project No. 19-08-00248.

DEPOSITION OF BORON FILMS BY DISCHARGE SYSTEM WITH HOT ANODE FROM BORON POWDER*

V.V. SHUGUROV, Yu.F. IVANOV

Institute of High Current Electronics, SB, RAS, Tomsk, Russia

e-mail: shugurov@inbox.ru

In this work, we have developed a discharge system for heating and evaporation of a boron powder target based on a non-self-sustaining arc discharge with a heated and hollow cathode and an uncooled combined anode. Experiments were carried out in a COMPLEX equipment [1]. The diagram of the electrode system is shown in Figure 1.

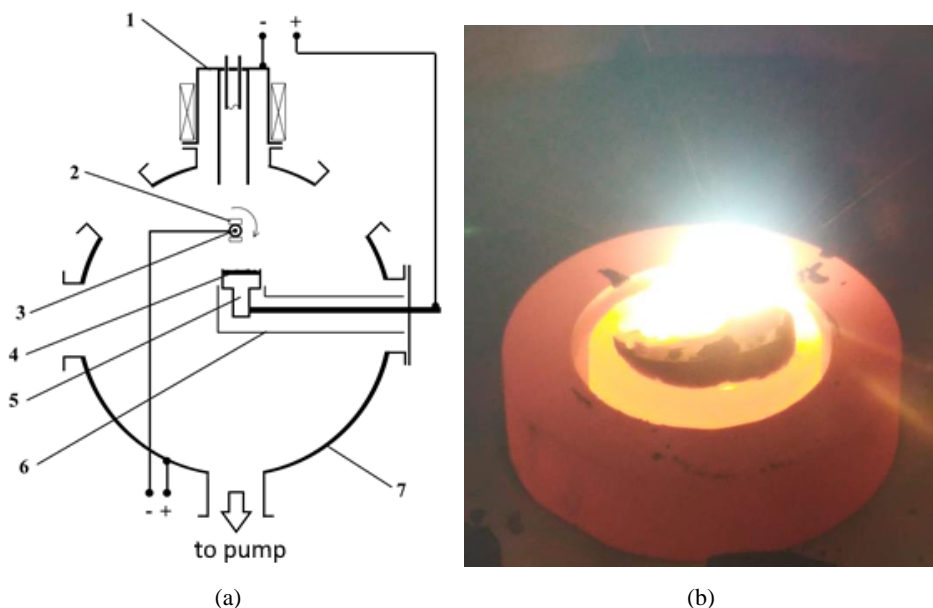


Fig. 1. Scheme of experiment (a): Hot anode electrode system. (b) Hot anode appearance.

1 - PINK gas plasma generator; 2 - samples; 3 - thermocouple; 4 - boron powder anode target; 5 - graphite crucible-anode; 6 - electric screen; 7 - working vacuum chamber.

The anode of the discharge system is made in the form of a cylindrical graphite crucible with a diameter of 40 mm and a height of 20 mm. On the upper end surface of the crucible, a recess with a diameter of 30 mm and a depth of 8 mm was made into which a sample of boron powder was placed. The target was amorphous boron, powder with "A" grade (TU 2112-001-49534204-2003) of the following composition (wt.%): B – 96.2, Fe – 0.3, Si – 0.2, H₂O – 0.3. The crucible was located at a distance of 100 mm from the outlet of the cathode cavity of the gas plasma generator. In the gap between the crucible-anode and the cathode cavity of the gas plasma generator, there was a holder with the processed samples, the temperature of which was controlled by a chromel-alumel thermocouple.

The results of a study of the current-voltage characteristics of a discharge with a hot anode and the dependence of the anode temperature on the discharge parameters are presented. The modes of deposition of boron films have been determined.

REFERENCES

- [1] Koval N. N., Ivanov Yu. F. // Russian Physics Journal. - 2019. - V. 62. - pp. 1161-1170.

* The work was supported by RSF project No. 19-19-00183.

MODIFICATION AND OPTICAL DEGRADATION OF THIN MULTILAYERS UNDER VUV/UV RADIATION FROM COMPRESSED PLASMA FLOWS*

A.S. SKRIABIN¹, V.D. TELEKH¹, A.V. PAVLOV¹, D.A. CHESNOKOV², V.G. ZHUPANOV², P.A. NOVIKOV²

¹*Bauman Moscow State Technical University, Moscow, Russia*

²*Luch Scientific Production Association, Podolsk, Russia*

e-mail: terra107@yandex.ru

The report presents the interaction features of high-power VUV/UV radiation with multilayer reflective and antireflection multilayer HfO₂/SiO₂ and ZrO₂/SiO₂ coatings. High-brightness radiation (with an intensity of 10⁵...10⁹ W/cm²) was generated with an erosive magnetoplasma compressor [1] at a discharge in air and neon (with a pressure of ≈ 300...400 Torr). In the case of neon, the energy of radiation quanta is limited from above by its ionization potential (≈ 21.55 eV), and in the case of air, by absorption in the Schumann-Runge bands (≈ 6.2 eV) [2]. The main features of a gas-dynamic response to the radiation were visualized by the schlieren photography [3]. It is shown that, in the case of high-energy quanta, evaporation of the coating and other effects, which lead to the degradation of optical characteristics, took place. Shock plasma front (1) and surface evaporation front (2) from the irradiated substrate (3) with the multilayer coating were recorded. For the antireflective coatings at the operating wavelength (≈ 527 nm), a decrease in the transmittance from 95 to 90% was recorded (under a single VUV/UV exposure). However, no gas-dynamics structures were recorded for a discharge in air. In this case, the changes in optical properties were minimal (0.5...1 %). Thus, it was concluded that high-energy quanta have a significant effect on the optical characteristics of coatings.

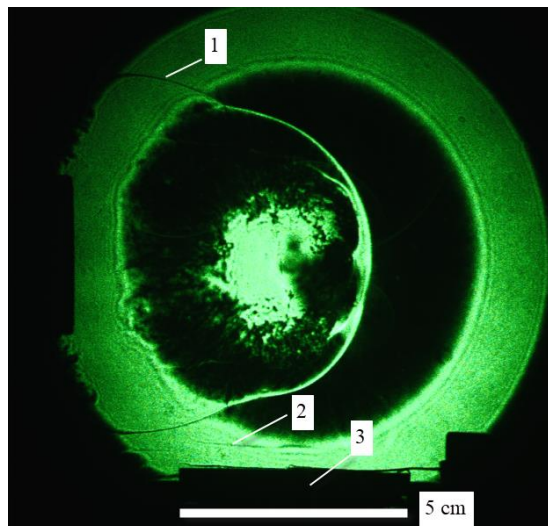


Fig. 1. Schlieren photography of gas-dynamic response from VUV/UV radiation: 1 – shock plasma front, 2 – surface evaporation front and 3 – substrate with coating.

REFERENCES

- [1] V. M. Astashinskii, “Formation of compression erosion plasma fluxes of a given composition in dense gases”, *J Appl Spectrosc.*, vol. 67, pp. 312-319., 2000.
- [2] K. Yoshino, D. E. Freeman, and W. H. Parkinson, “Atlas of the Schumann–Runge Absorption Bands of O₂ in the Wavelength Region 175–205 nm”, *J. Phys. Chem. Ref. Data*, vol. 13, no. 1, pp. 207-227.
- [3] A. S. Skryabin, A. V. Pavlov, A. M. Kartova, V. D. Telekh, A. E. Sytchev, N. V. Sachkova, M. M. Serov, “Experimental study of slow electrical explosion of thin titanium wires”, *J. Phys.: Conf. Ser.*, vol. 1250, pp. 012018, 2019.

* The work was funded by RFBR and ROSATOM, project number 20-21-00087 and has been performed at “Beam-M” facility of Bauman Moscow State Technical University.

PROCESSING OF THE TITANIUM ALLOY BY HIGH-SPEED STEEL TOOLS WITH COMBINE SURFACE TREATMENT*

S.V. FEDOROV, TET OO, E.S. MUSTAFAEV

*Moscow State University of Technology «STANKIN», Moscow, Russia
e-mail: sv.fedorov@icloud.com*

Today, a large share of the tool from high-speed steels, especially high-precision steels, is offered by the suppliers with various options for wear-resistant coatings based on refractory metal nitrides obtained by the PVD method. Nevertheless a significant difference in the physical and mechanical properties between the substrate and the coating often causes intense destruction of the working surfaces of the tool during plastic deformation of the substrate under the action of a high load. This disadvantage can be defeated by the formation of a particular transition layer, which can be obtained, for example, by preliminarily applying a wear-resistant coating of chemical-thermal treatment. In particular, a variety of methods for ion nitriding are widely used. The use of such processing allowed increasing the resistance of a high-speed tool several times in comparison with a tool that has only a PVD coating. It is possible to increase the thermal stability of the near-surface layer of the tool directly adjacent to the coating due to additional surface alloying of nitrided high-speed steel.

The workpieces, the milling process studied in this work, were obtained in the selective electron-beam melting unit Arcam A2. The workability of the workpiece obtained by additive technology compared with that of the forged one. As a tool material was chosen a medium-alloy high-speed steel AISI M2 after standard heat treatment.

Milling was carried out on a vertical console machine WF-1 using a dynamometer made by Kistler. The end milling process is modeled using a special holder and a unique metal-cutting insert. The scheme of counter milling is used.

Some of the experimental cutting inserts underwent an alloying operation of the near-surface layer before applying the wear-resistant coating. The treatment was carried out in the RHITHM-SP unit. The installation allows to apply films on the surface of the desired product and to mix this film and substrate materials by an intense pulsed electron beam. Nitriding of the tool before surface alloying performed using a two-stage vacuum-arc gas discharge.

The structure of the titanium Ti-6Al-4V alloy workpiece obtained using electron-beam melting differs significantly. Changing the properties of the material could affect the characteristics of its machinability, and the features of milling titanium alloy obtained by the electron beam melting method revealed - the component of cutting force F_T increases by approximately 15%. At the same time, a 20% drop in the force F_R was observed. Although the material is less flexible and harder and processing, it is somewhat more complicated, and the tendency to stick chips on the tool is significantly reduced.

Experiments have shown that it is possible to increase the durability of a unique tool made of high-speed steel up to six times when milling a titanium alloy both in the forged state and after obtaining the workpiece by electron-beam melting, which reduces the cost of tool production and increases processing productivity by 20%.

The service life of the tool affects its performance, which is directly related to the cutting speed. Unfortunately, the use of high-speed steel tools significantly limits the ability to increase it. Nevertheless, the use of complex surface treatment can give productivity increasing of up to 20% when the technological stability of the cutting tool is from 30 to 60 minutes.

* This research is funded under the state task of the Ministry of science and higher education of the Russian Federation, project no. 0707-2020-0025, and was carried out using the center of collective use of MSTU "STANKIN".

INTERACTION OF PLASMA WITH BERYLLIUM*

I.A. SOKOLOV¹, M.K. SKAKOV², A.Z. MINIYAZOV¹, T.R. TULENBERGENOV¹, G.K. ZHANBOLATOVA¹

¹*Institute of Atomic Energy NNC RK, Kurchatov, Kazakhstan*

²*National Nuclear Center of the Republic of Kazakhstan, Kurchatov, Kazakhstan*

e-mail: sokolov@nnc.kz

In ITER, there are two values of the heat load for the blanket, depending on the location on the sectional plane of the chamber [1]: “normal” – 2 MW/m² and “increased” – 4.7 MW/m². The aim of this work is to experimentally estimate the service life of a beryllium coating after irradiation with an electron beam, hydrogen and helium plasma under the operating conditions of a fusion reactor. The article presents the results of studies of beryllium grade TGP-56, carried out on a plasma-beam installation [2].

The joints between the panels of the first wall take place due to the location of the diagnostic and technological ports in the FWP. Plasma interaction is possible along the edges of the beryllium panels. These areas may be exposed to plasma and heat flux at angles from 15° to 90°, which can lead to local heat stress and possible melting of components. Higher surface temperatures at the edge of the tile and therefore the potential for erosion or melting of the material, together with increased atomization, can increase plasma contamination.

In this work, preliminary thermal calculations are carried out, which are based on literature sources and design characteristics at which the first ITER wall is operated. Fig. 1 shows some results of studying the microstructure of TPG-56 beryllium after plasma irradiation.

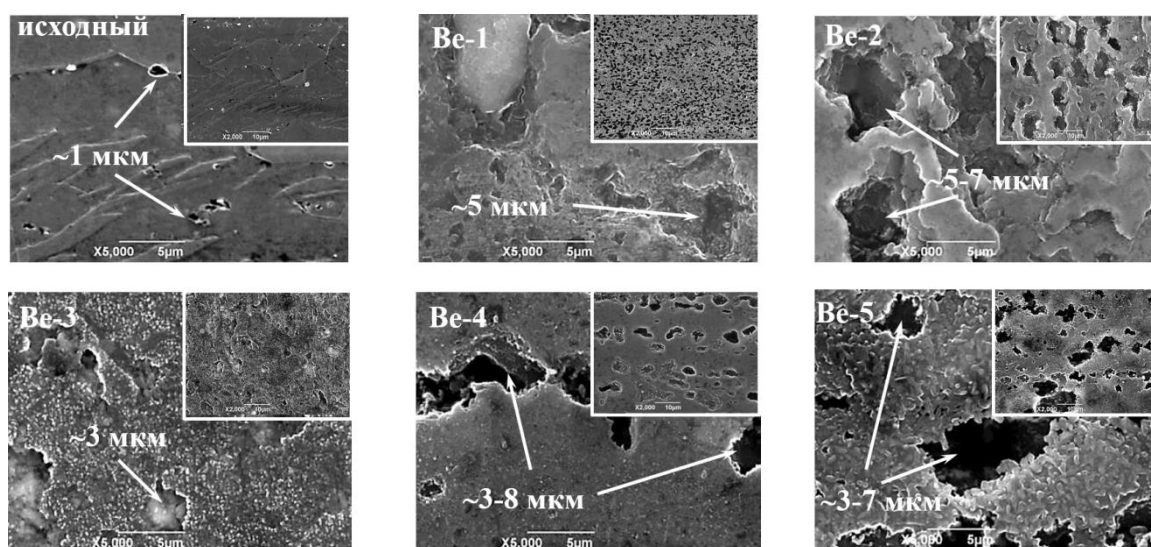


Fig. 1. Results of microstructural studies of beryllium.

The experiments revealed a change in the microstructure of beryllium after irradiation with hydrogen, deuterium and helium atoms. The pore diameter and their bulk density increase depending on the plasma parameters.

The results obtained make it possible to study in more detail the change in the properties of beryllium in the process of plasma interaction with the surface of the FWP of a thermonuclear reactor.

REFERENCES

- [1] Raffray A.R., Calcagno B., Chappuis P., Zhang Fu, [et al.], “The ITER blanket system design challenge”, *Nuclear Fusion*, vol. 54, no. 3, 2014.
- [2] Skakov M., Zhanbolatova G., Miniyaov A., Tulenbergenov T., Sokolov I., Sapatayev Y., “Impact of High-Power Heat Load and W Surface Carbide on Its Structural-Phase Composition and Properties”, *Fusion Science and Technology*, vol. 77, no. 1, pp. 57–66, 2021.

* This research has been/was/is funded by the Science Committee of the Ministry of Education and Science of the Republic of Kazakhstan (Grant No. AP08856026)

HYSTERESIS OF THE MAGNETRON DEPOSITION PROCESS WITH ALUMINUM AND ZINC TARGETS IN A REACTIVE MIXTURE OF GASES

D.G. AGEYCHENKOV¹, A.V. KAZIEV¹, D.V. KOLODKO^{1,2}, N.S. SERGEEV^{1,3}, A.S. ISAKOVA¹, A.V. TUMARKIN¹

¹National Research Nuclear University MEPhI, Moscow, Russia

²Kotelnikov Institute of Radio Engineering and Electronics, RAS, Fryazino, Moscow Region, Russia

³National Research Center "Kurchatov Institute", Moscow, Russia

e-mail: ageichenkovdmitry@yandex.ru

At the moment, obtaining transparent conductive coatings is an extremely relevant area. In addition to the various uses for transparent conductive coatings (TCO) in electronics, green energy and energy sources, there is the problem of switching the existing technology of TCO production from ITO coatings to the alternative ones, e.g., AZO, which are produced from more abundant elements [1]. There are two options for producing AZO films by magnetron sputtering - sputtering of sintered ceramic targets in an argon atmosphere and reactive sputtering of Zn and Al targets in an argon-oxygen atmosphere [2, 3]. The latter option is more promising for mass production. For its implementation, it is necessary to accurately select the ratio of the fluxes of aluminum and zinc incident at the substrate, for which it is necessary to obtain data on the target oxidation. In this work, we investigate the hysteresis of the magnetron deposition process with aluminum and zinc targets in a reactive argon-oxygen mixture of working gases.

All experiments were carried out in a setup with an ion beam extraction system and a magnetic sector mass analyzer, which enabled us to obtain mass spectra of the ion fluxes at various points of hysteresis. In addition, Extorr XT100 quadrupole residual gas analyzer and a quartz microbalance were used. The process of changing the ratio of gases in the working mixture was automated, as well as the measurement of the following parameters: total pressure, current and voltage of the discharge, mass spectra from the residual gas quadrupole analyzer, mass spectra of the ion flux from the magnetic sector mass analyzer, and the thickness of the obtained coatings measured by a quartz microbalance.

At the points characterizing the hysteresis, the flux densities of ions incident on the substrate, as well as the flux densities of neutral particles, were estimated.

REFERENCES

- [1] Y. Sun, H. Wang, J. Chen, L. Fang and L. Wang, "Structural and optoelectronic properties of AZO thin films prepared by RF magnetron sputtering at room temperature," *Trans. Nonferrous Met. Soc. China*, vol. 26, pp. 1655-1662, 2016.
- [2] E. G. Berasategui, C. Zubizarreta, R. Bayón, J. Barriga, R. Barros, R. Martins and E. Fortunato, "Study of the optical, electrical and corrosion resistance properties of AZO layers deposited by DC pulsed magnetron sputtering," *Surf. Coat. Technol.*, vol. 271, pp. 141-147, 2015.
- [3] H. Ko, W.-P. Tai, S.-H. K. S.-J. S. K.-C. Kim and Y.-S. Kim, "Growth of Al-doped ZnO thin films by pulsed DC magnetron sputtering," *Journal of Crystal Growth*, vol. 277, pp. 352-358, 2005.

EFFECT OF THE ANNEALING TEMPERATURE ON THE STRUCTURAL AND CHARACTERISTICS OF Hf NANOFILMS BY MAGNETRON SPUTTERING

A.P. KUZMENKO, THANT SIN WIN, A.S. PETROV, MYO MIN THAN

Southwest State University, Kursk, Russia

e-mail: thantsinwin2014@gmail.com

In previous works, nanostructured materials have become widely used in various fields of electronics, optics, for recording and storing data on magnetic media, as catalysts, in ceramic materials and nanocomposites by used HfO₂ films [1-5]. The electrical properties of hafnium oxide (HfO₂) and other metal oxides with high dielectric constants are currently being investigated with great interest, especially in connection with the promising possibilities that have been found by these materials to replace silicon oxide in the basis of metal oxide semiconductor (MOS) transistors, involved be used carbon nanotube [6-8].

Hf nanofilms were deposited on silicon substrates by direct current magnetron sputtering (DC MS) using a MVU TM Magna T. When the working chamber was evacuated, a vacuum of no more than 5×10^{-4} Pa was achieved in it. The magnetron discharge occurred at an Ar (99.998%) working pressure of 0.5 Pa. Before deposition, the substrates were heated to 130°C for 60 seconds, then ionic cleaning was carried out (60 mA, 120 s). The targets were products of GIRMET LLC made of Hf (99.99%). They were in the form of a disk with the following dimensions: diameter - 100 mm, thickness - 6 mm. Magnetron nanofilms were deposited on silicon wafers with dimensions of 18×5 mm. Sputtering was carried out at a power of 300 W for 300 s, an argon flow rate of 0.7 liter per hour (l/h).

X-ray structural analysis was performed on a GBC EMMA diffractometer with high temperature camera. Surface morphology was studied using an atomic force microscope (Smart SPM AistNT) minimum scanning area 1 μm² with spatial resolution along the Z coordinate - 30 pm. Changes in the chemical structure of nanofilms were studied by Raman scattering using an OmegaScope AIST-NT confocal Raman microspectrometer with high spatial and spectral resolutions: ~ 250 nm, 0.8 cm⁻¹, accordingly.

By analogy with earlier studies of degradation processes in metal magnetron nanofilms made of transition metals [9], oxidation and morphological changes of the surface were studied by nanofilms of metallic Hf with the same thickness (about 200 nm), each of which was annealed at a corresponding temperature, varied with a step of 100°C from room temperature to 700°C. A specific feature of magnetron nanofilms of Hf is an increase in surface roughness and coherence size *L* in the temperature range from room temperature to 300°C and decrease in the temperature range at 400-700°C. The fractal dimension of the analyzed surfaces of magnetron nanofilms of Hf changes insignificantly around 2.4, that is, it corresponded mainly to their three-dimensionality (planarity).

REFERENCES

- [1] R. Ananthakumar, K. Karthikeyan, J.K. Sang, "Novel synthesis of hafnium oxide nanoparticles by precipitation method and its characterization," *Materials Research Bulletin*, vol. 47, pp. 2680-2684, 2012.
- [2] S.B. Khan, W. Hui, L. Ma, M. Hou, Z. Zhang, "HfO₂ nanorod array as high-performance and high-temperature antireflective coating," *Adv. Mater. Interfaces*, vol. 4, pp. 1-9, 2017.
- [3] H. Iwai, S. Ohmi, "Silicon integrated circuit technology from past to future," *Microelectron. Reliab.*, vol. 42, pp. 465-491, 2002.
- [4] M. Vargas, N.R. Murphy, C.V. Ramana, "Structure and optical properties of nanocrystalline hafnium oxide thin films," *Opt. Mater.*, vol. 37, pp. 621-628, 2014.
- [5] S. Rudenja, A. Minko, D.A. Buchanan, "Low-temperature deposition of stoichiometric HfO₂ on silicon: analysis and quantification of the HfO₂/Si interface from electrical and XPS measurements," *Appl. Surf. Sci.*, vol. 257, pp. 17-21, 2010.
- [6] F.L. Marti'nez, M.L. Toledano, J.J. Gandi', J. Ca'ra'be, W. Bohne, J. Röhlich, E. Strub, I. Márti'l, "Optical properties and structure of HfO₂ thin films grown by high pressure reactive sputtering," *J. Phys. D: Appl. Phys.* vol. 40, pp. 5256-5265, 2007.
- [7] A.G. Khairnar, A.M. Mahajan, "Effect of post-deposition annealing temperature on RF-Sputtered HfO₂ thin film for advanced CMOS technology," *Solid State Sci.*, vol. 15, pp. 24-28, 2012.
- [8] F. Daneshvar, H. Chen, K. Noh, H.J. Sue, "Critical challenges and advances in the carbon nanotube-metal interface for next-generation electronics," *Nanoscale advances*, vol. 3, pp. 942- 962, 2021.
- [9] A.P. Kuzmenko, Thant Sin Win, Myo Min Than, Naw Dint, A.G. Besedin, "Degradation of Hf and Mo magnetron nanofilms under atmospheric annealing," *Bulletin of the South-West State University. Series: Engineering and technology*, vol 10, no. 3, pp. 86-104, 2020.

ELECTRON-BEAM DEPOSITION OF THERMOCONDUCTING CERAMIC COATINGS FOR MICROELECTRONIC DEVICES*

E.M. OKS^{1,2}, A.V. TYUNKOV¹, Yu.G. YUSHKOV¹, D.B. ZOLOTUKHIN¹

¹*Tomsk State University of Control Systems and Radioelectronics, Tomsk, Russia*

²*High Current Electronics Institute, RAS, Tomsk, Russia*

e-mail: tyunkov84@mail.ru

Long-term and reliable operation of semiconductor devices and integrated circuits is largely determined by the choice of the method of their protection. For protection and insulation of such devices, electrical insulating varnishes based on epoxy, organosilicon resins, polymers, or coatings with the inclusion of aluminum nitride fibers are often used [1, 2]. This category of materials has good dielectric properties, but their thermal conductivity does not exceed 1 W/mK, which makes it necessary to take special efforts to cool microelectronic devices. One of the modern trends in the production of protective coatings is the plasma-based technologies. However, the manufacturing of dielectric coatings that also have heat-conducting properties is complicated [3]. Electron-beam deposition of coatings by fore-vacuum plasma-cathode electron sources allows one to obtain dielectric coatings of thickness from several nanometers to tens of micrometers with all necessary properties for their use in microelectronic devices.

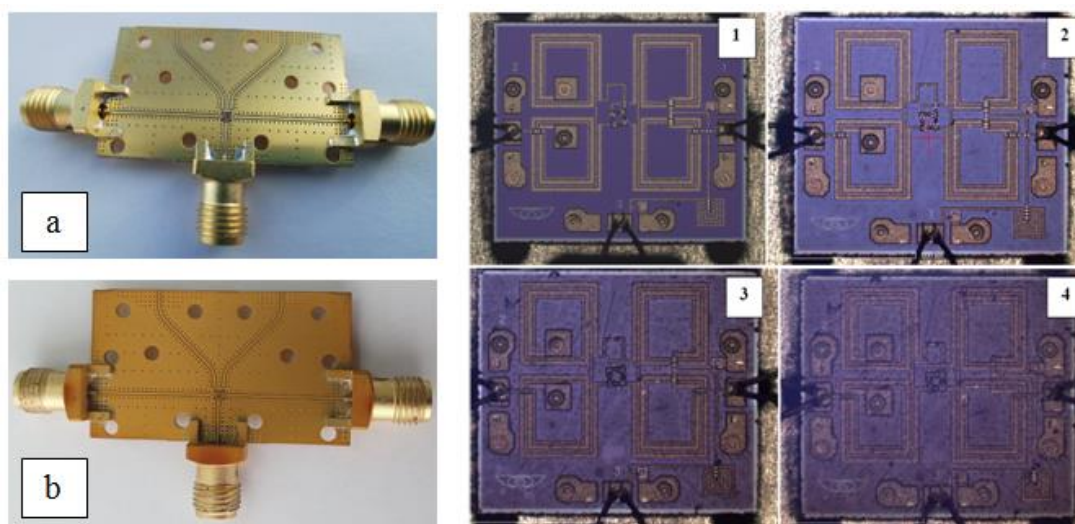


Fig. 1 – A chip with SMA-ports before the deposition of coatings (a) and after the deposition of the coating based on aluminum nitride ceramics (b); Photos of chip on all stages of coatings deposition: 1 – initial; 2 – after deposition of the first layer (coating thickness 0.5 μm); 3 – after deposition of the second layer (coating thickness 1 μm); 4 – after deposition of the third layer (coating thickness 1.5 μm).

In figure 1 one can see the photos of monolith integral circuit with alumina- and aluminum nitride-based coatings deposited on its surface. The deposition duration was 1 minute. Electron beam with power density of 8 kW/cm² in helium atmosphere evaporated the ceramic target, and its vapors then deposited on the surface of the circuit. One should note that the deposition of AlN and Al₂O₃ coatings has been conducted on a circuit which active parts were passivated by a dielectric (Si₃N₄). This allows one to conclude that these coatings can be used as constructive materials for the passivated monolith integrated circuits in high-frequency electronics. In our work, we show the results of our research on the regimes of electron-beam deposition of dielectric coatings in fore-vacuum, as well as diagnostics of their properties and characteristics.

REFERENCES

- [1] R. Prasher / Thermal interface materials: historical perspective, status, and future directions // Proc. IEEE. – 2006. – Vol. 94. –No. 8. – P. 1571-1586.
- [2] Sh. Xiao, R. Y.M. Huang, X. Feng / Synthetic 6FDA–ODA copolyimide membranes for gas separation and pervaporation: Functional groups and separation properties // Polymer. – 2007. – Vol. 48. Issue 18. – P. 5355-5368.
- [3] Yu.G. Yushkov, E.M. Oks, A.V. Tyunkov, D.B. Zolotukhin, A.Yu. Yushenko / Electron-beam deposition of heat-conducting ceramic coatings in the forevacuum pressure range // Ceramics International. – 2020. – Vol. 46, Issue 13. – P. 21190-21195.

* The work was supported by the Russian Foundation for Basic Research (grant # 18-29-11011 mk).

EVALUATION OF EFFECTIVE MAGNETIZATION OF THIN MAGNETO-DIELECTRIC FILMS DEPOSITED FROM BEAM PLASMA IN MEDIUM VACUUM*

A.V. TYUNKOV, Yu.G. YUSHKOV, D.B. ZOLOTUKHIN

Tomsk State University of Control Systems and Radioelectronics, Tomsk, Russia
e-mail: tyunkov84@mail.ru

Thin (with thickness of several μm) magneto-dielectric coatings have been used actively in high-frequency microelectronics due to their unique ability to ensure electrical isolation and exhibit magnetic properties with low eddy currents. In our previous work [1] we proposed a new method for obtaining such coatings. The method is based on sequential electron-beam evaporation of targets made of magnetic (such as ferrite or iron) and dielectric (alumina ceramic) materials by fore-vacuum plasma-cathode electron source, ionization of vapors and the working gas, with subsequent deposition a magneto-dielectric coating on a substrate from such multi-component beam-produced plasma in medium vacuum (several Pa). However, our previous estimation of magnetic properties of such coatings by inductive method was uncertain due to low sensitivity of this method for diagnostics of thin films. This fact stimulated the further research on methods for evaluation the magnetic properties (such as the effective magnetization) of the mentioned magneto-dielectric coatings.

In this study we consider the two methods for analysis of magneto-dielectric coatings: a method based on electromagnetic resonance in micro-strip resonator (MSR), and on ferromagnetic resonance (FMR) [2]. Fig. 1 below depicts the preliminary result obtained using MSR method.

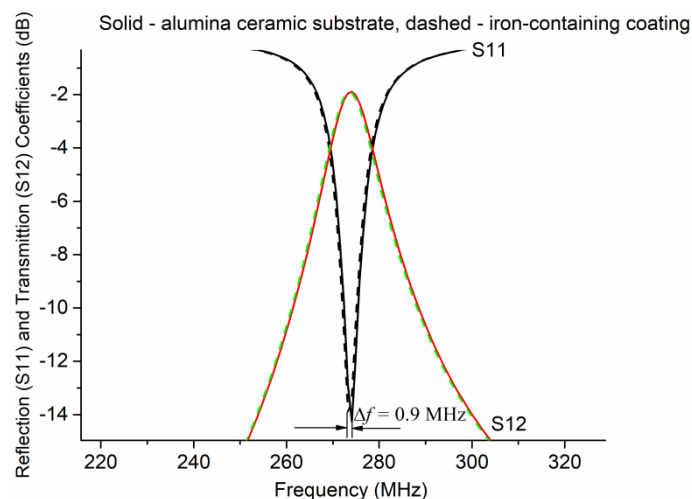


Fig. 1. Frequency dependences of S11, S12 coefficients near resonance peaks of the first mode of magnetic field oscillations, for the resonator with alumina substrate only (solid lines), and alumina substrate with iron-containing coating of 2.1 μm thickness (dashed lines).

Fig. 1 demonstrates that when an alumina ceramic substrate is placed into the micro-strip resonator, no change in the S11 and S12 coefficients occurs. However, when an alumina ceramic substrate with a thin iron-containing coating is placed into the gap, a small (0.9 MHz) left shift of the peak of the first mode of magnetic field oscillation occurs. This shift is also accompanied by a slight decrease in the peaks amplitude. The presence of this shift indicates that the deposited iron coating has a measurable non-zero magnetic permeability. However, the small value of the observed shift of the resonance peaks indicates the insufficient sensitivity of the MSR method. So, the further research of the coatings by a more sensitive FMR method is required.

REFERENCES

- [1] D.B. Zolotukhin, A.A. Klimov, E.M. Oks, A.V. Tyunkov, Yu.G. Yushkov, A.A. Zenin, "Electron-beam deposition of magneto-dielectric coatings in the forevacuum pressure range", *Vacuum*, vol.184, pp. 109944 (1-5), 2020.
- [2] A.G. Gurevich, G.A. Melkov, *Magnetic oscillations and waves*, Moscow: Fizmatlit, 1994.

* The work was supported by the Russian Foundation for Basic Research (grant # 20-08-00370 A) and by a Grant from the President of the Russian Federation (No. MK-154.2020.8).

TWO-STAGE PVD METHOD FOR PROTECTIVE COATINGS FORMATION*

V.A. BURDOVITSIN, A.V. TYUNKOV, Y.G. YUSHKOV, D.B. ZOLOTUKHIN

Tomsk State University of Control Systems and Radioelectronics, Tomsk, Russia

e-mail: tyunkov84@mail.ru

Aluminum oxide, being a simple chemical compound with high chemical inertia and temperature stability, is an ideal coating component for protecting various alloys from high temperature and chemical wear. Typically, for the formation of such coatings, CVD methods are used, since the aluminum oxide is a dielectric.

In this work, in order to improve the adhesion between the protective coating and the substrate material, thin intermediate layers (100-200 nm) based on titanium oxides and nitrides have been grown. The formation of intermediate layers is mainly carried out by PVD methods.

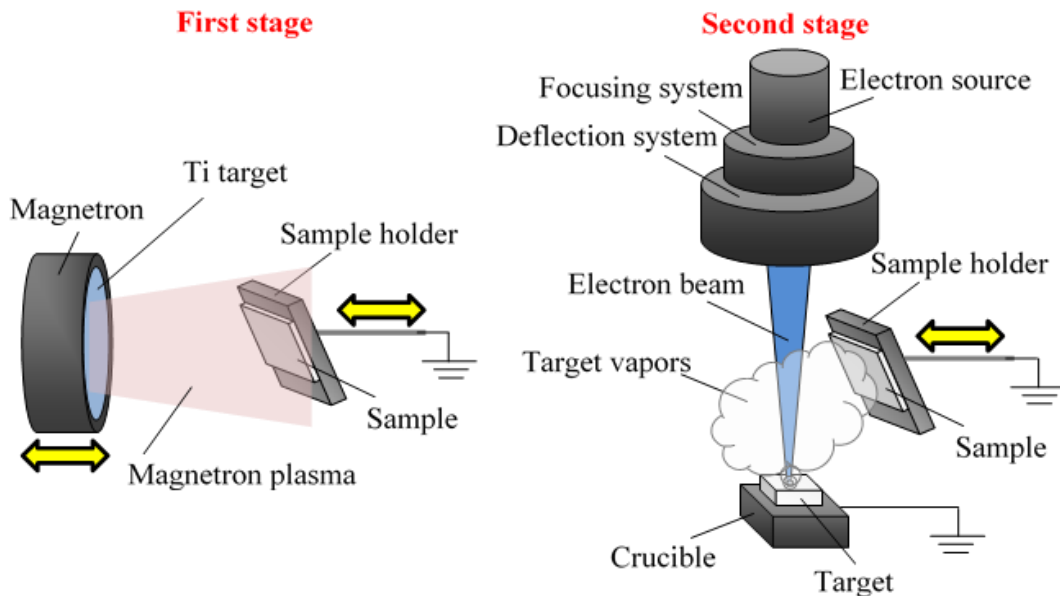


Fig. 1. Experimental setup.

This paper presents a two-stage PVD method for forming a layered structure on a titanium substrate. The formation of the intermediate layers was carried out by the magnetron method (first stage), and the main protective layer was deposited in the second stage using a fore-vacuum electronic source (Fig. 1). The use of an electronic source for the formation of the protective layer made it possible to avoid a large thermal load on the substrate typical for conventional CVD deposition methods. At the same time, the generation of dense beam plasma during the transport of an electron beam in a fore-vacuum gas medium compensates for the negative charge on the surface of the aluminum oxide target and promotes its effective evaporation.

The electrical properties of both the intermediate layers and the resulting layered coatings are investigated: the tangent of dielectric losses, the real and imaginary part of the conductivity and the dielectric constant versus the frequency.

REFERENCES

- [1] Oks E.M., Tyunkov A.V., Yushkov Y.G., Zolotukhin D.B. Ceramic coating deposition by electron beam evaporation // Surface and Coatings Technology. 2017. Vol. 325. P. 1–6.

* The work was supported by the Russian Foundation for Basic Research (grant # 20-58-00010 bel_a) and by a Grant from the President of the Russian Federation (No. MK-154.2020.8).

PLASMA NITRIDING IN COMPLEX POST-PROCESSING OF STAINLESS STEEL PARTS OBTAINED BY ADDITIVE LASER TECHNOLOGY*

A.V. MAKAROV¹, V.P. KUZNETSOV^{1,2}, P.A. SKORYNINA³, V.A. SIROSH¹, A.B. VLADIMIROV¹, N.V. LEZHININ¹,
S.V. KOLMAKOV²

¹*Institute of Metal Physics, UB, RAS, Yekaterinburg, Russia*

²*Ural Federal University, Yekaterinburg, Russia*

³*Institute of Engineering Science, UB, RAS, Yekaterinburg, Russia*

e-mail: sirosh@imp.uran.ru

Plasma nitriding coupled with deformation processing by a sliding indenter is an effective method for stainless steels surface hardening [1, 2]. This paper shows the possibility of ion-plasma nitriding application in the offered complex post-processing technology for a product produced by selective laser melting (SLM) using the PH1 high-chromium stainless steel powder. The complex post-processing technology for a part of isolating pipeline valves obtained by the SLM method includes heat treatment, plasma nitriding, burnishing with a sliding diamond indenter [3] and deposition of a multilayer (80 alternating layers of 25 nm thick from Ti_{0.2}C_{0.8} titanium carbide and diamond-like carbon) composite coating with a thickness of not less than 2 μm [4].

The multilayer coating deposited on the heat-treated substrate is characterized by significant divergency, with the average surface roughness Ra being 310 nm and 180 nm when measured, respectively, on surface areas with dimensions of 211.2×277.5 μm and 42.5×55.8 μm. The coating deposited on nitrided substrate at temperatures of 500-540°C shows less inhomogeneity, and the average Ra values are 230 nm and 180 nm. A thin-film coating deposited on a substrate subjected to nitriding and burnishing is characterized by the highest uniformity and the lowest average values of the roughness parameter, Ra=82-86 nm. X-ray diffraction analysis used after plasma nitriding revealed the α-phase, γ'-phase (Fe₄N), as well as chromium nitride inclusions CrN, in the surface layer structure. After the deposition of a multilayer thin-film coating on the surface, previously subjected to nitriding and burnishing, an additional TiC phase appears. The surface layer of the coated part received by the SLM method, forms favorable compressive stresses. The microhardness of a multilayer coating deposited on the heat-treated substrate reaches 1200 HV at a depth of 0.55 μm. The microhardness of the coating deposited on the sample, subjected to nitriding and subsequent burnishing, reaches 2500 HV at a depth of 0.50 μm. It is 500 HV higher than the microhardness of the coating deposited on the nitrided surface (without burnishing).

Thus, the complex application of plasma nitriding and burnishing with sliding diamond indenters takes on the role of a 'solid basis' contributing to the effective formation of high-strength thin-film 'titanium carbide – diamond-like carbon' coatings on the surface of stainless steel synthesized by the additive technology.

The authors express particular gratitude to A.G. Merkushev and I.Y. Malygina for their participation in the work.

REFERENCES

- [1] A.V. Makarov, G.V. Samoilova, N.V. Gavrilov, A.S. Mamayev, A.L. Osintseva, T.E. Kurennykh, R.A. Savrai, "Effect of Preliminary Nanostructuring Frictional Treatment on the Efficiency of Nitriding of Metastable Austenitic Steel in Electron Beam Plasma", AIP Conference Proceedings, vol. 1915, 030011, 5 p, 2017.
- [2] I.S. Zhidkov, A.I. Kukharenko, A.V. Makarov, R.A. Savrai, N.V. Gavrilov, S.O. Cholakh, E.Z. Kurmaev, "XPS characterization of surface layers of stainless steel nitrided in electron beam plasma at low temperature", Surf. Coat. Technol., vol. 386, No. 125492, 2020.
- [3] V.P. Kuznetsov, A.V. Makarov, S.G. Psakhie, R.A. Savrai, I.Yu. Malygina, N.A. Davydova, "Tribological aspects in nanostructuring burnishing of structural steels", Physical mesomechanics, vol. 17, pp. 250-264, 2014.
- [4] A.P. Rubshtein, A.B. Vladimirov, S.A. Plotnikov, "Specific Features of the Erosion Wear of Coatings with a Ti_{1-x}C_x – Diamond-Like Carbon Structure Forming Pair (x = 0.2, 0.8)", Physics of Metals and Metallography, vol. 12, pp. 1203-1210, 2020.

* The research was supported by RFBR and Sverdlovsk Oblast (project No. 20-48-660065).

AEROSOL ASSISTED ATMOSPHERIC PRESSURE PLASMA DEPOSITION FOR SILVER-CONTAINING ANTIBACTERIAL COATINGS*

L. WANG^{1,2}, C. LO PORTO³, F. PALUMBO^{3,4}, M. MODIC⁵, U. CVELBAR⁵, C. LEYS², A. NIKIFOROV²

¹College of Advanced Interdisciplinary Studies, National University of Defense Technology, Changsha, China

²Department of Applied Physics, Ghent University, Ghent, Belgium

³Department of Chemistry, University of Bari "Aldo Moro", Bari, Italy

⁴Institute of Nanotechnology, National Research Council of Italy, Bari, Italy

⁵Laboratory for Gaseous Electronics, Jozef Stefan Institute, Ljubljana, Slovenia

e-mail: wanglei09c@163.com

Fabrication of antibacterial coatings is an important strategy to prevent bacterial proliferation and infection [1, 2]. In this work, antibacterial coatings containing nanocapsules were synthesized in a single step by aerosol-assisted atmospheric pressure plasma deposition. It was observed that the formed nanocapsules were embedded in the polymer coating, which had a core-shell structure with silver as the core and polymer as the shell (see Fig. 1). The antibacterial coatings deposited on PET fabrics were then subjected to biological analysis, including Ag^+ ion release assays, antibacterial tests for *Escherichia coli* and *Staphylococcus aureus*, and cytotoxicity analysis of murine fibroblasts. A two-phase release kinetic process of Ag^+ ions was observed, i.e., from an initial short-term burst of release to a long-term slow release. It was shown that the coatings deposited on PET fabrics have high antibacterial efficiency and low cytotoxicity, which are promising for biomedical applications.

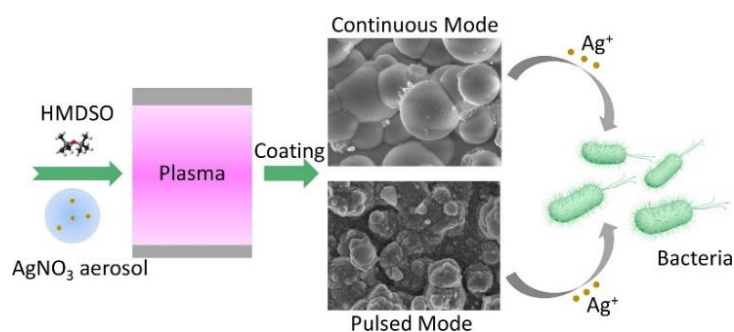


Fig. 1. Schematic of aerosol assisted atmospheric pressure plasma deposition for antibacterial coatings [3].

REFERENCES

- [1] M. Cloutier, D. Mantovani, F. Rosei, "Antibacterial coatings: challenges, perspectives, and opportunities", Trends in Biotechnology, vol. 33, pp. 637–652, 2015.
- [2] X. Li, B. Wu, H. Chen, K. Nan, Y. Jin, L. Sun, B. Wang, "Recent developments in smart antibacterial surfaces to inhibit biofilm formation and bacterial infections", J. Mater. Chem. B, vol. 6, pp. 4274–4292, 2018.
- [3] L. Wang, C. L. Porto, F. Palumbo, M. Modic, U. Cvelbar, R. Ghobeira, N. De Geyter, M. De Vrieze, Š. Kos, G. Serša, C. Leys, A. Nikiforov, "Synthesis of antibacterial composite coating containing nanocapsules in an atmospheric pressure plasma", Materials Science and Engineering: C, vol. 119, pp. 111496, 2021.

*This work was supported by the China Scholarship Council (File No.201503170253) and co-funding of Ghent University (Reference Code: DOZA/DDC/AM/006b-2016). The work was partially funded by the MEra-Net program, project "PlasmaTex", COST (European Cooperation in Science and Technology) AMiCI Action CA15114, and FWO/ARRS agencies project number G084917N and N3-0056.

FORMATION OF ALLOYED LAYERS ON THE SURFACE OF MA-2 MAGNESIUM ALLOY BY METHODS OF COMBINED ELECTRON-ION-PLASMA TREATMENT*

A.D. TERESOV, YU.A. DENISOVA, V.V. DENISOV, A.A. LEONOV, S.S. KOVALSKY

Institute of High Current Electronics, SB, RAS, Tomsk, Russia

e-mail: tad514@sibmail.com

The synthesis of the surface alloy was carried out as follows [1]. On the surface of flat specimens 15×15×5 mm in size made of MA-2 magnesium alloy (94.5–96.7% Mg, up to 0.05% Fe, up to 0.1% Si, 0.15–0.5% Mn, up to 0.005 % Ni, 3–4% Al, up to 0.05% Cu, up to 0.002% Be, 0.2–0.8% Zn) by the method of vacuum arc discharge sputtering of the cathode surface, a metal film 1 μm thick was deposited. A7 aluminum alloy was used as the cathode material (from 99.7% Al, up to 0.16% Fe, up to 0.15% Si, up to 0.03% Mn, up to 0.01% Ti, up to 0.01% Cu, up to 0.02% Mg, up to 0.04% Zn, up to 0.03% Ga). During the deposition of the coating, the surface temperature of the specimens was controlled (no more than 200°C) in order to exclude the degradation of the strength properties of the magnesium alloy in the bulk of the initial material as a result of annealing. Then the resulting “coating (A7)/substrate (MA-2)” system was irradiated with an intense pulsed electron beam of submillisecond duration. In the course of irradiation, the following parameters were varied: the energy density in the pulse was 3–12 J/cm², the pulse duration was 50–200 μs, and the number of pulses was 3–10. The impact of a pulsed electron beam on the “coating/substrate” system resulted in liquid-phase mixing of materials in the surface layer.

As a result of the studies carried out, the optimal modes of formation of the “Al (A7)/Mg (MA-2)” surface alloy were revealed, depending on the energy density in the pulse of the electron-beam and the pulse duration. It was shown that the combined surface treatment in the obtained modes allows increasing the microhardness and wear resistance of the modified layer up to 1.75 and 1.5 times, respectively (Fig. 1). X-ray diffraction analysis of the specimens showed that after pulsed electron-beam treatment, the particles of Mg₁₇Al₁₂ strengthening phase are formed in the surface layer, which is one of the reasons for the increase in the strength and tribological properties of the surface of the MA-2 magnesium alloy.

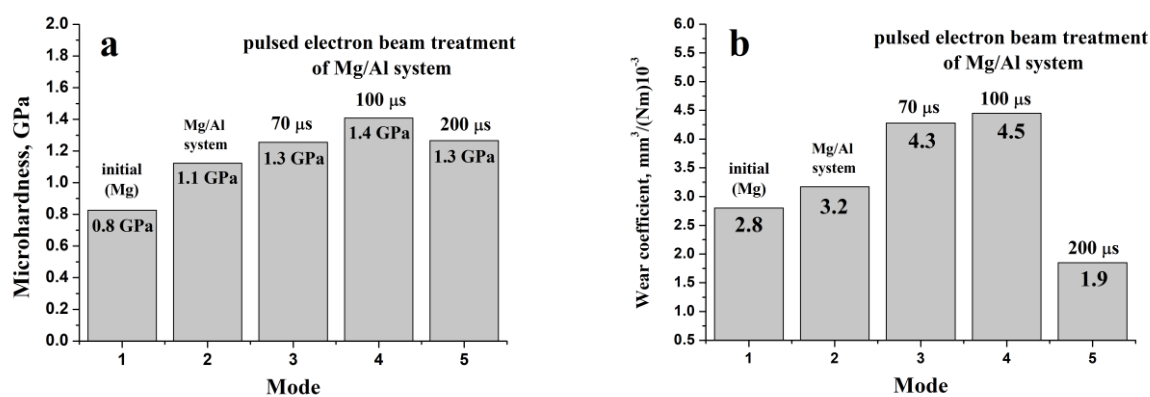


Fig. 1. Surface microhardness (a) and wear coefficient (b) of MA-2 magnesium alloy before and after combined electron-ion-plasma surface modification. Irradiation modes: 3 - 3.5 J/cm², 70 μs, 5 pulses; 4 - 5 J/cm², 100 μs, 5 pulses; 5 - 10 J/cm², 200 μs, 5 pulses.

REFERENCES

- [1] V.N. Devyatkov, Yu.F. Ivanov, O.V. Krysinina, N.N. Koval, E.A. Petrikova, V.V. Shugurov, “Equipment and processes of vacuum electron-ion plasma surface engineering,” *Vacuum*, Vol. 143, pp. 464-472, 2017.

* The work was performed under State Assignment of the Ministry of Science and Higher Education of the Russian Federation (project No. FWRM-2019-0002).

STRUCTURE AND MECHANICAL PROPERTIES OF STAINLESS-STEEL SPECIMENS, MADE BY ADDITIVE METHOD, AFTER PULSED ELECTRON BEAM TREATMENT*

A.D. TERESOV¹, Yu.H. AKHMADEEV¹, E.A. PETRIKOVA¹, O.V. KRYSINA¹, Yu.F. IVANOV¹, G.V. SEMENOV²

¹*Institute of High Current Electronics, SB, RAS, Tomsk, Russia*

²*LLC «TETA», Loskutovo, Tomsk, Russia*

e-mail: tad514@sibmail.com

A common problem, to some extent characteristic of all types of AM-technologies, is the problem of ensuring an appropriate microstructure of the synthesized material, eliminating porosity. Another disadvantage of AM-technologies is the anisotropy of the structure and properties of the material, high internal stresses, which is inevitable under the layer-by-layer principle of article creation. In order to solve these problems, the authors have proposed a method of finishing the surface of metal articles, produced using AM-technologies, with a pulsed electron beam in vacuum [1].

The purpose of the present work is to compare the structure and mechanical properties of AISI 308LSi stainless-steel specimens (0.01% C, 19.9% Cr, 0.1% Cu, 1.8% Mn, 0.15% Mo, 10.5% Ni, 0.9% Si, 9% Si+Fe, balance Fe) obtained by layer-by-layer electron-beam welding of wire with diameter of 1 mm in vacuum and subjected to subsequent pulse electron-beam treatment at SOLO setup [2]. During irradiation the following parameters were varied: energy density in pulse (12-40 J/cm²), pulse duration (50-150 μs), number of pulses (3-10).

Comparative analysis of the surface structure of the specimens after irradiation in some modes showed the formation of a uniform polycrystalline structure without cracks in contrast to the original samples (Fig. 1). Surface roughness decreased more than 2 times (R_a) and 3 times (R_z), at the same time, the microhardness of the surface remained equal to the initial (190 HV_{0.5}). Tribological tests showed a slight decrease in wear resistance (1.28 times) and friction coefficient (1.15 times), in contrast to the initial specimens. Thus, the surface treatment of AISI 308LSi stainless-steel specimens, made by AM-technologies, with a pulsed electron beam resulted in a uniform microstructure with significantly reduced roughness relative to the initial material.

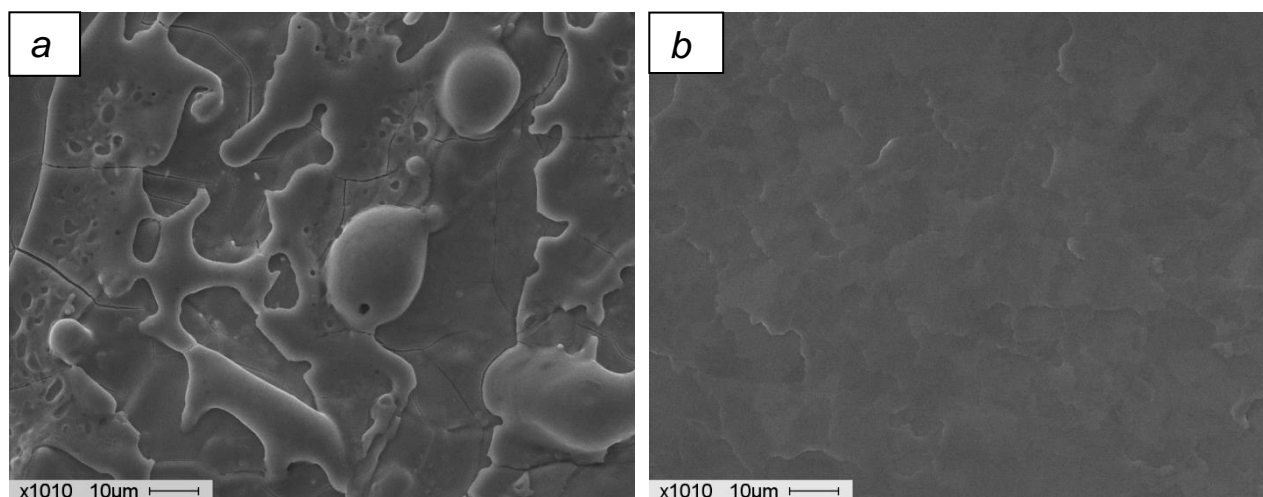


Fig. 1. SEM image of the surface structure of AISI 308LSi stainless-steel specimens manufactured by the additive method before (a) and after (b) pulsed electron beam treatment.

REFERENCES

- [1] A.D. Teresov, N.N. Koval, Yu.F. Ivanov, E.A. Petrikova, "Application of a pulsed electron beam for surface polishing of metal products obtained by laser or electron-beam powder sintering," *Izv. Vyssh. Uchebn. Zaved. Fiz.*, Vol. 59, No. 9/2, pp. 264–266, september 2016 [in Russian].
- [2] N.N. Koval, Yu.F. Ivanov, "Nanostructuring the surface of metal-ceramic and ceramic materials under pulsed electron-beam treatment," *Izv. Vyssh. Uchebn. Zaved. Fiz.*, Vol. 51, No. 5, pp. 60–70, may 2008 [in Russian].

* The reported study was funded by RFBR and Tomsk region according to the research project № 19-48-700021.

EFFECT OF ULTRAVIOLET IRRADIATION OR PLASMA OF DIFFUSE DISCHARGE ON THE SURFACE PROPERTIES OF MAO CALCIUM PHOSPHATE COATINGS*

E.G. KOMAROVA¹, E.A. KAZANTSEVA^{1,2}, V.S. RIPENKO³, A. ZHARIN⁴, Y.P. SHARKEEV¹

¹*Institute of Strength Physics and Materials Science, SB, RAS, Tomsk, Russia*

²*National Research Tomsk State University, Tomsk, Russia*

³*Institute of High Current Electronics, SB, RAS, Tomsk, Russia*

⁴*Belarussian National Technical University, Minsk, Belarus*

e-mail: katerina@ispms.ru

Recently, the effect of ultraviolet (UV) irradiation on titanium (Ti) [1] and hydroxyapatite [2] surfaces has been shown to induce photochemical and photocatalytic reactions, migration of the photoinduced charge carriers to the surface, the generation of hydrophilicity, a modification of the surface electrostatic properties and improvement their bioactivity and osteoconductive. Another surface treatment of metals in the plasma of a runaway electron preionized diffuse discharge (REP DD) in atmospheric pressure has been shown [3] to provide ultrafine surface cleaning of the treated metals from carbon and increases their surface free energy up to 3 times. However, the application of UV irradiation or REP DD for the functionalization of calcium phosphate (CaP) coatings on the Ti implants has not been reported. Therefore, the purpose of this work was to study effect of UV light or REP DD on the surface characteristics of CaP coatings formed by the micro-arc oxidation (MAO) on Ti substrates.

The coatings were deposited on samples from commercial pure Ti by the MAO method in anodic potentiostatic mode under standard conditions in the standard electrolyte described earlier [4]. Then, part of the CaP coated samples was irradiated with UV for 1, 5, 10, 15 and 20 min using a KrCl excilamp at 222 nm wavelength (exposure dose of 5.5 mW/cm²). Another part of the CaP coated samples was irradiated with REP DD under cathodic pulsed voltage of 12 kV, pulse duration of 4 ns, and varied pulses number from 10000 to 80000 with step of 20000 [4].

The SEM, EDX, XRD, and TEM data showed that the UV and REP DD treatments did not change the coating surface morphology, elemental and phase compositions, and microstructure. All the coatings were in amorphous-nanocrystalline state with incorporation (less than 8 vol.%) of nano-sized CaHPO₄ and β-Ca₂P₂O₇ phases. The surface electrical charge of the treated samples was measured by the contact potential difference method with a Kelvin scanning probe [5]. This study showed that both the untreated and treated CaP coatings have negative surface charge. It can be result of presence of negatively charged hydroxyl and phosphate groups on the coating surface observed with IRS. However, UV radiation and plasma exposure had different effects on the surface charge. With increasing UV exposure time, the surface negative charge increased from – 85 mV to – 105 mV. On the contrary, the REP DD led to a decrease in the negative charge from – 85 mV to – 40 mV. This was confirmed by the IRS data showing an increase in the intensity of the absorption bands of the P-O and O-H bonds because of UV irradiation with an increasing time exposure. In opposite, the intensity of adsorption bands of the P-O and O-H bonds decreased because of REP DD post-treatment with an increasing pulses number.

REFERENCES

- [1] Choi S.H., Jeong W.S., Cha J.Y., Lee J.H., Lee K.J., Yu H.S., Choi E.H., Kim K.M., Hwang C.H. Overcoming the biological aging of titanium using a wet storage method after ultraviolet treatment, *Scientific Reports*, 7, 3833, 2017.
- [2] Yasuda K., Okazaki Y., Abe Y., Tsuga K. Effective UV/Ozone irradiation method for decontamination of hydroxyapatite surfaces, *Heliyon*, 3, 00372, 2017.
- [3] Erofeev M., Ripenko V., Shulepov M., Tarasenko V. Surface tretment of metals in the plasma of a nanosecond diffuse discharge at atmospheric pressure, *Eur. J. D*, 71, 117, 2017.
- [4] Chebodaeva V.V., Komarova E.G., Erofeev M.V., Ripenko V.S., Sharkeev Yu.P. Effect of UV irradiation and diffuse plasma on surface properties of micro-arc calcium phosphate coatings, *J. Phys. Conf. Ser.* 1393, 012077, 2019.
- [5] Zharin A. “Contact Potential Difference Techniques as Probing Tools in Tribology and Surface Mapping”. In: *Scanning Probe Microscopy in Nanoscience and Nanotechnology*. NanoScience and Technology, Berlin, Heidelberg: Springer, 2010.

* The work was supported by the Government research assignment for ISPMS SB RAS, project FWRW-2021-0007.

LEAD EVAPORATION BY VUV RADIATION OF VARIOUS SPECTRAL RANGES*

A.V. PAVLOV, Y.Y. PROTASOV, V.D. TELEKH, T.S. SHCHEPANUK

Bauman Moscow State Technical University, Moscow, Russia

e-mail: telekh@bmstu.ru

The results of an experimental study of the plasma formed by the evaporation of the lead target in the field of powerful broadband VUV radiation are presented.

Similar processes take place during surface treatment with plasma and radiation flows during formation and modification of Nano-structured terrain on structural materials surfaces, as well as in various high-energy research facilities. Obtaining sufficient information about the effectiveness of such processing methods is unthinkable without studying the physics of impact on materials including studies of the gas-dynamic "response" of the target surface. At the same time, the task of switching to technological sources of plasma and radiation of a new generation with high energy conversion efficiency is urgent.

A pulse light-erosion magnetoplasma compressor (MPC's) discharge [1, 2] is used as a model source of VUV radiation. This discharge is stable and has a high light efficiency in shortwave spectrum (up to 20 – 30%). Capacitor stored energy is about 3.6 kJ ($U \sim 20$ kV, the maximum current is up to 200 kA). "Gas filtration" of radiation is used to control the spectral composition – the discharge takes place in pure inert gases: in argon at 200 Torr and neon at 400 Torr. This allows us to manage the spectral distribution of radiation energy and to limit the energy of quanta which irradiate the lead target with the first ionization potential of buffer gas.

A rectangular sample (50×30×10 mm) is set with a long side lengthways the discharge. The position of the sample is 45 mm from the axis and 10 mm from the face of MPC. Such placing additionally allows us to control the energy of falling radiation along the length of the sample.

Shadow photography, toeplergraphy, double exposure laser holographic interferometry are used for diagnostics [3].

Experimentally established different distribution of parameters in the lead plasma depending on the spectral composition of the impact radiation (the composition of buffer gas). It is shown that when the energy of quanta increases (above the lead second ionization potential), a more even heating of the plasma layer is realized.

REFERENCES

- [1] Pavlov A., Protasov Yu., Telekh V., Tshapanuk T., Experimental Research of Dynamics and Macrostructure of Light Erosion Radiative Plasmodynamic Discharges, *J. Phys.: Conf. Ser.*, V. 830, P. 012062 (2017).
- [2] Protasov Yu.S. Plasma radiation sources of high spectral brightness // in *Encyclopedia of Low Temperature Plasma. Introduction voluem. Vol IV.*- Moscow: Nauka, 2000.- P.232.
- [3] Pavlov A.V., Protasov Yu.Yu., Telekh V.D., Shchepanuk T. S., Laser holographic interferometry of high power density short ultraviolet radiation interaction with condensed matters, *Scientific Visualisation*, V.11, No. 3, P. 111-125 (2019).

* The reported study has been funded following the government task 0705-2020-0046 by the Russian Ministry of Education and Science and has been performed at large-scale research facilities "Beam-M" of Bauman Moscow State Technical University.

GAS-DISCHARGE PLASMA APPLICATION FOR ION-BEAM TREATMENT OF THE HOLES' INNER SURFACES*

D.O. SIVIN, O.S. KORNEVA, A.I. IVANOVA, D.O. VAKHRUSHEV

*National Research Tomsk Polytechnic University, Tomsk, Russia
e-mail: oskar@tpu.ru*

The development of method of the low energy high-intensity ion implantation (LEHI³) into various materials has shown that along with the formation of ion-doped layers with thicknesses of tens and hundreds of micrometers, the completely new possibilities for modifying the parts' surfaces have appeared. These possibilities were previously not available for traditional ion beam implantation.

The possibility to modify the holes and pipes' inner surface with focused high-intensity low-energy ion beams was first shown in this work. The studies were carried out using an axially symmetric single-grid system for the ions' extraction from a free plasma boundary with subsequent ballistic focusing of the ion beam. Ion implantation of the inner surface was carried out in the region of the ion beam defocusing.

The studies considered the effect of a nitrogen ions' beam with energy of 1.4 keV on the inner surface of a tube with a diameter of 25 mm made of stainless steel AISI 321. The beams were formed with a repetition rate of 40 kHz and pulse durations of 5, 7.5 and 10 μ s.

It is shown that the mutual deposition of the sputtered material on the tube' opposite sides compensates for ion sputtering. The possibility to use high-intensity low-energy ion beams for high-speed deposition of sputtered material has been studied.

As a result of implantation of the inner surface of a pipe made of stainless steel AISI 321, the nitride layers with a thickness of more than 20 microns with a nitrogen dopants content of 15-25 at.% were obtained.

* This work was carried out with the financial support of the russian science foundation (grant no. 17-19-01169 p).

HIGH-ENTROPY ZrTiCrNiCu COATING

V.M. YUROV¹, V.I. GONCHARENKO^{2,3}, V.S. OLESHKO²

¹Karaganda State University named after E.A. Buketov, Karaganda, Kazakhstan

²Moscow Aviation Institute (National Research University), Moscow, Russia

³Institute for Management Problems, V.A. Trapeznikov, RAS, Moscow, Russia

e-mail: exciton@list.ru

A high-entropy alloy ZrTiCrNiCu and coating are synthesized by mechanical alloying. A distinctive feature of high-entropy alloys (HEAs) from traditional alloys is that these alloys have a high entropy of mixing, which affects the formation of structures based on solid solutions.

For the formation of a 100% high-entropy phase of Laves the following conditions are required: the total negative enthalpy of alloy mixing at the level of -7 kJ/mol and below; pairs with an atomic difference of more than 12%; the presence in the alloy of two elements with a mixing enthalpy of less than -30 kJ/mol, the average electron concentration should be in the range of 6-7 electron/atom. It is shown that the ratio of the lattice parameters of solid-state HEA, determined in the experiment, to the lattice parameter of the most refractory metal of the HEA determine the magnitude of the elastic modulus.

We have investigated the phase composition of the coating. Let's discuss this composition.

The first is Cu_{1.5}ZrNi_{3.5} with a phase content of 10 at. % and with a lattice constant equal to $a = 6.7671 \text{ \AA}$. The structure of Cu_{1.5}ZrNi_{3.5} is B2 - a high-temperature austenitic phase ordered by the CsCl type (Pm3m-fcc). In second place is Cu with a phase content of 7.8 at. % and lattice constant $a = 3.6178 \text{ \AA}$. The unit cell of copper is fcc. Third place is Zr_{0.02}Ni_{0.98} with a phase content of 19.8 at. % and lattice constant $a = 3.3406 \text{ \AA}$. According to X-ray spectral analysis, the main component of the eutectic is the combination of nickel and zirconium. The eutectic component was identified as a ZrNi intermetallic compound with an fcc lattice corresponding to the space group F 43 m (sphalerite type). Fourth place is Cr₂Ti with a phase content of 29.5 at. % and lattice constant $a = 4.9076 \text{ \AA}$ and $c = 15.9700 \text{ \AA}$. Near the TiCr₂ composition, intermediate phases with the Laves structure are formed. In fifth place is NiTi with a phase content of 33 at. % and the lattice constant $a = 2.8007 \text{ \AA}$, $b = 4.6192 \text{ \AA}$, $c = 4.1824 \text{ \AA}$, $\beta = 97.5793$. The results of neutron diffraction studies of quenched alloys in the initial austenitic and martensitic states show that the Ti_{49.5}Ni_{50.5} alloy is in the austenitic state at room temperature. The parameter of its crystal lattice B2 (a) and the degree of long-range atomic order (η) turned out to be $a = 0.30125 \text{ nm}$; $\eta = 1.00 \pm 0.05$. In contrast, the Ti_{50.5}Ni_{49.5} alloy at room temperature is in the B19' martensite state, which unambiguously follows from the interpretation of the neutron diffraction pattern and allows one to determine its parameters: $a = 0.2903$, $b = 0.4112$, $c = 0.4636 \text{ nm}$, $\beta = 97.25$. The NiTi observed by us turns out to be martensite with the B19' structure.

Thus, of the five high entropy ZrTiCrNiCu coatings, three have an MCC structure, TiCr₂ gives the Laves phase, and NiTi gives martensite with the B19' structure.

Microhardness combined with a low coefficient of friction leads to good wear resistance of the ZrTiCrNiCu coating. The application of such a coating to parts of locomotives of rolling stock showed an increase in service life by 4 times. The coatings were made on steel parts DTRKZ4AC00446.

As for the contact potential difference and the electron work function for the ZrTiCrNiCu alloy, we can conclude that this alloy is not inferior to copper alloys in their electrical characteristics.

The very good performance of the coatings from the ZrTiCrNiCu target is most likely due to titanium and zirconium nickelides. These compounds have the property of shape memory. One of the most relevant areas of application of these materials is the so-called active devices (devices that perform mechanical work under the influence of heat, for example, drives). An alloy with a shape memory effect when operating in such devices is subjected to various thermomechanical influences, such as dynamic loading, a single or multiple temperature change through a full or incomplete temperature range of a reversible martensitic transformation.

Synthesis of a high-entropy alloy by mechanical alloying is more economically advantageous than remelting in a vacuum cast samples. We continue to study the ZrTiCrNiCu coating on the details of machines and mechanisms, but the preliminary results look encouraging.

EFFECT OF IRRADIATION WITH IONS OF DIFFERENT ATOMIC MASSES (Ar⁺ AND Xe⁺) ON THE PROPERTIES OF Co₉₀Fe₁₀/Cu MAGNETIC SUPERLATTICES*

N.V. GUSHCHINA¹, V.V. OVCHINNIKOV¹, K.V. SHALOMOV¹, N.S. BANNIKOVA², R.S. ZAVORNITSYN², M.A. MILYAEV²

¹Institute of Electrophysics, UB, RAS, Yekaterinburg, Russia

²Institute of Metal Physics, UB, RAS, Yekaterinburg, Russia

e-mail: icsartf@gmail.com

The work is to study the effect of irradiation with inert gas ions of different atomic masses on the magnetoresistance of Co₉₀Fe₁₀/Cu superlattices formed on three different substrates. This study is urgent for nanoelectronic devices with widely-used superlattices that exhibit a giant magnetoresistive effect, which can often be used under ionizing radiation. However, no data on the behavior of magnetic superlattices under radiation loading conditions are available.

Multilayered Co₉₀Fe₁₀/Cu magnetic nanostructures were prepared using a ULVAC MPS-4000-C6 high-vacuum deposition machine (Japan). The formula of the investigated superlattice is substrate/Ta (100 Å)/(Ni₈₀Fe₂₀)₆₀Cr₄₀(50 Å)/[Co₉₀Fe₁₀(14 Å)/Cu(23 Å)]₁₂/Ta(30 Å). Al₂O₃ (monocrystalline sapphire), glass and Si (monocrystalline silicon) were used as substrates.

The irradiation with continuous Ar⁺ and Xe⁺ ion beams was carried out on an ILM-1 implanter equipped with a PULSAR-1M ion source based on a low-pressure glow discharge with a hollow cold cathode [1]. Xe⁺ ions have an atomic mass that is more than three times greater than that of Ar⁺ ions. The energy for each of these ion types was 10 keV, the ion current density was 100 μA/cm², and the fluences were 1·10¹⁴–1·10¹⁷ cm⁻².

The magnetoresistance of the superlattices was measured in the initial state and after ion irradiation using an AVM-1 automated machine at the "Center for Technology of New Magnetic Materials" Physical-technological infrastructural complex, Institute of Metal Physics, UB RAS. The resistance of the superlattices in the magnetic field (to 19.5 kE) was measured using a four-contact method using clamped contacts. The magnetic vector and the current in the plane of the film layers were mutually perpendicular to each other during the measurements. The measurements were carried out at room temperature. The magnetoresistance was defined as the relative change in the electrical resistance of the material (R) when a magnetic field (H) was switched on: $\Delta R/R(H)=[(R(H)-R_s)/R_s]\cdot 100\%$, where R_s is the electrical resistivity of the sample in the case of magnetic saturation, when the magnetic moments of the ferromagnetic layers are parallel; $R(H)$ is the electrical resistivity in magnetic field H (value $(\Delta R/R)_{\max}$ is the maximum $\Delta R/R(H)$ value of the field dependence of magnetoresistance).

The Ar⁺ ion irradiation of the Co₉₀Fe₁₀/Cu superlattices (irrespective of the substrate material) from an ion fluence of 1·10¹⁶ cm⁻² has been found to decrease their magnetoresistance noticeably. Their maximum magnetoresistance $(\Delta R/R)_{\max}$ is 14.4% for glass substrate, 14.7% for Al₂O₃ substrate, and 10.9% for Si substrate ($(\Delta R/R)_{\max}$ for the initial samples are 28.6%, 22.9%, and 22.7% respectively). The transition to magnetic saturation becomes more abrupt. The above superlattices retain their functional characteristics at lower fluences (1.0·10¹⁴–1.25·10¹⁵ cm⁻²). The giant magnetoresistance effect disappears entirely at $F = 10^{17}$ cm⁻². Similar results were obtained upon Xe⁺ ion irradiation, but the magnetoresistance at the same fluence falls to lower values. For example, $(\Delta R/R)_{\max}$ at a xenon fluence of 1·10¹⁶ cm⁻² is 21.3% for the glass substrate, 20.4% for the Al₂O₃ substrate, and 17.4% for the Si substrate. This can be attributed to the greater average projective range R_p of Ar⁺ than for Xe⁺ ions (5–7 and 3–5 nm, respectively) and to the greater depth of the mixing zone of the substrate atoms, which is on the order of (2–3)× R_p .

According to the available literature and our data, the magnetoresistance of the Co₉₀Fe₁₀/Cu superlattices decreases when the argon and xenon ion fluence increases due to the partial in-depth mixing of atoms of different composition layers in the ion projective range, interlayer boundary state changes, and the formation of regions with ferromagnetic interaction between neighboring ferromagnetic layers in the superlattices under study.

REFERENCES

- [1] N.V. Gavrilov., G.A. Mesyats, S.P. Nikulin, G.V. Radkovskii, A. Eklind and A.J. Perry, "A New Broad Beam Gas Ion Source for Industrial Applications", J. Vac. Sci. Technol., vol. A 14, pp. 1050-1056, 1996.

* This work was supported by the Russian Scientific Foundation, project No. 19-79-20173.

INVESTIGATION OF THE EFFECT OF ION IRRADIATION ON THE PROCESS OF NANOCRYSTALLIZATION OF AN $\text{Fe}_{72.5}\text{Cu}_1\text{Nb}_2\text{Mo}_{1.5}\text{Si}_{14}\text{B}_9$ ALLOY USING THE IN SITU RESISTIVITY MEASUREMENT METHOD

K.V. SHALOMOV, V.V. OVCHINNIKOV

Institute of Electrophysics, UB RAS, Yekaterinburg, Russia

e-mail: icsartf@gmail.com

Recently, there is an increasing need to control the properties of soft magnetic materials due to the emergence of various new areas of their application. One of the most promising methods of modifying the properties of materials is ion-beam processing. At the same time, the complex processes that occur during ion-beam processing are still far from always exhaustively studied. This applies, in particular, to the modification of the properties of soft magnetic materials widely used in technology.

The soft magnetic alloy $\text{Fe}_{72.5}\text{Cu}_1\text{Nb}_2\text{Mo}_{1.5}\text{Si}_{14}\text{B}_9$ (Finemet) was chosen as the object of research. The measurement of the electrical resistivity ρ (in situ) of samples $10 \times 10 \times 0.025 \text{ mm}^3$ prepared from ribbons obtained by quenching from the melt was carried out using specially developed equipment that provides the determination of the ρ as well as the temperature T . Upon reaching thermal equilibrium, after applying the required operating current to the sample under conditions of a residual argon pressure of $\sim 4 \cdot 10^{-4} \text{ mm Hg}$, ion-beam treatment was performed with continuous beams of Ar^+ ions with an energy of 15 keV. In the experiments an ILM-1 ion implanter with a PULSAR-1M ion source based on a glow discharge with a cold hollow cathode was used [1]. The ion current density reached a value of $j = 300 \mu\text{A}/\text{cm}^2$.

The modes of target heating by an ion beam were reproduced (for comparison) using an IR heater made of FeCrAl alloy located in the implanter chamber at the required distance (up to 30 mm) from the irradiated targets.

Measurements of the dependence of the electrical resistivity on temperature $\rho(T)$, which is the most structurally sensitive quantity, provide express information on the temperature ranges of structural-phase and magnetic rearrangements in the materials under study under conditions of their heating by IR radiation and using ion beam at an identical temperature mode. After holding the samples of the $\text{Fe}_{72.5}\text{Cu}_1\text{Nb}_2\text{Mo}_{1.5}\text{Si}_{14}\text{B}_9$ alloy in the temperature ranges selected on the basis of the measured $\rho(T)$ dependences, their structure was investigated by X-ray structural analysis.

Previously obtained results on the effect of ion irradiation on the nanocrystallization process were confirmed [2]. Based on $\rho(T)$ measurements *in situ* it has been shown that irradiation causes the crystallization of the entire volume of ribbons of the amorphous $\text{Fe}_{72.5}\text{Cu}_1\text{Nb}_2\text{Mo}_{1.5}\text{Si}_{14}\text{B}_9$ alloy, when the temperature reaches only 350–420°C, which is significantly lower than the temperature of the thermal threshold for the onset of crystallization of this alloy. Despite the decrease in temperature, the rate and degree of completion of the process are many times higher compared to industrial annealing for 1 h at 570°C. The obtained results indicate the essential role of nanoscale dynamic effects leading to a decrease in temperature and acceleration of the processes of rearrangement of metastable media under the influence of cascade-forming types of radiation [3], in this case, ion bombardment.

REFERENCES

- [1] N.V. Gavrilov., G.A. Mesyats, S.P. Nikulin, G.V. Radkovskii, A. Eklind, A.J. Perry, "A New Broad Beam Gas Ion Source for Industrial Applications", *J. Vac. Sci. Technol.*, vol. A 14, pp. 1050-1056, 1996.
- [2] V.V. Ovchinnikov, F.F. Makhin'ko, N.V. Gushchina, A.V. Stepanov, A.I. Medvedev, V.A. Kataev, V.S. Tsepelev, Y.N. Starodubtsev, V.Y. Belozeroov, "Effect of ion irradiation on the nanocrystallization and magnetic properties of soft magnetic $\text{Fe}_{72.5}\text{Cu}_1\text{Nb}_2\text{Mo}_{1.5}\text{Si}_{14}\text{B}_9$ alloy," *The Physics of Metals and Metallography*, vol. 118, no. 2, pp.150-157, 2017.
- [3] V.V. Ovchinnikov, "Radiation-dynamics effects. Potential for producing condensed media with unique properties and structural states," *Phys. Usp.*, vol. 51, pp. 955-964, 2008.

FORMATION OF AUSTENITE PARTICLES ENRICHED IN MANGANESE UP TO 20 at.% AND MORE, IN VOLUME OF Fe-6.35 at.% Mn ALLOY IN TEMPERATURE RANGE OF 300-450°C DURING IRRADIATION WITH Ar⁺ 20 keV IONS*

E.V. MAKAROV, V.V. OVCHINNIKOV

Institute of Electrophysics, UB, RAS, Yekaterinburg, Russia

e-mail: efre-m@yandex.ru

High-purity alloys of the Fe-Mn system with 5-10 at.%, Mn, quenched from elevated temperatures (of the order of 800°C and higher), have a single-phase structure of a disordered bcc α -solid solution at room temperature [1]. Samples of these alloys subjected to cold plastic deformation also demonstrate the absence of both long-range and short-range atomic order in the distribution of atoms [2, 3]. It was shown [3] that at temperatures $T < 600^\circ\text{C}$ the diffusion mobility of atoms in these alloys is so low that it excludes the formation of zones or phases with a changed concentration of manganese in the course of thermally stimulated processes. In particular, it was found that the α (bcc) \rightarrow γ (fcc) transformation in alloys of the concentration range under consideration (however, without changing the composition) at $T < 600^\circ\text{C}$ can occur only as a result of severe plastic deformation.

Nevertheless, in [4], it was possible to initiate the process of precipitation of particles of the γ -phase with a composition of 17.1 at.% Mn, during ion bombardment of a cold-deformed Fe-6.29 at.% Mn alloy by Ar⁺ ions with an energy of 15 keV, for 4 s, at an abnormally low temperature: 299°C. This process is associated with a sharp increase in the low-temperature mobility of atoms due to cascade matter radiation shaking (by powerful post-cascade shock and/or elastic waves). In metastable media, such waves can propagate over unlimited distances, supported by the energy released as a result of collective rearrangements of atoms at their front [4].

For the purpose of further analysis of this phenomenon, similar experiments were carried out on a Fe-6.35 at.% Mn alloy. Foils with a thickness of 25 μm of the indicated alloy (prepared from cold-deformed strips using electrolytic and chemical etching) were heated for 4-7 seconds by an Ar⁺ ion beam ($E = 15$ keV, $j = 200$ $\mu\text{A}/\text{cm}^2$, $F = 3.75 \cdot 10^{15} - 3.75 \cdot 10^{16}$ cm^{-2}) to 311, 378, and 449°C without holding at these temperatures (the beam was switched off immediately after reaching these temperatures). For comparison, short-term heating of the samples to the indicated temperatures in a muffle furnace were also performed.

Irradiation was carried out on an ion implanter (ILM-1) equipped with a PULSAR-1M ion source [5]. Mössbauer spectra were recorded on an SM-2201 automatic NGR spectrometer. The source of gamma quanta was ⁵⁷Co in Rh. A description (fitting) of Mössbauer spectra has been performed using models of short-range atomic order (concentration delamination) [6] and in a two-phase model.

It was found that in the initial cold-deformed state the alloy is a completely disordered single-phase α -solid solution. After short heating in the furnace, the formation of short-range atomic order and the precipitation of any phases do not occur. Short-term heating to 311, 378, and 449°C in all three cases causes depletion of the α -solid solution to 4–5 at.% Mn and the formation of Fe-6.35 at.% Mn of austenite with a Mn content of up to 20 percent or more. This confirms the fact of the excitation of the low-temperature mobility of atoms in the iron-manganese alloy at anomalously low temperatures with the formation of a second phase - austenite with a significantly increased concentration of manganese. It is assumed that radiation shaking by powerful post-cascade waves plays the role of temperature in this case.

REFERENCES

- [1] O.A. Bannykh, P.B. Budberg, S.P. Alisova, Phase Diagrams of Binary and Multicomponent Iron-Based Systems, Moscow: Metallurgiya, 1986.
- [2] L.Yu. Pustov, S.D. Kaloshkin, V.V. Cherdynstev, E.V. Shelekhov, I.A. Tomlin, E.I. Estrin, "Phase transformations in iron-rich Fe-Mn alloys obtained by mechanical alloying", Phys. Met. Metallogr., vol. 95, no. 6, pp. 575–583, 2003.
- [3] V.A. Shabashov, K.A. Kozlov, V.V. Sagaradze, A.L. Nikolaev, K.A. Lyashkov, V.A. Semyonkin, V.I. Voronin, "Short-range order clustering in BCC Fe-Mn alloys induced by severe plastic deformation", Phil. Mag., vol. 98, pp. 560–576, 2018.
- [4] V.V. Ovchinnikov, E.V. Makarov, N.V. Gushchina, "Austenite Formation in α -Phase Fe-Mn Alloy after Cold Plastic Working and Fast Heating by an Ar⁺ Ion Beam to 299°C", Phys. Met. Metallogr., vol. 120, no. 12, pp. 1207–1212, 2019.
- [5] N.V. Gavrilov, G.A. Mesyats, S.P. Nikulin, G.V. Radkovskii, A. Eklind, A.J. Perry, R.A. Treglio, "A new broad beam gas ion source for industrial applications", J. Vac. Sci. Technol., no. 14, pp. 1050–1055, 1996.
- [6] M.A. Krivoglaz and A.A. Smirnov, The Theory of Order-Disorder in Alloys, New York: American Elsevier Publishing Co, 1965.

* This work was supported by the Russian Scientific Foundation, project no. 19-79-20173.

ELECTRONIC-ION-PLASMA MODIFICATION OF THE STRUCTURE AND PROPERTIES OF SILUMIN*

Yu.F. IVANOV¹, A.A. KLOPOTOV², A.M. USTINOV², D.V. ZAGULIAEV³, A.D. TERESOV¹, Yu.A. ABZAEV², O.M. LOSKUTOV²

¹*Institute of High Current Electronics, SB RAS, Tomsk, Russia*

²*Tomsk State University of Architecture and Building, Tomsk, Russia*

³*Siberian State Industrial University, Novokuznetsk, Russia*

e-mail: zagulyaev_dv@physics.sibsiu.ru

Silumins (Al-Si alloys) are now widely used in many industries. The main disadvantage of silumins is their increased fragility. This is due to the presence of micron-sized silicon inclusions in the material. One of the methods of substantial (down to the nanoscale) refinement of the structure of a material is irradiation with pulsed energy flows. The aim of this work is to analyze the structure and properties of silumin treated with a pulsed electron beam. The research material was silumin grade AK5M2 (5 wt.% Si) and AK10M2N (10 wt.% Si). Irradiation was carried out on a SOLO installation with an electronic source based on a low-pressure pulsed arc discharge with grid stabilization of the cathode plasma boundary and an open anode plasma boundary. Tensile testing of the samples was carried out on an INSTRON 3386 testing machine. The distribution of deformations in the near-surface layers of the sample under tension was obtained using an optical measuring system VIC-3D.

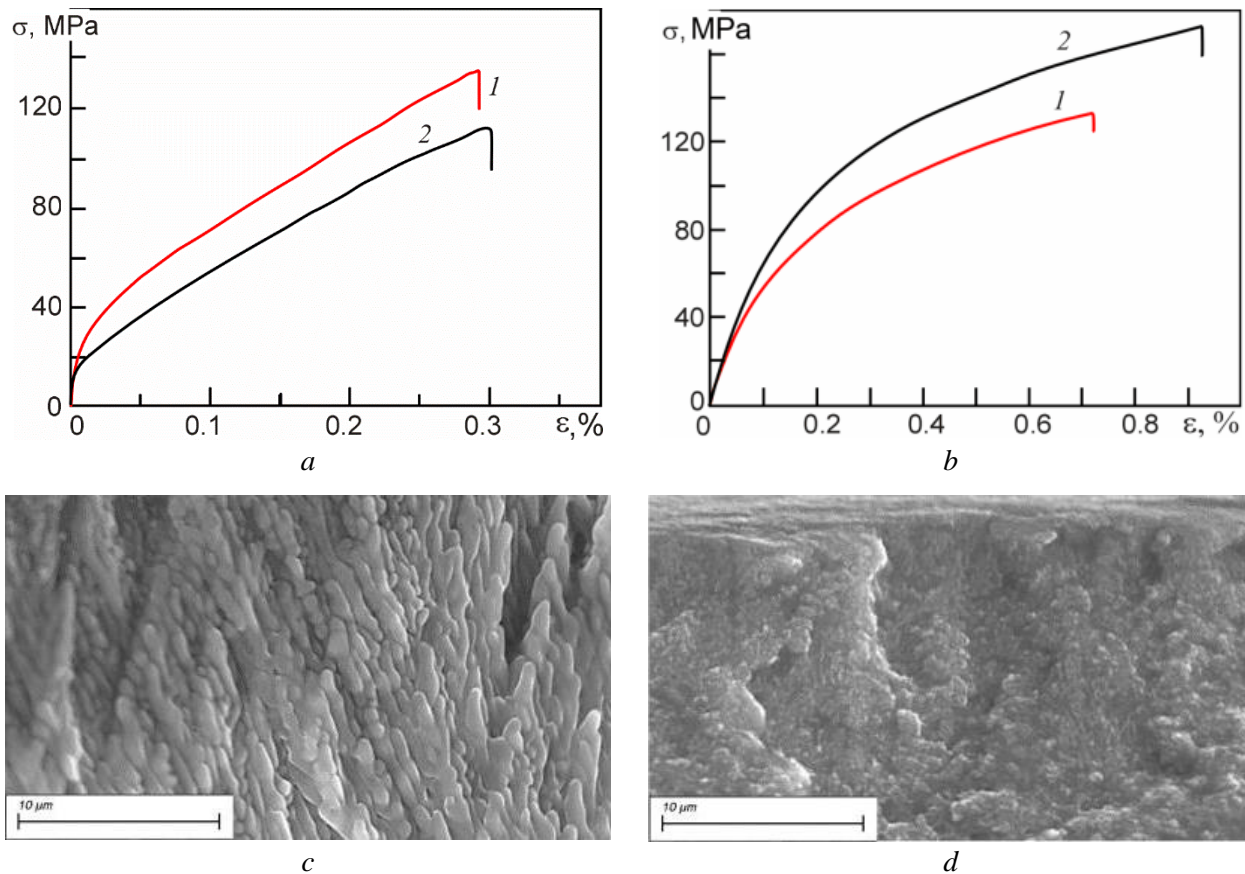


Fig. 1. Diagrams of deformation under uniaxial tension (a, b) and fracture surfaces (c, d) of silumin samples AK5M2 (a, c) and AK10M2N (b, d): 1 - initial state; 2 - irradiated with a pulsed electron beam (50 J/cm², 200 μs , 3 pulses, 0.3 s⁻¹).

Mechanical tests of AK5M2 silumin did not reveal an increase in properties after irradiation of the material with an electron beam (Fig. 1, a). Samples of silumin AK10M2N after irradiation showed an increase in strength and plasticity (Fig. 1, b). The main reason for the low mechanical properties of irradiated silumin AK5M2 is the formation of a columnar structure (Fig. 1, c). In silumin AK10M2N a columnar structure does not form upon irradiation (Fig. 1, d).

* The work was supported by RSF project No. 19-79-10059.

ADHESION STRENGTH OF $Ti_{1-x}C_x$ – DLC MULTILAYER NANOCOMPOSITE THIN FILMS COATED BY ION-PLASMA DEPOSITION ON MARTENSITIC STAINLESS STEEL PRODUCED BY SELECTIVE LASER MELTING FOLLOWED BY PLASMA-NITRIDING AND DIAMOND BURNISHING*

N.V. LEZHININ¹, A.V. MAKAROV¹, V.P. KUZNETSOV², A.B. VLADIMIROV¹, P.A. SKORYNINA³, V.A. SIROSH¹

¹*Institute of Metal Physics, UB, RAS, Yekaterinburg, Russia*

²*Ural Federal University, Yekaterinburg, Russia*

³*Institute of Engineering Science, UB, RAS, Yekaterinburg, Russia*

e-mail: nlezhnin@bk.ru

The multilayer coatings were deposited on a part of PH1 martensitic stainless steel (the chemical composition summarised in Table 1 formed by selective laser melting followed by one of post-processing schemes below:

1. oil quenching from 1040°C followed by tempering at 480°C for 4 hours and air cooling (HT), finishing milling (FM);
2. HT, FM, ion-plasma nitriding at a temperature of 500-540°C, multi-pass diamond burnishing.

Nanocomposite films were obtained by co-deposition of arc sputtered titanium and carbon cathodes. Multilayer coatings consisted of forty pairs of TiC and pure carbon layers 20-25 nm individual thick and a total thickness of about 2 µm. Titanium cathode was sputtered at a constant current of an arc source, and a graphite cathode was sputtered at a pulse transmission frequency ($f = 10$ Hz). Sputtering of carbon at such a pulse frequency made it possible to obtain TiC layers with an content of titanium and carbon of about 20 and 80 atomic percent, respectively.

Table. 1. Chemical composition of PH1 stainless steel.

Chemical element	C	Cr	Ni	Cu	Mn	Si	Mo	Nb	Fe
Content, mass.%	0.05	14.72	4.69	4.08	0.83	0.41	0.13	0.22	other

Scratch testing by indenter with diamond tip of 50 µm in diameter was used to evaluate the adhesion strength of coated films [1]. The normal load during test increased linearly up to 1000 mN.

The coating applied to the substrate treated according to scheme 1 shows the first signs of failure when the load reaches 320 mN. A typical for a hard coating on a ductile substrate, conformal cracking occurs as the coating is bent into the scratch track. Increasing of load leads to a gradual destruction of the coating layer-by-layer until 440 mN, when the moving indenter penetrate into the substrate and a total spallation takes place.

As for substrate treated according to scheme 2, coating failure mechanism changes. No conformal cracking detected, film detaches in buckling mode. Despite this mode still corresponds to hard coating on a ductile substrate, buckling only begins at about 920 mN.

Thus, the presented results indicate that post-processing including plasma-nitriding and multi-pass diamond burnishing of a part formed by additive laser technology increases significantly (up to 3 times) resistance of an ion-plasma deposited thin-film composite coating to contact loads.

The authors are grateful to A.G. Merkushev for his participation in the preparation of the part.

REFERENCES

- [1] N.V. Lezhnin, A.V. Makarov, N.V. Gavrilov, A.L. Osintseva, R.A. Savrai, "Improving the Scratch Test Properties of Plasma-Nitrided Stainless Austenitic Steel by Preliminary Nanostructuring Frictional Treatment", AIP Conference Proceedings, vol. 2053, pp. 40050-40054, 2018.

* The research was supported by RFBR and Sverdlovsk Oblast (project No. 20-48-660065).

Section 3

PLASMA-CHEMICAL, ELECTROPHYSICAL AND LASER TECHNOLOGIES:

environmental applications,
production of nanopowders
and functional materials.

ANALYSIS OF THE SIZE AND MORPHOLOGICAL COMPOSITION OF ABLATED CERIUM DIOXIDE NANOPARTICLES AFTER ULTRASONIC DISPERSION AND CENTRIFUGATION IN AQUATIC MEDIUM

M.A. PUGACHEVSKII, V.A. MAMONTOV, A.Yu. RYZHENKOVA

Southwest State University, Kursk, Russia

e-mail: vladimir-mamontov2013@yandex.ru

Explorations of the physicochemical properties of cerium dioxide nanoparticles are of interest in terms of practical application in a wide range of fields, in particular, biomedical. Nanosized cerium dioxide is capable of exhibiting antioxidant properties [1, 2], for example, ablated cerium dioxide nanoparticles inhibit the highly reactive short-lived hydroxyl radical in the process of oxidative degradation of the organic dye methylene blue by the Fenton reaction type [3]. Antioxidant properties are due to the presence of surface structural defects, such as an oxygen vacancy, and their number depends on the size of nanocrystalline cerium dioxide [4]. The composition distribution of centrifuged cerium dioxide nanoparticles was explored by scanning electron microscopy (see Fig. 1), atomic force microscopy, and X-ray structural analysis.

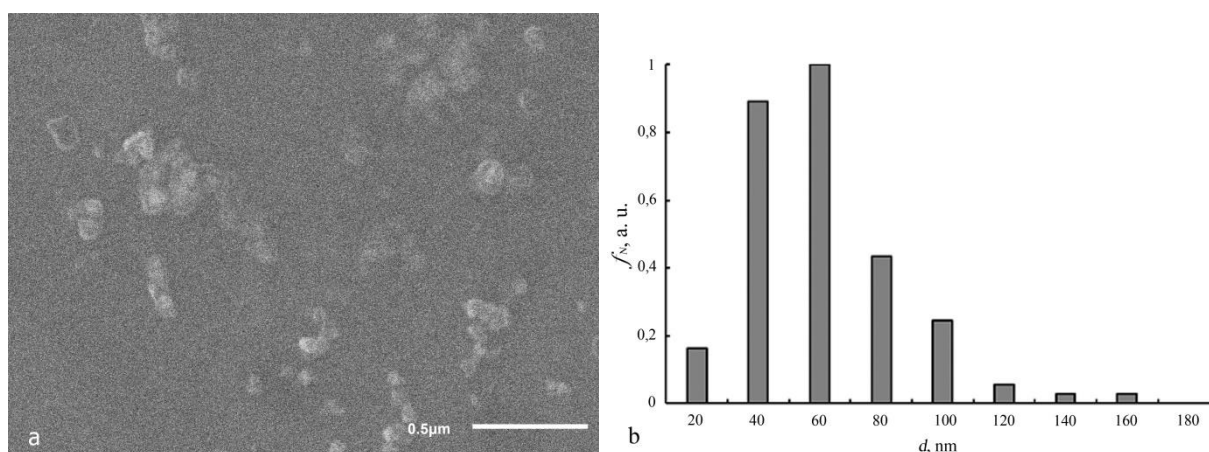


Fig. 1. Ablated cerium dioxide nanoparticles after centrifugation at 10 000 rpm, a - SEM images; b - granulometry.

In this work, the qualitative and quantitative composition of nanodispersed cerium dioxide was investigated under various modes of centrifugation, since, according to experiments on the study of the antioxidant properties of nanoparticles of cerium dioxide, it was revealed that during centrifugation their antioxidant capabilities increase due to an increase of the concentration of effective particles with a smaller size in the solution, despite of decrease of the concentration of cerium dioxide nanoparticles as a whole.

REFERENCES

- [1] A. Filippi, F. Liu, J. Wilson, eds., "Antioxidant activity of cerium dioxide nanoparticles and nanorods in scavenging hydroxyl radicals", RSC Advances, vol. 9, pp. 11077–11081, 2019.
- [2] P. Eriksson, A.A. Tal, A. Skallberget [et al.], "Cerium oxide nanoparticles with antioxidant capabilities and gadolinium integration for MRI contrast enhancement", Sci. Rep, vol. 8(1), pp. 1–12, 2018.
- [3] M.A. Pugachevskii, V.A. Mamontov, A.P. Kuz'menko, Y.A. Neruchev, "Study of antioxidant properties of ablated cerium dioxide nanoparticles in the oxidative reaction of Fenton", Izvestiya Yugo-Zapadnogo gosudarstvennogo universiteta, Series: Engineering and Technologies, vol. 11, no. 1, pp. 62–74, 2021.
- [4] M.A. Pugachevskii, V.A. Mamontov, Ney Vin Aung, A.S. Chekadanov, A.P. Kuz'menko, "Preparation of ablated CeO₂ particles with nanodisperse distribution by composition", Technical Physics Letters, vol. 46, no. 20, pp. 38–41, 2020.

INVESTIGATION OF EFFECTIVENESS OF ANTIMICROBIAL TREATMENT OF POULTRY PRODUCTS BY ELECTROPHYSICAL METHODS

R.A. VAZIROV¹, S.YU. SOKOVNIN^{1,2}, A.S. KRIVONOGOVA³, A.G. ISAEVA⁴

¹*Ural Federal University, Yekaterinburg, Russia*

²*Institute of Electrophysics, UB, RAS, Yekaterinburg, Russia*

³*Ural State Agrarian University Yekaterinburg, Russia*

⁴*Ural Scientific Research Veterinary Institute, Yekaterinburg, Russia*

e-mail: ruslan.vazirov@urfu.ru

Of particular interest in the modern food and agricultural industry is new methods of processing products to increase shelf life and the level of biological safety. Treatment with ionizing radiation (IR) [1], ultraviolet light (UV) [2] and plasma [3] is becoming more and more widespread. These electrophysical methods allow you to process products using low temperatures. Radiation treatment reduces microbiological contamination of products, however, due to the presence of radiation load, the nutritional value of the products decreases. At the same time, UV treatment is ineffective and requires long exposure. In radiobiology, methods of synergistic effect of two factors are widespread, in particular, the combination of IR, UV and plasma treatment.

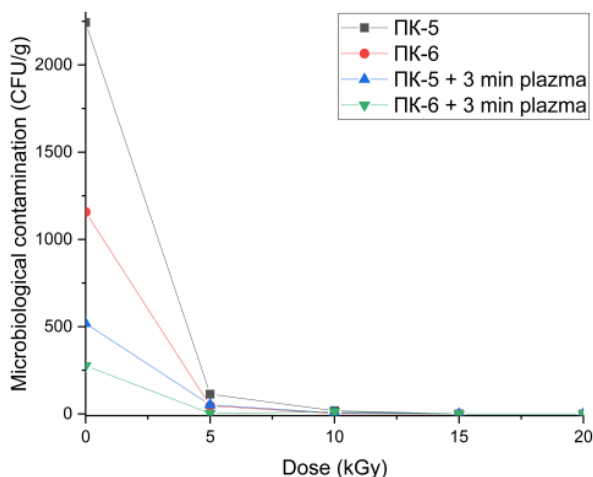


Fig. 1. Dose-effect relationship of microbiological contamination of combined fodders PK-5 and PK-6 with pretreatment of PRVD for GVI-150.

In the present work, in order to investigate the synergistic effect of IR treatment and high pressure gas discharge plasma radiation, combined feed of grade PK-5 and PK-6 was treated. Nanosecond electron beam (NEB) of accelerator URT-0.5 [4] was used as source of IR. High-voltage nanosecond GVI-150 generator [4] was used to create high-pressure nanosecond gas discharge plasma (HP PNGR).

Figure 1 shows the dependence of microbiological contamination of fodders on the amount of absorbed dose of NEB and treatment with HP PNGR radiation. Microbiological studies have shown an increase in the effectiveness of antimicrobial treatment, as a result of the possibility of using a smaller amount of absorbed dose.

There is an increased radio resistance of microorganisms of the genus *Penicillium* spp. и *Candida albicans*. Analysis of physicochemical properties of fodders showed preservation of the main parameters of production within the norm after joint treatment of NEB and HP PNGR radiation.

REFERENCES

- [1] Codex Alimentarius Commission. General Standard for Irradiated Foods CODEX STAN. — Rome: FAO. — 2003. — 22 p.
- [2] Bactericidal effectiveness of modulated UV light / H. L. Bank, J. John, M. K. Schmehl [et al.] // Applied and Environmental Microbiology. — 1990. — V. 56. — № 12. — P. 3888-3889.
- [3] Cold plasma: a novel non-thermal technology for food processing. Food biophysics / R. Thirumdas, C. Sarangapani, Annapure, U. S. — 2015. 10(1). — P. 1-11.
- [4] Sokovnin, S. Yu. Nanosecond electron accelerators for radiation technology / S.Yu. Sokovnin; UB RAS – Ekaterinburg. — 2007 — 225 p.

PREPARATION OF CERIUM (III) FLUORIDE NANOPOWDERS BY PULSED ELECTRON BEAM EVAPORATION IN VACUUM*

V.G. ILVES², S.Yu. SOKOVNIN^{1,2}, M.A. UIMIN^{1,3}

¹Ural Federal University, Yekaterinburg, Russia

²Institute of Electrophysics, UB, RAS, Yekaterinburg, Russia

³M.N. Mikheev Institute of Metal Physics, UB, RAS, Yekaterinburg, Russia

e-mail: ilves@iep.uran.ru

The method of pulsed electron evaporation in vacuum [1] was first used to obtain nanopowder (NP) CeF₃. When producing NP were observed a high evaporation rate of the target (~ 7 g/h) and a higher percentage of NP collection (> 72%), both for fluoride and the previously obtained CeO₂ oxide [2]. The main physicochemical characteristics of NP were studied: structure, porosity, thermal resistance, magnetic, luminescent and optical properties.

Was found, that the produced NP contains two crystalline phases: hexagonal CeF₃ (95 wt.%, CSR ≈ 8 nm) and [Ce-O-F] or [Ce-F]. The last phase is obtained only at a high temperature, which is characteristic for the used NP synthesis method.

The magnetic susceptibility of nanoparticles CeF₃ coincides with the susceptibility of micron particles, indicating the potential for using such nanoparticles as a contrast agent for tomography.

High specific surface area (CeO₂ - 270 m²/g, CeF₃ - 62 m²/g, large pore volume (0.35-0.11 cm³/g) allow to use NP as nanocontainers for drug delivery.

Good dispersibility, high sedimentation stability of both materials in different liquid media is established. Both materials showed excellent photocatalytic properties when exposed to visible light.

The obtained NP represents good matrices for creation of promising apconversion materials for medicine based on them, as indicated by recent studies of toxicity of fluoride [3] and cerium [4].



Fig. 1. the target from CeF₃ before (left) after evaporation (right).

REFERENCES

- [1] S.Yu. Sokovnin, V. Il'ves // Production of nanopowders using pulsed electron beam / *Ferroelectrics*, V. 436(1), p. 101-107.
- [2] V.G. Ilves, S.Y. Sokovnin // Production and studies of properties of nanopowders on the basis of CeO₂ / *Nanotechnologies in Russia*, vol. 7, pp. 213-226, 2012.
- [3] A.B. Shcherbakov, N.M. Zholobak, A.E. Baranchikov, A.V. Ryabova, V.K. Ivanov // Cerium fluoride nanoparticles protect cells against oxidative stress / *Materials Science and Engineering C*, vol. 50, pp.151-159, 2015.
- [4] N.M. Zholobak, A.B. Shcherbakov, O.S. Ivanova, V. Reukov, A.E. Baranchikov, V.K. Ivanov // Nanoceria-curcumin conjugate: Synthesis and selective cytotoxicity against cancer cells under oxidative / *Journal of Photochemistry and Photobiology B: Biology*, vol. 209, 111921, 2020.

* The work was supported by the RFBR and GACR Grants Nos. 20-58-26002.

PRODUCTION OF IRON OXIDE NANOPOWDERS BY RADIATION-CHEMICAL METHOD*

M.E. BALEZIN², S.YU. SOKOVNIN^{1,2}, M.A. UIMIN^{1,3}

¹Ural Federal University, Yekaterinburg, Russia

²Institute of Electrophysics, UB, RAS, Yekaterinburg, Russia

³M.N. Mikheev Institute of Metal Physics, UB, RAS, Yekaterinburg, Russia

e-mail: mk@iep.uran.ru

Radiation-chemical method [1] was used to obtain nanopowders (NP) of iron oxide. Irradiation of the iron cuprous solution (0.6 g FeSO₄ + 100 ml H₂O) was carried out on the accelerator URT-0.5 [2]. The absorbed dose from 41.5 to 2316 kGy was gained at different repetition rate of the accelerator - 3, 10 and 30 pps.

Were studied the main physical and chemical characteristics of NP: structure, porosity, thermal resistance and magnetic properties. The specific surface area of the NP was calculated from the isotherm of low-temperature sorption of nitrogen vapors and reached 12.5 m²/g. The pore volume was 0.06 cm³/g and the average pore size was 16.5 nm. According to the RFA, the NP is single-phase, maghemite C, γ -Fe_{21.33}O₃₂, the lattice is cubic ($a \approx 8.40 (\pm 0.57)$), CSR ≈ 2.3 nm.

By irradiating an iron nitrate solution (0.6 g Fe(NO₃)₃ + 100 ml isopropyl alcohol) under the same conditions were obtained amorphous particles with a specific surface area up to 185.7 m²/g.

The magnetic susceptibility of the NP depends on the composition of the irradiated solution. For NPs derived from iron nitrate in isopropyl alcohol, it has a reverse slope.

The produced NPs are good matrices for building on them promising upconversion materials for medicine.

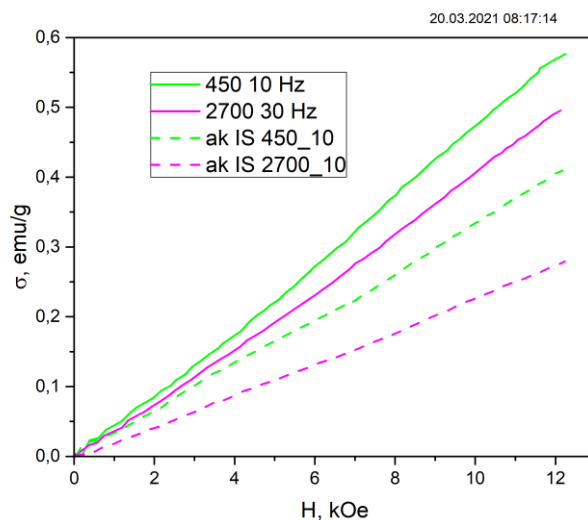


Fig. 1. Magnetic susceptibility of NP FeO in various production modes.

REFERENCES

- [1] S.Yu. Sokovnin, M. Balezin, "Production of nanopowders using nanosecond electron beam," *Ferroelectrics*, vol. 436, 01, pp. 108–111, 2012. DOI:10.1080/10584587.2012.731330.
- [2] S.Y. Sokovnin, M.E. Balezin, "Improving the Operating Characteristics of an URT-0.5 Accelerator," *Instrum Exp Tech*, vol. 48, pp. 392–396, 2005. <https://doi.org/10.1007/s10786-005-0068-0>.

* The work was supported by the RFBR and GACR Grants Nos. 20-58-26002.

INVESTIGATION OF BIOLOGICAL ACTIVITY OF NANOPOWDER DOPED WITH SILVER*

O.A. SVETLOVA^{1,2}, V.G. ILVES², M.V. ULITKO¹, S.YU. SOKOVNIN^{1,2}, T.R. SULTANOVA¹

¹*Ural Federal University, Yekaterinburg, Russia*

²*Institute of Electrophysics, UB, RAS, Yekaterinburg, Russia*

e-mail: olma_20@mail.ru

The silver coated bismuth oxide nanopowder is an interesting compound for using in the field of medicine due to its properties [1]. Mesoporous amorphous crystal NP Bi₂O₃ containing 1 and 5 wt% silver in the evaporable target was obtained by PEBE in vacuum [2].

The cytotoxic properties of oxide nanomaterials doped with silver were tested by assessing the safety of nanomaterials in model systems containing cultures of microorganisms. Studies were conducted at three concentrations (K): 1, 5 and 10 µg/ml.

It was revealed that all samples of NP Bi₂O₃ have cytotoxic effect on cells of tumoral and not tumoral origin. At the same time, an increase in the annealing temperature and the presence of silver amplify the cytotoxic effect of NP, both individually and jointly. At concentrations of 5 and 10 µg/ml, tumor cell viability is reduced by 25-40% compared to control. In the case of not tumoral cells, a 30-65% reduction in viability was observed at all concentrations (1, 5, 10 µg/ml) compared to the control.

REFERENCES

- [1] O.A. Malova, V.G. Ilves, S.YU. Sokovnin, «Investigation of photocatalytic activity nanopowders of bismuth oxide doped with silver by pulsed electron beam evaporation in vacuum», Abstract.
- [2] V.G. Ilves, S.YU. Sokovnin, M.A. Uimin, «Production of nanopowders of bismuth oxide doped with silver by pulsed electron beam evaporation in vacuum», Abstract.

* The work was supported by the RFBR and GACR Grants Nos. 20-58-26002.

MORPHOLOGY HIGHLY DISPERSED SiO₂ OBTAINED IN THERMAL PLASMA ENVIRONMENT*

V.V. SHEKHOVTSOV, O.G. VOLOKITIN, N.K. SKRIPNIKOVA, R.YU. BAKSHANSKIY

Tomsk State University of Architecture and Building, TSUAB, Tomsk, Russia

e-mail: shehovcov2010@yandex.ru

In connection with the constantly growing industry demand for various nanomaterials, various methods of their preparation are carried out [1-3]. In this article, experimentally, the possibility of obtaining nanopowder of SiO₂ particles from enriched natural silicon dioxide (quartz sand) in a plasma reactor is shown. Experimental studies were carried out in the "Plasma Technologies" laboratory of the Tomsk State University of Architecture and Building. The process of operation of an electroplasma installation is described in [4, 5] on the production of silicate melts from refractory oxide materials. The peculiarities of the operation of the installation when receiving nanopowder SiO₂ include: type and consumption of plasma-forming gas - nitrogen, 1 g/s, respectively; the diameter of the outlet section of the plasma torch nozzle is 10 mm.

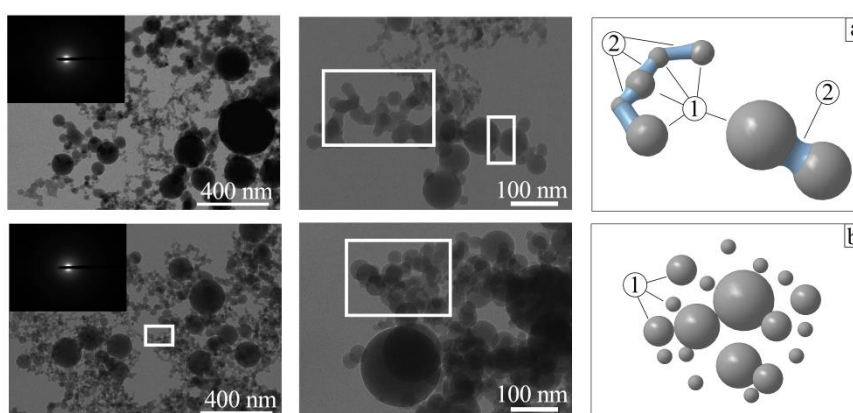


Fig. 1. Shape and size of synthesized SiO₂ powder particles: *a* – initial state; *b* – after thermal treatment at 1173 K.

According to the results of the BET analysis, the specific surface area of the obtained nanopowder is 68 ± 3 m²/g, in comparison with that of the calcined sample at temperature ($T_{\text{cal}}=1173$ K) of 163 ± 4 m²/g. Based on the results obtained, the following model representations of changes in the morphology of SiO₂ nanopowder can be presented:

-upon condensation of the gas phase into solid-phase particles, coalescence processes are developed, which make it possible to obtain polydisperse objects (Fig. 1, a). In the process of deposition of molecules on the cooled contact surface, deceleration and agglomeration of Si-O-Si bonds are carried out, there are no bright pronounced condensation nuclei. Under these conditions, the formed objects are prone to film condensation, where the growth of particles will be proportional to the rate of diffusion of the gas phase.

-repeated thermal exposure to T_{cal} leads to rupture of amorphous Si-O bonds in the solid. According to this model (Fig. 1, b), with an increase in temperature, a nonstoichiometric region is formed, in which broken bonds make it possible to group individual SiO₂ nanoclusters. It is also worth noting that repeated uniform heating / cooling allows initiating the crystallization process.

REFERENCES

- [1] C. Ojalvo, V. Zamora, R. Moreno, F. Guiberteau, and A. L.Ortiz, "Transient liquid-phase assisted spark-plasma sintering and dry sliding wear of B₄C ceramics fabricated from B₄C nanopowders," *J. Eur. Ceram. Soc.*, vol. 41, no. 3, pp. 1869–1877, Mar. 2021.
- [2] O. A. Hammadi, "Effects of extraction parameters on particle size of titanium dioxide nanopowders prepared by physical vapor deposition technique," *Plasmonics*, vol. 15, no. 6, pp. 1747–1754, Jun. 2020.
- [3] E. G. Kalinina, "Features of the electrophoretic formation of bulk compacts based on zirconium oxide nanopowder," *Russ. J. Phys. Chem.*, vol. 94, no. 10, pp. 2096–2102, Oct. 2020.
- [4] V. A. Vlasov, O. G. Volokitin, G. G. Volokitin, N. K. Skripnikova, and V. V. Shekhovtsov, "Calculation of the melting process of a quartz particle under low-temperature plasma conditions," *JEPT*, vol. 89, no. 1, pp. 152–156, Feb. 2016.
- [5] O. G. Volokitin and V. V. Shekhovtsov, "Prospects of application of low-temperature plasma in construction and architecture," *Glass Phys. Chem.*, vol. 44, no. 3, pp. 251–253, May 2018.

* This work was financially supported by Grant N 20-79-10102 from the Russian Science Foundation.

APPLICATION OF A NANOSECOND CORONA DISCHARGE GENERATOR FOR ELECTRICAL SEPARATION OF ORES

S.R. KORZHENEVSKIY, A.A. KOMARSKIY, A.V. PONOMAREV, A.S. CHEPUSOV, O.D. KRASNIY

*Institute of Electrophysics, UB, RAS, Yekaterinburg, Russia
e-mail: olegredman@gmail.com*

The paper proposes a new approach to the creation of drum electric corona separators for dry dressing of ores [1, 2]. The solution makes it possible to increase the specific productivity of concentration plants by 3-5 times. This is important for large-scale dressing of ferrous, non-ferrous, noble metal ores and for separation of biological mixtures and secondary resources. The nanosecond duration of corona discharge generation increases the strength of the interelectrode gap in comparison with the generation of corona discharge at constant voltage.

An increase in the electric strength of the interelectrode gap makes it possible to multiply the strength of the electric field in the area of a corona discharge. This leads to an increase in the mobility of ions [3] and increases the rate of transfer of charged particles from the active zone of the corona discharge to the collecting electrode. An increase in the specific power of the flow of charged particles makes it possible to reduce the time spent by the material in the corona discharge field, to increase the speed of movement of the ore, and to raise the upper limit of the particle size to be separated.

REFERENCES

- [1] I.P. Vereshchagin, "High voltage electrical technologies," Moscow, MPEI, 1999.
- [2] H.F. Olofinsky, "Electric enrichment methods," Moscow, 1977.
- [3] I.P. Vereshchagin, V.I. Levitov, G.Z. Mirzabekyan, M.M. Pashin, "Foundations of electrogasdynamics of dispersed systems," p. 480, Moscow: Energiya, 1974.

MECHANICAL PROPERTIES AND COMPOSITION OF TiSiCN COATINGS OBTAINED BY DECOMPOSITION OF HEXAMETHYLDISILAZANE AND ANODIC EVAPORATION OF TITANIUM IN A LOW PRESSURE ARC DISCHARGE*

A.I. MEN'SHAKOV^{1,2}, YU.A. BRYUHANOVA¹, I.S. ZHIDKOV², P.A. SKORYNINA³

¹ *Institute of Electrophysics UB RAS, Yekaterinburg, Russia*

² *Ural Federal University named after the first President of Russia B.N.Yeltsin, Yekaterinburg, Russia*

³ *Institute of Engineering Science UB RAS, Yekaterinburg, Russia*

e-mail: aim@iep.uran.ru

Method of deposition of TiSiCN-coatings by anodic evaporation of Ti and decomposition of organosilicon precursor (hexamethyldisilazane, HMDS) in nitrogen-argon low-pressure (~1 mTorr) hollow cathode arc discharge was investigated. On the samples made of stainless steel TiSiCN-coatings up to 6 μm thick with hardness up to 31 GPa were obtained in 1 hour. Coatings composition was analyzed by XPS method. The influence of discharge current (10-50 A), HMDS flow (1-10 g/h), N₂ flow (0-10 sccm) and Ti-vapors flow on the hardness and wear resistance of the resulting coatings was investigated.

* The study was financially supported by the Russian Science Fund, grant No. 20-79-10059.

SYNTHESIS OF METASTABLE CUBIC TUNGSTEN CARBIDE WITH A HIGH PURITY IN DISPERSED AND BULK FORMS BY THE PLASMA DYNAMIC METHOD *

A.A. SIVKOV^{1,2}, I.I. SHANENKOV^{1,2}, D.S. NIKITIN², A. NASSYRBAYEV²

¹Jilin University, Changchun, China

²Tomsk Polytechnic University, Tomsk, Russia

e-mail: shanenkovi@tpu.ru

Metastable compounds of various materials can potentially be of a great scientific interest, but their preparation is often associated with many nuances that impose serious restrictions on the synthesis procedure. These compounds include cubic tungsten carbide WC_{1-x} , which is supposed to be a highly active electrocatalyst [1, 2], but the synthesis of which is possible only in an extremely narrow temperature range (from 2798 K to 3033 K [3]). In addition, to stabilize this compound under normal conditions, it is necessary to achieve a high cooling rate when being crystallized from the melt (more than 10^7 K/s) in order to avoid phase transitions into hexagonal modifications of tungsten carbide [4]. All this imposes serious restrictions on the existing synthesis methods, as well as on studying the potential applications of this metastable phase.

By using the method of plasma dynamic synthesis [5], based on the generation, acceleration and sputtering of an electric-discharge tungsten-carbon plasma in an inert gas (argon) at normal pressure and temperature, cubic tungsten carbide with a yield of at least 98 wt.%, both in dispersed and bulk forms can be successfully obtained. The electric-discharge plasma was generated using a pulsed (less than 10^{-3} s) high-current (more than 10^5 A) high-voltage coaxial magnetoplasma accelerator of the erosion type with a graphite electrode system. A mixture of the initial reagents containing tungsten and carbon was placed into the plasma formation zone. After converting to the plasma state, accelerating and sputtering under ultrafast cooling conditions (more than 10^8 K/s), the necessary crystalline phase WC_{1-x} was formed. By changing the configuration of the plasma flow (into free space or onto a substrate), it was possible to obtain compounds based on cubic tungsten carbide, both in the form of a nanodispersed powder and in the form of a bulk coating with a thickness of up to several tens of micrometers.

Within the framework of exploratory studies, the influence of the system energy parameters, the ways of initiating an arc discharge, the precursors ratio on the phase composition and particle size distribution was studied. Various properties of the obtained materials were also analyzed, which made it possible to detect the high hardness of WC_{1-x} phase, its increased (in comparison with the hexagonal phases WC and W_2C) corrosion resistance, high catalytic activity after being slightly modified with platinum-containing nitrate ($Pt(NO_3)_2$).

Thus, within the framework of the study, the scientific and technical foundations of the plasma dynamic method for producing cubic tungsten carbide were developed, which make it possible to synthesize a unique metastable phase WC_{1-x} both in dispersed and bulk forms with a yield of at least 98 wt. %, and also obtained samples of nanodispersed powders and coatings, with the use of which complex studies of various application fields were carried out.

REFERENCES

- [1] D.V. Suetin, I.R. Shein, A.L. Ivanovskii, "Structural, electronic properties and stability of tungsten mono- and semi-carbides: A first principles investigation" // *Journal of Physics and Chemistry of Solids*, vol. 70, no. 1, pp. 64-71, 2009.
- [2] I. Shanenkov, A. Ivashutenko, Yu. Shanenkova, D. Nikitin, Y. Zhu, J. Li, W. Han, A. Sivkov, "Composite material $WC_{1-x}@C$ as a noble-metal-economic material for hydrogen evolution reaction" // *Journal of Alloys and Compounds*, vol. 834, p. 155116, 2020.
- [3] A.S. Kurlov, A.I. Gusev, "Phase equilibria in the W-C system and tungsten carbides" // *Russian Chemical Reviews*, vol. 75, no. 7, pp. 617-636, 2006.
- [4] F.G. Zhang, X.P. Zhu, M.K. Lei, "Microstructural evolution and its correlation with hardening of WC-Ni cemented carbides irradiated by high-intensity pulsed ion beam" // *Surface and Coatings Technology*, vol. 206, no. 19-20, pp. 4146-4155, 2012.
- [5] A.A. Sivkov, I.I. Shanenkov, Yu.L. Shanenkova, D.S. Nikitin, A.S. Ivashutenko, "Method for producing nanocrystalline cubic tungsten carbide" // *Russian Federation Patent No. 2730461 C1*, dated on 24.08.2020.

* The work was supported by the Russian Science Foundation (Grant No. 19-13-0020).

INFLUENCE OF THE SUPPLIED ENERGY ON THE PHASE CONTENT OF CRYSTALLINE DISPERSED TITANIUM DIOXIDE OBTAINED BY THE PLASMA DYNAMIC METHOD *

A.A. SIVKOV^{1,2}, Y.N. VYMPINA², I.A. RAKHMATULLIN², A.S. IVASHUTENKO², Y.L. SHANENKOVA²

¹College of Communication Engineering, Jilin University, Changchun, China

²School of Energy & Power Engineering, Tomsk Polytechnic University, Tomsk, Russia

e-mail: ynp2@tpu.ru

Through the direct use of sunlight, photocatalysis has become widely studied in recent years as a way to prevent further environmental pollution. The most famous photocatalyst is titanium dioxide (TiO₂) due to its high catalytic activity, chemical stability and low cost [1-4]. Unfortunately, there are two main restrictions on the use of titanium dioxide as a photocatalyst: the band gap, which makes it possible to use TiO₂ only in the ultraviolet region of the spectrum, and the high rate of recombination of electron-hole charge carriers [5].

In this regard, at present, many scientists are dealing with issues related to increasing the photocatalytic activity of titanium dioxide. Obviously, the properties of TiO₂ directly depend on the synthesis method. The synthesis of dispersed titanium dioxide by the plasma dynamic method is proposed in papers [6-7]. One of the parameters of the system, which primarily affect the phase content of the synthesized material and, as a consequence, its properties, is the amount of released energy. In this regard, we investigated the effect of this parameter on the phase content of the powder material in this work.

The paper shows the results of studying the value of released energy of the accelerator on the phase content of nanocrystalline titanium dioxide. It was found that the main crystalline phases are two modifications of TiO₂: anatase and rutile with a tetragonal system. It was revealed that the product can be synthesized with anatase content up to 80%. This factor is expected to have a positive effect on optical, semiconducting properties and, as a consequence, photocatalytic properties.

REFERENCES

- [1] I. Chung, B. Lee, J. He, R.P.H. Chang and M.G. Kanatzidis, "All-solid-state dye-sensitized solar cells with high efficiency," *Nat.*, vol. 485, No. 7399, pp. 486–489, 2012.
- [2] M. Tasbihi, K. Kočí, M. Edelmannová, I. Troppová, M. Reli and R. Schomäcke, "Pt/TiO₂ photocatalysts deposited on commercial support for photocatalytic reduction of CO₂," *J. Photochem. Photobiol. A: Chem.*, vol. 366, pp. 72–80, 2012.
- [3] L. Tian, L. Xing, X. Shen, Q. Li, S. Ge, B. Liu and L. Jie, "Visible light enhanced Fe–I–TiO₂ photocatalysts for the degradation of gaseous benzene" *Atmos. Pollut. Res.*, vol. 11, No. 1, pp. 179–185, 2020.
- [4] N. Sharotri, D. Sharma and D. Sud, "Experimental and theoretical investigations of Mn-N-co-doped TiO₂ photocatalyst for visible light induced degradation of organic pollutants" *J. Mater. Res. Tech.*, vol. 8, No. 5, pp. 3995–4009, 2019.
- [5] N.A. Jumat, P.S. Wai, J.J. Ching and W.J. Basirun, "Synthesis of polyaniline-TiO₂ nanocomposites and their application in photocatalytic degradation," *Polym. Polym. Compos.*, vol. 25, No. 7, pp. 507–514, 2017.
- [6] A.A. Sivkov, A.S. Ivashutenko, I.A. Rakhmatullin, Y.L. Shanenkova and Y.N. Vympina, "Possibility of obtaining TiO₂ material by plasma dynamic method into an air atmosphere," *J. Physics: Conference Series*, vol. 1, pp. 012136, 2019.
- [7] A.A. Sivkov, Yu.N. Vympina, I.A. Rakhmatullin, A.S. Ivashutenko and Yu.L. Shanenkova, "The possibility of obtaining materials by plasma dynamic synthesis in the Ti-O system," *IOP Conference Series: Mater. Sci. Eng.*, vol. 1019, No. 1, pp. 012094, 2021.

* Acknowledgments: The reported study was funded by RFBR, project number 20-33-90060.

SIALON SYNTHESIZED BY DC ARC PLASMA *

V.A. VLASOV¹, A.A. KLOPOTOV^{1,2}, K.A. BEZUKHOV¹, Yu.A. ABZAEV¹, N.N. GOLOBOKOV³, G.G. VOLOKITIN¹,
V.V. SHEKHOVTSOV¹, N.A. TSVETKOV¹

¹Tomsky State University of Architecture and Building, Tomsk, Russia

²National Research Tomsk State University, Tomsk, Russia

³Tomsk branch of the Institute of structural Macrokinetics, SB, RAS, Tomsk, Russia

e-mail: bezuhov_k@mail.ru

A promising area of research in the field of creating structural materials using SiAlON is the use of technology based on the energy of low-temperature plasma. Two types of SiAlON α and β phases are known in the literature. They are of great practical interest as structural ceramics. β -sialon is a compound with a wide area of homogeneity and is described by the formula $\text{Si}_{6-z}\text{Al}_z\text{O}_z\text{N}_{8-z}$ ($1 \leq z \leq 4.2$). This compound is isostructural to a two-component compound β - Si_3N_4 . α -SiAlON is a compound that already contains four formula units β - Si_3N_4 , and is described by the formula $\text{Me}_m\text{Si}_{12-(m+z)}\text{Al}_z\text{O}_z\text{N}_{16-z}$ (Me metal ion). It is known that the phase transition between the two types of SiAlON satisfies the conditions [1]: α -sialon + $\text{O}_2 \rightarrow \beta$ -sialon и β -sialon + $\text{N}_2 \rightarrow \alpha$ -sialon. The physical and mechanical properties of these two types of SiAlON are significantly different. Therefore, it is of interest from a fundamental and practical point of view to study the process of SiAlON synthesis using the action of low-temperature plasma.

The aim of this work was to study the features of the synthesis of SiAlON, carried out by the influence of the energy of a low-temperature plasma in a nitrogen atmosphere. The raw materials used were: β - Si_3N_4 , AlN, H_2NCoNH_2 (urea solution) and the binder - liquid glass.

Samples prepared for exposure to plasma were placed in an oven and sintered at 400°C for 30 minutes.

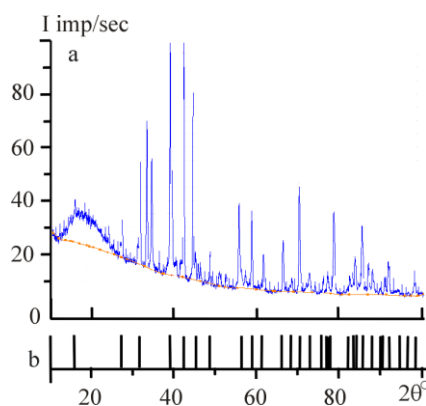


Fig. 1. Diffraction pattern of a sample recorded in $\text{CoK}\alpha$ radiation, synthesized using plasma energy (a). Sialon connection bar chart AlN_7OSi_5 (b)

The high-temperature effect on the sample was carried out in a plasma jet obtained in a plasma generator of the VPR-410 NPP type [2], supply voltage 380 V; nominal arc operating voltage 140 V; rated working current 220 A. Plasmatron power $P = 30$ kW and specific heat flux $q = 2.3 \times 10^6$ W/m². Plasma-forming gas – nitrogen with 14 l/min flow rate. Based on the results of colorimetry, the specific mass-average enthalpy Hg of the plasma jet was determined. Average mass temperature $T = 6100 \div 7300$ K. As a result of exposure to high-temperature plasma, the sample underwent sintering and melted along the contour. After plasma exposure, the sample was cooled to room temperature and then mechanically crushed for X-ray analysis and microscopy. The result of X-ray diffraction analysis showed the presence of the Si_5AlON_7 phase ($z=1$) (space group $P6_3$). This is reflected in the obtained diffractograms from the synthesized samples (Fig. 1). In addition to the crystalline phases, the diffraction patterns show a halo related to the X-ray amorphous phase.

REFERENCES

- [1] Lewis M.H., Bhatti A.R., Lumby R.J., North B.J., *Mare Sci.*, vol. 15, pp. 103-113, 1980.
- [2] Vlasov V.A., Volokitin G.G., Skripnikova N.K., Volokitin O.G., *Key Engineering Materials*, vol. 781, pp. 143-148, 2018.

* This work was supported by the state assignment of the Ministry of Science and Higher Education of the Russian Federation (project number FEMN-2020-0004).

EFFECT OF PULSED SOFT X-RAY RADIATION ON THE SURFACE TOPOGRAPHY OF SOME METALS*

A.E. LIGACHEV¹, M.V. ZHIDKOV², S.A. SOROKIN³, G.V. POTEKIN⁵, YU.R. KOLOBOV⁴

¹Prokhorov Institute of General Physics, RAS, Moscow, Russia

²Belgorod State National Research University, Belgorod, Russia

³Institute of High Current Electronics of Siberia Branch, RAS, Tomsk, Russia

⁴Institute of Problems of Chemical Physics, RAS, Chernogolovka, Russia

⁵Tomsk Polytechnic University, Tomsk, Russia

e-mail: carbin@yandex.ru

Effect of the pulsed soft X-ray fluxes on the surface topography of metals (Mg, Ti, Cr and Cu) has been investigated.

Soft pulse X-ray irradiation (energy quanta of 0.1-1.0 keV) were carried out on a high-current MIG generator. The sample of magnesium was located at a distance of 10 cm from the X-ray source. Since the distance to the sample significantly exceeded the size of the x-ray beam, it can be assumed that the density of the X-ray radiation flow to the magnesium sample was uniform. The duration of the radiation pulse was 100 ns, and the radiation energy density in the pulse varied from 13 to 19 J/cm².

As a result of melting and subsequent fast solidification, a wavy relief is formed on the surface of all metals after a single X-ray pulse.

Also of crater-like defects was observed on the irradiated surface. Small cracks are formed on the surface of magnesium due to the high cooling rate of the molten metal after exposure to pulsed X-rays.

* The work was supported by Program 11 of Russian Academy of Science.

STUDY OF METHANE STEAM REFORMING IN THE PLASMA OF A NANOSECOND SURFACE GAS DISCHARGE

I.E. FILATOV, D.L. KUZNETSOV, V.V. UVARIN

Institute of Electrophysics, UB, RAS, Yekaterinburg, Russia

e-mail: fil@iep.uran.ru

Steam reforming of methane ($\text{CH}_4 + \text{H}_2\text{O} \rightarrow \text{CO} + 3\text{H}_2$) is one of the main methane conversion reactions, along with the reactions of carbon dioxide (dry) reforming ($\text{CH}_4 + \text{CO}_2 \rightarrow 2\text{CO} + 2\text{H}_2$) and partial oxidation. In traditional methane processing technologies, complex chemical installations are used; high temperatures and pressures of the environment are required.

The developing gas-discharge methods of methane conversion are aimed at increasing the efficiency and reducing the capital costs. Typically, plasma-chemical studies of steam reforming use reactors based on arc and microwave discharges [1].

In this work, a powerful nanosecond discharge is used to create a plasma over the surface of water, which is one of the reacting substances. The use of such a discharge provides both a high excitation power and a high concentration of reactants.

The discharge power source is a high-voltage pulse generator with an output voltage of up to 100 kV, a pulse duration of 15 ns, and a pulse repetition rate of up to 50 Hz. The conversion reaction takes place in a 10^3 ml cylindrical chamber partially filled with water. The maximum methane pressure in the chamber is 5 atm. The discharge was carried out along the surface of the water between the central electrode partially placed in the water and the walls of the chamber. A spark or diffuse discharge was realized at different methane pressures, interelectrode gaps, and shapes of the central electrode.

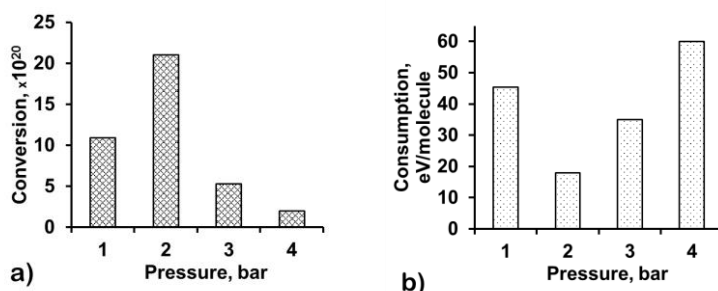


Fig. 1. Methane conversion (a) and specific energy consumption (b) at different pressures. 1.2×10^4 pulses with a duration of 15 ns.

The main determined characteristics were the conversion value and specific energy consumption under various discharge conditions (gas pressures, polarity, medium temperatures, interelectrode gaps, electrode shapes, etc.). In this work, the optimal conditions for steam conversion are determined and the data obtained are compared with the results of experiments on carbon dioxide conversion under similar discharge conditions [2]. For example, it has been shown that for a spark discharge from a blade cathode, the optimal methane pressure is approximately 2 bar, whereas the specific energy consumption is 20 eV/molecule (Fig. 1). As in the case of carbon dioxide reforming, an increase in pressure decreases the degree of methane conversion and increases energy consumption.

REFERENCES

- [1] Y.F. Wang, C.H. Tsai, W.Y. Chang, Y.M. Kuo, "Methane steam reforming for producing hydrogen in an atmospheric-pressure microwave plasma reactor", *Int J Hydrogen Energy*, vol. 35, no. 1, pp. 135-140, 2010.
- [2] I.E. Filatov, D.L. Kuznetsov, V.V. Uvarin, "Effect of gas pressure and pulse duration on dry reforming of methane in nanosecond spark discharge", *J. Phys. Conf. Ser.*, vol. 1393, 012081, 2019.

INVESTIGATION OF THE RELATIVE REACTIVITY OF VOLATILE ORGANIC COMPOUNDS IN THE AIR PLASMA OF A PULSED CORONA DISCHARGE BY THE METHOD OF COMPETING REACTIONS*

I.E. FILATOV, V.V. UVARIN, D.L. KUZNETSOV

Institute of Electrophysics, UB, RAS, Yekaterinburg, Russia

e-mail: fil@iep.ura.ru

Volatile organic compounds (VOCs) are important components of industrial emissions. One of the promising methods of air purification from VOCs vapors is plasma-chemical methods based on the treatment of air flows with non-equilibrium plasma discharges of various types [1]. To study such processes, the method of model mixtures is proposed [3]. Using multiple compounds instead of one allows you to calculate the parameters of the relative reactivity of compounds with high precision. These values are best suited for comparing the energy efficiency parameters of various methods using gas-discharge plasma and for bringing processes from laboratory up to industrial scale. The essence of the approach is to represent the process of removing impurities X_i (where i is the component number) by a system of equations of material and energy balance:

$$\begin{cases} \frac{d[X_i]}{dE} = -k_i[X_i][R] \\ \frac{d[R]}{dE} = G_R - \sum_{i=1}^N k_i[X_i][R] - k_d R \end{cases}, \quad (1)$$

where $[R]$ is the concentration of the formal reagent R , k_i – is the constants characterizing the reactivity of the impurity, N is the number of components, G_R – is the plasma chemical yield of the reagent R . E (J/l) – is energy input per unit volume of gas (specific energy). To estimate the values of the constants k_i , the experimental points of the dependences $[X_i]$ on E are used.

Due to the specifics of analytical methods, the absolute values of k_i , are difficult to calculate, but the relations of these constants to each other can be measured with high accuracy, which allows us to make a method of competing reactions [4]. As a measure of the efficiency of using the discharge energy, the concept of the plasma chemical yield G_R of the formal reagent R is used as a set of plasma components involved in the VOCs removal processes, while it is assumed that the formal reagent represents several different conversion mechanisms: $R = \sum_{j=1}^M R_j$, where M is the number of allocated processes. The formal reagent R can be apply to remove components, as shown in the lower part of the system of equations (1). Part of it is deactivated as a result of reactions with the walls of the plasma chemical reactor, side processes, etc. with the constant k_d . Thus, the task of optimizing air purification methods is both to increase the yield of the formal reagent G_R , and to increase the degree of its use (reducing the value of k_d).

Using the example of compounds of different classes, it is shown that the main active plasma particles participate with VOCs at different rates, which allowed us to distinguish several classes of functional compounds: 1. Widely used solvents, 2. Unsaturated compounds, 3. Halogenated unsaturated and other halogen-containing compounds.

REFERENCES

- [1] J. Schnelle, R. Dunn, M. Ternes, R.F. Dunn, and M.E. Ternes. Air Pollution Control Technology Handbook, Second Edition. CRC Press, 2015.
- [2] A.M. Vandenbroucke, R. Morent, N. De Geyter, and C. Leys. "Non-thermal plasmas for non-catalytic and catalytic VOC abatement", J. Hazard. Mater., vol. 195, pp. 30-54, 2011.
- [3] I.E. Filatov, V.V. Uvarin, and D.L. Kuznetsov. "Estimation of qualitative and quantitative parameters of air cleaning by a pulsed corona discharge using multicomponent standard mixtures", Technical Physics, vol. 63, pp. 680-688, 2019.
- [4] I.E. Filatov, V.V. Uvarin, and D.L. Kuznetsov. "The use of competitive reactions for studying the process of unsaturated organic compound vapor removal from air by pulsed discharge plasma", Technical Physics Letter, vol. 46, pp. 94-97, 2020.

* The work was supported in part by the RFBR Grant No. 20-08-00882 (methods) and RFBR & Sverdlovsk region, Grant No. 20-48-660062 r_a. (objects).

SYNTHESIS OF MULLITE FROM ALUMINOSILICATE RAW MATERIALS IN A THERMAL PLASMA FLOW*

R.E. GAFAROV, V.V. SHEKHOVTSOV, O.G. VOLOKITIN

Tomsk State University of Architecture and Building, TSUAB, Tomsk, Russia
e-mail: greexrayne@gmail.com

To identify the prospects for using plasma technologies in the production of mullite from various refractory materials, studies were carried out on its synthesis from enriched kaolin from the Zhuravliniy Log deposit. The chemical composition of the feedstock is characterized by a high content of SiO_2 and Al_2O_3 . However, for the synthesis of mullite of the general formula $3\text{Al}_2\text{O}_3\cdot 2\text{SiO}_2$, a higher content of Al_2O_3 is required, therefore, kaolin ground to a fraction of 2–5 microns was additionally mixed with aluminum oxide powder [1, 2].

The raw materials under study were melted in a graphite crucible using a plasma installation. The formation of a homogeneous melt occurred due to the action of a highly concentrated plasma flow on the prepared raw material.

It was found that the resulting melting product of kaolin is a glassy translucent material with white streaks. During the study of the product, its heterogeneous structure was found, including both residual quartz and amorphous regions. Elements of various shapes, partially soldered to each other, are randomly distributed in the glassy mass.

Figure 1 shows an XRD pattern of the resulting kaolin-based melt product.

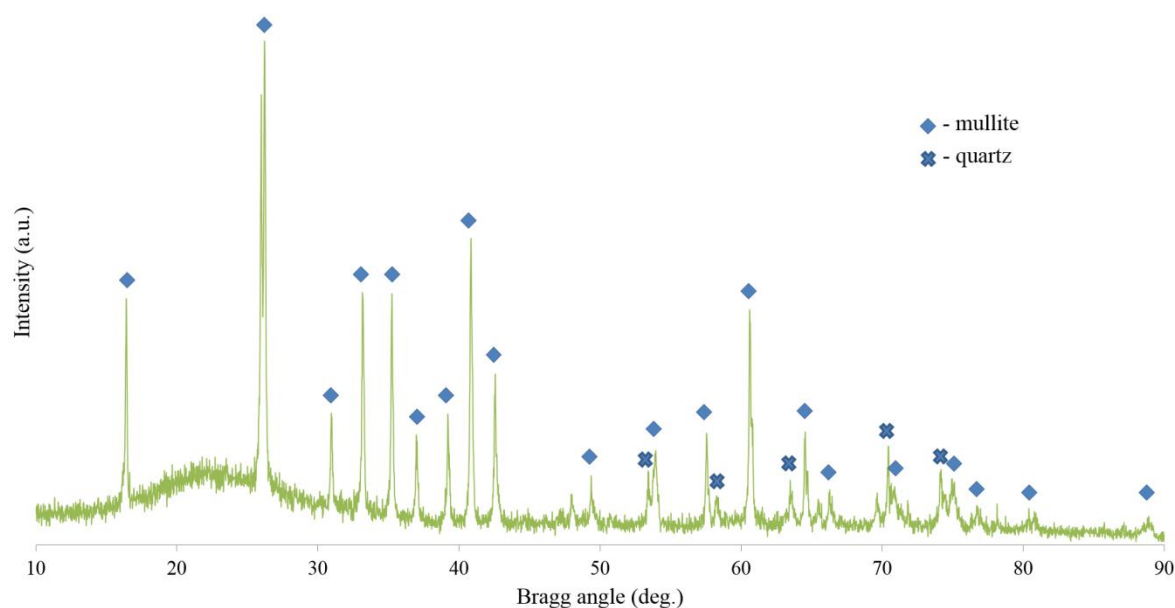


Fig. 1. XRD spectrum of the melting product based on kaolin

The XRD pattern of the crushed sample is represented by pronounced diffraction maxima corresponding to mullite of the composition $3\text{Al}_2\text{O}_3\cdot 2\text{SiO}_2$ and mainly by an amorphous glass phase, which is expressed as a characteristic halo.

Analysis of the data allows us to draw a conclusion about the possibility of obtaining high-quality mullite based on kaolin using the energy of low-temperature plasma and the prospect of its further application in composite materials.

REFERENCES

- [1] O.G. Volokitin, V.V. Shekhovtsov, M.A. Sheremet, N.S. Bondareva, V.I. Kuzmin, "Studying regimes of convective heat transfer in the production of high-temperature silicate melts", *Thermophysics and Aeromechanics*, vol. 23, no. 5, pp. 755 – 765, 2016.
- [2] O.G. Volokitin, V.V. Shekhovtsov, "Prospects of application of low-temperature plasma in construction and architecture", *Glass Physics and Chemistry*, vol. 44, no. 3, pp. 251 – 253, 2018.

* The work was supported by the grant from the Russian Science Foundation, Project No. 20-79-10102.

SYNTHESIS OF MAX-PHASES, STRUCTURE AND PHASE COMPOSITION OF MODIFIED LAYERS ON TITANIUM ALLOY VT-1 AS A RESULT OF ELECTRON-BEAM TREATMENT*

A.E. LAPINA¹, N.N. SMIRNYAGINA¹, V.M. KHALTANOVA²

¹Institute of Physical Materials Science, SB, RAS, Ulan-Ude, Russia

²Buryat State University, Ulan-Ude, Russia

e-mail: ann_lapin@mail.ru

Currently, MAX phases (double silicon carbides with various transition metals) synthesized by various methods in a nanostructured state in the form of films, layers, and ceramics are well studied, but little attention is paid to their thermodynamic properties [1]. The authors of the article revealed the optimal conditions for the formation of MAX phases during the treatment of titanium alloy VT-1 electron beam in a vacuum. The results of a study of strength characteristics, thermal properties of composite layers are presented. The article discusses the step-by-step construction of a mathematical model of thermal fields arising when exposed to a focused electron beam moving on the surface of a sample of titanium alloy VT-1 using the COMSOL Multiphysics software package. Calculations of heating and cooling rates in the electron beam exposure zone during sample processing reached the order of 10^4 - 10^5 K/s, which indicates that the process is high-speed. With the help of the TERRA software complex, phase equilibriums modeling was carried out in the Ti-B-C system [2]. The temperature range of the calculations was 300-4500 K. The total pressure in the system ranged from 10^5 to 10^{-3} Pa. Figure 1 shows isothermal section (1000 K) and isotherms at a pressure of 10^{-3} Pa (Fig. 2).

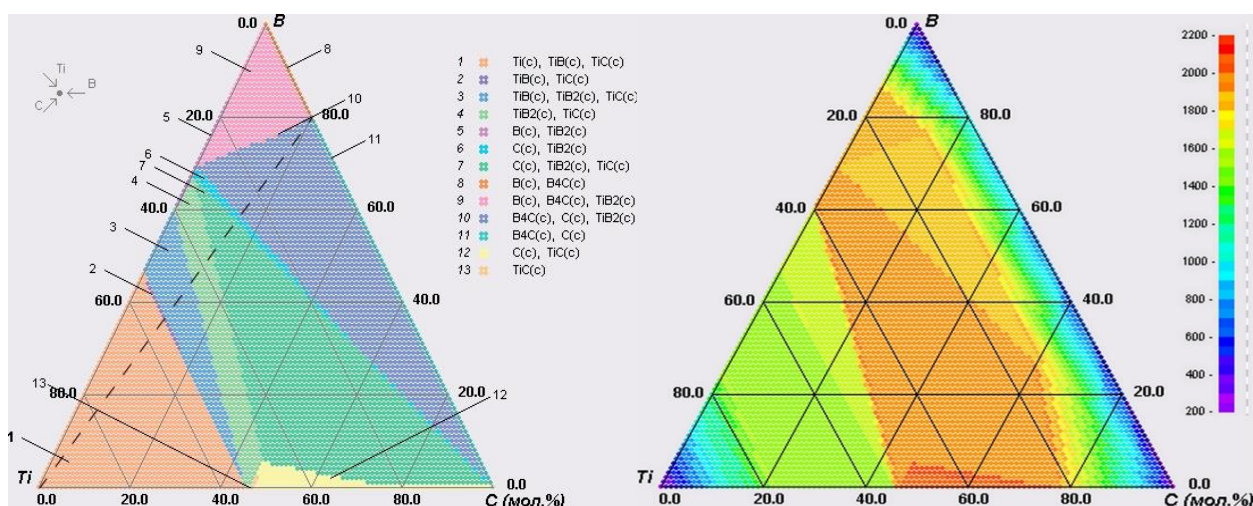


Fig. 1. Phase equilibrium in the system Ti-B-C at $P=10^{-3}$ Pa and $T=1000$ K.

Fig. 2. Isotherms in Ti-B-C system at $P=10^{-3}$ Pa.

The data presented are in accordance with the phase equilibrium in the Ti-B-C triple system at total atmospheric pressure ($P = 0.1$ MPa). Triple compounds (carbaborides or borocarbides) are not formed. The data confirm that the dual Ti-B₄C system is not a quasi-binary cut in the Ti-B-C triple system. In the Ti-B₄C system, the formation of titanium carbides, titanium borides, boron, carbon is possible. The processes of formation of titanium carbides and borides occur with the release of a significant amount of energy, thereby increasing the temperature in the system to 2000 – 2150 K ($P = 10^5$ Pa) and 1600 – 1725 K ($P = 10^{-3}$ Pa).

REFERENCES

- [1] Smetkin A. A., Mayorova Yu. K. Properties of materials based on MAX-phases (Review) // VESTNIK PNRPU. Mechanical engineering, materials science. 2015. Vol. 17, No. 4, pp. 120-138. DOI: 10.15593 / 2224-9877 / 2015.4.09.
- [2] Smirnyagina N. N., Khaltanova V. M., Dashev D. E., Lapina A. E. Phase equilibrium in system Ti-Si-C-B and synthesis of MAX phase layers in vacuum under the influence of electron beam. Journal of Physics: Conference Series. Vol. 830, pp. 012110. DOI: 10.1088/1742-6596/830/1/012110.
- [3] Lapina A. E. , Smirnyagina N. N., Dashev D. E. "Modeling of thermal processes in the processing of titanium alloy VT-1 with an electron beam in a vacuum", Vestnik of BSU. Chemistry. Physics. 2018. No. 2-3, pp. 55-63. DOI: 10.18101 / 2306-2363-2018-2-3-55-63.

* The work was carried out with the financial support of the state task of the Ministry of Science and Higher Education of the Russian Federation, topic No. 0270-2021-0001.

PLASMA-SOLUTION SYNTHESIS OF TRANSITION METAL OXIDES

K.V. SMIRNOVA, V.V. RYBKIN, D.A. SHUTOV, A.N. IVANOV

*Ivanovo State University of Chemistry and Technology, Ivanovo, Russia
e-mail: smirnovakv1@gmail.com*

Transition metal nanoparticles are used in various industrial and biological applications such as homogeneous and heterogeneous catalysis, fuel cell catalysis, sensors and biosensors. They are widely used as conductive pastes, battery materials, magnetic recording media, etc. Due to the semiconducting properties of oxide nanomaterials have been found their application in microelectromechanical systems and optoelectronics. Plasma-solution synthesis is one of the simple and effective methods for producing nanomaterials. In this work, we present the main results and regularities of the formation of a solid phase from a solution of transition metal salts under the action of direct current gas discharge in air.

The scheme of the plasma-solution cell and the experimental procedure are described in detail in [1]. The starting salts and products are shown in Table 1. The action of the discharge on the solution, which is the anode, led to the formation of colloidal particles. The rate of their formation, phase composition and elemental composition, the size of colloidal particles and sediment particles were investigated by the methods of turbidimetry, X-ray analysis, EDS, DLS, and SEM. It is shown that the formed colloidal particles are crystalline mixtures of hydroxides and hydroxonitrates. Calcining these substances, the kinetics of which was studied by DSC, led to the formation of the corresponding oxides. The properties of the obtained substances are shown in the Table 1.

A probable mechanism of the processes initiating the formation of insoluble hydroxo compounds is proposed. It is assumed that the discharge electrons, which bombard the surface of the liquid anode, form solvated electrons. Their rapid reaction with water molecules leads to the formation of OH⁻ ions, an increase in the pH of the solution, and the formation of insoluble hydroxo compounds.

Table 1: Oxide metal particles synthesis in plasma solution system. Discharge current 40 mA. The initial concentration is 5 mmol and 100 mmol.

Type of particles after calcination	Raw materials	Particle size		Rate constant, s ⁻¹		XRD and EDS of precursor
		The 1st fraction, nm	The 2nd fraction, μm	30 mA	70mA	
CoO	Co(NO ₃) ₂	50	1.2	9·10 ⁻³	10·10 ⁻³	Co(OH) ₂ ; Co(OH)(NO ₃)
NiO	Ni(NO ₃) ₂	73.5	1.2			β-Ni(OH) ₂
CuO	Cu(NO ₃) ₂	23	0.97	4,4·10 ⁻³	10·10 ⁻³	Cu(NO ₃)(OH) ₃
ZnO	Zn(NO ₃) ₂	95.4	1.8	15·10 ⁻³	22·10 ⁻³	Zn(OH) ₂ ; Zn(OH)(NO ₃)
CdO	Cd(NO ₃) ₂	57.3	2.7	10·10 ⁻³	22·10 ⁻³	Cd(OH) ₂ ; Cd(OH)(NO ₃)
(CoO)(Fe ₂ O ₃)	Co(NO ₃) ₂ with Fe(NO ₃) ₃	92.9	1.4	5.6·10 ⁻³	19·10 ⁻³	(CoO)(Fe ₂ O ₃)
(ZnO) _{0,92} (CdO) _{0,08}	Zn(NO ₃) ₂ with Cd(NO ₃) ₂	51	3.4	1.3·10 ⁻³	12·10 ⁻³	Zn(NO ₃)OH·H ₂ O, Zn(OH) ₂ , γ-Cd(OH) ₂ , β-Cd(NO ₃)OH·H ₂ O

REFERENCES

- [1] D.A. Shutov, K.V. Smirnova, M.V. Gromov, A.N. Ivanov, V.V. Rybkin, "Synthesis of CdO Ultradisperse Powders Using Atmospheric Pressure Glow Discharge in Contact With Solution and the Investigation of Intermediate Products," *Plasma Chem. Plasma Process*, 38, 107–121, 2018.

DROPLETS GENERATION CONDUCTING DURING LASER-PLASMA TREATING OF METALS IN ELECTRIC FIELD

A.YU. IVANOV, A.L. SITKEVICH, S.V. VASILIEV

Grodno State University, Grodno, Belarus

e-mail: ion_ne@mail.ru

In the publication [1] was shown that under the action of laser radiation with the mean radiation flux density $\sim 10^6$ W/cm² at the surface of some metals (Cu, Al, Sn, Pb, In) in the external electric field with different polarity and the strength up to 10^6 V/m the characteristic size of the target substance droplets, carried out of the irradiated zone, decreases by several times with increasing external electric field strength in spite of short duration of electric field existence. The aim of the present work is to study the influence of electric fields of different strength (from 0 to 10^6 V/m) on the spatial and temporal evolution of the laser plasma arising under the action of millisecond laser pulses at the surface of metals and to explain the mentioned effect.

The radiation of the GOR-100M ruby laser operating in the free oscillation regime (pulse duration ~ 1.2 mc) passed through the focusing system and was directed through the hole in the electrode onto the sample that served as the second electrode and was mounted in air at a pressure of 10^5 Pa. The energy of the laser pulses varied from 5 to 60 J. The voltage was applied to the electrodes from the source, built on the basis of the UN 9/27-13 voltage multiplier of the TVS-110 unit. The source allowed the voltage variation within 25 kV and its stabilization in the course of the experiment. To study the spatial and temporal evolution of the laser plasma torch in the course of laser radiation action on the sample, we used the method of high-speed holographic motion-picture recording. Presence of an external electric field weakly affects the concentration of electrons in the laser plasma plume. When either positive or negative potential is applied to the sample, many small droplets appear on its surface after the laser action. The droplets were seen at the distance up to ~ 1 cm from the crater centre. The primary plasma formation and the initial stage of the laser plume development, in principle, do not differ from those observed in the absence of the external electric field. The metal is melted and evaporated. As a result of local formation of steam and plasma, the erosion plume begins to form with the fine-dispersed liquid-drop phase. Note, that the bulk evaporation is promoted by the gases, diluted in the metal, and by the spatiotemporal non-uniformity of the laser radiation. At a radiation flux density $10^6 - 10^7$ W/cm² the bulk evaporation is typical of all metals used in the experiments. Obviously, the presence of the external electric field affects (increases or decreases depending on the direction of the field strength vector) the velocity of motion of the plasma front and causes some distortion of the plasma cloud shape. The significant difference in the characteristic size of droplets, observed on the surface of the irradiated sample in the presence of the external electric field (independent of the direction of the field strength vector) and in the absence of the field was observed. In particular, at the laser pulse energy 20 J, the diameter of the focusing spot 2 mm, and the electric field strength 10^6 V/cm we observed ejection of droplets having the mean characteristic size less than 0.1 mm to the distance up to 2 cm from the crater centre. The maximal characteristic size of drops was ~ 0.4 mm. In the absence of the external electric field the mean size of the droplets was ~ 0.4 mm.

It is essential that the mentioned differences (at the considered parameters of laser radiation) are observed only at the initial stage of the laser plume development, because after the steam-plasma cloud reaches the electrode an electric breakdown (short-circuit) occurs, and the external field in the interelectrode gap disappears.

Electric breakdown leads to the spasmodic increase of electron density and temperature of plasma and to effective absorption of laser radiation by plasma torch (shielding of the target). In consequence of shielding droplets generation happens only during electric field existence. This explains decrease by several times of the characteristic size of the target substance droplets in spite of short duration of electric field existence.

REFERENCES

- [1] Ivanov, A.Yu. Influence of an external electric field on particle generation during laser-plasma treating of metals / A.Yu. Ivanov, A.V. Kapyski, S.V. Vasiliev // Materials Physics and Mechanics. – 2019. – Vol. 41, No 1. – P. 97 – 102.

MODIFICATION OF THE SURFACE OF COPPER AND ITS ALLOYS DUE TO NANOSECOND ULTRAVIOLET LASER PULSES IMPACT*

T.V. MALINSKIY¹, V.E. ROGALIN¹, I.A. KAPLUNOV²

¹Institute of Electrophysics and Electric Power, RAS, St. Petersburg, Russia

²Tver State University, Tver, Russia

e-mail: v-rogalin@mail.ru

The impact of nanosecond UV laser pulses on polished samples of oxygen-free copper and its alloys (bronze and brass) has been studied. At the pre-threshold mode, in the absence of obvious traces of melting, at an energy density of $E = 0.1 - 1.0 \text{ J/cm}^2$, traces of high-temperature plastic deformation were found [1-3]. They manifest themselves as the results of sliding along grain boundaries and cracking along them, as well as traces of crystallographic sliding inside the grains (Fig. 1a). As a result, the metal in the irradiated zone distends. With an increase of the number of impacting impulses, accumulation of damage occurs, despite of the fact, that the surface completely cools down during the time between impulses. The height of the resulting uplift can reach $1 \text{ }\mu\text{m}$, and sometimes even slightly more (Fig. 1b). Exceeding the optical breakdown threshold ($E \sim 1.0 \text{ J/cm}^2$) leads to melting and evaporation of the metal with the formation of a crater. This stronger, oppositely directed process suppresses traces of plastic deformation.

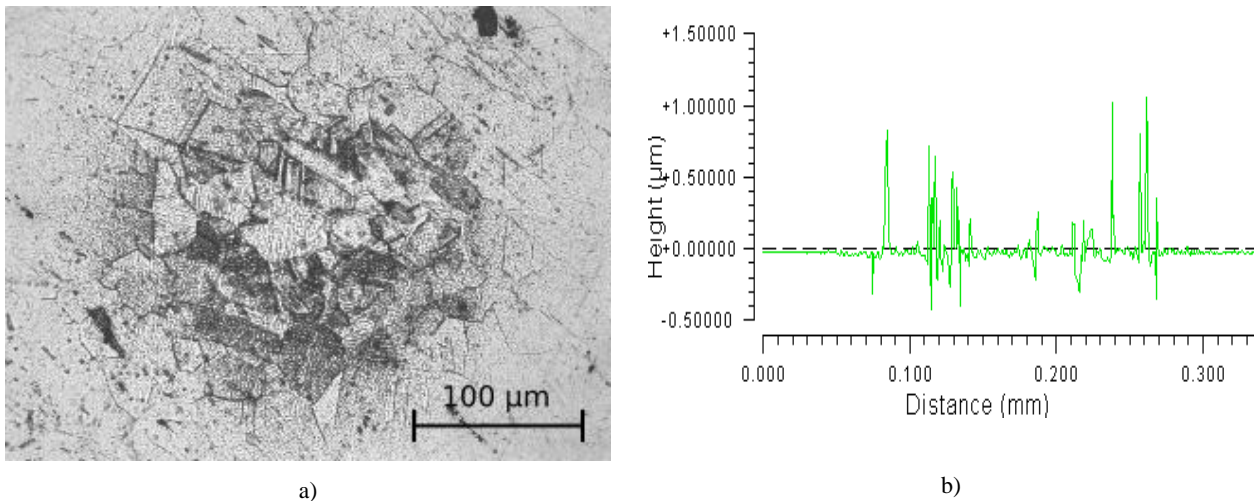


Fig. 1 Surface of a Cu-Cr bronze sample after impact to 25 UV Nd:YAG laser pulses, ($\lambda = 0.355 \text{ }\mu\text{m}$, pulse duration 10 ns, frequency 10 Hz, $E \sim 0.22 \text{ J/cm}^2$); a) micrograph; b) profilogram. Drawings were obtained using the Zygo New View 7300 profilometer.

The absorption of light by metals occurs because of the transfer of photon energy to the electronic component of the skin layer $\sim 15 \text{ nm}$, which significantly overheats the electronic subsystem. During the electron-ion relaxation time (2 - 3 ps), the absorbed energy is transferred to the phonon subsystem. Therefore, the near-surface layer is heated during the laser pulse action time - 10 ns.

The effect of impact of radiation on the surface, associated with the occurrence of plastic deformation, is similar to the electroplastic and magnetoplastic effects. By analogy, it is proposed to call the discovered effect optoplastic.

REFERENCES

- [1] T V Malinskiy, S I Mikolutskiy, V E Rogalin, Yu V Khomich, V A Yamshchikov, I A Kaplunov, and A I Ivanova "Plastic Deformation of Copper under the Action of High-Power Nanosecond UV Laser Pulse" *Technical Physics Letters* 46(8) 831–834. 2020.
- [2] Yu Khomich, T Malinskiy, V Rogalin, I Kaplunov, and A Ivanova "Features of microrelief formation during laser treatment of Cu-Cr-Zr alloy surface for diffusion welding" *IOP Conf. Series: Materials Science and Engineering* 939 012035. 2020.
- [3] Yu V Khomich, T V Malinskiy, S I Mikolutskiy, V E Rogalin, V A Yamshchikov, I A Kaplunov, and A I Ivanova "Powerful ultraviolet laser pulse impact on polished metals and semiconductors" *J of Physics: Conf. Ser.* 1697 012254. 2020.

* This study was supported in part by the Ministry of Science and Higher Education of the Russian Federation within project № 0057-2019-0005.

THE STUDY OF AN INSTABILITIES ROLE OF PLASMA IN THE HIGH-VOLTAGE DISCHARGE FORMATION INITIATED BY OPTICAL RADIATION AT HIGH PRESSURES IN HIGH-VOLTAGE OPTICALLY TRIGGERED SWITCHES

A.I. LIPCHAK, S.V. BARAKHVOSTOV, N.B. VOLKOV, E.A. CHINGINA, I.S. TURMYSHEV

Institute of Electrophysics of the UB, RAS, Yekaterinburg, Russia

e-mail: lipchak@iep.uran.ru

High-voltage switches are an important part of a broad range of modern equipment from scientific experimental setups to industrial power equipment. The improvement of their efficiency (reducing switching losses) and stability of triggering determines the relevance of the investigation. Switches with optical (laser) triggering have an important practical advantage in comparison with analogs with the electrical method of triggering due to the galvanic isolation of switched circuits and control circuits. When a laser-plasma is generated, oscillations of its front may occur [1], such phenomenon was explained by the occurrence of Richtmyer – Meshkov instability [2]. However, estimation shows this model does not describe instability in the switches in the range at characteristic times from tenths of a nanosecond or less. So the aim of the present investigations is a study the processes in high-voltage high-current high-pressure switches with optical triggering. The operation regime of the laser triggered gas discharge gap, when the instability (jitter) is minimal was found experimentally. Fig. 1 shows the non-monotonic dependence of jitter Δt on the normalized voltage $\sigma = (U_s - U_b)/U_s$, where U_b is the voltage when the spark gap is triggered, U_s is the self-breakdown voltage.

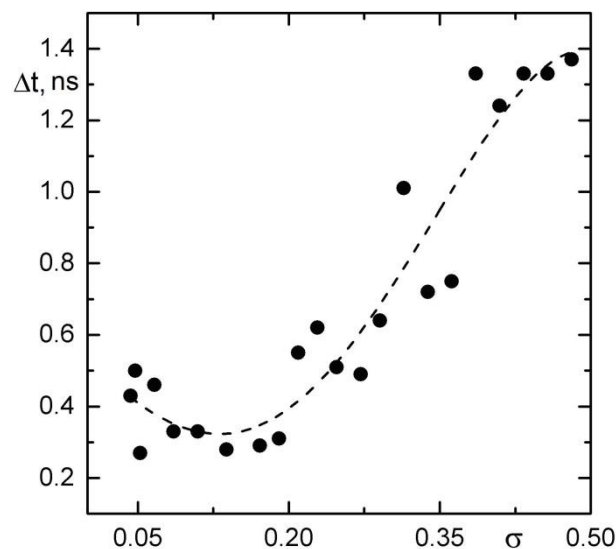


Fig. 1. The dependence of jitter vs the normalized operation voltage σ at nitrogen pressure of 4MPa.

Each point on fig. 1 was obtained by averaging of 30 measurements. One can see the 0.3 ns jitter in range 0.05 – 0.2 of σ .

REFERENCES

- [1] Lipchak A.I., Solomonov V.I., Osipov V.V., Tel'nov V.A. Spectral-temporal characteristics of a laser-plasma. *Quantum Electronics (Rus)*, 22, no. 4, pp. 367-373, 1995.
- [2] Mesyats G.A., Osipov V.V., Volkov N.B., Platonov V.V., Ivanov M.G. Nonlinear dynamics a plasma torch generated by a laser pulse of long duration. *Letters of ZhTF*, 29, iss. 18, pp. 54-60, 2003.

FEATURES OF THE GAS-PHASE SYNTHESIS OF OXIDE NANOPOWDERS USING HIGH-POWER LASERS*

V.V. OSIPOV, V.V. LISENKOV, V.V. PLATONOV, E.V. TIKHONOV

Institute of Electrophysics UB RAS, Yekaterinburg, Russia

e-mail: platonov@iep.uran.ru

The main peculiarity of obtaining of refractory oxide nanopowders using a CW ytterbium fiber laser (1.06 μm) with a radiation power of up to 700 W and a repetitively-pulsed CO_2 -laser (10.6 μm) with an average radiation power of 500 W are considered in report. The role of buffer gas pressure, its composition and average radiation power on the size of nanoparticles and the productivity of their obtaining were studied. It was shown that in relation to thermophysical properties of the material, in the environment of atmospheric pressure air the productivity of nanopowder synthesis varies from 15-23 g / h (YSZ) to 350 g / h (WO_3). The mass yield of nanopowder obtained in result of evaporation of one target is usually is 30 wt% from the weight of initial target. The obtained nanopowders contain weakly agglomerated nanoparticles of spherical shape. The average size of nanoparticles (11–20 nm) weakly depends on material.

It was shown that the most important features of using a CW ytterbium laser to obtain nanopowders of refractory oxides are their high transparency for radiation of 1.06 μm , as well as the spraying of many melt droplets. These features led to a reduction in the productivity of nanopowder production and its mass yield. Another important feature is the scattering of laser radiation in porous of the initial target and its concentration in some regions. This mechanism makes it possible to efficiently evaporate oxide targets from materials with a refractive index of more than $1.7 \div 1.75$. The transition to a repetitively-pulsed mode of radiation (pulse duration 120 μs , square waveform, and peak power 600 W), an increase in the spot diameter and the speed of beam movement over the target surface made it possible to significantly reduce droplet spattering and increase the yield of Nd: Y_2O_3 nanopowder from 9.7 wt.% to 30 wt.% of the weight of the initial target. However, a twofold decrease in the average radiation power led to the fact that the productivity of obtaining the nanopowder was only 15 g / h. Based on the above, to obtain nanopowders of refractory oxides, it is desirable to use a quasi-CW fiber ytterbium laser, which is specially designed for operation in a repetitively pulsed mode.

* The work was performed as part of State Task № 0389-2019-0003, was supported in part by RFBR Grant № 20-08-00054 A.

THE POSSIBLE CHEMICAL PATHWAYS IN NRP PLASMA-ASSISTED AMMONIA SYNTHESIS AND NITROGEN FIXATION*

SHUAI ZHANG^{1,2}, XIN ZENG^{1,2}, LIJUN ZONG¹, XIUCUI HU¹, TAO SHAO^{1,2}

¹ Beijing International S&T Cooperation Base for Plasma Science and Energy Conversion, Institute of Electrical Engineering, Chinese Academy of Sciences, China

² University of Chinese Academy of Sciences, Beijing, China
e-mail: st@mail.iee.ac.cn

Recently, many green and sustainable approaches beyond fossil fuel-driven nitrogen transformations (i.e. ammonia synthesis and nitrogen fixation) has been widely explored to challenge the industrialized Haber-Bosch process, such as nitrogenase enzymes, heterogeneous catalysts, non-thermal plasma and electrocatalysis [1-3]. The non-thermal plasma technology has the unique advantages in high energy efficiency, miniaturization, easy to coupling and so on, especially when the reactor was driven by a nanosecond repetitively pulse (NRP) power source [4]. However, further parameter optimizations should be proceeded to promoting the energy efficiency, based on the knowledge of underlying chemical reaction processes. In this paper, we attempt to solve the above problem by combining with online product measurements, optical diagnosis and reaction kinetic simulations.

Plasma-assisted ammonia synthesis (with and without Ru/CeO₂ catalysts) has been implemented in a NRP coaxial dielectric barrier discharge. The synergistic effect of plasma and catalysts is more likely to appear in a lower temperature condition (less than 500°C) and a lower ratio of N₂/H₂ gaseous mixture, with the maximum NH₃ concentration of ~ 5000 ppm at a total gas flow rate of 90 mL/min. The reaction kinetic model indicates that the high vibrational excited states may play an important role in the synergistic activation of nitrogen molecules, with a mean electron energy of ~ 3 eV, an average electron density of ~10¹³ cm⁻³ and a vibrational temperature of ~ 3000 K. The corresponding optical diagnosis is also proceeded to support the above speculation.

Plasma-assisted nitrogen fixation has been implemented in a plate-to-plate NRP spark discharge. The NO_x energy efficiency and concentration can reach to about 4-11 g/kWh and 960-10900 ppm varies as air flow rate of 40-340 mL/min, respectively. The reaction kinetic model indicates that more than 50% NO is contributed by the chain reactions of O and N radicals with vibrationally excited N₂ and O₂ molecules (O+N₂(v)→NO+N and N+O₂(v)→NO+O) while most of NO₂ is formatted by the oxidation of NO (NO+O→NO₂). The appearance of O and N spectral line peaks at the post-discharge stage indirectly proves that the chain reactions have taken place. Furthermore, the oxynitrides after NRP spark discharge can be translated into ammonium by coupling an electrocatalysis reactor [5].

REFERENCES

- [1] J.G. Chen, R.M. Crooks, L.C. Seefeldt, K.L. Bren, R.M. Bullock, M.Y. Darensbourg, P.L. Holland, B. Hoffman, M.J. Janik, A.K. Jones, M.G. Kanatzidis, P. King, K.M. Lancaster, S.V. Lyman, P. Pfromm, W.F. Schneider, R.R. Schrock, Beyond fossil fuel-driven nitrogen transformations, *Science*, 360, 873, 2018.
- [2] P. Mehta, P. Barboun, F.A. Herrera, J. Kim, P. Rumbach, D.B. Go, J.C. Hicks, W.F. Schneider, Overcoming ammonia synthesis scaling relations with plasma-enabled catalysis, *Nat. Catal.*, 1, 269-275, 2018.
- [3] X. Pei, D. Gidon, Y.-J. Yang, Z. Xiong, D.B. Graves, Reducing energy cost of NO_x production in air plasmas, *Chem. Eng. J.*, 362, 217-228, 2019.
- [4] T. Shao, R. Wang, C. Zhang, P. Yan, Atmospheric-pressure pulsed discharges and plasmas: mechanism, characteristics and applications, *High Vol.*, 3, 14-20, 2018.
- [5] J. Sun, D. Alam, R. Daiyan, H. Masood, T. Zhang, R. Zhou, P. Cullen, E.C. Lovell, A.R. Jalili, R. Amal, A hybrid plasma electrocatalytic process for sustainable ammonia production, *Energy Environ. Sci.*, 14, 865-872, 2021.

* This work was supported by the National Science Fund for Distinguished Young Scholars (Grant No. 51925703), the National Natural Science Foundation of China (Grant No. 52077205), and the Royal Society–Newton Advanced Fellowship, UK (Grant No. NAF\R2\192117).

INVESTIGATION OF THE EFFECT OF WATER VAPOR AND CONDENSED PHASE ON THE ENERGY CONDITIONS FOR THE INITIATION OF THE PLASMA-CHEMICAL PROCESS OF FLUE GAS PURIFICATION BY A PULSED ELECTRON BEAM*

R. SAZONOV, G. KHOLODNAYA, D. PONOMAREV, I. EGOROV, A. POLOSKOV, M. SEREBRENNIKOV

Tomsk Polytechnic University, Tomsk, Russia

e-mail: galina_holodnaya@mail.ru

Polluted atmospheric air is one of the main factors of anthropogenic impact on the environment. Despite the implementation of various air protection programs, its current state, both in Russia and abroad, remains unsatisfactory, which is primarily due to growing emissions from industrial facilities and road transport. As a result of an increase in the content of pollutants in the atmospheric air, the process of destruction of the Earth's ozone screen is intensively developing, acid rain is observed, causing damage to all living things, land fertility decreases, water is poisoned, and deforestation of the earth's surface occurs. There is currently a significant number of reports devoted to the purification of flue gases by pulsed electron accelerators.

However, one of the important factors hindering the development of flue gas purification using pulsed electron accelerators is the lack of an appropriate physical model based on experimental data of the processes occurring during the interaction of pulsed electron beams not only with model objects in the condensed and gas phase, but also with objects with complex chemical composition, which are basic in technological processes. A significant role in solving this problem is assigned to experimental data both from the point of view of providing results for the formation of a model and its testing, and from the point of view of a quantitative description of the processes accompanying the development of specific technological processes.

The work investigates the processes of dissipation of the charge and energy of a pulsed electron beam in gas compositions (nitrogen, carbon dioxide and oxygen) in the presence of water vapor, ammonium sulfate and nitrate. A pulsed electron beam generated by the TEA-500 accelerator with an electron energy of 450 keV, a beam current of 10×10^3 A (I_0), and a pulse duration $t = 60 \times 10^{-9}$ s was injected into a 46 cm long drift chamber filled with a gas mixture. An electron beam current (I_{FC}), which passed through the drift chamber, was recorded using a sectioned calorimeter with beam charge monitor function, and the efficiency of the current passage of the beam was determined as the ratio q_{FC}/q_0 , where q_0 is the beam current measured at its injection into the drift chamber. The pressure and concentration of water vapor in the drift chamber varied (375, 560, and 760 Torr; humidity value $15\% \pm 5\%$ and $50\% \pm 15\%$). It is shown that an increase in the efficiency of current passage of a pulsed electron beam is observed in the drift chamber at a humidity of $50\% \pm 15\%$. When ammonium sulfate and nitrate are added to the drift chamber, the ratio of the charge of the pulsed electron beam that reached the collector of the Faraday cup (q_{FC}) to the charge of the pulsed electron beam introduced into the drift chamber (q_0) decreases.

* This work was supported by RFBR according to the research project № 18-32-20066.

CREATING NANOSCALE LUMINESCENCE CENTRES IN SILVER HALIDES SUITABLE FOR INFRARED APPLICATION

E.A. KORSAKOVA², V.V. LISENKOV¹, L.V. ZHUKOVA², A.N. ORLOV¹, A.S. KORSAKOV², V.V. OSIPOV¹, A.E. LVOV²,
V.V. PLATONOV¹, D.D. SALIMGAREEV²

¹*Institute of Electrophysics, UB, RAS, Yekaterinburg, Russia*

²*Institute of New Materials and Technologies, Ural federal university, Yekaterinburg, Russia*

e-mail: orlov@iep.uran.ru

The task of creating simple, compact, and high-power sources of coherent radiation in the range of 5 - 1000 μm has become more and more urgent with the active development of lasers for the wide range of wavelengths. These lasers can be used in medicine, military technology, for probing samples at checkpoints, etc. The lasers' active media are transparent at the radiating wavelength and have inclusions in the form of ions luminescent upon pumping. In general, the active substances are transparent merely in the visible and near-IR spectral regions. There are practically no natural substances luminescent within the entire optical region mentioned above. However, this issue can be solved not only by creating new materials but also by introducing active centres of luminescence (in the form of particles) into existing optically transparent materials. These materials include silicon oxide, germanium, silver halides, to name but a few. The question to be addressed here is how much the materials and the embedded nanoparticles reciprocally impair each other's optical properties, particularly their transparency and luminescence nature.

This study shows the possibility of creating luminescence centres in silver halide media using substances based on rare-earth elements such as neodymium, ytterbium and dysprosium. These luminescent substances in the form of fine particles of both nanoscale and microscale dimensions can be introduced into the $\text{AgCl}_{0.25}\text{Br}_{0.75}$ ceramic matrix highly transparent in the spectral range of 0.5-35 μm .

First, we carried out the theoretical characterization of the luminescent nanoparticles in terms of Rayleigh scattering. We also numerically solved the Helmholtz equation [1] for an alternating electromagnetic field applied to AgCl-AgBr ceramic medium with Y_2O_3 particles embedded. Then, the transmission and luminescence spectra of $\text{AgCl}_{0.25}\text{Br}_{0.75}$ samples were experimentally measured. To obtain the samples, we utilized the method of thermozone crystallization-synthesis (TZKS) [2], which is based on different solubility of substances in acid solutions at the same temperature.

The empirical data showed that the attenuation we observed in the samples was mostly caused by absorption on the structural defects rather than by Rayleigh scattering. And expectedly, experimental losses are still much higher than theoretical ones, confirming the substantial contribution of absorption to the overall losses. However, we revealed that scattering manifests itself as well and the microscale particles scatter radiation larger than nanoparticles.

Furthermore, our theoretical and experimental studies showed that the introduction of luminescent nanoparticles or microparticles at the amount of 0.5 wt% into $\text{AgCl}_{0.25}\text{Br}_{0.75}$ ceramics neither reduces the level of its transmission in the MIR region nor shortens the range of transmission. What is more, we proved that the luminescent properties of nanoparticles remain well preserved after doping silver halide ceramic media with them. Therefore, silver halides doped with rare-earth elements in question can be used for developing the sources of coherent middle infrared radiation, with appropriate energy levels being excited by optical radiation or pulsed electric field.

REFERENCES

- [1] V.V. Osipov, V.V. Lisenkov, V.V. Platonov, E.V. Tikhonov, Processes of interaction of laser radiation with porous transparent materials during their ablation, *Quantum Electronics*, vol. 48 (3), p. 235–243 (2018).
- [2] A.S. Korsakov, L.V. Zhukova, E. Korsakova, E. Zharikov, Structure modeling and growing $\text{AgCl}_x\text{Br}_{1-x}$, $\text{Ag}_{1-x}\text{Ti}_x\text{Br}_{1-x}\text{I}_x$, and $\text{Ag}_{1-x}\text{Ti}_x\text{Cl}_y\text{Br}_{1-y-z}$ crystals for infrared fiber optics, *Journal of Crystal Growth*, vol. 386, p. 94–99 (2014).

EVALUATION OF THE EFFECT OF PRE-SOWING ELECTRON IRRADIATION OF BARLEY SEEDS ON PLANT DEVELOPMENT AND DISEASE INCIDENCE

N. N. LOY¹, N. I. SANZHAROVA¹, S. N. GULINA¹, O. V. SUSLOVA¹, T. V. CHIZH¹, M. S. VOROBYOV², S. YU. DOROSHKEVICH²

¹*Federal State Scientific Institution «Russian Institute of Radiology and agroecology», Obninsk, Russia*

²*Institute of High Current Electronics SB RAS, Tomsk, Russia*

e-mail: loy.nad@yandex.ru

The use of low-energy electron radiation for pre-sowing irradiation of seeds of various crops in laboratory experiments has shown that this technique is promising for increasing the sowing qualities of seeds and reducing the incidence of diseases [1-3]. When using electron irradiation of seeds for further growing plants before harvest under the conditions of a growing experiment, it was not clear to what extent the positive effects noted on seedlings would remain on adult plants during the growing season.

The studies were carried out on spring barley of the Vladimir variety (*Hordeum vulgare* L.). The grain was irradiated on a Duet wide-aperture electron accelerator with a grid plasma cathode and the output of a generated beam with a large cross section into the ambient atmosphere [4]. The rate of surface absorbed radiation dose was about 3000 Gy/pulse, the accelerating voltage was 130 kV (mode 1) and 160 kV (mode 2). In this case, the dose absorption depth did not exceed 300 µm.

After irradiation, the seeds were sown in vessels with sod-podzolic soil and grown until harvest. The experiments were repeated 3 times. The morphometric and biochemical parameters of the development of vegetative plants, the structure of the yield and the susceptibility of barley to root rot (*Bipolaris sorokiniana*) were studied according to generally accepted methods.

The study of the biological effectiveness of pre-sowing electron irradiation of barley seeds showed that low-energy electron radiation influenced the morphometric and biochemical parameters of plant development. Analysis of the development of plants in the tillering phase revealed the absence of a significant effect of irradiation on all biometric indicators at irradiation mode 1 and inhibition of barley development at mode 2 in terms of the following indicators: "plant height" by 20-26% (doses of 90-150 kGy and "leaf surface area", "wet and dry biomass" by 35% at a dose of 150 kGy.

When assessing the development of plants by the same indicators in the heading phase, a significant increase of 41-71% in dry biomass and a decrease in leaf surface area by 25-44% were noted, regardless of the dose and irradiation regime. Determination of the photosynthetic activity of barley in the tillering phase showed that electron irradiation inhibits (decrease by 9-25%) the formation of chlorophyll a and b and carotenoids in leaves at all doses and modes of irradiation.

The data from the records of the infestation of barley by root rot indicate that irradiation promoted, at the level of a tendency, a decrease in the infestation of plants by the disease in the tillering phase at doses of 60-120 kGy (mode 1) and a dose of 30 kGy (mode 2), in the heading phase at doses 60 and 120 kGy (mode 1) and at doses of 60, 120 and 150 kGy (mode 2). In the phase of full ripeness, the effect of irradiation on the infestation of barley by root rot was almost completely leveled out in comparison with the non-irradiated control.

Electron irradiation of seeds caused an increase in the total tillering of plants (especially in mode 2), but at the same time reduced productive tillering, except for a dose of 120 kGy (mode 1) and a dose of 60 kGy (mode 2), where the growth of productive stems was noted. The weight of grain and straw per 1 plant did not differ from the control, but the weight of 1000 grains increased in almost all variants with irradiation by an average of 10-15%.

Thus, the positive effects on plant development noted under the action of low-energy electron radiation on barley seeds require further research in order to clarify the dose range and irradiation mode.

REFERENCES

- [1] T.V. Chizh, N.N. Loy, A.N. Pavlov, M.S. Vorobyev, S.Yu. Doroshkevich, "Low-energy electron beams for protection of grain crops from insect pests and diseases", IOP Conf. Series: Journal of Physics: Conf. Series, 1115 (2018) 022025, doi :10.1088/1742-6596/1115/2/022025.
- [2] N.N. Loy, N.I. Sanzharova, S.N. Gulina, M.S. Vorobyov, N.N. Koval, S.Yu. Doroshkevich, T.V. Chizh, O.V. Suslova, "Influence of electronic irradiation on the affection of barley by root rot", IOP Conf. Series: Journal of Physics: Conf. Series 1393 (2019) 012107 doi:10.1088/1742-6596/1393/1/012107.
- [3] N.N. Loy, S.Yu. Doroshkevich, N.I. Sanzharova, O.V. Suslova, M.S. Vorobyov, S.N. Gulina, T.V. Chizh, "Effectiveness of electron-beam radiation presowing treatment of spring wheat", Book Series: 7th International Congress "Energy Fluxes and Radiation Effects" (EFRE-2020). PP. 750-755.
- [4] M.S. Vorobyov, N.N. Koval, S.A. Sulakshin, Instrum. Exp. Tech, 58, no. 5 (2015) 687.

INVESTIGATION OF HYDROXYL GROUP RADICALS GENERATION AT INTERACTION OF A COLD ATMOSPHERIC PLASMA JET WITH AN ENVIRONMENT*

P.P. GUGIN¹, D.E. ZAKREVSKY^{1,2}, E.V. MILAKHINA^{1,2}

¹A. V. Rzhanov Institute of Semiconductor Physics SB RAS, Novosibirsk, Russia

²Novosibirsk State Technical University, Novosibirsk, Russia

e-mail: [lena.yelak@gmail.com](mailto:lana.yelak@gmail.com)

Reactive oxygen species affect the biological processes in living tissues. The main chemical reagents are particles such as hydroxide OH, hydrogen peroxide H₂O₂ and oxygen O₂. At present, a spectral analysis of a cold atmospheric plasma jet (CAPJ) in the area of interaction with a target has been carried out, the conditions of changing the OH hydroxide generation, which actively interacts with cancer cells through chemical reactions, have been investigated [1]. It was assumed that the effect of CAPJ in the flow of a mixture of helium with oxygen and CAPJ generated at an increased concentration of water vapor would make it possible to control the hydroxyl radical generation process. The analysis of the CAPJ emission spectrum was carried out above the target, which was exposed to water vapor at a distance of 2–5 mm. The natural relative humidity of the environment indoors near the interaction area of the CAPJ with the target was ~ 30%. In Fig. 1 the spectrum fragments in the UV range: (a) depending on the relative humidity level of the environment above the target; (b, c) in conditions of high humidity of the environment ~ 55%: depending on the amplitude of the applied voltage (b); depending on the pumping rate of the working gas He (c) are shown.

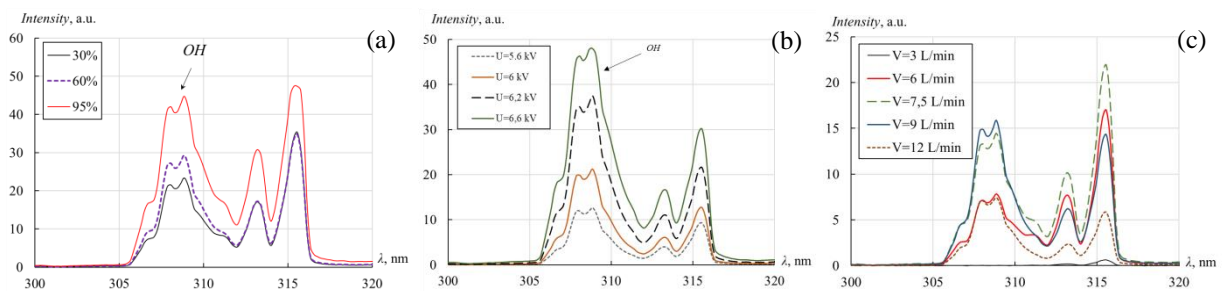


Fig. 1. The spectra of a CAPJ, $f = 13$ kHz (a) $U = 5.6$ kV, (b) $v = 9$ L/min, (c) $U = 5.6$ kV.

It was found that the spectral lines intensity of OH hydroxide ($\lambda = 309$ nm) was increased proportionally the humidity growth in the interaction area; the intensity of OH spectral lines increases with the applied voltage growth and is the extreme function of the pumping speed with the optimum at $v = 9$ L/min.

The OH radical generation process upon the addition of O₂ into the CAPJ has been investigated. According to the experimental results, it was revealed that the addition of O₂ at a rate of $v = 1.5$ – 9 ml/min together with He $v = 6$ – 9 L/min, significantly reduced the radiation intensity of the OH spectral line. With an increase in the pumping rate of O₂ more than $v > 9$ mL/min the discharge was extinguished. In Fig. 2 a fragment of the spectrum of CAPJ without O₂, and CAPJ with addition of O₂ (1.5; 7.5 mL/min) is shown.

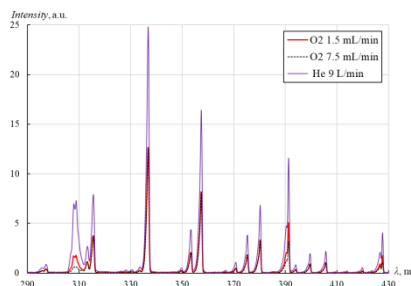


Fig. 2. The spectra of a CAPJs without O₂ and with addition of O₂

REFERENCES

- [1] D. Xu, D. Liu, B. Wang, C. Chen, Z. Chen, D. Li, Y. Yang, H. Chen, M. G. Kong “*In situ* OH generation from O₂ - and H₂O₂ plays a critical role in plasma-induced cell death,” PLoS One, vol. 10, p. e0128205, 2015.

* The work was supported by the NSTU Grants No. C21-22.

IMPULSE LASER APPLICATION FOR SURFACE MODIFICATION OF TOOL STEEL WITH B₄C-AL POWDERS

U.L. MISHIGDORZHIYN¹, N.S. ULAKHANOV^{1,2}, A.V. NOMOEV¹

¹ *Institute of Physical Materials Science of the SB, RAS, Ulan-Ude, Russia*

² *East Siberia State University of Technology and Management, Ulan-Ude, Russia*

e-mail: druh@mail.ru

The paper deals with the issues of Ytterbium Picosecond Pulsed Fiber Laser application in surface modification of hot-work tool steel 3Kh2V8F (the analog of AISI H21 steel). Surface modification was conducted by B₄C-Al powders injected in the surface from preplaced pastes followed by laser heating. The ratio of B₄C-Al powders was taken as 5/1 by weight and the paste thickness was approximately 1 mm. Laser treatment was conducted according to the following parameters: wavelength - 1070 Nm, power - 50 W, pulse energy - 1 mJ, pulse duration - 100 ns, and pulse frequency range - 50 kHz - 90 kHz. Several tracks with different widths were obtained as a result of treatment depending on the velocity of laser moving. EDS analysis showed that B₄C particles were not completely dissolved in the weld beads. However, an enhanced concentration of boron (8-12 wt.%) was revealed in the vicinity of B₄C particles. The aluminum concentration was low (up to 0.79 wt.%) on the surface of the weld beads.

THE STUDY OF RADIATION DAMAGE ASSESSMENT ON FUEL CLAD OF MNSR USING COMPUTATIONAL TOOLS*

A. SAMIRU, V.N. NESTEROV

National Research Tomsk Polytechnic University, Tomsk, Russia
e-mail: alhassan@tpu.ru

The focus on this article is to study the neutron flux distribution in the reactor core including radiation damage assessment on the clad. The GHARR-1 research reactor operates at maximum power of 30 kW in order to attain the flux of 10^{12} n.cm⁻².s⁻¹ as the nominal flux of the HEU core. The core excess reactivity of 4 mK, 348 fuel pins would be proven to be appropriate for the GHARR-1 LEU core. Due to its inherent safety features, stability of flux and moderate cost, the MNSR has recently found enormous application in various fields of science [1].

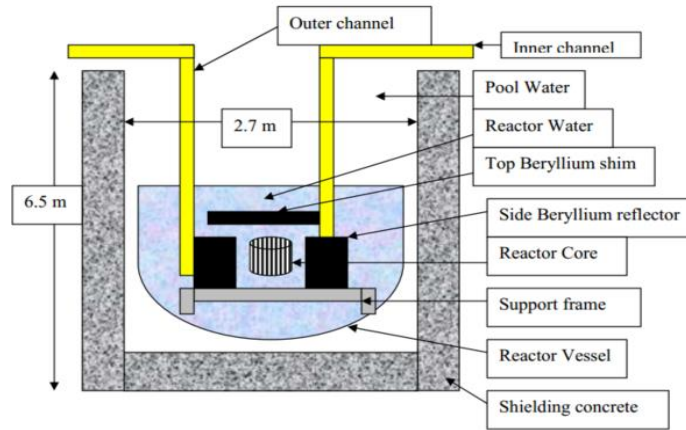


Fig. 1. Schematic view of the core of the MNSR- GHARR-1 [2].

The first calculation was intended to derive the flux of neutrons within the reactor core. This involved the calculation of all cross-sections \sum_a, \sum_{tr} :

$$-D^i \cdot B_i^2 \cdot \phi^i - \sum_a^i \phi^i - \sum_{k=i+1}^I \sum_R^{i \rightarrow k} \phi^i + \sum_{k=1}^{i-1} \sum_R^{k \rightarrow i} \phi^k + \varepsilon^i \cdot \sum_{k=1}^I \vartheta_f^k \cdot \sum_f^k \phi^k = 0, \quad (1)$$

The calculation of the K_{eff} is determined and compared to the enrichment at 10%, 12.5%, 16%, 20%, 30% and 90.2%. The K_{eff} calculation is also compared to the flux generation and burnup of the reactor. In this condition, the neutron flux at the various enrichment are used on the TRIM code for the radiation damage assessment to establish Zircaloy-4 clad as the best clad material. The replacement collisions, recoiling energy, interstitial energy and point defects created are used for the radiation assessment. The displacement per atom is estimated using the Norgett –Robinson Torrens model.

$$k_{NRT} \cong \phi_i \frac{\sigma_s(\bar{E}_n)}{5E_d} \Lambda \bar{E}_n. \quad (2)$$

REFERENCES

- [1] G.I. Balogun, "Automating some analysis and design calculation of Miniature Neutron Source Reactors", CERT (1), Annals of Nuclear Energy, 30, 81-92, 2003.
- [2] Y.A. Ahmed, T. Bezboruah, M. Johri, E.H.K. Akaho, "The low Power Miniature Neutron Source Reactors: Design, Safety and Applications", The Abdus Salam International Centre for Theoretical Physics, IAEA, 4, 2006.

* The work was supported in part by the RFBR Grants Nos. 20-08-00172 (theory) and 20-08-00249 (experiment).

EFFECT OF PLASMA ON PROLIFIRATION RATE OF HUMAN CELLS*

E.A. SHERSHUNOVA¹, S.I. MOSHKUNOV¹, S.V. NEBOGATKIN¹, O.S. ROGOVAYA²

¹*Institute for Electrophysics and Electric Power, RAS, Saint-Petersburg, Russia*

²*Koltzov Institute of Developmental Biology, RAS, Moscow, Russia*

e-mail: eshershunova@ieeras.ru

Today there is a growing interest in plasma medicine, which not only makes it possible to effectively treat bacterial diseases, but also shows encouraging results in oncology. It has been shown that oxygen and nitrogen radicals generated in plasma affect the DNA of cancer cells [1]. However, the mechanism of this effect is still being studied. In addition, there are no unambiguous data on the effect of plasma on healthy cells during plasma exposure. In this regard, we studied the effect of cold plasma on human skin cells: healthy keratinocytes of the HaCaT line and A431 human carcinoma cells from the Collection of Cell Cultures of the IDB RAS.

An argon DBD-based plasma jet was used as a plasma source [2]. The high-voltage pulse generator developed at IEE RAS served as a power source. It supplied the plasma reactor with 7 kV pulses of 1.5 μ s duration with a repetition rate of 3 kHz.

The cells had been growing in DMEM medium in an incubator for several days. Plasma treatment took place in vitro in Petri dishes at a distance of 30 mm to the medium surface from the reactor nozzle. The power density of the jet, estimated from the volt-coulomb characteristic based on the oscillograms data, was 0.72 mW/cm^2 . In the UV spectrum of the jet, there were lines of N_2 , OH , NO , N_2^+ with high reactivity. The result of exposure was estimated by the cell viability, a number of surviving cells and through the proliferation rate, the level of cell proliferation in 24 hours after treatment. The cell viability was assessed by staining cells with a vital dye, propidium iodide. The proliferation rate was assessed by measuring the amount of the specific protein ki-67, a marker of tumor growth in oncology.

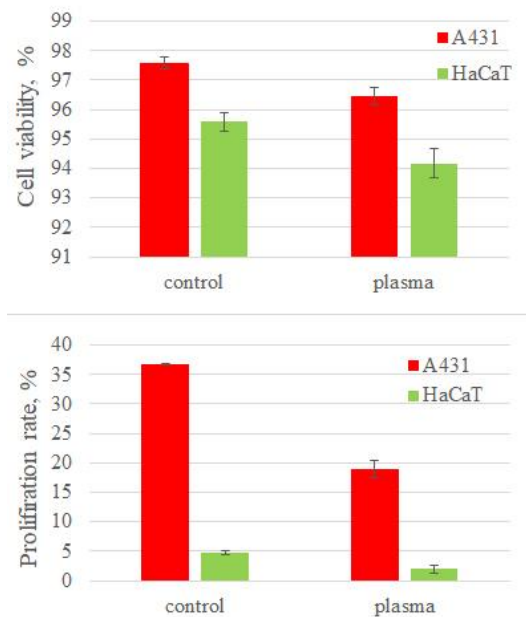


Fig. 1. Survival and proliferation rates of human keratinocytes and carcinoma cells without and after plasma exposure.

According to the obtained results (Fig. 1), it can be concluded that the effect of argon plasma on the viability of both cell lines is insignificant, while plasma strongly suppresses cell growth. With a minute exposure under described conditions, the growth of cancer cells slowed down almost 2 times in 24 hours.

REFERENCES

- [1] M. Keidar et al., "Cold atmospheric plasma in cancer therapy", *Physics of Plasmas*, vol. 20, n. 5, p. 057101, 2013.
- [2] E.A. Shershunova., S.I. Moshkunov, V.Yu. Khomich, "Features of Pulsed Argon Plasma Jet Impinging on Grounded Target", *IEEE Transactions on Plasma Science*, vol. 47, n. 11, p. 4909-4914, 2019.

* This work was partially supported by the Russian Foundation for Basic Research, grant 19-08-00069a.

THE DC PULSE CURRENT PATTERN INFLUENCE DURING SPARK PLASMA SINTERING

THET NAING SOE, I.M. MAKHADILOV, N.W. SOLIS PINARGOTE

Moscow State Technological University "STANKIN", Moscow, Russia

e-mail: kothetnaingsoe6151@gmail.com

Spark Plasma Sintering (SPS) is one of the most advanced nanopowder consolidation methods, which apply a uniaxial pressure and thermal expansion between the raw powder and the matrix using high heating rates (from 100 to 1000°C/min). The heating used for the sintering is mainly generated by Joule heating in a graphite matrix when a DC pulse current, created during the SPS process, crosses through them. Thanks to this, the thermal field in the sample is caused mostly by heat conduction from the matrix and others heating mechanisms as Joule heating, electrical discharges, and high-temperature plasma, associated with the electric current. The current is created by a DC pulse current generator, which can control the ON-OFF parameters of the DC pulses. Thereby, the use of pulse current during sintering promotes the appearance of spark discharges in the gap or at the point of contact between the material particles. The temperature in the spark discharge zones is in the order of about 1000°C, which leads to local melting and/or evaporation of the raw material in very short periods of time. This leads the formation of a neck in the contact zones between the powder particles due to the mass transfer process during sintering [1]. For this reason, the study of the influence of the pulse current form on the mechanical properties of sintered samples is a very interesting field of research, which requires a lot of attention due to its practical application. Unfortunately, only few research groups are carried out investigations in this field, and they established some dependence for the sintering of specific materials under certain conditions. For instance, Xie et al [2], showed that the frequency is a factor that influences on the homogenous temperature distribution through sintering raw powder, but it have not influence on the sintered sample material properties. On the other hand, a pulsed DC current during sintering can generate very high heating and cooling rates, which enhance the diffusion mechanism of the raw material, which in turn permit the grain growth control process, and leads to a combined improvement of different material properties that include high-temperature strength and good mechanical properties such as density, toughness, flexural strength and good surface stability at the high-temperature environment [3].

REFERENCES

- [1] D B Kumar, B S Babu, K M Aravind Jerrin, N Joseph, A Jiss. Review of Spark Plasma Sintering Process. IOP Conf. Series: Materials Science and Engineering 993. 2020.
- [2] G Xie, O Ohashi, K Chiba, N Yamaguchi, M H Song, K Furuya, T Noda. Frequency effect on pulse electric current sintering process of pure alumina. Materials Science and Engineering A359, 384-390, 2003.
- [3] N Sahed, Z Iqbal, A Khalil, A S Hakeem, N A Aqeeli, T Laoui, A Al-Qutub, R Kirchner. Spark Plasma Sintering of Metals and Metal Matrix Nanocomposites: A Review. Journal of Nanomaterials 2012, 983470, 4 June 2012.

CARBON NANOPARTICLES (CNP) COATED COPPER OXIDE (CuO) BY ELECTROPHORETIC SYNTHESIS

NAY WINAUNG, V.A. MAMONTOV, MYO MIN THAN, M.A. PUGACHEVSKII, THET PHYO NAING

Southwest State University, Kursk, Russia

e-mail: naywinaungnano@gmail.com

The nanocomposite film of Carbon Nanoparticles (CNP) coated with Copper Oxide (CuO) prepared by using the electrophoretic method [1]. The Single-wall Carbon Nanotubes (SWCNT) solution were centrifuged in miniSpin and the process of electric field used by confocal microscope [1]. The sizes and morphology of CNP-CuO nanocomposite particles determined from Atomic Force microscope (AFM) and Scanning Electron Microscope (SEM), the establishment of chemical structures determined by using Raman Spectroscopy.

Carbon Nanoparticles (CNP) solution are produced from SWCNT by using centrifugation method. During the electrophoretic forces process, the carbon nanoparticles coated copper oxide from the copper electrode. After evaporation process of CNP solution, CNP-CuO nanocomposite film were appeared between two copper electrodes under the electrophoretic forces [2]. The CNP-CuO nanoparticles size ranging from 16 – 38 nm using Atomic Force Microscope (AFM) (See Fig. 1).

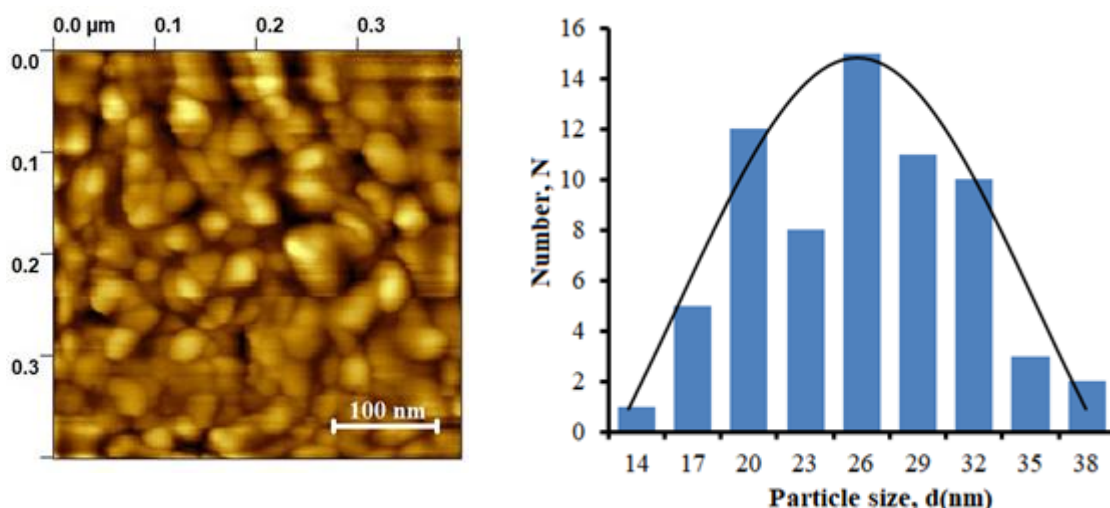


Fig. 1. AFM image of CNP-CuO nanoparticles film and the size of nanoparticles.

The chemical, vibrational and electronic properties of CNPs and the vibrational spectra of CuO can be distinguished from the Raman Spectroscopy [3]. The present of carbon, oxygen, copper in CNP-CuO are confirmed by elemental analysis using an energy dispersive attachment on a Scanning Electron microscope.

The method of electrophoretic synthesis makes it possible to obtain nanofilms based on carbon nanoparticles with a high degree of continuity. This technology can be applied to obtain film materials for infrared sensors with distinctive optical and operational characteristics.

REFERENCES

- [1] N.Q. Dung, D. Patil, H. Jung and D. Kim, "A high-performance nonenzymatic glucose sensor made of CuO-SWCNT nanocomposites," *Biosensors and Bioelectronics*, vol. 42, pp. 280–286, 2013.
- [2] M.T. Colel, V. Ciantanni and W.I. Milne, "Horizontal Carbon Nanotube Alignment," *Nanoscale*, pp. 1–12, 2016.
- [3] J. Maultzsch, H. Telg, S. Reich and C. Thomsen, "Radial breathing mode of single-walled carbon nanotubes: Optical transition energies and chiral-index assignment," *PHYSICAL REVIEW*, vol. 72, pp. 205438(1)–205438(16), 2005.

INFLUENCE OF THE CATALYST PACKING CONFIGURATION ON THE DISCHARGE CHARACTERISTICS AND CO₂ REDUCTION IN A PACKED BED PLASMA REACTOR*

M. ZHU¹, F.F. WU², H. MA², S.Y. XIE², C.H. ZHANG¹

¹Jiangsu Key Laboratory of New Energy Generation and Power Conversion, Nanjing University of Aeronautics and Astronautics, Nanjing, China

²Zhejiang Key Laboratory for Protection Technology of High-Rise Operation, ZheJiang HuaDian Equipment Testing and Research Institute Co., Ltd, Hangzhou, China
e-mail: zhumin@nuaa.edu.cn

Packed bed dielectric barrier discharge reactor (PB-DBD) is commonly used non-thermal plasma catalytic unit, mainly attribute to its simple structure, easy amplification, mild operating conditions. A PB-DBD in molecular gases at atmospheric pressure may show three types of discharges, i.e. streamer discharges, filamentary microdischarges, and surface discharges (so-called surface ionization waves) [1]. To be sure that these discharge types are closely related to the packing configuration of catalyst, especially for streamer and surface ionization waves, which are considered to be the key to excite plasma chemical reactions [2]. In literature, however, researchers are accustomed to using granular catalysts and packing them directly in the discharge gap, which makes it difficult to precisely adjust the structural characteristics of the catalyst. In this study, an array rod structure catalyst was proposed and used in the low-temperature plasma CO₂ reduction reaction. The array rods are arranged in the discharge gap in an orderly manner, with the aid of two 3D printing supports. The experimental device diagram is shown in Fig. 1. Al₂O₃ dielectric rods is used and the diameter of those are 0.5 mm, 0.8mm and 1mm. The filling numbers of 1 mm rods are set from 6 to 24, and the filling position of 0.5 mm rods are shown in Fig.2. It can be observed that the filling of Al₂O₃ dielectric rods in the discharge gap changes the characteristics of plasma discharge and CO₂ conversion. The closer the filling position of the dielectric rod is to the high-voltage electrode, the more conducive to the formation of the streamer discharge which benefits to improve CO₂ conversion. However, increasing the number of dielectric rods along the direction of the electric field is not conducive to the formation of discharges on the surface of the dielectric rods, but instead promotes the formation of streamer between the dielectric rods.

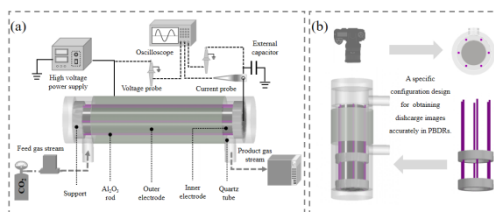


Fig. 1. Experimental device diagram.

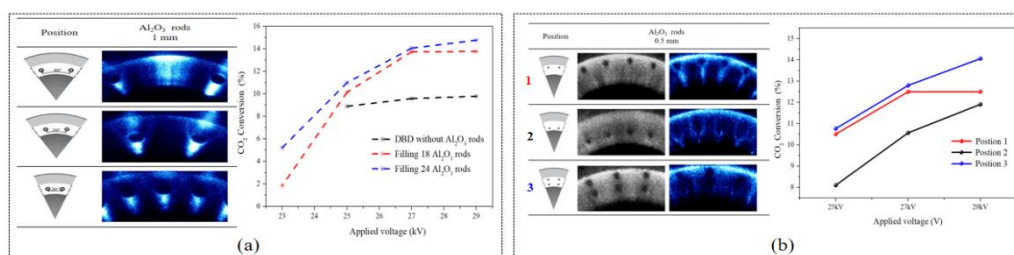


Fig. 2. Effect of filling number (a) and filling position (b) of Al₂O₃ rods on plasma discharge characteristics and CO₂ conversion.

REFERENCES

- [1] W. Z. Wang, H. H. Kim, K. Van Laer, and A. Bogaerts, "Streamer propagation in a packed bed plasma reactor for plasma catalysis applications," *Chem Eng J* 334, 2467-2479 (2018).
- [2] K. W. Engeling, J. Kruszelnicki, M. J. Kushner, and J. E. Foster, "Time-resolved evolution of micro-discharges, surface ionization waves and plasma propagation in a two-dimensional packed bed reactor," *Plasma Sources Sci* 27 (8) (2018).

* The work was supported by supported by the leading innovation and entrepreneurship team in Zhejiang Province (Project No.: 2019R01014); Natural Science Foundation of Jiangsu Province (Project No.:BK20200452); China Postdoctoral Science Foundation Funded Project (Project No.: 2020M681584).

INVESTIGATION OF PHOTOCATALYTIC ACTIVITY OF NANOPOWDER DOPED WITH SILVER OBTAINED BY PULSED ELECTRON BEAM EVAPORATION IN VACUUM*

O.A. SVETLOVA^{1,2}, V.G. ILVES², S.YU. SOKOVNIN^{1,2}

¹*Ural Federal University, Yekaterinburg, Russia*

²*Institute of Electrophysics, UB, RAS, Yekaterinburg, Russia*

e-mail: olma_20@mail.ru

Nanopowders doped with silver are promising materials for use in the medical and pharmaceutical sphere due to the antimicrobial, antitumor and other properties of the shell and bioinert nucleus.

Bismuth oxide often acts as an object in the creation of photocatalysts, an increase in stability is created due to silver, whose nanoparticles have bactericidal properties.

Were examined the photocatalytic properties of nanopowders obtained by PEBE in vacuum [1] from silver doped targets (1 and 5 wt%). The textural properties of the NP were studied by the BET method on the analyzer Micromeritics TriStar 3000 V 6.03 A. The pore sizes of the NP were 25.1 - 32.5 nm, volume 0.069-1.121 cm³/g, specific surface area (SSA) of the target 1.4 m²/g, SSA of samples 10 - 23 m²/g.

Nanopowders were annealed at a temperature from 0°C to 500°C, which reduced the defects in the structure of the test samples.

The photocatalytic activity of nanopowders was evaluated in comparison with the decomposition of methyl violet when irradiated with ultraviolet light. The rate of decomposition of MV from the time of exposure to UV radiation can be described by the linear equation $y = kx + b$, where the coefficient k is the rate of photodegradation (discoloration). The higher is the coefficient k , the faster is the solution discolored.

The results of the experiments are shown in Table.

Coefficient k value for NP Bi₂O₃ and Bi₂O₃+ Ag.

Sample (Bi ₂ O ₃ + Ag, mass. 1 %)	k		Sample (Bi ₂ O ₃ + Ag, mass. 5 %)	k	
	100 mkg/ml	300 mkg/ml		100 mkg/ml	300 mkg/ml
Test	-0.0134 (1)	-0.0134 (1)	Test	-0.0148 (1)	-0.0146 (1)
S0	-0.0139 (1.03)	-0.0261 (1.9)	S0	-0.0246 (1.66)	-0.031 (2.12)
S200	-0.0076 (0.57)	-0.016 (1.19)	S200	-0.0178 (1.20)	-0.0156 (1.06)
			S300	-0.0156 (1.18)	-0.031 (2.12)
S500	-0.0077 (0.57)	-0.0086 (0.64)	S400	-0.0175 (1.18)	-0.0168 (1.15)
			S500	-0.0149 (1.01)	-0.0126 (0.86)

* between parentheses relative values k

It was found that a sample with a firing temperature 300°C at the concentration 300 mkg/ml had the best values, among all the samples studied in the work. It is worth to note that in samples S300 and S200 there is a noticeable discoloration of the solution.

REFERENCES

- [1] V.G. Ilves, S.YU. Sokovnin, M.A. Uimin, «Production of nanopowders of bismuth oxide doped with silver by pulsed electron beam evaporation in vacuum». Abstract.

* The work was supported by the RFBR and GACR Grants Nos. 20-58-26002.

PLASMA SYSTEMS FOR FORMATION OF ELECTROHYDRODYNAMIC FLOWS

V.A. YAMSHCHIKOV, V.YU. KHOMICH

Institute for Electrophysics and Electric Power, RAS, Saint Petersburg, Russia
e-mail: yamshchikov@ras.ru

The work is devoted to the problem of obtaining electrohydrodynamic (EHD) flows formed during the interaction of plasma with the surrounding gas. It presents a theoretical model and the results of numerical simulation of EHD flows. Experimental dependences of the spatial profiles of the air flow velocity on frequency, voltage amplitude, average supply power, and dielectric substrate thickness have been obtained. The developed systems for the formation of EHD flows both based on barrier and corona discharges and examples of their application for pumping gas mixtures of electric-discharge lasers are considered. Special attention is paid to the possibility of active control of aerodynamic flows by plasma methods. The results of studies on the creation of multi-discharge actuator systems (MAS) for the formation of a flow in the boundary layer on extended aerodynamic surfaces are presented, and the promising nature of the method for controlling laminar flow on a swept wing using the developed MAS and their high-voltage power supply systems is demonstrated. In the final part, an ionocraft device is considered, in which a corona discharge is used to create a lifting force. Due to the achieved high thrust-to-power ratio of 6 N / kW, a thrust was obtained sufficient to lift an ionocraft with a mass of 35 g with an autonomous power supply unit on board weighing 20.5 g. Such devices can be useful for observation and communication facilities.

REFERENCES

- [1] Khomich V.Yu., Yamshchikov V.A. // *Phys. Usp.* 2017. V. 60. No. 6. P. 608-620.
- [2] Khomich V.Yu., Rebrov I.E. In-atmosphere electrohydrodynamic propulsion aircraft with wireless supply onboard // *Journal of Electrostatics.* 2018. V. 95. P. 1-12.
- [3] Khomich V.Yu., Yamshchikov V.A., Chernyshev S.L., Kuryachy A.P. // *Acta Astronautica.* 2021. V. 181. P. 292-300.

PRODUCTION OF NANOPOWDERS OF BISMUTH OXIDE DOPED WITH SILVER BY PULSED ELECTRON BEAM EVAPORATION IN VACUUM

V.G. ILVES², S.Yu. SOKOVNIN^{1,2}, M.A. UIMIN^{1,3}

¹*Ural Federal University, Yekaterinburg, Russia*

²*Institute of Electrophysics, UB, RAS, Yekaterinburg, Russia*

³*M.N. Mikheev Institute of Metal Physics, UB, RAS, Yekaterinburg, Russia*

e-mail: ilves@iep.uran.ru

Various bismuth containing compounds are promising in many applications, including for creating photocatalysts based on them using a visible range of light. Bismuth oxide is the simplest of the large family of bismuth oxides, so it most often acts as an object when creating new photocatalysts [1]. However, strong polymorphism (are known 9 polymorphic phases of Bi₂O₃), thermal instability and changes in the properties of bismuth oxide during long-term storage significantly complicate work with it. One way to increase stability and improve photocatalytic properties is by doping Bi₂O₃ with various metals, in particular Ag, which has bactericidal properties. Ag doped Bi₂O₃ nanoparticles are typically produced using chemical techniques often associated with the presence of toxic chemicals.

The present paper used an environmentally friendly method of producing Ag doped Bi₂O₃ nanopowders using the method of pulsed electron evaporation in vacuum. The evaporation target was obtained by solid phase synthesis in an electric furnace on air using silver nitrate additives (1 and 5 wt%).

Textural, thermal and magnetic properties of the obtained NP have been studied. Was found that the Ag- Bi₂O₃ NPs have a specific surface area (SSA) of 23.7 m²/g, which was almost 2 times bigger than the SSA of the pure Bi₂O₃ (13.2 m²/g) obtained previously [2].

DSC-TG analysis showed the presence of an amorphous fraction and impurity carbon in the NP, however, annealing at a relatively low temperature of 200°C led to degassing and improved crystallinity, SSA growth of all NP without exception. The thermal stability of the pure and Ag-doped Bi₂O₃ samples was maintained to the temperature 300-350°C. While further heating on air took place the phase transition $\beta \rightarrow \alpha$.

REFERENCES

- [1] T.O. Ajiboye, O.A. Oyewo, D.C. Onwudiwe, "The performance of bismuth-based compounds in photocatalytic applications", Surf. Interfaces, vol. 23, pp. 100927-1-100927-19, 2021.
- [2] S.Yu. Sokovnin, V. Il'ves, "Production of nanopowders using pulsed electron beam," Ferroelectrics, vol. 436(1), pp. 101-107, 2012.

INFLUENCE OF RESIDUAL GAS ON THE FIELD ELECTRON EMISSION CHARACTERISTICS OF GRAINED STRUCTURAL GRAPHITE

A.S. CHEPUSOV, A.A. KOMARSKIY, S.R. KORZHENEVSKIY

*Institute of electrophysics UB RAS, Ekaterinburg, Russia
e-mail: chepusov@iep.uran.ru*

Field electron emission plays an important role in the operation of electro-vacuum devices. It can operate as an independent electrode as well as be a source of electrons leading to a decrease in the dielectric strength of the gap [1]. Thus, the study of the field emission properties of various materials is a significant issue of vacuum electronics and devices associated with various kinds of discharges.

In recent decades, carbon cold emitters have been of great interest: thin films, nanotubes, diamond-like structures, etc. The level of the achieved emission current makes it possible to initiate a discharge [2, 3]. Also, massive cathodes made of structural graphite are considered as promising field emitters [4].

A study of field emission cathodes made of granular structural graphite of GMZ, MG and MPG-7 grades operating under technical vacuum conditions, at a pressure of $2 \cdot 10^{-4}$ Pa \div 10^{-2} Pa (in an argon atmosphere) was carried out. Experiments with recording current-voltage characteristics (CVC), long-term studies (LTS) under various vacuum levels have been provided.

The results show a change in the emission characteristics of cathodes after long-term operation under technical vacuum conditions: increase in threshold voltage of CVC, oscillations of the LTS are observed. Calculations of the field enhancement factor β for all stages have been carried out. The results show that the field enhancement factor for CVCs in Ar is 20% lower than for ones under the best vacuum level (10^{-4} Pa) (see Fig. 1).

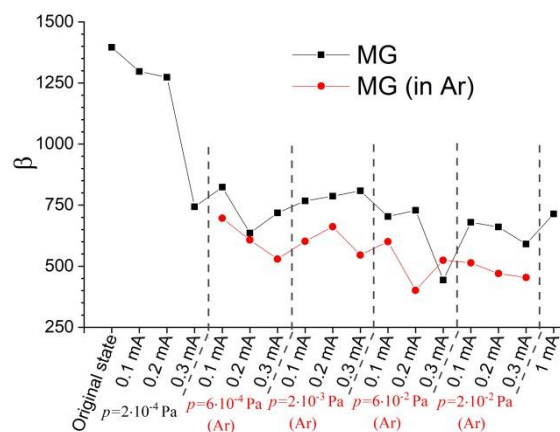


Fig. 1. Dynamics of field enhancement factor for MG sample.

The experimental results demonstrate the effect of vacuum conditions on the field emission properties of carbon cathodes. One of the factors is the residual gas ions impact and consequently a change in the field amplification factor.

REFERENCES

- [1] J.W. Flowers, "The Initiation of Electrical Discharges by Field Emission", Phys. Rev., 48, 954. 1935.
- [2] S.S. Baturin, T. Nikhar, S.V. Baryshev, "Field electron emission induced glow discharge in a nanodiamond vacuum diode", J. Phys. D: Appl. Phys., 52, 325301, 2019.
- [3] D. Wenger, W. Knapp, B. Hensel, S.F. Tedde, "Evidences for Field Emission Initiated Glow Discharge at High Currents", Technical Digest 27th International Vacuum Nanoelectronics Conference, Engelberg, Switzerland, 2014.
- [4] E.P. Sheshin, "Surface structure and field emission properties of carbon materials", Moscow: MIPT Publishing, 2001.

PHOTOCHEMICAL CONVERSION PROCESSES IN PETROLEUM

U.J. YOLCHUEVA, R.A. JAFAROVA, S.Y. RASHIDOVA, Z.F. HASHIMZADE SEYID, S.A. SULEYMANOVA

Y.H. Mamedaliyev's Institute of Petrochemical Processes, ANAS, Baku, Azerbaijan
e-mail: u.jevhunzade@gmail.com

In petroleum, several photophysical and photochemical transformations can run over time as a result of photorays as well as sunlight and molecular oxygen effect, and the study of these processes is quite important from the point of petroleum storage and their efficient use. Irradiation with light and especially UV rays is an effective means of initiating organic compounds. In accordance with the laws of photochemistry, the absorption of one quantum of light can activate one molecule and, therefore, initiate one chain. Thus, the prerequisite for initiating the process is the absorption of light. Note that, in contrast to simple olefinic hydrocarbons, aromatic compounds, as well as polyenes with conjugated double bonds, easily absorb light in the UV part of the spectrum. It is well known that the effect of ultraviolet (UV) radiation on polyaromatic hydrocarbons (PAHs) is accompanied by chemical reactions - dimerization, formation of excimers, addition, etc. Photooxidation of PAHs is most often manifested [1, 2].

The composition of crude oil is extremely complex and varies depending on the oil sample. The composition of the oil can change even over a certain period of time for samples taken from the same well. In oils in the presence of molecular oxygen under the influence of ultraviolet and visible radiation, photophysical and photochemical processes occur, which lead to structural changes in the molecules of hydrocarbons present in them.

Studies show that, in contrast to secondary products of oil refining, the content and degree of condensation of aromatic hydrocarbons (AH) in the primary products of refining is less. These products are more stable than secondary products and have large raw materials. Therefore, the study of photochemical processes and their mechanisms in primary oil products is very important for the rational use of oil products isolated from them as raw materials for oil refining, petrochemical, and other industries.

This article presents the results of studies of the oxidation of aromatic hydrocarbons, isolated from natural heavy oil from the Balakhani field of the Absheron Peninsula of Azerbaijan, by atmospheric oxygen.

Particular aromatic group hydrocarbons have been separated according to refractive indices by using the adsorption column with purpose of more accurate studying of conversion processes occurring under impact of ultraviolet rays in Balakhany petroleum (from the oil field near Baku) hydrocarbons of aromatic group and their mechanisms were studied by spectral methods (ultraviolet-visible and infrared spectrophotometry): Aromatic hydrocarbons of I group, aromatic hydrocarbons of II group, aromatic hydrocarbons of III group, aromatic hydrocarbons of IV group. In sequence of these groups, it has been established that the petroleum composition is constituted properly by mono-, bi-, tri- and tetracyclic aromatic hydrocarbons (AH). It has been determined that optical densities of absorption bands compatible to bi- and tricyclic polycyclic aromatic hydrocarbons decrease with an increase of period of photoirradiation affecting the aromatic group hydrocarbon components, and their absorption bands maxima undergo the hypsochromatic shift that is characteristic for electronodonor substances and change its position in the direction of spectral region of high energy, meanwhile the absorption maxima (243, 244, 247, 248 and 250 nm) relating to quinone compounds are recorded. In this process, the increase of optical density of absorption band maximum at about 200 nm shows the formation of endoperoxides. It has been established that the photochemical conversion processes in the shown petroleum occur by chain-radical and molecular mechanisms.

REFERENCES

- [1] U.J. Yolchuyeva, R.A. Jafarova, Ch.K. Salmanova, M. Khamiyev, "Photochemical investigation of aromatic hydrocarbons of Balakhani crude oil as petroleum luminophores", *Applied Petrochemical Research*, No. 3, pp. 139-148, 2020.
- [2] U.J. Yolchuyeva, R.A. Jafarova, M. Khamiyev, "Investigation of photochemical conversion processes in aromatic hydrocarbons of Balakhani oil", *Journal of Petroleum Science and Engineering*, V. 196, 2021.

INVESTIGATION OF THE ROLE OF CHEMICALLY ACTIVE RADICALS IN THE ANTIBACTERIAL PROPERTIES OF A LOW-TEMPERATURE PLASMA JET AT AMBIENT PRESSURE MIXED WITH ARGON AND AIR*

N.A. ASHURBEKOV¹, Z.M. ISAEVA¹, G.S. SHAKHSINOV¹, K.M. RABADANOV¹, A.A. MURTAZAEVA^{1,2}, E.KH. ISRAPOV²

¹*Dagestan State University, Makhachkala, Russia*
²*Institute of Physics, DFRC of RAS, Makhachkala, Russia*
e-mail: nashurb@mail.ru

The authors investigate the antibacterial effect on biological tissues of a low-temperature atmospheric pressure plasma-jet mixed with air and argon and used in plasma medicine [1-4].

An atmospheric pressure plasma-jet was produced by a nanosecond barrier discharge in a flow of air mixed with argon in a quartz tube with an inner diameter of 1 mm and an outer diameter of 7 mm.

Placed inside the tube was a needle electrode with a diameter of 0.5 mm, to which voltage pulses with an amplitude of up to 12 kV with the frequency of 100 Hz, and a front duration of about 100 ns were applied. On the outside of the quartz tube, at a distance of 60 mm from the high-voltage electrode, was a grounded ring-shaped metal electrode. Argon was pumped through the air tube with an adjustable gas flow rate in the range of 0.2-1 l/min.

The relationship between the antibacterial properties of the plasma-jet and the intensity of the spectral emission lines of OH-(309 nm), N₂ (337 nm), N₂ (356 nm) was investigated depending on argon flowrate and the amplitude of voltage pulses on the electrodes at different segments of the plasma-jet.

To analyze the kinetic processes in the plasma source in the current study, the numerical simulation of ionization processes was carried out with Comsol Multiphysics software using its Plasma Module. The numerical model consists of several interconnected physical interfaces, including the kinetics of the plasma model and the model of flow dynamics. In the plasma model, the continuity equation (1), the electron energy conservation equation (2), and the Poisson equation (3) were applied.

$$\frac{\partial}{\partial t}(n_e) + \nabla \cdot \Gamma_e = R_e, \quad (1)$$

$$\frac{\partial}{\partial t}(n_e) + \nabla \cdot \Gamma_e + \mathbf{E} \cdot \Gamma_e = S_{en}, \quad (2)$$

$$\nabla^2 V = -\frac{q}{\epsilon_0} \left(\sum_i N_j^+ - n_e \right). \quad (3)$$

The geometry of the simulation area was chosen based on the actual size of the discharge tube and the configuration of the electrode system.

The dynamics of the distribution of excited molecules and atoms in the plasma-jet, as well as the kinetic plasma processes inside the plasma-jet, affecting the antibacterial effect of the plasma-jet on biological tissues with pathology, are analyzed.

REFERENCES

- [1] Z. Xu, et.al., "Applications of atmospheric pressure plasma in microbial inactivation and cancer therapy: a brief review," *Plas. Sc. and Tech.*, vol. 22, no. 10, p. 103001, 2020.
- [2] E. Sysolyatina, M. Vasiliev, M. Kurnaeva, I. Kornienko, O. Petrov, V. Fortov, A. Gintsburg, E. Petersen, and S. Ermolaeva, "Frequency of cell treatment with cold microwave argon plasma is important for the final outcome," *J. of Phys. D: Appl. Phys.*, vol. 49, no. 29, p. 294002, 2016.
- [3] N.Y. Babaeva and G.V. Naidis, "Modeling of Plasmas for Biomedicine," *Trends in Biotechnology*, vol. 36, no. 6, pp. 603–614, 2018.
- [4] N.A. Ashurbekov, K.M. Giraev, G.S. Shakhshinov, E.K. Israpov, Z.M. Isaeva, A.A. Murtazaeva, and K.M. Rabadanov, "Interaction of low-temperature atmospheric pressure plasma jet mixed with argon and air with living tissues," *J. of Phys.: Conf. Ser.*, vol. 1697, p. 012044, 2020.

* The work was partially funded by RFBR grant № 19-32-90180.

ELECTRIC ARC IN PLASMA FLOW OF GAS DISCHARGE WITH A LIQUID ELECTROLYTE CATHODE

G.K. TAZMEEV¹, A.K. TAZMEEV¹, B.K. TAZMEEV²

¹Kazan Federal University, Naberezhnye Chelny Institute, Naberezhnye Chelny, Russia

²Kuban State Agrarian University named after I.T. Trubilin, Krasnodar, Russia

e-mail: gktazmeev@kpfu.ru

A distinctive feature of gas discharge with liquid electrolyte cathode is multi-channel nature in region of binding to electrolyte. As the current increases, discharge channels become larger. In the ranges of currents of amperes and tens of amperes, they are clearly recorded in high-speed video frames [1, 2]. Under certain conditions, a contracted channel is formed in discharge gap [3, 4]. At the same time, the general multichannel is preserved. The contracted channel appears and disappears randomly. In this work, the possibility of formation of contracted channel in controlled mode is investigated.

The gas discharge was ignited between the metal anode 1 and the liquid electrolyte 2, which flowed out from the vessel 3 in the form of a glass (Fig. 1). A graphite plate 4 was located inside the vessel for supplying a negative potential from a power source. The electric arc was ignited between the metal anode 1 and the cathode 5. The current was regulated by a step change in ballast resistors 6 and 7. The power source was a three-phase full-wave rectifier with an output voltage of 1200 V.

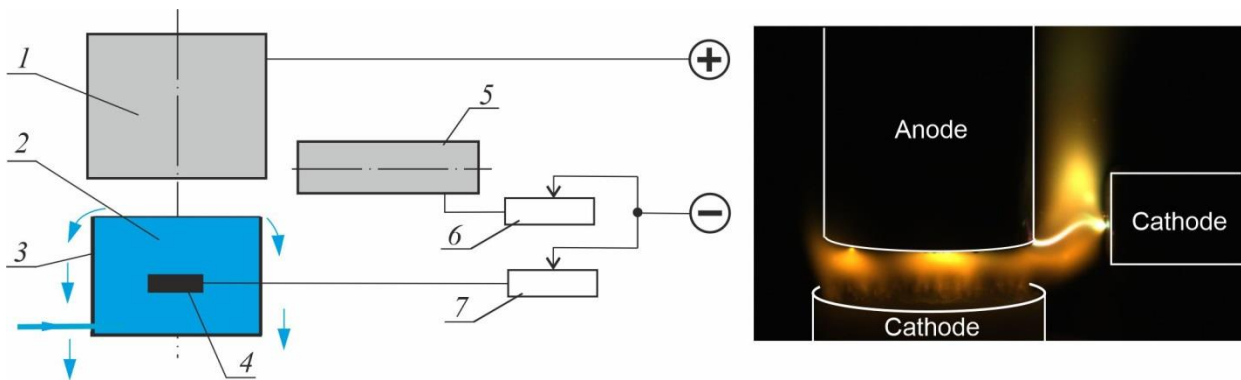


Fig. 1. Diagram of the experimental setup and snapshot of the discharges.

The gas discharge current with a liquid electrolyte cathode was set in the range of 5-10 A, and arc current varied in the range of 1-10 A. Aqueous solutions of sodium chloride with a specific electrical conductivity of 10-15 mS/cm were used as a liquid electrolyte. Spectra of radiation of plasma were investigated. Intense spectral lines of hydrogen were recorded.

In configuration of the electrodes shown in fig. 1, the electric arc was displaced upward under influence of plasma flow and heated gases. Its spatial position was constantly changing. In this work, other options for location of electrodes were investigated. The search for conditions under which the steady burning electric arc occurs was carried out.

REFERENCES

- [1] G.K. Tazmeev, B.A. Timerkaev and K.K. Tazmeev, "Study of the binding zone of electrical discharge to the liquid cathode by high-speed visualization," *Journal of Physics: Conference Series*, vol. 789, p. 012059, 2017.
- [2] R.N. Tazmeeva and B.K. Tazmeev, "Development features of the plasma flow in the gas discharge with the liquid electrolyte cathode", *Journal of Physics: Conference Series*, vol. 1328, p. 012074, 2019.
- [3] Kh.K. Tazmeev and A.Kh. Tazmeev, "Gas discharge with liquid electrolyte cathode in the mode of occurrence of the constricted channels", *Journal of Physics: Conference Series*, vol. 5677, p. 012035, 2014.
- [4] G.K. Tazmeev, B.A. Timerkaev and A.K. Tazmeev, "The emergence and development of spark channels in the plasma column of a gas discharge between water-solution cathode and a copper anode," *Journal of Physics: Conference Series*, vol. 927, p. 012064, 2017.

PECULIARITIES OF ELECTROPHORETIC DEPOSITION OF NANOPOWDERS OF VARIOUS MORPHOLOGIES USED FOR OPTICAL CERAMICS FABRICATION*

E.G. KALININA^{1,2}, M.G. IVANOV^{1,2}, D.S. RUSAKOVA¹

¹*Institute of Electrophysics, UB RAS, Yekaterinburg, Russia*

²*G.G. Devyatikh Institute of Chemistry of High-Purity Substances, RAS, Nizhny Novgorod, Russia*

e-mail: jelen456@yandex.ru

A promising colloidal method for compacting powder materials that does not require expensive technological equipment is electrophoretic deposition (EPD) [1]. This method gives a chance to control easily the thickness, morphology, and microstructure of EPD green body by changing the composition of the suspension, deposition time, applied voltage and / or current. The advantages of the EPD determine the prospects for its application in the fabrication of bulk elements of optical ceramics.

The aim of this work is to study the formation of bulk elements of scintillation and magneto-optical ceramics by the EPD from non-aqueous suspensions of nanopowders with different morphologies obtained by laser evaporation method – $\text{Ce}^{3+}:(\text{La}_x\text{Y}_{1-x})_2\text{O}_3$ (YLaCe) and self-propagating high-temperature synthesis (SHS) – 5% $\text{La}:\text{Ho}_2\text{O}_3$ (HoLa) and $(\text{Dy}_{0.7}\text{Y}_{0.25}\text{La}_{0.05})_2\text{O}_3$ (DyLaYO). Powders obtained by the laser evaporation consist of spherical, weakly agglomerated nanoparticles ($S_{\text{BET}} = 76 \text{ m}^2/\text{g}$). SHS powder is a mixture of lamellar nanoparticles ($S_{\text{BET}} = 36 \text{ m}^2/\text{g}$). The choice of a dispersion medium, as well as the use of dispersants, is one of the most important factors affecting the deposition efficiency and characteristics of the green body. Acetylacetone and polyethyleneimine (PEI) additives, which were selected according to electrokinetic studies (zeta potential and pH), were used in nanopowder suspensions. The main tasks of the work were to determine the effect of the composition of the dispersion medium, the time of sedimentation, the aging of the suspension on the zeta potential and pH of the suspensions, the current during EPD, mass deposition rate of the green body, the thickness and density of dry compacts. The peculiarities of the kinetics of the current and the morphology of the sediment were investigated for different geometry of the EPD electrodes. It was found that the configuration of the EPD cell significantly affects the kinetics of the current at the initial period of the EPD (about 30 min). In the case of vertical deposition, an increase in the current was observed, after which a further decrease occurs. For horizontal deposition there is an unambiguous trend towards a decrease of the current. It is shown that the optimal EPD for the formation of a homogeneous dense green body is vertical deposition from nanopowder suspensions in isopropyl alcohol at an electric field strength of 20 V/cm. The density of the obtained compacts with a thickness of 2.4 mm after drying reached 37% of the theoretical value.

REFERENCES

- [1] E.G. Kalinina, E.Yu. Pikalova, "New trends in the development of electrophoretic deposition method in the solid oxide fuel cell technology: theoretical approaches, experimental solutions and development prospects", *Russ. Chem. Rev.*, vol. 88, pp. 1179-1219, 2019.

* The work was supported by the Russian Science Foundation (research project No. 18-13-00355).

ONE OF THE METHODS OF NUMERICAL OPTIMIZATION IN CHEMICAL KINETICS PROBLEMS*

L.N. KASHAPOV, N.F. KASHAPOV, V.YU. CHEBAKOVA

Kazan Federal University, Kazan, Russian Federation

e-mail: vchebakova@mail.ru

This paper shows the application of numerical optimization methods to the solution of inverse problems, arising when predicting the current yield of substances. In this paper, the inverse kinetic problem that arises when modeling cathodic during the obtaining hydrogen by electrolysis were set. An algorithm for its solution based on numerical optimization methods is proposed. The proposed algorithm is based on the direct Hook-Jeeves method, supplemented by constraints check, and the Runge-Kutta method used to solve the kinetic equations system describing consecutive electrochemical reactions. The solution method was tested on the full-scale experiment data, and it showed close quantitative and qualitative agreement of the numerical result with the presented experimental data.

According to [1], the electrolyzer has an internal diameter of 50 mm, the working area of the electrodes is 60 cm², and the height of the electrolyte level is 300 mm. The electrolyte is 30% KOH solution. Since the temperature in the cell was kept constant by means of a regulating potentiometer, the equation of the electrolyte temperature is considered constant according to the data of [1]. Table 1 shows the experimental results of work [1] and calculation results of the present work, minimization was carried out using a single value of the hydrogen concentration at the time $t = 0.28$ (of an hour), and the relative calculation results deviation from the experimental data.

t, hour	0.5 A, T=60°C			1 A, T=60°C		
	Work [1] experiments, %	Calculated values, %	Relative deviation	Work [1] experiments, %	Calculated values, %	Relative deviation
0.07	0.00874	0.0086	1.6	0.0172	0.0162	5.8
0.14	0.01672	0.0173	3.4	0.0352	0.0325	0
0.21	0.0292	0.0260	10.9	0.052	0.0489	6
0.28	0.0348	0.0348	0	0.0654	0.0654	0
0.35	0.04	0.0436	9	0.08	0.0820	2.5
0.42	0.0484	0.0525	8.4	0.0892	0.0988	10.7

Table 1. Comparison of the experimental data of [1] with the calculations of this work, minimization was carried out according to the hydrogen concentration at the time $t = 0.28$.

This numerical algorithm makes it possible to find the constants rates during electrode processes in accordance with the specified experimental data on the yield, and to calculate the concentrations of substances participating in the near-electrode processes at the required time points. The proposed numerical algorithm makes it possible to reduce the amount of experimental data required for predicting, and can also be generalized to predict the yield of the deposited material in electroplating and discharge with liquid electrodes [2, 3].

REFERENCES

- [1] Babaev, R.K., Aliev, S.A. "Kinetics investigation of hydrogen production by water electrolysis", Problems of Science, no. 4 (28), p. 31-33, 2018.
- [2] Kashapov, R.N., Kashapov, L.N., Kashapov, N.F. "Investigation of CoCr micropowder obtaining process in gas discharge with liquid electrodes", Journal of Physics: Conference Series, vol.1328(1), art. 012105, 2019.
- [3] Kashapov, R.N., Kashapov, L.N., Kashapov, N.F. "Investigation of parameters of low-temperature gas discharge plasma with liquid electrodes upon receipt of metal powder", Journal of Physics: Conference Series, vol. 1328(1), art.012104, 2019.

* This work was supported by the Russian Foundation for Basic Research (№ 20-08-01005, 19-08-01184, № 18-48-160041 p_a)

LASER PLUME GLOW ON A SURFACE OF NON-ROTATING AND FAST-ROTATING TARGET

V.A. SHITOV

Institute of Electrophysics UB, RAS, Yekaterinburg, Russia

e-mail: vlad@iep.uran.ru

The purpose of this work was to investigate the glow dynamics of a plasma plume under the action of laser radiation on non-rotating and fast-rotating target.

An electroionization CO₂-laser operating in a single-pulse mode with predetermined amplitude and pulse duration was used as a source of radiation. The glow of plasma formed near the surface of a stainless steel disk was registered by a photo camera using an optical light filter. Time of exposure was 33.3 ms.

The laser plume spreads perpendicular to the disk surface at low levels of power density. The plume height and the plasma glow intensity increased with an increase in the power density. It was found that a component directed along the laser beam is released in the erosion plume when the power density reaches $5.5 \cdot 10^6$ W/cm², which can be interpreted as the formation of a low-threshold optical discharge (breakdown) in the erosion plume. With a further increase in the power density the plasma component directed along the beam increases and, finally, becomes dominant (fig. 1).

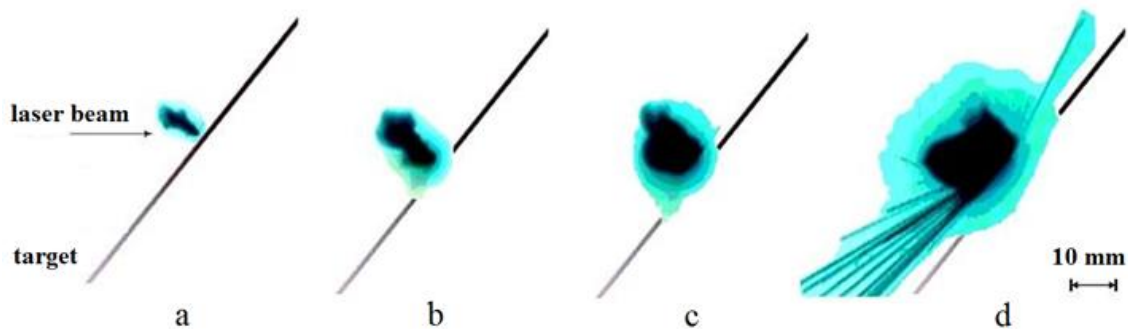


Fig. 1. Photograph of plasma glow. Power density of laser radiation:

a – $2.1 \cdot 10^6$ W/cm²; b – $5.5 \cdot 10^6$ W/cm²; c – $6.2 \cdot 10^6$ W/cm²; d – $7.3 \cdot 10^6$ W/cm².

Rotation of the disk, linear speed of which was 50 m/s relative to the laser beam dramatically changed the situation. No breakdown phenomena were observed when the power density reached $7.3 \cdot 10^6$ W/cm² at which the optical breakdown was recorded in the experiments with the non-rotating target. Moreover, a further increase in the power density up to $5 \cdot 10^7$ W/cm² did not cause the optical breakdown.

The absence of breakdown in vapors of the target material is an obvious fact and is due to the lower heating of the vapors in this case. It would seem that breakdown in air is not related to target evaporation, but in fact it usually occurs directly near the surface where the power density increases upon reflection. However, the gas layer near the target surface is not only the place of breakdown initiation, but also the boundary layer, which is captured by the target under moving conditions. The constant change of gas at a speed of 50 m/s prevents it from heating up in the place of the expected breakdown and inhibits the development of ionization processes causing optical breakdown. From this it follows that for each specific case (power and duration of radiation, type of target) it is possible to choose the speed of the beam movement relative to the target, at which there will be no optical breakdown.

SYNTHESIS OF CEMENT CLINKER USING PLASMA TECHNOLOGY*

N.K. SKRIPNIKOVA, V.V. SHEKHOVTSOV, M.A. SEMENOVYKH, R.YU. BAKSHANSKIY

Tomsk State University of Architecture and Building, TSUAB, Tomsk, Russia
e-mail: shehovcov2010@yandex.ru

The synthesis of cement clinker is complex, multifactorial process, where the line between its constituent factors is very thin and undergoes systematic changes associated with deviations in the chemical and granulometric compositions of the raw mixture technological regime of its preparation and firing. To obtain cement clinker using traditional technology, which has the necessary qualities and required technical properties (optimal mineralogical composition, structure and hydraulic activity), raw mixtures go through number of complex, energy-intensive processes, including the regulation of chemical and particle size distribution, homogenization, heat treatment, cooling of cement clinker, etc. However, even the constancy of technological modes is unable to ensure the stable quality of synthesized clinker minerals. This indicates the influence on the kinetics of the clinker formation process main, fundamental factors - the physicochemical characteristics of raw materials, which include the nature of raw materials, the dispersion and structure of their minerals, and chemical composition. In this regard, the proposed design of the installation (Fig. 1) for the production of cement clinker [1-3].

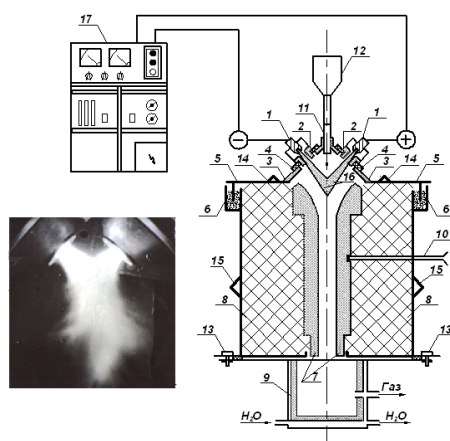


Fig. 1. Diagram of the experimental setup - plasma-chemical reactor: 1 - electrode; 2 - nozzle; 3 - pyramid; 4 - insulator; 5 - cover; 6 - sand gate; 7 - graphite reactor; 8 - lining; 9 - refrigerator; 10 - tungsten-rhenium thermocouple; 11 - water-cooled powder feed tube; 12 - vibrating dispenser of granular raw mixture; 13 - rubber seal; 14 - water pipe for cooling the reactor lid; 15 - water conduit for cooling the side walls of the reactor; 16 - plasma arc; 17 - power supply UPR-4011.

The presented installation of plasma-chemical reactor (Fig. 1) is thermal unit consisting of direct-flow electrode assemblies (1) - cathode and anode, located symmetrically in the vertical plane at an angle of 30–45° to the reactor axis. The experimental installation of plasma-chemical reactor allows obtaining high concentration of energy in small volumes and is characterized by compactness, with capacity of 60 kg of cement clinker per hour. The use of plasma-chemical reactor makes it possible to produce small batches of cement clinker with different mineralogical composition for the production of special types cement (fast-hardening, plasticized, hydrophobic, expanding, stressing, etc.) with the introduction of appropriate additives, which is unprofitable with traditional technology.

REFERENCES

- [1] N. Skripnikova, G. Volokitin, M. Semenovikh, and V. Shekhovtsov, "Features of synthesis of clink minerals under conditions of high-concentrated heat flows," *Proceedings - 2020 7th International Congress on Energy Fluxes and Radiation Effects, EFRE 2020*, 9241998, pp. 769-772, 2020.
- [2] N.K. Skripnikova, V.V. Shekhovtsov, V.A. Vlasov, O.G. Volokitin, and G.G. Volokitin, "Thermodynamic analysis of cement clinker formation using low temperature plasma," *Journal of Physics: Conference Series*, V. 1393, no. 1, Art. 012137, 2019.
- [3] V.V. Shekhovtsov, O.G. Volokitin, V.I. Otmakhov, G.G. Volokitin, and N.K. Skripnikova, "Investigation of Hollow Microspheres Obtained in Thermal Plasma Jet Using Ash-Slag Wastes from CHP in Kemerovo Oblast," *Glass and Ceramics*, V. 75, no. 1-2, pp. 32-35, 2018.

* The work has been conducted with the financial support of the Government Assignment of the Ministry of Education and Science of the Russian Federation (project No. FEMN-2020-0004).

OBTAINING GLASS-CRYSTALLINE MATERIALS USING ARC PLASMA*

G.G. VOLOKITIN, N.K. SKRIPNIKOVA, V.V. SHEKHOVTSOV, M.A. SEMENOVYKH, R.YU. BAKSHANSKIY

Tomsk State University of Architecture and Building, TSUAB, Tomsk, Russia
e-mail: shehovcov2010@yandex.ru

Glass-crystalline materials can be considered as monolithic composites consisting of fine-grained crystals evenly distributed in the glassy phase. The disordered orientation of the crystals means that the properties of glass-crystalline materials are independent of the direction in which they are measured. The most important characteristics of glass-crystalline materials are their exceptional fineness and ideal polycrystalline structure. The technological process of plasma production of glass-crystalline materials consists in grinding and thorough mixing of components, melting and forming products [1].

To study the influence of the technological features of the plasma melting method on the quality of the resulting silicate melt, an experimental setup was created at the Department of Applied Mechanics and Materials Science of TSUAB [2]. In fig. 1, *a* shows the curves of the dependence of the high-temperature viscosity on the temperature synthesized silicate melt based on the raw mixture and the ash-and-slag waste melt without correcting additives. In fig. 1, *b* shows the dependence of the amount formed melt on the time of exposure to plasma flows.

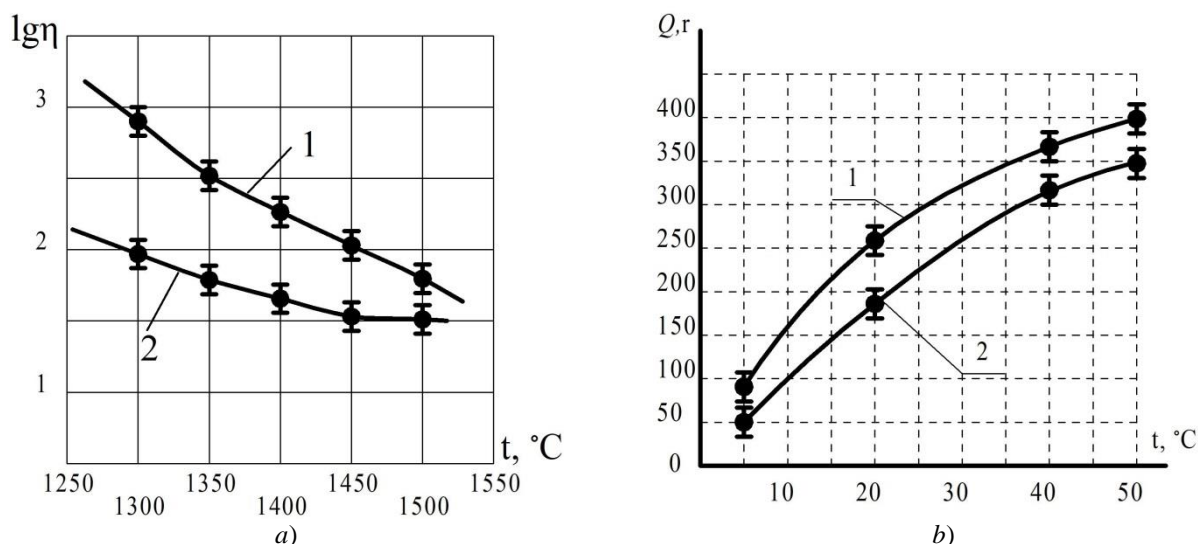


Fig. 1. *a*) Temperature dependence of the melt viscosity in the molding region;
b) Dependence of the amount of formed melt on the time of exposure to plasma flows ($P = 50$ kW).
1 - amount of the melt raw mixture; 2 - the amount of TPP ash melt without corrective additives.

Analysis of the values viscosity resulting melt makes it possible to recommend it for production by casting and pressing. This will have positive effect on the manufacturability melt and will make it possible to obtain products by the free casting method. It was also found that the melting of the studied raw mixtures at specific heat fluxes $q = 1.8-2.6 \cdot 10^6$ W/m², and temperature of 2000-3000°C, volt-ampere characteristics are in the range: $I=240-260$ A, $U=120-140$ V, makes it possible to obtain a silicate melt enriched with anorthite of the following chemical composition: $SiO_2 - 61.89 \div 40.22$; $Al_2O_3 - 20.4 \div 30.3$; $CO - 9.8 \div 20$; $MgO - 1.7 \div 1.89$; $Fe_2O_3 - 4.9 \div 5.32$; $NaO - 0.51 \div 1.15$; $TiO_2 - 0.8 \div 1.12$.

REFERENCES

- [1] O. G. Volokitin and V. V. Shekhovtsov, "Prospects of application of low-temperature plasma in construction and architecture," *Glass Phys. Chem.*, vol. 44, no. 3, pp. 251–253, May 2018.
- [2] V. A. Vlasov, O. G. Volokitin, G. G. Volokitin, N. K. Skripnikova, and V. V. Shekhovtsov, "Calculation of the melting process of a quartz particle under low-temperature plasma conditions," *JEPT*, vol. 89, no. 1, pp. 152–156, Feb. 2016.

* The work has been conducted with the financial support of the Government Assignment of the Ministry of Education and Science of the Russian Federation (project No. FEMN-2020-0004).

Section 4

SOURCES OF LOW-TEMPERATURE PLASMA:

generators of continuous,
pulse-periodic
and pulsed action,
gas switches,
power supply

THE 40 YEARS TO RADAN – COMPACT MULTI-PURPOSED SOURCES FOR VARIOUS PULSE POWER INVESTIGATIONS*

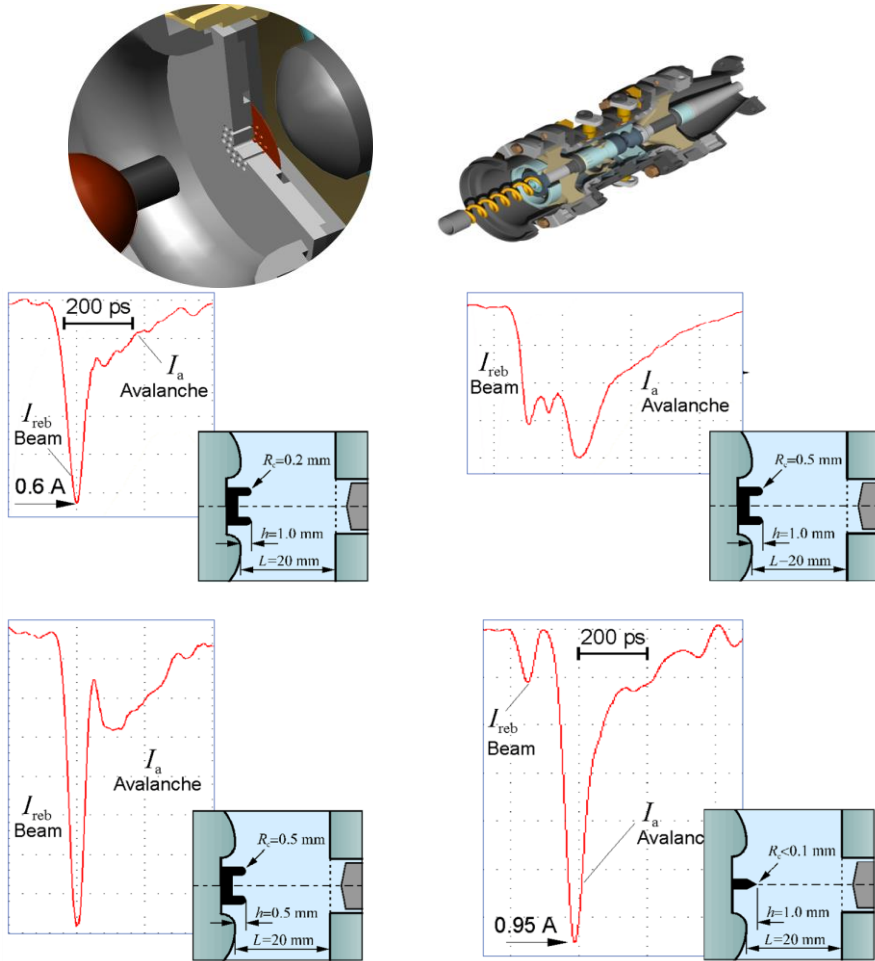
V.G. SHPAK, S.A. SHUNAILOV, M.I. YALANDIN

Institute of Electrophysics, UB, RAS, Yekaterinburg, Russia

e-mail: radan@iep.uran.ru

Pulse sources of RADAN series have been used for many years to study fast-flowing processes in gases and vacuum. Simple and reliable in operation, they have become an effective tool in various fields of scientific research. Desktop devices powered by a conventional wall socket generate pulses with amplitude of 40 to 300 kV, a current of several kiloamperes and a duration of 0.1-4 ns with a repetition rate from a single pulses to 100 pps. The RADAN sources are based on Tesla transformer combined with single or double forming coaxial line. The primary circuit switch is a fast thyristor. High-pressure gas spark gap connects the forming line to the load. This allows one to obtain a pulse shape close to rectangular. RADAN-series pulsers produce low interferences, do not require highly qualified personnel, specially equipped room and are safe in operation.

The report presents some of the numerous pulse devices based on RADAN sources, as well as the results obtained for the first time using them in the nano- and subnanosecond range of durations. A special attention is paid for prospective applications of the RADAN-based systems in the tasks of high-gradient electron acceleration, formation a magnetized flows of runaway electrons, peak power enhancement of the ultrashort microwave pulses, etc.



* This work in part of prospective applications of the RADAN-based systems for high-gradient electron acceleration is supported by the Russian Science Foundation, Grant No 21-19-00260.

COMBINED ELECTRIC DISCHARGE "ARC + DISCHARGE WITH LIQUID ELECTROLYTE CATHODE"

G.K. TAZMEEV¹, B.A. TIMERKAEV², K.K. TAZMEEV¹

¹Kazan Federal University, Naberezhnye Chelny Institute, Naberezhnye Chelny, Russia

²Kazan National Research Technical University named after A.N. Tupolev, Kazan, Russia

e-mail: gktazmeev@kpfu.ru

One of the features of discharge with liquid electrolyte cathode is volumetric combustion. By changing geometry of cathode zone on electrolyte surface, it is possible to give plasma column various shapes, in particular, it is possible to form a "flat wall" [1, 2]. In this work, a device that allows to create plasma column in form of a "hollow cylinder" has been developed. It contains one anode 1 and two cathodes: metal 2 and electrolyte 3 (Fig. 1). An aqueous solution of sodium chloride is used as an electrolyte cathode. It flows out of the annular channel 4 with dielectric walls. A negative potential is fed to the graphite ring 5, mounted inside the channel. The discharge between the electrolyte cathode 2 and the metal anode 1 is volumetric and forms a "hollow cylinder". The arc burns between metal electrodes 1 and 2 inside the "hollow cylinder". Electrical power is supplied from a single source. The currents flowing in the device are regulated by two ballast resistors 6 and 7.

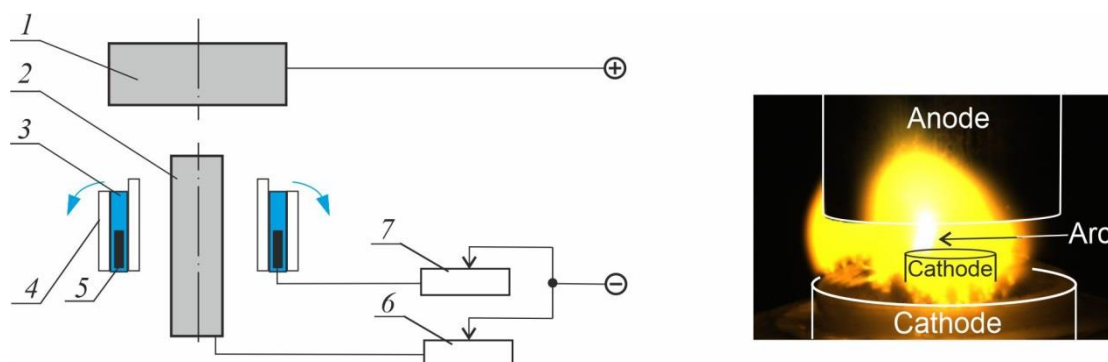


Fig. 1. Diagram of the experimental setup and snapshot of the discharges.

The gas discharge current with liquid electrolyte cathode was set in the range of 5-10 A, and arc current varied in range of 1-10 A. Metallic cathodes made of copper and duralumin were used. At elevated currents, the duralumin cathode was underwent to intense destruction. This result is quite expected, since arc burns in an oxidising environment.

Oscillograms of currents and voltages were obtained. Stable current regimes with small-scale pulsations have been recorded. Spectral studies in visible range have been carried out. A characteristic feature of the spectra was presence of the Balmer lines H_{α} and H_{β} .

REFERENCES

- [1] G.K. Tazmeev, B.A. Timerkaev and K.K. Tazmeev, "Study of the binding zone of electrical discharge to the liquid cathode by high-speed visualization," *Journal of Physics: Conference Series*, vol. 789, p. 012059, 2017.
- [2] R.N. Tazmeeva and B.K. Tazmeev, "Development features of the plasma flow in the gas discharge with the liquid electrolyte cathode", *Journal of Physics: Conference Series*, vol. 1328, p. 012074, 2019.

SIMULATION OF CHARGED PARTICLE BEAM DYNAMICS EXTRACTED FROM A PLASMA SOURCE

I.A. KANSHIN

Dukhov Automatics Research Institute (VNIIA), Moscow, Russia
e-mail: ilia.kanshshin2011@yandex.ru

The Penning-type plasma source is one of the components of a small linear ion accelerator designed for neutron generation [1-3]. In this source, plasma is generated in a pulsed mode in a medium of hydrogen isotopes, from which hydrogen isotope ions are extracted by applying a constant negative potential relative to the earth to the electrodes of the accelerating system. Further, the ions are accelerated to the target, where reactions occur with the formation of neutrons [4].

This paper presents the results of computer simulation in COMSOL Multiphysics of the hydrogen isotopes beam dynamics extracted from a plasma source. The simulation was carried out taking into account the charge exchange of ions on neutral gas molecules in the accelerating system [5]. At the same time, the calculations took into account the process of secondary ion-electron emission (SIEE) from the surfaces of the accelerating system that are bombarded with both fast and slow ions. An example of the simulation results is shown in Figure 1. Consideration of the SIEE process made it possible to determine the value of the electronic load, which leads to a decrease in the value of the neutron flux generated by the linear accelerator. The dynamics of the electron beam in the absence of its suppression system is shown (Fig. 1b).

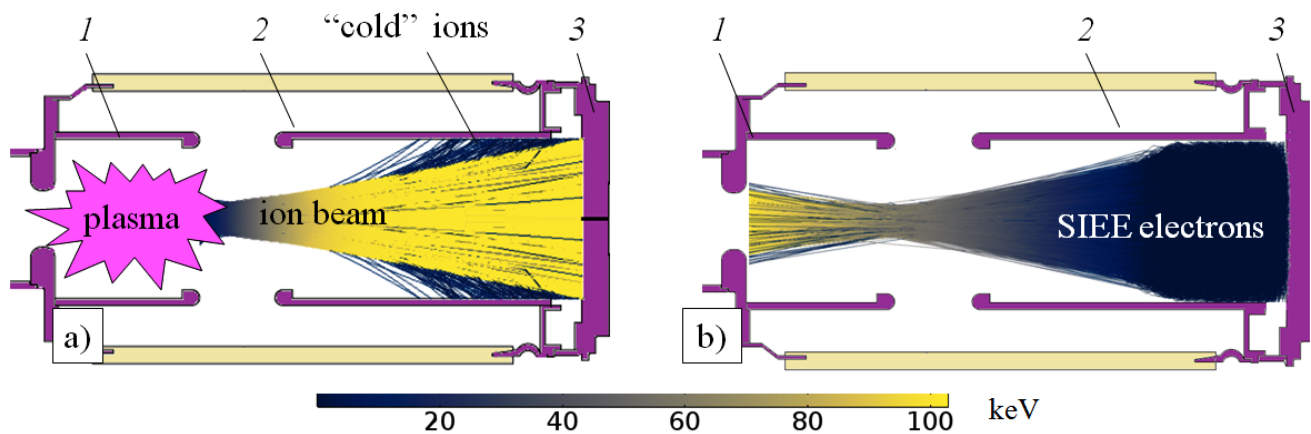


Fig. 1. (a) Trajectories of the ion beam and "cold" charge exchange ions in the accelerating system and the trajectories of secondary electrons in the absence of a system for their suppression at the target assembly of the accelerator (b).
1 – plasma source, 2 – high-voltage electrode of the accelerating system, 3 – target assembly

The inclusion in the trajectory analysis process the magnetic field simulation in the target assembly made it possible to evaluate its effect on the electronic load value in the linear ion accelerator accelerating system.

REFERENCES

- [1] N.V. Mamedov, D.E. Prokhorovich, D.I. Yurkov, I.A. Kanshin, A.A. Solodovnikov, D.V. Kolodko, and I.A. Sorokin, "Measurements of the Ion-Beam Current Distribution over a Target Surface under a High Bias Potential", *Instruments and Experimental Techniques*, vol. 61, no. 4, pp. 530–537, 2018, DOI: 10.1134/S0020441218030223.
- [2] N.V. Mamedov, N.N. Shchitov, and I.A. Kan'shin, "An Experimental Apparatus for Penning Ion Source Research", *Instruments and Experimental Techniques*, vol. 59, no. 6, pp. 870–878, 2016, DOI: 10.1134/S002044121606004X.
- [3] N.V. Mamedov, D.V. Kolodko, I.A. Sorokin, I.A. Kanshin and D.N. Sineelnikov, "Energy & mass-charge distribution peculiarities of ion emitted from penning source", *IOP Conf. Series: J. Physics Conf. Series*, vol. 830, p. 012063, 2017, <https://doi.org/10.1088/1742-6596/830/1/012063>.
- [4] I.A. Kanshin, "Increase of gas-filled neutron tubes dielectric strength to ensure stability of generated neutron pulses", *Tekhnol. Elektromagn. Sovmestimosti*, vol. 3 (66), 2018, pp. 26-35.
- [5] V.S. Boldasov, S.V. Denbnoveckij, and A.I. Kuz'michyov. *Simulation of low-pressure gas-discharge switching devices. Electrical strength of devices in the pre-discharge period*. Kiev, 1996, 140 p.

THRUST CHARACTERISTICS OF COMPACT HIGH-VOLTAGE PULSED PLASMA THRUSTER UTILIZING LIQUID PROPELLANT*

S.A. BULDASHEV¹, R.V. EMLIN², P.A. MOROZOV², I.F. PUNANOV², Y.N. SHCHERBAKOV², L.Y. YASHNOV¹

¹Research and Development Institute of Mechanical Engineering, Nizhnyaya Salda, Russia

²Institute of Electrophysics, UB, RAS, Yekaterinburg, Russia

e-mail: ivan.punanov@gmail.com

Development of compact low-mass thrusters is an important issue in space industry. It gained the second breath as the Cubesats and similar devices occurred [1]. Very low values of thrust bits necessary for orbit correction of small satellites can be provided by the pulsed thrusters. By now, the most developed pulsed systems have capacitors storing ~ 5-10 J of energy, which discharge at rate of ~ 1-2 pps and provide current of ~ 10-20 kA. The weak point of this design is relatively high mass of the capacitor. Energy capacity of a typical capacitor is ~ 25 J/kg. If we use such a capacitor, the thruster would have mass of ~ 0.5 kg, which is too much for a micro-satellite. One of the solutions is to use storage with lower energy capacity but capable of working at high frequency.

We have developed the pulsed plasma thruster (PPT) with a lower energy capacity (~ 0.2 J) which is capable of work at 400 Hz. The discharge current is also lower (~ 1 kA), to be compared to the analogues. Nevertheless, at lower density of current we get relatively high velocity of ejecting plasma. The high-voltage generator of the thruster produces pulses of voltage of ~ 25 kV. It charges up the storage with capacity of ~ 700 pF. The discharge of the coaxial capacitor in self-breakdown mode provides the train of pulses of current of ~ 1 kA. The discharge unit has a valve for liquid propellant supply. The discharge starts on the surface of the solid dielectric, whereas the liquid propellant is injected in the gap between the batches of the discharges (400 pulses in each).

In this work, we present the results on measurements of thrust and mass consumption of this PPT prototype. Thrust measurements are carried out in vacuum at pressure of 10^{-4} mm Hg. The assembly of pulsed transformer, discharge unit, electronic controller and the stack of batteries for independent power supply are mounted on a platform which is hanged on a thin metal thread. The thrust is calculated from the rotation angle of the platform. This measuring technique provides relatively high sensitivity and noise immunity.

The series of 400 shots is initiated by irradiating of IR-receiver on a controller by an IR-LED. In case of vacuum oil as a propellant, we obtained values of thrust of ~ 20 $\mu\text{N}\cdot\text{s}$ and the specific mass loss of ~ 0.1 $\mu\text{g}/\text{shot}$. Also, we measured full current of the ion component of the plasma bunch, electron density at 100 mm from the discharge and the ionization degree in plasma.

REFERENCES

- [1] I. Levchenko et al., "Space micropropulsion system for Cubesats and small satellites: From proximate targets to furthestmost frontiers", Appl. Phys. Rev., no. 5, p. 011104, 2018.

* The work was supported by the Russian Foundation for Basic Research, grant No 18-08-000185.

MEASUREMENT OF THE ELECTRON BEAM ENERGY IN A SOURCE WITH A PLASMA ANODE AND THE BEAM EXTRACTION INTO THE ATMOSPHERE THROUGH A FOIL WINDOW*

E.N. ABDULLIN, G.F. BASOV

Institute of High Current Electronics, SB, RAS, Tomsk, Russia

e-mail: abdullin@ihfe.hcei.tsc.ru

Earlier, a version of an electron beam source with an explosive-emission cathode, a plasma anode and a foil window for obtaining and ejecting electron beams with a cross section of up to 200 cm² into the atmosphere was presented [1]. The high voltage source was a previously developed Marx generator with matched loads [2]. The use of a plasma anode and the generator made it possible to obtain quasi-rectangular microsecond pulses of the voltage and electron beam current without the formation of a breakdown in the interelectrode gap. In this work, we present the data of experiments on measuring the energy of an electron beam aimed at increasing the energy efficiency of an electron beam source.

REFERENCES

- [1] Abdullin E.N., Basov G.F., Obtainig of high-power electron beams in a plasma anode source powered by the Marx generator with matched loads, *Izv. Vuzov. Fizika*, 2019, vol. 62, no. 11, pp. 156–160.
- [2] Abdullin E.N. , Basov G.F., Shershnev S.I., Marx generator for rectangular microsecond voltage pulses production at constant arbitrary resistive load, *Izv. Vuzov. Fizika*, 2017, vol. 60, no. 10/2, pp. 5–11.

* The work was supported by the Russian Foundation for Basic Research (RFBR Grant # 18-48-700034 r-a).

SUPPRESSION OF THE GENERATION OF HEAVY IONS IN VACUUM DIODE WITH PASSIVE ANODE*

A.I. PUSHKAREV^{1,2}, A.I. PRIMA², X.P. ZHU¹, C.C. ZHANG¹, Y. LI¹, YU. EGOROVA², M.K. LEI¹

¹ Dalian University of Technology, Dalian, China

² Tomsk Polytechnic University, Tomsk, Russia

e-mail: aipush@mail.ru

The results of the experimental study and simulation of the high-intensity pulsed ion beam (HIPIB) generation in an ion diode with passive anode (250-300 kV, 150 ns) are presented. The experiments were conducted using a pulsed accelerator TEMP-6 [1] which consist of a Marx generator, a pulsed forming line and a vacuum ion diode with self-magnetic insulation of electrons. The studies of diodes with graphite and stainless steel anodes during operation in double-pulse mode and the formation of anode plasma at explosive emission of electrons during the first pulse. Time-of-flight (TOF) diagnostics were used to determine the composition of the ion beam. The ion beam energy density measurements confirm the correctness of the TOF diagnostics.

Our studies have shown that the ion diode with a stainless steel anode generates nitrogen ions; the content of heavier ions of the anode material (Fe+) in HIPIB is negligible, see Fig. 1a.

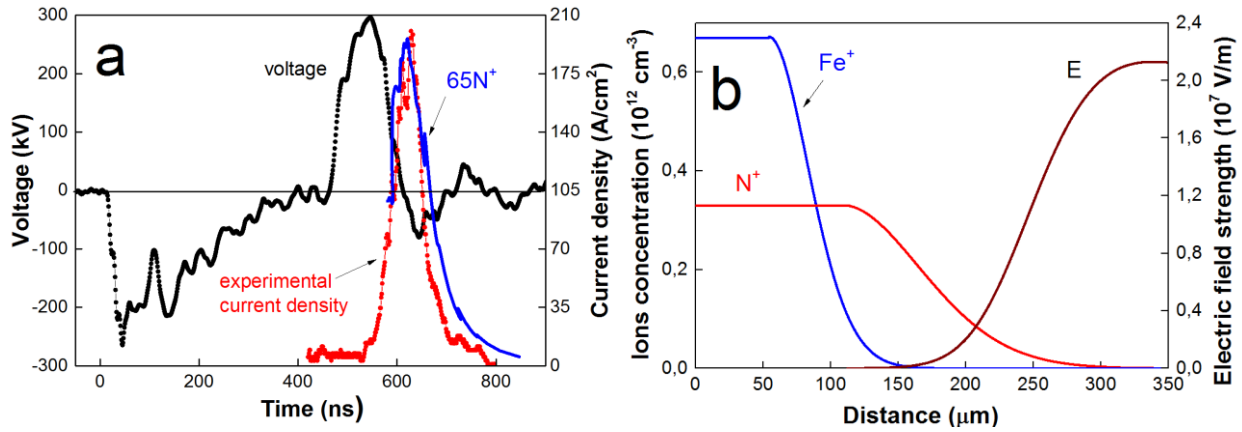


Fig. 1. Waveforms of accelerating voltage, experimental (points) and calculated (lines) ion current density (a). Distribution of ions concentration and electric field strength in A-K gap (b). Diode with a stainless steel anode

The suppression of the heavy ions generation in an ion diode with a passive anode can be caused by different expansion rates of various components of the anode plasma [2]. The anode plasma, which is formed by the explosive emission of electrons during the first pulse, will have the same ion temperature during the HIPIB generation. Heavier ions have a lower velocity and when the anode plasma expands, its external (emission) boundary will contain mainly light ions. The penetration depth of the electric field into the anode plasma is less than the thickness of the layer of lighter ions at its emission boundary (see Fig. 1b), so during the whole time of HIPIB generation, the emission from the anode plasma of lighter ions and their acceleration in the A-K gap mainly occurs.

The suppression of the heavy ions generation in a diode with a passive anode is a positive effect; it provides an increase in the ion current density when operating in the mode of space charge limitation, increasing the purity of HIPIB and high shot-to-shot stability of its parameters.

REFERENCES

- [1] X.P. Zhu, M.K. Lei, and T.C. Ma, Characterization of a high-intensity bipolar-mode pulsed ion source for surface modification of materials // *Rev. Sci. Instrum.* 73, 1728 (2002).
- [2] Q. Xu and L. Liu, Simulative research on the expansion of cathode plasma in high-current electron beam diode // *Phys. Plasmas.* 19, 093111 (2012).

* The work was supported by the Russian Foundation for Basic Research, projects no. 19-38-90001.

CATHODIC ARC DISCHARGE SYSTEM WITH LANTHANUM HEXABORIDE CATHODE FOR BORON-CONTAINING PLASMA GENERATION*

A.S. BUGAEV¹, V.I. GUSHENETS¹, E.M. OKS^{1,2}, V.P. FROLOVA^{1,2}

¹Institute of High Current Electronics, SB, RAS, Tomsk, Russia

²State University of Control Systems and Radioelectronics, Tomsk, Russia

e-mail: gvi@opee.hcei.tsc.ru

The paper reports on experimental studies of a cathodic arc discharge system with lanthanum hexaboride cathodes differing in density (4 g/cm and 4.65 g/cm) and geometry (plane and conical) for the generation of boron-containing plasma (Fig. 1). Lanthanum hexaboride, being a widely used material for field emission and thermionic cathodes, compares with metals in conductivity and resistivity, and therefore, the behavior of a cathodic arc with lanthanum hexaboride is very similar to its behavior with metals. However, during the operation of a cathodic arc, the cathode loses its mass in the form of vapors, plasma (ions and electrons), hot macroparticles, liquid droplets, and even solid small fragments, and such a loss of mass for lanthanum hexaboride, compared to many metals, is much higher: 220 $\mu\text{g}/\text{C}$ according to experimental data. The studies reported here show that the flow of hot microparticles from a lanthanum hexaboride cathode strongly affects the breakdown strength of the high-voltage acceleration gap and that the number of breakdowns can be reduced many times by using a direct-flow filter with a magnetic island at floating potential.

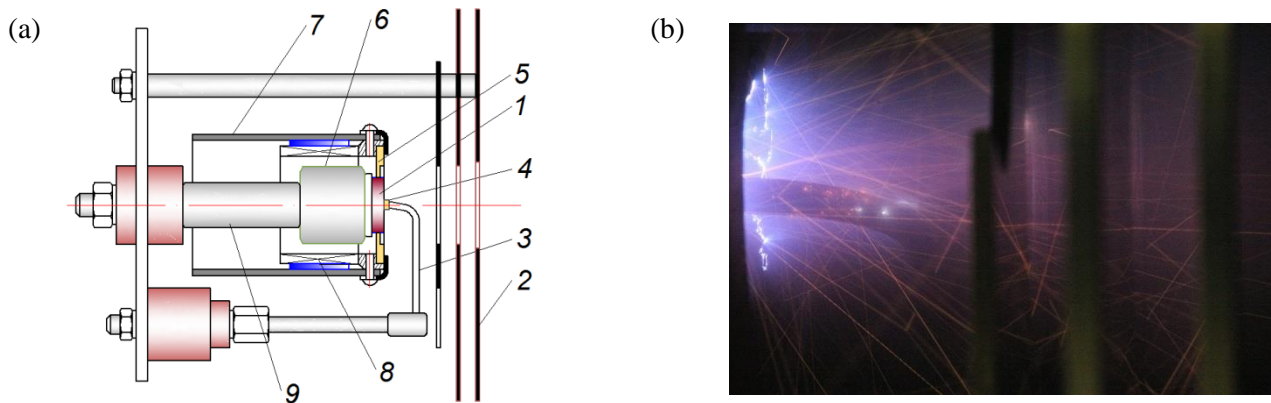


Fig. 1. (a) Sketch of the cathodic arc discharge system with flat lanthanum hexaboride cathode and (b) photo of the hot macroparticle flow.

* The work was supported in part the state assignment project FWRM-2021-0006.

EFFICIENCY OF ELECTRON BEAM EXTRACTION TO THE AMBIENT ATMOSPHERE IN AN ELECTRON ACCELERATOR BASED ON ION-ELECTRON EMISSION*

S.YU. DOROSHKEVICH, M.S. VOROBYOV, M.S. TORBA, N.N. KOVAL, S.A. SULAKSHIN, V.A. LEVANISOV

*Institute of High Current Electronics, SB, RAS, Tomsk, Russia
e-mail: doroshkevich096@gmail.com*

One of the important characteristics of all accelerators capable of extracting an electron beam into the ambient atmosphere is the efficiency of extraction this beam. Coefficient describing the efficiency of beam extraction is defined as the ratio of beam current in the ambient atmosphere to current in the accelerating gap [1]. To increase the extraction coefficient, the geometry of the electrodes is calculated and selected so as to provide the optimal ion-electron optical system (IEOS) of the accelerator. However, it is known that in electron accelerators based on ion-electron emission with a non-self-sustaining high-voltage glow discharge, the IEOS can have a strong dependence on the parameters of generated electron beam. A change in the IEOS in such systems leads to a change in the efficiency of electron beam extraction into the ambient atmosphere. In this case, the efficiency can both increase and decrease, which, first of all, is determined by the position of the emission plasma boundary [2].

The use of a modern element base makes it possible to create power supplies with a transition from a continuous mode of generation of an auxiliary discharge to a pulse-periodic mode with a pulse repetition rate at the level of several tens of kHz. This allows for a more flexible adjustment of the discharge parameters, keeping the average value of its current, but changing its amplitude with a corresponding change in the pulse duty cycle.

In this work, using an electron accelerator based on ion-electron emission [3], generating a wide-aperture (450×650 mm) electron beam, we research the effect of auxiliary discharge generation mode (continuous and pulse-periodic) (Fig. 1) on the efficiency of electron beam extraction into the ambient atmosphere, as well as the dynamics of development of a pulsed electron beam using an automated sectioned collector is investigated.

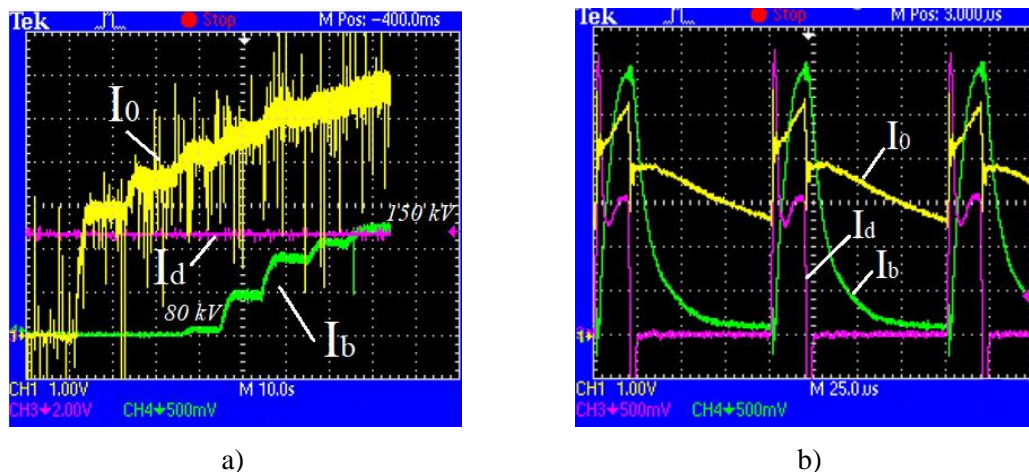


Fig. 1. Oscillograms of currents: CH1– current in the accelerating gap I_0 (10 mA/div), CH3– auxiliary discharge current I_d (50 mA/div), CH4– beam current I_b (5 mA/div) at the continuous (50, 70, 80, 100, 120, 140, 150 kV) (a) and pulse-periodic (150 kV) (b) generation mode.

REFERENCES

- [1] M. S. Vorobyov, N. N. Koval and S. A. Sulakshin 2015 Instrum. Exp. Tech. 58 (5) 687–695 pp.
- [2] E. M. Oks, Plasma cathode electron sources: Physics, Technology, Applications. Wiley-VCH, 2006.
- [3] Sergey Doroshkevich, Stepan Sulakshin, Maksim Vorobyov, Aram Ekavyan, Nikolay Koval, Aleksey Chistyakov. Electron Accelerator Based on Ion-Electron Emission for Generation of a Wide-Aperture Beam. IEEE2020, Proceedings of 7th International Congress on Energy Fluxes and Radiation Effects (EFRE) - 21st International Symposium on High-Current Elec-tronics - Tomsk – 2020, P. 42–45.

* This work was supported by the Russian Science Foundation (project No. 20-79-10015).

INVESTIGATION OF SEPARATE DISCHARGE PROCESSES IN A HIGH-VOLTAGE NANOSECOND COMBINED SWITCH.*

P.A. BOKHAN¹, N.A. GLUBOKOV², P.P. GUGIN¹, D.E. ZAKREVSKY^{1,2}

¹*Rzhanov Institute of Semiconductor Physics, SB, RAS, Novosibirsk, Russia*

²*Novosibirsk State Technical University, Novosibirsk, Russia*

e-mail: gugin@isp.nsc.ru

The high voltage switching device based on a combination of open and capillary discharges was presented in [1, 2]. An open discharge is used as a plasma cathode and it generates an intense electron beam, due to which the plasma is generated and power is switched. The capillary provides a breakdown delay increase by more than an order of magnitude in comparison with an open discharge and ones allows the device operating voltage an increase without a significant increase in the switching time. Another important property of the capillary is the rapid pulsed electric strength recovery, which makes it possible to work with this device up to a pulse repetition rate of at least 100 kHz.

The disadvantages of this discharges operation scheme are the non-optimal open discharge combustion mode, as a result the switching efficiency decreases, as well as the capillary breakdown instability increases, reaching 100 ns at low (<1 kHz) pulse repetition rates. This work is devoted to solving these problems. The open discharge modernization was carried out by implementing an external preliminary ignition with a controlled breakdown moment and pulse energy. This made it possible to increase the efficiency of switching power into active and capacitive loads by 20 percent or more. In [1], a shield with a cathode potential along the capillary is used to increase the pulsed electrical strength and the frequency characteristics. In this work, it is proposed to apply a positive pulse on the shield. The influence of this pulse on the stability of the capillary breakdown is investigated depending on its parameters. In general, the work demonstrates a combined gas discharge switch efficiency and stability increasing when operating at low pulse repetition rates at voltages up to 200 kV.

REFERENCES

- [1] P.A. Bokhan, P.P. Gugin, M.A.Lavrukhin, D.E. Zakrevsky, "Gas discharge switch" patent RU2734730, 2020.04.10
- [2] P.A. Bokhan, P.P. Gugin, M.A.Lavrukhin, D.E. Zakrevsky, "A high-voltage subnanosecond sharpener based on a combination of 'open'and capillary discharges", Journal of Physics D: Applied Physics, vol. 51, no 36, pp. 364001, 2018.

* The work was supported by the RSF Grants No. 19-19-00069.

THE MEASUREMENTS OF PLASMA EXPANSION PROCESSES OF HIGH CURRENT VACUUM ARC

I.L. MUZYUKIN, P.S. MIKHAILOV, S.A. CHAIKOVSKY, I.V. UIMANOV, D.L. SHMELEV, YU.A. ZEMSKOV

Institute of Electrophysics, UB, RAS, Yekaterinburg, Russia

e-mail: plasmon@mail.ru

The measurements of ion flow of pulsed high current vacuum arc (15 mks, 10 kA) with using of a set of small sized ion collectors were done. These collectors were placed at different distances from vacuum arc plasma source and moved around it at 0-110° angle range. The waveforms of ion detectors contain the relatively smooth signal and intensive peaks. These peaks retain their form during propagation from the vacuum arc plasma source. The amplitudes of peaks decrease and velocities can rise or drop with the distance from the source. The smooth signal stretches with increasing distance. It can be assumed that the propagation of plasma is accompanied by intense wave phenomena.

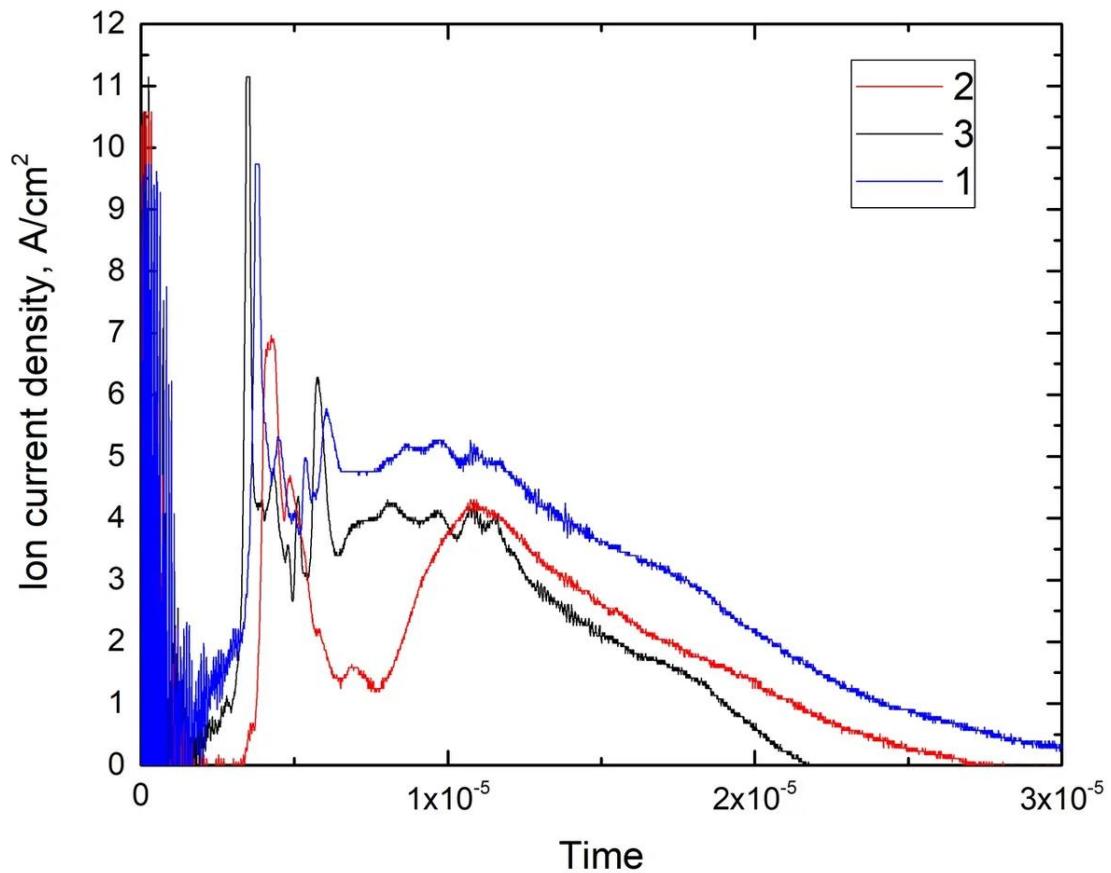


Fig. 1. The waveforms of three ion current collectors.

EXPERIMENTAL STUDY OF MICRO PULSED PLASMA THRUSTER

I.L. MUZYUKIN, P.S. MIKHAILOV

Institute of Electrophysics, UB, RAS, Yekaterinburg, Russia

e-mail: gmgm01@mail.ru

Currently, the space industry is actively developing, and with it, the demand for different space thrusters is growing [1]. In this work, a prototype of a small size pulsed plasma engine is described and investigated. The main idea was to make a small electric propulsion system that could be used on CubeSat and other small satellites. It follows that the mass of the propulsion system should not exceed 250 g and the power consumption of 5 W [2].

The design of the thruster is simple; it consists of a metal cathode and anode and a solid insulator between them as a propellant. Thrust is produced by plasma flow generated by pulsed vacuum flashover discharge. In this prototype, a coaxial and planar electrode design with a gap of about 0.3 mm was used. As the material for the electrodes, Cu or Al can be used. In addition to the thruster, it was necessary to develop a Power processing unit (PPU) that could generate high voltage impulses with an amplitude of several kV. By changing the frequency of the generator, thrust can be adjusted. With the right pulse parameters, it is possible to achieve a working model with minimal cathode erosion, to ensure high system stability.

Several high voltage generators were used in the tests. With a pulse length from 5 μ s to 200 ns and impulse amplitude from 4.5 to 10 kV. As a result, the obtained thrust values were about 7 μ N / W.

REFERENCES

- [1] Levchenko I. et al., "Space micropropulsion systems for Cubesats and small satellites: from proximate targets to furthestmost frontiers", Appl. Phys. Rev., 5, 011104 (2018).
- [2] CubeSat Design Specification (2014) Rev. 13, The CubeSat program, Cal Poly SLO, February 2014.

EFFECT OF EXTINCTION BEAM-PLASMA DISCHARGE WHILE THE INJECTION THERMOELECTRONS DURING TRANSPORTATION OF THE ELECTRON BEAM IN THE FOREVACUUM PRESSURE RANGE*

A.A. ZENIN, I.YU. BAKEEV, A.S. KLIMOV

Tomsk State University of Control Systems and Radioelectronics, Tomsk, Russia
e-mail: zenin1988@gmail.com

Forevacuum plasma electron sources [1] are of great interest for various technological operations. The features of operation such electron sources provide the possibility of direct electron-beam processing of both metallic materials and dielectrics. At the present time, the forevacuum plasma sources of electrons developed at the Department of Physics of TUSUR have reached a power of more than 5 kW [2]. However, during the transportation of such beams at elevated pressures of the working gas, a beam-plasma discharge is ignited, which hinders the effective transportation of the beam. The experiments have shown that, as a result of the emission of thermo electrons to the region of electron beam transportation, the parameters of the generated plasma change significantly, which can lead to the extinction of the beam-plasma discharge. This paper presents the results of these studies.

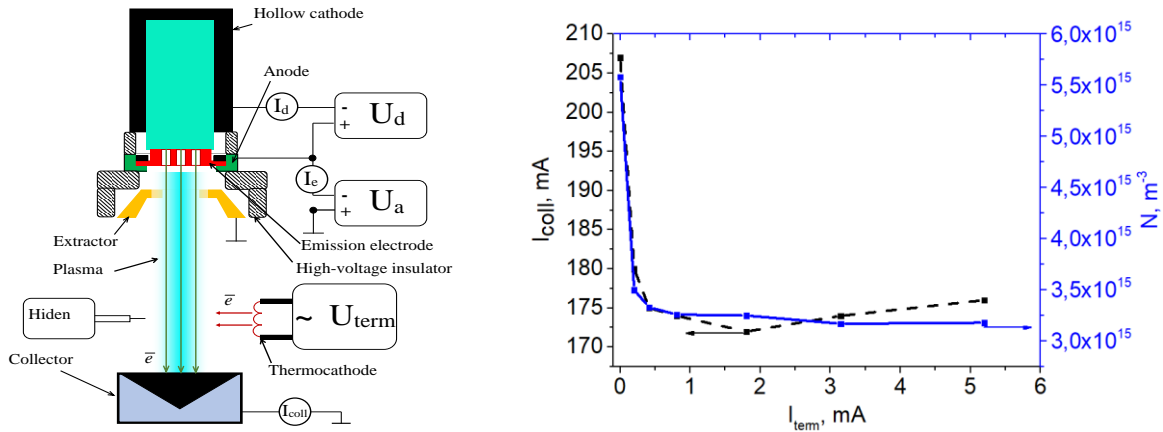


Fig. 1. (a) Schematic of the experimental setup, and (b) collector current and plasma concentration vs thermal emission current.

All experiments were carried out with the electron beam with the energy of 10 kV at an operating helium pressure of 30 Pa. A direct-heated hot cathode was used as a source of low-energy electrons. From the diagram shown in Fig. 1 (b) of the dependence of the collector current on the thermionic emission current, it can be seen that a sufficiently low current of thermionic electrons (less than mA) leads to a noticeable decrease in the current to the collector from 205-210 mA to 175-180 mA, which is associated with the extinction of the beam-plasma discharge, and improving the conditions for the transport of the electron beam.

REFERENCES

- [1] Oks E. Plasma Cathode Electron Sources: Physics, Technology, Applications. Weinheim: Wiley - VCH Verlag GmbH & CO. KGaA, 2006. 171 p. DOI 10.1002/9783527609413.
- [2] A. A. Zenin, I. Y. Bakeev, A. S. Klimov, E. M. Oks, V. T. Tran, "Forevacuum-pressure plasma-cathode high-power continuous electron beam source", Review of Scientific Instruments, Vol. 91, No 3, P. 033303, 2020.

* The work was supported by the RFBR Grant № 19-48-700004 r_a.

FEATURES OF GLOW DISCHARGE IGNITION THROUGH A SMALL HOLE IN THE HOLLOW CATHODE OF A LARGE VOLUME*

A.S. KLIMOV¹, I.YU. BAKEEV¹, V.T. TRAN², E.M. OKS^{1,2}, A.A. ZENIN¹

¹Tomsk State University of Control Systems and Radioelectronics, Tomsk, Russia

²Institute of High Current Electronics, SB, RAS, Tomsk, Russia

e-mail: klimov680@gmail.com

The ignition of a glow discharge through a narrow extended gap in the cathode cavity of a large volume in the discharge system of a forevacuum plasma electron source is investigated. For the experiments, a plasma source of a ribbon electron beam operating in the forevacuum pressure region was used [1]. The electron source is shown in Figure 1. It is established that the current at which the discharge switches to the hollow cathode mode is determined by the length l of the slit aperture in the cathode cavity, as well as by the gas pressure, Figure 2.

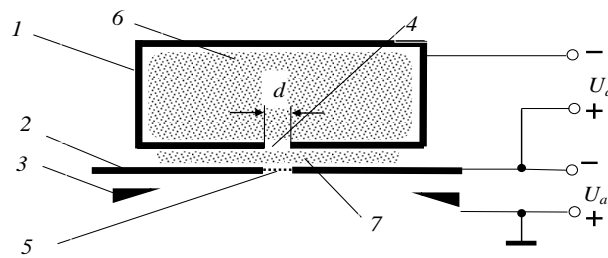


Fig. 1. Discharge emission system of a ribbon electron beam source: 1 – hollow cathode; 2 – anode; 3 – extractor; 4 – split aperture; 5 – emission grid; 6 – hollow cathode glow discharge plasma; 7 – glow discharge plasma

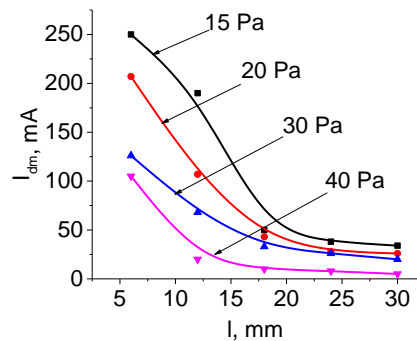


Fig. 2. Dependence of the switching current on the length of the gap in the cathode.

At low currents, the glow discharge exists between the flat parts of the cathode and the anode and does not penetrate into the cathode cavity. The plasma concentration is not sufficient to break the ion layer and allow the plasma to enter the cathode cavity. An increase in the plasma concentration due to an increase in the discharge current or gas pressure leads to a decrease in the layer separating the plasma from the cathode walls. When the threshold value of the discharge current is reached, which is determined primarily by the length of the gap in the cathode, the discharge penetrates into the cathode cavity.

Figure 2 shows the dependence of the current at which the discharge is switched to the hollow cathode. The width of the gap in the cathode is 1.5 mm. It can be seen that with an increase in the length of the gap in the cathode, the transition current decreases.

REFERENCES

- [1] A.S. Klimov, I.Yu. Bakeev, E.M. Oks, A.A. Zenin, Laser Part. Beams, 37, 203-208 (2019).

* The work was supported under the state task of the Ministry of Education and Science of the Russian Federation, Project FEWM -2020-0038.

HIGH VOLTAGE CAPACITOR FOR POWER SUPPLY SYSTEM*

A.D. LENSKIY, D.V. MOLCHANOV, D.V. RYBKA

Institute of High Current Electronics, SB, RAS, Tomsk, Russia

e-mail: denmolw@gmail.com

The creation of a LTD-generator based on the developed new type of CSA [1], with an electric power of ~ 250 TW at a load impedance of 0.165 Ohm, requires the development of new capacitive storage devices with special electrical parameters, shape and sizes. Despite the large number of generator layout variants for obtaining the specified parameters, there are only a few solutions that allow using the minimum number of capacitors and easy-to-manufacture and maintenance dimensions of the generator [2].

This paper describes the development and testing results of the new high-voltage pulse capacitor «HCEIcap 100-0.1» with a nominal operating voltage of 100 kV and a capacity of 100 nF. The calculated inductance of the capacitor is 50 nH, the outer diameter is 25 cm, the height is 13.5 cm, and the diameter of the inner hole for the gas spark gap is 8 cm. The capacitor plates are insulated with a combined paper-polymer film impregnated with castor oil. To reduce the electric field at the edge of the plates and increase the capacitor operation life, the method of field equalization by displacement of capacitor plates was used [3]. Preliminary tests have shown that when operating on a matched load of one section of such a capacitor, the operational life is $\sim 2 \times 10^6$ imp.

REFERENCES

- [1] Lavrinovich I.V., Molchanov D.V., Zharova N.V. "New capacitor-switch assembly for pulsed power generators and compact LTD-stages", *Prikl. Fiz.*, No. 2, 2018.
- [2] Lavrinovich I.V., Rybka D.V., Lenskiy A.D., Vagaytsev S.A., Molchanov D.V. "Architecture of a 100-ns LTD generator based on a new type of capacitor-switch assemblies", 7th International Congress on Energy Fluxes and Radiation Effects (EFRE 2020). IEEE. 2020.
- [3] Greisukh M.A., Kuchinsky G.S., Kaplan D.A., Messerman G.T. "Paper-oil insulation in high voltage designs", Leningrad: Gosenergoizdat, 1963.

* The work was supported by the Russian Foundation for Basic Research (grant No. 19-48-700017).

METHODS FOR INCREASING THE ELECTRICAL BREAKDOWN STRENGTH OF THE ACCELERATING GAP IN AN ELECTRON SOURCE WITH A PLASMA CATHODE*

P.V. MOSKVIN, V.N. DEVYATKOV, I.V. LOPATIN, V.I. SHIN

*Institute of High Current Electronics, SB, RAS, Tomsk, Russia
e-mail: pavelmoskvin@mail.ru*

For the electron source SOLO with a plasma cathode and grid stabilization of the emission plasma boundary [1, 2], several approaches were used that reduce the breakdown probability of the high-voltage accelerating gap. It is the breakdown of the gap that prevents the increase in use of electron beams for pulsed surface treatment of metal products to increase operational characteristics. As part of this work, we individually increased the length of the drift space, used a deflection system for transporting the electron beam, created additional anode plasma before generating the beam, and changed the rising-edge of arc discharge current in plasma emitter.

It was found that an increase in the length of the transport channel from 30 to 80 cm [3] makes it possible most of all to increase the limiting mode for longer beam pulses formed at a higher accelerating voltage. For example, for an aluminum target at an argon pressure of 25 mPa, an accelerating voltage of 20 kV, and a pulse duration of 150 μ s, the maximum integral energy in the accelerating gap doubled from 300 to 600 J. Turning the transport channel with a channel length of 80 cm in the same mode makes it possible to increase the energy by another 20% to 740 J. With increased pressure up to 45 mPa and for shorter durations, the difference between the limiting mode of the deflection and direct transport system may not be in favor of the last one. However, the shape of the current pulse in the limiting mode becomes more controllable and repeatable.

It is shown that a plasma with a concentration of 10^{11} cm^{-3} created in the drift space by a special discharge cell [4] 1 ms before the arc pulse reduces the probability of breakdown of the accelerating gap for pulses with a duration of 15 μ s. So, at a pressure of 65 mPa for a current of 400 A, when exposed to molybdenum, the probability of breakdown decreases from 19% to about 3%. At a pressure of 20 mPa, the probability of breakdown decreased from 20% to 13%. In the first case, the source was pre-trained with 5000 pulses, and in the second case less than 1000 pulses.

It was found that a decreasing the rising-edge of the current in the accelerating gap from 65 to 9 A/ μ s due to a change in the rising-edge of the discharge current in plasma emitter when exposed to pulses with a current in the accelerating gap of 200 A, duration 100 μ s, an initial accelerating voltage of 17 kV and the argon pressure 37 mPa on the surface of steel SUS316, leads to a decrease in the breakdown probability from 25 to 8%.

The presented experimental data are of practical value and can be useful in the design of plasma electron sources.

REFERENCES

- [1] Yu.H. Akhmadeev, S.V. Grigoriev, N.N. Koval, P.M. Schanin, Plasma sources based on a low-pressure arc discharge, *Laser Part. Beams*. 21 (2003) 249–254. <https://doi.org/10.1017/S0263034603212131>.
- [2] N.N. Koval, S.V. Grigoryev, V.N. Devyatkov, A.D. Teresov, P.M. Schanin, Effect of Intensified Emission During the Generation of a Submillisecond Low-Energy Electron Beam in a Plasma-Cathode Diode, *IEEE Trans. Plasma Sci.* 37 (2009) 1890–1896. <https://doi.org/10.1109/TPS.2009.2023412>.
- [3] V.I. Shin, P.V. Moskvina, M.S. Vorobyov, V.N. Devyatkov, S.Y. Doroshkevich. The deflection of a wide electron beam from the longitudinal axis of the source with a plasma cathode and plasma anode, *J. Phys. Conf. Ser.*, IOP Publishing, 2019: Vol. 1393, No. 1, p. 012055. <https://doi.org/10.1088/1742-6596/1393/1/012055>.
- [4] P.V. Moskvina, V.N. Devyatkov, I.V. Lopatin, M.S. Vorobyov, Plasma source for auxiliary anode plasma generation in the electron source with grid plasma cathode, in: *J. Phys. Conf. Ser.*, Institute of Physics Publishing, 2019: p. 12049. <https://doi.org/10.1088/1742-6596/1393/1/012049>.

* The work was supported by the Russian Science Foundation (project No. 20-79-10015).

SUBNANOSECOND SWITCHING OF STANDARD THYRISTORS TRIGGERED IN IMPACT-IONIZATION WAVE MODE BY A HIGH-VOLTAGE PCSS DRIVER*

A. GUSEV¹, I. PRUDAEV², I. LAVRINOVICH¹, A. DE FERRON¹, B. NOVAC^{1,3}, L. PECASTAING¹

¹ *Universite de Pau et des Pays de l'Adour, E2S UPPA, SIAME, Pau, France*

² *Functional Electronics Laboratory, Tomsk State University, Tomsk, Russia*

³ *Wolfson School of Mechanical, Electrical and Manufacturing Engineering, Loughborough University, Loughborough, United Kingdom*

e-mail: anton.gusev@univ-pau.fr

Fast rise time high-voltage pulses are required for the generation of a transient plasma that is used in various pulsed power applications [1], that need a reliable, long lifetime pulse generator based on solid-state switches. Therefore, modern research is focused on improving their switching characteristics, such as current rise rate dI/dt and switching time t_s , by using a gate-boosting circuit [2] or an integrated structure [3].

The promising technique of subnanosecond switching of the high-voltage semiconductor devices is the initiation of the impact-ionization wave in a low doped region by applying a fast rise time overvoltage pulse [4]. This triggering technique has been recently validated for commercial power thyristors; this achievement increases the dI/dt by two orders of magnitude when comparing to the standard triggering through a gate electrode [5].

In this work we investigate the low-power thyristors triggered in impact ionization wave mode using a pulse generator based on a high-voltage PCSS (Photoconductive Semiconductor Switch), which is running by a commercial laser diode feed by an S-diode [6] (as shown in Fig. 1). The test bench allows gradually changing parameters of the trigger generator and discharge circuit.

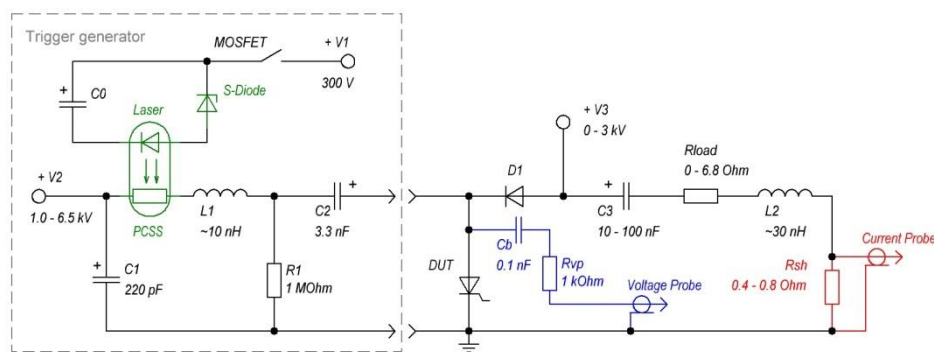


Fig. 1. A simplified electrical diagram of the experimental setup.

Several TO-220 package thyristors with a rated voltage of 0.6-2.2 kV have been tested. For the 1.6 kV thyristor 30TPS16, the following results have been obtained: triggering pulse $dV/dt \sim 5$ kV/ns, switching time ~ 300 ps, current amplitude ~ 400 A, current rise rate $dI/dt_{0.1-0.9} \sim 10$ kA/ μ s and current pulse duration ~ 170 ns.

REFERENCES

- [1] I. Adamovich et al., "The 2017 Plasma Roadmap: Low temperature plasma science and technology," *J. Phys. D. Appl. Phys.*, vol. 50, no. 32, 2017.
- [2] M. Hochberg, M. Sack, and G. Mueller, "Analyzing a gate-boosting circuit for fast switching," 2016 IEEE Int. Power Modul. High Volt. Conf. IPMHVC 2016, pp. 171-175, 2017.
- [3] J. Waldron, K. Brandmier, and V. Temple, "Ultra-fast, high reliability solid state thyatron, ignitron and thyristor replacement," in 2015 IEEE Pulsed Power Conference (PPC), 2015, vol. 2015-October, pp. 1-5.
- [4] I.V. Grekhov, "Pulse Power Generation in Nano- and Subnanosecond Range by Means of Ionizing Fronts in Semiconductors: The State of the Art and Future Prospects," *IEEE Trans. Plasma Sci.*, vol. 38, no. 5, pp. 1118-1123, May 2010.
- [5] A.I. Gusev, S. K. Lyubutin, S. N. Rukin, and S. N. Tsyranov, "Superfast Thyristor-Based Switches Operating in Impact-Ionization Wave Mode," *IEEE Trans. Plasma Sci.*, vol. 44, no. 10, pp. 1888-1893, Oct. 2016.
- [6] I.A. Prudaev et al., "The Mechanism of Superfast Switching of Avalanche S-Diodes Based on GaAs Doped with Cr and Fe," *IEEE Trans. Electron Devices*, vol. 65, no. 8, pp. 3339-3344, Aug. 2018.

* This research was carried under the framework of E2S UPPA (PULPA chair and S2P2 chair) supported by the "Investissements d'Avenir" French programme managed by ANR (ANR-16-IDEX-0002).

HIGH-POWER RADIO FREQUENCY GENERATOR FOR PLASMA APPLICATIONS

V.E. PATRAKOV, D.A. LISOVSKY

Ural Federal University, Yekaterinburg, Russia

e-mail: vitpatrakov@gmail.com

Radio frequency (RF) energy finds many uses, for example in the generation of plasma for technological purposes [1, 2]. Usually RF generators utilize vacuum tubes or RF transistors as a main active component. [3]. Transistor-based generators have advantages of being compact, easy to use, and may achieve high efficiency values, but generally they require usage of specialized RF transistor assemblies, which significantly increases the cost of such generator.

In this work the possibility of creating a high-power RF generator using non-specialized general-purpose field effect transistors (MOSFETs) was studied. The generator was constructed based on IRFB4020 MOSFETs manufactured by Infineon. Operating frequency was chosen to be 13.56 MHz, as that is one of the widely spread industrial RF frequencies. The generator can provide power to a standard 50 Ohm load.

The main obstacle to high-efficiency RF operation of general-purpose MOSFETs is repeated charging and discharging of their parasitic drain-source capacitance that occurs during switching, which rapidly increases energy losses at RF frequencies. To overcome this problem and minimize switching losses, the RF generator was built using Current-Mode Class D circuit [3]. This circuit provides zero-voltage switching condition on the drains of the transistors, which reduces capacitance-caused losses to a negligible value. This circuit also provides the advantage of suppressing higher-order harmonics on the output.

The constructed RF generator supplies continuous RF power of up to 200 W to a 50 Ohm load. The efficiency of the generator is in the 90-95% range, and total harmonic distortion (THD) of the output signal is 2.5%.

REFERENCES

- [1] Akitsu T. et al. "Plasma sterilization using glow discharge at atmospheric pressure," *Surface and Coatings Technology*, vol. 193, pp. 29-34, 2005.
- [2] Smirnov A.V. et al. "Surface modification of polystyrene thin films by RF plasma treatment," *BioNanoScience*, vol. 7, pp. 680-685, 2017.
- [3] Gupta A. et al. "A 13.56 MHz high power and high efficiency RF source," 2013 IEEE MTT-S International Microwave Symposium Digest (MTT), pp. 1-4, IEEE, 2013.

WIDE RADIATION BANDS OF SUB-NANOSECOND DISCHARGE IN XENON AND INACCURACIES IN THEIR MEASUREMENTS*

V.F. TARASENKO, A.N. PANCHENKO, D.V. BELOPLOTOV, D.A. SOROKIN, M.I. LOMAEV, V.V. KOZEVNIKOV

Institute of High-Current Electronics, SB, RAS, Tomsk, Russia

e-mail: VFT@loi.hcei.tsc.ru

The parameters of a discharge in xenon formed by voltage pulses with a duration at half-maximum of 0.7 ns are studied. It has been confirmed that the main part of the energy emitted by the diffuse discharge of xenon in the range of 120–850 nm is ensured by the spectral transitions of xenon dimers (the second continuum with a maximum at the wavelength of 172 nm). Similar results were obtained earlier in [1]. Waveforms of the voltage and radiation pulses at 172 nm and in the region 200–600 nm for two xenon pressures are shown in Fig. 1.

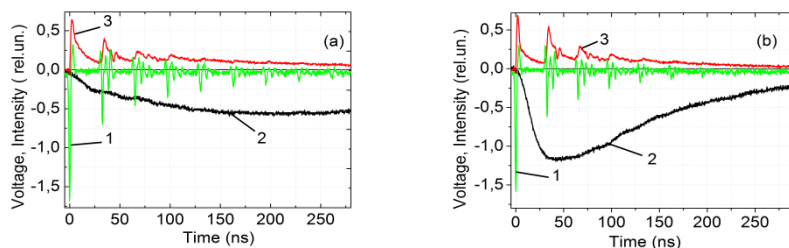


Fig. 1. Waveforms of voltage (1), radiation at 172 nm (2) and in the spectral range 200-600 nm pulses (3). Xenon pressures are 0.6 atm. (a) and 1.8 atm. (b).

During the first 30 ns before the arrival of the first voltage pulse reflected from the generator, the only by the voltage pulse with the duration of ≈ 0.7 ns (FWHM) is determined plasma glow. As a result, intense emission of the second continuum of xenon dimers is observed. The radiation pulse duration at the wavelength of 172 nm with xenon pressures of 0.3–3 atm, significantly exceeds the duration of the voltage pulse. The time until the peak radiation intensity of Xe_2^* molecules is reached decreases with increasing pressure.

Broadband radiation in the visible and UV spectral regions from the spark discharge is mainly associated with the recombination radiation [2]. It was found that recombination continua appear after the discharge contraction, which occurs faster with a decrease in the interelectrode distance or an increase in the input energy from the voltage pulse.

In the paper [3], V.I. Baryshnikov with coauthors claim that there is no radiation of the second continuum in a diffuse discharge of xenon. Our results indicate that the data given in article [3] require additional verification of the measurement procedure of VUV radiation, as well as, the voltage across the gap and discharge current. We assume that the authors of [3] did not take into account the effect of the capacitive current at the front of the voltage pulse, which was measured by the pin-diode. It is known that current collectors [4] and photodetectors [5] can detect the displacement current, including the dynamic displacement current when a voltage pulse with a subnanosecond rise time is applied to a discharge gap.

REFERENCES

- [1] E.K. Baksht, M.I. Lomaev, D.V. Rybka, V.F. Tarasenko, "Study of emission of a volume nanosecond discharge plasma in xenon, krypton and argon at high pressures", *Quantum Electronics*, vol. 36, no. 6, pp. 576-580, 2006.
- [2] E.Kh. Baksht, A.M. Boichenko, I.V. Galakhov, V.I. Zolotovskii, M.I. Lomaev, V.A. Osin, D.V. Rybka, V.F. Tarasenko, A.N. Tkachev, S.I. Yakovlenko, "Spectral characteristics of a high-current pulsed discharge in xenon", *Laser physics*, vol. 17, no. 6, pp. 782-797, 2007.
- [3] V.I. Baryshnikov, V.L. Paperny, A.Y. Chernykh, "Small-Sized nanosecond source of powerful wide-band VUV-UV radiation", in 7th International Congress on Energy Fluxes and Radiation Effects (EFRE), Tomsk, Russia, 14-26 Sept. 2020, pp. 107-110, 2020.
- [4] T. Shao, V. F. Tarasenko, C. Zhang, A.G. Burachenko, D.V. Rybka, I.D. Kostyrya, M.I. Lomaev, E.Kh. Baksht, P. Yan, "Application of dynamic displacement current for diagnostics of subnanosecond breakdowns in an inhomogeneous electric field", *Rev. Sci. Instrum.*, vol. 84, no. 5, 053506 (7 pp), 2013.
- [5] V.F. Tarasenko, E.K. Baksht, A.G. Burachenko, D.V. Beloplotov, A.V. Kozyrev, "Luminescence of polymethyl methacrylate excited by a runaway electron beam and by a KrCl excilamp", *IEEE Transactions on Plasma Science*, vol. 45, no. 1, pp. 76-84.

* The work is performed in the framework of the State task FWRM-2021-0014 for HCEI SB RAS.

INFLUENCE OF PLANAR MAGNETRON DISCHARGE PARAMETERS ON SPATIAL DISTRIBUTION OF ION CURRENT DENSITY AND SUBSTRATE TEMPERATURE *

M.V. SHANDRIKOV¹, E.M. OKS^{1,2}, A.V. VIZIR¹, G.YU. YUSHKOV¹

¹ Institute of High Current Electronics, SB, RAS, Tomsk, Russia

² Tomsk State University of Control Systems and Radioelectronics, Tomsk, Russia.

e-mail: shandrikov@opee.hcei.tsc.ru

In a planar magnetron with a copper target 125 mm in diameter, the influence of the operating pressure and discharge current on the spatial distribution of the ion current density, as well as the substrate temperature in the drift space, is studied. The working pressure of argon in the experiments was 0.07÷0.3 Pa. The discharge current was 0.1÷1 A in continuous mode. The ion current was measured with a movable flat Langmuir probe with a guard ring. It is shown that at distances of 1÷3 target diameters in the radial direction, there is a Gaussian distribution of the ion current density. An increase in the discharge current does not lead to a significant transformation of the shape of the radial distribution. The effect of the discharge current on the temperature of a dielectric and also a metal substrate is investigated, depending on its potential. It is shown that the maximum temperature of the grounded substrate compared to the temperature of the insulated substrate at the same value of the discharge current is approximately 40÷45°C higher. At a magnetron discharge power of 250 W in a continuous mode, at a distance of 25 cm from the target, the steady-state temperature of the substrate under the floating potential is about 100°C.

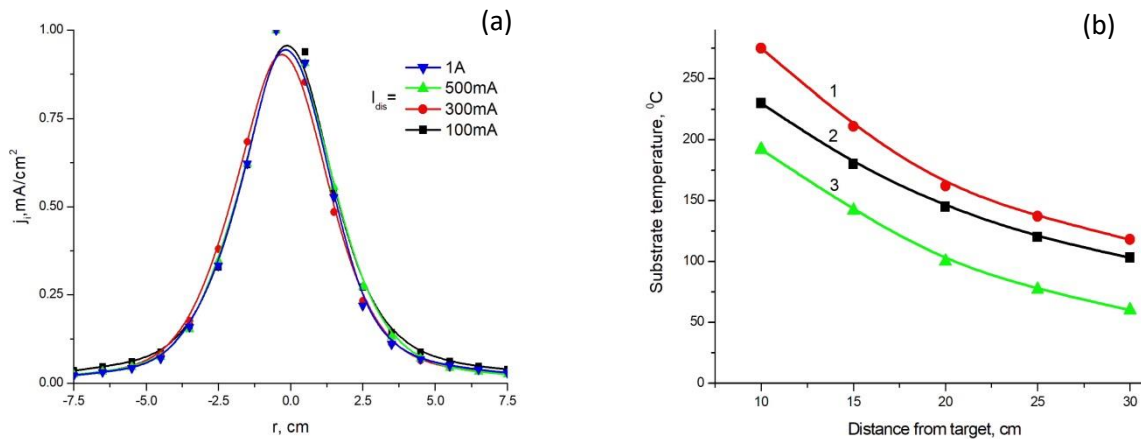


Fig. 1. Normalized radial ion current density distribution for different magnetron discharge current at a distance of 10 cm (a) and substrate temperature for different target-to-substrate distance (b):

1 – $I_{dis}=1$ A, floating potential; 2 - $I_{dis}=0.5$ A, “ground” potential; 3 - $I_{dis}=0.5$ A, floating potential ($p=0.13$ Pa).

* The reported study was funded by RFBR and Tomsk Region according to the research project № 19-48-700003.

INFLUENCE OF WORKING PRESSURE ON MASS-TO-CHARGE ION STATE IN A HIGH-CURRENT PULSED PLANAR MAGNETRON DISCHARGE PLASMA *

M.V. SHANDRIKOV¹, E.M. OKS^{1,2}, A.V. VIZIR¹, G.YU. YUSHKOV¹

¹ *Institute of High Current Electronics, SB, RAS, Tomsk, Russia*

² *Tomsk State University of Control Systems and Radioelectronics, Tomsk, Russia.*

e-mail: shandrikov@opee.hcei.tsc.ru

We have analyzed the mass-to-charge spectra of ions in the plasma of a planar magnetron. The measurements were made by using a modified quadruple mass spectrometer and time-of-flight spectrometer. Experiments were carried out with copper magnetron cathode (target) and argon as operating gas. The operating pressure range was 0.15÷1.3 Pa. The discharge current was 10÷20 A at a pulse duration 50÷100 μ s. As expected, increasing the amplitude of the magnetron discharge current increases the Cu ion fraction and decreases the Ar ion fraction in a drift space plasma. At a distance from magnetron target more than 20 cm the plasma mainly consists of metal ions (the Cu ion fraction is greater than 50%). Somewhat unexpected result is that an increase of operating pressure increases the Cu ion fraction in a drift space plasma. We suppose that prevalence of the metal component in the plasma at high currents can be explained by cooling of plasma electrons despite the fact that Cu has a much lower ionization potential (7.7 eV) compared to Ar (15.5 eV). The same results were observed in magnetron discharges with boron targets (8.3 eV) for operating gases such as argon (15.5 eV) and krypton (14 eV). An additional factor influencing the increase in the fraction of metal ions can be Penning ionization by excited metastable argon atoms (excitation potential 11.5 eV).

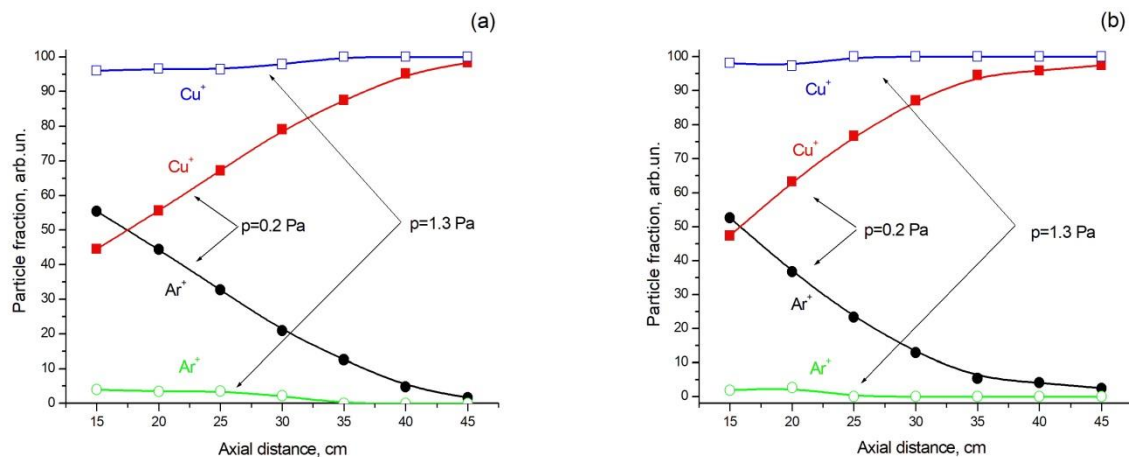


Fig. 1. Axial distribution of mass-to-charge ion state depending of operating pressure in a drift space plasma for magnetron discharge current of 10 A (a) and 20 A (b), $\tau = 50 \mu$ s, $f = 200$ Hz.

* The work was supported by the RSF Grant 21-19-00136.

INCREASING THE OPERATION STABILITY OF THE ELECTRON ACCELERATOR BASED ON ION-ELECTRON EMISSION

M.S. TORBA, S.YU. DOROSHKEVICH, M.S. VOROBYOV, N.N. KOVAL, S.A. SULAKSHIN, V.A. LEVANISOV

*Institute of High Current Electronics, SB, RAS, Tomsk, Russia
e-mail: mtorba9@gmail.com*

In electron accelerators based on ion-electron emission and non-self-sustaining high-voltage glow discharge (HVGD), the stability of operation is determined by the probability of HVGD transition to the arc form. The transition of the HVGD to the arc form of discharge burning can be due to several reasons, namely, the exacerbation of the electric field at the cathode of the HVGD (due to the presence of micropoints or charge accumulation on any dielectric inclusions), violation of gas conditions (uncontrolled increase in the pressure of the working gas) malfunction of the plasma emitter [1]. In the latter case, when used as an auxiliary glow discharge, instabilities can be associated with the appearance of cathode spots on the walls of a hollow cathode and the transition of a glow discharge into an arc [2], which leads to a local increase in the concentration of the emission plasma, disruption of ion-electron optics, and an increase in the ion current density at the cathode HVGD, when exceeding a certain value of which an electrical breakdown of the high-voltage accelerating gap occurs.

In this work, in the electrode system of an electron accelerator based on ion-electron emission [3], we present the results of studying the stability of the plasma emitter during the transition from continuous to frequency (up to 50 kHz) repetitively pulsed generation of a self-sustained glow discharge with a hollow cathode. Thus, the work investigated the dependences of the number of cathode spots on the operating modes of the plasma emitter, as well as the pressure and type of gas in the working region of the auxiliary discharge generation.

In fig. 1 shows the graphs of the dependences of the number of cathode spots depending on the operation time of the accelerator (a), the pressure of the working gas in the system and the modes of discharge generation (b) and when using nitrogen as the working gas. It can be seen from the graphs below that the use of a pulse-frequency mode of beam generation, as well as an increase in pressure in the system, increases the stability of its operation, due to a decrease in both the total number of cathode spots and their increase over time (the slope of the constructed straight line). The main reasons for the appearance of cathode spots in the plasma emitter are discussed.

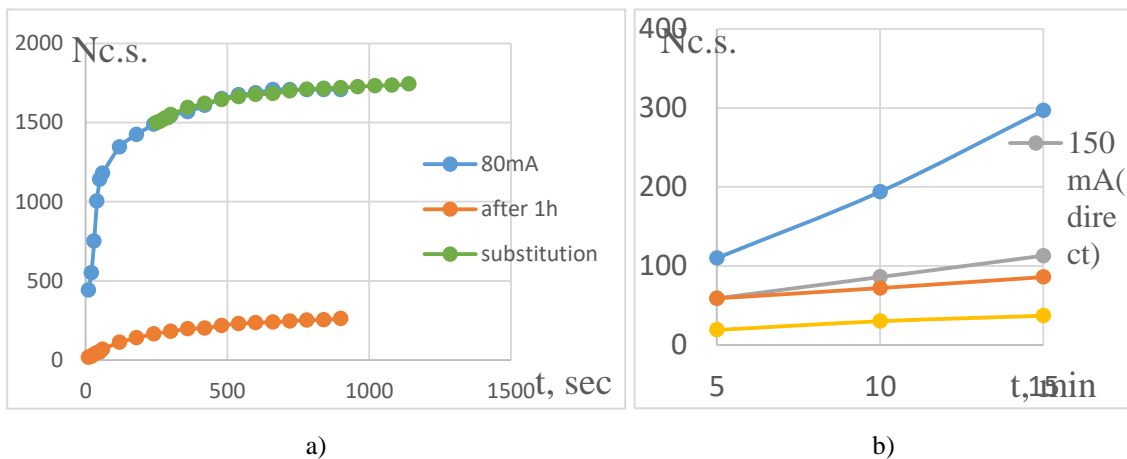


Fig. 1. Dependence of the number of cathode spots (Nc.s.) on the operating time of the system in a continuous mode (a) and at different pressures (0.4 and 0.8 Pa) and discharge combustion modes (with the same average current of 150 mA) (b)

REFERENCES

- [1] E. M. Oks, Plasma cathode electron sources: Physics, Technology, Applications. Wiley-VCH, 2006.
- [2] S. Schiller, K. Goedicke, J. Reschke, V. Kirchhoff, S. Schneider and F. Milde. Pulsed magnetron sputter technology // – Surface and Coatings Technology, 1993 – V.61. – P. 331-337.
- [3] Sergey Doroshkevich, Stepan Sulakshin, Maksim Vorobyov, Aram Ekavyan, Nikolay Koval, Aleksey Chistyakov. Electron Accelerator Based on Ion-Electron Emission for Generation of a Wide-Aperture Beam. IEEE2020, Proceedings of 7th International Congress on Energy Fluxes and Radiation Effects (EFRE) - 21st International Symposium on High-Current Electronics - Tomsk – 2020, P. 42–45.

NON-SELF-SUSTAINING HIGH-VOLTAGE DISCHARGE WITH HOLLOW CATHODE AND PLASMA ANODE*

V.I. GUSHENETS¹, E.M. OKS^{1,2}, A.S. BUGAEV¹

¹Institute of High Current Electronics, SB, RAS, Tomsk, Russia

²State University of Control Systems and Radioelectronics, Tomsk, Russia

e-mail: gvi@opee.hcei.tsc.ru

We demonstrate the experimental studies of a non-self-sustained pulsed high-voltage discharge (HVD). A distinctive feature of the high-voltage discharge geometry is the use of a hollow cathode, instead of a flat cathode, and a plasma anode without rigid fixation of the plasma surface position. A toroidal plasma generator (plasma anode) based on a geometry of a closed-drift plasma thruster with a short acceleration zone (plasma thruster with anode layer) creates the anode plasma emitting ions into cathode region. In the pulsed operation mode the high-voltage discharge current reaches 10 A with a pulse duration of 200 μ s and a voltage across the high-voltage gap of 35 kV. Pulse mode is implemented due to the pulsed operation of the anode plasma generator. The HVD current is proportional to the current of the anode plasma generator and does not depend on the pressure of the working gas. The working gas pressure has a strong effect on the operation of the plasma anode generator - determining the generator discharge current and the duration of the discharge current pulse. Argon, nitrogen, and air were used as a working gas in the experiments. It is shown that the current of the non-self-sustained pulsed high-voltage glow discharge with a hollow cathode increases by one and a half times in comparison with the discharge current with a flat cathode. Under certain experimental conditions, the self-oscillation excitation in the MHz-frequency range of the discharge current is observed.

* The work was supported in part by the Russian Foundation for Basic Research (RFBR) under Grant 19-08-00315 and the state assignment project FWRM-2021-0006.

INFLUENCE OF ACCELERATING GAP CONFIGURATION ON PARAMETERS OF A FOREVACUUM PLASMA-CATHODE SOURCE OF PULSED ELECTRON BEAM*

A.V. KAZAKOV¹, A.V. MEDOVNIK¹, E.M. OKS^{1,2}, N.A. PANCHENKO¹

¹Tomsk State University of Control Systems and Radioelectronics, Tomsk, Russia

²Institute of High Current Electronics, Siberian Branch of the Russian Academy of Sciences, Tomsk, Russia

e-mail: andrykazakov@gmail.com

Ceramics, polymers and glasses, which are usually dielectrics, are widely used in various fields of industry and medicine [1–4]. Therefore, different methods of treatment of these dielectric materials are developed and improved [4–6]. Forevacuum plasma-cathode sources of low-energy (up to 20 keV) electron beams provide treatment of different dielectric material by electron beams at gas pressure 3–50 Pa (negative charge appearing on dielectric surface is compensated by ion flow from beam-produced plasma) [7, 8]. In particular, the forevacuum sources of pulsed electron beams provide surface modification of dielectric materials [8]. The characteristics of plasma-cathode electron sources are determined by the type of discharge used to generate the emission plasma, the electrode configuration of the accelerating gap, and some other parameters and conditions [9]. The purpose of this work is to investigate influence of the configuration of the accelerating gap of the source and the processes occurring in this gap on the parameters of the plasma-cathode electron source generating the pulsed low-energy electron beam in the forevacuum pressure range of 3–30 Pa.

Influence of configuration of the accelerating gap on the parameters of the forevacuum plasma-cathode electron source generating low-energy (up to 10 keV) electron beam in the pressure range of 3–20 Pa has been investigated. Electrode system of the pulsed forevacuum plasma-cathode electron source based on a cathodic arc has been used in the experiments. The plane-parallel accelerating gap is formed by a fine mesh emission electrode and a mesh extractor (accelerating electrode). An increase in the length of the accelerating gap, i.e. the distance between the emission electrode and the extractor leads first to an increase in the electron emission efficiency η , but when a certain optimal value is reached, a further increase in the length leads to a decrease in the efficiency η . The electron emission efficiency has been estimated as the ratio of the emission current I_e to the arc discharge current I_d ($\eta = I_e/I_d$). The optimal value of the length of the accelerating gap, at which the maximum emission efficiency is provided, depends on the pressure and the type of working gas. In addition, the length of the acceleration gap influences the maximum working gas pressure. The influence of the length of the accelerating gap on the parameters of the forevacuum plasma-cathode electron source is caused by a change in the value of the back-streaming ion flow moving towards discharge gap and by change in the electric field pressure at the boundary of the emission plasma.

REFERENCES

- [1] N.P. Bansal, and R.H. Doremus, Handbook of glass properties, Orlando, Florida: Academic Press Inc., 1986.
- [2] E. El-Meliegy, and R. Van Noort, Glasses and glass ceramics for medical applications, London: Springer science & business media, 2011.
- [3] S. Somiya, Handbook of advanced ceramics: materials, applications, processing, and properties, Waltham, USA: Academic press, 2013.
- [4] M.A. Spalding, and A. Chatterjee, Handbook of Industrial Polyethylene and Technology: Definitive Guide to Manufacturing, Properties, Processing, Applications and Markets, Hoboken: John Wiley & Sons, 2017.
- [5] C.J. McHargue, “Ion beam modification of ceramics,” Mater. Sci. Eng. A., vol. 253, pp. 94–105, 1998.
- [6] V.S. Bessmertnyi, “Plasma treatment of glasses (A review),” Glass Ceram., vol. 58, no. 3-4, pp. 121–124, 2001.
- [7] A.V. Burdovitsin, A.S. Klimov, A.V. Medovnik, and E.M. Oks, “Electron beam treatment of non-conducting materials by a fore-pump-pressure plasma-cathode electron beam source,” Plasma Sources Sci. Technol., vol. 19, no. 5, Art. 055003, 2010.
- [8] V.A. Burdovitsin, E.S. Dvilis, A.V. Medovnik, E.M. Oks, O.L. Khasanov, and G.Yu Yushkov, “Surface structure of alumina ceramics during irradiation by a pulsed electron beam,” Tech. Phys., vol. 58, no. 1, pp. 111–113, 2013.
- [9] E. Oks, Plasma Cathode Electron Sources: Physics, Technology, Applications, Berlin, Germany: Wiley, 2006.

* The work was supported by the Ministry of Science and Higher Education, project FEWM -2020-0038.

INFLUENCE OF ELECTRON EMISSION ON OPERATION OF A CONSTRICTED ARC DISCHARGE IN A PULSED FOREVACUUM PLASMA-CATHODE ELECTRON SOURCE*

A.V. KAZAKOV¹, E.M. OKS^{1,2}, N.A. PANCHENKO¹

¹*Tomsk State University of Control Systems and Radioelectronics, Tomsk, Russia*

²*Institute of High Current Electronics, Siberian Branch of the Russian Academy of Sciences, Tomsk, Russia*

e-mail: andrykazakov@gmail.com

Pulsed plasma-cathode sources of large-radius (or large area) low-energy (up to about 30 keV) electron beams are used for surface treatment of materials and for other applications [1–3]. The characteristics of the plasma-cathode electron sources are largely determined by the parameters of the emission plasma generated by the gas discharge [4]. An arc discharge with cathode spots also called vacuum arc is often used to generate emission plasma in the pulsed electron beam sources. This type of discharge provides high current and long pulse duration of the discharge current, and, accordingly, of the electron beam. However, the arc discharge with cathode spots has disadvantages caused by the chaotic movement and instabilities of the cathode spots, and by formation of vapors and microdroplets of the cathode material during operation of the cathode spots [5]. More over the vapors and microdroplets of the cathode material may penetrate into the accelerating gap of the source and the region of electron beam propagation. These disadvantages affect the characteristics of the plasma-cathode electron sources (for example, it leads to decrease of electric strength of an accelerating gap). A constricted arc discharge is used to eliminate the negative influence of the cathode spots operation in the sources generating electron beams in the traditional gas pressure range 10^{-3} – 10^{-1} Pa [6]. The operation of the constricted arc discharge and features of electron emission from plasma formed by this type of arc have been studied in detail for the traditional plasma-cathode electron sources. The research of constricted arc operation in a forevacuum plasma-cathode electron source operating at pressure 5–20 Pa have demonstrated some features of formation of the emission plasma [7]. The aim of this work is to research influence of electron emission on the constricted arc discharge forming emission plasma in the forevacuum plasma-cathode source of the pulsed electron beam.

The research of influence of electron emission on the pulsed constricted arc discharge forming emission plasma in the forevacuum plasma-cathode source generating low-energy (up to 10 keV) electron beam in pressure range 5–20 Pa is presented. The electron emission from plasma formed by the constricted arc leads to a change in the discharge operation voltage. An increase in the gas pressure and an increase in the accelerating voltage lead to a decrease in the constricted arc voltage. In case of use nitrogen as working gas, an increase in gas pressure from 7 to 20 Pa leads to a decrease in the pulse-averaged voltage of the contracted arc from 90–100 V to 60–70 V ($U_a = 2$ kV). The use a working gas with a larger ionization cross section (for example, argon) provides lower arc voltage and a sharper decrease in the constricted arc voltage with increasing gas pressure. The decrease in the voltage of the constricted arc discharge observed during the electron emission is caused by a change in the discharge operation conditions due to the penetration of the back-streaming ion flow into discharge system of the forevacuum plasma-cathode electron source. The value of the back-streaming ion flow, which propagates towards a mesh emission electrode and penetrates into the discharge system, increases with increasing gas pressure and with increasing accelerating voltage.

REFERENCES

- [1] D.I. Proskurovsky, V.P. Rotshtein, G.E. Ozur, A.B. Markov, D.S. Nazarov, V.A. Shulov, and R.G. Buchheit, "Pulsed electron-beam technology for surface modification of metallic materials," *J. Vac. Sci. Technol. A*, vol. 16, no. 4, pp. 2480–2488, 2001.
- [2] A.V. Burdovitsin, A.S. Klimov, A.V. Medovnik, and E.M. Oks, "Electron beam treatment of non-conducting materials by a fore-pump-pressure plasma-cathode electron beam source," *Plasma Sources Sci. Technol.*, vol. 19, no. 5, Art. 055003, 2010.
- [3] V.I. Engelko, G. Mueller, "Microsecond intense electron beams for industrial applications," *IEEE Trans. Plasma Sci.*, vol. 41, no 10, pp. 2769–2773, 2013.
- [4] E. Oks, *Plasma Cathode Electron Sources: Physics, Technology, Applications*. Berlin, Germany: Wiley, 2006.
- [5] A. Anders, *Cathodic Arcs: From Fractal Spots to Energetic Condensation*. New York, NY, USA: Springer, 2008.
- [6] A.F. Zlobina, G.S. Kazmin, N.N. Koval, and B.E. Kreindel, "Plasma parameters in the expander of an electron emitter with a constricted arc discharge," *Sov. Phys. Tech. Phys.*, vol. 25, no. 6, pp. 689–691, 1980.
- [7] A.V. Kazakov, A.V. Medovnik, E.M. Oks, and N.A. Panchenko, "Parameters and characteristics of a pulsed constricted arc discharge operating in a forevacuum-pressure plasma-cathode electron beam source," *Vacuum*, vol. 186, Art. 110071, 2021.

* The work was supported by the Russian Foundation for Basic Research (RFBR) under the Grant No. 20-08-00123.

PROPERTIES OF PULSED MAGNETRON DISCHARGE PLASMA IN HELIUM

A.V. KAZIEV¹, D.V. KOLODKO^{1,2}, G.I. RYKUNOV¹, N.S. SERGEEV^{1,3}

¹National Research Nuclear University MEPhI (Moscow Engineering Physics Institute), Moscow, Russia

²Kotelnikov Institute of Radio Engineering and Electronics, RAS, Fryazino, Russia

³National Research Center "Kurchatov Institute", Moscow, Russia

e-mail: kaziev@plasma.mephi.ru

Nowadays, a lot of practical applications—such as material etching; electric propulsion (plasma thrusters); material testing under high thermal and plasma loads; plasma separation of spent nuclear fuel—demand having efficient sources of highly ionized metal-free plasma. It could be convenient to utilize commercially available high-power impulse magnetron sputtering (HiPIMS [1]) technique for this purpose. However, originally HiPIMS is being used for coating deposition and thus in its conventional form is not suitable for generating plasma free of metal species. The usage of light working gas (e. g. helium) can significantly reduce the sputtering effects and turn this type of discharge into highly efficient generator of metal-free plasmas.

Depending on operating conditions (including pulse duration), it is possible to transform long HiPIMS regime (L-HiPIMS) into the non-sputtering low-voltage mode at the same power level. This mode is known as non-sputtering magnetron discharge (NSMD) [2–4]. Introducing helium into NSMD might result in high density plasma generation with extremely low cathode material erosion rate.

In this study the operation of millisecond-scale impulse magnetron discharges in helium has been examined. The pulse duration was varied from 1 ms to 20 ms, and the maximum pulse energy was 6 kJ. We measured the deposition rates of target materials (Al, Ti, Cu) in L-HiPIMS, as well as the content of metallic species in plasma. The plasma parameters were monitored with a Langmuir probe.

The use of the long-pulsed modes enables achieving high plasma density (up to 10^{15} cm⁻³) and accelerating the ion flux with a peak energy distribution of 20–30 eV, which corresponds to 30–40 km/s for a helium ion.

REFERENCES

- [1] Gudmundsson J.T., Brenning N., Lundin D., Helmersson U. 2012 J. Vac. Sci. Technol. A 30(3), 030801.
- [2] Khodachenko G.V. et al. 2012 Plasma Phys. Rep. 38, 71.
- [3] Kaziev A.V. 2018 Vacuum 158, 191.
- [4] Sommerer T.J. et al. 2019 J. Phys. D: Appl. Phys. 52, 435202.

OPERATING PARAMETERS OF HIGH PULSE REPETITION FREQUENCY CAPILLARY GAS DISCHARGE SWITCH AND ITS APPLICATION FOR ION SELF-TERMINATING LASERS PUMPING*

P.A. BOKHAN, P.P. GUGIN, M.A. LAVRUKHIN, D.E. ZAKREVSKY

A. V. Rzhanov Institute of Semiconductor Physics SB RAS, Novosibirsk, Russia

e-mail: lavrukhin@isp.nsc.ru

Studies of an high-voltage switch based on a capillary discharge with a plasma cathode - an eptron [1, 2] were carried out in the burst mode operation. The characteristic features of this type of switch are short times of transition into the conducting state (fractions, units of nanoseconds), high pulse repetition frequency (PRF) (tens of kHz and more), long breakdown delays after the moment of voltage applying (hundreds of nanoseconds and more), a wide range of operating voltages (from units to hundreds of kV). The study of the structural and other parameters influence on the switch maximum achievable PRF at voltages of tens of kV was carried out, changes in the operating parameters of the switch (switching time, efficiency, breakdown delay) were also investigated with an increase in the operating PRF up to 200 kHz. The considered factors, that significantly affect the ultimate PRF of an eptron, in particular, include the dimensions of the conducting shield around the capillary part of the switch and the reverse voltage applied to the electrodes in the period between pulses.

One of the developed fast high-voltage switch applications is gas-discharge lasers pumping, in particular, lasers on self-terminating transitions in atoms and ions. The prospect of studying gas-discharge lasers on ion self-terminating transitions lies in the possibility of realizing relatively efficient and affordable sources of coherent UV radiation [3]. However, the achievement of significant values of the efficiency and average power is possible only at high pumping PRFs, under conditions when most of the ions in the active medium don't recombine between pumping pulses, and with a rapid increase in the voltage across the active element, which ensures fast heating of electrons to the optimal temperature, at which the population of the upper laser level prevails over the lower one.

The results of the frequency-energy characteristics studies of lasers on self-terminating transitions of Ba^+ ($\lambda = 614.2$ nm) and Ca^+ ($\lambda = 854.2$ and 866.2 nm) up to 60 kHz and Hg^+ ($\lambda = 398.4$ nm) up to 200 kHz are presented. A comparison of various electrical circuits for pumping lasers using magnetic pulse compression (MPC) and an eptron was performed. In the first case, the voltage pulse edge on the gas discharge tube equaled ~ 30 ns, in the second, it was less than 2 ns. A significant increase in the laser pulse energy and optimal PRF was experimentally demonstrated when the eptron was introduced into the lasers pumping circuit (Fig. 1).

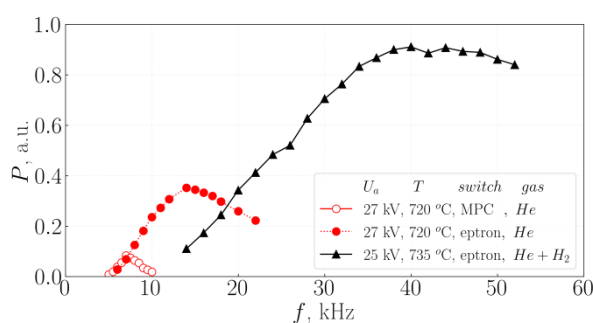


Fig. 1. Average Ba^+ laser ($\lambda = 614.2$ nm) output power versus pulse repetition frequency for different pumping electrical circuits with pure He and He + H_2 mixture as a buffer gas.

REFERENCES

- [1] Bokhan P.A., Gugin P.P., Lavrukhin M.A., Schweigert I.V., Alexandrov A.L., Zakrevsky D.E. J. Phys. D: Appl. Phys., vol. 51, p. 404002, 2018.
- [2] Bokhan P.A., Belskaya E.V., Gugin P.P., Lavrukhin M.A., Zakrevsky D.E., Schweigert I.V. Plasma Sources Sci. Technol., no. 8 (29), p. 84001, 2020.
- [3] Little C.E. Metal vapour lasers : physics, engineering and applications, Chichester New York: Wiley-VCH, 1999.

* The work was supported by the Russian Science Foundation under grant No. 19-19-00069.

INFLUENCE OF THE CATHODE REGION PREIONIZATION ON THE OPERATING PARAMETERS OF THE EPTRON

P.A. BOKHAN, P.P. GUGIN, M.A. LAVRUKHIN, D.E. ZAKREVSKY

A. V. Rzhzanov Institute of Semiconductor Physics, SB, RAS, Novosibirsk, Russia
e-mail: lavrukhin@isp.nsc.ru

The results of studies of a new type of switch [1, 2] based on a capillary discharge with a preionization of a cathode region are presented. The cathode region of the switch consists of two flat rectangular SiC cathodes with a total area of 22 cm² and two grids remote from the cathodes by a distance of 3 mm each and forming a 6 mm region between each other. A capillary of rectangular cross section with dimensions of 10x0.3 mm and a length of 35 mm is located at the side of cathode region. The inner surface of the capillary has a meander shape with a period of 2 mm, which avoids surface breakdowns along the walls of the capillary. Two copper plates connected to the cathodes of the device are attached to the outer surface of the capillary through an additional insulator. Such a configuration allows to reduce the inductance of the switch and has a great influence on providing a large breakdown development time t_d at high pulse repetition frequency (PRF) [2].

The positive voltage pulses from the generator and following magnetic compression line were applied to the anode of the switch, the cathode of the device was grounded. The charging time of the working capacitance was ~ 200 ns. The load resistance R_L varied from 24.5 to 98 Ohms. Parameters were measured in the burst operation mode at a PRF inside the burst f of 5 to 50 kHz. A positive pulse with an amplitude of up to 8 kV was applied between the grids and cathodes to preionize the cathode region 1 μ s before each of the pulses in the burst. Current measurements were carried out using two low-inductance shunts.

The dependences of the switching efficiency η and the time of breakdown development delay t_d in the switch on the energy of the preionization pulse, PRF, pressure and type of working gas, and the amplitude of the switched voltage U_A are obtained. It is demonstrated that at low PRF the starting losses in the switch significantly depend on the energy of the preionization pulse of the cathode region W_{pre} (Fig. 1). An increase in the amplitude of the charging voltage U_A leads to an increase in the efficiency of the switch η . For example, with a low load resistance of 24.5 Ohms, the efficiency η increases from 0.45 to 0.54 when voltage rises from 10 to 16 kV in helium. It was shown that in helium for PRF up to 50 kHz, with a switching time of $t_{sw} \sim 1.5$ ns, the compression ratio of the leading edge of the voltage pulse exceeds $S = t_d / t_{sw} = 300$ at $U_A = 16$ kV.

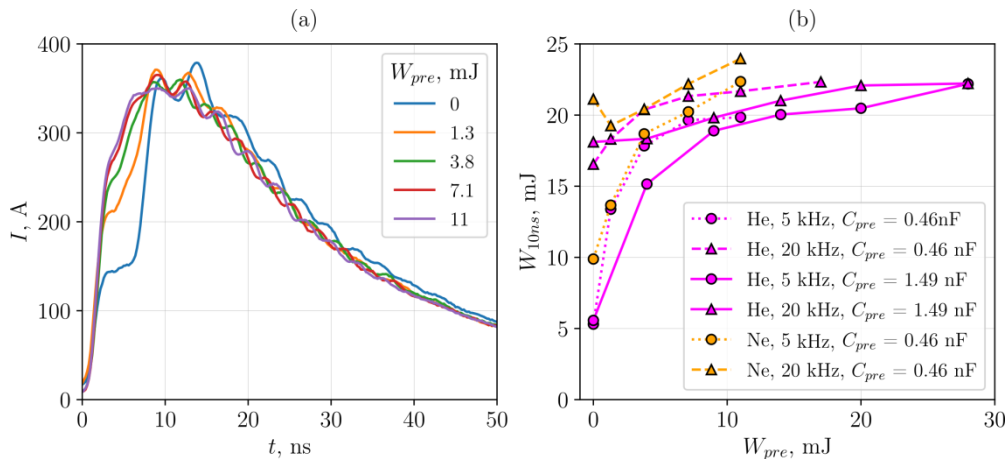


Fig. 1. (a) - oscillograms of current I through the load at different values of the preionization pulse energy of the switch W_{pre} (He , $P = 10$ Torr, $U_A = 16$ kV, $f = 5$ kHz, $R_L = 24.5$ Ohm, $C_{pre} = 0.46$ nF); (b) - dependences of the energy W_{10ns} deposited into the load during the first 10 ns on W_{pre} ($U_A = 16$ kV, $R_L = 24.5$ Ohm).

REFERENCES

- [1] P.A. Bokhan, P.P. Gugin, M.A. Lavrukhin, I.V. Schweigert, A.L. Alexandrov, D.E. Zakrevsky, J. Phys. D: Appl. Phys., vol. 51, p. 404002, 2018.
- [2] P.A. Bokhan, P.P. Gugin, D.E. Zakrevsky, M.A. Lavrukhin, Russian Physics Journal, vol. 62, no. 11, p. 2059, 2020.

FORMATION OF THE VOLTAGE PULSES UP TO 400 KILOVOLTS WITH FRONT PULSE LESS THAN 10 NANoseconds

B.A. KOZLOV¹, D.S. MAKHANKO²

¹Ryazan State Radio Engineering University, Ryazan, Russia

²PLASMA, JSC Research Institute of Gas-Discharge Devices, Ryazan, Russia

e-mail: mahdim@rambler.ru

The purpose of this work is to provide basic information about the manufacturing technology of sealed-off spark gaps in metal-ceramic design with hydrogen filling and pressures up to 120 atmospheres at an operating voltages of 150-400 kV. The results of an experimental investigation of the switching characteristics of the RO-49 spark gap-sharpeners are also presented.

Figure 1 shows the design of the RO-49 spark gap (1) located inside the body of the X-ray device (2). The spark gap contains a metal body (3) in the form of a cylinder and a ceramic insulator (4) located in it in the form of a truncated cone, two electrodes – the anode (5), fixed to the inner surface of the lid, and the cathode (6) together with the contact rod (7), located on the surface of the smaller base of the insulator (4) [1].

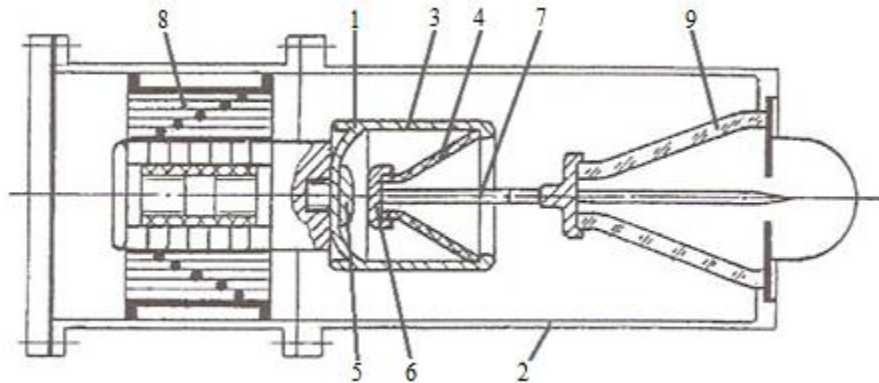


Fig. 1. The scheme of the compact pulse X-ray device.

After assembly the spark gap is filled with a mixture of N_2 and SF_6 gases to the required pressure and the device is initially trained to improve the electrical strength of the inner surface of the insulator. This mixture is then released and the spark gap is filled with high-purity hydrogen to a pressure that provides the required breakdown voltage.

The pulse transformer (8) after influence on the its primary winding to a voltage pulse of 15-20 kilovolts, charges the constructive capacitance between the spark gap corps and the X-ray device body in a time of 1-2 μs . After the spark gap is triggered, the constructive capacity is discharged to the X-ray tube IMA5-320 (9) along the contour with a minimum inductance.

Measurements of the switching characteristics of spark gaps were carried out on a similar stand, in which instead of an X-ray tube, a set of low-inductive resistors of the TVO-60 type and a resistive current shunt with $R = 0.01$ Ohms were installed. A constructive capacitive divider used to register the temporary behavior of the voltage on the spark gap.

The results of the investigations showed that the development of the discharge in the RO-49 spark gap-sharpeners is determined by the composition of the working mixture and its pressure and they times have of $\approx 2-10$ nanoseconds at the anode voltages in the range of 150-400 kV.

The resource of the RO-49 spark gap is 3×10^6 pulses.

REFERENCES

- [1] B.P. Merkulov, V.G. Samorodov, D.S. Makhanko, N.I. Cherepennikova, Gas-filled spark gap, Patent RU № 111715 U1 H01J 17/02, 2011.

GENERATION OF A COLD ATMOSPHERIC PLASMA JET IN A PLANAR MULTICHANNEL DEVICE*

P.P. GUGIN¹, D.E. ZAKREVSKY^{1,2}, E.V. MILAKHINA^{1,2}

¹A. V. Rzhanov Institute of Semiconductor Physics, SB, RAS, Novosibirsk, Russia

²Novosibirsk State Technical University, Novosibirsk, Russia

e-mail: lena.yelak@gmail.com

Plasma devices for a cold atmospheric plasma jet (CAPJ) generation in a mixture of inert gases and air are widely used in medicine [1]. To increase the exposure area of CAPJ to the target, a planar multichannel device was developed (see Fig. 1), and its functional parameters were investigated. The design was a dielectric box (1) in which between a quartz plates (2) formed flat discharge channels (3). Dielectric plates (4) at the outlet of the discharge channels formed a gap of 2 mm — a nozzle. The discharge area was formed by an internal copper saw-shape electrode (5) 40 mm in length, located along the gaps, and an external grounded electrode (6). A sinusoidal voltage $U = 0-10$ kV with a frequency of $f = 10-50$ kHz was applied to the internal potential electrode.

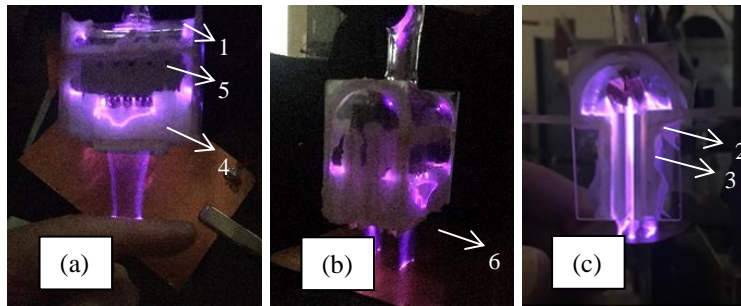


Fig. 1. Planar devices (a) single-channel, (b) two-channel, (c) three-channel.

The typical dependence of the current on the voltage $I(U)$ of the CAPJ generated in a single-channel device at a gas flow rate $v = 15$ L/min and a sinusoidal voltage frequency of $f = 13$ kHz had a sublinear character (see Fig. 2 (a)). When a sinusoidal voltage is applied to all interconnected potential electrodes, plasma jets are formed, which are determined by the stochastic generation of streamers from the tips of the potential electrode. Experiments have shown that the current is generated at each positive half-wave of the applied sinusoidal voltage, and its propagation both within one channel and through different channels are independent of each other (see Fig. 2 (b)).

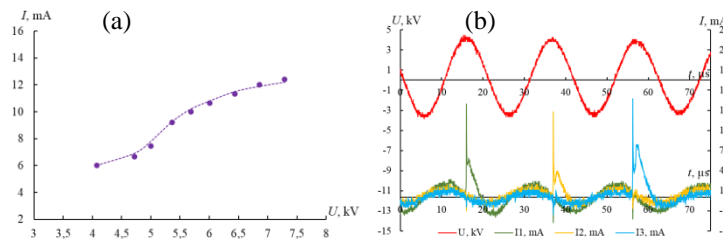


Fig. 2. (a) The typical dependence of the current on the voltage, (b) measured voltage (red) and currents recorded from different channels (green, yellow, blue).

It was shown that at each moment of time, a separate streamer appears. Thus, the larger area and jet uniformity is determined by the multifrequency overlap of current pulses.

REFERENCES

- [1] M. Keidar, "Plasma for cancer treatment," *Plasma Sources Science and Technology*, vol. 24, 1 3, p. 033001, 2015.

* The work was supported by the RSF Grants No. 19-19-00255.

PICOSECOND SEMICONDUCTOR GENERATOR FOR CAPACITIVE SENSORS CALIBRATION

V.E. PATRAKOV^{1,2}, M.S. PEDOS¹, S.N. RUKIN¹

¹*Institute of Electrophysics, UB, RAS, Yekaterinburg, Russia*

²*Ural Federal University, Yekaterinburg, Russia*

e-mail: vitpatrakov@gmail.com

Experimental studies of ultrafast processes of electrical discharges development in gases, for example, at runaway electron flows generating in air [1], require the use of sources of powerful short pulses. The voltage pulse amplitude at pulse duration of 100–200 ps can reach 1–2 MV [2, 3]. The pulses affecting the gas gap are transmitted along a coaxial line and are recorded by capacitive voltage dividers (sensors), the division factor of which, as a rule, is $\sim 10^3$ – 10^4 . Such sensors require preliminary calibration with pulses, the front and duration of which are shorter than the corresponding parameters of the measured pulse.

The paper describes a semiconductor picosecond pulse generator that can be used to calibrate capacitive voltage sensors. The generator is designed as a base unit, to which additional external sharpeners and pulse converters are connected. In the base unit, semiconductor devices – first a semiconductor opening switch (SOS) and then a semiconductor sharpener (SS) – generate an output pulse with a front of 210 ps and a subsequent plateau of 2 ns in duration. The pulse amplitude is 970 V across 50-Ω load. An external diode sharpener generates a pulse with 155-ps front and 500-ps plateau at the amplitude of 820 V. To switch the semiconductor sharpeners to the conducting state, the shock-ionization wave mode is used. External converters make it possible to generate output pulses across 50-Ω load with the front of 105–155 ps, the pulse duration of 160–310 ps, and the amplitude of 180–500 V.

The electrical diagram of the generator, waveforms of the output pulses of the base unit and after external sharpeners and converters are presented. An example of the calibration of capacitive sensors located in the measuring section of a powerful picosecond generator is also shown.

REFERENCES

- [1] G.A. Mesyats, M.S. Pedos, S.N. Rukin, V.V. Rostov, I.V. Romanchenko, A.G. Sadykova, K.A. Sharypov, V.G. Shpak, S.A. Shunailov, M.R. Ulmasculov, and M.I. Yalandin, “Formation of 1.4 MeV runaway electron flows in air using a solid-state generator with 10 MV/ns voltage rise rate,” *Applied Physics Letters*, vol. 112, pp. 163501, 2018.
- [2] E.A. Alichkin, M.S. Pedos, A.V. Ponomarev, S.N. Rukin, S.P. Timoshenkov, and S.Y. Karelin, “Picosecond solid-state generator with a peak power of 50 GW,” *Review of Scientific Instruments*, vol. 91, pp. 104705, 2020.
- [3] S.N. Rukin, A.V. Ponomarev, E.A. Alichkin, S.P. Timoshenkov, M.S. Pedos, and K.A. Sharypov, “Generation of multi-gigawatt picosecond pulses by magnetic compression lines,” *Proc. 7th Int. Congress on Energy Fluxes and Radiation Effects (EFRE)*, Tomsk, Russia, pp. 92–97, 2020.

SPATIAL DISTRIBUTION AND TIME EVOLUTION OF A METAL-CONTAINING PLASMA OF A LOW-CURRENT ATMOSPHERIC PRESSURE DISCHARGE*

K.P. SAVKIN, D.A. SOROKIN, G.YU. YUSHKOV

Institute of High Current Electronics, SB, RAS, Tomsk, Russia

e-mail: savkinkp@mail2000.ru

The spatial distribution of the intensity and the temporal dynamics of the plasma generated by atmospheric pressure with a magnesium cathode in an argon flow are experimentally investigated. A discharge system of coaxial geometry was used in the work [1]. In the center was a cathode placed inside a ceramic tube. There was a hole in the anode through which the plasma was forced out of the discharge system by the flow of the working gas. The repetition rate of unipolar quasi-rectangular pulses was 56 kHz, with a pulse duration of 12 μ s. The amplitude of the discharge current in the steady-state mode was 100 mA, at a voltage of about 130 V. In this mode, local melting of the active cathode surface occurred. The evaporated magnesium atoms were captured by the working gas flow and formed a green glow plume around the positive discharge column outside the anode nozzle. The image of the plasma formation was projected onto the entrance slit of the monochromator, with the help of which the spatial distribution of the radiation intensity and its evolution in time of the selected monochromatic components were measured. The spectrum of this radiation contained groups of lines of ions and magnesium atoms with wavelengths 285.21 nm (singlet resonant Mg I); 383.08, 383.36, 383.9 nm (triplet Mg I); 516.8, 517.4, 518.5 nm (triplet Mg I) [2].

The results of this work are promising from the point of view of studying open-type spontaneous radiation sources, as well as the generation of combined gas-metal plasma flows [3] at atmospheric pressure.

REFERENCES

- [1] K.P. Savkin, E.M. Oks, G.Yu. Yushkov, Yu.F. Ivanov, "A low-current atmospheric pressure discharge generating atomic magnesium fluxes," *J. Appl. Phys.*, 213303 (2020).
- [2] Y.M. Smimov, "Electron-impact excitation cross sections of triplet levels of magnesium atom," *High Temperature*, vol. 37, iss. 3, pp. 359-365 (1999).
- [3] K.P. Savkin, A.S. Bugaev, V.I. Gushenets, A.G.Nikolaev, Y.F. Ivanov, E.M. Oks, V.P. Frolova, M.V. Shandrikov, G.Yu.Yushkov, "Generation of micron and submicron particles in atmospheric pressure discharge in argon flow with magnesium, zinc, and boron carbide electrodes," *Surf. Coat. Technol.*, vol. 389, 125578 (2020).

* The reported study was funded in part by RFBR and Tomsk Region according to the research project № 19-48-700019 (investigation of spatial distribution) and .and partially by state assignment project FWRM-2021-0014 (investigation of time evolution).

MINICP DEVICE FOR INVESTIGATION OF THE PLASMA-SURFACE INTERACTIONS*

N.S. SERGEEV^{1,2}, A.V. KAZIEV¹, M.M. KHARKOV^{1,3}, YU.M. GASPARYAN¹, A.YU. KHOMYAKOV¹

¹*National Research Nuclear University MEPhI (Moscow Engineering Physics Institute), Moscow, Russia*

²*National Research Center "Kurchatov Institute", Moscow, Russia*

³*A.A. Bochvar High-Technology Scientific Research Institute for Inorganic Materials, Moscow, Russia*

e-mail: nickbebeskis@gmail.com

The radio frequency (RF) inductively coupled plasma (ICP) is a universal tool for studying the erosion and surface modification processes [1]. Because of its unique properties, ICP discharge can be used in two different pressure regimes: at high pressure ($p_g \sim 100$ torr) it can produce equilibrium plasmas, whereas at low pressure values ($p_g \sim 0.01$ torr) its plasma is non-equilibrium [2]. Moreover, it is possible to regulate the values of the basic plasma parameters, such as electron temperature, T_e , and electron density, n_e , in a wide range. All described features are making ICP discharge a promising tool for plasma-surface interaction studies including LIBS, LIAS measurements in presence of background plasma.

In this work, the change of the spectral lines ratio of the H impurity radiation and He/Ar plasma emission spectrum of the ICP discharge was studied in a newly designed and built device (see Fig. 1). In order to do so, the measurements of Balmer series lines intensities ($n' = 2$ и $n = 3, 4, 5$) were considered. The measurements were carried out with a different impurity to working gas percentage ratio. Methods for increasing the signal to noise ratio of LIBS/LIAS measurements in the ICP background plasma discharge are studied.

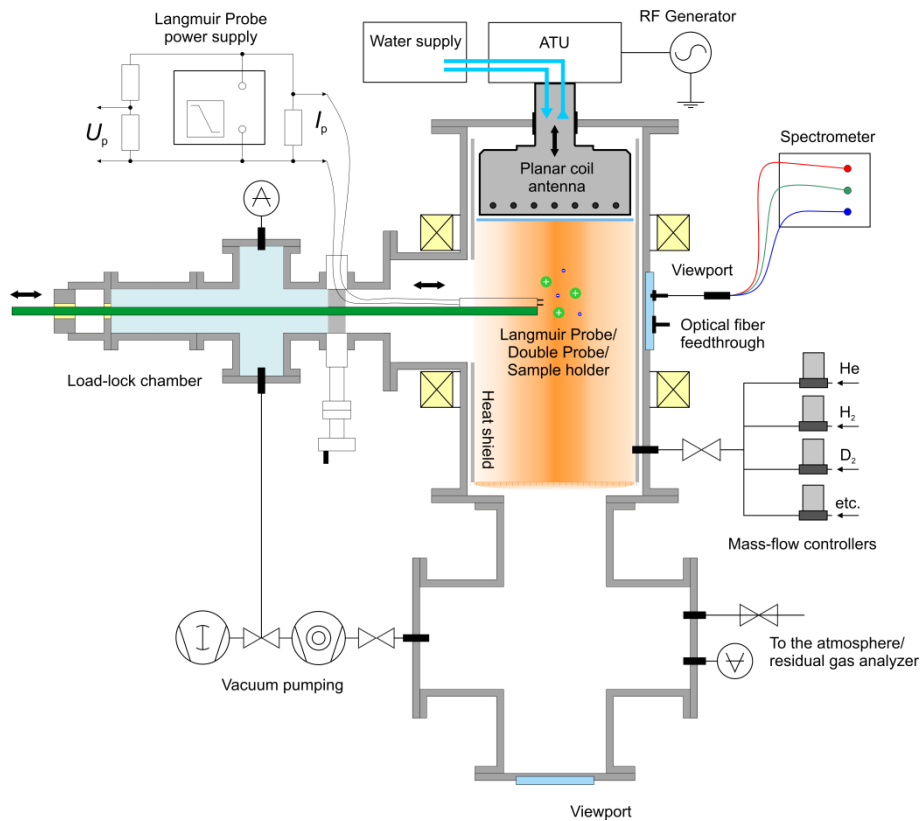


Fig. 1. Sketch of the minICP device

REFERENCES

- [1] Hyo-Chang Lee. Review of inductively coupled plasmas: Nano-applications and bistable hysteresis physics // *Applied Physics Reviews* 5, 011108 (2018).
- [2] T Czerwiec and D B Graves // *J. Phys. D: Appl. Phys.* 37 2827 (2004).

*The work was supported by the Ministry of Science and Higher Education of the Russian Federation (project No. 0723-2020-0043).

COLD PLASMA SOURCE BASED ON THE APOKAMPIC DISCHARGE IN ATMOSPHERIC-PRESSURE AIR*

D.A. SOROKIN, V.A. PANARIN, E.A. SOSNIN, V.S. KUZNETSOV, V.S. SKAKUN

Institute of High Current Electronics, SB, RAS, Tomsk, Russia
e-mail: SDmA-70@loi.hcei.tsc.ru

To date, the problem of creating a source of non-equilibrium low-temperature plasma, formed upon excitation of the air around us and having a temperature of the order of room one or slightly higher, continues to be extremely urgent. Despite the huge amount of research in this direction, such a plasma source has not yet been implemented. However, such a source is extremely promising from a practical point of view and can be used in various fields [1, 2].

The study deals with the results of studies of the characteristics of a source of cold air plasma based on the relatively recently discovered phenomenon of the gas discharge physics – an apokampic discharge (Fig. 1a) [3, 4]. This type of discharge is implemented when voltage pulses of microsecond duration with an amplitude of tens of kilovolts, following with a frequency of tens of kilohertz, are applied to the gap formed by electrodes (1 and 2 in Fig. 1a) located at a certain angle to each other (one must have a capacitive decoupling with respect to the ground), and it allows to form plasma plume (5 на Fig. 1a) of relatively low temperature in atmospheric pressure air. Its formation is due to streamers propagating at a high speed from the bright branch (3 in Fig. 1a) of the pulse discharge channel (2 in Fig. 1a).

A design is proposed that makes it possible to localize and stabilize the discharge channels, which are the centers of the formation of plasma plumes. Measurements of electronic, vibrational, rotational, and gas temperatures in plasma in various zones of the discharge formed in this design were carried out by optical emission spectroscopy techniques [5, 6]. It is shown that everywhere plasma is strongly non-equilibrium – there is a strong difference between the electronic temperature (several eV) and the temperature of heavy particles (hundreds to thousands of K, depending on the measurement zone). Thus, a cold air plasma jet based on the apokampic discharge has been realized (Fig. 1b).



Fig. 1. (a) Apokampic discharge. 1, 2 – electrodes; 3 – discharge channel; 4 – bright branch; 5 – plasma plume. (b) Cold air plasma jet.

REFERENCES

- [1] I. Adamovich, S.D. Baalrud, A. Bogaerts, et al., “The Plasma Roadmap. Low temperature plasma science and technology,” *J. Phys. D: Appl. Phys.*, Vol. 50, art. no. 323001, 2017.
- [2] S. Reuter, et al., “The kINPen – a review on physics and chemistry of the atmospheric pressure plasma jet and its applications,” *J. Phys. D: Appl. Phys.*, Vol. 51, art. no. 233001, 2018.
- [3] V.F. Tarasenko, E.A. Sosnin, V.S. Skakun, V.A. Panarin, M.V. Trigub, G. S. Evtushenko, “Dynamics of apokamp-type atmospheric pressure plasma jets initiated in air by a repetitive pulsed discharge,” *Phys. Plasmas*, Vol. 24, art. no. 043514, 2017.
- [4] E.A. Sosnin, N.Yu. Babaeva, V.Yu. Kozhevnikov, A.V. Kozyrev, G.V. Naidis, V.A. Panarin, V.S. Skakun, V.F. Tarasenko, “Modeling of transient luminous events in Earth’s middle atmosphere with apokamp discharge,” *Phys. Usp.*, Vol. 64, no. 2, 2021.
- [5] H. Nassar, S. Pellerin, K. Musiol, O. Martinie, N. Pellerin, J.-M. Cormier, “ N_2^+/N_2 ratio and temperature measurements based on the first negative N_2^+ and second positive N_2 overlapped molecular emission spectra,” *J. Phys. D: Appl. Phys.*, Vol. 37, no. 14, pp. 1904–1916, 2004.
- [6] D.M. Phillips, “Determination of gas temperature from unresolved bands in the spectrum from a nitrogen discharge,” *J. Phys. D: Appl. Phys.*, Vol. 9, no. 3, pp. 507–521, 1976.

* The work was performed in the framework of the State Task for IHCE SB RAS, # FWRM-2021-0014.

OPTIMUM TRANSFER CHARACTERISTICS OF THE TESLA TRANSFORMER ON THE FIRST AND SECOND HALF-WAVES OF OUTPUT VOLTAGE

V.V. KLADUKHIN, S.P. KHRAMTSOV

Institute of Electrophysics, UB, RAS, Yekaterinburg, Russia

e-mail: laepr@iep.uran.ru

Tesla transformers, the equivalent circuit of which is shown on Fig. 1, are widely used in the design of high-voltage power supplies.

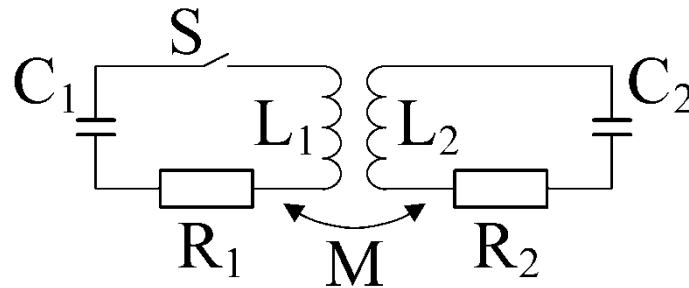


Fig. 1. Equivalent circuit of Tesla transformers.

Many publications are devoted to the analysis of the operating modes of the Tesla transformer, for example [1-4], however, the optimal transfer properties of the transformer were considered, either with incomplete variation of the parameters, or using approximations.

In the present work, the optimal processes of charging the capacitance of the output oscillatory circuit at the first and second half-waves are considered, based on the exact solution of the transformer equations with varying of Q-factors ($Q_1 = \sqrt{L_1/C_1}/R_1$, $Q_2 = \sqrt{L_2/C_2}/R_2$), of coupling factor ($k = M/\sqrt{L_1L_2}$) and of mismatching factor of the natural resonance frequencies of the circuits ($\omega_{01} = 1/\sqrt{L_1C_1}$, $\omega_{02} = 1/\sqrt{L_2C_2}$).

REFERENCES

- [1] P. Drude, "Über induktive Erregung zweier elektrischer Schwingungskreise mit Anwendung auf Perioden- und Dämpfungsmessung, Teslatransformatoren und drahtlose Telegraphie," *Annalen der Physik*, vol. 13, pp.512-561, 1904, DOI: 10.1002/andp.18943180306.
- [2] C.R.J. Hoffman, "A Tesla Transformer High-Voltage Generator," *Rev. Sci. Instrum.*, vol. 46, no. 1, pp.1-4, 1975, DOI: 10.1063/1.1134057.
- [3] H. Matsuzawa, S. Suganomata, "Design Charts for Tesla-transformer-type relativistic electron beam generators," *Rev. Sci. Instrum.*, vol. 53, no. 5, pp.694-696, 1982, DOI: 10.1063/1.1137044.
- [4] E.I. Palchikov, A.M. Ryabchun, "Analysis of the Tesla transformer operation at the first half-wave of the output voltage taking into account ohmic losses," *Technical Physics*, vol. 61, no. 6, pp. 919-923, 2016, DOI: 10.1134/S1063784216060165.

INVESTIGATION OF COLD ATMOSPHERIC PLASMA JET GENERATION EXCITED BY SQUARE-WAVE PULSE*

P.P. GUGIN¹, D.E. ZAKREVSKY^{1,2}, E.V. MILAKHINA^{1,2}

¹A. V. Rzhanov Institute of Semiconductor Physics, SB, RAS, Novosibirsk, Russia

²Novosibirsk State Technical University, Novosibirsk, Russia

e-mail: zakrdm@isp.nsc.ru

Interest in the investigation of a cold atmospheric pressure plasma and its parameters, in particular a plasma jet, is associated, on the one hand, with the fact that it is an interesting physical object, and on the other hand, with its active application as a tool for cold plasma medicine. The impact of a cold atmospheric plasma jet (CAPJ) on biological objects activates the processes of viability reducing of cancer cells and suppressing the development rate of malignant tumors. Non-equilibrium plasma state allows the production of chemically active species without excessive gas heating and affects to targets, including living organisms that are sensitive to heat. An increase in temperature in the contact area between plasma and biological object may not exceed several degrees, which is not a destructive parameter of plasma exposure. In most cases, during biophysical experiments, a source of cold plasma jet is used, generated when a sinusoidal voltage is applied to the potential inner electrode. The streamers generated at each positive half-wave of the applied voltage propagated along the gas flow into the surrounding space and formed a plasma jet.

The aim of this research was to investigate the parameters of CAPJ generation excited by unipolar positive pulses. In this work, we used a coaxial device with a potential internal electrode [1], and a source of positive square-wave pulses with $U = 0-10$ kV and an adjustable frequency of $f = 3-30$ kHz was used as an excitation source.

When pumping a working gas helium grade A (99.995%) through the gas-discharge cell with flow rates $\nu = 1.5-12$ L/min ($\nu > 1$ L/min) and applying a voltage of $U \approx 0.7$ kV to the electrodes, the discharge was ignited. When the voltage was exceeded $U > 0.7$ kV, a CAPJ was formed that propagated beyond the channel and spread in free space. Oscillograms of voltage and current are shown in Fig. 1 (a). In Fig. 1 (b, c) the typical dependences of the current amplitude on the voltage $I(U)$ are shown, which has a saturating form with increasing U , and an exponentially decreasing dependence of the current on the pulse repetition rate $I(f)$. In contrast to research [2], in which the CAPJ was generated by a sinusoidal voltage, in the present case (excitation by square-wave pulses) the previously discovered effect of frequency changing during the generation of current pulses, different from the frequency of the applied sinusoidal voltage, was not observed.

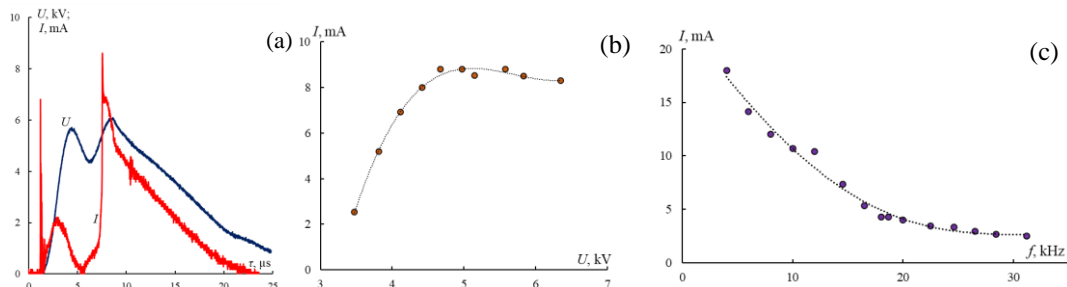


Fig. 1. (a) Oscillograms of U, I : He, $\nu = 4.5$ L/min, $U = 5$ kV и $f = 13.4$ kHz; (b) dependence $I(U)$ $\nu = 4.5$ L/min; (c) dependence $I(f)$ $\nu = 4.5$ L/min $U = 5.6$ kV.

An increase in the pulse repetition rate leads to the growth of target temperature over 40°C , which limits the application of CAPJ at biomedical purposes. A specially developed device limiting the duration of the current pulse $\leq 2 \mu\text{s}$ made it possible to lower the target temperature by 10°C .

REFERENCES

- [1] I. Schweigert, D. Zakrevsky, P. Gugin, E. Yelak, E. Golubitskaya, O. Troitskaya, O. Koval, "Interaction of Cold Atmospheric Argon and Helium Plasma Jets with Bio-Target with Grounded Substrate Beneath," *Applied Sciences*, vol. 9, p. 4528, 2019.
- [2] I.V. Schweigert, A.L. Alexandrov, D.E. Zakrevsky, "Self-organization of touching-target current with ac voltage in atmospheric pressure plasma jet for medical application parameters," *Plasma Sources Science and Technology*, vol. 29, p. 12LT02, 2020.

* The research was founded by RFBR and Novosibirsk region, project number 20-48-540019.

DYNAMICS OF THE TARGET TEMPERATURE CHANGE UNDER DIRECT IMPACT OF A COLD ATMOSPHERIC PLASMA JET*

P.P. GUGIN¹, D.E. ZAKREVSKY^{1,2}, E.V. MILAKHINA^{1,2}

¹A. V. Rzhanov Institute of Semiconductor Physics SB RAS, Novosibirsk, Russia

²Novosibirsk State Technical University, Novosibirsk, Russia

e-mail: [lena.yelak@gmail.com](mailto:lana.yelak@gmail.com)

The impact of a cold atmospheric plasma jet (CAPJ) on biological objects is a developing area of plasma medicine. Until now, the mechanisms of the CAPJ effect on biological objects have not been unambiguously defined. To use CAPJ in biomedical research, it is necessary to control the temperature rise in the contact area of the CAPJ with the target at different He gas flow rates, amplitudes of the applied sinusoidal voltage U , and distances to the target. The target was an Al_2O_3 plate ($1 \times 25 \times 34$ mm) placed on an auxiliary grounded electrode at a distance of 20 mm and 30 mm from the nozzle [1].

The temperature measurements in the contact area of the plasma jet with the surface were carried out when a sinusoidal voltage was applied with a frequency of $f = 13; 23$ kHz in the range of He flow rates $\nu = 1,5\text{--}13,5$ L/min and voltages $U = 2,7\text{--}6,5$ kV. The target was positioned at a distance of 20 mm and 30 mm from the nozzle (see Fig. 1).

It was found that the temperature in the contact area of the CAPJ with the target was established in a constant state within 60-120 s of exposure. The temperature of the dielectric plate reached $T \sim 100^\circ\text{C}$ at $\nu = 6$ L/min, $U = 6,5$ kV at a distance of 20 mm from the nozzle.

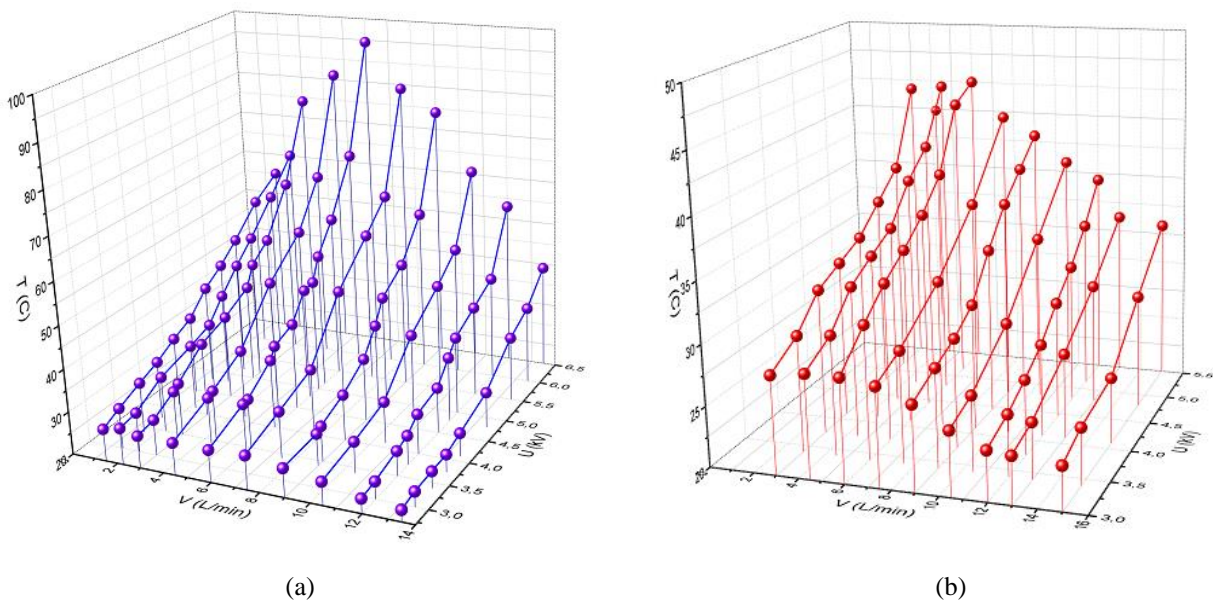


Fig. 1. The temperature in the contact area of a CAPJ with a dielectric surface at distance (a) 20 mm, (b) 30 mm.

In the contact area between the CAPJ and the target, the temperature increases with voltage growth at the same He flow rate. The dependences of the temperature to the gas flow rate at constant voltage is an extreme function, more pronounced at higher voltages. The right side of the dependence demonstrates that the temperature of the target decreases with an increase in the flow rate, and the left side of the dependence is determined that with flow rate decreasing the CAPJ length shorten and the contact between the jet and the target disappear. With an increase in the distance from the nozzle to the target under similar conditions, the temperature reached is lower. Thus, from the graphs it is possible to determine the conditions for the functioning of the CAPJ source and the necessary conditions for the effect on living tissues.

REFERENCES

- [1] I. Schweigert, Dm. Zakrevsky, E. Milakhina (Yelak), P. Gugin, E. Golubitskaya, O. Troitskaya, O. Koval, "Interaction of cold atmospheric argon and helium plasma jets with bio-target with grounded substrate beneath," *Applied Sciences*, vol. 9, p. 4528, 2019.

* The work was supported the RSF Grants No. 19-19-00255.

PLASMA GENERATION IN A HIGH-CURRENT GLOW DISCHARGE WITH A HOLLOW CATHODE IN AN AXIALLY SYMMETRICAL SYSTEM USING TWO ELECTRON SOURCES*

E.V. OSTROVERKHOV, V.V. DENISOV

Institute of High Current Electronics, SB, RAS, Tomsk, Russia
e-mail: evgeniy86evgeniy@mail.ru

A non-self-sustained low-pressure glow discharge with a hollow cathode makes it possible to efficiently generate plasma in large ($> 0.1 \text{ m}^3$) vacuum volumes [1]. In this paper, we present the results of probe measurements of the main parameters of the glow discharge plasma in the case of separate and joint operation of electron sources supporting the combustion of the glow discharge. The validity of the application of the principle of superposition of the distributions of the main plasma parameters in a hollow cathode of a glow discharge with currents up to 200 A, obtained using two electron sources based on an arc discharge with an arc spot [2] was investigated. The studies were carried out for a hollow cathode with a diameter to length ratio of 2:1 and a volume of 0.34 m^3 .

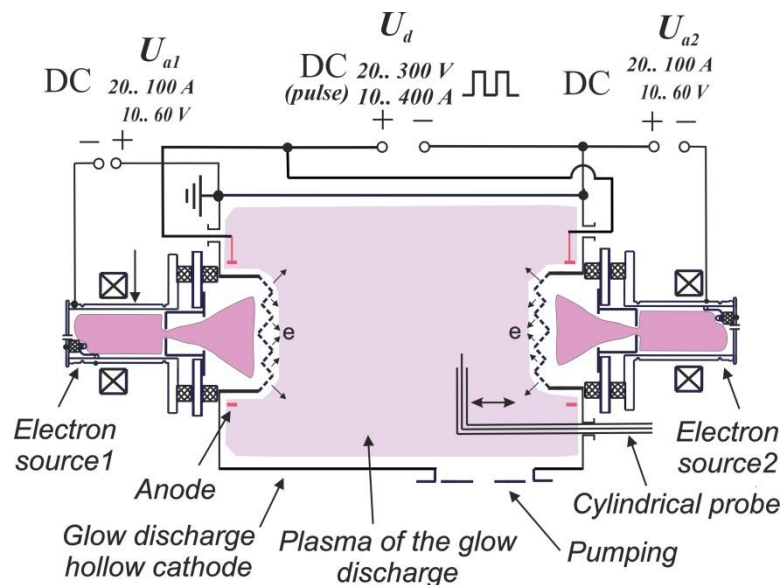


Fig. 1. The experimental assembly.

REFERENCES

- [1] V.V. Denisov, Yu.H. Akhmadeev, N.N. Koval, S.S. Kovalsky, I.V. Lopatin, E.V. Ostroverkhov, N.N. Pedin, V.V. Yakovlev, and P.M. Schanin. The source of volume beam-plasma formations based on a high current non-self-sustained glow discharge with a large hollow cathode // *Phys. Plasmas* 26, 123510 (2019).
- [2] V.V. Denisov, Yu.H. Akhmadeev, N.N. Koval and E.V. Ostroverkhov // *High Temp. Mater. Process.* 20(4), 309–316 (2016).

* The work was performed under State Assignment of the Ministry of Science and Higher Education of the Russian Federation (project No. FWRM-2019-0002).

ATMOSPHERIC COLD PLASMA JET GENERATED BY MICROWAVE ELECTRODE DISCHARGE: SOME DIAGNOSTIC TECHNIQUES*

S.N. ANTIPOV, V.M. CHEPELEV, M.A. SARGSYAN, M.KH. GADZHIEV

Joint Institute for High Temperatures, RAS, Moscow, Russia

e-mail: antipov@ihed.ras.ru

Microwave-driven cold plasma jets based on atmospheric-pressure discharges are intensively investigated for purposes of plasma modification in practical medicine, microbiology, agriculture and the food industry [1-3]. The experimental setup based on the previously developed multipurpose 2.45-Hz-plasmatron was used [4] (see Fig. 1). The plasmatron has a microwave power in the waveguide of up to 2.5 kW and a power in the torch of up to couple of hundreds of watts. The plasma torch consists of cylindrical common chamber with 6 rod-like electrodes forming a regular hexagon in a cross-section (MicroPlaSter device arrangement [5]). Discharge channels are formed between the ends of the electrodes and the inner wall of the torch close to the torch outlet. Argon of high purity (99.998%) was used with the flow rate in the range from 0 to 10 standard liters per minute.

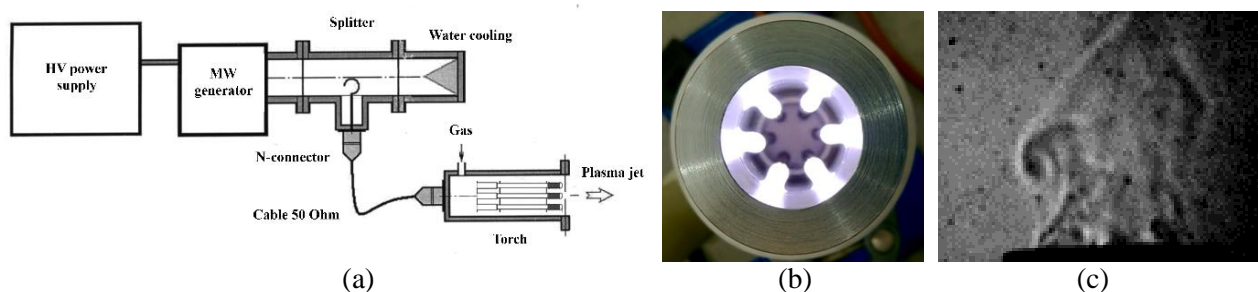


Fig. 1. (a) Sketch of the 2.45-GHz-plasmatron, (b) discharges in the plasma torch (view from the outlet), (c) side view of the plasma jet (shadow imaging).

Cold plasma jet generated by the torch is a discharge streaming-afterglow which is rather weak and not distinguished by naked eye. In the present work, the new collection of experimental diagnostic techniques has been developed to explore and characterize such plasma jets. The measurements and analysis of the emission spectra were conducted. Probe floating potential in the plasma jet was investigated by means of oscilloscope. The spatial structure and dynamics of the cold plasma jet were studied using the shadowgraphy and high-speed video filming. Thermocouple and thermal imaging measurements of the plasma jet temperature were conducted.

REFERENCES

- [1] Kong M.G., Kroesen G., Morfill G. et al. Plasma medicine: an introductory review // *New Journal of Physics*. 2009. V. 11, no. 11, P. 115012.
- [2] Levshenko M.T., Filippovich V.P., Prokopenko A.V. et al. Investigation of the effect of a microwave discharge plasma at asepsis packaging // *Storage and processing of farm products*. 2011. No. 10, P. 13–16.
- [3] Ermolaeva S., Petrov O., Zigangirova N. et al. Low temperature atmospheric argon plasma: Diagnostics and medical applications // in *NATO Science for Peace and Security Series A: Chemistry and Biology / Plasma for Bio-Decontamination, Medicine and Food Security* (Z. Machala et al., eds.). Dordrecht: Springer. 2012. P. 163–177
- [4] Chepelev V.M., Chistolinov A.V., Khromov M.A. et al. Thermocouple and electric probe measurements in a cold atmospheric-pressure microwave plasma jet // *J. Phys.: Conf. Ser.* 2020. V. 1556, P. 012091
- [5] Shimizu T., Steffes B., Pompl R. et al. Characterization of microwave plasma torch for decontamination // *Plasma Processes and Polymers*. 2008. V. 5, iss. 6. P. 577–582.

* The work was supported by the RFBR Grant No. 19-08-00844.

FEATURES OF PLASMA GENERATION IN A PULSED MODE OF A NON-SELF-SUSTAINED ARC DISCHARGE*

S.S. KOVALSKY, V.V. DENISOV, E.V. OSTROVERKHOV, V.E. PROKOP'EV

Institute of High Current Electronics, SB, RAS, Tomsk, Russia
 e-mail: kovalsky@opee.hcei.tsc.ru

Plasma of the non-self-sustained arc discharge generated by a PINK plasma generator with a thermionic and hollow cathode in a system with a hollow anode is widely used in such processes of surface treatment of the materials as nitriding and plasma-assisted deposition of functional coatings [1]. One of the main factors complicating the treatment process is a significant inhomogeneity of the distribution of plasma parameters over the volume of the vacuum chamber. The pulsed mode of a non-self-sustained arc discharge is promising to reduce the degree of inhomogeneity of the distributions of plasma parameters.

The paper presents the results of measurements of plasma parameters over the volume of a hollow anode formed by the inner walls of a cylindrical vacuum chamber 1200 mm high and 600 mm in diameter. The inhomogeneity of the plasma concentration distribution decreases 1.5-2 times with a decrease in the pulse duration from 500 μ s to 200 μ s, and also 15-30 times with an increase in the discharge voltage from 100 V up to 300 V for the same pulse discharge power (30 kW). The required average discharge power for processing can be obtained by changing the pulse repetition rate.

In this work, we also studied the optical emission spectra of the plasma at a distance of about 300 mm from the output aperture of the plasma generator. A significant increase in the intensity of the spectral emission lines of atomic nitrogen N* and molecular nitrogen ion N₂⁺, which have the main effect on the nitriding process, with an increase in the pulse power for a short pulse duration (600 μ s) is shown. This effect for a doubled pulse duration (1200 μ s) at the same average power is not observed.

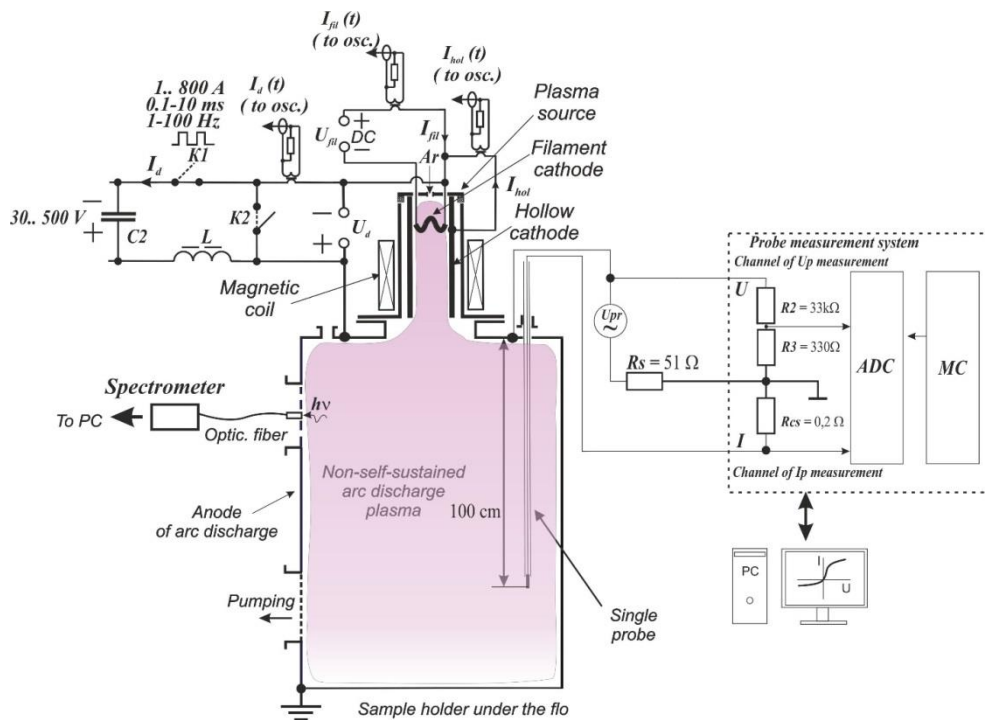


Fig. 1. The experimental bench.

REFERENCES

- [1] N.N. Koval, Yu.F. Ivanov, I.V. Lopatin, Yu.H. Akhmadeev, V.V. Shugurov, O.V. Krysinina, V.V. Denisov. Generation of low-temperature gas discharge plasma in large vacuum volumes for plasma chemical processes // Russian Journal of General Chemistry, 2015, V. 85, no. 5, pp. 1326-1338.

* The work was performed under State Assignment of the Ministry of Science and Higher Education of the Russian Federation (project No. FWRM-2019-0002).

GENERATION OF ION AND ELECTRON BEAMS AND PLASMA FLOWS IN SPECIAL CONDITIONS WITH "EXTREME" PARAMETERS AND SOME EXAMPLES OF ITS APPLICATIONS

E.M. OKS^{1,2}

¹ *Institute of High Current Electronics, SB, RAS, Tomsk, Russia*

² *Tomsk State University of Control Systems and Radioelectronics Tomsk, Russia*

email: oks@opee.hcei.tsc.ru

The report provides an overview of recent research conducted at the integrated plasma electronics laboratory of High Current Electronics Institute, Russian Academy of Science (HCEI) And Tomsk State University of Control Systems and Radioelectronics (TUSUR) Tomsk, Siberia, Russia. The subject of investigation in the laboratory is associated with the development of unique plasma sources of electron beams, ion sources, and also plasma generators operating in extreme conditions or providing extreme output parameters. The physical principles of the functioning of the such devices and systems will be presented and described.

FPGA BASED DEVELOPMENTS FOR HIGH SWITCHING FREQUENCY POWER MODULES BASED ON WIDE BAND GAP SEMICONDUCTORS

R. RUSCASSIE¹, J. M. LARBAIG¹, R. LEDUC¹, J. M. DIENOT^{1,2}

¹ Université de Pau et des Pays de l'Adour, E2S UPPA, SIAME, Pau, France

² Université de Toulouse III, LABCEEM, Tarbes, France

e-mail: robert.ruscassie@univ-pau.fr

These last years have seen the growing interest of electrical engineering community for wide band gap semiconductors (Silicon Carbide, but also Gallium Nitride more recently) which will gradually spread over more and more converters designs, especially in the pulsed power area [1].

Within the frame of a project based on a SiC converter development, we initiated the development of a test bench based on FPGA-SoC (System on a Chip) technology, allowing the combination of FPGA fast synchronous features together with a ARM micro-processor operated OS together in one single chip.

These fast and powerful devices [2] are a very appropriate solution to generate the driving commands of numerous semiconductor switches at increasing speeds, as well as to set their security routine. In addition, since the available resources of such systems remain significant, the development of Human Machine Interface (HMI) was also implemented and the development of an integrated data acquisition solution is currently under development.

The idea behind this concept is to progressively establish our own all in one open system adapted to the specific requirements of pulsed power environment applications. In order to achieve this purpose, several EMC concerns will have to be investigated and avoided by the use of specific shielding and protection techniques.

In our paper, we will describe in details the system we designed (Fig. 1) and present the first conclusions that were driven regarding the benefits of such solutions for pulsed power, as well as the road map ahead.

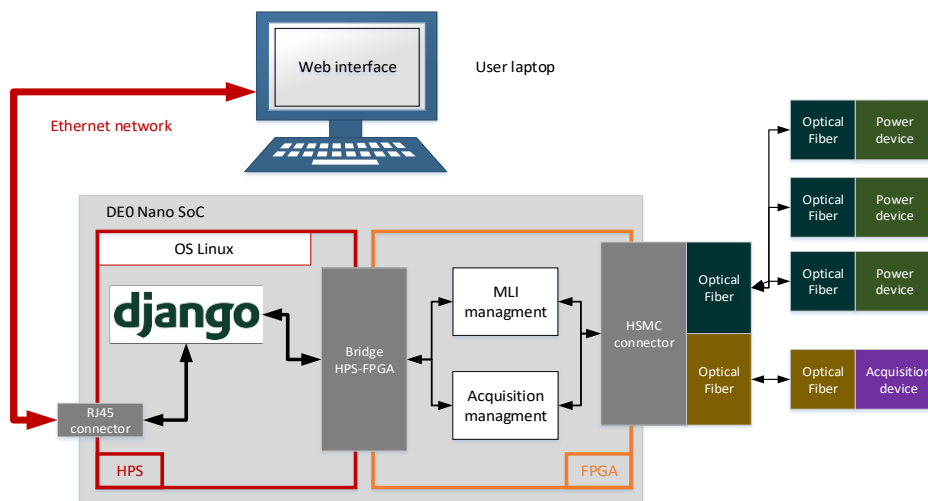


Fig. 1. Architecture diagram of the developed FPGA SoC based test bench.

REFERENCES

- [1] M. Samizadeh Nikoo, A. Jafari and E. Matioli, "GaN Transistors for Miniaturized Pulsed-Power Sources," in IEEE Transactions on Plasma Science, vol. 47, no. 7, pp. 3241-3245, July 2019, doi: 10.1109/TPS.2019.2917657.
- [2] J.J. Rodríguez-Andina, M. D. Valdés-Peña and M. J. Moure, "Advanced Features and Industrial Applications of FPGAs—A Review," in IEEE Transactions on Industrial Informatics, vol. 11, no. 4, pp. 853-864, Aug. 2015, doi: 10.1109/TII.2015.2431223.

A NEW TYPE OF NON-THERMAL ATMOSPHERIC PRESSURE PLASMA SOURCE BASED ON A WAVEGUIDE BRIDGE *

V.N. TIKHONOV, S.A. GORBATOV, I.A. IVANOV, A.V. TIKHONOV

Russian Institute of Radiology and Agroecology, RAS, Obninsk, Russia
e-mail: v.n.tihonov@yandex.ru

Recently, intensive development of plasma-chemical methods for modifying the surfaces of synthetic and natural polymers, has been carried out. For this purpose, low-current discharges - corona and dielectric barrier discharge (DBD) - with limited gas activation efficiency were initially used as sources of non-equilibrium atmospheric pressure plasma of non-destructive action. The microwave discharge of atmospheric pressure removes the restrictions on the specific power. However, at atmospheric pressure, the microwave plasma torch of the "classical" electrodeless design forms a plasma jet with a temperature of several thousand degrees or more. Known electrode microwave dischargers [1] form argon plasma with a temperature of tens of degrees Celsius, but such plasma may contain products of destruction of the electrode material. The new type of non-destructive plasma microwave source presented in [2] has both the characteristics of DBD (in terms of configuration and low gas temperature) and the ability to form a "clean" plasma jet like a classical microwave plasmatron. The temperature of the plasma jet in this case is on average about 2000C, which does not have a destructive thermal effect on many polymers in the case when a short processing time is sufficient. However, the need to use a circulator leads to a significant increase in the complexity, cost and weight of the installation as a whole (see Fig. 1a).

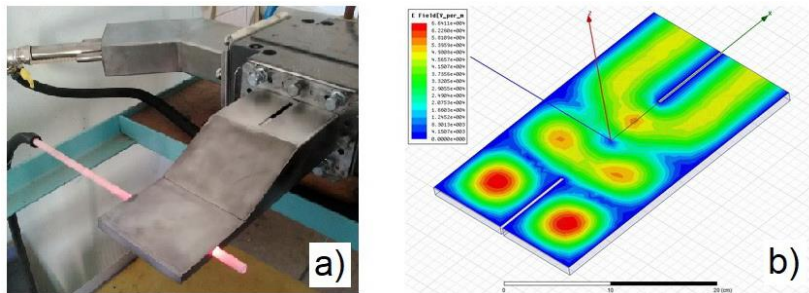


Fig. 1. (a) Fragment of the experimental setup, and (b) longitudinal section of the calculated model.

The basis of the presented plasma source is a three-decibel waveguide bridge with a connection along a narrow wall. Both output arms of the bridge are loaded on identical short-circuited segments of waveguides. At a distance of a quarter of the wavelength from the short circuits, a discharge tube passes across the waveguides. In this case, the vector of the E-component in the antinode of the standing electromagnetic wave is perpendicular to the axis of the dielectric tube and, accordingly, the geometric conditions for the formation of DBD are met. In addition, since the output arms of the bridge are always loaded symmetrically, the generator power reflected from the short circuits (in the absence of a discharge) or not absorbed in the microwave discharge enters the decoupled arm of the bridge to which the matched load is connected. Thus, in any case, the magnetron is protected from the reflected wave without the need for an expensive circulator. For geometric parameters and their subsequent optimization calculation were using the HFSS – electrostatics modeling of microwave structures program. A longitudinal section in plane H of the calculated model of the electromagnetic structure is shown in Figure 1b. As a source of microwave power, a budget generator can be used, built on the basis of components for household microwave ovens [3].

REFERENCES

- [1] V. Tikhonov, S. Gorbatov, I. Ivanov and A. Tikhonov, The Low-Cost Microwave Source of Non-Thermal Plasma, 2020 7th International Congress on Energy Fluxes and Radiation Effects (EFRE), Tomsk, Russia, 2020, pp. 596-599, doi: 10.1109/EFRE47760.2020.9242089
- [2] V.N. Tikhonov, I.A. Ivanov and A.V. Tikhonov, A new type of non-thermal atmospheric pressure plasma source // J. Phys.: Conf. Ser. 1393 (2019) 012062 doi:10.1088/1742-6596/1393/1/012062
- [3] V.N. Tikhonov, S.N. Aleshin, I.A. Ivanov and A.V. Tikhonov, The low-cost microwave plasma sources for science and industry applications // J. Phys.: Conf. Ser. 927 (2017) 012067 doi:10.1088/1742-6596/927/1/012067

* This work was supported by the Russian Foundation for Basic Research (project No. 20-08-00894).

“OVERHEATING” INSTABILITY FOR AN HF ARC DISCHARGE IN AIR AT ELEVATED PRESSURES

A.F. KOKORIN

Ural Federal University, Yekaterinburg, Russia
e-mail: a.f.kokorin@urfu.ru

During theoretical and experimental research of a high-frequency arc discharge [1] in air at pressures above atmospheric, instability was found, which manifests itself in the appearance of jumps in the current and plasma temperature.

Loop-shaped sections appear on the current-voltage characteristics of the arc. The appearance of "overheating" instability can be explained by the non-monotonic dependence of the coefficient of thermal conductivity of air on temperature. The non-monotonic nature of thermal conductivity is associated with the dissociation of nitrogen and oxygen molecules and has two peaks: in the temperature range (3500-4500) K and (7000-10000) K. The position of the peaks depends on pressure. As it increases, the peaks shift towards higher temperatures.

This type of instability was confirmed in an experimental study of an HF arc discharge. In this case, the current jumps were accompanied by a sharp increase in the plasma temperature and radiation from the discharge region. The active power of the discharge increased, but the reactive power of the discharge increased especially strongly, which was explained by an increase in the discharge inductance caused by a decrease in the radius of the conductive zone.

REFERENCES

- [1] A.F. Kokorin, Vestnik UGTU-UPI, Vol. 231, No. 2, 326-329, 1976.

Author Index

Abdullin E.N.	215
Abzaev Yu.A.	163, 176
Ageychenkov D.G.	133, 147
Ahmetshin S.A.	101
Akhmadeev Yu.H.	66, 104, 155
Akishev Yu.S.	28, 56
Alexeenko V.M.	37
Andreev M.V.	36
Anshakov A.S.	48
Antipov S.N.	248
Argunov G.A.	20, 29
Armyninov S.M.	60
Arslanov K.P.	116
Artyomov A.P.	25, 42, 49
Ashurbekov N.A.	38, 203
Ashurova K.T.	100
Asylbaev A.V.	115
Avtaeva S.V.	45
Babinets I.S.	126
Bakeev I.Yu.	108, 109, 222, 223
Baklanov V.V.	122
Baksh E.Kh.	19
Bakshanskiy R.Yu.	171, 208, 209
Balezin M.E.	169
Bannikova N.S.	160
Barakhvostov S.V.	185
Barengolts S.A.	73
Baryshnikov V.I.	30
Basov G.F.	215
Bazhin P.S.	75
Belomytsev S.Ya.	84
Beloplotov D.V.	19, 31, 32, 228

Belskaya E.V.	21, 50
Benard N.	41
Beschapov P.P.	126
Bestetti M.	138
Bezrukov V.O.	87
Bezukhov K.A.	176
Bleykher G.A.	98
Bobrovskii V.I.	132
Bocong Zheng	85
Bokhan P.A.	21, 33, 50, 219, 236, 237
Bozhko I.A.	137
Bryuhanova Yu.A.	102, 173
Bugaev A.S.	217, 232
Bukina O.S.	118, 122
Buldashev S.A.	214
Bunin I.Zh.	124
Buntov E.A.	116
Burachenko A.G.	19
Burdovitsin V.A.	151
Chaikovsky S.A.	35, 47, 65, 72, 220
Chebakova V.Yu.	206
Cheng Zhang	106
Chengyan Ren	106
Chepelev V.M.	248
Chepusov A.S.	172, 201
Chernyshov S.V.	126
Chesnokov D.A.	144
Chikhachev A.S.	90
Chingina E.A.	185
Chizh T.V.	190
Cholakh S.O.	103
Chuansheng Zhang	106

Chukin A.V.	102, 105, 107
Cvelbar U.	153
Dasheev D.E.	110
Datsko I.M.	34, 35, 65
De Ferron A.	226
Defoort E.	40
Denisov V.V.	82, 117, 121, 123, 154, 247, 249
Denisova Yu.A.	117, 123, 154
Devyatkov V.N.	44, 141, 225
Dienot J.M.	251
Domarov P.V.	48
Doroshkevich S.Yu.	190, 218, 231
Dutov V.A.	116
Dyatlov A.V.	74
Egorov A.O.	121
Egorov I.S.	81, 188
Egorova Yu.	216
Emlin R.V.	214
Erzunov D.A.	103
Esipov R.S.	115
Fedorov S.V.	145
Filatov I.E.	178, 179
Frants O.B.	20, 29
Franz S.	138
Frolova V.P.	217
Gadzhiev M.Kh.	248
Gafarov R.E.	180
Gasparyan Yu.M.	242
Gavrilov N.V.	103, 105, 107
Gelchinski B.R.	99, 101

Geyman V.G.	20, 29
Glubokov N.A.	33, 219
Golobokov N.N.	176
Goncharenko V.I.	159
Gorbatov S.A.	252
Gorlov E.V.	36
Grishkov A.A.	84
Grudin V.A.	98
Gugin P.P.	21, 33, 50, 191, 219, 236, 237, 239, 245, 246
Gulina S.N.	190
Gusev A.	226
Gushchina N.V.	131, 132, 160
Gushenets V.I.	217, 232
Haiyun Luo	27
Handong Li	27, 83
Hashimzade Z.F.	202
Ignatov D.Y.	59, 66
Ilves V.G.	168, 170, 198, 200
Il'inyh S.A.	101
Iminov K.O.	38
Isaeva A.G.	167
Isaeva Z.M.	203
Isakova A.S.	147
Israpov E.Kh.	203
Ivanov A.N.	182
Ivanov A.Yu.	183
Ivanov I.A.	252
Ivanov S.N.	86
Ivanov Yu.F.	94, 95, 96, 104, 112, 128, 140, 142, 143, 155, 163
Ivanov M.G.	205

Ivanova A.I.	137, 158
Ivashutenko A.S.	175
Jafarova R.A.	202
Kaigorodova L.I.	131
Kalinina E.G.	205
Kamenetskikh A.S.	105, 107
Kanshin I.A.	213
Kaplunov I.A.	184
Karalnik V.B.	28, 56
Kashapov L.N.	206
Kashapov N.F.	206
Kashlev A.R.	87
Kasyanov V.S.	58
Kazakov A.V.	233, 234
Kazantseva E.A.	125, 156
Kaziev A.V.	126, 127, 133, 147, 235, 242
Khabarova I.A.	124
Khairtdinov E.F.	115
Khaltanova V.M.	181
Kharkov M.M.	126, 127, 133, 242
Khimich M.A.	127
Kholodnaya G.	188
Khomich V.Yu.	199
Khomyakov A.Yu.	242
Khramtsov S.P.	244
Kim V.A.	21
Kiryukhantsev-Korneev Ph.	134
Kladukhin V.V.	244
Klimkin A.V.	81
Klimov A.S.	108, 109, 222, 223
Klopotov A.A.	163, 176
Kokorin A.F.	253

Kokovin A.O.	61, 62
Kokshenev V.A.	77, 78
Kolmakov S.V.	152
Kolobov Yu.R.	177
Kolodko D.V.	126, 133, 147, 235
Komarova E.G.	125, 156
Komarskiy A.A.	172, 201
Kondratiev S.S.	37
Korneva O.S.	137, 158
Korolev Y.D.	20, 29, 58
Korsakov A.S.	189
Korsakova E.A.	189
Korzhenevskiy S.R.	172, 201
Koval N.N.	44, 94, 100, 128, 141, 142, 218, 231
Koval T.V.	100
Kovalsky S.S.	58, 59, 66, 82, 117, 154, 249
Kozevnikov V.V.	228
Kozhahmetov Ye.A.	118, 122
Kozhevnikov V.Y.	61, 62
Kozlov B.A.	63, 64, 238
Kozyrev A.V.	37, 61, 62
Krashaninin V.A.	101
Krasniy O.D.	172
Krivobokov V.P.	98
Krivonogova A.S.	167
Krivoshapko S.V.	105, 107
Krysin O.V.	95, 104, 112, 128, 155
Kukhareno A.I.	103
Kukushkina M.S.	126, 127
Kun Xie	106
Kurmaev E.Z.	103

Kurmaev N.E.	77, 78
Kustova E.V.	70
Kuzmenko A.P.	148
Kuznetsov D.L.	178, 179
Kuznetsov V.P.	152, 164
Kuznetsov V.S.	243
Kvashnina A.A.	50
Labetskaya N.A.	34, 35, 65
Landl N.V.	20, 29, 58
Lapina A.E.	110, 181
Larbaig J.M.	251
Lavrinovich I.	226
Lavrukhin M.A.	236, 237
Leduc R.	251
Lei M.K.	216
Lenskiy A.D.	224
Leonov A.A.	117, 121, 123, 154
Levanisov V.A.	218, 231
Levashov E.	134
Leys C.	153
Lezhnin N.V.	152, 164
Li Y.	216
Ligachev A.E.	135, 177
Lijun Zong	187
Lipchak A.I.	185
Lisenkov V.V.	51, 53, 60, 86, 186, 189
Lisovsky D.A.	227
Lo Porto C.	153
Loginov S.V.	54
Lomaev M.I.	19, 32, 74, 228
Lopatin I.V.	58, 59, 66, 104, 137, 225
Loskutov O.M.	163

Loy N.N.	190
Lutsenko Y.Y.	55
Lvov A.E.	189
Lykov S.V.	96
Ma H.	197
Makarov A.V.	152, 164
Makarov E.V.	162
Makhadilov I.M.	195
Makhanko D.S.	63, 238
Malinskiy T.V.	184
Mamedov N.V.	88
Mamontov D.V.	115
Mamontov V.A.	166, 196
Mamontov Y.I.	24, 51, 52, 53, 86
Markov A.B.	129, 136
Maslov A.A.	111, 113, 114
Matitsev A.I.	116
Medovnik A.V.	233
Men'shakov A.I.	102, 173
Meschanov A.V.	75
Mesyats G.A.	23, 26, 46, 80
Mikhailov P.S.	39, 130, 220, 221
Milakhina E.V.	191, 239, 245, 246
Milonov A.S.	110
Milyaev M.A.	160
Miniyazov A.Zh.	118, 146
Mishigdorzhyn U.L.	192
Modic M.	153
Molchanov D.V.	224
Moreau E.	40, 41
Morini F.	138
Morozov P.A.	214

Moshkunov S.I.	76, 194
Moskvin P.V.	44, 100, 141, 225
Murtazaeva A.A.	203
Mustafaev E.S.	145
Muzyukin I.L.	39, 130, 220, 221
My Kim An Tran	100
Myo Min Than	148, 196
Myusova A.E.	55
Nagimov R.Sh.	111, 113, 139
Nassyrbayev A.	174
Nay Win Aung	196
Nazarov A.Yu.	111, 113, 114, 139
Nebogatkin S.V.	76, 194
Nekhoroshev V.O.	20, 29, 58
Nesterov V.N.	193
Nikiforov A.	153
Nikitin D.S.	174
Nikolaev A.A.	139
Nikolaev E.O.	97, 119
Nikulin S.P.	91
Nomoev A.V.	192
Novac B.	226
Novikov P.A.	144
Oks E.M.	149, 217, 223, 229, 230, 232, 233, 234, 250
Okulov R.A.	99
Oleinik A.V.	139
Oleshko V.S.	159
Orazgaliev N.A.	122
Oreshkin E.V.	47, 65, 92
Oreshkin V.I.	25, 35, 42, 43, 47, 49, 65

Orlov A.N.	60, 189
Osipenko E.A.	23
Osipov V.V.	60, 186, 189
Ostroverkhov E.V.	82, 117, 247, 249
Ovchinnikov V.V.	131, 132, 160, 161, 162
Palmeri A.	138
Palumbo F.	153
Panarin V.A.	243
Panchenko A.N.	228
Panchenko N.A.	233, 234
Panchenko Yu.N.	36
Paperny V.L.	30
Patrakov V.E.	227, 240
Pavlov A.V.	144, 157
Pecastaing L.	226
Pedos M.S.	240
Peng Zhang	85
Pesterev E.A.	129, 136
Petrikova E.A.	94, 96, 104, 112, 140, 142, 155
Petrov A.S.	148
Petrov V.I.	136
Petryakov A.V.	28, 56
Platonov V.V.	186, 189
Poloskov A.	188
Poloskov A.V.	81
Ponomarev A.V.	172
Ponomarev D.	188
Poplavsky V.V.	120
Popov E.V.	99
Potemkin G.V.	135, 177
Prima A.I.	89, 216
Prokopenko N.A.	112, 128, 140

Prokop'ev V.E.	82, 95, 249
Prosolov K.A.	127
Protasov Y.Y.	157
Prozhega M.V.	126
Prudaev I.	226
Puchikin A.V.	36
Pugachevskii M.A.	166, 196
Punanov I.F.	214
Pushkarev A.I.	89, 216
Qi Hua Fan	85
Raab G.I.	115
Rabadanov K.M.	38, 203
Rakhmatullin I.A.	175
Ramazanov K.N.	113
Rashidova S.Y.	202
Rasposienko D.Y.	131
Remnev G.E.	135
Rempel A.A.	99, 101
Reschikov E.O.	126
Ripenko V.S.	156
Rogalin V.E.	184
Rogovaya O.S.	194
Rohmanenkov A.S.	88
Romanov K.I.	76
Rousskikh A.G.	25, 42, 43, 49
Rousskikh I.A.	42
Rukin S.N.	240
Rusakova D.S.	205
Ruscassie R.	251
Ryabchikov A.I.	137
Rybka D.V.	224
Rybkin V.V.	182
Rygina M.E.	96, 104, 112
Rykunov G.I.	126, 127, 235

Ryzhenkova A.Yu.	166
Saifutdinov A.I.	69, 70, 71
Saifutdinova A.A.	69, 71
Salimgareev D.D.	189
Samiru A.	193
Sanzharova N.I.	190
Sargsyan M.A.	248
Savchuk M.V.	121, 123
Savkin K.P.	241
Sazonov R.	188
Semeniuk N.S.	37
Semenov A.P.	97, 119
Semenov G.V.	155
Semenova I.A.	97
Semenovych M.A.	208, 209
Serebrennikov M.A.	81, 188
Sergeev N.S.	133, 147, 235, 242
Serushkin S.V.	57
Shakhsinov G.S.	38, 203
Shakreev Y.P.	125
Shalomov K.V.	160, 161
Shandrikov M.V.	229, 230
Shanenkov I.I.	174
Shanenkova Y.L.	175
Sharkeev Y.P.	156
Sharkeev Yu.P.	127
Sharypov K.A.	23, 26
Shchepanuk T.S.	157
Shcherbakov Y.N.	214
Shekhovtsov V.V.	171, 176, 180, 208, 209
Shershunova E.A.	76, 194
Shevchenko G.V.	21
Shin V.I.	44, 100, 141, 225

Shishpanov A.I.	75
Shitov V.A.	207
Shklyayev V.A.	31, 84
Shmelev D.L.	72, 73, 220
Shpak V.G.	23, 26, 211
Shuai Zhang	187
Shugurov V.V.	94, 95, 112, 128, 142, 143
Shunailov S.A.	23, 26, 211
Shutov D.A.	182
Sidelev D.V.	98
Sirosh V.A.	152, 164
Sitkevich A.L.	183
Sivin D.O.	137, 158
Sivkov A.A.	174, 175
Skakov M.K.	118, 122, 146
Skakun V.S.	243
Sklizkov I.D.	115
Skorynina P.A.	152, 164, 173
Skriabin A.S.	144
Skripnikova N.K.	171, 208, 209
Slobodyan M.S.	136
Smirnova K.V.	182
Smirnyagina N.N.	110, 181
Sokolov I.A.	118, 122, 146
Sokovnin S.Yu.	167, 168, 169, 170, 198, 200
Solis N.W.	195
Solodovnikov A.A.	88
Solovev A.V.	129, 136
Sorokin D.A.	19, 31, 32, 74, 228, 241, 243
Sorokin S.A.	177

Sorokina A.R.	69
Sosnin E.A.	243
Stasenko A.M.	126
Sulakshin S.A.	218, 231
Suleymanova S.A.	202
Sultanova T.R.	170
Surkov Yu.S.	102
Suslova O.V.	190
Svetlova O.A.	170, 198
Tao Shao	106, 187
Tarasenko V.F.	19, 31, 32, 74, 228
Tazmееv A.K.	204
Tazmееv B.K.	204
Tazmееv G.K.	204, 212
Tazmееv K.K.	212
Telekh V.D.	144, 157
Teresov A.D.	94, 96, 140, 142, 154, 155, 163
Tet Oo	145
Thant Sin Win	148
Thet Naing Soe	195
Thet Phyto Naing	196
Tikhonov A.V.	252
Tikhonov E.V.	186
Tikhonov V.N.	252
Timerkaev B.A.	69, 71, 212
Tishchenko V.N.	117, 123
Tolkachev O.S.	112
Torba M.S.	218, 231
Tran V.T.	223
Tretnikov P.V.	105, 107
Trigub M.V.	81
Tsvetoukh M.M.	67, 68, 73
Tsvetkov N.A.	176

Tsyrenov D.B-D.	97, 119
Tulenbergenov T.R.	118, 146
Tumarkin A.V.	133, 147
Turmyshev I.S.	185
Tyukavkin A.G.	42
Tyunkov A.V.	149, 150, 151
Uimanov I.V.	22, 24, 46, 52, 72, 73, 220
Uimin M.A.	168, 169, 200
Ulakhanov N.S.	119, 192
Ulitko M.V.	170
Ustinov A.M.	163
Uvarin V.V.	178, 179
Vafin R.K.	115
Vakhrushev D.O.	158
Van'kevich V.A.	34, 35, 65
Vardanyan E.L.	111, 113, 114, 139
Vasiliev S.V.	183
Vazirov R.A.	167
Verboncoeur John P.	85
Vicenzo A.	138
Vichuzhanin D.I.	131
Vizir A.V.	229, 230
Vladimirov A.B.	152, 164
Vlasov V.A.	176
Volkov N.B.	185
Volokitin G.G.	176, 209
Volokitin O.G.	171, 180
Vorobyov M.S.	44, 100, 141, 190, 218, 231
Voronin V.I.	132
Vympina Y.N.	175
Wang L.	153

Wu F.F.	197
Xiaobing Zou	83
Xie S.Y.	197
Xin Zeng	187
Xinxin Wang	27, 83, 85
Xiucui Hu	187
Yakovlev E.A.	87
Yakovlev E.V.	129, 136
Yakovlev V.V.	117, 121
Yalandin M.I.	23, 26, 211
Yampolskaya S.A.	79
Yamshchikov V.A.	199
Yan H.	41
Yangyang Fu	83, 85
Yashnov L. Y.	214
Yastremskii A.G.	79
Yolchueva U.J.	202
Yugay V.V.	87
Yurov V.M.	159
Yushkov G.Yu.	229, 230, 241
Yushkov Yu.G.	149, 150, 151
Yutai Li	27, 83
Zaguliaev D.V.	163
Zakaryaeva M.Z.	38
Zakrevsky D.E.	21, 33, 50, 191, 219, 236, 237, 239, 245, 246

Zatsepin A.F.	116
Zavornitsyn R.S.	160
Zemskov Yu.A.	22, 24, 220
Zenin A.A.	108, 109, 222, 223
Zhanbolatova G.K.	118, 122, 146
Zhang C.H.	197
Zhang C.C.	216
Zharin A.	156
Zharkov V.I.	36
Zherlitsyn A.A.	37
Zhidkov I.S.	103, 173
Zhidkov M.V.	135, 177
Zhigalin A.S.	25, 42, 43, 49
Zhigang Liu	83
Zhu M.	197
Zhu X.P.	216
Zhukova L.V.	189
Zhupanov V.G.	144
Zinovyev L.A.	87
Zolotukhin D.B.	149, 150, 151
Zubarev N.M.	23, 26, 80

Научное издание

**15-Я МЕЖДУНАРОДНАЯ КОНФЕРЕНЦИЯ
"ГАЗОРАЗРЯДНАЯ ПЛАЗМА И ЕЁ ПРИМЕНЕНИЕ"
(GDP 2021)**

Тезисы

**УДК 533.9
ББК 22.333.3
ISBN 978-5-6046849-0-0**

Материалы публикуются в авторской редакции.
Верстка: Чингина Е.А., Крутикова И.В., Болтачев Г.Ш.
Дизайн обложки: Уйманова Е.Ю.

Ответственный за выпуск Н.М. Зубарев

Подписано в печать 09.08.2021.
Формат 60x90 1/8. Тираж 20 экз.

Участок оперативной полиграфии Уральского отделения РАН
620049, г. Екатеринбург, ул. Первомайская, д. 91.

© Институт электрофизики Уральского отделения Российской академии наук